LEABHARLANN CHOLÁISTE NA TRÍONÓIDE, BAILE ÁTHA CLIATH | TRINITY COLLEGE LIBRARY DUBLIN
Ollscoil Átha Cliath | The University of Dublin

Terms and Conditions of Use of Digitised Theses from Trinity College Library Dublin

Copyright statement

All material supplied by Trinity College Library is protected by copyright (under the Copyright and Related Rights Act, 2000 as amended) and other relevant Intellectual Property Rights. By accessing and using a Digitised Thesis from Trinity College Library you acknowledge that all Intellectual Property Rights in any Works supplied are the sole and exclusive property of the copyright and/or other IPR holder. Specific copyright holders may not be explicitly identified. Use of materials from other sources within a thesis should not be construed as a claim over them.

A non-exclusive, non-transferable licence is hereby granted to those using or reproducing, in whole or in part, the material for valid purposes, providing the copyright owners are acknowledged using the normal conventions. Where specific permission to use material is required, this is identified and such permission must be sought from the copyright holder or agency cited.

Liability statement

By using a Digitised Thesis, I accept that Trinity College Dublin bears no legal responsibility for the accuracy, legality or comprehensiveness of materials contained within the thesis, and that Trinity College Dublin accepts no liability for indirect, consequential, or incidental, damages or losses arising from use of the thesis for whatever reason. Information located in a thesis may be subject to specific use constraints, details of which may not be explicitly described. It is the responsibility of potential and actual users to be aware of such constraints and to abide by them. By making use of material from a digitised thesis, you accept these copyright and disclaimer provisions. Where it is brought to the attention of Trinity College Library that there may be a breach of copyright or other restraint, it is the policy to withdraw or take down access to a thesis while the issue is being resolved.

Access Agreement

By using a Digitised Thesis from Trinity College Library you are bound by the following Terms & Conditions. Please read them carefully.

I have read and I understand the following statement: All material supplied via a Digitised Thesis from Trinity College Library is protected by copyright and other intellectual property rights, and duplication or sale of all or part of any of a thesis is not permitted, except that material may be duplicated by you for your research use or for educational purposes in electronic or print form providing the copyright owners are acknowledged using the normal conventions. You must obtain permission for any other use. Electronic or print copies may not be offered, whether for sale or otherwise to anyone. This copy has been supplied on the understanding that it is copyright material and that no quotation from the thesis may be published without proper acknowledgement.

Identification of novel targets for cancer chemotherapeutic agents: Design, synthesis and evaluation of chromene based compounds with affinity for steroid hormone receptors

Billy Egan (B.Sc.)

A thesis submitted to the University of Dublin for the degree of Doctor of Philosophy.
Based on research carried out under the supervision of Prof. Mary J. Meegan

School of Pharmacy and Pharmaceutical Sciences
University of Dublin
Trinity College

May 2013

Declaration

I declare that this thesis has not been submitted as an exercise for a degree at this or any other university and it is entirely my own work.

I agree to deposit this thesis in the University's open access institutional repository or allow the library to do so on my behalf, subject to Irish Copyright Legislation and Trinity College Library conditions of use and acknowledgement.

Signed

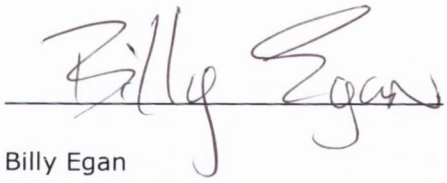

Billy Egan

TRINITY COLLEGE
- 4 MAR 2014
LIBRARY DUBLIN

Thesis 10991

Abstract

Breast cancer is the second most common cancer in Ireland and accounts for 28% of all cancers in women in Ireland, with an average of 1726 new diagnosis each year. One of the major therapeutic advances in clinical treatment of breast cancer has been the introduction of selective estrogen receptor modulators (SERMs). Tamoxifen is a selective estrogen receptor modulator (SERM) with a triarylethylene structure which acts as an estrogen antagonist in the breast. This drug is used extensively and successfully as an endocrine treatment for breast cancer. However, it can also act as an agonist in endometrial tissue resulting in unwanted side effects including endometrial cancer. A variety of modified triarylethylene SERM structures have been developed based on the non-isomerisable scaffold structures such as raloxifene. The vast majority of early stage breast cancers, in both pre- and postmenopausal women, are hormone-dependent. The human hormone estradiol has an important role in the progression of breast cancer. The key feature of the SERMs, which are chemically diverse compounds, is that they contain a tertiary structure that enables them to bind to the estrogen receptor.

The successful discovery of new drugs for cancer chemotherapy requires a combination of chemical and biochemical data and is both a costly and challenging task. Using *in silico* high throughput screening (HTS) methods, a novel series of estrogen receptor antagonists featuring the chromene scaffold has been discovered. In this thesis a comprehensive library of structurally related chromene compounds has been synthesised and evaluated. These compounds provide a resource of small-molecule SAR (structure–activity relationship) data, which can be used to guide lead compound identification in the area of drug discovery for estrogen receptor antagonists. These novel structures are designed to incorporate the potent chromene scaffold structure, and the data provides promising evidence for use of the benzopyran and pyranocoumarin ring scaffolds as an effective method for producing large libraries of novel compounds with interesting biochemical activities. Thirteen different libraries of benzopyran and pyranocoumarin compounds were synthesised (Chapter 2) and evaluated for antiproliferative activity *in vitro* in MCF-7 estrogen receptor positive human breast cancer cells (Chapter 3). These compounds bind to the estrogen receptor, while also inhibiting the proliferation of a human MCF-7 breast carcinoma cell

line with a considerably higher potency than tamoxifen. The most potent compound in the entire library of products evaluated was identified as 2-ethoxyethyl 2-amino-7-(dimethylamino)-4-{4-[(4 methylphenyl)methoxy] pheny -4*H*-chromene-3-carboxylate (BE97). This compound displays an IC_{50} value of 0.92 μM in the antiproliferative assay in MCF-7 breast cancer cells. The combination of the effects of the 4-methylbenzyloxyaryl ether at C4, the ethoxyethyl ester at C-3 and the N,N-dimethylamino substituent at C-7 contributes to optimise the structural requirements for activity. A number of the chromene products also displayed potent activity as estrogen receptor antagonists in a competitive binding assay. The results from the biochemical analysis are rationalized using molecular modelling studies. Additionally, in Chapter 4, the synthesis and structural characterisation of a series of novel naphthalene-2-carbohydrazide derivatives are described as novel non-ligand binding pocket androgen receptor antagonists. X-ray analysis of two examples of these compounds is presented and the structure–activity relationships for these compounds as potential therapies for prostate cancer is discussed.

Acknowledgements

I would like to thank first and foremost my supervisor Prof Mary Meegan. Thank you for all for your help not only in meticulously writing the thesis but all of the help and guidance in the lab throughout the past 4 years when I needed it. Thanks for your incredible patience, your invaluable knowledge and expertise on the many areas of chemistry covered throughout the duration of this project. Thank you for giving me the support and confidence in my work!

A big thank you also to Dr Cormac O'Donohoe for much of the help and support you have given me throughout the course of my project. From the first day you helped me get set up and more recently your experience especially to process the data from the NCI was really appreciated.

A special thank you to Dr. Fernando Blanco for the constant motivation, and to the rest of "team hydrazine" in the Molecular Design Group. Thanks you to Prof David Lloyd for collaborating with us to publish the papers.

Thanks also to those who provided spectroscopy and chromatography data for all the compounds that were synthesised in this project, including Dr. John O'Brien, Dr. Manuel Ruether and Dr. Martin Feeney in the School of Chemistry, and Mr. Brian Talbot in the School of Pharmacy, Trinity College Dublin. Thank you to Dr. Tom Mc Cabe in the X-Ray crystallography facility for all of the cystal data provided. Thanks to Dr. Stephen Hynes (Henkel Ltd.) for donation of the various cyanoacetate esters which were used in the synthesis of each chromene products.

Thanks to all of my colleagues in the medicinal chemistry labs in the School of Pharmacy for their support, help in every area, coffee chats and humourous observations! I can't name everyone but you all know who you are, especially Pat, Shu, Conor, Tadgh, Jun, Andy, Jason, Sid, Yvonne, Mike and Ferenc. Thank you to all of the technicians and to all the staff and in the School of Pharmacy Trinity College Dublin and to anyone else who has been helpful during my time there.

I would like to thank my family for their encouragement, support and patience throughout my studies. To my dad, Bill who has always helped me regardless of any

challenges, and Marguerite, I really appreciate all the helpful support you have given me. To my sisters Nicky, Suzi and Clodagh (and families!) for your support and encouragement. A huge and very special thank you to my late mother Mary Egan, to whom this thesis is dedicated.

Thank you to my Italian family, la famiglia Caboni for welcoming me to my second home in Sardegna. To Giorgio, Angela and Paolo for your love, support, and encouragement. You always have been so kind, generous, and fun spirited!

Finally to my new wife Dr. Laura Caboni (Egan), thanks you so much for all of the support you given me thoughout the PhD process. We have encouraged each other by both undertaking PhD projects at the same time, and at times the levels of compassion and empathy for each others daily predicaments were truly tested, I was always glad both of us were in similar situatiuons. Laura I am overjoyed to have married you and we can look forward to our new life together with many more adventures to share on the horizon. *Grazie di esistere!*

Table of Contents

Declaration ii

Abstract iii

Acknowledgements v

Table of Figures xiv

Table of Schemes xx

Table of Tables xxi

Table of Abbreviations: xxiii

Chapter 1: Introduction xxvi

1.1 Introduction and Background 1

1.1 .2 Cancer 1

1.2 Breast Cancer 5

1.2.1 Types of Breast Cancer 6

1.2.2 Irish statistics of breast cancer occurrences 10

1.2.3 Estrogens and Breast Cancer 13

1.2.4 ER antagonists *general* 18

1.3 Nonsteroidal antiestrogens (SERMs) 18

1.3.1 Tamoxifen 19

1.3.2 SERDs 27

1.4 HMR 3339 28

1.5 Aromatase Inhibitors 28

1.5.1 The Steroid Tree 31

1.5.2 Novel SERMs and related compounds 32

1.5.3 Pyrazole SERMs 32

1.5.4 General biological activity of Benzopyrans and Chromenes 34

1.6 Chromenes as SERMs with breast cancer activity 36

1.6.1 Chromenes and coumarins targeting ERβ- SERBAs 37

1.6.2 Chromanes 39

1.7 Biologically active coumarins 42

1.7.1 Chromene scaffold in tubulin targetting 44

1.8 Androgen receptor - Nonsteroidal AR Ligands 47

1.8.1 Discovery of nonsteroidal SARMs- Propionanilides 48

1.8.2 Quinolinone, Coumarin and Chromeno-Benzazepines; AR Antagonists 50

1.9 Targeting the Nuclear Receptor –Cofactor 51

1.9.1 Hydrazides targeting AR 51

1.10 Virtual high throughput screening (*v*HTS) 53

1.11 Objectives 57

Chapter 2: 4*H*-Chromene ring as a Scaffold for Design of Selective Estrogen Receptor Modulators (SERMs): Synthesis of Tamoxifen analogues 58

2 Results and Discussion 59

2.0 Benzopyrans 61

2.01 Development of chromenes as SERMs in breast cancer therapy 64

2.02 Knoevenagel condensation as a synthetic route to novel Chromene type SERMs 68

2.1 Section 1,4-Aryl-4*H*-chromenes 69

2.1.1 Results series 1: Synthesis of the library of chromene compounds 69

2.1.2 Spectroscopic Identification 73

2.1.3 XRD Crystallography study of structure BE11 77

2.2: Series 2; Synthesis of 2-amino-7-hydroxy-4*H*-chromene carboxylates using a two step method 79

2.3 Series 3: Discovery of novel adduct, pyranodiethyldiamino-4*H*-chromene dicarboxylate. 82

2.3.1 Synthetic route to novel adduct pyranochromene BE33 82

2.3.2 Spectroscopic Identification 84

2.3.3 XRD Crystallography study of BE33- Novel adduct pyrano chromene 87

2.4 Series 4: Chromenes with variation of the ester substituent at the C-3 position of the chromene..... 89

2.4.1 Results series 4: Synthesis of the library of chromene compounds..... 89

2.4.2 Spectroscopic identification 90

2.5 Series 5: 4-Hydroxyphenyl chromenes with variation on the C-3 ester side chain 93

2.5.1 Results series 5..... 93

2.5.2 Spectroscopic identification 95

2.6 Series 6: 4-Benzyloxyphenyl chromenes with variation in the structure on the C-3 ester side chain 98

2.6.1 Results series 6: Synthesis of the library of chromene compounds..... 99

2.6.2 Spectroscopic identification 101

2.6.3 XRD Crystallography Structure of 4-(3-Benzyloxyphenyl)-*4H*- chromene BE70..... 103

2.7 Series 7: 4-(3,4,5-Trimethoxyphenyl)-4*H*-chromenes with variation of the R_2 ester at C-3 106

2.7.1 Results series 7 Synthesis of the library of 3,4,5-trimethoxyphenyl chromene compounds 106

2.7.2 Spectroscopic identification 108

2.7.3 XRD Crystallography Study of 4-(3,4,5-trimethoxyphenyl)-2-amino-4*H*-chromene carboxylate ester BE79..... 110

2.8 Series 8: 2,7-Diamino-4*H*-chromenes with arylbenzyloxy ether substituent at C-4 and selected esters at C-3. 114

2.8.1 Results series 8: Synthesis of the library of 2,7-diamino chromene compounds 114

2.8.2 Spectroscopic identification 116

2.9 Series 9: 4-Benzyloxyaryl chromenes with N,N-dimethylamino substituent group at C-7 118

2.9.1 Results series 9..... 119

2.9.2 Spectroscopic identification 120

2.10 Series 10: 4-Arylchromene compounds synthesised with ester subsuituents introduced at C-7 123

2.10.1 Results series 10 124

2.10.2 Synthesis of4*H*-chromene ester BE108.....125

2.10.3 Spectroscopic identification.....125

2.11 Series 11: *Bis* 4*H*-chromene compounds 128

2.11.1 Results series 11 *bis* chromenes.....130

2.11.2 Spectroscopic Identification 131

2.12 Coumarin ring as a scaffold for design of Selective Estrogen Receptor Modulators (SERMS) 133

2.12.1 Introduction.....133

2.12.2 Series 12, Pyranocoumarin (pyrano[3,2-c]benzopyran-5-one) precursors: Benzylidene malononitrile intermediates.....139

2.12.3 Results series 12 Synthesis of the library of malononitrile intermediates BE116-BE129.....140

2.12.4 Synthetic route to 2-(4-methoxybenzylidene)malononitrile.....141

2.12.5 Spectroscopic identification.....141

2.13 Series 13, Pyranocoumarin (pyrano[3,2-c]benzopyran-5-one) synthesis 144

2.13.1 Results series 13 Synthesis of the library of 4-arylpyrancoumarin (pyrano[3,2-c]benzopyran-5-one) products 145

2.13.2 Synthetic route to *pyranocoumarin BE130* 146

2.13.3 Spectroscopic identification.....147

2.14 Series 14 Synthesis of the library of pyranoocoumarins (pyrano[3,2-c]benzopyran-5-ones) substituted with basic ether chains 149

2.14.1 Results Series 14 150

2.14.2 Synthetic route to basic ether substituted pyranocoumarins 151

2.14.3 Spectroscopic identification.....152

2.15 Conclusion.....155

Chapter 3 *4H*-Chromenes and pyranocoumarins: Biochemical activity and molecular modelling 156

3. Introduction: Biochemical activity of 4*H*-Chromenes 157

3.1 Experimental details 157

3.1.1 MCF-7 human breast cancer cell lines 158

3.1.2 LNCaP human prostate cancer cell lines 158

3.1.3 Storage and breaking out of cells 159

3.1.4 Growth and maintenance of cells 160

3.1.5 Counting cells 160

3.1.7 Measurement of growth inhibitory effects: the alamarBlue assay 162

3.2 Biochemical evaluation of chromene products for antiproliferative activity 163

3.2.1 Results series 1: 4-Aryl substituted 4*H*-chromenes with varied aryl and benzyloxy substitutions.; type1 166

3.2.2 Results series 2: 4*H*-Chromenes synthesised using a 2 step method. 170

3.2.3 Results series 3: 4*H*,6*H*-pyrano[3,2-g]chromene product BE33. 171

3.2.4 Results series 4: 3-Phenyl-4*H*-chromenes with C-3 ester substituents 172

3.2.5 Results series 5: 4-Hydroxyphenyl-4*H*-chromenes with ester substituents chain. 174

3.2.6 Results series 6: 4-Benzyloxyphenyl-4*H*-chromenes with various C-3 esters. 176

3.2.7 Results series 7: 3,4,5-Trimethoxyphenyl substituted chromenes with variation on the C-3 ester 180

3.2.8 Results series 8: 2,7-Diaminochromene compounds 182

3.2.9 Results series 9: 4-Benzyloxyarylchromenes with N,N-dimethylamino substituent at C-7 184

3.2.10 Results series 10: Chromenes with ester substituent at C-7 186

3.2.11 Results series 11: *bis* 4-aryl-4*H*-chromenes 188

3.2.12 Results series 13: Pyranocoumarin (pyrano[3,2-c]benzopyran-5-one) products. 189

3.2.13 Results series 14: Pyranocoumarins (pyrano[3,2-*c*]benzopyran-5-ones) with substituted antagonistic type basic ether chains 191

3.3 Antiproliferative results of LNCaP Assays 192

3.4 Molecular Modelling 195

3.5 ER binding assays 201

3.5.1 Time Resolved Fluorescence Resonance Energy Transfer (TR-FRET) 201

3.5.2 Fluorescence Polarization (FP) 202

3.5.3 Estrogen receptor binding activity results 204

3.5.31 ERα binding assay results 205

3.5.32 ERβ binding assay results 206

3.5.4 FRET ER binding assay in agonist and antagonist mode 210

3.6 The NCI-60 human tumour cell line drug screen and the COMPARE algorithm 211

3.6.1 Compounds submitted to NCI-DTP 212

3.6.2 COMPARE algorithm 220

3.7 Conclusions 222

Chapter 4 Synthesis of novel non-ligand binding pocket androgen receptor antagonists 224

4.1 Introduction 225

4.2. Synthesis of 3-hydroxy-N'-((naphthalen-2yl)methylene)naphthalene-2-carbohydrazide derivatives 228

4.3. NMR spectroscopic characterization 229

4.4. X-ray analysis 233

4.5. Biochemical study 235

4.6 Qualitative SAR analysis 237

4.7 Structural Basis of AR-Antagonism by Diarylhydrazides 239

4.8. Synthesis of Diarylhydrazides (Panel 2) 240

4.9 X-ray analysis 243

4.10 Biochemical Evaluation of AR Modulation 245

4.11 Structure Activity Relationship Study (Panel 2) 246

4.12 Molecular Modelling study of Diarylhydrazides into AR AF-2. 248

4.13 Conclusions 251

5.1 Chemistry Experimental Section..... 253

5.2 Synthesis of Chromenes using one-pot *piperidine*-catalyzed *Knoevenagel* condensations 254

5.3 Synthesis of Diamino-chromenes using one-pot *piperidine*-catalyzed *Knoevenagel* condensation reactions 339

Esterification of benzopyrans 350

5.4 Coupling reaction of Ethyl 2-amino-7-hydroxy-4-(4-methoxyphenyl)-4H-chromene-3-carboxylate with 3,4,5-Trimethoxybenzoic acid 360

5.5 Synthesis of benzyloxyaldehydes 369

5.6 Synthesis of Benzyloxy-benzopyrans, using one-pot piperidine-catalyzed Knoevenagel condensations 374

5.7 Synthesis of Dimethylamino-chromenes using one-pot piperidine-catalyzed Knoevenagel condensations 374

5.8 Synthesis of Benzylidene intermediates using malononitrile intermediates..... 375

5.9 Coumarin Products 383

5.10 Alkylation of Coumarins 393

5.11 Synthesis of Naphthohydrazides..... 396

6.0 Bibliography 423

Appendix: X-Ray crystallography data

Table of Figures

Figure 1. 1 Tumorigenesis 2
Figure 1. 2 Not all tumors are cancerous; tumors can be benign or malignant 3
Figure 1. 3 Selection of chemotherapeutics specifically targeting ER positive breast cancer 8
Figure 1. 4 Ranking of the most commonly diagnosed invasive cancers in Ireland (excluding NMSC), 2007-2009 [36] 10
Figure 1. 5 Person-years of life lost due to cancer in Ireland, 1996 and 2006 [36] 11
Figure 1. 6 Estimated cancer incidence and mortality in Europe 2008 – female breast cancer[36] 12
Figure 1. 7 Domain-structure representation of human ERα and ERb isoforms [44] ... 13
Figure 1. 8 Estrogen receptor mechanism of action 15
Figure 1. 9 Binding of agonists and antagonists to the ER 16
Figure 1. 10 The binding of estradiol in the estrogen receptor LBP. The region of the binding cavity above the plane of the bound hormone is referred to as the β-face, whereas the area below the plane is referred to as the α-face [52] 17
Figure 1. 11 (a) ERα-selective ligand: Propyl pyrazole triol; (b) ERβ-selective ligand: Genistein 17
Figure 1. 12 Raloxifene (a) and Arzoxifene (b) 25
Figure 1. 13 New generation SERMs: lasofoxifene (left); bazedoxifene (right) 26
Figure 1. 14 Structure of Fulvestrant 27
Figure 1. 15 HMR 3339 28
Figure 1. 16 Structures of Aromatase Inhibitors, (a) Steroidal aromatase inactivator and (b) Non-steroidal aromatase inhibitors [1] 30
Figure 1. 17 The Steroid Tree [89] 31
Figure 1. 18 Pyrazole agonist (a) and corresponding antagonist (b) 33
Figure 1. 19 Indolazine ER modulators 33
Figure 1. 20 Biologically active chromenes 36
Figure 1. 21 EM 800 (a) and EM 652 (b) 37
Figure 1. 22 3,8-Dihydroxy-6H-benzochromen-6-one scaffold 38
Figure 1. 23 ERβ selective benzochromene structures 38
Figure 1. 24 Benzopyranobenzopyran 12, and Benzopyranobenzoxepane 13 39
Figure 1. 25 Partial estrogen receptor antagonists 40
Figure 1. 26 SERBA 18 [109] 42
Figure 1. 27 Two new coumarins, glaumacidines (19) and (20) 43

Figure 1. 28 Coumarin-3(N-aryl)carboxamides investigated for antiproliferation activity 43
Figure 1. 29 Tubulin targeting agents , including CA-4P, ZD6126 and 4-aryl-4H-chromenes 46
Figure 1. 30 Structures of 4H-chromene-3-carboxylate compounds 26 and 27. 47
Figure 1. 31 Anilide derivatives as antiandrogens 47
Figure 1. 32 SARM 31, incorporating the chromene scaffold 48
Figure 1. 33 Discovery of propionanilide AR agonists with in vitro and in vivo activity 49
Figure 1. 34 Selection of Coumarin, Quinolinone and Chromene Antagonists 37[127], 38[128], 39[120, 129] and 40[130, 131] 50
Figure 1. 35 Cofactor AR Antagonists 41, 42 and 43 52
Figure 1. 36 Residue ligand interactions of the agonist Estradiol in ERα and antagonist Raloxifene in ERα [139] 54
Figure 1. 37 Examples of scaffolds identified through the vHTS protocol 55
Figure 1. 38 Schematic of target specific virtual screening (TS-VS) filtering procedure with lead chromene compound 47 55
Figure 1. 39 A total of 7 hits were identified by vHTS and chosen for biochemical evaluation [139] 56

Figure 2. 1 SERMs Tamoxifen, Raloxifeen and Bazedoxifen in clinical use 59
Figure 2. 2 Structural isomers of Benzopyran 61
Figure 2. 3 Drugs containing the chromene (benzopyran) ring system and related scaffolds 63
Figure 2. 4 Chromene scaffold (A) indicating position of R group substitutions. R_1, R_2, , and Pyranocoumarin scaffold (B) displaying position of R group substitution. 67
Figure 2. 5 ^{1}H NMR spectrum for benzopyran BE2 73
Figure 2. 6 ^{13}C NMR (upper) and DEPT 135 (lower) spectra for benzopyran BE2 75
Figure 2. 7 Crystal structure of BE11 77
Figure 2. 8 ORTEP representation of the X-Ray crystal structure of BE11, ellipsoids at 50% probability 77
Figure 2. 9 ^{1}H NMR spectrum for pyranodiethyldiamino-4H-chromene, BE33 84
Figure 2. 10 ^{13}C NMR (upper) and DEPT 135 (lower) spectra for pyranodiethyldiamino-4H-chromene, BE33 85
Figure 2. 11 Crystal structure of pyranodiethyldiamino-4H-chromene, Compound BE33 87

Figure 2. 12 ORTEP representation of the X-ray crystal structure of BE33, the thermal ellipsoids are set at 50% probability 87
Figure 2. 13 ^{1}H NMRspectrum for compound BE35 91
Figure 2. 14 ^{13}C NMR (upper) and DEPT-135 (lower) spectra for benzopyran compound BE35 92
Figure 2. 15 ^{1}H NMR spectrum for compound BE54 95
Figure 2. 16 ^{13}C NMR (upper) and DEPT 135 (lower) spectra for benzopyran BE54.... 96
Figure 2. 17 The selection of 4-(benzyloxyaryl)chromene compounds BE57-BE69 and BE70-BE75 with variation of the ester substituents at the C-3 position 100
Figure 2. 18 ^{1}H NMR spectrum for compound BE69 101
Figure 2. 19 ^{13}C NMR (upper) and DEPT-135 (lower) spectra for benzopyran BE69 ..102
Figure 2. 20 Crystal structure of BE70 104
Figure 2. 21 ORTEP representation of the X-ray crystal structure of BE70, the thermal ellipsoids are set at 50% probability 104
Figure 2. 22 ^{1}H NMR Spectrum BE76 108
Figure 2. 23 ^{13}C NMR (upper) and DEPT 135 (lower) spectra for benzopyran BE76...109
Figure 2. 24(a) BE79 X-Ray Crystal Structure showing enantiomers (b) ORTEP representation of the X-ray crystal structure of BE79 showing both R and S isomers with 50% thermal ellipsoids; (c) Crystal structure of compound BE79 (Blue) flexibly aligned over energy minimised structure of BE79 (yellow)obtained with MOE software 112
Figure 2. 25 2,7-Diamino-4-benzyloxyphenyl-4H-chromenes BE88-BE91 115
Figure 2. 26 ^{1}H NMR spectrum of BE89 116
Figure 2. 27 ^{13}C NMR (upper) and DEPT-135 (lower) spectra for benzopyran compound BE89 117
Figure 2. 28 Dimethylamino-4-(4-benzyloxyphenyl)-4H-chromenes BE93-BE98 119
Figure 2. 29 ^{1}H NMR Spectrum for compound BE93 120
Figure 2. 30 ^{13}C NMR (upper) and DEPT 135 (lower) spectra for benzopyran BE93...121
Figure 2. 31 ^{1}H NMR spectrum for BE108 126
Figure 2. 32 ^{13}C NMR (upper) and DEPT 135 (lower) spectra for benzopyran BE108.127
Figure 2. 33 Bis 4H-chromene compounds BE112-115 130
Figure 2. 34 ^{1}H NMR spectrum for BE113 131
Figure 2. 35 ^{13}C NMR (upper) and DEPT 135 (lower) spectra for benzopyran diester BE113 132
Figure 2. 36 Pyranocoumarins (pyrano[3,2-c]benzopyran-5-ones) BE130-139 145

Figure 3. 1 Images of MCF-7 cells at low and high cell densities 158
Figure 3. 2 Images of LNCaP cells at low and high cell densities 159
Figure 3. 3 A representative haemocytometer grid. Cells falling in the five squares marked with a red 'X' are counted 161
Figure 3. 4 A representative 96-well plate showing the pattern of dosing. The concentrations shown are the final concentration of the drug diluted in the well 161
Figure 3. 5 Alamarblue as an indicator of cell viability 162
Figure 3. 6 Tamoxifen standard cell viability assay performed 164
Figure 3. 7 Cell viability assay for chromenes BE8 and BE9, (Series 1-Type I) 167
Figure 3. 8 Cell viability assay for compounds BE15 and BE16 showing IC_{50} results. 169
Figure 3. 9 Antiproliferative results of compound BE32, with dose-response curve for BE32 and IC_{50} value 170
Figure 3. 10 Results of 4H,6H-pyrano[3,2-g]chromene compound BE33 171
Figure 3. 11 Cell viability assay and IC_{50} value for compound BE52 175
Figure 3. 12 Cell viability assays and IC_{50} values for compounds BE62 and BE65 177
Figure 3. 13 Antiproliferative results of chromene compounds, series 6b, IC_{50} in (μM), PSA values ($Å^2$)and CLogP values 178
Figure 3. 14 Cell viability assay and IC_{50} value for compound BE71 179
Figure 3. 15 Cell viability assay and IC_{50} value for compound BE79 180
Figure 3. 16 Antiproliferative results of chromene compounds series 8 IC_{50} (μM),PSA values ($Å^2$)and CLogP values 182
Figure 3. 17 Cell viability assay and IC_{50} value for compound BE91 183
Figure 3. 18 Antiproliferative results of chromene compounds series 9 IC_{50} in (μM), PSA values ($Å^2$)and CLogP values 184
Figure 3. 19 Cell viability assay and IC_{50} value for compound BE97 185
Figure 3. 20 Cell viability assay and IC_{50} value for compound BE102 187
Figure 3. 21 Antiproliferative results of bischromene compounds series 11 IC_{50} in (μM), PSA values ($Å^2$)and CLogP values 188
Figure 3. 22 Antiproliferative results of pyranocoumarin compounds series 11 IC_{50} in(μM), PSA values ($Å^2$)and CLogP values 189
Figure 3. 23 Cell viability assay and IC_{50} value for compound BE131 190
Figure 3. 24 Antiproliferative results of coumarin compounds series 14 IC_{50} in (μM), PSA values ($Å^2$)and CLogP values 191
Figure 3. 25 Cell viability assay and IC_{50} value for compound BE140 191

Figure 3. 26 LNCaP cell preliminary viability screening, ...193
Figure 3. 27 LNCaP Dose-response curve and IC50 value for compounds BE69 and BE92.....194
Figure 3. 28 Top-ranking docked conformation of BE65 (yellow) in ERα, 3ERT.pdb. overlapped with 4-hydroxytamoxifen (green).....196
Figure 3. 29 2D representation of binding interactions of BE65 in the LBD ERα binding site (pdb 3ERT). 2-D rendering of ligand-protein interactions using LigX module of MOE used to create docked structure of BE65 in the LBD ERα binding site. 197
Figure 3. 30 Top-ranking docked conformation of B140 (yellow) in ERα, (1ERR.pdb). overlaid with Raloxifene(RAL) (blue) 198
Figure 3. 31 2D representation of binding interactions of BE140 in the LBD ERα binding site (pdb 1ERR). 2-D rendering of ligand-protein interactions using LigX module of MOE used to create docked structure of BE140 in the LBD ERα binding site. 199
Figure 3. 32 2D representation of binding interactions of BE141 in the LBD ERα binding site (pdb 3ERT). 2-D rendering of ligand-protein interactions using LigX module of MOE used to create docked structure of BE140 in the LBD ERα binding site. 200
Figure 3. 33 2D representation of binding interactions of BE137 in the LBD ERα binding site (pdb 3ERT). 2-D rendering of ligand-protein interactions using LigX module of MOE used to create docked structure of BE137 in the LBD ERa binding site. 200
Figure 3. 34 Time-resolved measurement allows the signal to be cleared of background fluorescence; the energy pulse from the excitation source (flash lamp, laser) is immediately followed by a time delay, allowing interfering short-lived fluorescence to decay [170].....202
Figure 3. 35 PolarscreenTM fluorescence assay principle for ER 204
Figure 3. 36 ERα and ERβ binding results for compound BE7 207
Figure 3. 37 ERα and ERβ binding results for compound BE16 207
Figure 3. 38 ERα and ERβ binding results for compound BE36 208
Figure 3. 39 BE140 ERα binding curve of compound BE140 208
Figure 3. 40 ERβ binding result for compound BE91 209
Figure 3. 41 ER-α/ER-β TR-FRET binding assay in antagonist mode 210
Figure 3. 42 (a) Number of samples screened by the NCI from 1989 - 2007; (b) source of samples between 1999 - 2005 212
Figure 3. 43 5 dose NCI results for compound BE65 (Sample S767434) for 60 cell lines (Log10 of sample concentration plotted against percentage growth). 215
Figure 3. 44 Growth percentage results for compound BE36 on 9 cell lines 216

Figure 3. 45 Mean GI50, TGI and LC50 results for BE36 on 60 cell lines 217
Figure 3. 46 GI50, TGI and LC50 results for BE36 on 60 cell lines 219

Figure 4. 1 Hydrazone Types A to E 227
Figure 4. 2 Compounds studied in this work 227
Figure 4. 3 E/Z isomerism in 3-hydroxy-N'-(naphthalen-2-ylmethylene)-2-naphthohydrazide derivatives 228
Figure 4. 4 ^{1}H NMR spectrum of compound 7 229
Figure 4. 5 ^{13}C NMR spectrum of compound 7 230
Figure 4. 6 ^{1}H NMR spectra of compounds 7, 8 and 9 231
Figure 4. 7 Relevant spectroscopic data used for NMR structure elucidation 232
Figure 4. 8 ORTEP representation of the crystal structure of compounds 7, with the thermal ellipsoids at 50% probability 233
Figure 4. 9 Series of diarylhydrazides assayed on AR TR-FRET 235
Figure 4. 10 Dose response curve and IC50 values for hydrazides (5) and (7) 236
Figure 4. 11 Diarylhydrazides: Selection of Analogues as AR Antagonists (Panel 1). 238
Figure 4. 12 Diarylhydrazides: General Structure and SAR Guidelines. I. Significance of OH group in the C3 position of ring A; II. Significance of OH group in the C2'/C3' position of ring B (for phenyl/naphthyl analogues respectively); III. Substitution effects at th 239
Figure 4. 13 Diarylhydrazides 26-45 (Panel 2) 241
Figure 4. 14 ^{1}H and ^{13}C NMR spectra of compound 37 242
Figure 4. 15 Ortep representation of the X-ray structure of compound 42, ellipsoids set at 50% probability. 243
Figure 4. 16 Biological Characterization of Active Ligands (28, 31-34 and 36-38).... 246
Figure 4. 17 Structures selected for Molecular Modeling 249
Figure 4. 18 Role of Hydroxylation and Methoxylation: Effect on Bioactive Conformation P1 (MD Study). Before and after conformations over the 40 ns of production dynamics are represented in yellow and magenta respectively. Images were generated by MOE [54] 250

Table of Schemes

Scheme 1. 1 Interconversion between E2 and the less active hormone 14
Scheme 1. 2 Epoxidation of 17β-estradiol shown, with Tamoxifen (a), and metabolites: 4-hydroxytamoxifen (b) and endoxifen (c)..... 20
Scheme 1. 3 Mechanism proposed to explain tamoxifen long-term toxicity 22
Scheme 1. 4 Carbocation derived from toremifene..... 23
Scheme 1. 5 Mechanism of aromatase activity [1]..... 29
Scheme 1. 6 Synthesis of two partial estrogen receptor antagonists 16 and 17 (i) NaH, DMF, N,N-dimethylthiocarbamoyl chloride; (ii) 260 °C, diphenyl ether; (iii) $LiAlH_4$, THF; (iv) N-(2 chloroethyl)pyrrolidine hydrochloride, or N-(2 chloroethyl)piperidine hydrochloride K_2CO_3, NaI, zinc dust, acetone, (v) BBr_3, CH_2Cl_2..... 41
Scheme 1. 7 Reagents and conditions: (a) piperidine/EtOH/HOAc; (b) $HCl/H_2O/EtOH$; (c) $SOCl_2$; (d) $PhNH_2$/pyridine/dioxane [111] 44

Scheme 2. 1 Synthesis of 4-Hydroxytamoxifen..... 60
Scheme 2. 2 (a) K_2CO_3, allyl bromide, acetone, 60 °C; (b) $Cu(OAc)_2$, $Sn(vinyl)_4$, acetonitrile, O_2, rt; (c) 5% catalyst,,toluene, 60 °C 63
Scheme 2. 3 Synthesis of substituted 4H-pyrans 7 64
Scheme 2. 4 Synthesis of EM-652 and EM-800, (a) $BF_3 \bullet Et_2O$, toluene; (b) DHP, TsOH, 0°C; (c) 4-hydroxybenzaldehyde, piperidine, benzene; (d) 1-(2-chloroethyl)dialkylamine hydrochloride, Cs_2CO_3, acetone, H_2O, reflux, 19 h; (e)(i) MeLi, THF, -78 °C; (ii) CH_3CO_2H, aq, 90 °C (f) $(CH_3)_3CCOCl$, Et_3N, CH_2Cl_2. 65
Scheme 2. 5 General one pot synthetic reaction for 4H-chromenes..... 67
Scheme 2. 6 Knoevenagel condensation reaction for synthesis of the chromene products..... 68

Scheme 4. 1 General synthetic pathway of 3-hydroxy-N'-(naphthalen-2-ylmethylene)-2-aromatic hydrazides derivatives 2,3,6-9(R = H, CH_3, Ph)(Panel 1).....229
Scheme 4. 2 Synthesis of Diarylhydrazides 26-45, (Panel 2).....240

Table of Tables

Table 2. 1 Library of chromene compounds produced with variation at C-4 (Type I).. 70
Table 2. 2 Library of chromene compounds produced with variation on C-4 aryl ring substituents (Type II) 71
Table 2. 3 Crystal data and structure refinement for BE11. 78
Table 2. 4 Crystal data and structure refinement for BE33 88
Table 2. 5 Chromene esters compounds with variation in R2 substituent 90
Table 2. 6 The library of 4-(4-hydroxyphenyl)chromenes synthesised 94
Table 2. 7 Series of 4-benzyloxyaryl-4H-chromenes 99
Table 2. 8 Crystal data and structure refinement for shelxl. BE70 105
Table 2. 9 The selection of 4-(3,4,5-trimethoxyphenyl)-4H-chromene compounds BE76-BE87 with variation in the structure of the ester substituent R2. 107
Table 2. 10 Crystal data and structure refinement for shelxl. BE79 113
Table 2. 11 Library of chromene compounds BE98-BE111 produced with structural variation in the ester substituent at C-7 124
Table 2. 12 Benzylidene malononitrile intermediates BE116-BE129 140

Table 3. 1 Antiproliferative results of chromene compounds series 1 type I, with IC_{50} values(μM and TSA values ($Å^2$) 166
Table 3. 2 Antiproliferative results of chromene compounds series 1 type II, with IC_{50} values (μM), and PSA values ($Å^2$) 168
Table 3. 3 Antiproliferative results of chromene compounds series 4 IC50 in (μM), PSA values ($Å^2$)and CLogP values 172
Table 3. 4 Cell viability assay and IC_{50} value for compounds BE36 and BE37 172
Table 3. 5 Antiproliferative results of chromene compounds series 5 IC50 in (μM), PSA values ($Å^2$)and CLogP values 174
Table 3. 6 Antiproliferative results of chromene compounds series 6a IC50 in (μM), PSA values ($Å^2$)and CLogP values 176
Table 3. 7 Antiproliferative results of chromene compounds series 7 IC_{50} in (μM), PSA values ($Å^2$)and CLogP values 180
Table 3. 8 Antiproliferative results of chromene compounds series 10 IC_{50} in (μM), PSA values ($Å^2$)and CLogP values 186
Table 3. 9 ERα binding results for selected compounds (IC50 μM) 205
Table 3. 10 ERβ binding results for selected compounds (IC50 mM) 206
Table 3. 11 One Dose Screen (10 mM) result for compound BE65 (767434) 213

Table 3. 12 Leukaemia growth activity (%) on full panel of compounds screened 214
Table 3. 13 Standard COMPARE Analysis of chromene BE36.....221

Table 4. 1 Crystal data and structure refinement for compound 7 234
Table 4. 2 Crystal data and structure refinement for 42.....244
Table 4. 3 Quantification of the AR-Antagonism of Diarylhydrazides by AR TR-FRET Assays 245

Tables 5.1 – 5.36 X-Ray Crystal ORTEP DATA ..... Appendix Supplemental CD

Table of Abbreviations:

ACAT	Acyl Coenzyme A: cholesterol acyl Transferase
AF-2	Activation Function 2
AMBER	Assisted Model Building with Energy Refinement
AR	Androgen Receptor
AEBS	Antiestrogen Binding Sites
ADT	Androgen Deprivation Therapy
BBB	Blood Brain Barrier
BRCA1 and BRCA2	Breast Cancer susceptibility genes
CPA, CPRC	Castration Resistant Prostate Cancer; Cyproterone Acetate
CA4	Combretastatin
DCM	Dichloromethane
DHT	Dihydrotestosterone
DMSO	Dimethyl sulfoxide
DHEA	Dehydroepiandrosterone
DNA	Deoxyribonucleic acid
DMF	Dimethylformamide
EC_{50}	Half maximal Effective Concentration
ER-α	Estrogen Receptor-alpha
ER-β	Estrogen Receptor-beta
EGFR	Epidermal Growth Factor Receptor
E_1	Estrone
E_2	Estradiol
EPB	Poisson-Boltzmann Energy Binding
ET_A	Endothelin-A receptor
EtOH	Ethanol
FBS	Fetal Bovine Serum
FP	Fluorescence Polarization
GR	Glucocorticoid Receptor
HB	Hydrogen Bond
HCL	Hydrochloric acid
HER 2	Human Epidermal Growth Factor Receptor 2
HRMS	High Resolution Mass Spectrometry analysis

HTS	High-Throughput Screening
HRMS	High Resolution Mass Spectrometry
HTRF	Homogeneous Time Resolved Fluorescence
HTS	High Throughput Screening
IC_{50}	Half maximal Inhibitory Concentration
IGF-I	Insulin-like Growth Factor I
IMHB	Intramolecular Hydrogen Bond
IR	Infrared spectroscopy
IUPAC	International Union of Pure and Applied Chemistry
LBD	Ligand Binding Domain
LBP	Ligand Binding Pocket
LNCaP	Prostate cancer adenocarcinoma human cell line
MAPK	Mitogen-Activated Protein Kinase pathway
MCF-7	Michigan Cancer Foundation-7 human breast cancer cell line
MD	Molecular Dynamics
MeOH	Methanol
MEME	Minimum Essential Medium Eagle
MDR	Multi Drug Resistance
MMPs	Matrix Metalloproteases
MMPBSA	Molecular Mechanics/Poisson-Boltzmann Surface Area
MOE	Molecular Operating Environment
mP	Millipolarisation units
mRNA	Messenger Ribonucleic acid
NaH	Sodium hydride
NB	Nuclear Box
NCI	National Cancer Institute
NMR	Nuclear Magnetic Resonance
NR	Nuclear Receptor
Ns	Nano seconds
ORTEP	Oak Ridge Thermal Ellipsoid Plot
PDB	Protein Data Bank
P	Pose
PSA	Polar Surface Area
RAL	Raloxifene

RPMI	Roswell Park Memorial Institute
SAR	Structure Activity Relationship
SARMs	Selective Androgen Receptor Modulators
SAPK	Stress Activated Protein Kinase
SERBa	Selective Estrogen Receptor βeta agonist
SERDs	Selective Estrogen Receptor Downregulators
SERMs	Selective Estrogen Receptor Modulators
Sp	Single point
SBMA	Spinal Bulbar Muscular Atrophy
SRC	Steroid Receptor Coactivator
S	Subpocket
TAM	Tamoxifen
Tb	Terbium
TGF-β	Transforming Growth Factor *beta*
Tes	Testosterone
THF	Tetrahydrofuran
TLC	Thin Layer Chromatography
TR-FRET	Time Resolved Fluorescence Resonance Energy Transfer
TS-VS	Target Selective-Virtual Screening
*v*HTS	Virtual High-Throughput Screening
wt	wild type
XRD	Xray Diffraction crystallography

Chapter 1: Introduction

1.1 Introduction and Background

1.1 .2 Cancer

Cancer is a term used for diseases in which abnormal cells divide without control and are able to invade other tissues. Cancer cells can spread to other parts of the body through the blood and lymph systems through a process known as metastasis, which is the cause of 90% of cancer deaths. Cancer remains one of the most difficult diseases to treat and is responsible for about 13% of all deaths worldwide, and this incidence is increasing due to ageing of population in most countries, but especially in the developed ones[1].

Cancer is not just one disease but many diseases. There are more than 100 different types of cancer. Most cancers are named for the organ or type of cell in which they start; for example, cancer that begins in the colon is classified as colon cancer; cancer that begins in basal cells of the skin is classified as basal cell carcinoma. [2]

Cancer is normally caused by abnormalities of the genetic material of the affected cells. Tumorigenesis is a multistep process that involves the accumulation of successive mutations in oncogenes and suppressor genes that deregulate the cell cycle. Tumorigenic events include the small scale changes in DNA sequences such as mutations; larger scale chromosomal aberrations, such as translocations, deletions, and amplifications; and changes that affect the chromatin structure and are associated with dysfunctional epigenetic control, such as aberrant methylation of DNA or acetylation of histones[3]. About 2,000-3,000 proteins may have a potential role in the regulation of gene transcription and in the complex signal-transduction cascades that regulate the activity of these regulators. Cancer is a disease of the tissue in which the normal relationships between epithelial cells and their underlying stromal cells are altered[4].

The human body naturally produce new cells. In fact, during the course of a year, almost every single cell in the body is replaced. The frequency of this turnover depends on the location. For example, stomach cells divide rapidly because of the wear and tear they receive from stomach acid. However, normally cells die off as new ones replace them in order to keep the body at a normal size. Sometimes, though, this growth can become unregulated and lead to a mass of cells, see figure 1.1.

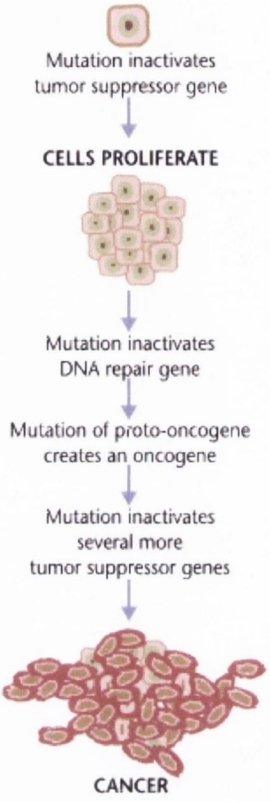

Figure 1. 1 Tumorigenesis

Proteins in the body signal cells when they should grow, double their chromosomes, and divide into distinct cells. In somatic cells, or the cells of the body besides egg and sperm, this process is called mitosis. Because each cycle of mitosis leads to one cell becoming two, this growth can quickly accumulate if unrestricted (see Figure 1.1).

Cells lose the ability to regulate growth if their genetic information is mutated, or changed, due to exposure to carcinogens such as radiation or exposure to asbestos. This mutation can lead to two different types of tumours, benign and malignant. The form of the tumour depends on the type of growth that it undergoes.

Cancer types can be grouped into broad categories as follows:

- Carcinoma is a cancer that begins in the skin or in tissues that line or cover internal organs.
- Sarcoma is a cancer of bone, cartilage, fat, muscle, blood vessels, or other connective or supportive tissue.

- Central nervous system cancers are cancers that originate in the tissues of the brain and spinal cord.
- Lymphoma and multiple myeloma are cancers that develop in the cells of the immune system.
- Leukaemia is a cancer that starts in blood-forming tissue such as the bone marrow, and causes large numbers of abnormal blood cells to be produced and enter the blood stream. [5]

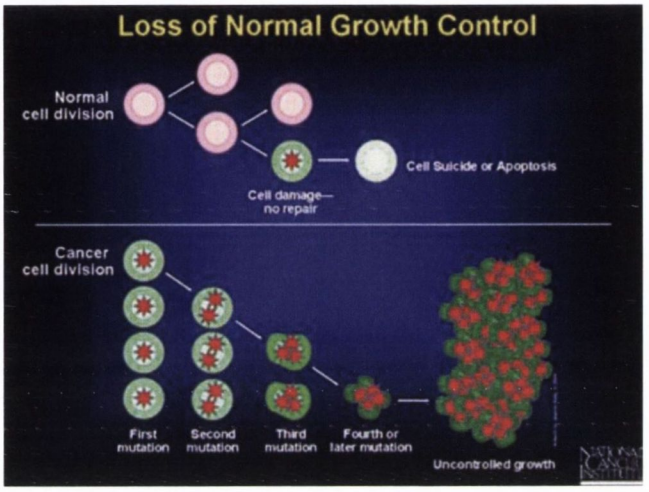

Figure 1. 2 Not all tumors are cancerous; tumors can be benign or malignant

Benign tumors are not cancerous. They can often be removed, and in most cases, they do not recur. Cells in benign tumors do not spread to other parts of the body. Malignant tumors are cancerous. Cells in these tumors can invade nearby tissues and spread to other parts of the body (see Fig 1.2).

Cancer therapy is based on surgery and radiotherapy, (which are, when possible, rather successful regional interventions), and on systemic chemotherapy. Approximately half of patients are not cured by these treatments and may obtain only a prolonged survival or no benefit at all. The aim of most cancer chemotherapeutic drugs currently in clinical use is to destroy malignant tumor cells by inhibiting some of the mechanisms implicated in cellular division. Accordingly, the antitumor compounds developed through this approach are cytostatic or cytotoxic. However, the knowledge of tumor biology has exploded in the past decades and this may pave the way for more active, targeted anticancer drugs[6]. The introduction of the tyrosine kinase inhibitor imatinib as a highly effective drug in chronic myeloid leukemia and gastrointestinal

stromal tumors [7] was a proof of the concept of effective drug development based on the knowledge of tumor biology[8].

Effective targeted therapies may be suitable only for small subgroups of patients[9]. Pharmacogenetics, which focuses on intersubject variation in therapeutic drug effects and toxicity depending of polymorphisms, is particularly interesting in oncology since anticancer drugs usually have a narrow margin of safety. The dose of chemotherapeutic agents is generally adjusted by body surface area, but this parameter is not sufficient to overcome differences in drug disposition[10]. DNA micro array technology permits study of alterations in the transcriptional level of entire genomes, and may become an important tool for predicting the chemosensitivity of tumors before treatment.

Cancer chemotherapy is in fact a very difficult task. One of its main associated problems is the nonspecific toxicity of most anticancer drugs due to their biodistribution throughout the body, which requires the administration of a large total dose to achieve high local concentrations in a tumor. Drug targeting aims at preferred drug accumulation in the target cells independently of the method and route of drug administration[11]. One approach that allows improving the selectivity of cytotoxic compounds is the use of prodrugs that are selectively activated in tumor tissues, taking advantage of some unique aspects of tumor physiology, such as selective enzyme expression, hypoxia, and extracellular pH. More sophisticated tumor-specific delivery techniques allow the selective activation of prodrugs by exogenous enzymes (gene-directed and antibody-directed enzyme prodrug therapy, eg. prodrugs based on Tamoxifen and Doxorubicin[12]). Furthermore, the increased permeability of vascular endothelium in tumors (enhanced permeability and retention, EPR effect) permits that nanoparticles loaded with an antitumor drug can flow and accumulate inside the interstitial space, where the drug can be released as a result of normal carrier degradation[13].

Another problem of cancer chemotherapy is drug resistance. After the development of a resistance mechanism in response to a single drug, cells can display cross-resistance to other structural and mechanistically unrelated drugs, a phenomenon known as multidrug resistance (MDR) in which the ATP-dependent transporters have a significant role[14].

Finally, a major problem in the development of anticancer drugs is the large gap from promising findings in preclinical *in vitro* and *in vivo* models to the results of clinical trials. The problems found in this transition arise because experimental cancer models greatly differ from human patients, who very often suffer from a much more complex therapeutic situation. Although a large number of clinical trials are in progress and new results are continuously being published, the real clinical efficacy of most of these treatments is usually disappointing and a statistically significant benefit is observed for very few of them[15]. It has been claimed that development and utilisation of more clinically relevant cancer models would represent a major advance for anticancer drug research[1].

1.2 Breast Cancer

In Ireland, in 2007, there were 2,463 new cases of breast cancer diagnosed making it the most common invasive cancer for Irish women. A significant increase was also seen in the number of breast cancer cases between 1994 and 2001 [16]. Breast cancer is the most common cancer in females in Europe. Breast cancer is responsible for 26.5% of all new cancer cases among women in Europe, and 17.5% of cancer deaths[17].

Aetiology of breast cancer

There are several factors, both endo- and exogenous, which are known to affect the risk of breast cancer in the population. These include lifestyle factors (i.e. childbearing, breastfeeding, type of diet and obesity, use of alcohol and tobacco), hormonal status (influencing age at menarche and menstrual cycle, and determined by endogenous hormones, oral contraceptives use, and hormone replacement therapy), individual physical human characteristics, radiation, and genetic predisposition[18]. Finally, mortality from breast cancer may be influenced by prevention (e.g. chemoprevention using tamoxifen or raloxifene) and screening[19, 20]. Women with a family history of breast cancer are at increased risk of the disease. It was estimated, based on the 52 epidemiological studies, which having one first-degree relative with breast cancer increases risk by about 80%, two first-degree relatives increases risk approximately 3-fold, and in those with 3 or more first-degree relatives the risk is elevated 4 fold[21]. About 10% of breast cancers in developed countries may be due to genetic

predisposition[18]. The lifetime risks of developing breast cancer for BRCA1 and BRCA2 (breast cancer susceptibility genes) mutation carriers is 80-85% [22].

Over the past two decades understanding and knowledge of breast cancer has evolved resulting in better management of the disease. There has been a shift from a largely surgical therapeutic approach to treatment regimens that involve less radical surgical intervention and the increased use of radiotherapy and/or systemic therapies for oestrogen receptor positive tumours [23].

1.2.1 Types of Breast Cancer

Breast cancer is currently classified into several sub-types based mainly on hormone and growth-factor receptor status. Classifications also include clinical categories that share DNA damage repair defects, classifications between endogenous and exogenous factors, and methods based upon micro-array or tissue-array data and associated cell type of origin [24].
Classification based on hormone receptor status involves the identification of the presence or absence of estrogen receptors (ER) and/or progesterone receptors (PR). The human epidermal growth factor receptor 2 (HER 2/neu) is a well characterised tumour marker and is used in conjunction with the identification of hormone receptors to classify breast cancer. The expression of HER 2 indicates a more aggressive cancer.
After immunohistochemical testing for these breast cancer markers the classification may be further divided into: (1) ER/PR positive; (2) ER/PR negative with HER 2 over expression; or (3) "triple negative" (breast cancer with the absence of any of the above three receptors). The triple negative type breast cancer frequently contains a defected BRAC1 gene [24].

In general, surgical and radiation treatments are similar for these different types of breast cancer. But drug treatments – such as chemotherapy, endocrine therapies, and other medications are usually different. These treatments are targeted to the specific type of cancer [25]. The specific drugs which are clinically approved for targeting ER positive breast cancer will be discussed below. Taxol (see structure figure 1.3) is a chemotherapeutic agent given for early stage and metastatic breast cancer and is also given as adjuvant treatment. Taxol (trade name Paclitaxel) is a mitotic inhibitor. Taxol targets tubulin in rapidly growing cancer cells, and adheres to them while they are

trying to divide, which prevents mitosis. This in turn prevents metastasis [26]. Adriamycin (Doxorubicin, see structure figure 1.3) can be used to treat early-stage or node-postive breast cancer, HER2-positive breast cancer, and metastatic disease. Adriamycin is also used to treat cancer by slowing or stopping the growth of cancer cells. This drug intercalates the DNA of cancer cells and prevents cell replication by inhibiting protein synthesis and acts as an inhibitor of topoisomerase [12, 27]. Methotrexate (see structure figure 1.3) is an anti-metabolite chemotherapy. It prevents cells from using folate to synthesise DNA and RNA. Methotrexate helps to stop the growth of cancer cells and metastasis [27-29]. Fluorouracil (see figure 1.3) is a fluorinated pyrimidine antimetabolite that resembles uracil, where a fluorine atom is substituted for the 5-methyl group[30]. Cancer cells take up Fluorouracil (trade name Adrucil) and this interferes with their growth, preventing metastasis[27, 30]. Gemcitabine (trade name Gemzar, for intravenous injection) is a nucleoside metabolic inhibitor that exhibits antitumor activity. Gemcitabine (see figure 1.3 for structure) is 2'-deoxy-2',2'-difluorocytidine monohydrochloride [31]. As with fluorouracil and other analogues of pyrimidines, the triphosphate analogue of gemcitabine replaces one of the nucleoside building blocks of nucleic acids, in this case cytidine, during DNA replication. The process arrests tumor growth, by incorporation of the "faulty" nucleoside, resulting in apoptosis[27, 31].

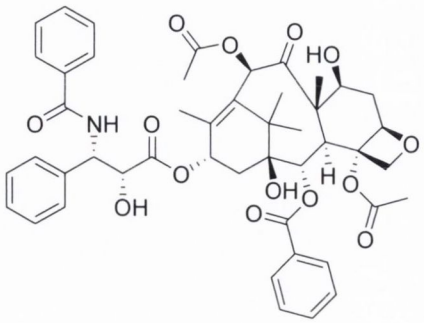

Taxol

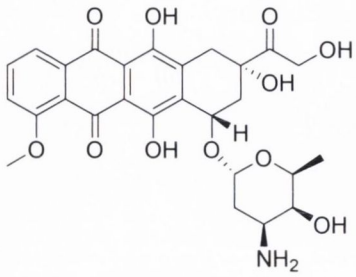

Adriamycin

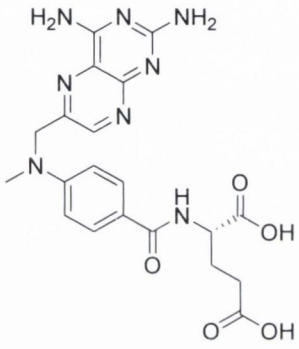

Methotrexate

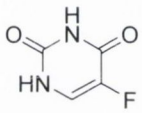

Fluorouracil

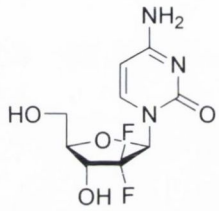

Gemcitabine

Figure 1. 3 Selection of chemotherapeutics specifically targeting ER positive breast cancer

ER positive Breast Cancer

About 75% of all breast cancers are ER positive. These tumours grow in response to the hormone estrogen. About 65% of these are also PR positive, which develop in response to the hormone progesterone. If breast cancer cells have a significant number of receptors for either estrogen or progesterone, the cancer is considered hormone-receptor positive and is likely to respond to endocrine therapies, i.e. treatments that block or remove hormones[32]. Tumours that are ER/PR-positive are 60% likely to respond to endocrine therapy [25]. Endocrine therapies for breast cancer are treatments usually required after surgery, chemotherapy, and/or radiation are completed. They are designed to help prevent recurrence of the disease by blocking the effects of estrogen.

- The drug Tamoxifen, used to treat some women for up to five years after initial treatment for breast cancer, helps prevent recurrence of the disease by blocking the estrogen receptors on breast cancer cells and preventing estrogen from binding to them.
- A class of drugs called Aromatase Inhibitors(AIs) actually stops estrogen production in post-menopausal women. These drugs are not effective for women who have not yet gone through menopause[33].

HER2-Positive Breast Cancer

In about 20% to 25% of breast cancers, the cancer cells produce excessive amounts of a protein known as HER2/neu. These breast cancers tend to be much more aggressive and fast-growing. The drug Herceptin (trastuzumab) has been shown to dramatically reduce the risk of recurrence. It has now become standard treatment to give Herceptin along with adjuvant (after-surgery) chemotherapy in those women with metastatic breast cancer[32]. Trastuzumab is a recombinant DNA derived humanised-monoclonal antibody that selectively targets the extracellular domain of the human epidermal growth factor receptor 2 protein (HER2). Trastuzumab is composed of 1,328 amino acids and has a molecular weight of ~ 148 kDa [34].

Triple negative Breast Cancer

Some breast cancers; estimates range between 10% and 17%, are known as "triple negative" because they lack estrogen and progesterone receptors and do not overexpress the HER2 protein. The majority of breast cancers associated with the breast cancer gene known as BRCA1 are triple negative. These cancers generally respond well to adjuvant chemotherapy[32]. Overall, however, they have a poorer prognosis than other types of breast cancer. So far, no targeted therapies like Tamoxifen or Herceptin have been developed to help prevent recurrence in women with triple-negative breast cancer. Cancer researchers are studying several promising targeted strategies aimed at triple-negative breast cancer [25].

1.2.2 Irish statistics of breast cancer occurrences

At present breast cancer accounts for about 18% of all cancers in women in Ireland and in 2009 there were 2,740 new cases diagnosed [35]. Its incidence continues to rise and according to the Irish National Cancer Registry the number of new cases recorded in Ireland each year will increase to approximately 5,000 by 2020 [23]. Breast cancer remains the biggest cause of death from cancer for women in Ireland. In Ireland, excluding NMSC (non melanoma skin cancer), female breast alone comprised almost one third of all cancers diagnosed in women respectively in females from the year 2007 to 2009 (Figure 1. 4)

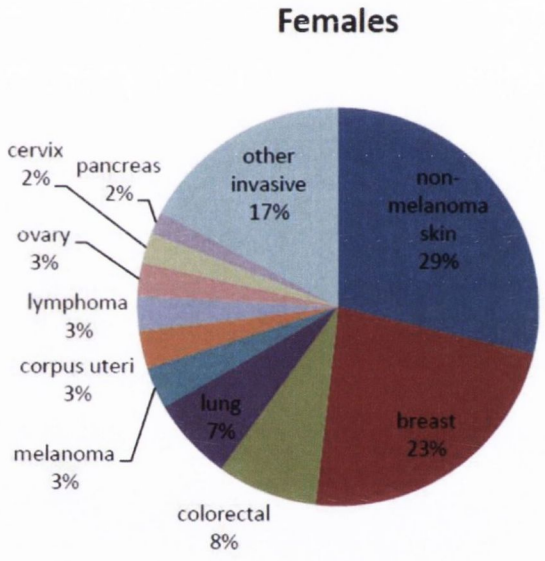

Figure 1. 4 Ranking of the most commonly diagnosed invasive cancers in Ireland (excluding NMSC), 2007-2009 [36]

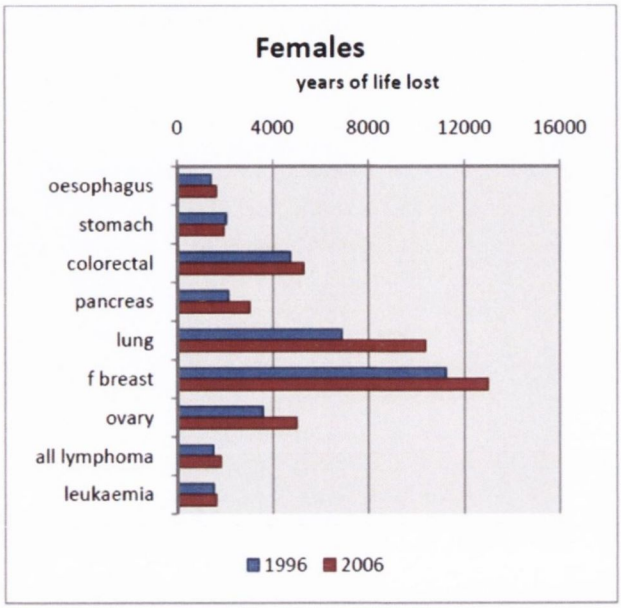

Figure 1. 5 Person-years of life lost due to cancer in Ireland, 1996 and 2006 [36]

In Ireland in 2006, of the 8,141 cancer deaths were responsible for over 120,000 years of life lost. Breast cancer had the greatest impact for women[36], representing 21% of all years of life lost (Figure 1. 5).

European variation of breast cancer incidence

Female breast cancer incidence in Ireland ranked 4th highest of the 30 European countries surveyed, after Belgium, France and the Netherlands (Figure 1. 6). Some of the lowest European incidence rates were found in eastern European countries. It is likely that the comparatively high incidence rates in Ireland are linked to the development of organised screening here in recent years – some of the lowest ranked countries have recently been identified as not having yet introduced a national screening programme [37]. Ireland also ranked 4th highest in terms of mortality, behind Belgium, Denmark and Netherlands with the same mortality rate as Malta and Hungary [36].

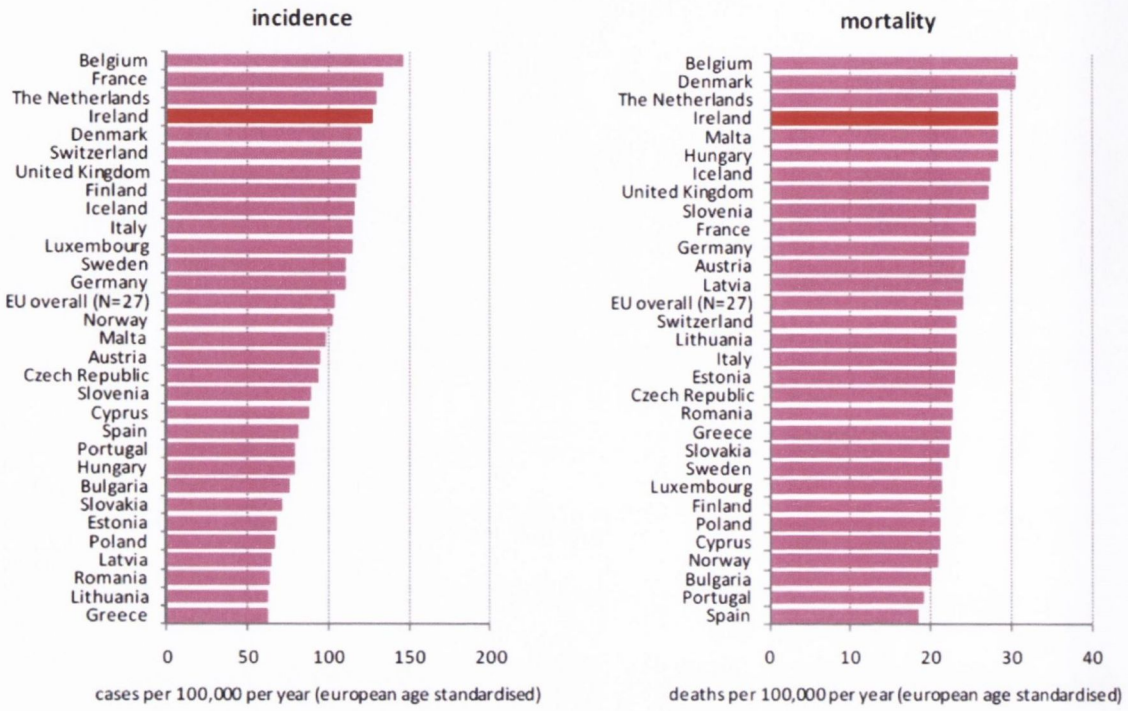

Figure 1. 6 Estimated cancer incidence and mortality in Europe 2008 – female breast cancer[36]

Around the world incidence rates vary greatly, but they are increasing in regions that until now had relatively low rates of the disease. The WHO International Agency for Research on Cancer estimates that in 2008, up to 400,000 women died with breast cancer throughout the world [38, 39]. Worldwide, more than a million women are diagnosed with breast cancer every year, accounting for a tenth of all new cancers and 23% of all female cancer cases. Breast cancer is the most frequent cancer found in women worldwide. Breast cancer incidence rates vary considerably, with the highest rates in North America and the lowest rates in Africa and Asia [40].

Of the best cancer survival rates of cancers after 5 years, breast cancer is at 86% on the list. Many would be surprised to see breast cancer in the top 5. It has good survival figures but is still responsible for thousands of deaths as it is also a very common cancer. These figures do not indicate the number of people killed by these diseases, only survival rates once a diagnosis is made. It is also important to point out that the reasons these figures are so good is because of modern cancer screening and innovations in treatments [41].

1.2.3 Estrogens and Breast Cancer

Endogenous estrogens are thought to play a major role in the development of breast cancers and estrogen receptor blockers are important drugs in its treatment. It has been shown that longer exposures to estrogens result in an increased risk for breast cancer. Estrogens have effects on many organ systems, beyond the reproductive system, in both females and males. Breast tissue is particularly dependent on circulating estrogens since there is no breast development in aromatase-deficient women and estrogen therapy of these patients leads to normal pre- and postpubertal breast development. Estrogen effects are exerted through two types of specific receptor: estrogen receptor alpha (ERα) and beta (ERβ). These nuclear receptors are ligand-dependent transcription factors that mediate the biological effects of estrogens and anti-estrogens[42]. ERα and ERβ represent two separate gene products. The hERα protein consists of 596 amino acids with a molecular weight of 66 kDa and is located on chromosome 6, while the hERβ sequence encodes a protein of 530 amino acid residues with a molecular weight of 59 kDa and is positioned on chromosome 14. Like other nuclear receptors, the ER has a multidomain structure consisting of six functional regions, from the N-terminal A/B domain to the C-terminal F domain, which show various degrees of sequence conservation (see Figure 1. 7)[43].

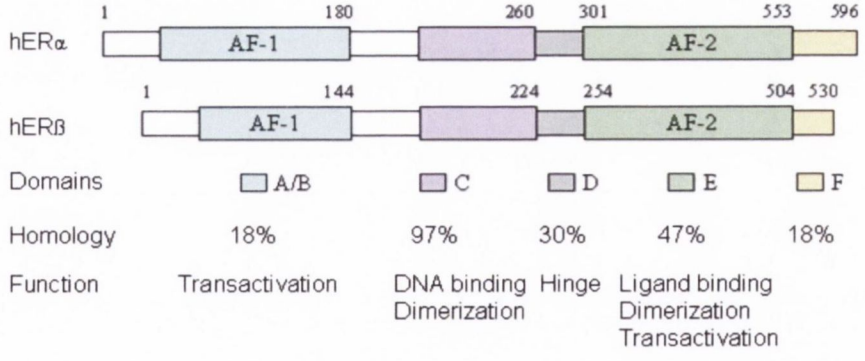

Figure 1. 7 Domain-structure representation of human ERα and ERb isoforms [44]

The "dependent" natural female sex hormone means primarily estrogen, 17β-estradiol (E2), which plays a prominent role in mediating the maturation, proliferation, differentiation, apoptosis, inflammation, metabolism, homeostasis, and brain function and also influences the growth and development of breast cancer [43, 45-47]. The biological activity of E2 in hormone sensitive tissues is actively regulated by the

interconversion by 17β-hydroxysteroid dehydrogenase between E2 and the less active hormone, estrone[48]

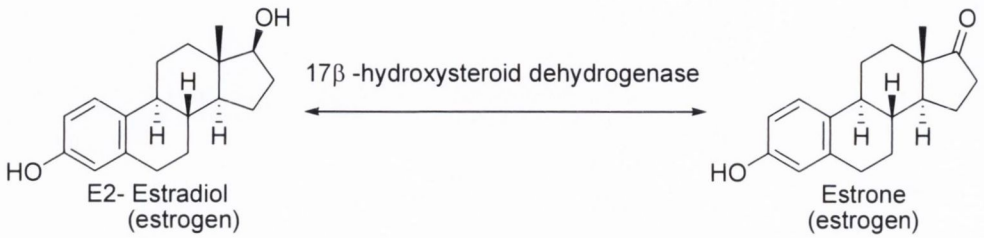

Scheme 1. 1 Interconversion between E2 and the less active hormone

Mechanism of action of Estrogen

The mechanism of action for all steroid hormones follows the same general activation, involving the regulation of gene expression[49]. Estrogen being a small lipophilic molecule is carried in the blood stream bound to carrier proteins. The free steroid diffuses through the lipid membrane and either acts at the cytosol or in the nucleus to become bound to the estrogen receptor; the estrogen-estrogen receptor complex then passes into the nucleus to act at a genetic level. The complex initiates a conformational change that involves a dimerization, to activate the complex which in turn interacts with specific regions on the DNA. It acts on hormone response elements. This initiates the transcription and translation of new proteins. These proteins regulate cell function, growth differentiation, etc. So it is by the process of expression of these proteins that hormones such as estrogen function. The Figure 1. 8 shows the estrogen receptor mechanism of action.

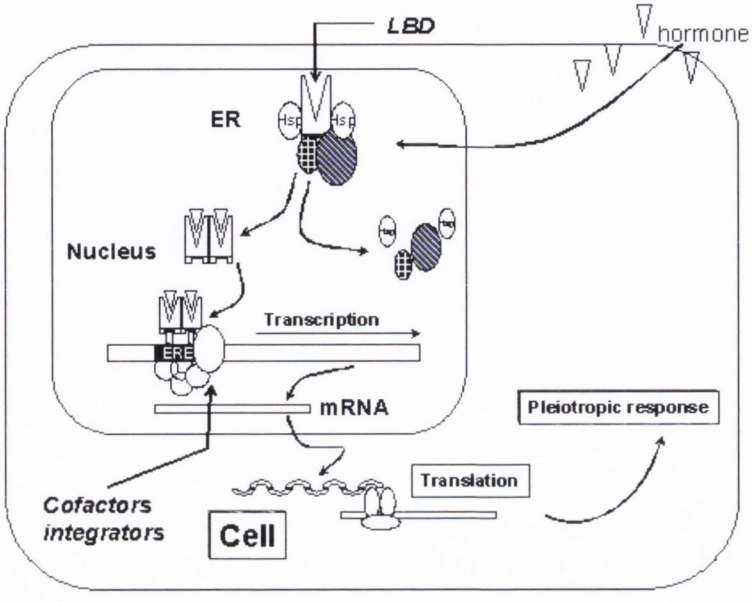

Figure 1. 8 Estrogen receptor mechanism of action

Agonists such as β-estradiol act at the Ligand Binding Domain (LBP) of the receptor and induce a conformational change involving 4α helices H3, H4, H5 and H12. The estrogen receptor-agonist complex is characterised by alignment of helix 12 across the LBP. This conformation favours docking of co-activators and facilitates gene transcription following ER dimerization and binding of the receptor dimer to target sites on DNA. In both normal and malignant cells, the estrogen-receptor complex binds DNA causing genomic effects i.e.: gene transcription or gene repression and also activates growth-regulatory genes.[50, 51] In contrast, an antagonist such as 4-hydoxytamoxifen (tissue selective antagonist) binds the ER but disrupts the binding of helix 12 across the LBP and the receptor-antagonist complex formed does not facilitate recruitment of co-activators. Instead co-repressor interaction is favoured and the antagonist blocks estrogens from binding to the receptor. [23] In both cases, the AF2 domain of the receptor is primarily involved in the recruitment of the co-regulatory proteins. The binding of agonists and antagonists to the ER is illustrated in Figure 1. 9.

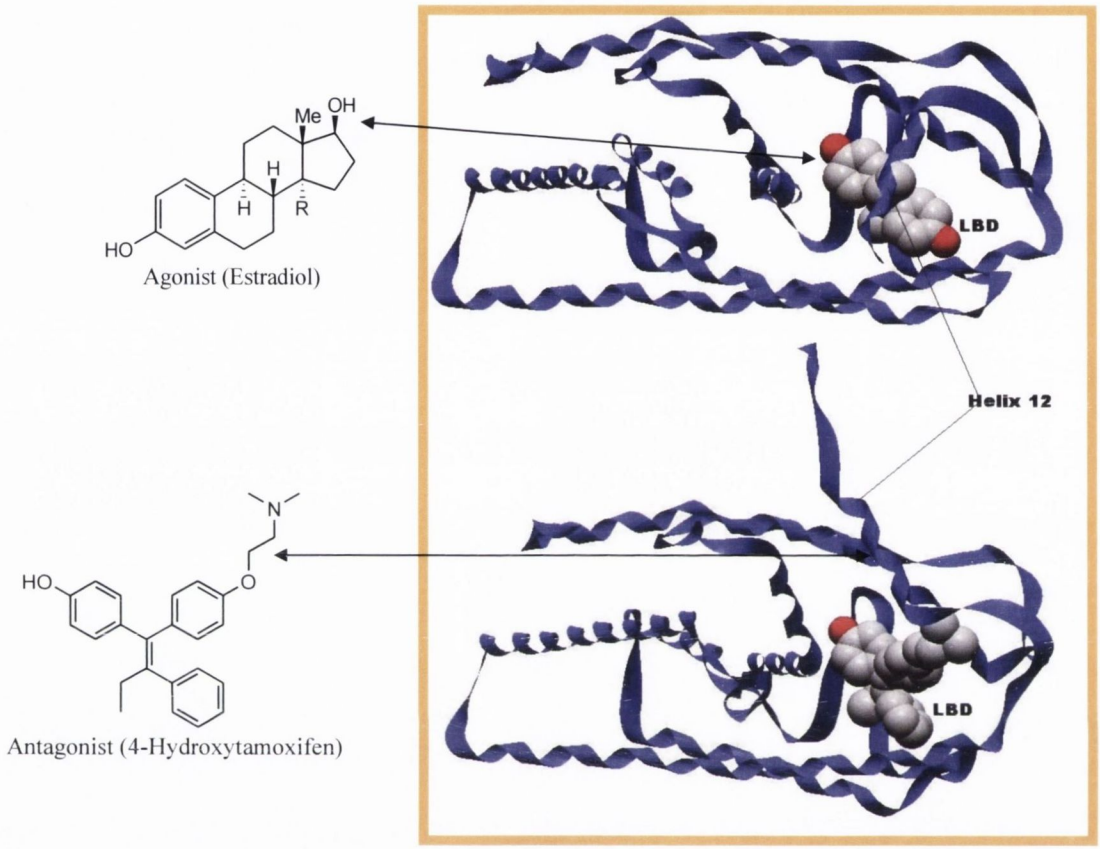

Figure 1. 9 Binding of agonists and antagonists to the ER

A number of key amino acid residues are present within the LBP that interact with ligand substituents (e.g.: *via* H-bonding). These include Glu353, Arg394 and His524. Recognition of estradiol and other agonists by the LBP of the receptor involves a combination of polar and nonpolar interactions. The Glu353 and Arg394 residues form hydrogen bonds to the phenolic hydroxyl at the 3-position of estradiol, while the 17β-hydroxyl group of estradiol forms a hydrogen bond with the His524 residue in the LBP of the receptor. The remainder of the LBP consists of hydrophobic amino acid residues which align with the hydrophobic core of the estradiol molecule, (Figure 1. 10). Antagonists, such as tamoxifen or raloxifene occupy the same binding sites but the interaction is different. A strong hydrogen bond also forms between the basic group present in the side chain and the residue Asp351. [1]

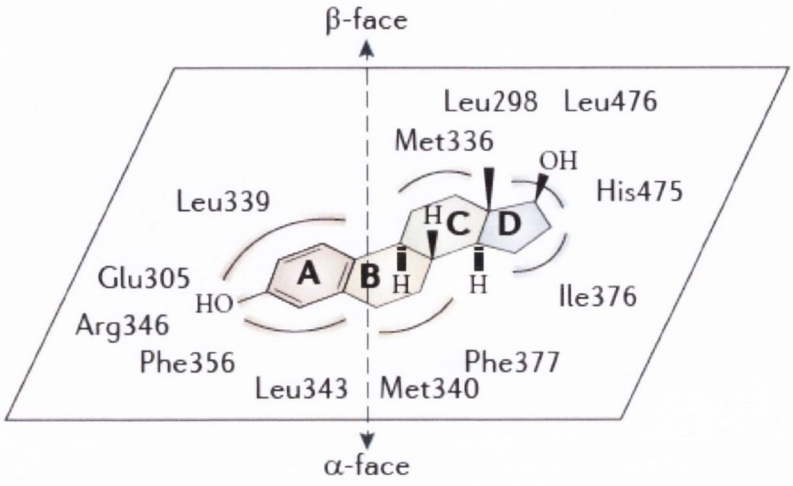

Figure 1. 10 The binding of estradiol in the estrogen receptor LBP. The region of the binding cavity above the plane of the bound hormone is referred to as the β-face, whereas the area below the plane is referred to as the α-face [52]

A comparison of the ligand binding domains of the ER subtypes shows that they differ by only two conservative amino acids, i.e. two binding amino acid residues present in the ERα LBP namely Leu384 and Met421 are replaced in the ERβ LBP by Met336 and Ile373 respectively. The agonist estradiol and classical selective estrogen modulators (SERMs) like tamoxifen bind both receptor subtypes but the development of ligands which are subtype-selective may lead to a more optimal approach for the treatment of diseases associated with the ER in the future. Examples of ERα-selective and ERβ-selective ligands are illustrated below. (Figure 1. 11) [52]

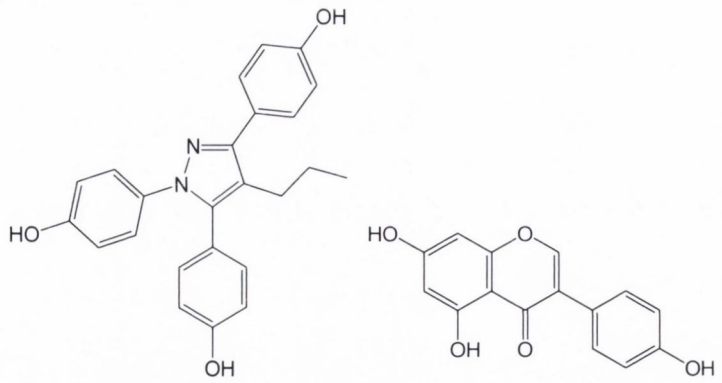

Figure 1. 11 (a) ERα-selective ligand: Propyl pyrazole triol; (b) ERβ-selective ligand: Genistein

1.2.4 ER antagonists *general*

Estradiol (E2) regulates the growth, differentiation, and physiology of the reproductive process through the estrogen receptor (ER). E2 also affects other tissues, such as bone, liver, brain and the cardiovascular system. Because of the functional diversity displayed by estrogens through the ER, much of the current interest in understanding the basis of ER actions at the molecular level is focused towards the goal of therapeutic intervention[53].

1.3 Nonsteroidal antiestrogens (SERMs)

The discovery of this group of compounds is a good example of serendipity. Estrogen has been a major target in the treatment of breast cancer since the end of the 19th century. In 1896, George Beatson first demonstrated the beneficial role of oophorectomy for the treatment of premenopausal women with metastatic breast cancer; removal of the ovaries was shown to regress the disease and improve the prognosis of the patient in some cases [54]. In 1936, a French physician named Lacassagne suggested that if breast cancer was caused by a hereditary sensitivity to estrogen then an antagonist to estrogen action could be used to prevent the disease. His proposal to use an antiestrogen for the treatment of breast cancer was finally realised by the development of tamoxifen, the first selective ER modulator (SERM)[55].

SERMs are derivatives of the triphenylethylene system, developed by molecular manipulation of diethylstilbestrol, the prototype nonsteroidal estrogen agonist. The key structural features of this group of compounds, which are essential for activity, are the presence of a triphenylethylene core and a basic aminoether side chain at the 4-position of one of the phenyl rings[56].

1.3.1 Tamoxifen

Tamoxifen, 2-(4-((Z)-1,2-diphenylbut-1-enyl)phenoxy)-N,N-dimethylethanamine (for structure (TAM) see structure scheme 1.2, a) is a synthetic non-steroidal triphenylethylene derivative that is an antiestrogen, and was approved by the Food and Drug administration in 1977 for the treatment of women with advanced breast cancer and several years later for adjuvant treatment of primary cancer[57]. Tamoxifen is a prodrug that has increased activity after activation *in vivo*. Tamoxifen is extensively metabolised by the human cytochrome P450 enzyme system into several metabolites that have variable potencies towards the estrogen receptor. Of these, 4-hydroxytamoxifen (see structure scheme 1.2, b) is an active metabolite which has greater anti-estrogenic potency than the parent drug, tamoxifen. 4-Hydroxytamoxifen was considered the most important active metabolite until recently, when it was found that another active metabolite, endoxifen (see structure scheme 1.2, c), is present in higher concentration in human plasma of breast cancer patients receiving chronic tamoxifen[58]. These results provide evidence that endoxifen is important as, or more important than, 4- hydroxytamoxifen to the the anti-estrogenic action of tamoxifen[59]. Tamoxifen is largely inhibitory and functions as estrogen antagonist in breast cancer cells, but it also functions as an agonist in some tissues including the bone, uterus, liver, and the cardiovascular system. These estrogen-like activities of tamoxifen are significant for woman taking the anti-estrogen against breast cancer. Its stimulatory effects on uterus and liver may underlie the increased incidence of endometrial hyperplasia that may lead to cancer, as well as alterations in liver function. The agonistic effects of tamoxifen in bone cells and in the cardiovascular system enhance bone maintenance, preserve a favorable blood-lipid profile, and reduce the risk of coronary problems. However, the latest results of several major international trials showed that aromatase inhibitors work better than tamoxifen in post-menopausal women with early-stage breast cancer that is ER positive, progesterone receptor positive, or both. So, in the near future, it may be possible that aromatase inhibitors will be the new standard of care for post-menopausal women with invasive hormone-receptor-positive breast cancer, both early and advanced-stage.

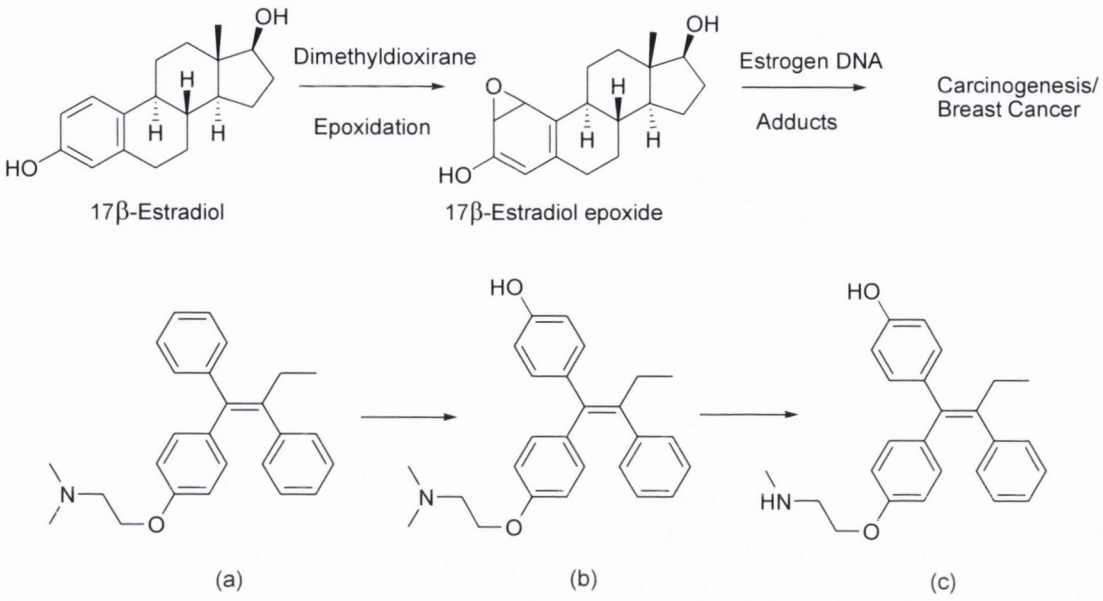

Scheme 1. 2 Epoxidation of 17β-estradiol shown, with Tamoxifen (a), and metabolites: 4-hydroxytamoxifen (b) and endoxifen (c)

Proposed mechanism of action of Tamoxifen

Tamoxifen (TAM) is known to have a dual mechanism of action: (1) to compete with 17β-estradiol (E_2) at the receptor site and to block the promotional role of E_2 in breast cancer; and (2) to bind DNA after metabolic activation and to initiate carcinogenesis. Recent large scale clinical trials indicate that TAM is also an effective chemopreventive agent against breast cancer. Because E_2 requires activation by epoxidation to bind DNA forming DNA adducts[60, 61] (see scheme 1.2), and the same is true for TAM [62], the question is whether this preventive effect of TAM against breast cancer is contributory to the possibility that TAM, as an effective competitor for epoxidation, prevents the formation of E_2 epoxide and consequently breast cancer. When incubated together with E_2 for epoxidation, TAM was able to dramatically reduce the formation of E_2 epoxide as measured by both the loss of the ability of E_2 to inhibit nuclear RNA synthesis, and the reduced binding of [^{3}H]labeled E_2 to nuclear DNA. Identical results were obtained when TAM and estrone (E_1) were used. These results suggest that the breast cancer preventive effect of TAM is through a competitive epoxidation mechanism with E_1/E_2.[63]

It is true that the mechanism of action of tamoxifen is complex. Clearly, its principal mechanism of action is mediated by its binding to the estrogen receptor and the blocking of the proliferative actions of estrogen on mammary epithelium[64]. One suggested mechanism for this antiproliferative action is the induction by tamoxifen of the synthesis of the cytokine transforming growth factor-β (TGF-β), which acts as a negative autocrine regulatory molecule.[65] However, it has also been shown that tamoxifen can induce synthesis of TGF-β in estrogen receptor-negative cells, such as fetal fibroblasts.[66] Moreover, immunohistochemical studies have shown that tamoxifen induces the synthesis of TGF-β in the stromal (mesenchymal) compartment of breast cancers, suggesting a paracrine as well as autocrine mechanism of action, independent of an interaction with the estrogen receptor.[67] Reports of some clinical efficacy of tamoxifen in the treatment of women with estrogen receptor-negative breast carcinomas would appear to be in accord with these mechanistic conclusions.[68] Other studies that are in accord with these observations are the findings that tamoxifen can lower the circulating levels of insulin-like growth factor I (IGF-I) in breast cancer patients.[69, 70] IGF-I is a potent mitogen for breast cancer cells and may act by endocrine, paracrine, and autocrine routes to stimulate their growth.[64]

Most of the antiestrogen type compounds may lead to long-term toxic effects. For instance, tamoxifen induces liver cancer in rats after prolonged administration, which has been attributed to the generation of DNA-alkylating species from the metabolism of the stilbene framework. It has been proposed that cytochrome P450 hydroxylates tamoxifen at the allylic position of the ethyl side chain, leading to an alcohol, which can generate a highly delocalised allylic cation (a, scheme 1.3) and therefore alkylate DNA to give product (b) (see scheme 1.3).

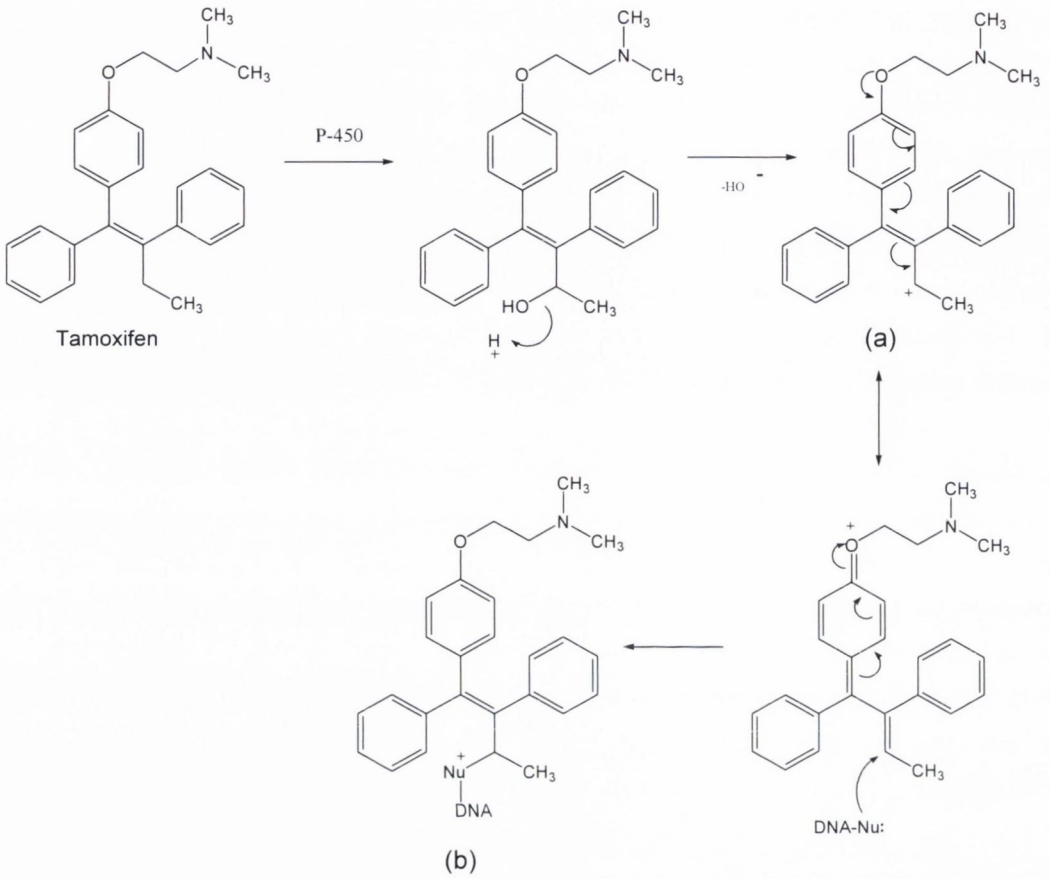

Scheme 1. 3 Mechanism proposed to explain tamoxifen long-term toxicity

This proposal also explains the lack of carcinogenicity of the related antiestrogen toremifene, which can be attributed to destabilisation of the positive charge in b (scheme 1.3) by the inductive effect of the chlorine substituent at the position adjacent to the allylic carbon[1].

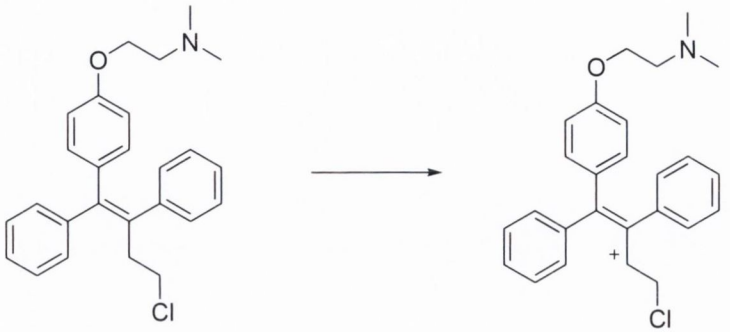

Toremifene (b)

Scheme 1. 4 Carbocation derived from toremifene

Tamoxifen has become the standard therapy for all types of ER-positive breast cancer. In the 1990's, it was also the first cancer chemopreventative agent approved by the FDA for the reduction of breast cancer in pre- and postmenopausal women with high risk[71]. Tamoxifen also binds with high affinity to other targets, such as microsomal antiestrogen binding sites (AEBS), protein kinase C, calmodulin (CaM)-dependent enzymes, and acyl coenzyme A:cholesterol acyl transferase (ACAT)[72].

The reversible pharmacological action of tamoxifen as an antiestrogen was first described *in vitro* using the MCF-7 human breast cancer cell line. Tamoxifen blocked cell replication but subsequent addition of estrogen restored cell growth. Similarly, Tamoxifen significantly reduced the induction and growth of tumors in a carcinogen-induced rat mammary carcinoma model[55]. However, the drug showed paradoxical species-specific effects. Tamoxifen acted as an estrogen in dog and mouse, a pure antiestrogen in chick, and had both agonist and antagonist actions in humans and rats. Initially, the species-specific actions of tamoxifen were thought to result from species-specific metabolism, but no species difference in the metabolites of the drug was found. Two important observations in the laboratory laid the foundation for the concept of SERMs. In an athymic mouse model transplanted with both a breast (MCF-7) tumor on one side of mammary fat pads and an endometrial (EnCa101) tumor on the other side, tamoxifen produced the same spectrum of metabolites in both tumors, but had different actions on the growth of each tumor. Tamoxifen inhibited growth of breast cancer, but stimulated the growth of endometrial cancer. In addition, tamoxifen caused the growth of the mouse uterus but did not cause the growth of a breast tumor despite the presence of the same metabolites. These data raised the possibility that the mode of action of tamoxifen is not specific to a species, but specific to a target tissue. Finally, and perhaps most importantly, nonsteroidal antiestrogens maintained bone density in

the ovariectomized rat at doses known to prevent rat mammary cancer [55]. Although the risks are actually quite small, there is major concern about the safety of the use of tamoxifen as a chemopreventive agent for the prophylaxis of breast cancer, because of its estrogenic effect on uterine epithelium and the attendant increased risk for development of uterine cancer. Thus, there has been a search for new agents that would resemble tamoxifen in their overall mechanism of action, but would be inhibitory to the growth of uterine epithelium[64].

Toremifene

Toremifene is a structural analogue of Tamoxifen [73]. It contains a chlorine moiety not found on Tamoxifen. Toremifene is an antiestrogen which has been shown to inhibit the simulative effects of estrogens on breast cancer growth. Toremifene causes growth inhibition of estrogen-sensitive breast cancer cells by inducing some cells to undergo apoptosis and by inhibiting other cells from entering mitosis. It has been used in clinical practice for the treatment of ER-positive breast cancer (see structure in scheme 1.4). It displays similar properties and side-effects to tamoxifen but does not appear to increase the risk of endometrial cancer in post-menopausal females[51]. Studies have shown that toremifene is as effective as tamoxifen in advanced breast cancer. Like tamoxifen, the antiproliferative effect of toremifene on breast cancer cells is mediated by its competitive binding to the ER [74]. However, the long term side effect of liver cancer associated with tamoxifen is not evident in the case of toremifene as metabolism of toremifene does not lead to the generation of DNA-alkylating species [1].

Raloxifene

Because of the toxic effects associated to the central double bond in triphenylethylene derivatives, a new family of antiestrogens has been developed where the incorporation of this double bond into a more conformationally restricted cyclic system increases its chemical and metabolic stability. Another structural difference of these compounds with the traditional triphenylethylene derivatives is the presence of a ketone bridging group linking the phenyl ring that contains the basic side chain. The main representative of this family is raloxifene, containing a benzothiophene ring system (Figure 1. 12, a), which was approved by the FDA for osteoporosis, while studies as a treatment for breast cancer were discontinued. However, there is a recent renewal of the interest in raloxifene as a means for breast cancer prevention, with a very large

clinical study in progress involving more than 19,000 postmenopausal women at increased risk of breast cancer, aimed at comparing the efficacy of tamoxifen and raloxifene in chemoprevention[1, 75].

Raloxifene has been shown to function as an antagonist in the breast and uterus, while functioning as an estrogen in the bone and cardiovascular system. Raloxifene was developed initially as an anti-estrogen for breast cancer in the late 1980s, but since it was found to maintain bone density, to prevent rodent breast cancer, and to inhibit tamoxifen stimulated endometrial cancer growth, it was developed for osteoporosis, for which it is now an established drug. Raloxifene is an inhibitor of cultured breast cancer cells and, *in vivo*, it possesses antitumor activity. Like tamoxifen, raloxifene reduces total cholesterol but does not increase high-density lipoprotein cholesterol, a feature that may lessen any cardioprotective effects. Furthermore, it was demonstrated that raloxifene has a potential in the treatment of myocardial ischemia. It is able to relax porcine coronary arteries *in vitro* due to activation of the mitogen-activated protein kinase (MAPK) pathway. P38 MAPK activation has been shown to be responsible for cardioprotection during ischemic preconditioning[43].

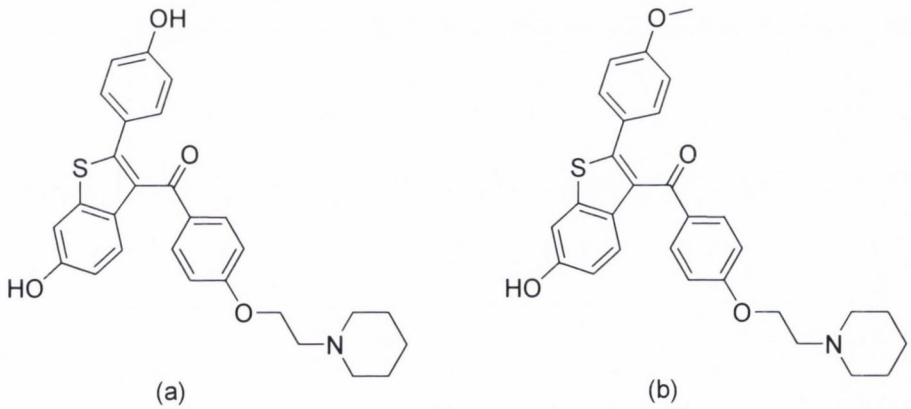

Figure 1. 12 Raloxifene (a) and Arzoxifene (b)

Arzoxifene, one of a number of newer type ER antagonists, is a benzothiophene analogue SERM candidate. Replacement of the carbonyl group with an electron withdrawing oxygen results in an improved oral bioavailability and a 10-fold increase in *in vitro* estrogen antagonist potency relative to raloxifene. Arzoxifene (Figure 1. 12, b) also inhibited uterine proliferation response, produced a significant decrease in total cholesterol levels and showed protective effect on bone. Phase II clinical trials showed

significant response rates to arzoxifene [76] in tamoxifen resistant patients with locally advanced metastatic breast cancer. Arzoxifene is currently undergoing phase III trials for breast cancer therapy[77, 78].

Lasofoxifene and Bazedoxifene

Researchers have developed the concept of the 'ideal' SERM. [79] The 'ideal' SERM is one that mimics estrogen's beneficial effects in the body by acting as an agonist in the bone and cardiovascular system but that counteracts estrogen's harmful effects in the breast and uterus by acting as an antagonist in these tissues. Several compounds with 'ideal' SERM characteristics are currently being developed for the treatment and prevention of breast cancer. These include other triphenylethylenes (droloxifene, idoxifene), arzoxifene (a long-acting raloxifene analogue), benzopyrans (EM-800), naphthalenes (CP-336, 156) and pyrazoles [10] [80, 81]. Other new generation SERMs include the tetrahydronaphthalene compound lasofoxifene and the indole compound bazedoxifene, (see structures, Figure 1. 13). Lasofoxifene and bazedoxifene have recently undergone large phase III clinical trials and are now approved for use in the EU for the treatment of osteoporosis[82]. The development of ERα-selective SERMs could offer an alternative approach for the treatment of breast cancer and other diseases in the future and such agents could replace the non-subtype-selective SERMs which have been used up until now [9].

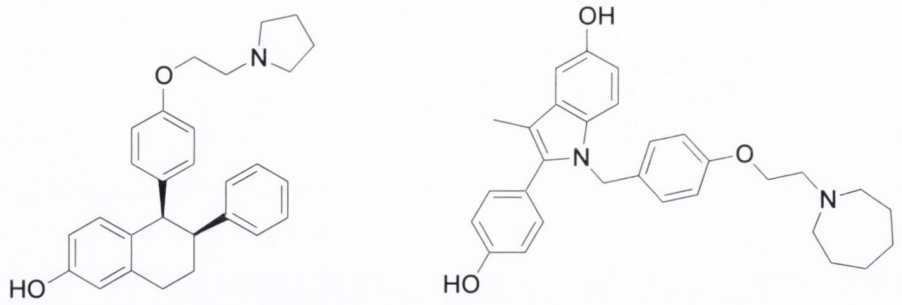

Figure 1. 13 New generation SERMs: lasofoxifene (left); bazedoxifene (right)

1.3.2 SERDs

In addition to SERMs, 'pure' antiestrogens or selective estrogen downregulators (SERDs) have also been developed to target the ER. With the advent of drug resistance, particularly resistance to tamoxifen, interest in this class of drug has grown. One such agent, Fulvestrant has been approved as a third line drug for treatment of ER-positive metastatic breast cancer and is illustrated in Figure 1. 14 [74]. Fulvestrant is a steroidal antiestrogen with a hydrophobic side chain in the 7α position. The mechanism of action of fulvestrant involves the competitive inhibition of estradiol binding at the ER. Once bound to the ER, fulvestrant impairs dimerisation of the receptor ultimately leading to receptor degradation. The long side chain of fulvestrant also obstructs the folding of the Helix 12 of the ER resulting in the inhibition co-activator recruitment [1].

Initial studies of the drug *in vitro* and in animal models showed that it effectively down-regulated the ER and inhibited tamoxifen-resistant breast tumour cells. However, fulvestrant has yielded less promising results in clinical practice and this has been blamed on the poor oral bioavailability of the drug in humans and resulting low levels of the drug reaching the tumour site. Fulvestrant is therefore administered by intramuscular injection. Current research in this area is focused on developing SERDs which exhibit more favourable pharmaceutical properties [74].

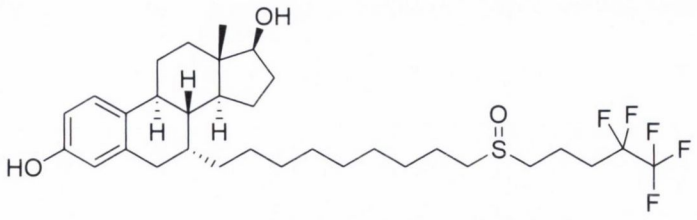

Figure 1. 14 Structure of Fulvestrant

1.4 HMR 3339

Unlike the other SERMs, HMR 3339 (Figure 1. 15) is a steroid. It is currently under clinical development for the prevention of osteoporosis and coronary heart disease. In rats, the SERM HMR 3339 completely prevented bone mineral density loss and even increased it following ovariectomy. Furthermore, HMR 3339 also increased bone mechanical strength at multiple sites following ovariectomy. The increases in bone mineral density and bone strength induced by HMR 3339 were more pronounced than raloxifene on cortical bone. In healthy postmenopausal women, HMR 3339 promoted an antiatherogenic lipid profile by reducing total LDL cholesterol, and decreased homocysteine levels, while not influencing HDL cholesterol and lipoprotein(a), whereas raloxifene showed similar effects but did not reduce homocysteine levels. In healthy postmenopausal women, HMR 3339 at the highest dosage (50 mg daily) reduced antithrombosin, protein C, and fibrinogen compared to placebo. Hence, HMR 3339 shows promise for protection of coronary heart disease, and perhaps osteoporosis.

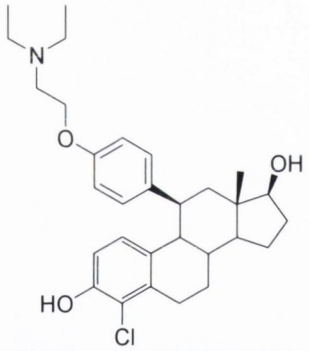

Figure 1. 15 HMR 3339

1.5 Aromatase Inhibitors

An alternative strategy for achieving antiestrogenic effects is the inhibition of aromatase, the enzyme responsible for biosynthesis of estradiol and estrone from androgens[83]. In principal, this strategy has the advantage over the use of antiestrogens of blocking the two pathways involved in the generation of tumours by the estrogenic hormones, namely ER activation and the generation of carcinogenic metabolites, see scheme 1.5.

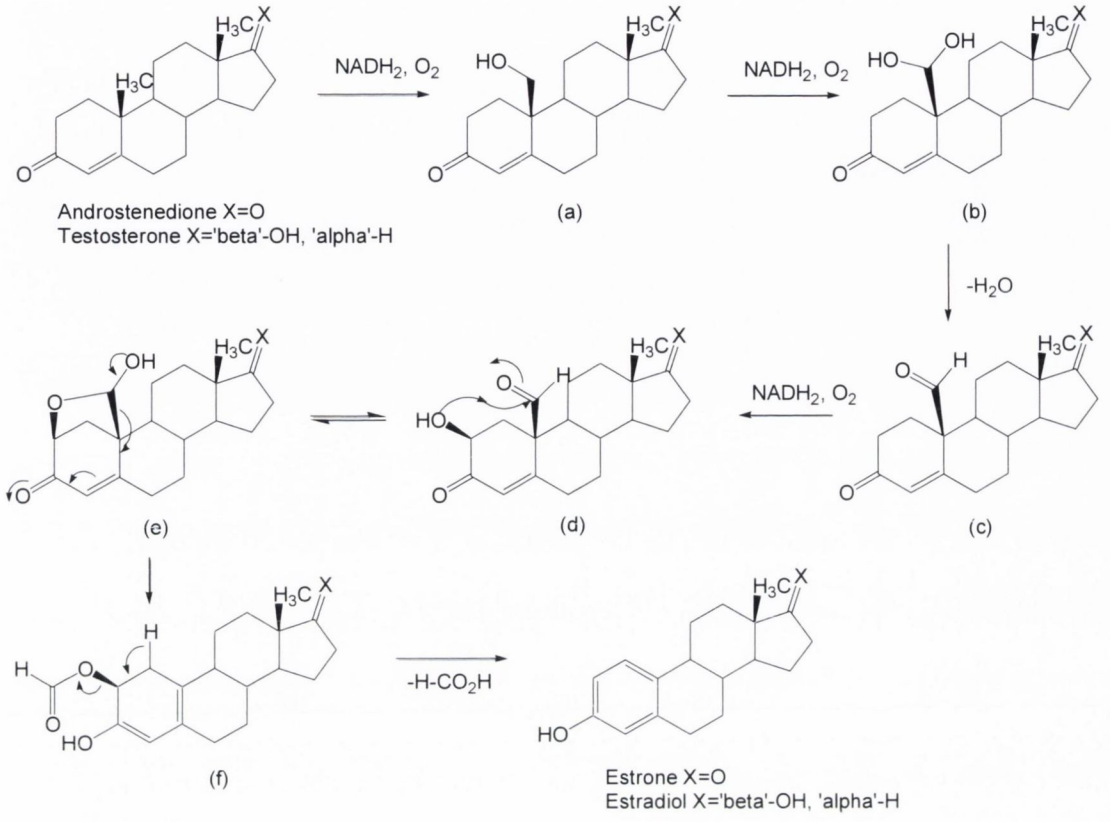

Scheme 1. 5 Mechanism of aromatase activity [1]

Aromatase belongs to the group of microsomal cytochrome P450 enzymes responsible for the hydroxylation metabolic process. The overall process catalysed by aromatase comprises a series of three oxidative steps. The first two are the insertion of two hydroxyl groups at the C-19 methyl group of its substrates leading to (a, scheme 1.5) and to *gem*-diol (b, scheme 1.5), which is dehydrated to aldehyde (c, scheme 1.5). The third reaction is only partially understood, and involves loss of the C-19 carbon atom as a molecule of formic acid, with concomitant aromatisation of ring A. One mechanistic possibility is that the third hydroxylation takes place at C-2β, yielding intermediate (d, scheme 1.5), which can be postulated to rearrange to (f), through the intermediacy of the cyclic hemiacetal (e). Loss of a molecule of formic acid, driven by the generation of the aromatic A ring, would finally culminate the process, yielding the estrogens estradiol and estrone (scheme 1.5). However the experiments with [2β-^{18}O-,19-^{3}H]-2β-hydroxy-10β-formylandrost-4-ene-3,17-dione failed to show incorporation of the β-hydroxyl to formic acid under enzymatic and nonenzymatic conditions [1, 84].

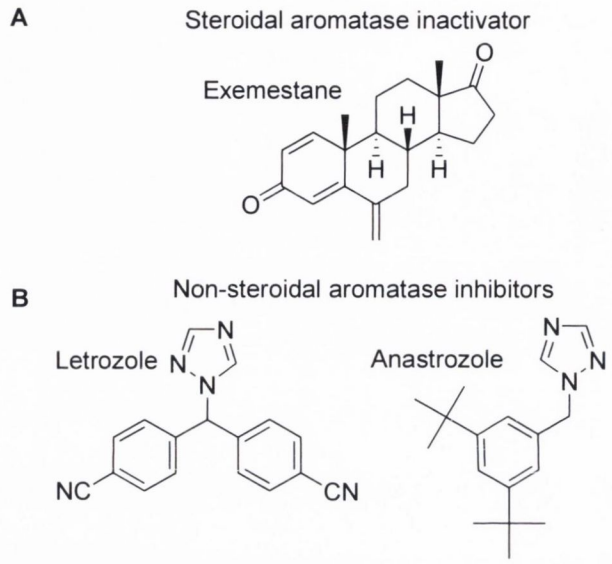

Figure 1. 16 Structures of Aromatase Inhibitors, (a) Steroidal aromatase inactivator and (b) Non-steroidal aromatase inhibitors [1]

Exemestane (marketed as Aromasin see Figure 1. 16) is indicated for the adjuvant treatment of postmenopausal women with estrogen-receptor positive early breast cancer who have received two to three years of tamoxifen and are switched to it for completion of a total of five consecutive years of adjuvant hormonal therapy [85]. Exemestane is an aromatase inhibitor and had a steroidal structure similar to estrogen (estradiol). The mechanism of action of exemestane is by inhibiting the action of the enzyme aromatase, which converts androgens into estrogens by a process called aromatization (see steroid tree Figure 1. 17). Other non-steroidal aromatase inhibitors include Letrozole and Anastrozole (see Figure 1. 16 for structures).

Exemestane, Letrozole, Anastrozole and Tamoxifen are used as adjuvant breast cancer treatments. Long-term follow-up data from a large international phase III trial shows that postmenopausal women with early-stage hormone receptor-positive breast cancer who received 2 to 3 years of tamoxifen and then switched to the drug exemestane for a total of 5 years of adjuvant hormone therapy experienced a delay in disease recurrence and a survival advantage, compared with women who took tamoxifen on its own for 5 years [86-88]

1.5.1 The Steroid Tree

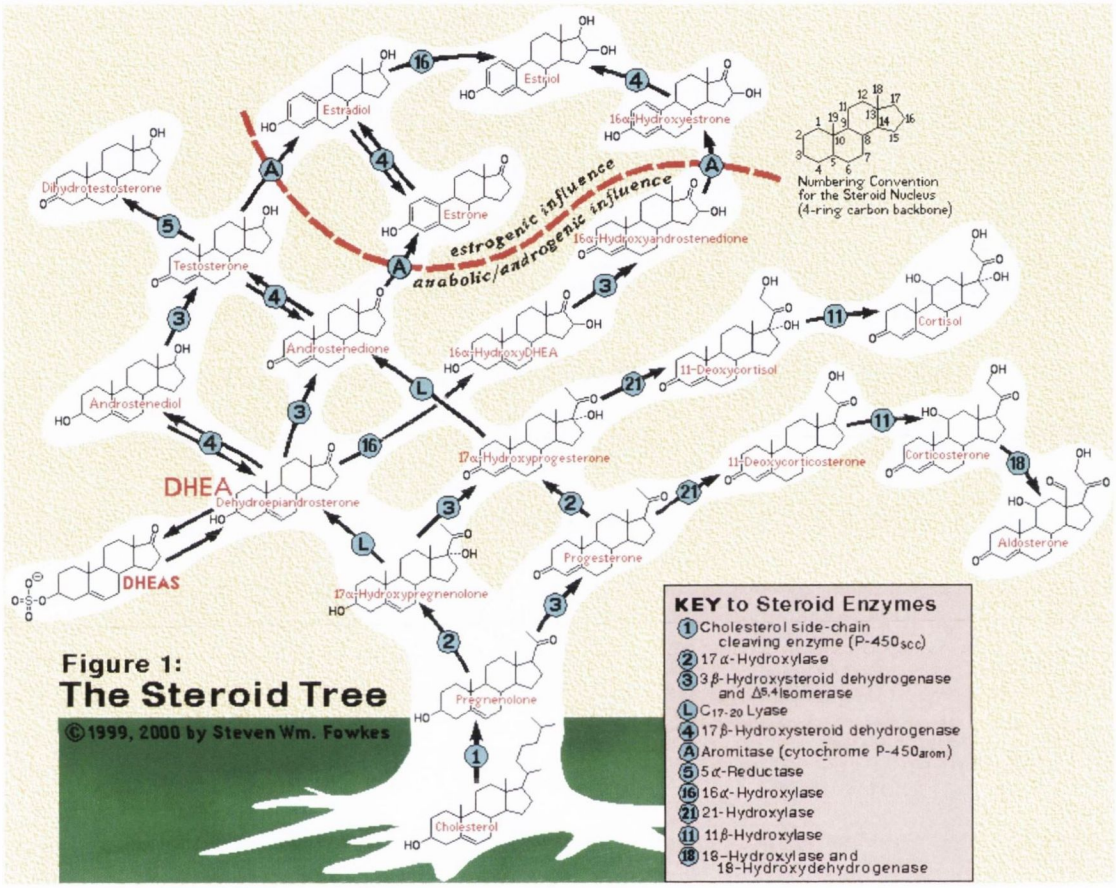

Figure 1. 17 The Steroid Tree [89]

Any steroid precursor can be metabolized into estrogen (estradiol, estrone and estriol). If the many steroids in the steroid tree are examined (see Figure 1. 17), most lead to estrogens [89]. The key enzyme in the production of estrogens is aromatase (the A-marked **[blue]** circles). If a line is drawn through the aromatase-catalyzed reactions, all of the estrogens are on one side of the line, and the anabolic and androgenic steroids are on the other side (see **[red]** dashed line). This means that aromatase is the gatekeeper that influences the relative dominance of estrogenic versus anabolic/androgenic influences within the steroidal hormonal system.

The two primary aromatase pathways are 1) the conversion of androstenedione to estrone, and 2) the conversion of testosterone to estradiol (the leftmost arrows crossing the dashed line). Since estradiol and estrone readily interconvert (note the

bidirectional arrows, Figure 1. 17), the particular pathway to estrogen is not very significant from the estrogen perspective (on the estrogen side of the line). There is, however, a major difference on the androgen/anabolic side of the line. Aromatase has a tenfold higher affinity for androstenedione than testosterone. This puts androstenedione at a distinct disadvantage compared to testosterone regarding potential estrogenic side effects[90].

This estrogenic disadvantage of androstenedione is not shared by androstenediol. Androstenediol is not a direct substrate for aromatase and must first be 1) converted to testosterone, 2) converted to DHEA and then to androstenedione, or 3) converted to testosterone and then to androstenedione before it can be converted to estrogens by aromatase. One of the key enzymes in these three alternatives is 17-beta-hydroxysteroid dehydrogenase, the same enzyme that interconverts estradiol and estrone. This enzyme allows androstenediol and DHEA to interconvert, and testosterone and androstenedione to interconvert[89].

1.5.2 Novel SERMs and related compounds

Many novel heterocyclic SERM compounds have been investigated and reported in recent years. The following is a minor selection of the diverse and varied therapeutics investigated that target the estrogen receptor and are potentially of interest for the development of breast cancer chemotherapy.

1.5.3 Pyrazole SERMs

There is much interest in fixed ring scaffold structures for SERMs and the pyrazole ring has been demonstrated as a suitable candidate. Pyrazole rings have been used by Stauffer *et al* as a scaffold for the synthesis of SERMs, (see Figure 1. 18, a) and were claimed as the first ERα specific agonists showing 410 fold affinity for α over β. Four analogues were designed to explore the four possible orientations that the pyrazole core structure might adopt the ER ligand binding pocket, and thereby identifying which site on the pyrazole could best accommodate the rather large, basic side chain substituent [78]. The C(5) piperidinyl-ethoxy-substituted pyrazole (Figure 1. 18, b) was found to have the highest affinity for ERα. Compound b (Figure 1. 18) is an

antagonist on both ERα and ERβ, but its potency on ERα is somewhat higher, reflecting its ERα affinity selectivity[91].

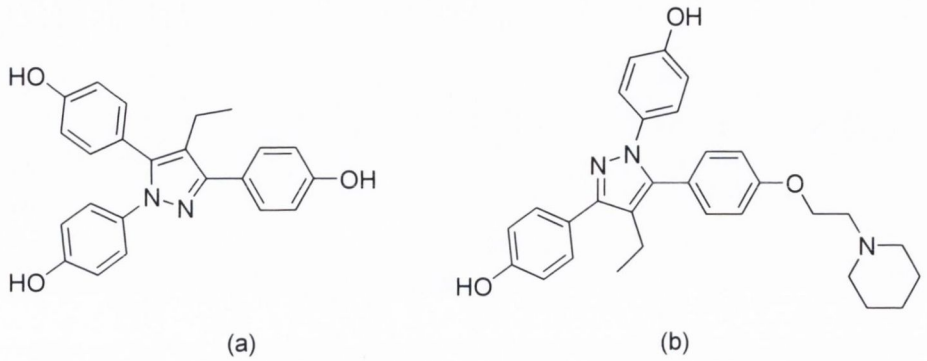

(a) (b)

Figure 1. 18 Pyrazole agonist (a) and corresponding antagonist (b)

Indolazines are novel heterocyclic ER targeting derivatives, designed to be unable to undergo isomerisation but where the double bond character of the aromatic indolazine nucleus is utilsed to take the place of the olefinic bond in tamoxifen. They showed low relative binding affinity to the ER[92]. NCC 45-0095 (see Figure 1. 19, (a)) is a novel pyrrolo[2,1,5-cd]indolizine compound which showed high receptor binging affinity. NCC 45-0095 is the parent pharmacophore and showed full agonist effects in the endometrium for the skeleton non-steroidal ER ligand[93]. It is expected that this compound would have antagonist activity if the 4-hydroxy group were replaced with a suitable extended basic side chain ether (e.g. (b), see Figure 1. 19).

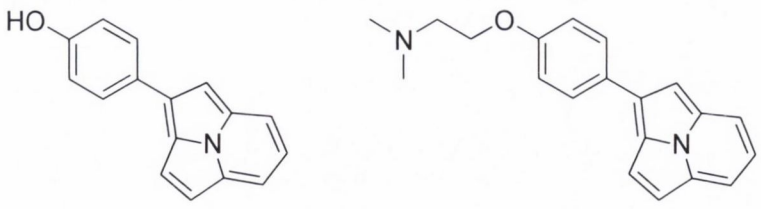

(a) (b)

Figure 1. 19 Indolazine ER modulators

1.5.4 General biological activity of Benzopyrans and Chromenes

The benzopyran and chromene ring systems have been identified as core scaffolds for many biologically active compounds and a brief review of their diverse activities is now presented. Researchers have used *In silico* screening [94] of a collection of 1584 academic compounds to identify a small molecule hit for the human adenosine A_{2A} receptor (pK_i = 6.2) containing a novel chromene scaffold (Figure 1. 20, **1a-d**). These researchers undertook a structure–activity relationship study of the chemical series for adenosine receptors, and a focused library of 43 2*H*-chromene-3-carboxamide derivatives was synthesised and tested in radioligand binding assays at human adenosine A_1, A_{2A}, A_{2B} and A_3 receptors. The series was found to be enriched with bioactive compounds for adenosine receptors, with 14 molecules showing submicromolar affinity ($pK_i \geq 6.0$) for at least one adenosine receptor subtype.

A conformational study of potent and selective endothelin-A (ET_A) receptor antagonists, 4 substituted (R)-2-(benzo[1,3]- dioxol-5-yl)-6-isopropoxy-2H-chromene-3-carboxylic acids was reported by Ishizuka *et al*. These 2H-chromene derivatives were bound to an ETA receptor and were found with IC_{50} values of less than 1 nM. These were shown to be effective for use on endothelins (ETs), which are endogenous vasoconstrictive peptides containing 21 amino acids. ET_A receptor antagonists have been developed for treating various cardiovascular diseases in various disease states[95]. In particular, the 4-anisyl derivative **2** (S-1255, see Figure 1. 20), was found to be a highly potent and orally active antagonist and was selected as a clinical candidate [94].

Akritopoulou-Zanze et al have reported the discovery of a novel class of glucocorticoid receptor (GR) antagonists based on the chromene molecular scaffold[96]. Glucocorticoid receptor antagonists such as RU-486 (**3,** see Figure 1. 20) have been shown to be effective at blocking gene-transcription mediated by endogenous glucocorticoids such as cortisone (**4**) One of the derivatives in this group's effort to improve lead to hit compound (**5**) had a IC_{50} of 2 nM. The utility of GR-antagonists in treating conditions that result from high levels of circulating glucocorticoids has been demonstrated by the use of RU-486 for the treatment of the Cushing's syndrome, diabetes, glaucoma, and depression [96].

Another group of chromenes has been found with activity as calcium channel blocking agents. These have been used in the management as angina pectoris and hypertension. Within this class of cardiovascular agents, dihydro(benzopyran)pyridine

calcium antagonists have found widespread use in the clinic and have served as important tools for the study of calcium channel structure and function [97]. In the search for new and better Nifedipene analogues as antagonists, the replacement of the 4-substituent, i.e. the phenyl ring has been examined further. The benzopyran structure (**6**, see Figure 1. 20) is among those described in the literature [97] as a calcium channel antagonist.

Benzopyrans have also been described as histamine-3-receptor antagonists. H_3 receptors are found primarily in the brain, where they negatively regulate the synthesis and release of histamine. The spirobenzopyran piperidine ether analogs demonstrated excellent H_3 receptor affinity and selectivity (see compound **7**, Figure 1. 20). The 1'-cyclobutyl-6-(4-piperidyloxy)spiro[benzopyran]-2,4'-piperidine] derivative **10,** exhibited high affinities for human and rat H_3 receptors with low nanomolar activity [98]. The potential uses of modulating this target are in the areas of ADHD, Alzheimers disease and schizophrenia. Benzopyrans have also been found as potential H_1-antihistaminic agents. This has been known to be effective in therapy for respiritory distress [99].

Coumarin and chromene derivatives have been used as cannabinoid receptor antagonists and inverse agonists[100]. Antagonistic/inverse agonising of these receptors has the potential to be effective in treatment of Tourettes syndrome tics, multiple sclerosis and neuropathic pain [100]. A series of benzopyran and 3-benzylcoumarin derivatives were synthesised, (see the structure **8**, Figure 1. 20, as an example) and were found with high affinities of 0.738 μM at CB_1 and 0.944 μM at CB_2 receptors [100]. The *2H*-chromene derivative showed good affinity for the CB_1 receptor, with K_i values of 1.37 μM. A series of benzopyranopyridines have been reported as the first small molecule inhibitors of mitogen-activated protein kinase activated protein kinase 2 (MK-2) and may have a role in the treatment of TNFα mediated inflammatory disease. Compound **9** demonstrated IC_{50} value for MK-2 inhibition of 0.13 μM and IC_{50} value of 0.92 μM for reduction of TNFα expression[101].

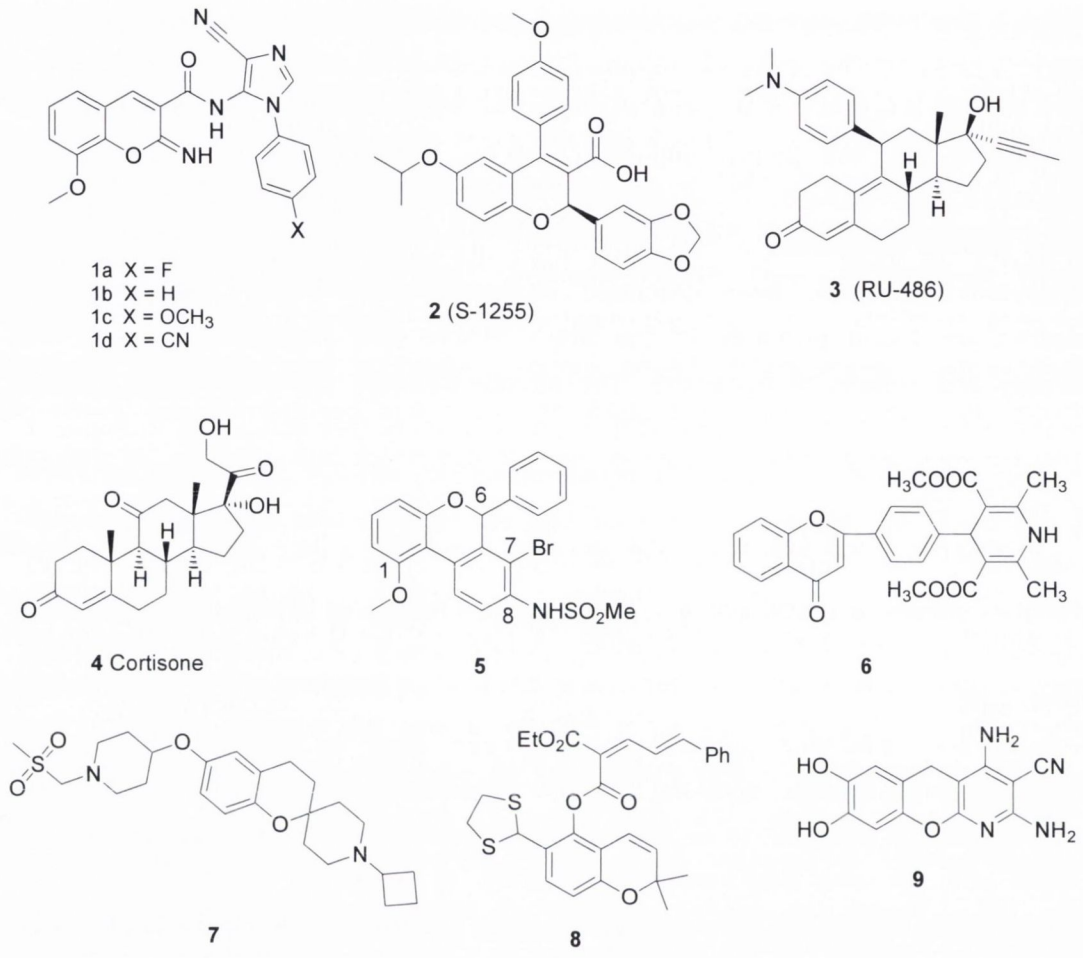

Figure 1. 20 Biologically active chromenes

These results provide evidence that the chromene scaffold, a core structure present in natural products from a wide variety of plants sources constitutes a valuable source for novel therapeutic agents [94].

1.6 Chromenes as SERMs with breast cancer activity

The interactions of various flavones, isoflavones and other plant derived estrogens with estrogen receptors for prevention and treatment of breast cancer have been recently reviewed[102]. EM 800 (Figure 1. 21, a), converted *in vivo* to its active metabolite EM 652, Acolbifene (Figure 1. 21, b) is an orally active benzopyran derivative with SERM properties. It has shown good activity in breast cancer, in both prevention and treatment models in animals, and acts as a potent estrogen-antagonist on the uterus in the ovary-intact animal with no estrogenic-agonist activity. The orientation of the

basic side chain in these compounds is similar to that of raloxifene, and is thought to account for the tissue selectivity profile of these compounds when compared to Tamoxifen. Compound (b)(Figure 1. 21) is reported to exhibit a higher binding affinity than any known antiestrogen and possesses a 2.9 fold higher receptor affinity than estradiol. It also shows agonist effects on bone and lipids and thus appears to have an 'ideal' SERM profile. It is currently in clinical trials for the treatment of estrogen sensitive breast and endometrial cancers[103].

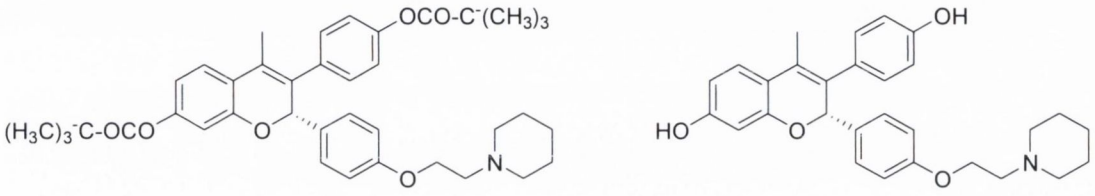

(a) (b)

Figure 1. 21 EM 800 (a) and EM 652 (b)

1.6.1 Chromenes and coumarins targeting ERβ- SERBAs

Until 1996, estrogens were assumed to mediate their effects through a single nuclear receptor (now called ERα). The discovery of a new estrogen receptor named ERβ, in 1996[104], followed by tissue distribution studies[105] which showed that the expression of the two ERs is not coincident in tissues, has led to renewed interest in estrogen receptor modulators, especially compounds that are selective for the two subtypes ERα and ERβ. X-Ray crystal structures of receptor–ligand complexes of ERα and ERβ[106] show that the binding pockets of the two receptors are very similar and differ by only two amino acids. The leucine present at position 384 in ERα is replaced by a methionine in ERβ (Met 336) and the methionine in position 421 is replaced by an isoleucine in ERβ (Ile373). In light of this it is not surprising that most previously known estrogens and SERMs bind fairly non-selectively to the two receptors. However, recent reports have described chromene type compounds that bind selectively to ERα and ERβ[104].

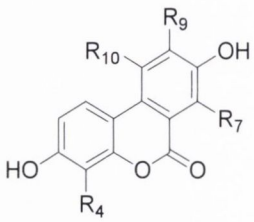

Figure 1. 22 3,8-Dihydroxy-6H-benzochromen-6-one scaffold

Benzochromene derivatives have been reported as selective ERβ agonists. Sun *et al.* prepared a series of 6*H*-benzo[*c*]chromene derivatives. Many of the analogs were found to be potent and selective ERβ agonists. Bis phenolic hydroxyls at positions 3 and 8 (see Figure 1. 22) are essential for activity in a HTRF coactivator recruitment assay. Additional modifications at both phenyl rings led to compounds (see Figure 1. 23, structures **10** and **11**) with ERβ <10 nM potency and >100-fold selectivity over ERα [104].

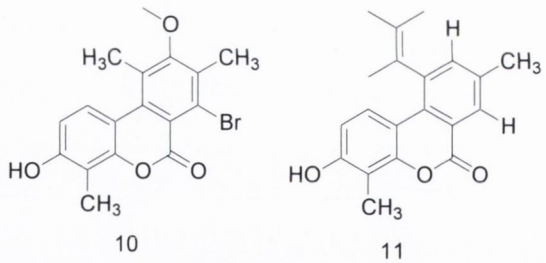

	IC_{50} (nM)		ERα/ERβ
	ERβ	ERα	
10	1.15	225	150
11	10	10,000	1000

Figure 1. 23 ERβ selective benzochromene structures

A number of tetracyclic benzopyranobenzopyrans and benzopyranobenzoxepanes were also synthesised and evaluated as SERM ligands. These chromene rings are excellent at mimicking natural ligands as estrogen modulators. Figure 1. 24 shows benzopyranobenzopyran **12**, and benzopyranobenzoxpane **13** [107]. The aminoalkylethers of **12** and **13** were also investigated for ER antagonistic activity.

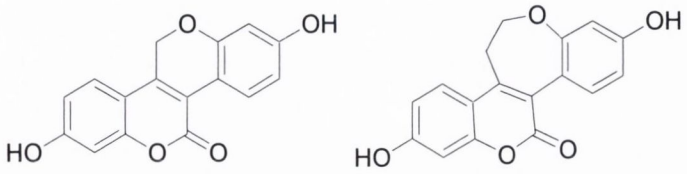

12 13

Figure 1. 24 Benzopyranobenzopyran 12, and Benzopyranobenzoxepane 13

1.6.2 Chromanes

As previously described, the significant benefits of estrogen replacement therapy are achieved at the expense of an increased risk of endometrial hyperplasia and breast cancer. Levormeloxifene (Figure 1. 25) may largely lack the estrogenic activity on the endometrium and appear to act as an anti-resorptive agent on bone in preclinical and clinical studies. In 2002 a group of related chromanes were demonstrated to be very potent binding ligands to the estrogen receptor [108]. Among these were (±)-*cis*-7-hydroxy-3-phenyl-4-(4-(2-pyrrolidinoethoxy)phenyl)chromane (**14**, Figure 1. 25) and (±)-*cis*-7-hydroxy-3-phenyl-4-(4-(2-piperidinoethoxy)phenyl)chromane (**15**, Figure 1. 25). This compound was further demonstrated to completely prevent the loss of total bone mineral density of the tibiae in the ovariectomised rat. In addition the unwanted uterotrophic changes normally observed with estradiol treatment, and in particular the dangerous proliferative effects on endometrial tissue, were not observed. The synthesis of some novel related thio-analogues is illustrated (see scheme 1.6, compounds **16** and **17)**. *In vitro* biological data for these compounds were also reported. The estrogen receptor ligand binding affinity (ER-LBA) value for compound **16** was IC_{50} (nM) 9.7 ± 2.5, for compound **17**was IC_{50} (nM) 6.5 ± 6.4, for compound **14** was IC_{50} (nM) 19.0 ± 1.4 and for compound **15** was IC_{50} (nM) 3.1 ± 1.4.

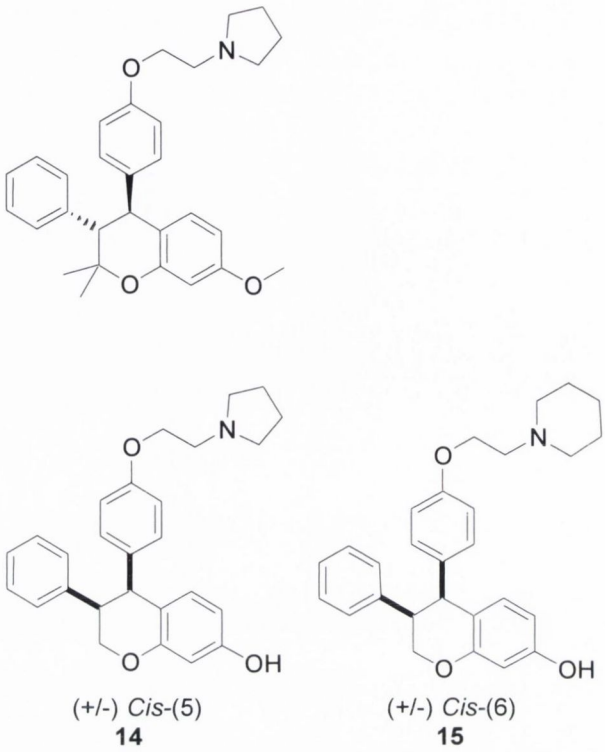

(+/-) *Cis*-(5)
14

(+/-) *Cis*-(6)
15

Figure 1. 25 Partial estrogen receptor antagonists

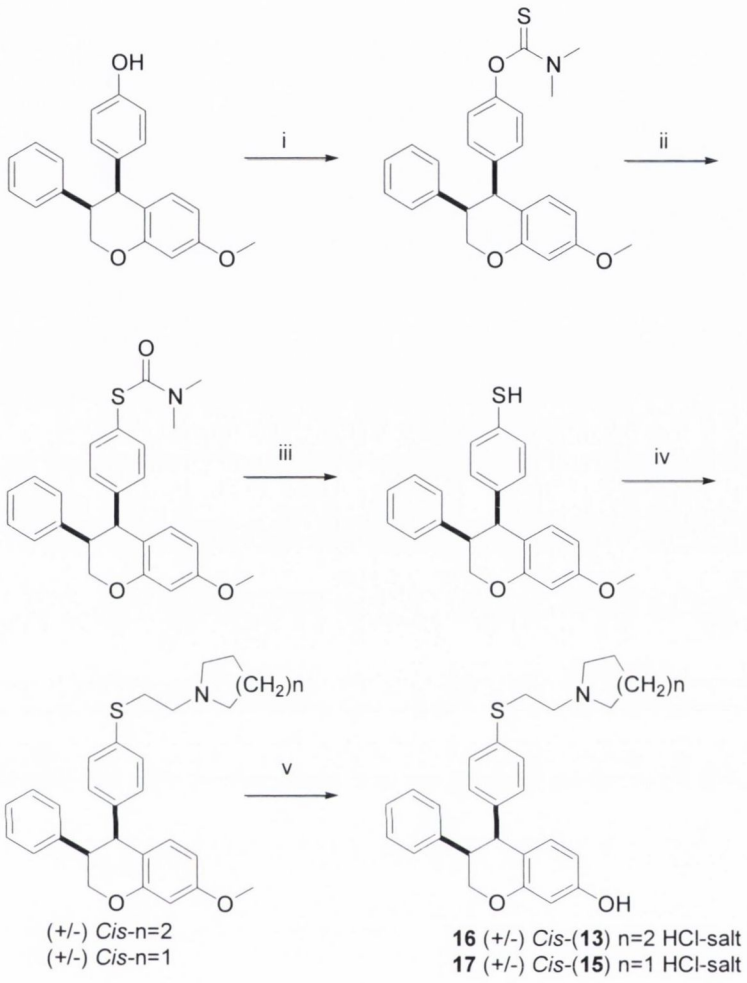

Scheme 1. 6 Synthesis of two partial estrogen receptor antagonists 16 and 17 (i) NaH, DMF, N,N-dimethylthiocarbamoyl chloride; (ii) 260 °C, diphenyl ether; (iii) $LiAlH_4$, THF; (iv) N-(2 chloroethyl)pyrrolidine hydrochloride, or N-(2 chloroethyl)piperidine hydrochloride K_2CO_3, NaI, zinc dust, acetone, (v) BBr_3, CH_2Cl_2

A series of benzopyrans have been shown to be specifically selective for estrogen receptor beta, (ERβ) as agonists (SERBAs)[109], and bind to ER subtypes α and β in opposite orientations. ERα and ERβ function as ligand-activated gene transcription factors and mediate a number of important physiological processes with the classical receptor, ERα, being most important for development and regulation of the female reproductive system as well as maintenance of the skeletal and cardiovascular systems. It has been proven possible to develop synthetic estrogen agonists that have

tissue type selectivity [109]. Figure 1. 26 shows benzopyran **18** was shown with binding values on ERβ of 0.47 μM ± 0.18, a 9-fold selectivity for ERβ over ERα.

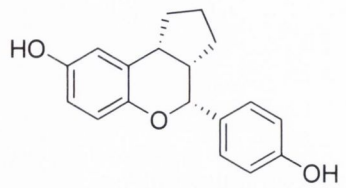

Figure 1. 26 SERBA 18 [109]

1.7 Biologically active coumarins

Coumarins are structurally simple compounds belonging to a large class of molecules known as benzopyrones[110]. Coumarins and related compounds have diverse biological activities, including anti-coagulant and anti-thrombotic properties. Coumarin derivatives have also been shown to be novel lipid lowering agents that possess moderate triglyceride lowering activity[111]. Many coumarin derivatives have the unique ability to scavenge reactive oxygen species such as hydroxyl free radicals, superoxide radicals, or hypochlorous acid to prevent free radical injury [112]. Recently, certain coumarin derivatives have been shown to function as human immunodeficiency virus integrase inhibitors and have been evaluated in treatment of HIV infection. Others have been evaluated as anti-invasive compounds due to their inhibitory activity against some serine proteases and matrix metalloproteases (MMPs) [113]. Recently, it has been shown that 6-nitro-7-hydroxy coumarin acts as a selective anti-proliferative agent by activating p38, stress activated protein kinase (SAPK) and the p21 cyclin dependent kinase inhibitor, in the human renal cell carcinoma cell line, A-498 [113]. More recently, two new naturally occurring coumarins (Figure 1. 27, **19** and **20**) have been isolated and shown to inhibit the polymerisation of tubulin and arrest cells in mitotic phase by inhibiting microtubule formation[114]. These coumarins were found to act synergistically with paclitaxel in inhibiting KB (human epidermoid carcinoma) cell proliferation[108].

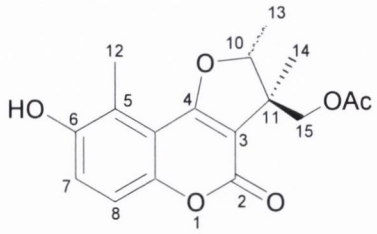

19: 10S11R
20: 10R11R

Figure 1. 27 Two new coumarins, glaumacidines (19) and (20)

Recently, studies have described the growth inhibitory properties of novel coumarin sulfonamides using a panel of cancer cell lines. These coumarin derivatives up-regulated the activity of c-Jun NH_2 terminal kinase 1 (JNK1), which is a member of the stress activated protein kinases (SAPKs) that are involved in apoptotic signaling[115]. Based on the diverse biological activities of coumarins and their derivatives, a series of novel coumarin 3-carboxamides were synthesised and examined in different cancer cell lines (Figure 1. 28, Scheme 1.7). Results show that these coumarin 3-carboxamides selectively inhibit the tumor cells that have higher levels of epidermal growth factor receptor (EGFR or erbB1) and erbB2 (HER2) receptor expression[113].

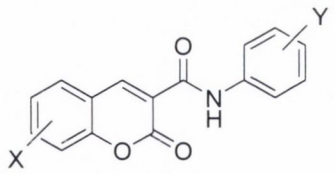

X = H, EtO, Cl, Br
Y = Br, I, NO_2, Cl, NH_2

Figure 1. 28 Coumarin-3(N-aryl)carboxamides investigated for antiproliferation activity

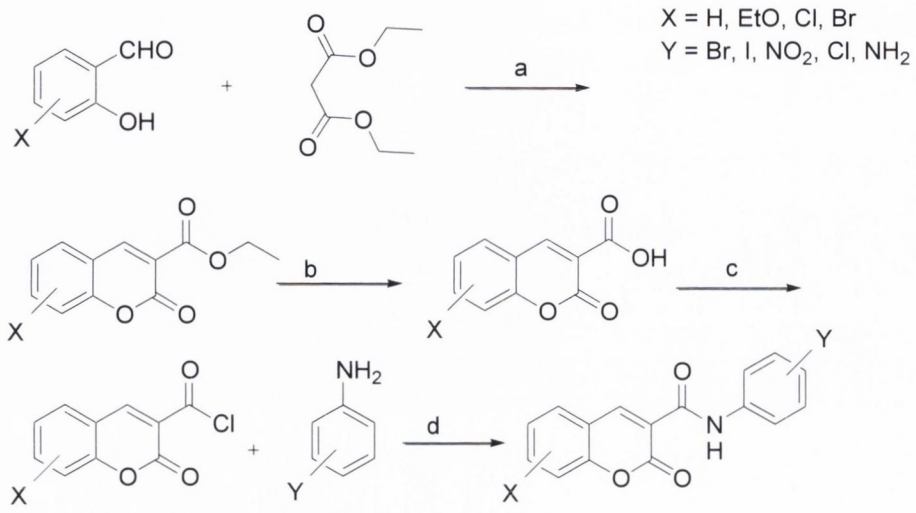

Scheme 1. 7 Reagents and conditions: (a) piperidine/EtOH/HOAc; (b) HCl/H_2O/EtOH; (c) $SOCl_2$; (d) $PhNH_2$/pyridine/dioxane [111]

The coumarin compounds have demonstrated a 4–5-fold increase in cytotoxic activity [113]. These results show that substitutions on the coumarin ring and also on the phenyl group can drastically alter the cytotoxic property of the compounds. Coumarin carboxamides with increased potency can be designed and synthesised by analysing the structure–activity relationship observed. Such molecules may possess much higher ErbB-2 and ERK1 MAPK inhibitory activities, which in turn could result in enhanced anti-tumor activity[113]

1.7.1 Chromene scaffold in tubulin targetting

Studies have reported the discovery, (from a cell- and caspase-based high-throughput screening (HTS) assay), of 4-aryl-4*H*-chromenes as a new series of potent apoptosis inducing agents possessing vascular targeting activity[116]. These compounds were found to be tubulin destabilisers, binding at or close to the binding site of Colchicine. The tubulin targeting agents are shown in Figure 1. 29 together with CA4-P (phosphate derivative of combretastatin CA4) and the phosphate ester of colchicine ZD6126, both currently in clinical trials. The chromenes were also active in drug-resistant cancer cell lines including the paclitaxel-resistant, multi-drug-resistant MES-SA/DX5 tumor cells, and were found to be highly active in several anticancer animal models [117]. The 4-aryl-4*H*-chromenes, therefore, represent a promising series of novel apoptosis inducers

that could be developed into new therapeutic anticancer agents. The structure–activity relationship (SAR) of the 4-aryl ring substituents of these 4-aryl-4*H*-chromenes have also been reported[116]. Starting from a screening hit, 2-amino-3-cyano-7-dimethylamino-4-(3-methoxy-4,5-methylenedioxyphenyl)-4*H*-chromene (Figure 1. 29**, 21**), by maintaining the 2-amino, 3-cyano, and 7-dimethylamino substituent groups of (**21)**,the compound 2-amino-4-(3-bromo-4,5-dimethoxyphenyl)-3-cyano-7-dimethylamino-4*H* chromene (**22**) was identified as a lead compound (Figure 1. 29). As a continuation of these efforts to develop the apoptosis inducing 4-aryl-4*H*-chromenes as potential anticancer therapeutics, a further study of the SAR of 4-aryl-4*H*- chromenes (**23-25**) with modifications at the 7- and 5-, 6-, 8-positions was reported. [116].

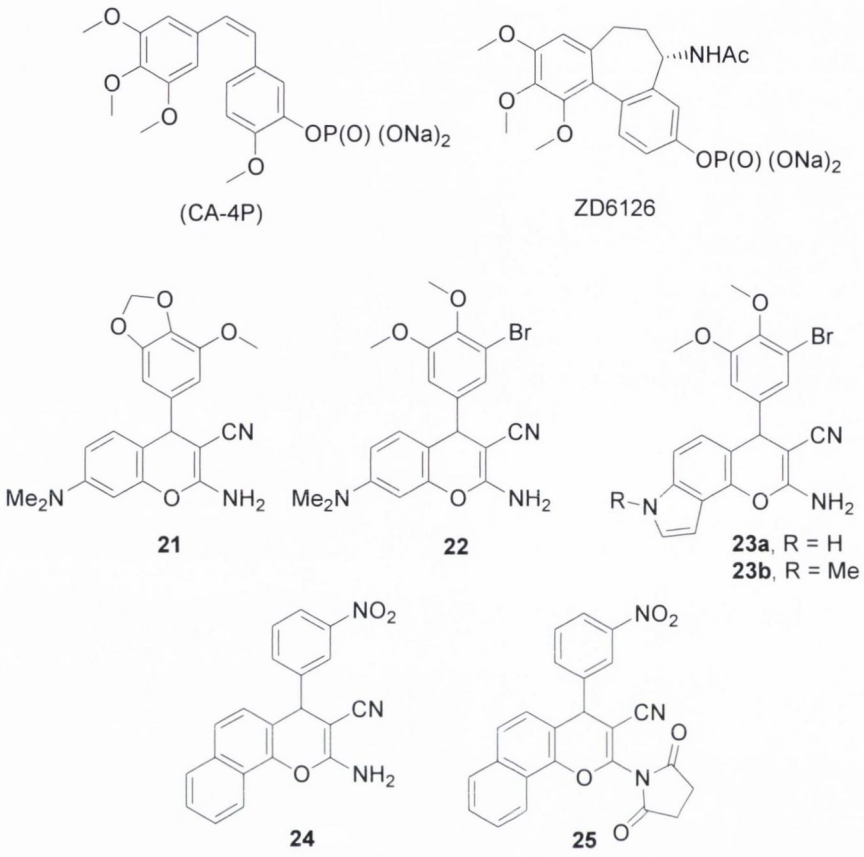

Figure 1. 29 Tubulin targeting agents , including CA-4P, ZD6126 and 4-aryl-4H-chromenes

The issue of multiple drug resistance (MDR) in cancer is a phenomenon in which administration of a single chemotherapeutic agent causes cross-resistance of cancer cells to a variety of therapies even with different mechanisms of action. Therefore anticancer agents that can overcome this resistance to therapy is of much interest. The design and SAR of a series of 6-aryl-4*H*-chromenes such as **26** (see Figure 1. 30) and related derivatives, was based on the hypothesis that the removal of the nitrile group present in the lead compound, would lead to an analogues that selectively target drug-resistant cancer cells with the potential for the treatment of multiple drug-resistant cancers[118]. Further SAR studies led to the development of a more potent analogue, compound **27** with low micromolar cytotoxicity against a wide range of haematological and solid tumour cells[118].

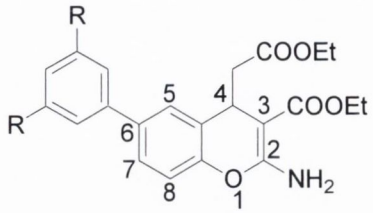

26 R= H
27 R = OMe

Figure 1. 30 Structures of 4H-chromene-3-carboxylate compounds 26 and 27.

1.8 Androgen receptor - Nonsteroidal AR Ligands

Prostate cancer is a major cause of death in men worldwide[119]. Key molecular targets in prostate cancer therapy are the androgen receptor (AR) and its endogenous ligands, such as dihydrotestosterone (DHT). AR antagonists, also referred to as antiandrogens or 'pure' antagonists, are compounds that antagonise the biological responses induced by endogenous or exogenous androgens by competitively inhibiting their binding to AR. Although steroidal antiandrogens such as cyproterone acetate (potent antiandrogen, antiprogestin and antiglucocorticoid) are known, they are no longer used clinically. Nonsteroidal androgen antagonists were first reported in the 1980s. Three anilide derivatives include, flutamide (**28**), nilutamide (**29**), and bicalutamide (**10**), were successfully commercialised for the treatment of prostate cancer (Figure 1. 31) [120].

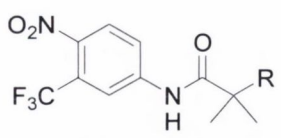

Flutamide (R = H) (**28**)
Hydroxyflutamide (R = OH)

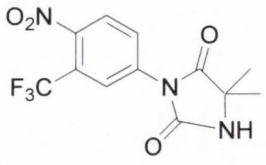

Nilutamide (**29**)

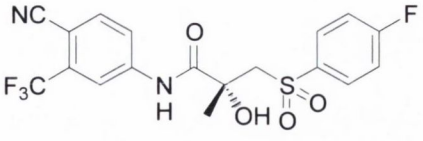

R-Bicalutamide (**130**)

Figure 1. 31 Anilide derivatives as antiandrogens

Currently, clinically available antagonists such as Flutamide (**28**) and Bicalutamide (**30**) are used as small-molecule antiandrogens. Although these therapies possess minimal side effects and relatively good bioavailability, resistance to antiandrogen therapy has been reported, particularly after long term drug treatment for prostate

cancer. One proposed mechanism in which AR resistance occurs is through AR mutation, causing the antiandrogens to function as agonists rather than antagonists[121]. As an example, a focused library of 19 derivatives was then synthesized and evaluated in vitro against LNCaP prostate cancer cell line[122]. A novel compound (Figure 1. 32, **31**) was identified as a promising lead compound for the further development of new therapeutic agents against hormone-refractory prostate cancer. Chromene structure **31** was shown to be active on LNCaP cell line with 10μM, at 87% relative luciferase antagonistic activity[122].

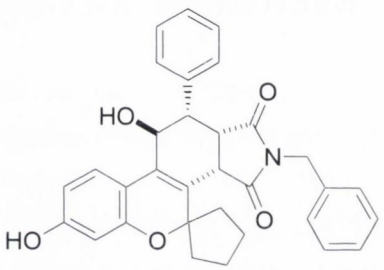

31

Figure 1. 32 SARM 31, incorporating the chromene scaffold

1.8.1 Discovery of nonsteroidal SARMs- Propionanilides

The field of SARMs was stimulated by the early discoveries of Miller and Dalton at the *University of Tennessee Health Science Center* focusing on chiral synthesis [123] and characterisation of electrophilic analogs of bicalutamide as potential irreversible antiandrogens [124]. Dalton *et al.* unexpectedly discovered several nonsteroidal ligands with the ability to fully stimulate *in vitro* AR-dependent transcriptional activation. This unprecedented activity was observed for propionanilidines (**32**) and (**33**)(Figure 1. 33) that differed from hydroxyflutamide and bicalutamide by addition of halogen to the terminal methyl of hydroxyflutamide and changing the linker sulfone of bicalutamide to a thioether (various *para* B-ring substituents), respectively (Figure 1. 33). Ligand Pharmaceuticals, a contemporaneous group, also reported *in vitro* agonist activity immediately thereafter [125, 126]. Structure-activity relationship (SAR) inquiries explored the *para* B-ring positions, thus improving the *in vitro* agonist activity while eliminating reactivity at the *para* B-ring position (e.g. thioacetolutamide **34,** Figure 1. 33)[120]. Hydroxyflutamide analogs and nonprionanilide templates were also explored with less success. These thio-ether linked propionanilides seemed very promising, but suffered from a lack of the expected androgenic or anabolic activity *in*

vivo due to metabolic oxidation of the thioether to the partials agonist/antagonist sulfoxides or sulfones[120]. Traditional medicinal chemistry design methods were used to elimate the site of metabolism and enhance the binding affinity by changing the linker heterogroup from thioether to ether. An *in vivo* pilot study in castrated rats demonstrated that these AR ligands were capable of tissue-selective AR-dependant full agonist activity. The ether linked propionanilides were full anabolic agonists with the ability to fully support the weight of the *androgen*-dependent levator ani (LA) muscle, but weak partial agonists (or antagonists) in androgenic tissues such as ventral prostate (VP) and seminal vesicle (SV) (see Figure 1. 33, (**35**) and (**36**). Molecules such as these were termed SARMs in analogy to selective ER modulators (SERMs) where tissue-specific anabolic (bone maintenance) and estrogenic (breast and /or uterine maintenance) activities have been separated.

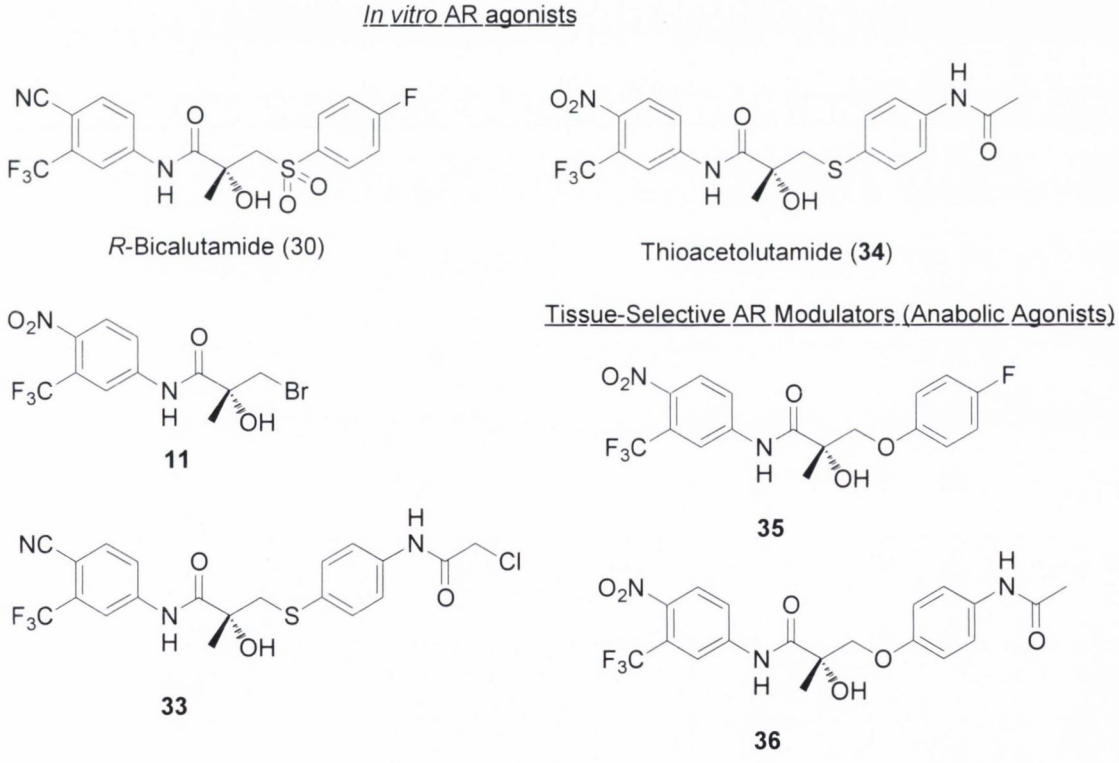

Figure 1. 33 Discovery of propionanilide AR agonists with in vitro and in vivo activity

1.8.2 Quinolinone, Coumarin and Chromeno-Benzazepines; AR Antagonists

Pfizer developed and patented a series of AR ligands which are analogs of the Ligand Pharmaceuticals 6-quinoline templates. These AR ligands are of three distinct templates: (i) 6-substituted quinolone sulfonamides [127], (ii) benzyl urea quinolones [128] and (iii) benzyl coumarins [129] that appear to be weak affinity (micromolar) antagonists which are illustrated as representative examples **37**, **38** and **39** respectively[120], in figure 1.34. Conspicuously absent from these quinolinones is the aniline moiety, which may explain the low affinity and lack of agonist activity. Merck patented a handful of anthracene-based chromeno and quinolinyl benzazepines (e.g. compound **40** in figure 1.34) These compounds are reportedly SARMs that were tested by the same panel of assays as for Merck patents; however, no activity is reported[130].

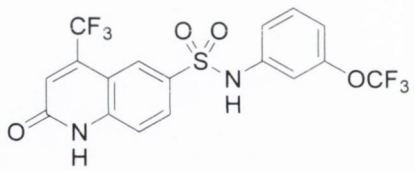

(37) Quinolone sulfonamide

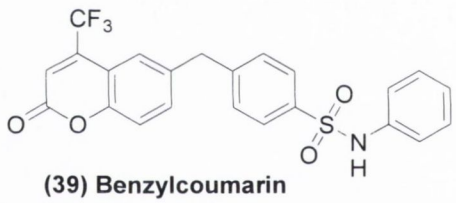

(39) Benzylcoumarin

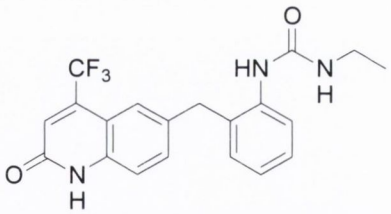

(38) Benzylurea quinolone

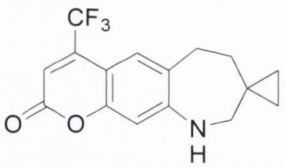

(40) Chromeno-benzazepine

Figure 1. 34 Selection of Coumarin, Quinolinone and Chromene Antagonists 37[127], 38[128], 39[120, 129] and 40[130, 131]

1.9 Targeting the Nuclear Receptor –Cofactor

The development and physiological processes regulated by nuclear receptors are the result of the interplay between the receptors, their small-molecule ligands (hormones), their response elements on the DNA and a large set of interecting proteins, the so-called cofactors [132]. Up to recently, the modulation of the function of nuclear receptors concentrated mainly on ligands with agonistic, antagonistic or partial (ant)agonistic properties that bind in the binding pocket of the ligand-binding domain (LBP), also occupied by the natural ligands. These ligand types have proven very beneficial for the treatment of various diseases and the regulation of hormone functioning, as illustrated by many examples in the previous sections[120]. Some of these ligands have been shown to feature tissue-specific or selective (ant)agonistic properties, which is often of crucial importance for the separation of the beneficial effects of nuclear receptor stimulation or inhibition from unwanted side-effects, regulated by the same receptor[133]. Nethertheless, predictability and control over tissue specificity of these classical ligands is difficult. The physiological effects of some of the nuclear receptor ligands are sometimes altered over a period of time. A typical example of this is the transition of nuclear receptors ligands used for the treatment of specific cancers from an antagonistic profile into and agonistic profile[134]. Interestingly, there are also nuclear receptors for which, up to now, no ligand, neither of natural nor of synthetic origin, has been found. Examples of orphan receptors include nuclear receptors and G-protein coupled receptors. These so-called orphan receptors seem not to be amendable to modulation by classical ligands.[120]

1.9.1 Hydrazides targeting AR

It is evident that issues such as tissue specificity, detrimental side effects, and a loss of the pharmacological effect (acquired drug resistance) over time are major and ongoing concerns with such LBP targeting treatment regimes[135]. The discovery and characterisation of a novel class of selective non-LBP targeted "true" antiandrogens, characterised by full AR antagonism in inhibiting the recruitment of coactivators and lacking intrinsic partial agonistic properties are an active area of pharmaceutical research. As an example, diarylhydrazides have been recently reported as non-LBP targeted "true" antiandrogens [121].

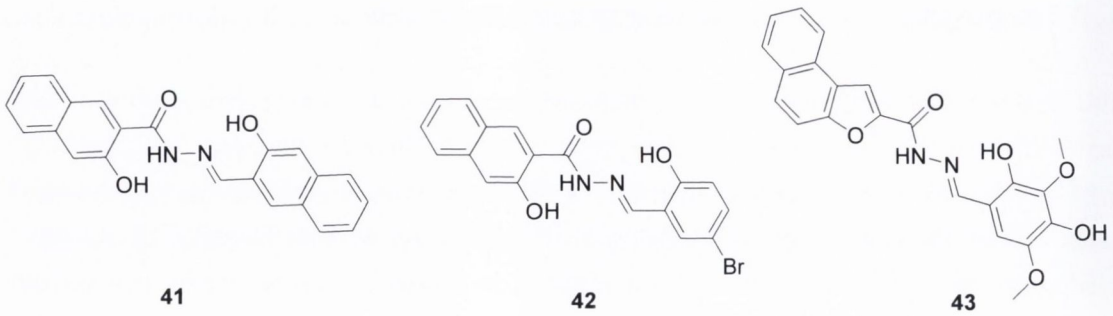

Figure 1. 35 Cofactor AR Antagonists 41, 42 and 43

The selectivity of the diarylhydrazide scaffold for the AR was demonstrated through TR-FRET evaluation in the estrogen and glucocorticoid receptors, where agonist bound receptor recruitment of coactivator was unimpaired at screening concentrations up to 100 μM. The diaryl-substituted hydrazides inhibited coactivator binding in the micromolar range, acting as full AR antagonists in TR-FRET assays with compound **41** (see Figure 1. 35) at 11.1 ± 3.2 μM, compound **42** at 12.4 ± 2.2 μM, and compound **43** at 33.2 ± 5.9 μM [121].

The limitations of the current nuclear receptor ligands generate a continuous quest for new ligands with optimized profiles in both industry and academic research. The requirements of the effects of these ligands on the level of the organism are usually quite clear; the translation of these requirements to the level of the conformation of the protein structure of the ligand is, however, usually not evident. This is due to a major extent to the large number of protein-protein interactions between nuclear receptors and their many cofactors[132, 133]. Binding of the ligand results in a change of the conformation of the LBP and with that it influences the dimerization of the nuclear receptor with other proteins[136].

In chapter 4 of this thesis, a further development and evaluation of a series of hydrazide type compounds which target the interaction of the AR with a cofactor is described. This approach offers an alternative to the classical therapeutic method of targeting the ligand binding domain, used as a measure to prevent drug resistance and long-term toxicity in the treatment of prostate cancer.

1.10 Virtual high throughput screening (*v*HTS)

In the early 1990s, the advent of high-throughput screening (HTS) increased dramatically the capacity for testing compounds. The implementation of advanced computational methods in the pharmaceutical industry, and in clinical research, was beneficial as it gave an increase in the capacity for testing compounds and a reduction in time required for testing the diverse screening of chemical libraries[137]. It became clear that augmenting the capacity for testing alone was not sufficient for delivering high quality leads, and that more data was required in balancing the composition of the screening collections with compounds containing features compatible with the nature of the targets or target classes. Novel strategies were undertaken to design chemical libraries focused on a particular target, including the collection and storing of prior knowledge either from bioactive ligands or crystallographic data in the literature.

In previous research, a number of target scaffold structures were identified as potential ER ligands by virtual high throughput screening. Computational drug design techniques are used frequently in the development of new ER antagonists. Virtual screening is an *in silico* approach complementary to experimental high-throughput screening (HTS). When the structure of the target protein is known, structure-based virtual screening (SBVS) is the method of choice. SBVS involves molecular docking of each ligand into the binding site of the target, producing a predicted binding mode and a measure of quality of the fit of the compound into the binding site. This information is used to rank the compounds in order to select a small subset for biological evaluation[138]. A complementary method to SBVS is the ligand-based virtual screening (LBVS) which uses information provided by known active compounds to identify other compounds with similar properties. This can be accomplished by the implementation of a variety of techniques, one of which is 3D pharmacophore development[139].

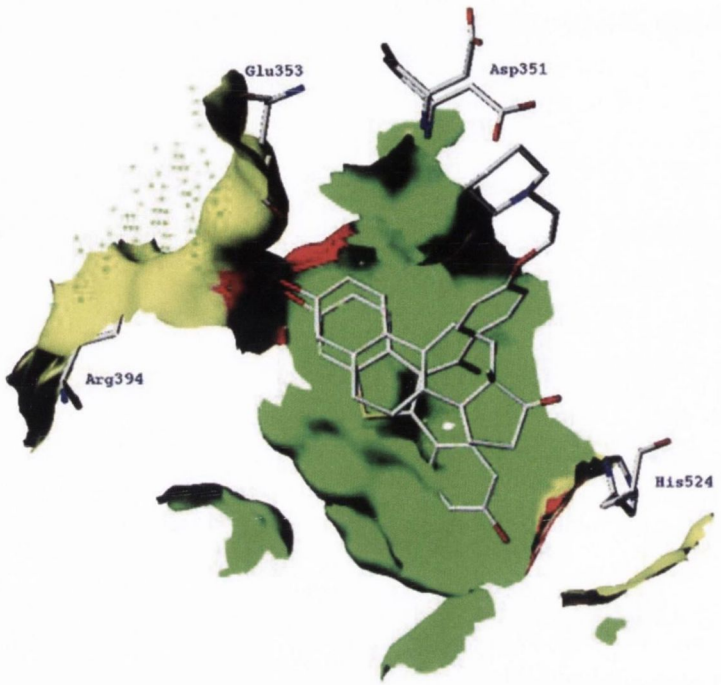

Figure 1. 36 Residue ligand interactions of the agonist Estradiol in ERα and antagonist Raloxifene in ERα [139]

The large quantity of co-crystal data from the estrogen nuclear receptor family, including data obtained which was previously performed within the Meegan research group[139] was collected and utilised. A comprehensive *In silico* screening was performed targeting novel compounds with potential antagonistic activity on the ER, utilising knowledge about its modulation through key antagonistic interactions with protein residues including Glu353, Arg394, His524, and Asp351 (see Figure 1. 36). Several well known scaffolds(**A-F**) were identified from the initial ER antagonistic screening (see figure 1.37), and advantages can be gained here as all scaffolds that adopt the correct shape within the active site can be retained. While these ligands may not currently possess the appropriate H-bonding substituents to be immediate binders with potent activity in the ER LBP, they can be designed to do so using organic synthetic chemistry methods. Thus, TS-VS (Target Selective-Virtual Screening) serves to suggest novel scaffolds for follow-up studies and synthesis[139].

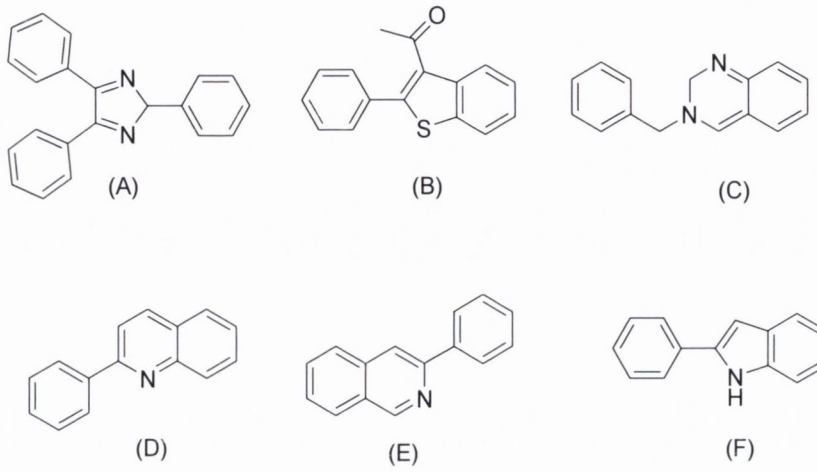

Figure 1. 37 Examples of scaffolds identified through the vHTS protocol

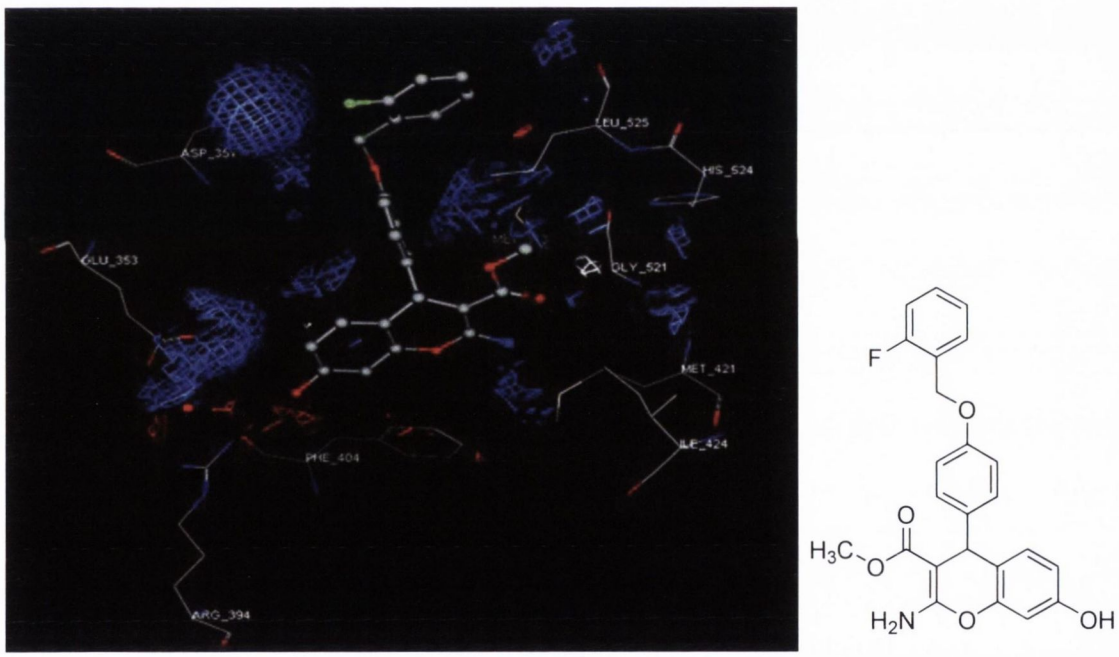

Figure 1. 38 Schematic of target specific virtual screening (TS-VS) filtering procedure with lead chromene compound 47

The four-step scoring and filtering procedure, produced a target specific virtual screening protocol (TS-VS, Figure 1. 38) and minimised false positives resulting from conformational artifacts of the docking process. The protocol was optimised to converge on novel scaffold structures as ligands of estrogen receptor alpha (ERα). [139].

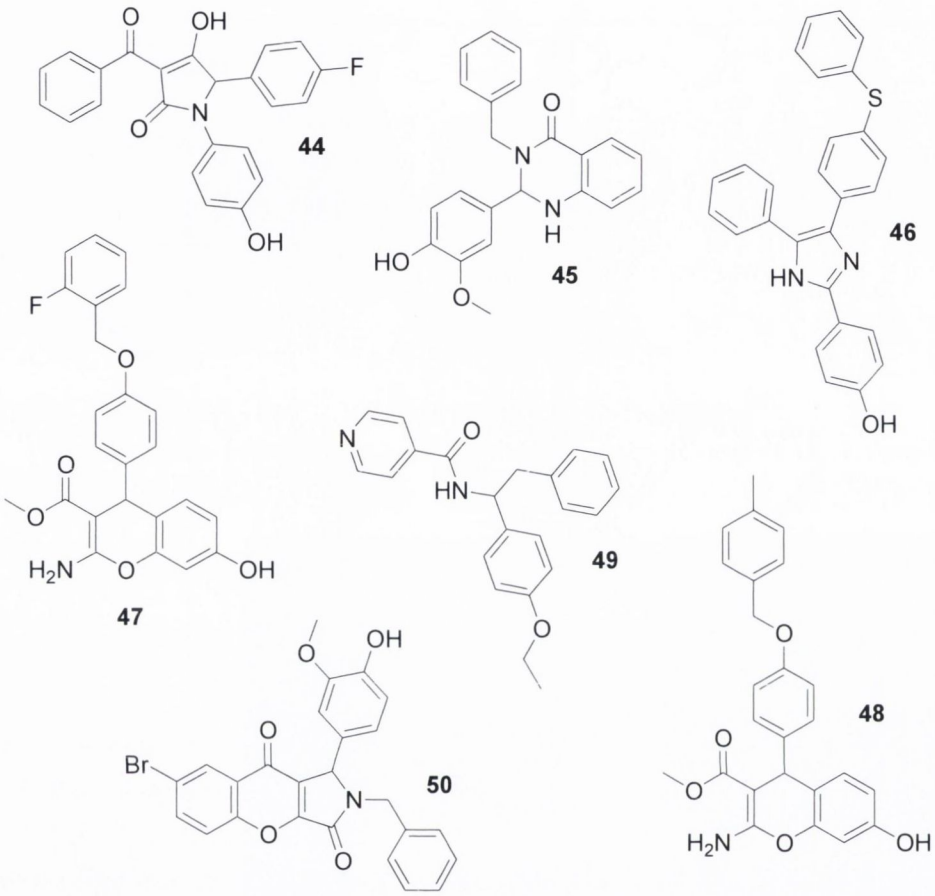

Figure 1. 39 A total of 7 hits were identified by vHTS and chosen for biochemical evaluation [139]

Following visual inspection (compounds selected based on number of interactions with key residues) of the 13 ranked compounds remaining. As a proof of concept, a set of seven compounds from the original database of >200,000 (Figure 1. 39) were selected, purchased, and evaluated for their ability to bind to the ER by fluorescence binding assay using 10 μM as an activity cutoff. Of these seven tested ligands, three demonstrated ERα binding affinities below the 10 μM cutoff, with measured binding affinity IC_{50} values of 1.1 μM (compound **45**, see Figure 1. 39), 53 nM (compound **47**), and 56 nM (compound **48**) for human ERα[139]. The compounds showed selectivity for ERα over ERβ, with compound **48** showing the greatest α/β selectivity(17 fold). These compounds also demonstrated antiproliferative effects in the MCF-7 breast cancer cell line at low micromolar levels.

The research in this thesis is based on these selected chromene derivatives, with attention currently focused on synthesis of novel derivatives of products **47** and **48** (Figure 1. 39). These novel compounds are designed to incorporate the potent chromene scaffold structure and to obtain maximum cellular cytotoxic effects.

1.11 Objectives

The effective targeting of the estrogen receptor is essential in the development of estrogen receptor positive breast cancer therapy. The androgen receptor is also a focus in designing treatments for prostate cancer. Resistance to treatment and rapid invasion of cancer cells are the main causes of cancer mortality.

Despite intense research efforts, the development of new therapeutic treatments for breast and prostate cancers have been demonstrated to have poor outcomes in clinical applications. This is often due to side effects associated with ineffective targeting of the nuclear receptor (ER and AR) and therefore resulting in damage to other tissues and toxic side effects.

The specific objectives of this research are summarised as follows:

1. Synthesis of a library of chromene compounds, based on hit vHTS structure scaffolds identified from *in silico* screening for ER ligands.
2. Synthesis of a comprehensive library of ester derivatives of chromene products.
3. Investigation of related coumarin based compounds.
4. Biochemical antiproliferation assays of a series of chromene products on MCF-7 breast cancer cell line using cell culturing techniques.
5. Structure-activity relationship evaluation study for the series of chromene compounds.
6. Design, synthesis and structure-activity relationship evaluation of a series of naphthylhydrazide androgen receptor targeted compounds.
7. Estrogen receptor (ER) and androgen receptor (AR) receptor binding assays of groups of synthesised chromene based, coumarin based and naphthylhydrazide compounds.

Chapter 2: 4*H*-Chromene ring as a Scaffold for Design of Selective Estrogen Receptor Modulators (SERMs): Synthesis of Tamoxifen analogues

2 Results and Discussion

Introduction

Many different modifications to Tamoxifen have been attempted in an effort to improve its effectiveness as an antiestrogen and to try and reduce the side effects attributed to it, and examples being Raloxifene and Bazedoxifene (see figure 2.1)[103, 140]. Due to the increased risk of endometrial cancer with the use of tamoxifen, a rigid structure in place of the ethylene double bond to prevent E/Z isomerisation is found to be effective [141]. There are many examples of different ring structures being used to form non-isomerisable SERMs(See Chapter 1). Generally SERMs contain a core non-steroidal scaffold with a triaryl arrangement positioned around this structure.

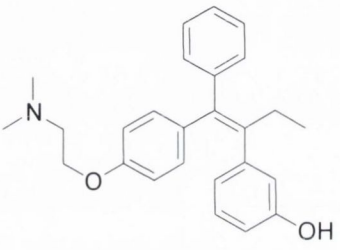

4-Hydroxytamoxifen

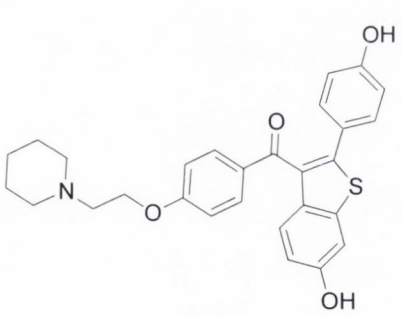

Raloxifene

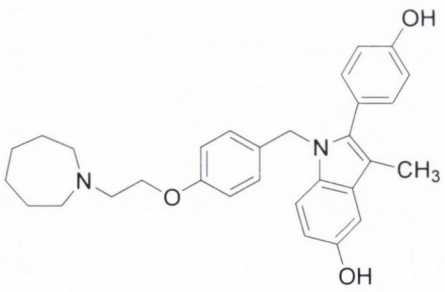

Bazedoxifene

Figure 2. 1 SERMs Tamoxifen, Raloxifeen and Bazedoxifen in clinical use

There is much interest in the design and synthesis of SERMs with alternative scaffolds to drugs such as Tamoxifen. Because of the toxic effects associated with the central double bond in the triphenylethylene derivatives, designing new groups of antiestrogens incorporating the double bond into a cyclic system may increase its chemical and metabolic stability. Many synthetic mechanism for the preparation of tamoxifen have been reported. Production of libraries of related antiestrogens mimicking the structure of the the triphenylethylene scaffold of tamoxifen derivatives have been reported. Scheme 2.1 outlines one example of the synthetic route for preparation of 4-hydroxytamoxifen.

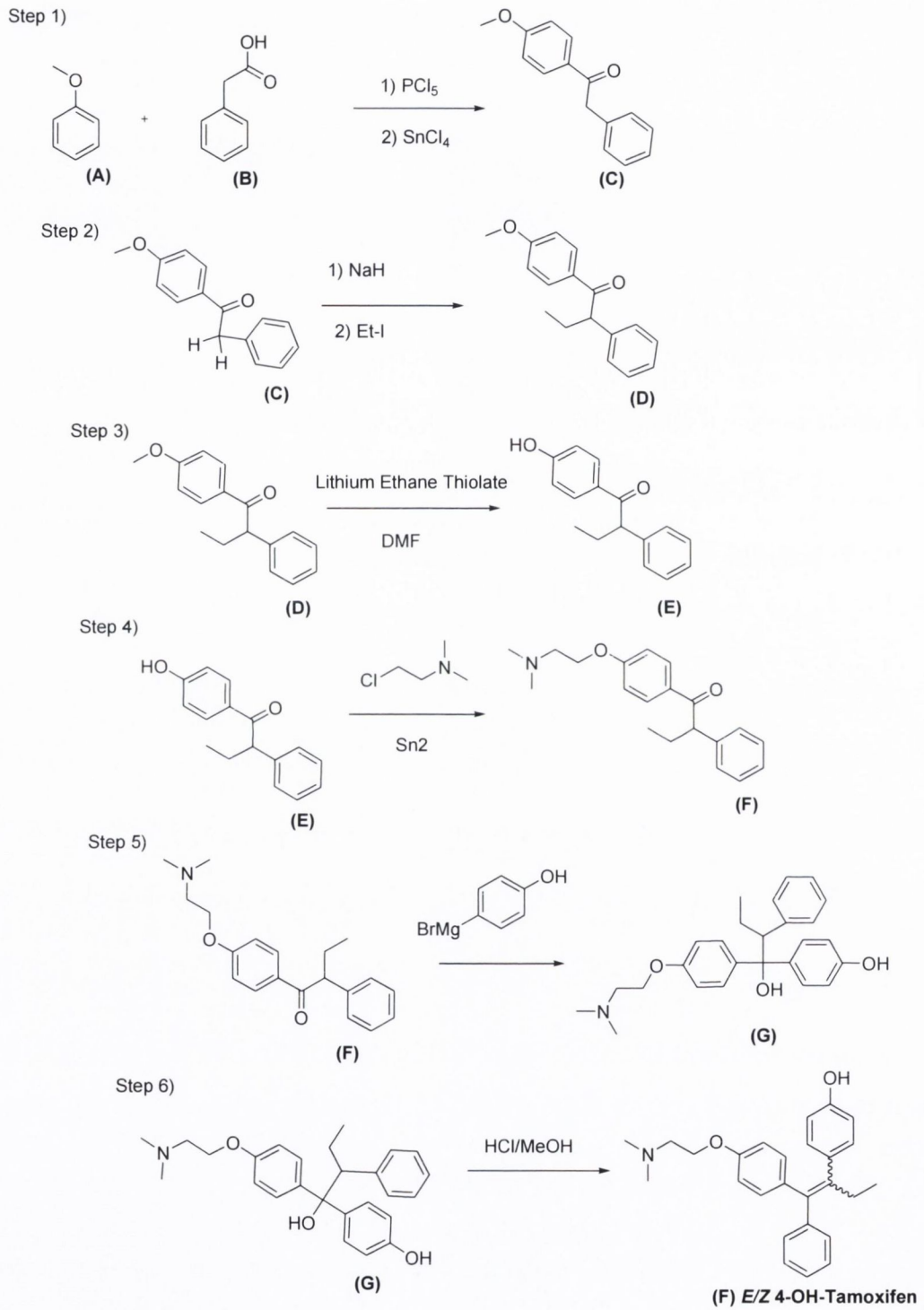

Scheme2. 1 ***Synthesis of 4-Hydroxytamoxifen***

In scheme 2.1, step 1 shows the use of a simple Friedel-Craft acylation involving anisole(A) and phenylacetic acid (B) to afford the ketone C. In step 2, alkylation is

promoted by treating the ketone C with sodium hydride (NaH). This reagent removes the acidic protons (located on the position alpha to the carbonyl group) to produce the enolate ion. The sodium enolate of the ketone on treatment with ethyl iodide resulting in the formation of compound (D). The ethyl iodide is chosen as the alkylating agent as it contains the iodide moiety, which is an excellent leaving group. It can therefore facilitate the substitution reaction with relative ease. In step 3 the phenol is deprotected using lithium ethanthiolate in DMF. This reagent facilitates the demethylation to form the phenol compound (E) in good yield. This is a key step as the phenol group can then be used to build up the characteristic dimethylamino-ethyl group of the tamoxifen molecule. Then in step 4 product (E) is alkylated on the phenolic OH group by treatment with 2-(dimethylamino)ethyl chloride. The above reaction gives product (F) in 70% yield. In step 5, product (F) on treatment with the Grignard reagent 4-OHPhMgBr to form the tertiary alcohol (G). In step 6 the dehydration of compound (F) is initiated by treatment of methanolic hydrogen chloride. This gives the required product, 4-hydroxytamoxifen, as a mixture of *E* and *Z* isomers.

2.0 Benzopyrans

Benzopyran is an polycyclic organic compound that results from the fusion of a benzene ring to a heterocyclic pyran ring. According to IUPAC nomenclature it is called chromene. There are two isomers of benzopyran that vary by the orientation of the fusion of the two rings compared to the oxygen, resulting in 1-benzopyran (chromene) and 2-benzopyran (isochromene); the number denotes where the oxygen atom is located by standard naphthalene-like nomenclature, Figure 2.2.

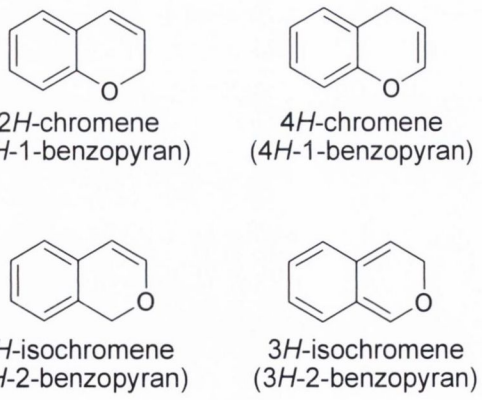

Figure 2. 2 Structural isomers of Benzopyran

Having examined the variety of ring systems that have been used as scaffolds for SERMs, it was decided to design SERMs based on the benzopyran fixed ring scaffold. The benzopyran structure was chosen for this purpose mainly because it is easily manipulated to incorporate the triaryl system necessary for ER activity. Another advantage of the benzopyran scaffold is its chemical stability.

Synthetic methods for chromene synthesis

There are many biologically active therapeutic agents that contain the chromene(benzopyran) ring system and related scaffolds. Some examples are illustrated in Figure 2.3. Khellin is a natural product which has been used since ancient times as a folk remedy, and is known as a bronchodilator and antispasmotic agent[142]. Cromoglycic acid, incorporating the chromone moiety is a synthetic drug providing an effective treatment for the bronchial spasms associated with asthma. The ability of cromoglycic acid as an inhibitor of mediators of anaphylaxis has resulted in many attempts to improve the antiasthmatic properties of cromoglycic acid. In the design of the drug cromitrile, the tetrazole ring is introduced to replace one of the carboxylic acids, and the two aromatic rings are different from one another. The enzyme aldose reductase catalyses the reduction of glucose to sorbitol [142]. Excess sorbitol is believed to contribute to cataracts and to neuropathy by deposition in the lens and nerves of the eye in the latter stages of *diabetes mellitus*. Spirohydantoins such as (*S*)-Sorbinil have been found to inhibit this enzyme, and so are of potential value in delaying or inhibiting this problem. Cannabinoids have been used in medicine as their crude extracts for many centuries. Many potentially useful cannabinoids have been reported to be devoid of abuse potential such as nabilone, a synthetic 9-ketocannabinoid with antiemetic properties[142]. The amino alkylether bucromanone shows promising activity as an antiarrhythmic agent, while the benzopyran provides the scaffold for the leukotriene antagonist ablukast[142]. The ethanolamine functional group characteristic of the β-blocker class can be incorporated in a benzopyran containing scaffold as in nebivolol. The oxypropanolamine functionality has also been incorporated into the antihypertensive agent flavodilol[142].

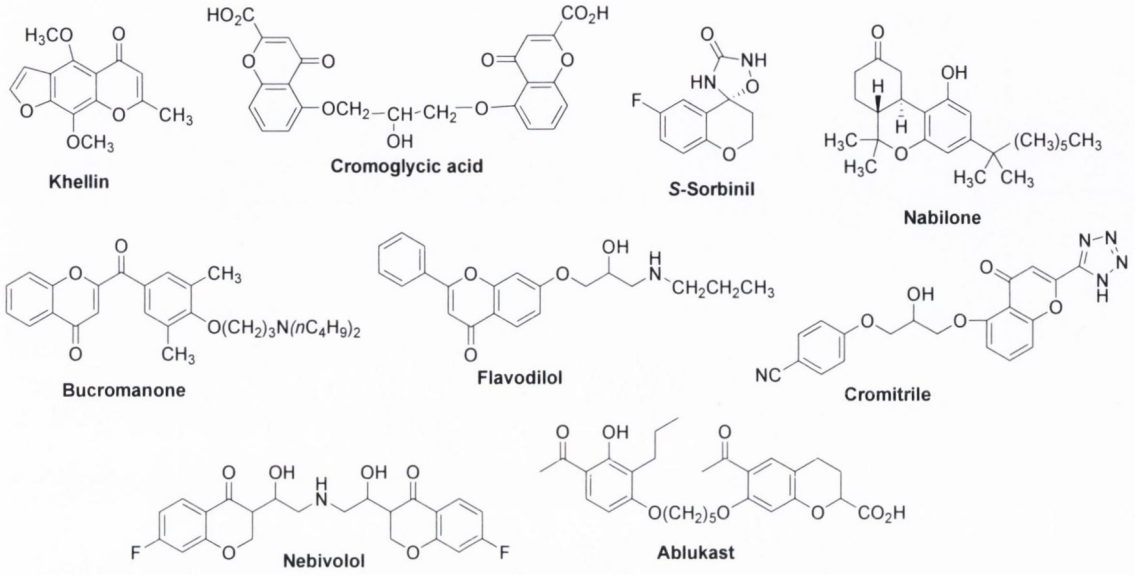

Figure 2. 3 Drugs containing the chromene (benzopyran) ring system and related scaffolds

Because of the importance of chromenes (benzopyrans) in pharmaceuticals their varied synthetic methods have attracted considerable attention. A number of routes to the synthesis of these compounds are displayed in scheme 2.2, 2.3, 2.4, and 2.5.

4*H*-Chromenes can be synthesised by way of an *O*-vinylation followed by a ring-closing metathesis using a Grubbs catalyst, (see Figure 2.2)[143].

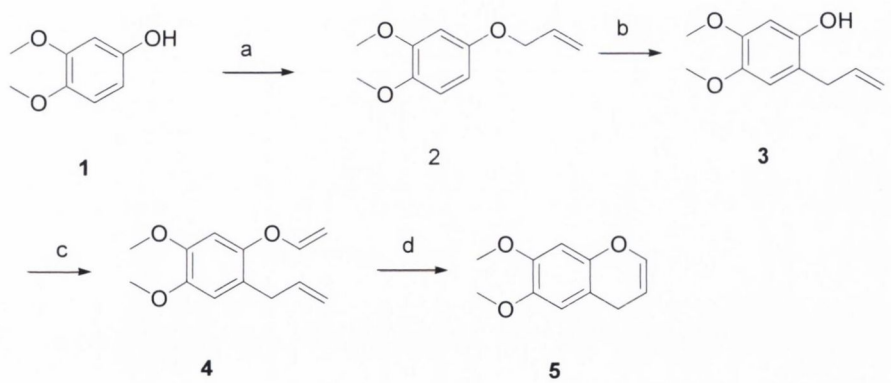

Scheme 2. 2 (a) K_2CO_3, allyl bromide, acetone, 60 °C; (b)Δ, 180-240 °C (c)$Cu(OAc)_2$, $Sn(vinyl)_4$, acetonitrile, O_2, rt; (d) 5% ruthenium Grubb's catalyst,toluene, 60 °C

Substituted phenol **1** was initially converted into the corresponding aryl allyl ether **2.** Subsequent thermal Claisen rearrangement then gave the substituted phenol **3** in acceptable yields over two steps[143]. The compounds were then converted into the respective aryl vinyl ethers **4**, also in excellent yield, using a copper-mediated procedure. The crucial ruthenium-mediated ring-closing metathesis reaction on compounds **4** was highly successful, affording the 4*H*-chromene **5** in a 90% yield[143].

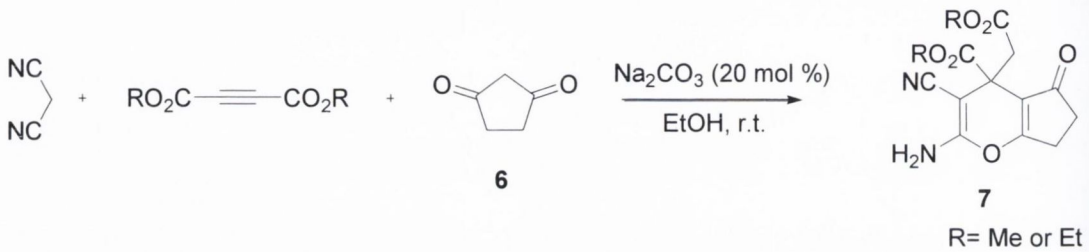

Scheme2. 3 Synthesis of substituted 4H-pyrans 7

Scheme 2.3 displays a synthesis of related 4*H*-pyrans **7**, in which a strategy of Michael addition and cyclization between malononitrile, various dialkyl acetylendicarboxylates, and structurally diverse 1,3-diketones such as **6**, catalyzed by sodium carbonate affords the desired products. The milder conditions use the inexpensive and environmentally safe sodium carbonate catalyst, with high reaction rates, excellent yields, and a simple work-up to make this procedure an efficient process[144]. This chemistry is relevant for the subsequent chemistry required for the target compounds prepared in this chapter of the thesis.

2.01 Development of chromenes as SERMs in breast cancer therapy

EM-652 (Acolbifene), is the active metabolite of EM-800, a novel nonsteroidal antiestrogen compound, scheme 2.4. It is clinically available and used in breast cancer therapy. This chromene compound acts as a pure and highly potent antiestrogen in human breast and uterine cancer cells *in vitro* as well as *in vivo*. EM-800 is the most potent of the known antiestrogens, it is the only nonsteroidal antiestrogen shown to have no estrogenic activity either in human Ishikawa endometrial carcinoma cells[145], EM-800 blocks both the AF-1 and AF-2 activities of the estrogen receptor, thus potentially decreasing the resistance to hormonal therapy[145].

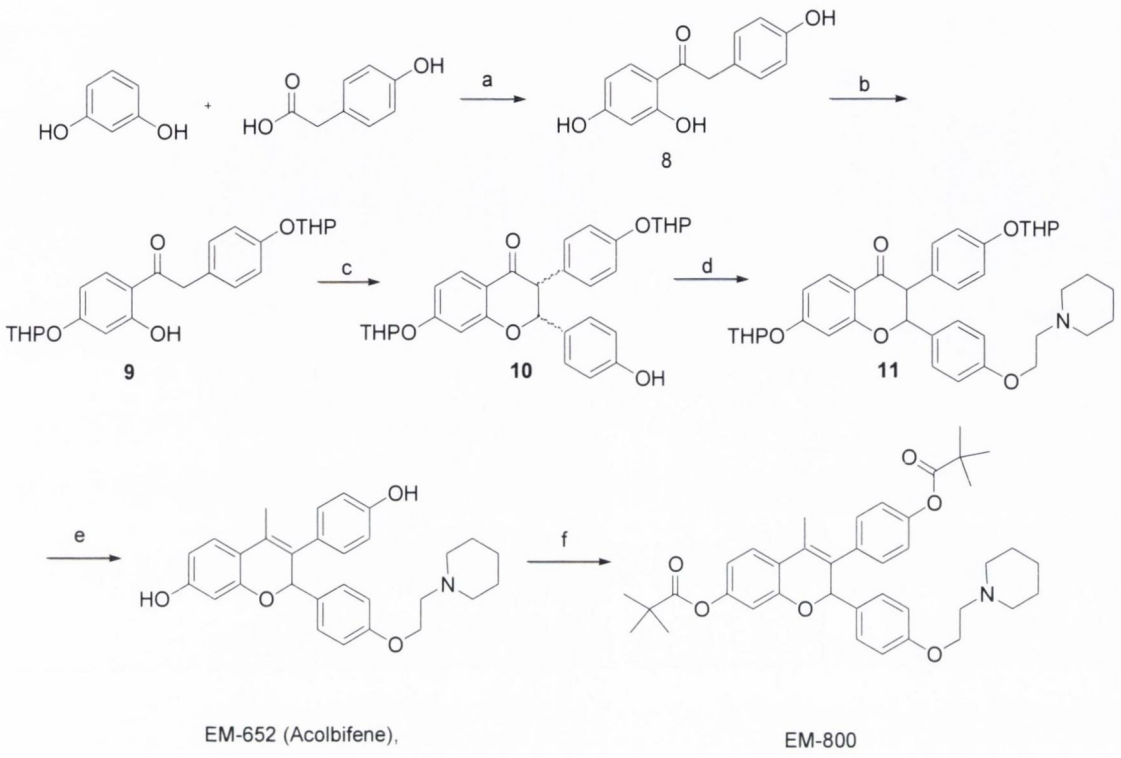

Scheme2. 4 Synthesis of EM-652 and EM-800, (a) BF_3•Et_2O, toluene; (b) DHP, TsOH, 0 °C; (c) 4-hydroxybenzaldehyde, piperidine, benzene; (d) 1-(2-chloroethyl)dialkylamine hydrochloride, Cs_2CO_3, acetone, H_2O, reflux, 19 h; (e)(i) MeLi, THF, -78 °C; (ii) CH_3CO_2H, aq, 90 °C (f) $(CH_3)_3CCOCl$, Et_3N, CH_2Cl_2.

The synthesis of 2*H*-1-benzopyrans and is shown in scheme 2.4. In the first step a Friedel-Crafts reaction uses $BF_3 \cdot Et_2O$ as catalyst in toluene at 100 °C. Resorcinol is acylated with 4-hydroxyphenylacetic acid to yield trihydroxydeoxybenzoin (**8**) in an 81% yield. In step two the trihydroxydeoxybenzoin **8** is then protected with DHP, in the presence of TsOH as a catalyst, to give the bis-THP ether **9** in 69% yield. The third step is a Knoevenagel condensation reaction of *bis*-THP ether **9** with 4-hydroxybenzaldehyde, in the presence of piperidine in refluxing benzene which gives quantitatively the chromanone **10**. The crude intermediate **10** is then alkylated with 1-(2 chloroethyl)dialkylamine hydrochloride in the presence of Cs_2CO_3 in a mixture of refluxing acetone and water, to yield the chromanone **11** in 40–90% yields[146]. The chromanone **11** is then alkylated with methyllithium at -78 °C to room temperature, to give tertiary alcohol intermediates. The crude alcohols are then dehydrated and deprotected in 90% aqueous acetic acid at 90 °C to yield 2*H*-1-benzopyran **EM 652** in

80% yields. The obtained 2*H*-1-benzopyran **EM-652** is then derivatized to improve bioavailability to the corresponding dipivaloate **EM-800** under standard conditions in 50–80% yields[146].

By reviewing some synthetic methods for the synthesis of chromenes, benzopyrans and pyrans reported in the literature and also considering the heterocyclic SERMs which are clinically available, the 4*H*-chromene scaffold was chosen to undertake and produce structurally varied libraries of compounds. It was decided to implement the Knoevenagel condensation reaction method (see scheme 2.5) for production of the compounds. The chromenes investigated in this study were divided into 14 structural varied series. The general structural scaffolds **A** and **B** chosen for synthesis are illustrated in Figure 2.4 and listed below.

Series 1: 4-Aryl substituted 4*H*-chromenes with varied aryl and benzyloxy substitutions.

Series 2: 4*H* Chromenes synthesised using a 2 step method.

Series 3: Production of the benzopyran adduct.

Series 4: Phenyl-4*H*-chromenes with substituted cyanoacetate esters substituents.

Series 5: 4-Hydroxyphenyl-4*H*-chromenes with substitutions on the ester side chain.

Series 6: 4-Benzyloxyphenyl chromenes with variation in the structure on the C-3 ester side chain.

Series 7: 3,4,5-Trimethoxyphenyl chromenes with variation on the R_2 ester side chain.

Series 8: 2,7-Diaminochromene compounds.

Series 9: Benzyloxy-4-phenyl chromenes with N,N-dimethylamino substituent group at C-7.

Series 10: Chromene compounds synthesised with 4-methoxyphenyl group on R_1 and substituted ester chemistry on the chromene OH group C-7,

Series 11: Series of novel *bis* 4*H*-chromene compounds synthesised from the phenolic chromenes using bis acid chlorides.

Series 12: Pyranocoumarin precursors: benzylidene malononitrile intermediates.

Series 13: Pyranocoumarin product synthesis.

Series 14: Pyranocoumarin with substituted antagonistic type basic ether chains.

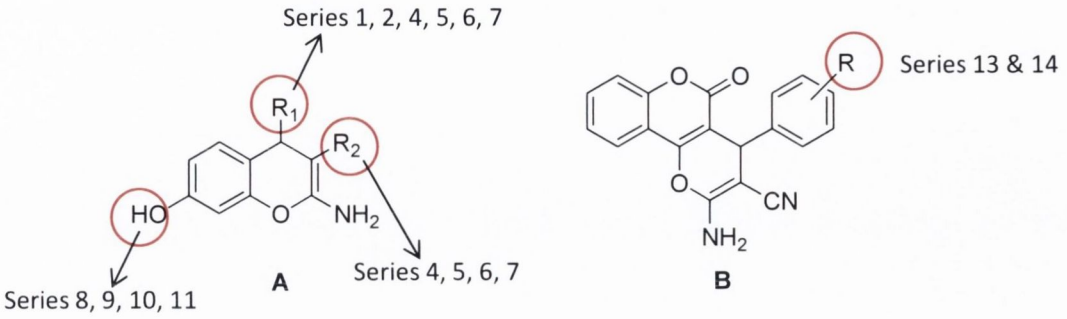

Figure 2. 4 Chromene scaffold (A) indicating position of R group substitutions. R_1, R_2, and Pyranocoumarin scaffold (B) displaying position of R group substitution.

<u>Series 1</u>: 4-Aryl substituted 4*H*-chromenes with varied aryl and benzyloxy substitutions.

An initial series of chromene compounds was synthesised by reaction of diverse substituted benzaldehydes, resorcinol and ethyl cyanoacetate in the presence of the base piperidine (scheme 2.5). Yields were in the range 40-90%. A comprehensive library of compounds with variation of substituents on C-4 aryl ring was prepared, with 28 compounds produced in this series. The novel compounds were characterised by ^{1}H, ^{13}C NMR and IR spectroscopy and High Resolution Mass Spectrometry (HRMS). The molecular modelling study of the products has been carried out to determine the three-dimensional topography and minimised energy structural characteristics of the chromene compounds (see chapter 3).

In this section, the synthesis of a series of chromenes (**BE1 – BE28**) is presented by reaction of benzaldehyde, ethyl cyanoacetate and resorcinol is discussed.

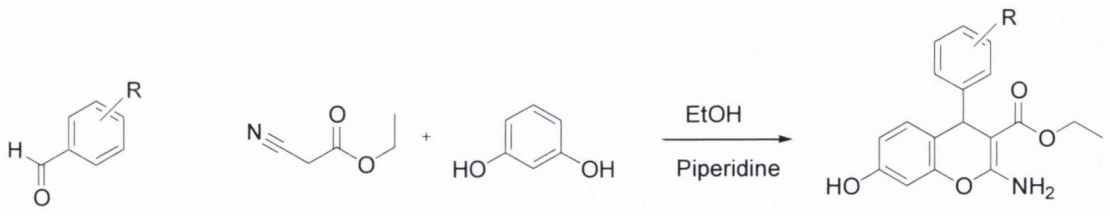

Scheme2. 5 General one pot synthetic reaction for 4H-chromenes

2.02 Knoevenagel condensation as a synthetic route to novel Chromene type SERMs

Scheme 2.6 shows the general mechanism proposed for the synthesis of the 4*H*-chromenes in this project. It is proposed that the reaction occurs in two steps, the first being the formation of the alkyl cyano intermediate before a cyclisation of the benzyl aldehyde group to give the product. This is a Knoevenagel condensation and can be performed as a one pot synthesis[116].

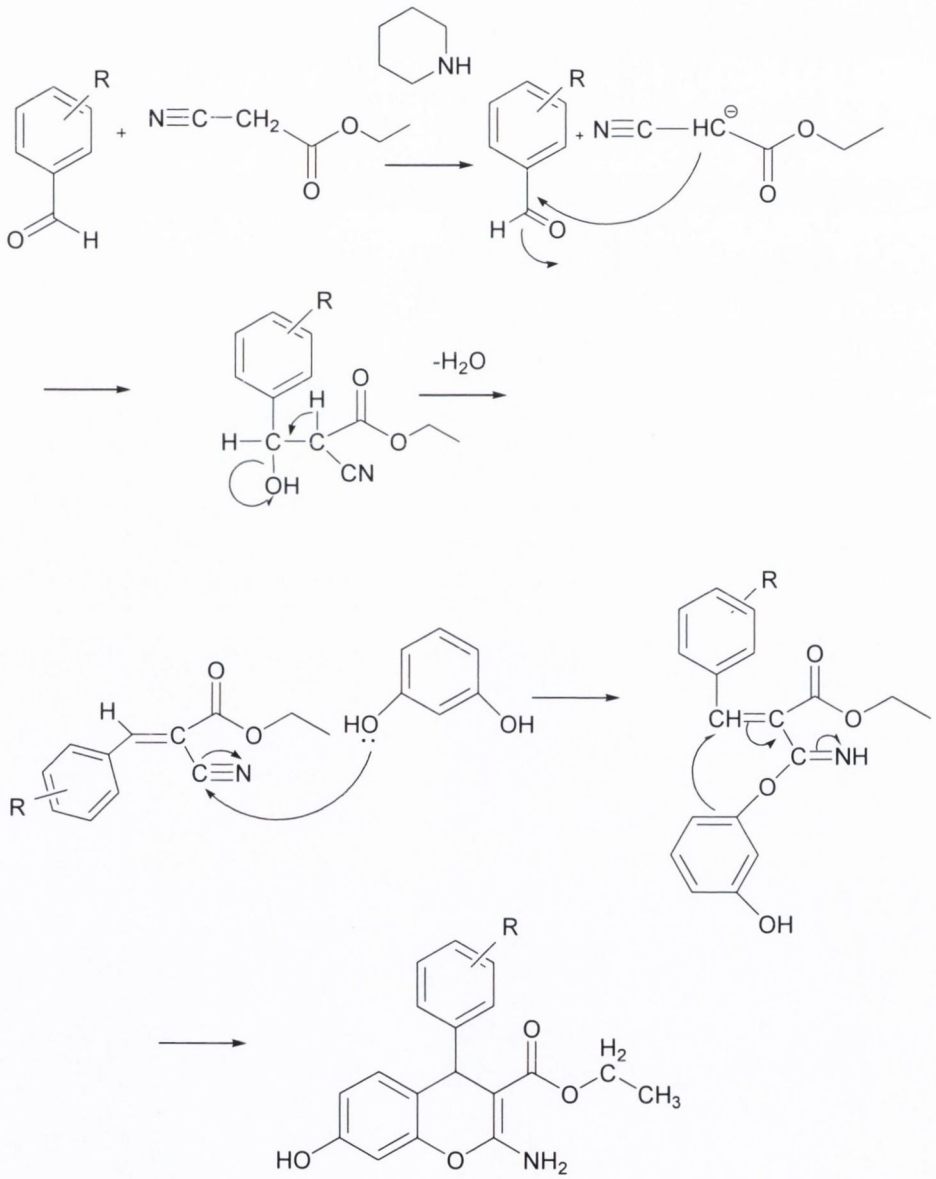

Scheme2. 6 Knoevenagel condensation reaction for synthesis of the chromene products

2.1 Section 1,4-Aryl-4*H*-chromenes

The highly efficient one pot synthesis Knoevenagel condensation reaction[116] was used as product was afforded in good yield, usually by recrystallisation from EtOH. A series of chromene compounds were synthesised by reaction of different benzaldehydes, resorcinol and ethyl cyanoacetate in base piperidine (scheme 2.6). The common core structure of these compounds is a 4*H*-chromene. Yields were in the range 40-90%. A comprehensive library of compounds with variation of substituents on C-4 aryl ring was thus obtained.

2.1.1 Results series 1: Synthesis of the library of chromene compounds

Synthesis of chromenes **BE1 – BE28,** illustrated in table 2.1 and table 2.2 was achieved using the general reaction scheme (Scheme 2.5). The products were obtained as racemic mixtures and the yields are listed below.

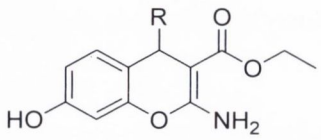

No.	R Group	% Yield	CLogP*	No.	R Group	% Yield	CLogP*
BE1	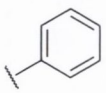	*45*	4.52	**BE7**	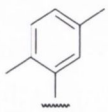	*32*	5.47
BE2	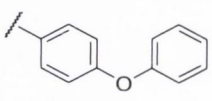	*43*	6.62	**BE8**	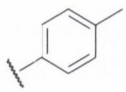	*29*	5.02
BE3	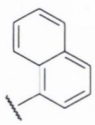	*31*	5.69	**BE9**	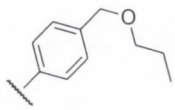	*44*	5.35
BE4	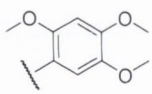	*39*	3.77	**BE10**	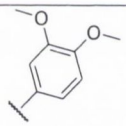	*2*	4.18
BE5	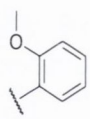	*26*	4.04	**BE11**	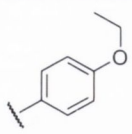	*22*	4.97
BE6	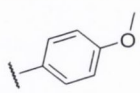	*62*	4.44	**BE12**	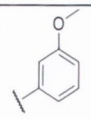	*80*	4.44

Table 2. 1 Library of chromene compounds produced with variation at C-4 (Type I)

*CLogP calculated using Chemdraw Ultra version.

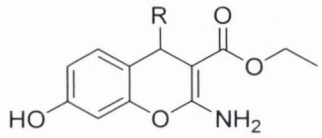

No.	R Group	% Yield	CLogP*	No.	R Group	% Yield	CLogP*
BE13	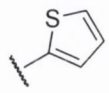	*31*	4.16	**BE21**	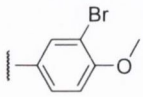	*30*	5.21
BE14	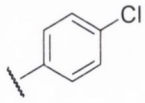	*45*	5.23	**BE22**	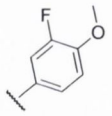	*42*	4.52
BE15	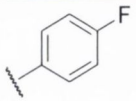	*33*	4.66	**BE23**	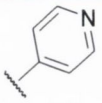	*28*	3.02
BE16	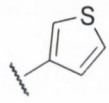	*27*	4.16	**BE24**	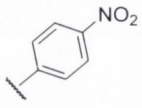	*7*	4.26
BE17	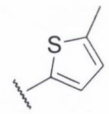	*10*	4.66	**BE25**	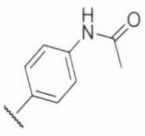	*49*	3.54
BE18	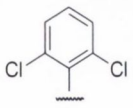	*51*	5.94	**BE26**	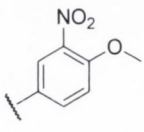	*98*	4.20
BE19	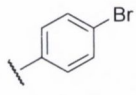	*42*	5.38	**BE27**	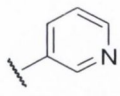	*53*	3.02
BE20	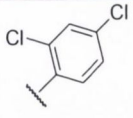	*88*	5.94	**BE28**	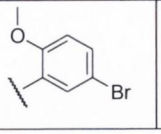	*55*	5.04

Table 2. 2 Library of chromene compounds produced with variation on C-4 aryl ring substituents (Type II)

*CLogP calculated using Chemdraw Ultra version.

For table 2.1 (Type I) a library of 12 different chromene compounds **(BE1-BE12)** was produced with variation of substituents on C-4 aryl ring obtained using various methoxy, dimethoxy, trimethoxy, phenoxy, methyl, dimethyl and naphthyl groups. These substituent groups were of interest for synthesis for Type I in observing if final compounds would display an agonistic or antagonistic feature in response to the estrogen receptor in a biochemical assay. Yields ranged from 2% - 80%.

The synthesis of compounds **(BE13-BE28),** table 2.2 (Type II) was implemented using the same one pot synthesis condensation reaction, however synthesis was focused on inclusion of various halogen and nitro substituent groups. The library of 16 different halogenated 4*H*-chromene compounds was produced with variation of substituents on C-4 aryl ring using groups such as chloro, fluoro, bromo, nitro, together with thiophene and pyridine heterocycles . These Type II halogenated and heterocycle containing chromene compounds were closely examined for activity in the LBP as possible ER agonistists. CLogP values were all within oral bioavailablity standards(The optimum cLogP value for orally active drugs is <5) and scored better in type II, compared to Type I. Isolated yields ranged from 7% - 98%. All were crystalline products.

The products were purified by flash column chromatography over silica gel with eluent solvents CH_2Cl_2 – MeOH in varied proportions depending on polarity of the products. Crystallisation and recrystallisation from EtOH was also used to purify the library of chromene compounds. Purity was checked by thin layer chromatography (TLC) and HPLC(see experimental details in Chapter 5). TLC Rf values were determined between 0.3 - 0.5. Pure crystalline product was then characterised by ^{1}H, ^{13}C, and DEPT NMR spectroscopy. High Resolution Mass Spectrometry analysis (HRMS) was also carried out to confirm the identity of the purified novel compounds.

2.1.2 Spectroscopic Identification

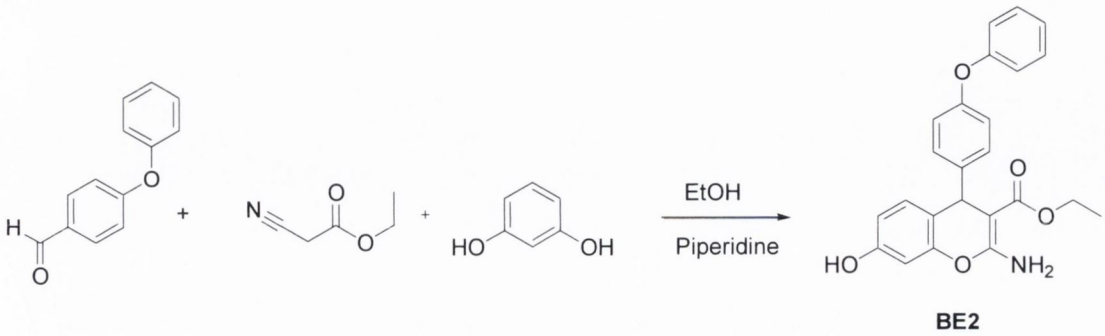

Scheme 2. 7 Reaction scheme for synthesis of 4H-chromene compound BE2

As an example of the analytical characterisation, compound **BE2** will be discussed. The benzyloxy chromene was obtained using reaction scheme 2.7. Identification of the chromene compound was achieved using Nuclear Magnetic Resonance (NMR) spectroscopy, Infrared (IR) spectroscopy, and Mass spectrometry. The following Figures 2.5 and 2.6 illustrate the ^{1}H and ^{13}C NMR spectra for compound **BE2**. Discussion of the ^{1}H and ^{13}C NMR spectra is used as an example of how each compound was identified in this series.

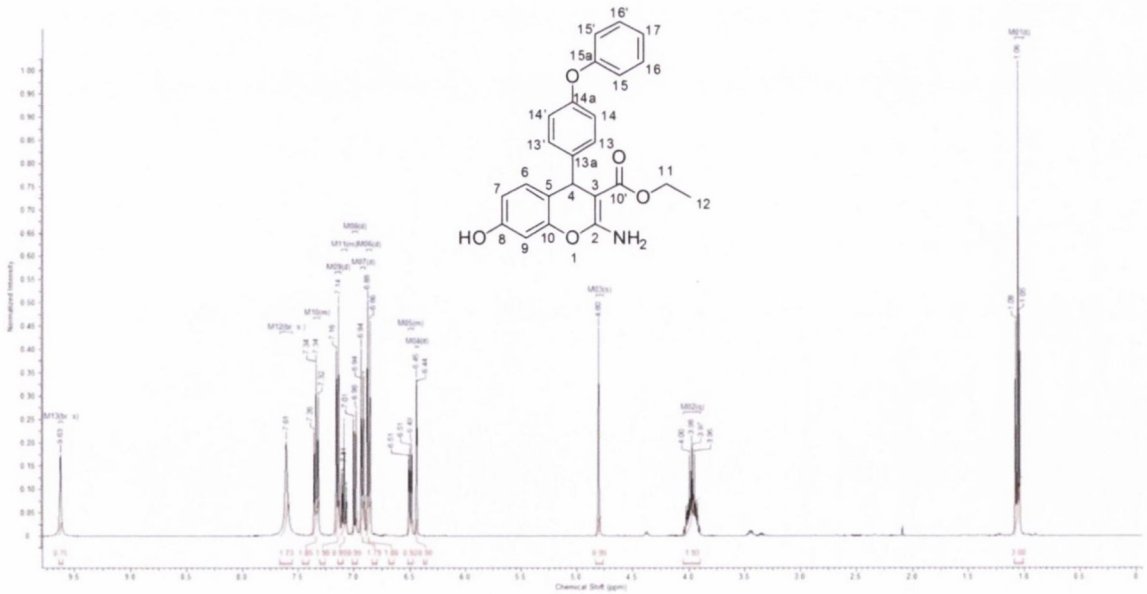

Figure 2. 5 ^{1}H NMR spectrum for benzopyran BE2

For the ^{1}H NMR spectrum of compound **BE2** in figure 2.5, the CH_3 at C12 on the ethyl side chain appeared at δ ppm 1.06 as a triplet integrated for 3 protons, J=7.03 Hz. This signal was usually the reference used for identification of the compound series. The C11 CH_2 group signal is observed at δ 3.98 and this consistently appeared as a quartet absorbance, with a J=value of 7.02 Hz. At δ 4.80 a singlet peak for the CH proton of C4 at the chiral centre is observed, integrated for 1H. At 6.44 a doublet is observed, J=7.42 Hz and is integrated for 1H, indicating the Ar-H at C9. At δ 6.51 a multiplet is observed integrated for 1H, this indicates the Ar-H proton at C7. At δ 6.86 a doublet absorbance is observed, integrating for 2H, J=8.54 Hz, for the Ar-H proton at C14 and C14'. At δ 6.94 there is a doublet, 2H, J=8.03 Hz, indicating the Ar-H protons at C15 and C15' and at δ 7.01 a doublet is assigned to C6 1H, J=8.54 Hz, Ar-H . A multiplet absorbance is observed between δ 7.07 to 7.11 integrated for 1H, indicating the Ar-H proton at C17. At δ 7.14 a doublet is seen, 2H, J=7.04 Hz, indicating the Ar-H protons at C13 and C13'. From δ 7.32 to 7.36 there is a multiplet, 2H, for the Ar-H proton at C16 and C16'. At δ 7.61 a broad singlet peak is characteristic of an amine absorbance, 2H, NH_2, and at δ 9.63 another broad singlet,integrating for 1H, and assigned to the OH.

The alcohol and amino group protons were usually identified as broad singlet signals. Solvents used for sample preparation of samples for ^{1}H and ^{13}C NMR spectroscopy were $CDCl_3$, MeOH-d_6, or $(CH_3)_2SO$-d_6.

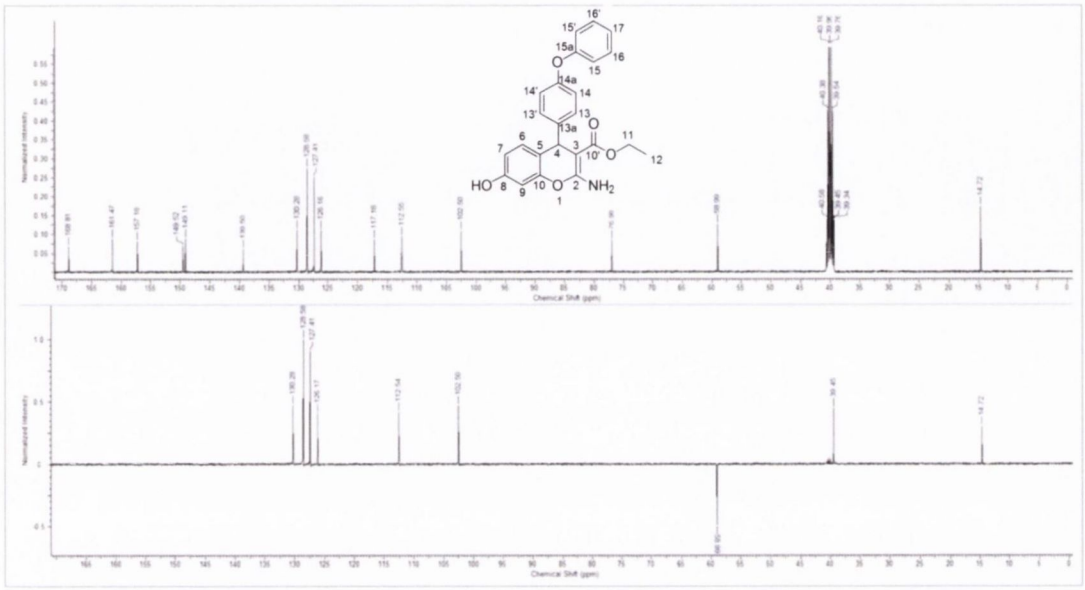

Figure 2. 6 ^{13}C NMR (upper) and DEPT 135 (lower) spectra for benzopyran BE2

In ^{13}C and DEPT-135 carbon NMR spectra (Figure 2. 6) of compound **BE2**, the ethyl ester C12 CH_3 was observed at 14.72 ppm. The chiral C4 CH signal can just be seen at 39.34 ppm in the ^{13}C spectrum, in this case it is nearly hidden, overlapped by the large residual DMSO solvent peak always occurring at 40 ppm. However it is confirmed to be present by viewing the DEPT-135 spectrum, and the absorbance is at 39 ppm. The C11 CH_2 peak can be identified in the ^{13}C spectrum at 58.99 ppm as a positive peak, and in the carbon DEPT-135 spectrum at 58.99 ppm as a negative peak. At 76.98 ppm the carbon C3 attached to the side chain is identified in the ^{13}C spectrum. The aryl ring-hydrogens are seen in the region 102 to 130 ppm and totalling 12. There is one carbon observed at 117.18 ppm and the rest occur in the upper range values from 149 ppm to 168 ppm. CH at C9 is identified at 102.50 ppm and the signal at 112.55 ppm is assigned for the CH at C7. The following aromatic signals were also assigned: the signal at 117.18 ppm indicating the quaternary C at C5 position, the CHs at C15 and C15' were assigned at 126.16 ppm, at 127.41 ppm the CH at C17, at 128.58 ppm the CHs at C13 and C13' and at 130.28 ppm the CH at C6. The following quaternary signals were assigned: at 139.50 ppm the C at position C13a, at 149.11 ppm the C-O at C14a, at 149.52 ppm the C-OH at C8, at 157.18 ppm the C-O at C15a, at 161.47

ppm the O-C-N at C2, at 168.81 ppm the C=O at C10'. These values were typical of this library of chromene compounds.

The IR spectrum absorbances for compound **BE2** were identified as follows; 3480.76 cm^{-1},(OH), 3414.57 and 3387.63 cm^{-1}(NH_2), 1676.55 cm^{-1},(C=O) and 1649.70 and 1631.85 cm^{-1}, (C=C).

The HRMS (EI) for compound **BE2** $C_{24}H_{21}NO_5$ [M^+ + Na] requires (m/e) 426.1317; the value found was 426.1326, (2.0 ppm). The analysis confirmed the structural identification of the novel ethyl 2-amino-7-hydroxy-4-(4-phenoxyphenyl)-4*H*-chromene carboxylate compound, **BE2.**

2.1.3 XRD Crystallography study of structure BE11

The single crystal X-Ray tructure of compound **BE11** was determined and is displayed in Figure 2.7. The ORTEP representation is shown in Figure 2.8 (thermal ellipsoids at 50% probability). The relevant crystal structure data is displayed in Table 2.3.

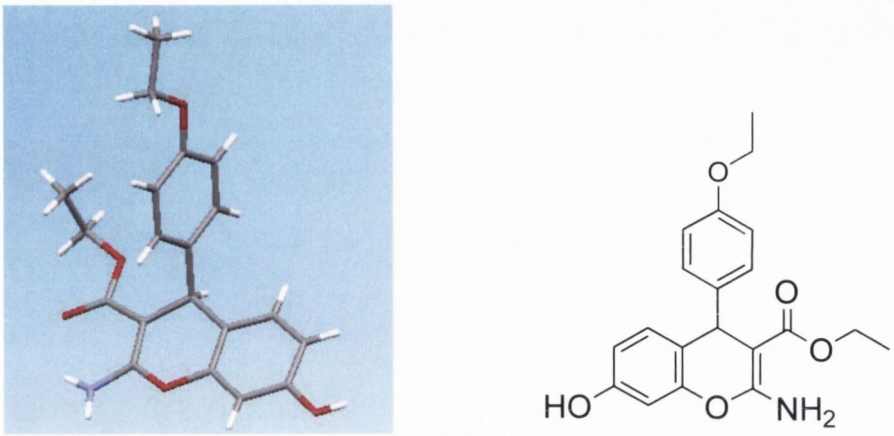

Figure 2. 7 Crystal structure of BE11

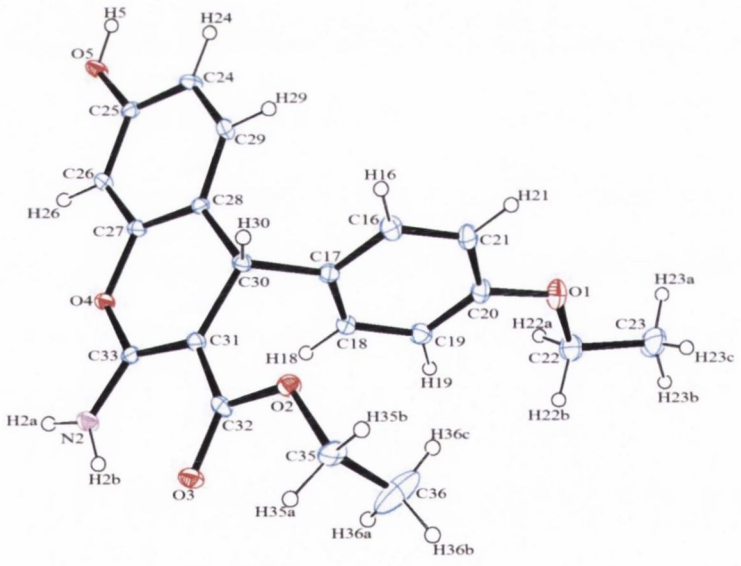

Figure 2. 8 ORTEP representation of the X-Ray crystal structure of BE11, ellipsoids at 50% probability

Identification code		shelxl
Empirical formula	C80 H0 N4 O20	
Formula weight	1336.84	
Temperature	158(2) K	
Wavelength	0.71075 Å	
Crystal system	monoclinic	
Space group	P2/c	
Unit cell dimensions	a = 16.982(7) Å	
	b = 5.340(2) Å	α= 90°.
	c = 20.683(9) Å	β= 91.189(6)°.
Volume	1875.2(13) $Å^3$	γ = 90°.
Z	1	
Density (calculated)	1.184 Mg/m^3	
Absorption coefficient	0.088 mm-1	
F(000)	668	
Crystal size	0.20 x 0.20 x 0.20 mm3	
Theta range for data collection	1.20 to 25.00°.	
Index ranges	-20<=h<=20, -5<=k<=6, -23<=l<=24	
Reflections collected	13694	
Independent reflections	3251 [R(int) = 0.0641]	
Completeness to theta = 25.00°	98.10%	
Refinement method	Full-matrix least-squares on F^2	
Data / restraints / parameters	3251 / 0 / 238	
Goodness-of-fit on F^2	1.353	
Final R indices [I>2sigma(I)]	R1 = 0.0885, wR2 = 0.2513	
R indices (all data)	R1 = 0.1237, wR2 = 0.3027	
Largest diff. peak and hole	0.562 and -0.663 $e.Å^{-3}$	

Table 2. 3 Crystal data and structure refinement for BE11.

2.2: Series 2; Synthesis of 2-amino-7-hydroxy-4*H*-chromene carboxylates using a two step method

A two step method for synthesis of some of the chromene products was proposed when product was not achieved using the one pot method. It was possible to produce a selection of chromenes through a two step synthesis, stopping after the first step to purify the afforded acrylate compounds **BE29** and **BE31** with slow recrystallisation, then following step two for reaction with resorcinol to obtain the final 4*H*-chromene products **BE30** and **BE32**.

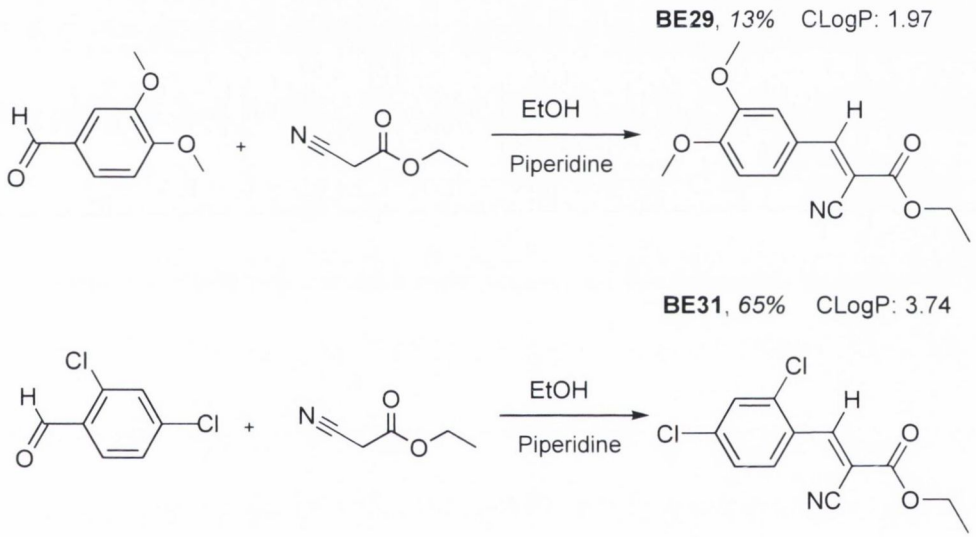

Scheme2. 8 Synthesis of cyanocrylate intermediates

As illustrated in scheme 2.8, the appropriate aldehyde was reacted with the desired ethyl cyanoacetate, in solvent ethanol and catalysed with base piperidine. After 6 hours reflux, the afforded product was the cyanoacrylate intermediates **BE29** and **BE31**. The products were purified by recrystallisation from EtOH.

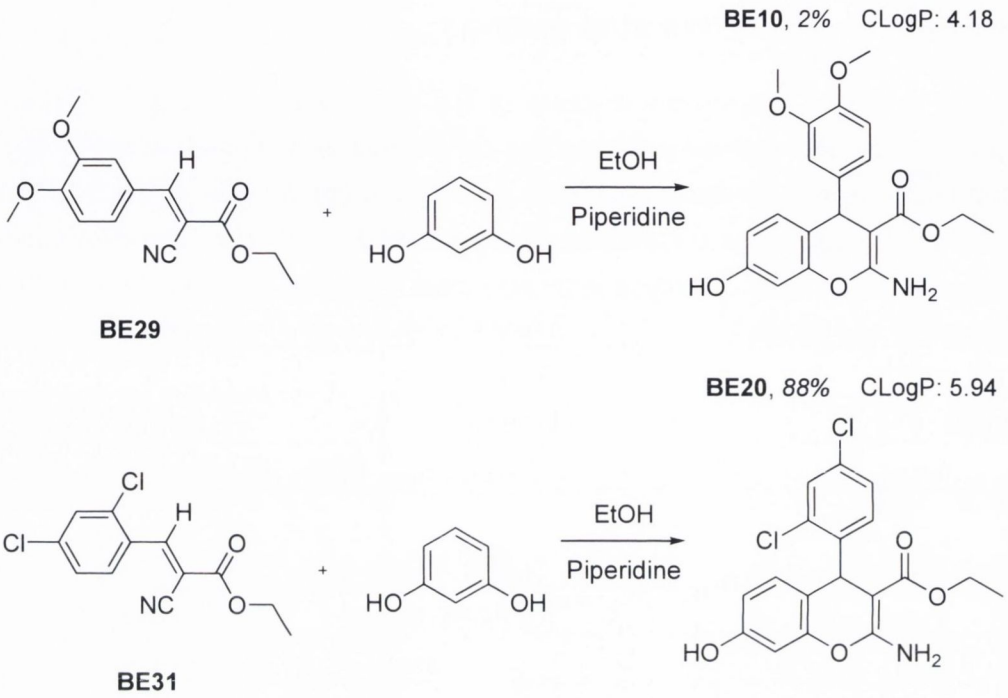

Scheme2. 9 Synthesis of 4H-chromenes from cyanoacrylate intermediates

The intermediate cyanoacrylate esters **BE29 and BE31** were refluxed (step 2, scheme 2.9) with resorcinol for 6 hours, and the reaction was monitored by thin layer chromatography (TLC). Afterwards the desired chromenes **BE30 and BE32** were purified by recrystallisation from EtOH. By carrying out the synthesis in 2 steps, it avoided unwanted side products and gave a cleaner final product for selected reactions. This method also avoided unwanted over-reaction of materials i.e. in the case for the adduct chromene **BE33** (see section 2.3), where the CN group of two acrylate ester molecules reacts with both OH groups of the diphenol resorcinol group to produce an unexpected adduct.

Scheme 2.10 shows the two step general mechanism outline for the synthesis of 4*H*-chromenes., **BE30** and **BE32**. The first step that takes place here is with the aldehyde and the ethyl cyanoacetate, to form the cyanoacrylate intermediate. This is followed in the second step by cyclisation of the OH group of the resorcinol to afford the cyanoacrylate intermediate and finally to give the desired product. It was demonstrated that the Knoevenagel condensation reaction can afford chromene products via a two step synthesis route.

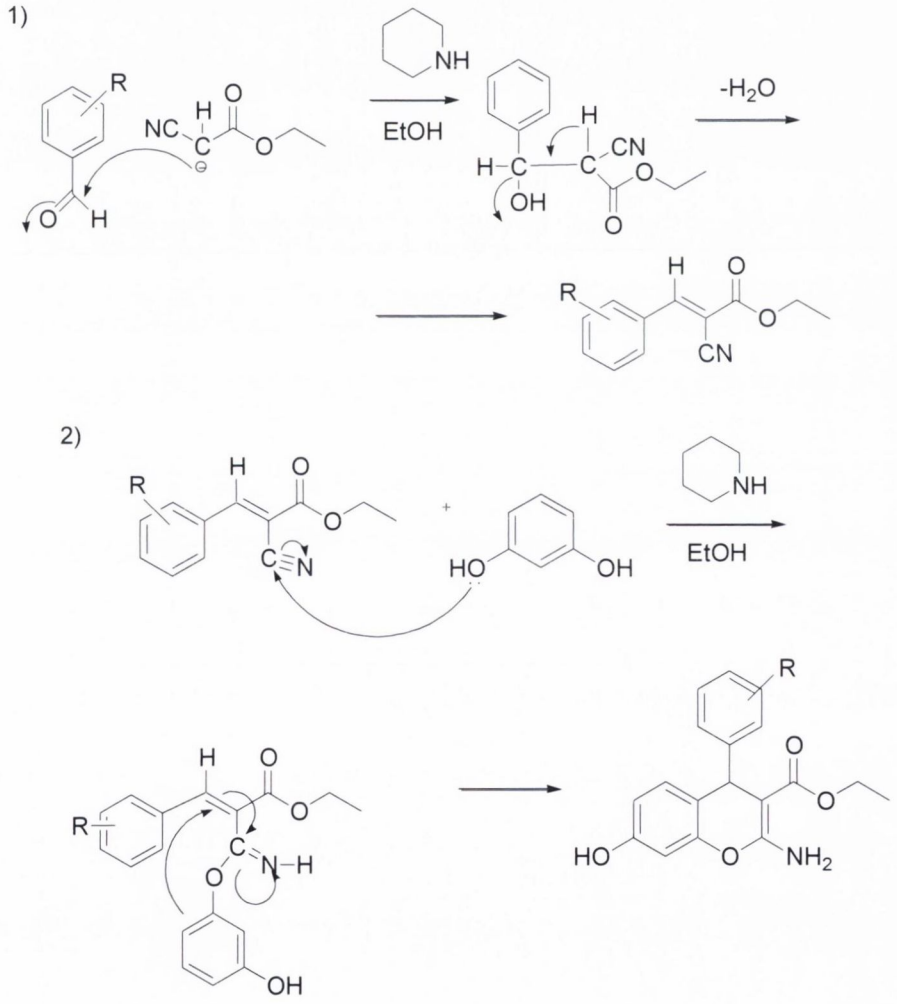

Scheme2. 10 The two step reaction for the synthesis of BE30 & BE32

2.3 Series 3: Discovery of novel adduct, pyranodiethyldiamino-4*H*-chromene dicarboxylate.

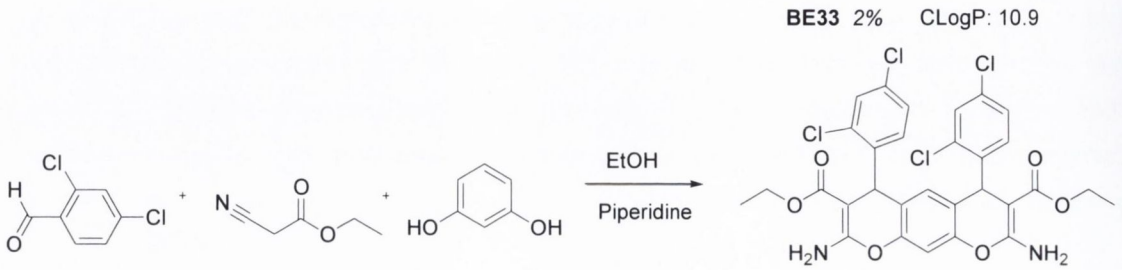

Scheme2. 11 Synthesis of pyranodiethyldiamino-4H-chromene, BE33

Scheme 2.11 displays the reaction to afford the novel adduct pyrano 4*H*-chromene-dicarboxylate **BE33**. It is carried out by reaction of 2,4-dichlorobenzaldehyde, ethyl cyanoacetate and resorcinol. Solvent used was ethanol and reaction was catalysed with base piperidine. Reaction mixture was refluxed for 6 hours. Afterwards the product was recrystallised using slow solvent evaporation techniques in EtOH, this was performed in conditions at constant room temperature and absent from light, and crystals were afforded after 2 weeks. Product was obtained in a 2% yield and it was apparent that it was not the expected 4*H*-chromene, but a novel pyranochromene **BE33** had been formed.

2.3.1 Synthetic route to novel adduct pyranochromene BE33

Scheme 2.12 displays the proposed reaction mechanism for the synthesis of the novel adduct, 4*H*,6*H*-pyrano[3,2-g]chromene-3,7-dicarboxylate (**BE33**). There are two reaction steps proposed to take place here. The first step is reaction of the aldehyde with ethyl cyanoacetate, to form the cyanoacrylate intermediate. This is then followed by reaction of the cyanoacrylate intermediate with both OH groups of the diphenol resorcinol group to give the dimer product. This is a Knoevenagel condensation and can be performed in a one pot synthesis, before a slow recrystallisation from ethanol. This novel product type was not detected in similar reactions outlined for preparation of compounds in series 1 and 2 above, but may be present.

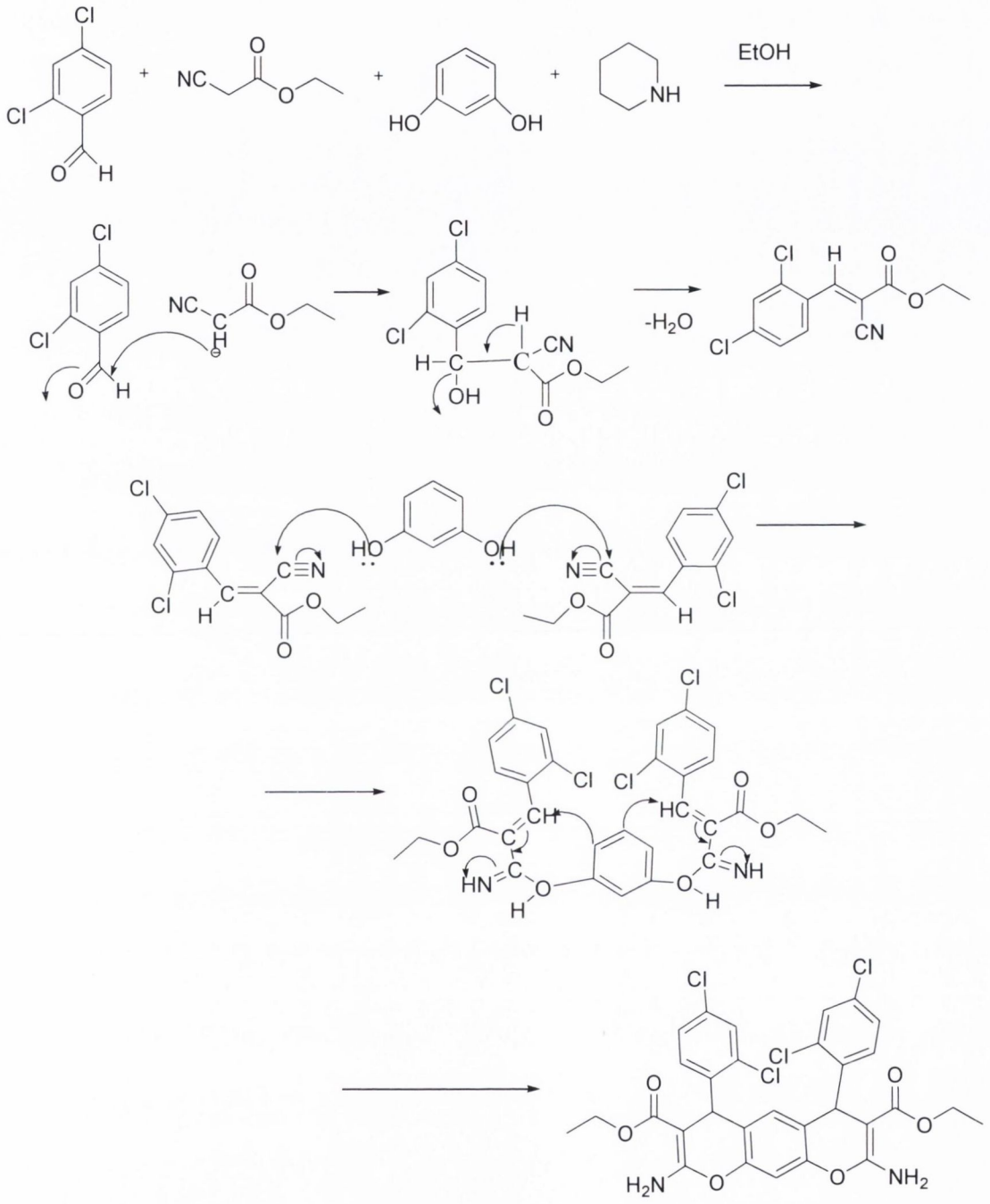

Scheme2. 12 Reaction sequence for synthesis of novel pyranodiethyldiamino-4H-chromene, BE33

2.3.2 Spectroscopic Identification

The characterisation of the novel chromene adduct compound **BE33** was achieved using Nuclear Magnetic Resonance (NMR) spectroscopy, Infared spectroscopy (IR), and Mass spectrometry(MS). The novel structure was also confirmed using X-Ray diffraction crystallography, and the ORTEP structure is shown in figure 2.11. The following figures 2.9 and 2.10 display NMR spectra for compound **BE33**

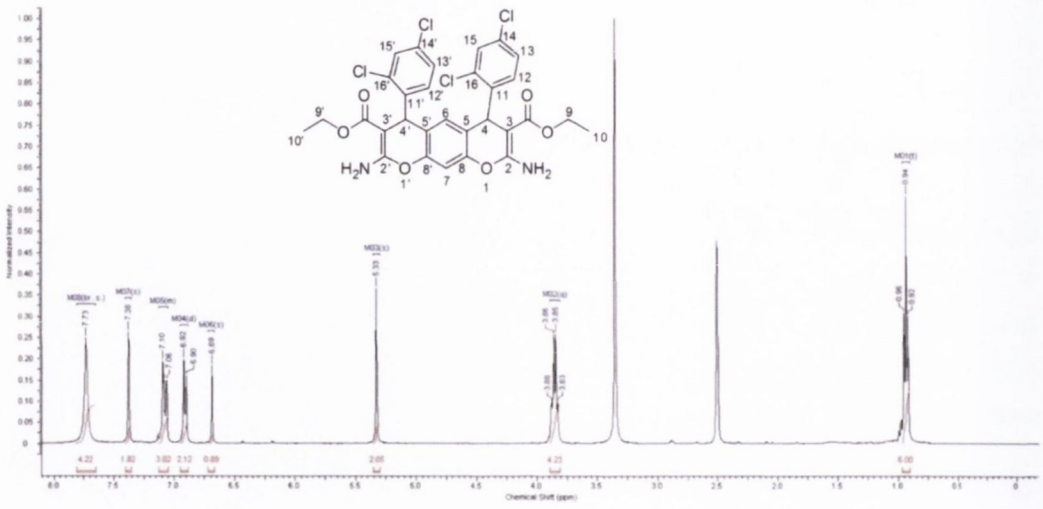

Figure 2. 9 ^{1}H NMR spectrum for pyranodiethyldiamino-4H-chromene, BE33

^{1}H NMR characterisation was required for unambiguous identification of product **BE33**. For the spectrum displayed in (Figure 2. 9), each of the two CH_3 groups on the both of the ethyl ester side chains at C10 and C10′ appear as an identical signal δ 0.94, and this overlapping is typical of the novel symmetrical 'dimer like' adduct compound. This signal was observed as a triplet with a *J* coupling constant of 7.02 Hz, and is integrated to 6H protons. At δ 3.83 a quartet absorbance was observed indicating the two CH_2 groups at C9 and C9′ with a *J* coupling constant value of 6.76 Hz, and integrating for 4H. At δ 5.33 there is a singlet for the 2xCH groups at C4 and C4′ attaching each of the aryl rings, and are integrated for 2H. At δ 6.69 another singlet is observed, integrated for 1H, indicating the Ar-H at C7. At δ 6.90, there was a doublet signal,

J=8.56, integrated to 2H, and this is assigned to the two Ar-H protons at C12 an C12′. From δ 7.06 to 7.10 there was observed a multiplet, integrated for 3H, and this indicates the two Ar-H protons at C13 and C13′ and the single Ar-H of C6 which can be seen as an overlapping singlet. At δ 7.38 there was a singlet absorbance, integrating for 2H, indicating the two Ar-H groups at the C15 and C15′ positions. At δ 7.73 a broad singlet absorbance is observed, integrated to 4H and assigned to the two NH_2 groups protons of the novel pyrano adduct.

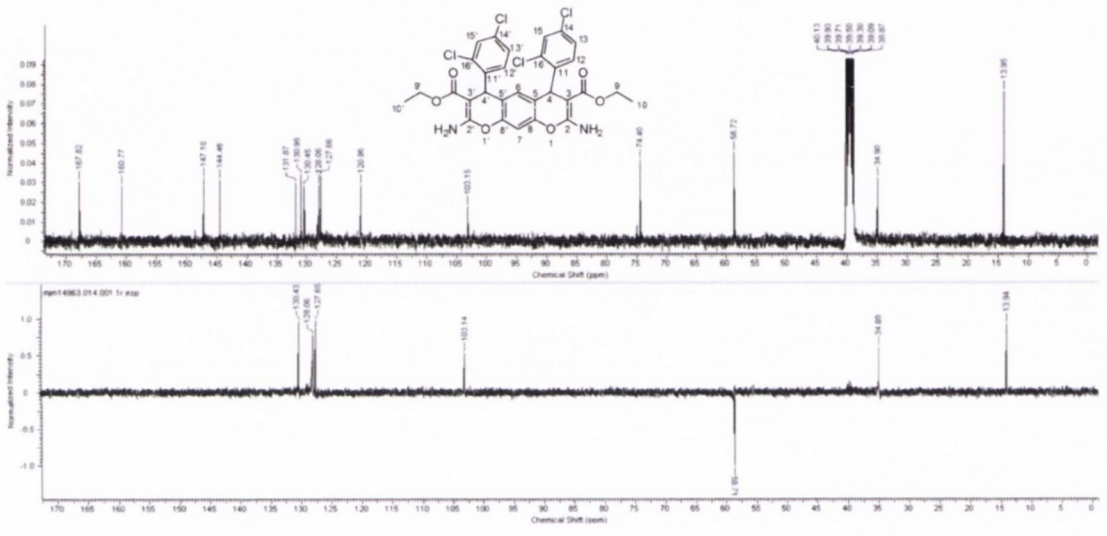

Figure 2. 10 ^{13}C NMR (upper) and DEPT 135 (lower) spectra for pyranodiethyldiamino-4H-chromene, BE33

In the ^{13}C and DEPT-135 carbon NMR spectra (Figure 2. 10) of **BE33** the two ethyl ester CH_3 groups at C10 and C10′ were seen as an identical signal at 13.95 ppm. Signals for the chiral CH carbons of C4 and C4′ can be seen at 34.90 ppm in both ^{13}C and DEPT 135 spectra. At 58.72 ppm, the signal indicating the CH_2 of C9 and C9′ are seen as a positive peak in the ^{13}C spectrum and a negative peak in the DEPT 135 spectrum. At 74.40 ppm the signal indicating the quaternary carbons at C3 and C3′ are observed. Between 103 and 130 ppm the aryl CH signals are seen in both spectra, with the remaining carbons of the molecule observed as signals from 130 ppm to ppm 167 and shown as positive peaks in the ^{13}C spectrum. At 103.15 ppm the signal is observed for the CH carcon at C7, at 120.96 ppm the signal for the CH at C5 and C5′, at 127.64 ppm the CH groups of C13 and C13′. At 128.06 ppm a signal is observed for the CH

carbons at C6, C15 and C15'. At 130.45 ppm a signal indicating the CH assigned at C12 and C12' is observed. At 130.95 ppm the carbon at C14 and C14' is assigned, and at 131.87 another signal indicating the carbons of positions C16 and C16' are observed. The quaternary signal is assigned at 144.46 ppm indicating the C of C11 and C11', and at 147.18 ppm the signal for the C-O carbon of positions C8 and C8' is observed. At 160.77 ppm there is a signal for the O-C-N of C2 and C2', and finally at ppm 167.82 the signal indicating the quaternary carbonyl C=O is observed.
The IR spectrum absorbances for compound **BE33** were assigned as follows; 3481.93 and 3416.35 cm^{-1},(NH_2), 1683.33 cm^{-1}, (C=O) and 1634.97 and 1624.62 cm^{-1}, (C=C)

The mass spectrum HRMS (EI) for compound **BE33** was determined: $C_{30}H_{24}{}^{37}Cl_4N_2O_6$ [M^- - H] requires (m/e) 647.0310; the value found was 647.0313, (+0.4 ppm), confirming the identity of the 2,8-diamino-4,6-bis(2,4-dichlorophenyl)-4*H*,6*H*-pyrano[3,2-g]chromene-3,7-dicarboxylic acid ethyl ester, **BE33.**.
The formation of the dimer like adduct compound **BE33** was an isolated observation, and only specific to this compound. This type of adduct was not observed to take place in the synthesis of any other chromene in the project.

2.3.3 XRD Crystallography study of BE33- Novel adduct pyrano chromene

The novel pyrano[3,2-g]chromene **BE33** was identified and characterised by single crystal X-ray analysis, see Figures 2.11 and 2.12. The crystal data for compound BE33 iis displayed in Table 2.4.

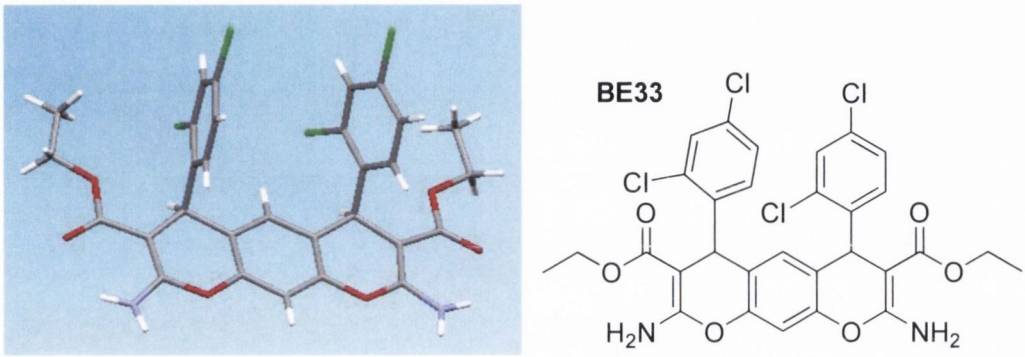

Figure 2. 11 Crystal structure of pyranodiethyldiamino-4H-chromene, Compound BE33

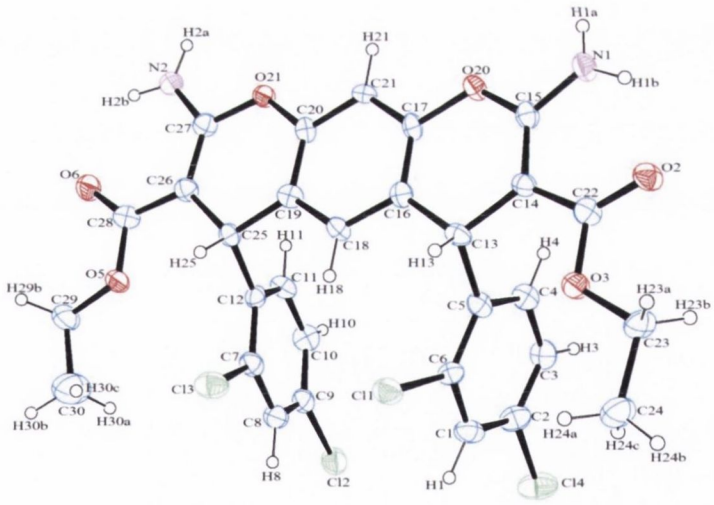

Figure 2. 12 ORTEP representation of the X-ray crystal structure of BE33, the thermal ellipsoids are set at 50% probability

Identification code	shelxl	
Empirical formula	C30 H24 Cl4 N2 O6	
Formula weight	650.31	
Temperature	150(2) K	
Wavelength	0.71075 Å	
Crystal system	monoclinic	
Space group	P2(1)/c	
Unit cell dimensions	a = 10.055(10) Å	α= 90°.
	b = 26.93(2) Å	β= 111.425(18)°
	c = 11.955(11) Å	γ = 90°.
Volume	3014(5) $Å^3$	
Z	4	
Density (calculated)	1.433 Mg/m^3	
Absorption coefficient	0.439 mm^{-1}	
F(000)	1336	
Crystal size	0.20 x 0.20 x 0.04 mm^3	
Theta range for data collection	1.51 to 25.00°.	
Index ranges	-11<=h<=11,-32<=k<=32, -14<=l<=14	
Reflections collected	22261	
Independent reflections	5260 [R(int) = 0.1005]	
Completeness to theta = 25.00°	99.40%	
Max. and min. transmission	0.9827 and 0.9174	
Refinement method	Full-matrix least-squares on F^2	
Data / restraints / parameters	5260 / 0 / 382	
Goodness-of-fit on F_2	1.201	
Final R indices [I>2sigma(I)]	R1 = 0.1200, wR2 = 0.3106	

Table 2. 4 Crystal data and structure refinement for BE33

2.4 Series 4: Chromenes with variation of the ester substituent at the C-3 position of the chromene.

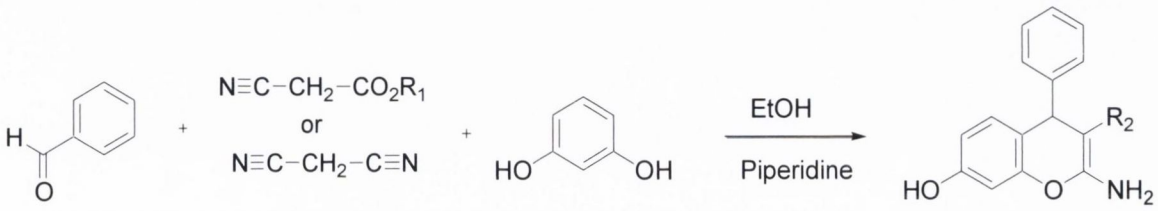

Scheme2. 13 Synthesis of 4-phenyl-4H-chromenes BE34-BE40 using malononitrile and varied cyanoacetate esters

The further series of six substituted 4*H*-chromenes (**BE35-BE40**) was prepared by the one-pot synthesis as previously stated, however this series was obtained using benzaldehyde and required reaction of substituted cyanoacrylate esters. Reagents benzaldehyde, resorcinol and varied alkyl cyanoacetates were reacted in the presence of base piperidine (see scheme 2.13). A library of compounds with variation of substituents R_2 at the C-3 ester was produced (see table 2.3). Substituted 4*H*-chromenes were varied with C-3 esters to include methyl ester, allyl acetate, benzyl, isopentyl and methylpentyl substituents. The C-3 nitrile substituted 4*H*-chromene **BE34** was also obtained using malononitrile as the methylene component in the Knovenagel reaction.

2.4.1 Results series 4: Synthesis of the library of chromene compounds

Synthesis of ester compounds (**BE34 – BE40**) in table 2.5 was achieved using the general reaction scheme (Scheme 2.13). The products obtained are illustrated in table 2.5.

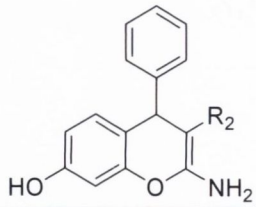

No.	R_2 Group	*% Yield*	CLogP	No.	R_2 Group	*% Yield*	CLogP
BE34		*83*	2.91	**BE38**	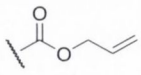	*33*	4.76
BE35	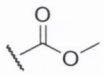	*12*	3.99	**BE39**	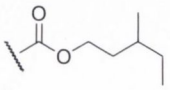	*40*	6.50
BE36	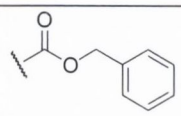	*26*	5.76	**BE40**	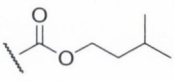	*32*	5.98
BE37	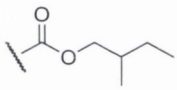	*92*	5.98				

Table 2. 5 Chromene esters compounds with variation in R2 substituent

*CLogP calculated using Chemdraw Ultra version.

A one pot Knoevenagel condensation synthesis was implemented. For table 2.5, a library of 7 different chromene compounds (**BE34 – BE40**) was produced with variation of substituents on the C-3 ester(R_2) using a selection of alkyl cyanoacetates and also malononitrile. Yields ranged from 12% - 83%. This reaction allowed preparation of potential ER agonistic 4*H*-chromenes with introduction of varied length ester side chains at C-3 including benzyl, allyl and alkyl. The cLog P values for the compounds of series 4 were in the range 2.9 for the 3-cyano substituted compound **BE34** to 6.5 for the 3-methylpentyl ester compound **BE39**.

2.4.2 Spectroscopic identification

Analysis for identification of each chromene compound was completed using Nuclear Magnetic Resonance (NMR) spectroscopy, Infared (IR) spectroscopy, and Mass spectrometry(MS). The following figures 2.13 and 2.14 display NMR spectra for compound **BE35**. Discussion of the NMR spectra for **BE35** is used as an example of the identification for each molecule in this series.

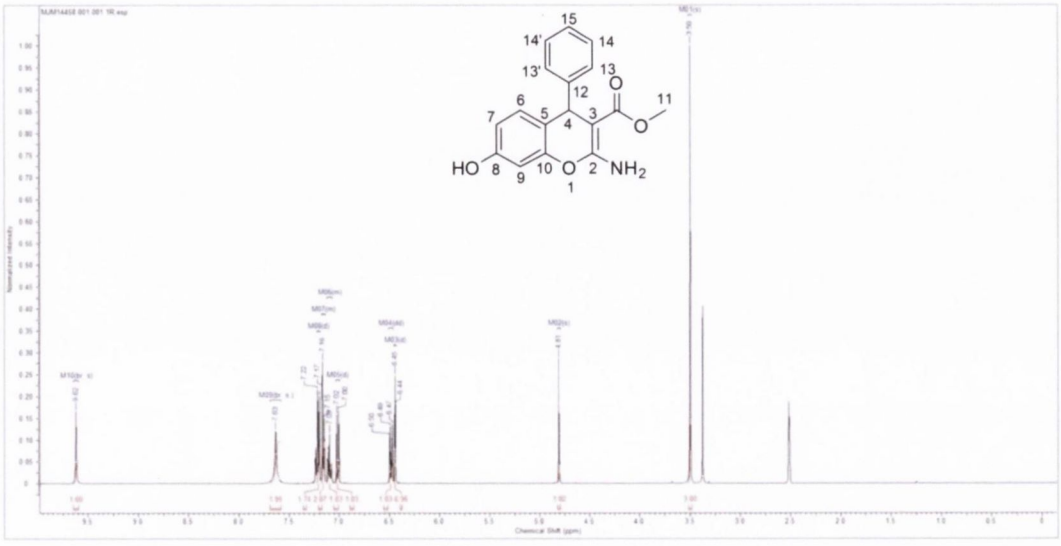

Figure 2. 13 ^{1}H NMRspectrum for compound BE35

For the ^{1}H NMR spectrum (fig 2.13) for compound **BE35**, the singlet for the CH_3 on the methyl ester side chain, at position C11, can be seen at δ 3.50 and integrated for 3 protons. Next there is the absorption for the chiral CH proton at the C4 position occurring as a singlet at δ 4.81 and integrating for 1H. At δ 6.44 there is a doublet, integrated for 1H proton, with a coupling constant value J=7.52 Hz, and this is assigned to the aromatic H at position C9. In the region δ 6.47 and 6.50 a multiplet is observed, integrating for 1H, indicative of the Ar-H at C7 position. At δ 7.00, a doublet is observed, 1H, J=8.28 Hz, indicating the Ar-H at C6. In the region δ 7.07 to 7.11 there is another multiplet observed, integrating for 1H, for the Ar-H at C15. There is a multiplet observed between δ 7.15 to 7.16, integrated for 2H, and this is assigned to the Ar-H of positions C13 and C13'. Another multiplet occurs between δ 7.17 and 7.22, integrated for 2H protons, indicating the Ar-H protons of the C14 and C14' positions. There is a broad singlet peak observed at δ 7.63 indicating the NH_2 group integrated for 2 protons. Finally at δ 9.62 there is a broad singlet absorbance which is integrated for 1 proton and is assigned to the OH group.

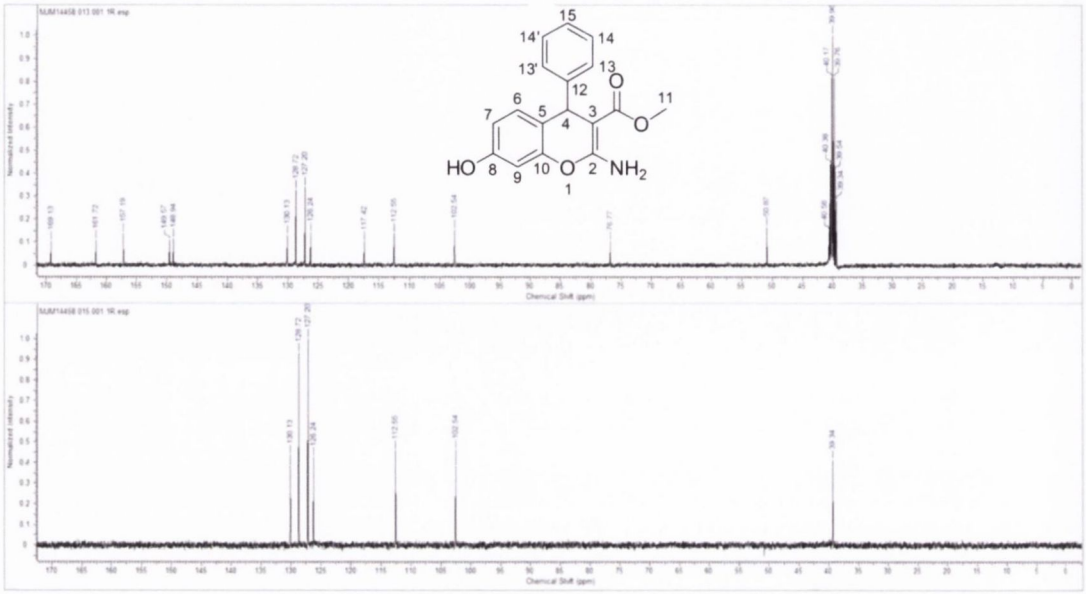

Figure 2. 14 ***^{13}C NMR (upper) and DEPT-135 (lower) spectra for benzopyran compound BE35***

In ^{13}C and DEPT-135 carbon NMR spectra (fig 2.14) for compound **BE35** the signal for the chiral carbon CH of the C4 position can be seen at 39.96 ppm. The signal for the methyl ester CH_3 at C11 can be seen at 50.87 ppm in the ^{13}C spectrum. At 76.77 ppm an absorbance occurs for the carbon attached to the carbon at position C3, seen in the ^{13}C spectrum. The aryl ring-hydrogen signals are seen from 102 to 130 ppm and totalling 12 carbons. At 102.54 ppm the signal indicating the CH group at C9 is identified, at 112.55 ppm the CH signal assigned to C7 is observed. The signal for the carbon of C5 is assigned 117.42 ppm while at 126.24 ppm there is the signal indicating the CH at position C14. At ppm 127.20 there is a signal assigned to the CH carbons of the C12 and C12′ positions. The signal at 128.72 ppm is assigned to the CH of positions C13 and C13′ while at 130.13 ppm there is a signal observed indicating the CH of C6. The following quaternary carbon signals are assigned: the carbon of position C12is observed at 148.94 ppm; the signal at 149.57 ppm is assigned to the C-O of the C10 position. At ppm 157.19 is observed a signal indicating the C-OH of C8. At ppm 161.72 a signal is assigned to the O-C-N of C2, and finally at ppm 169.13 there is an absorbance signal assigned to the carbonyl C=O group. This assignment was typical for the library of chromene compounds in this series.

In the IR spectrum of compound **BE35**, the absorbances were assigned as follows; 3418.27 cm^{-1},(OH), 3378.45 and 3227.45 cm^{-1}, (NH_2), 1669.51 cm^{-1},(C=O) and for the (C=C) group 1634.81, 1629.69 cm^{-1}.

The mass spectrum HRMS (EI) for compound **BE35,** $C_{17}H_{15}NNaO_4$, [M^+ + Na] requires (m/e) 320.0899; the value found was 320.0900, (+0.4 ppm). This confirmed the structural identification of the methyl 2-amino-4-phenyl-4*H*-chromene-3-carboxylate compound, **BE35**

2.5 Series 5: 4-Hydroxyphenyl chromenes with variation on the C-3 ester side chain

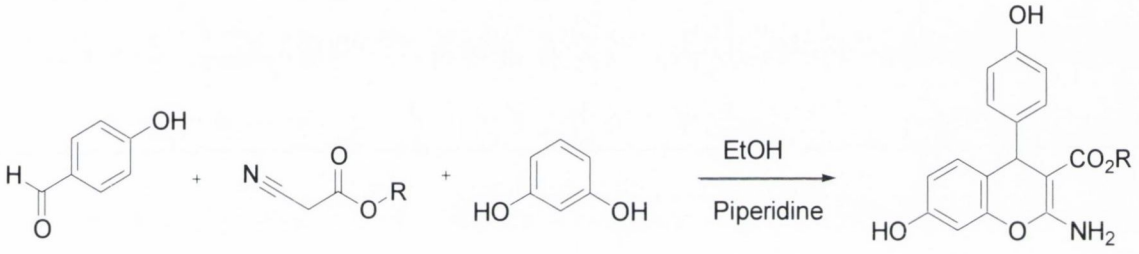

Scheme 2. 14 Synthesis of 4-hydroxyphenyl-4H-chromenes

The series 5 substituted 4 hydroxyphenyl 4*H*-chromenes were prepared by a one-pot reaction using 4-hydroxybenzaldehyde, resorcinol and a selection of varied alkyl cyanoacetates in the presence of base piperidine (scheme 2.14). A library of compounds was produced (**BE41-BE54**), all with 4-hydroxy phenolic substituents at C-4 of the chromene ring, and with variation of ester substituents R at C-3 of the chromene ring, (see table 2.6). The 4-hydroxyphenyl substituent at C-4 was introduced to facilitate additional interactions of these compounds with the ligand binding domain of the estrogen receptor (as predicted from *in silico* modelling discussed in Chapter 1).

2.5.1 Results series 5

The library of 4-hydroxyphenyl chromenes with variation on the R_2 ester side chain at C-3 is illustrated in table 2.6.

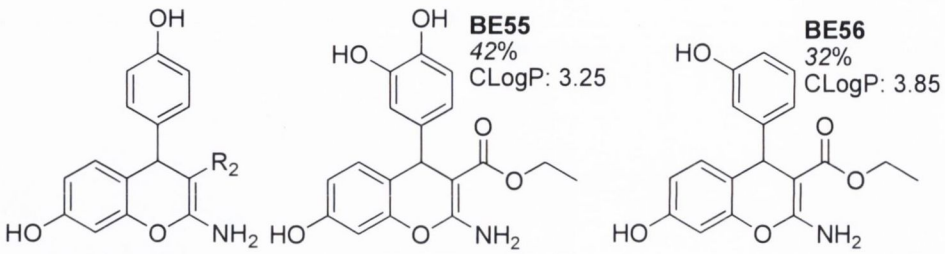

No.	R_2	% Yield	CLogP	No.	R_2	% Yield	CLogP
BE41	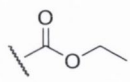	*32*	3.85	**BE48**	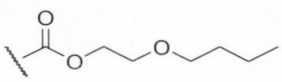	*82*	4.73
BE42	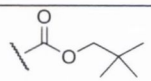	*65*	5.18	**BE49**	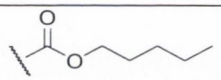	*92*	5.44
BE43	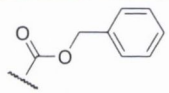	*3*	5.09	**BE50**	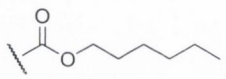	*15*	5.97
BE44	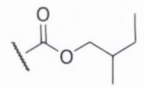	*42*	5.31	**BE51**	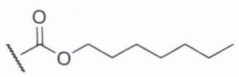	*12*	6.50
BE45	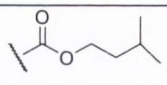	*4*	5.31	**BE52**	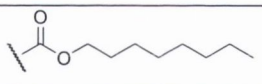	*36*	7.03
BE46	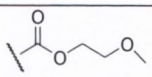	*42*	3.28	**BE53**	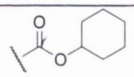	*7*	5.35
BE47	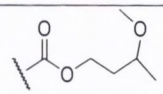	*9*	3.96	**BE54**	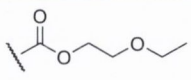	*11*	3.67

Table 2. 6 The library of 4-(4-hydroxyphenyl)chromenes synthesised

*CLogP calculated using Chemdraw Ultra version.

Synthesis of the products illustrated in table 2.6 was achieved using the general reaction scheme 2.14. For table 2.6 a library of 14 different chromene compounds was produced with variation of substituents of the R2 at C-3 of the chromene ring using a wide selection of alkyl cyanoacetates together with a 4-hydroxy phenyl substituent at C-4. The structures were varied to include examples of the alkyl esters, cycloalkyl esters, allyl ether esters and benzyloxy esters at C-3. Yields ranged from 3% - 92%. CLogP values ranged from 3.28 to 7.03 in this series. Results displayed in the table 2.6

indicate the versatility of synthesising the 4*H*-chromenes using the 1 step Knoevenagel reaction. All the 4-OH-phenyl chromenes were purified using flash column chromatography on silica gel, and afterwards recrystallised from EtOH affording the pure product.

2.5.2 Spectroscopic identification

Analysis for identification of each chromene compound was achieved using Nuclear Magnetic Resonance (NMR) spectroscopy, Infared (IR) spectroscopy, and Mass spectrometry. The following figures 2.15 and 2.16 illustrate NMR spectra for compound **BE54**. Discussion of the NMR spectra for **BE54** is used as an example on how each molecule was identified in this series.

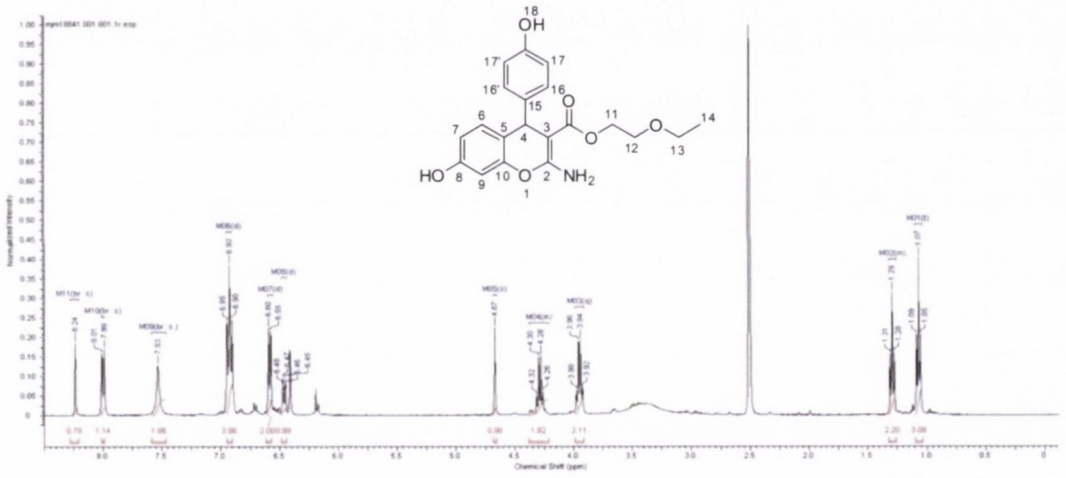

Figure 2. 15 ^{1}H NMR spectrum for compound BE54

In the ^{1}H NMR spectrum (fig 2.15) for compound **BE54**, the triplet observed at δ 1.07 is assigned to the CH_3 on the ester side chain at the C14 position, and is integrating for 3H, with a *J* coupling value of 7.03 Hz. Following this, a multiplet for the CH2 group on the ester chain of the C13 position, occurring between δ 1.29 and 1.34, is observed integrating for 2H. At δ 3.95 there is a quartet, integrating for 2H, with a coupling value of *J*=7.04 Hz, assigned to the CH_2 group at the C12 position. Another CH_2 at the C11 position, can be observed occurring as a multiplet between 4.29 to 4.34, and is integrating for 2H. The chiral CH of the C4 position, occurs at δ 4.67 as a singlet, integrated for 1H. At δ 6.46 there is a doublet, integrating for 1H, with a coupling constant of J=8.28 Hz, indicating the Ar-H group at C9. At δ 6.59 there is a doublet

absorbance, integrating for 2H, J=8.53 Hz, and this is assigned to the Ar-H protons at C6 and C7 positions. At δ 6.92 there is a multiplet observed, integrating for 4H protons, with a coupling value of J=8.03, assigned to the Ar-H protons at positions C17, C17′, and C16, C16′. At δ 7.53 a broad singlet absorbance is observed integrating for 2H, and this is assigned to the NH_2. At δ 8.01, a broad singlet is shown, integrating for 1H integrating for 1H, is assigned to the OH at position C8. Finally at δ 8.24, another broad singlet is observed and assigned to the OH group at position C18.

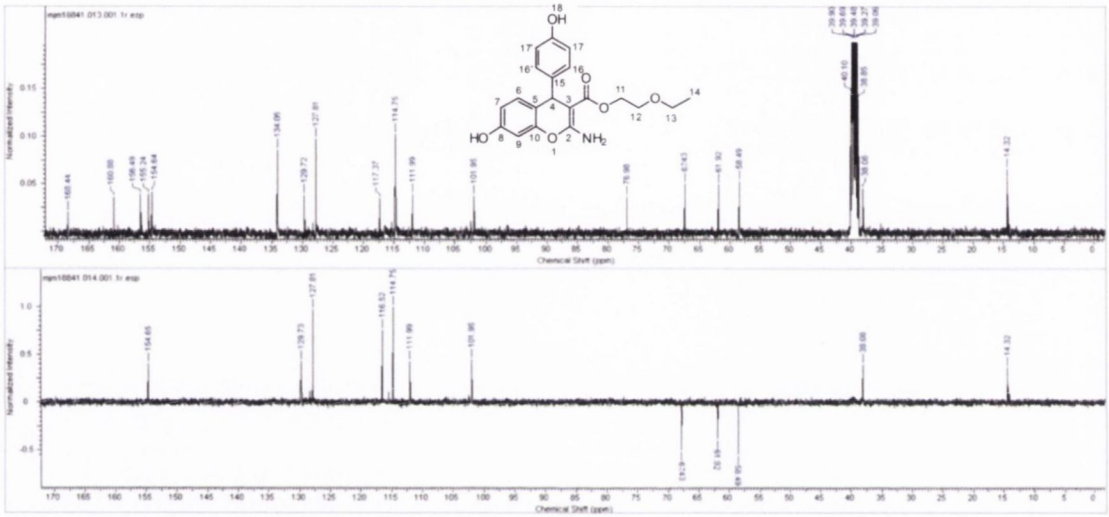

Figure 2. 16 ^{13}C NMR (upper) and DEPT 135 (lower) spectra for benzopyran BE54

In ^{13}C and DEPT carbon NMR spectra in fig 2.16 for compound **BE54**, the CH_3 on the ester chain at C14 can be seen at 14.32 ppm. At 38.08 ppm there is a signal assigned to the chiral CH at C4 position. Following this, three signals are assigned for each of the three CH_2 groups, and are observed as positive absorbances in the ^{13}C spectrum and negative absorbances in the DEPT 135 spectrum, at 58.49 ppm for the CH_2 group of the C11 position, at 61.92 ppm for the CH_2 of the C13 position and at 67.43 ppm for the CH_2 group at the C12 position. At 76.98 ppm an absorbance occurs for the C3 carbon attached to the side chain seen in the ^{13}C spectrum. Five separate absorbances are seen from 101 ppm to 129 ppm, indicating the 7 aryl CH carbons. There is one carbon(C) seen at 134.06 ppm and the remaining quaternary carbons occur in the upper range ppm values from 154 ppm to 168 ppm. The tertiary(CH) and quaternary carbons (C) are assigned as follows: at 101.95 ppm the signal is assigned to the CH at C9, at 111.99 ppm indicating the CH group of the C7, at 114.75 ppm the carbon(C) of

C5, at 117.37 ppm the CH groups of C17 and C17', at 127.81 ppm the CH of C16 and at 129.72 ppm the CH group of C6. The remaining quaternary carbons are identified as follows: at 134.06 ppm the carbon of C15, at 154.64 ppm the C-O of C10, at 155.24 ppm for the C-OH of C18, at 156.49 ppm the C-OH of C8, at 160.88 ppm is assigned to the O-C-N of position C2, and finally at 168.44 ppm is assigned to the C=O. These assignments were typical of the compounds of this library of chromene compounds.

In the IR spectrum of **BE54** the following absorbances were observed; 3529.04 and 3499.62 cm^{-1}(OH), 3439.26 and 3409.61 cm^{-1} (NH_2), 1667.07,(C=O) and 1632.53 and 1624.48 cm^{-1}, (C=C).

The mass spectrum HRMS (EI) for compound **BE54** $C_{20}H_{21}NNaO_6$ [M^+ + Na] requires (m/e) 394.1267; the value found was 394.1258, (-2.2 ppm). The analysis confirmed the structural identification of the novel ethoxyethyl amino (4-hydroxyphenyl)-4*H* chromene carboxylate compound **BE54**.

2.6 Series 6: 4-Benzyloxyphenyl chromenes with variation in the structure on the C-3 ester side chain

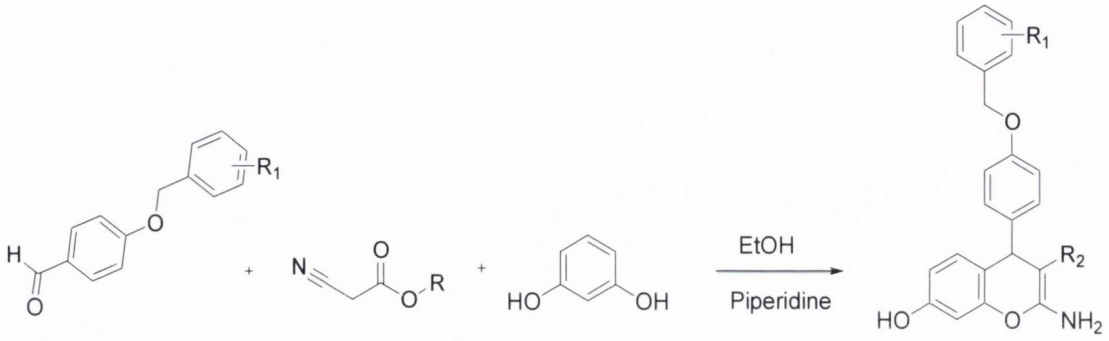

Scheme2. 15 Synthesis of benzyloxyphenyl-4H-chromenes using varied alkyl cyanoacetate esters BE57-BE69

The type 6 series of substituted 4-benzyloxy-4*H*-chromenes **BE57-BE69** were prepared by a one-pot reaction using 4-benzyloxybenzaldehyde, resorcinol and a selection of varied alkyl cyanoacetates in the presence of base piperidine (see scheme 2.15) involving reaction of substituted esters. A library (see table 2.7). of benzyloxy chromene compounds with variation of substituents on R_2 C-3 aryl ring, was produced. These specific compounds were of interest because of the promising biochemical results obtained in the initial *in silico* study (section 1), predicting optimum interaction of the benxyloxy substituted 4-arylchromenes wuth the ligand binding domain of the estrogen receptor.

2.6.1 Results series 6: Synthesis of the library of chromene compounds

Synthesis of the 4-benzyloxy-4*H*-chromenes **BE57-BE69** illustrated in Table 2.7 was carried out using the general reaction scheme (Scheme 2.15). The products obtained are illustrated in Table 2.7, together with the % yields and CLogP values.

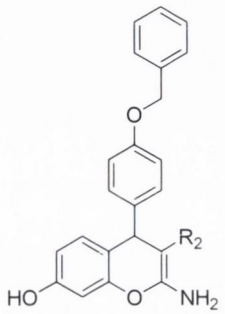

BE57-BE69

No.	R_2 Group	% Yield	CLogP	No.	R_2 Group	% Yield	CLogP
BE57	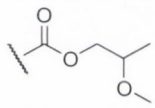	*6*	5.95	**BE64**	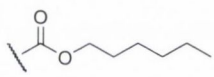	*34*	8.32
BE58	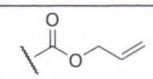	*38*	6.45	**BE65**	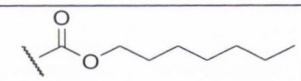	*37*	8.85
BE59	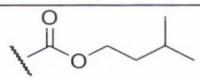	*33*	7.66	**BE66**	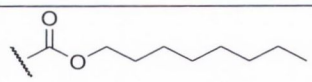	*45*	9.38
BE60	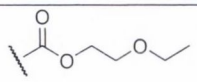	*32*	6.03	**BE67**	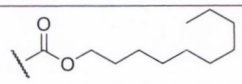	*56*	10.44
BE61	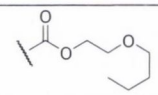	*40*	7.08	**BE68**	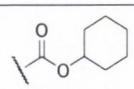	*50*	7.71
BE62	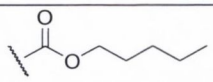	*41*	7.79	**BE69**	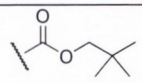	*13*	7.53
BE63	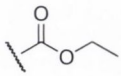	*47*	6.21				

Table 2. 7 Series of 4-benzyloxyaryl-4H-chromenes

*CLogP calculated using Chemdraw Ultra version.

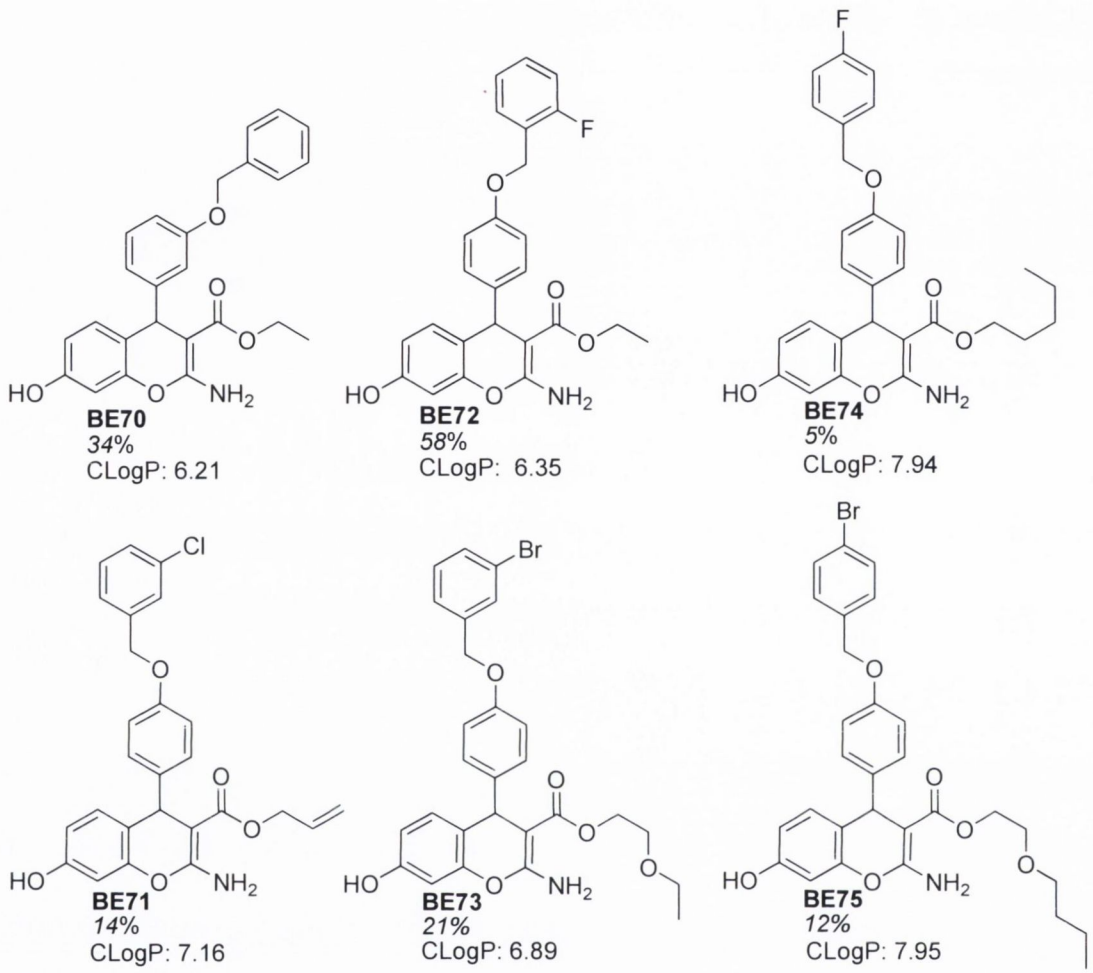

Figure 2. 17 The selection of 4-(benzyloxyaryl)chromene compounds BE57-BE69 and BE70-BE75 with variation of the ester substituents at the C-3 position

*CLogP calculated using Chemdraw Ultra version.

Synthesis of the chromene products **BE57- BE75** illustrated in table 2.7 was achieved by using the general reaction scheme (Scheme 2.15). Yields are seen in the range from 6 to 58%. In table 2.7 a library of 13 different chromene compounds was produced, again with variation of the R_2 substituent located at the C-3 position of the aryl ring using a wide selection of alkyl cyanoacetate esters. In addition, a benzyloxyphenyl moiety was now introduced on the chromene at the C4 position. There are 6 additional compounds in the library table 2.7, compounds **BE70 – BE75** (illustrated separately in Figure 2.17), and these have further variation on the 4-arylbenzyloxy group including fluoro, chloro and bromo substituents. In this series yields ranged from 5% - 56%. CLogP values are shown and are in the range 5.9 to 9.3

for the series, and these values are considerably higher than the previous series. The introduction of the benzyloxy type substituents on the chromene C4 aryl ring together with a wide variation of lipophilic esters on the C3 position allowed production of a library of molecules with a potentially greater antagonistic potential for these molecules in targeting the highly lipophilic ER-LBP.

2.6.2 Spectroscopic identification

Identification of each chromene compound in this series was achieved using Nuclear Magnetic Resonance (NMR) spectroscopy, Infared (IR) spectroscopy, and Mass spectrometry(MS). The following figures 2.18 and 2.19 illustrate NMR spectra for compound **BE69**. Discussion of the NMR spectra is used as an example on how each molecule was identified in this series.

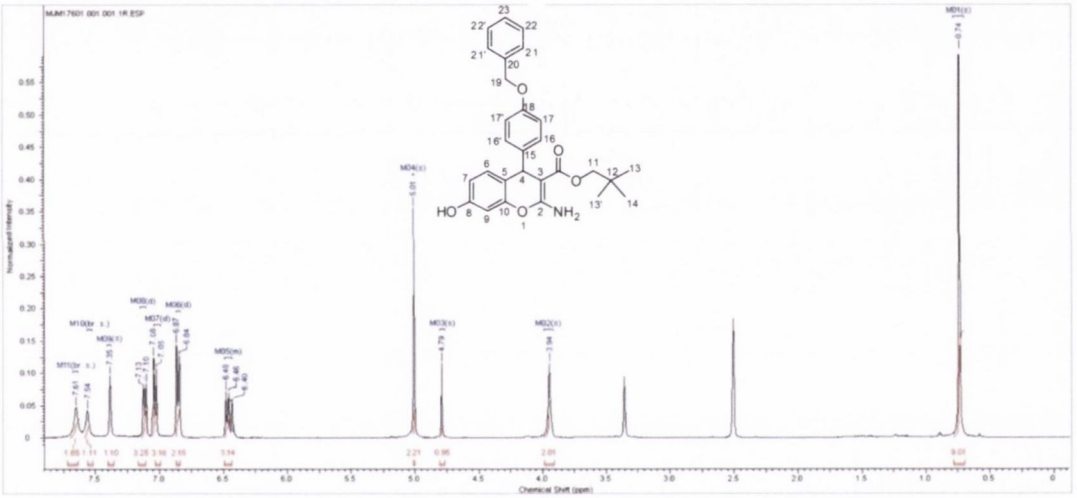

Figure 2. 18 ^{1}H NMR spectrum for compound BE69

In the proton NMR spectrum illustrated in fig 2.18 for compound **BE69**, the tertiary butyl methyl group protons at positions C13, C13′ and C14 on the ester side chain are indicated by the singlet absorption occurring at δ 0.74, and this is integrated for 9H. The next absorbance is assigned to the ester OCH_2 at C11 at δ 3.94, observed as a singlet, and is integrated for 2H. Following this, there is a singlet peak at δ 4.79, indicating the C4 chiral CH and is integrating for 1H. Another singlet peak can be seen at δ 5.01 for the benzyloxy OCH_2 at the C19 position, and integrating to 2H. Between δ 6.40 and 6.49 there is a multiplet absorbance, of three aromatic protons, and assigned to positions C9, C7 and C6. At δ 6.84 there is a doublet absorbance, integrating for 2H,

with a coupling constant value of J=8.04 Hz, indicating the Ar-H protons at C17 and C17′. At δ 7.05, a doublet is observed, integrating for 3H, J=8.80 Hz, indicating the Ar-H protons at positions C16, C16′ and C21. At δ 7.10. an apparant doublet is observed, integrating for 3H, with a coupling value of J=7.24 Hz, and is assigned to the Ar-H protons at C21′, C22 and C22′. At δ 7.35, a singlet is observed, integrated for 1H, for the Ar-H proton at C23. At δ 7.54 a broad singlet integrating for 1H is assigned to the OH group at the C8 position. Finally at δ 7.61 another broad singlet is observed, integrating for 2H, which is attributed to the NH_2 protons at the C2 position.

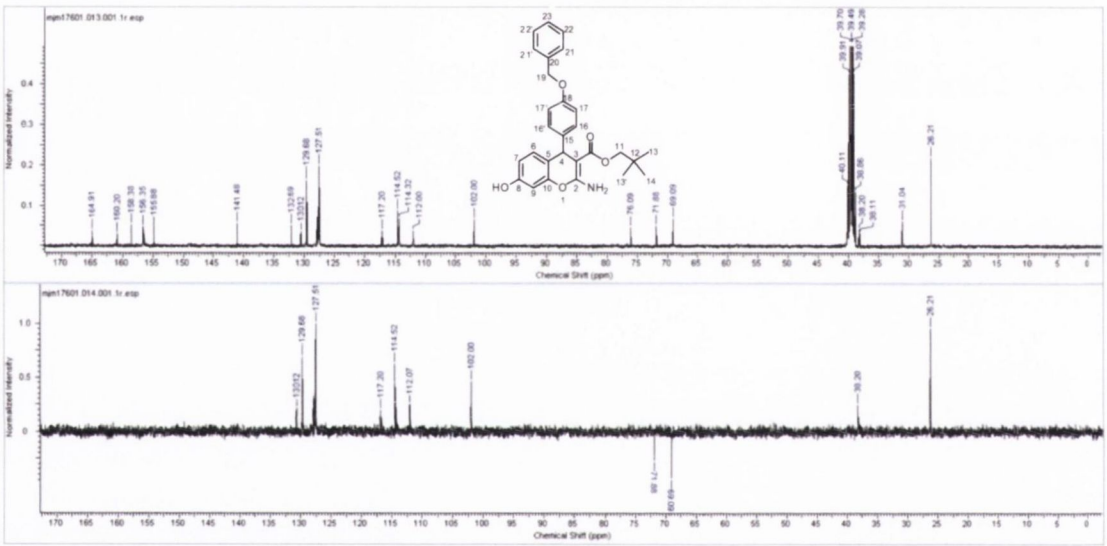

Figure 2. 19 ^{13}C NMR (upper) and DEPT-135 (lower) spectra for benzopyran BE69

In ^{13}C and DEPT-135 carbon NMR spectra shown in figure 2.19 for compound **BE69**, the tertiary butyl CH_3 groups at positions C13, C13′ and C14 on the ester chain can be observed at ppm 26.21. At 31.04 ppm a signal is assigned to the quaternary carbon at C12. The C4 chiral CH is observed at 38.16 ppm. At 69.09 ppm the benzyloxy CH_2 of the C19 position is seen as a positive peak in the ^{13}C, and as a negative peak in the DEPT 135 spectrum. Similarily at 71.88 ppm the OCH_2 of the C11 position on the ester side chain is confirmed. At 76.09 ppm the carbon C3 at the ester chain is indicated. All of the signals assigned for the aryl CH carbons are observed between 102 ppm to 130 ppm, with the remaining quaternary carbon signals observed from 132 ppm to 164 ppm. The following tertiary and quaternary carbon signals are assigned:at 102.00 ppm the CH of the C9 position, at 112.06 ppm the CH of C7, at 114.32 ppm the carbon at C5, at 114.52 ppm the CH signal of C17 and C17′ positions, at 117.20 ppm the CH of

positions C21, C21' and C23, at 127.51 ppm the CH of C22, at 129.62 ppm the CH of C16, at 130.12 ppm the CH of C6. The following quaternary carbon signals are assigned: at 132.69 ppm the C of C15, at 141.48 ppm the C of position C20, at 155.88 ppm the C-O of C10, at 156.35 ppm the C-OH group at C8, at 158.38 ppm the Bn-C-O at position C18, at 160.20 ppm the O-C-N of the C2 position, and finally at 164.91 ppm the carbonyl C=O signal is identified.

In the IR spectrum the absorbances for **BE69** were consistent with the structure and were assigned as follows; 3483.73 cm^{-1}, (OH); 3465.83 and 3386.24 cm^{-1}, (NH_2); 1685.80 cm^{-1}, (C=O);and 1669.72 and 1636.22 cm^{-1},(C=C).

The mass spec HRMS (EI) for for **BE69** , $C_{28}H_{30}NO_5$ [M^+ + Na] requires (m/e) 460.2124; the value found was 460.2114, (+2.17 ppm). The novel neopentyl 2-amino-benzyloxyphenyl-4*H* chromene carboxylate for **BE69** was thus identified.

2.6.3 XRD Crystallography Structure of 4-(3-Benzyloxyphenyl)-*4H*- chromene BE70

The X-Ray structure for an example of the series of 4-(benzyloxyphenyl)-*4H*-chromene **BE70** was determined. The results are illustrated in Figures 2.20 and the ORTEP representation of the X-Ray structure (Thermal ellipsoids set at 50% probability) is shown in Figure 2.21. The crystal data and structure refinement for **BE70** is displayed in Table 2.8.

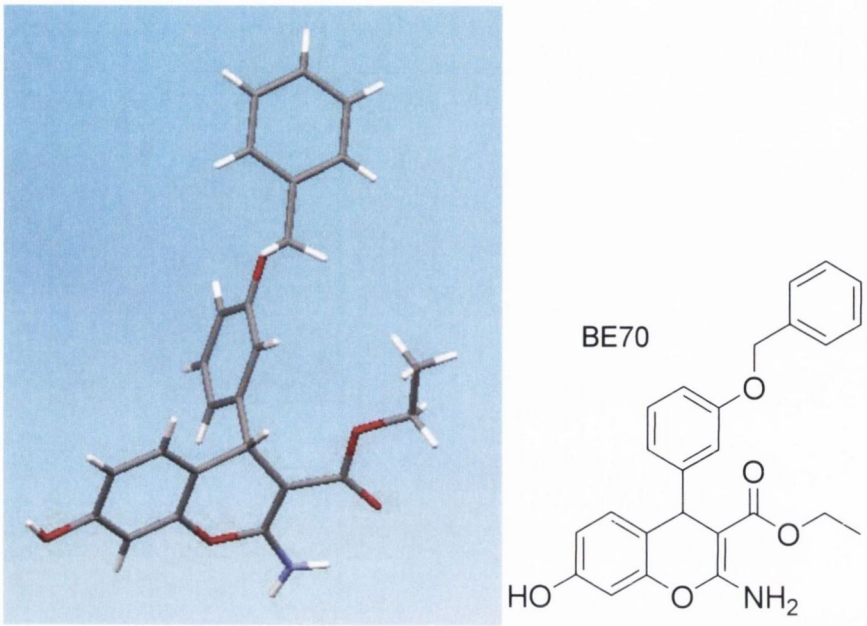

Figure 2. 20 Crystal structure of BE70

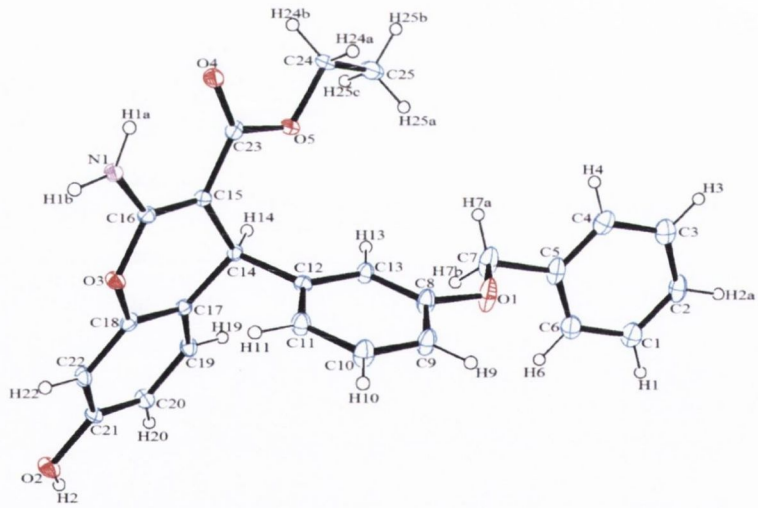

Figure 2. 21 ORTEP representation of the X-ray crystal structure of BE70, the thermal ellipsoids are set at 50% probability

Identification code	shelxl	
Empirical formula	C200 H184 N8 O40	
Formula weight	3339.55	
Temperature	158(2) K	
Wavelength	0.71075 Å	
Crystal system	monoclinic	
Space group	C2/c	
Unit cell dimensions	a = 36.706(14) Å	α= 90°.
	b = 10.491(4) Å	β= 102.505(6)°.
	c = 11.178(4) Å	γ = 90°.
Volume	4202(3) $Å^3$	
Z	1	
Density (calculated)	1.320 Mg/m^3	
Absorption coefficient	0.092 mm^{-1}	
F(000)	1760	
Crystal size	0.40 x 0.30 x 0.20 mm3	
Theta range for data collection	1.14 to 25.00°.	
Index ranges	-43<=h<=43, -12<=k<=12, -13<=l<=13	
Reflections collected	14801	
Independent reflections	3644 [R(int) = 0.0526]	
Completeness to theta = 25.00°	98.20%	
Refinement method	Full-matrix least-squares on F^2	
Data / restraints / parameters	3644 / 0 / 282	
Goodness-of-fit on F2	1.289	
Final R indices [I>2sigma(I)]	R1 = 0.0711, wR2 = 0.2162	
R indices (all data)	R1 = 0.0956, wR2 = 0.2652	

Table 2. 8 Crystal data and structure refinement for shelxl. BE70

2.7 Series 7: 4-(3,4,5-Trimethoxyphenyl)-4*H*-chromenes with variation of the R_2 ester at C-3

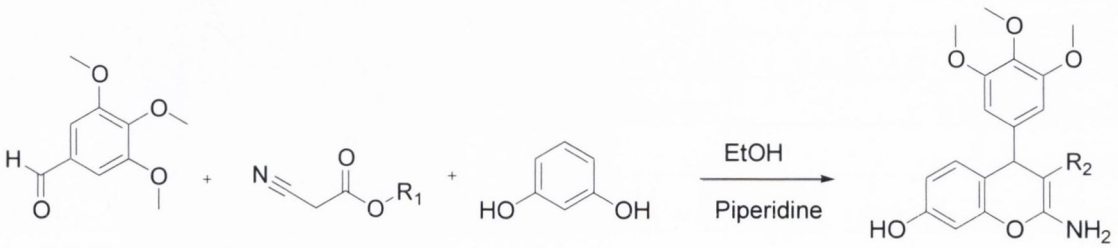

Scheme2. 16 General synthetic scheme for 4-(3,4,5-trimethoxyphenyl)-4H- chromenes BE76-BE87 using varied alkyl cyanoacetate esters

This series of substituted 4-(3,4,5–trimethoxyphenyl)-4*H*-chromenes were prepared by a one-pot reaction using 3,4,5 trimethoxybenzaldehyde, resorcinol and a selection of varied alkyl cyanoacetates in the presence of base piperidine (scheme 2.16). This reaction gave good yields of products in the range 18-80% (see table 2.9). A library of 9 trimethoxy 4*H*-chromene compounds with variation of substituents on R_2 C-3 aryl ring, was produced. This series was of interest as it was proposed that these compound structures may contribute additional potency due to known affinity of the 3,4,5-trimethoxyphenyl substituent for tubulin (as observed for combretastatin type stilbenes) and may contribute to the increased and complimentary antiproliferative ativity for these compounds[147].

2.7.1 Results series 7 Synthesis of the library of 3,4,5-trimethoxyphenyl chromene compound*s*

Synthesis of compounds **BE76-BE87** illustrated in Table 2.9 was achieved by using the general reaction scheme (Scheme 2.16). The products obtained are illustrated in Table 2.9, below.

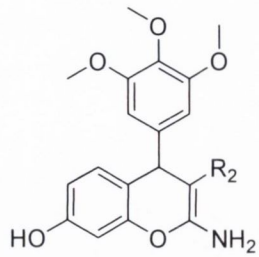

BE86
60%
CLogP: 7.18

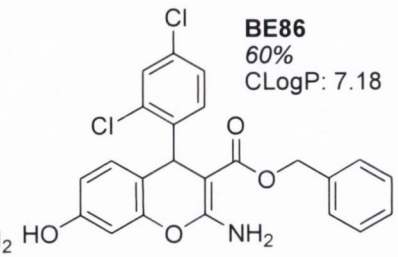

BE87
49%
CLogP: 7.40

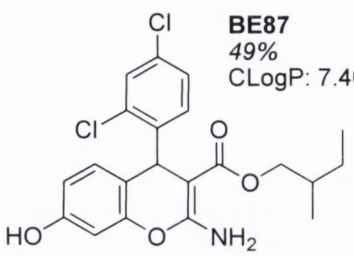

BE76-BE85

No.	R_2 Group	*% Yield*	CLogP	**No.**	R_2 Group	*% Yield*	CLog P
BE76	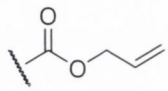	*46*	4.06	**BE81**	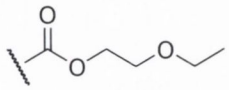	*42*	3.64
BE77	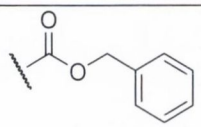	*32*	5.06	**BE82**	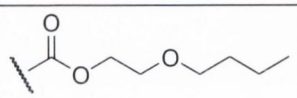	*35*	4.70
BE78	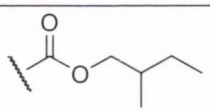	*56*	5.28	**BE83**	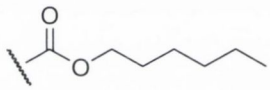	*18*	5.93
BE79	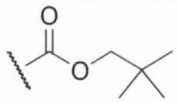	*23*	5.15	**BE84**	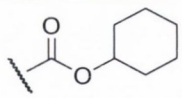	*80*	5.32
BE80	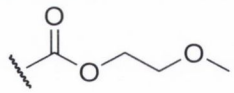	*41*	3.25	**BE85**	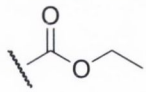	*39*	3.82

Table 2. 9 The selection of 4-(3,4,5-trimethoxyphenyl)-4H-chromene compounds BE76-BE87 with variation in the structure of the ester substituent R2.

*CLogP calculated using Chemdraw Ultra version.

The results obtained (shown in table 2.9) are a selection of 4-(3,4,5-trimethoxyphenyl)-4*H*-chromenes **BE76-BE85** with yields ranging from 18 to 80%. There was also an additional subset of 4-(2,4-dichlorophenyl)-4H-chromenes synthesised **BE86** and **BE87**. The selection of compounds in table 2.9 have an extensive variation in the type of esters substituent located at the chromene C3 position, some of which include lipophilic and stericallly hindered groups which may potentially contribute to selectivity in ER antagonistic activity such as observed for

fulvestrant[74]. CLogP values were in the range 3.2 – 5.9 in this series and higher CLogP values were calculated for the compounds **BE86** and **BE87**(CLogP = 7.18 and 7.40 respectively) due to the lipophilic ester and dichlorophenyl substituents.

2.7.2 Spectroscopic identification

Identification of each chromene compound was achieved using Nuclear Magnetic Resonance (NMR) spectroscopy, Infared (IR) spectroscopy, and Mass spectrometry(MS). The following figures 2.22 and 2.23 present the NMR spectra for compound **BE76**. Discussion of the NMR spectra for compound **BE76** as an example is useful to illustrate the identification of each compound in this series.

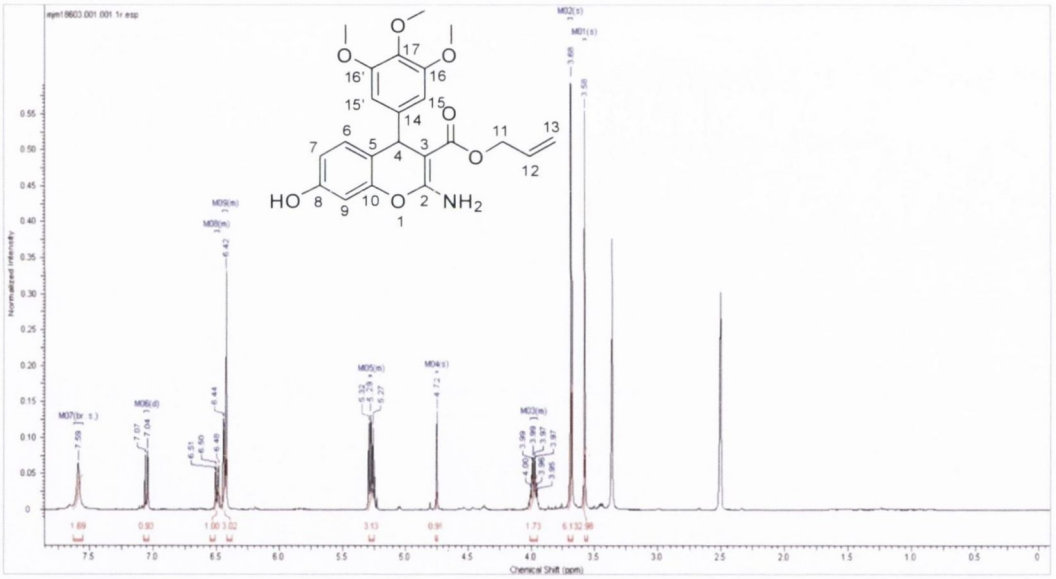

Figure 2. 22 ^{1}H NMR Spectrum BE76

In the ^{1}H NMR spectrum in figure 2.22 for compound **BE76**, the 2,3,4-trimethoxy group protons are identified between δ ppm 3.58 and δ 3.68, with the OCH_3 of the C17 position at δ 3.58 as a singlet integrated to 3H, and the two other OCH_3 groups of the C16 and C16′ positions at δ 3.68 as a singlet integrating for 6 protons. Next is the OCH_2 group of C11 on the ester side chain observed as a multiplet between δ 3.95 to 4.00, and integrating for 2H. The chiral CH at the C4 position is observed at 4.72 ppm as a singlet absorbance, and is integrating for 1H. The 3x CH protons on the double bond of the ester side chain, one at C12 and two at C13 are seen here occurring as a

multiplet absorbance between δ 5.27 to 5.32, integrating for 3H. Between δ 6.42 to 6.44 a multiplet absorbance is observed, integrating to 3H and this peak is assigned to the Ar-H groups at positions C15, C15′ and C9. Between δ 6.44 to 6.49, anothermultiplet is observed, integrating for 1H, and assigned to the Ar-H at C7. At δ 7.04 a doublet is observed, with a *J* coupling constant of 8.53 Hz, integrating for 1H, and is assigned to the Ar-H proton at C6. Finally at δ 7.59 a broad singlet absorbance can be assigned to the NH_2 group protons at C2, integrated for 2H. The signal corresponding to the OH group was not observed.

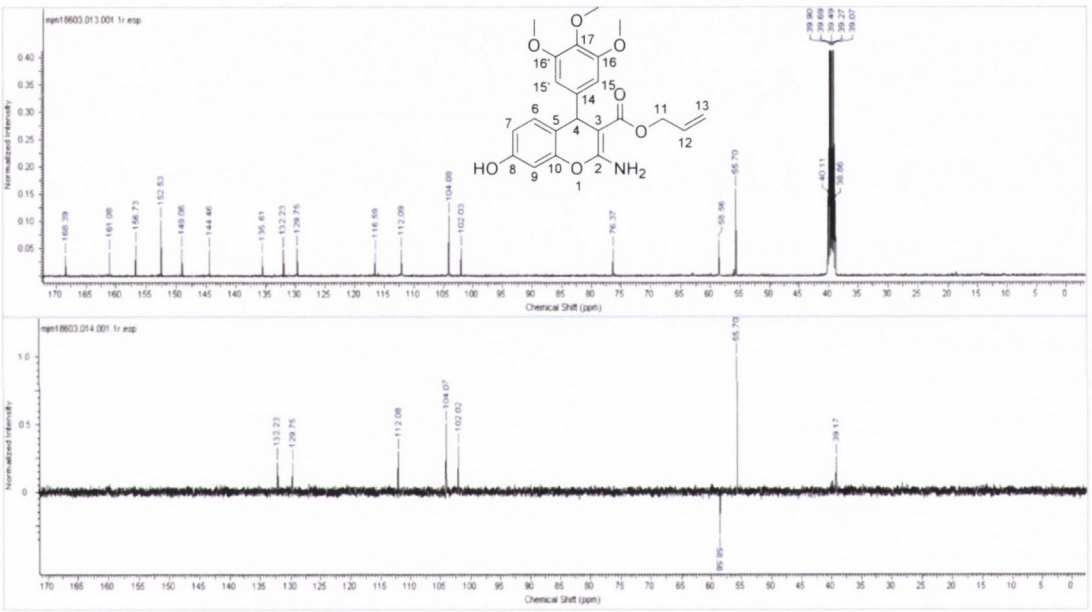

Figure 2. 23 ^{13}C NMR (upper) and DEPT 135 (lower) spectra for benzopyran BE76

In ^{13}C and DEPT-135 carbon NMR spectra (Fig 2.23) for compound **BE76** the chiral CH at C4 is observed at 38.86 ppm in the ^{13}C and 39.17 ppm in the Dept 135 spectrum. The absorption at 55.70 ppm is assigned to the three OCH_3 groups C16, C16′ and C17. At 58.56 ppm a positive signal is observed in the ^{13}CNMR for the CH_2 group at C11 and a negative peak in the DEPT 135. At 76.37 ppm the signal for the carbon on the C3 side chain is observed in the ^{13}C spectrum. From 102 ppm to 135 ppm the aryl CH carbons were assigned and the quaternary carbons were observed between 144 ppm to 168 ppm. The tertiary carbons (CH) were assigned as follows: at 102.03 ppm the CH at C9, at 104.08 ppm the CH at C15 and C15′, at 116.59 ppm the carbon at the C5 position, at 129.75 ppm the CH at C13 and at 132.23 ppm the CH at C6. The

quaternary carcons were assigned as follows: at 135.61 ppm the C at C14, at 144.46 ppm the C-OCH_3 at C17, at 149.06 ppm the C-OCH_3 at C16, C16', at 152.53 ppm the C-O at C10, at 156.73 ppm the C-OH at C8, at 161.08 ppm the O-C-N at C2, and lastly at 168.39 ppm the C=O group was observed.

The IR spectrum absorbances for compound **BE76** were identiifed as follows: the characteristic OH absorption was noted at 3560.58 cm^{-1}; for the NH_2 group, the absorbances at 3464.12 cm^{-1} and 3379.72 cm^{-1} were observed, and for the C=O group, the characteristic absorbance at 1671.47 was noted, while the absorbances at 1645.91, 1636.49 and 1628.93 cm^{-1}.were attributed to the C=C and aromatic functional groups.

In the mass spectrum HRMS (EI) for **BE76,** the molecular ion for $C_{22}H_{23}NNaO_7$ [M^+ + Na] requires (m/e) 436.1372; the value found was 436.1382, (+2.2 ppm). The structure of the novel allyl 4-(3,4,5-trimethoxyphenyl)-2-amino-4*H*-chromene carboxylate ester **BE76** was thus confirmed.

2.7.3 XRD Crystallography Study of 4-(3,4,5-trimethoxyphenyl)-2-amino-4*H*-chromene carboxylate ester BE79

Figure 2.24 (a) shows the crystal structure of chromene compound **BE79** which was obtained after purification and recrystallisation using slow solvent evaporation. As with all of the compounds produced in this series, compound **BE79** is chiral and therefore is obtained as a racemic mixture (50:50) ratio as can be seen below. The ORTEP representation of compound **BE79** is displayed in Figure 2.24(b) clearly showing the two enantiomers.. The crystal data and structure refinement for **BE79** are displayed in Table 2.10.

(a)

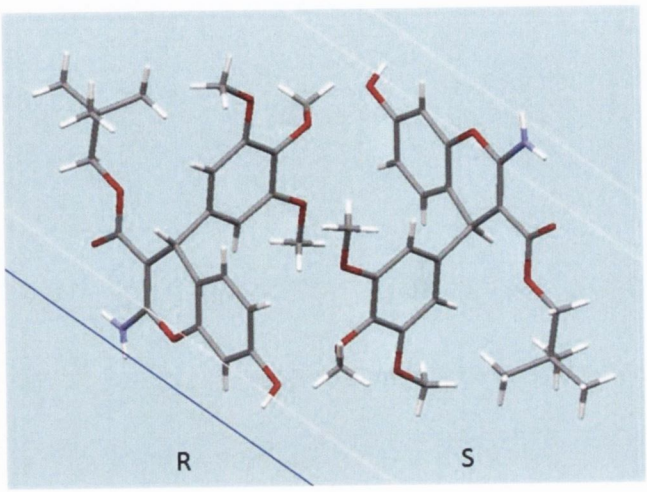

(b)

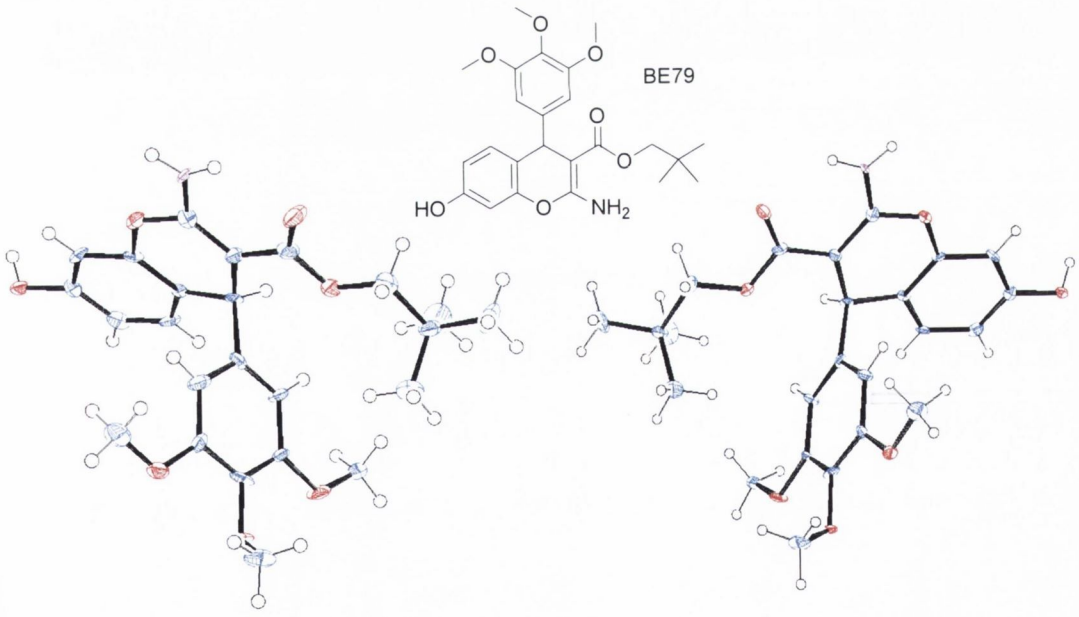

(c)

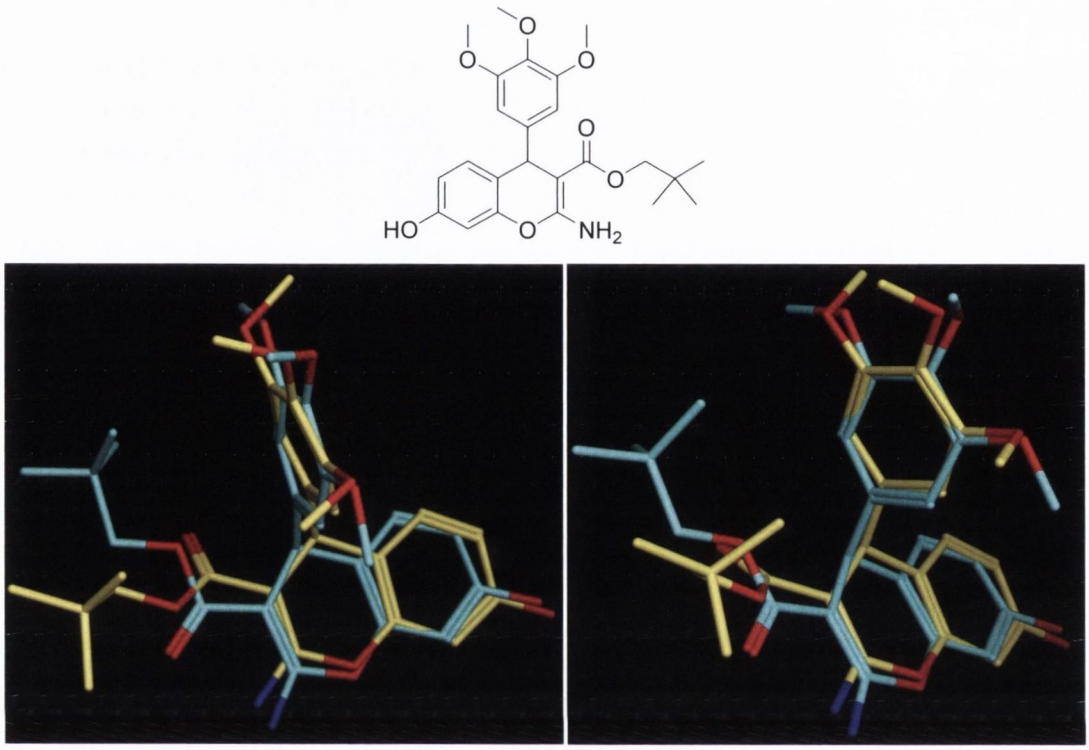

Figure 2. 24(a) BE79 X-Ray Crystal Structure showing enantiomers (b) ORTEP representation of the X-ray crystal structure of BE79 showing both R and S isomers with 50% thermal ellipsoids; (c) Crystal structure of compound BE79 (Blue) flexibly aligned over energy minimised structure of BE79 (yellow)obtained with MOE software

The XRD crystal structure of **BE79** was compared with an energy minimised conformer of compound **BE79** using the MOE (Molecular Operating Environment software; see Chapter 3). Figure 2.24(c) shows the XRD crystal structure of **BE79** (blue) flexibly aligned over energy minimised version of **BE79** (yellow). Both structures are fixed. As can be seen both crystal structure and energy minimised structure are a very similar fit over each other. However, minor differences can be seen in the conformations of the trimethoxy substituent of the aryl ring and a more noticeable difference can be seen in the conformations of the *tert*butyl ester feature on the C-3 side chain. In the MOE energy minimised model (yellow) the side chain ester is positioned at a 180° angle but on the actual crystal structure image (blue) the side chain can be seen to be at a 90° angle.

Identification code	shelxl	
Empirical formula	C96 H116 N4 O28	
Formula weight	1773.93	
Temperature	150(2) K	
Wavelength	0.71073 Å	
Crystal system	Monoclinic	
Space group	P2(1)/c	
Unit cell dimensions	a = 6.2430(12) Å	α= 90°.
	b = 11.639(2) Å	β= 99.61(3)°.
	c = 30.160(7) Å	γ = 90°.
Volume	2160.7(7) Å3	
Z	1	
Density (calculated)	1.363 Mg/m3	
Absorption coefficient	0.100 mm-1	
F(000)	944	
Crystal size	0.40 x 0.20 x 0.10 mm3	
Theta range for data collection	1.37 to 25.00°.	
Index ranges	-7<=h<=5, -13<=k<=13, -35<=l<=35	
Reflections collected	16248	
Independent reflections	3730 [R(int) = 0.1125]	
Completeness to theta = 25.00°	97.70%	
Absorption correction	Semi-empirical from equivalents	
Max. and min. transmission	1.0000 and 0.5919	
Refinement method	Full-matrix least-squares on F2	
Data / restraints / parameters	3730 / 0 / 297	
Goodness-of-fit on F2	1.365	
Final R indices [I>2sigma(I)]	R1 = 0.1714, wR2 = 0.4146	
R indices (all data)	R1 = 0.1942, wR2 = 0.4423	
Largest diff. peak and hole	0.621 and -0.702 e.Å-3	

Table 2. 10 Crystal data and structure refinement for shelxl. BE79

2.8 Series 8: 2,7-Diamino-4*H*-chromenes with arylbenzyloxy ether substituent at C-4 and selected esters at C-3.

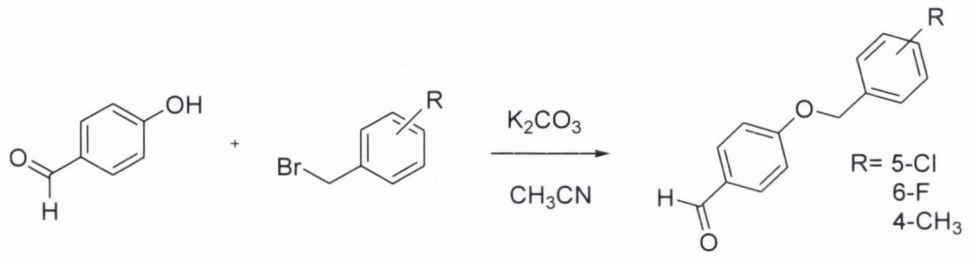

Scheme2. 17 General synthesis of benzyloxybenzaldehydes

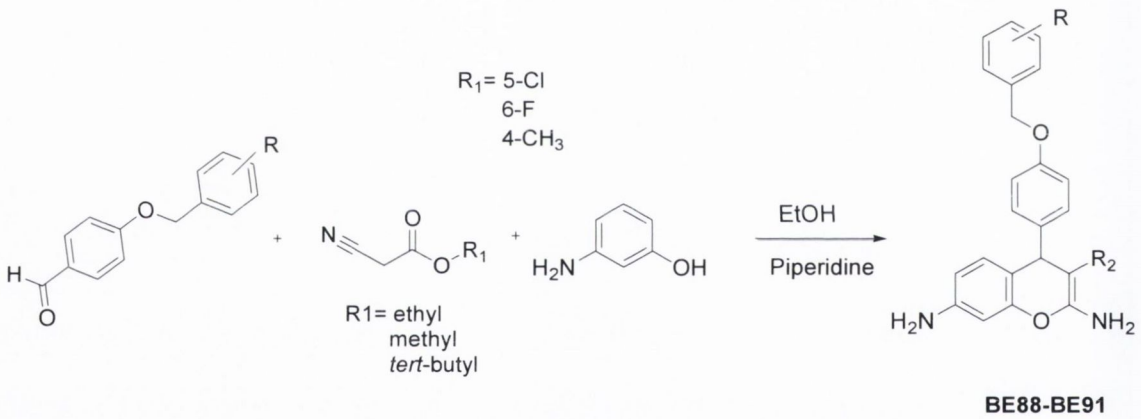

BE88-BE91

Scheme2. 18 General synthesis of 2,7-diamino-4-benzyloxyphenyl-4H-chromenes BE88-BE91

2.8.1 Results series 8: Synthesis of the library of 2,7-diamino chromene compounds

Series 8 compounds **BE88-BE91** (2,7-diamino- 4-benzyloxyaryl)-4*H*-chromenes) were prepared to investigate the effect on biological activity of the introduction of the primary amine(NH_2) in place of the phenolic group at positopn 7 of the chromene scaffold. The desired chromenes were prepared firstly by synthesis of the appropriate benzyloxybenzaldehydes by reaction of 4-hydroxybenzaldehyde, the appropriate benzyl bromide and potassium carbonate in acetonitrile (scheme 2.17). The appropriate benzyloxybenzaldehyde was then reacted with 3-aminophenol and a

selection of varied alkyl cyanoacetates in the presence of base piperidine (scheme 2.18.) in solvent ethanol. This reaction gave good yields in the range 11-64% (see results Figure 2.25). A selection of substituted 4-benzyloxyaryl- 4*H*-chromene compounds was produced with variation of substituents (R_2) at position C-3 of the chromene ring system.

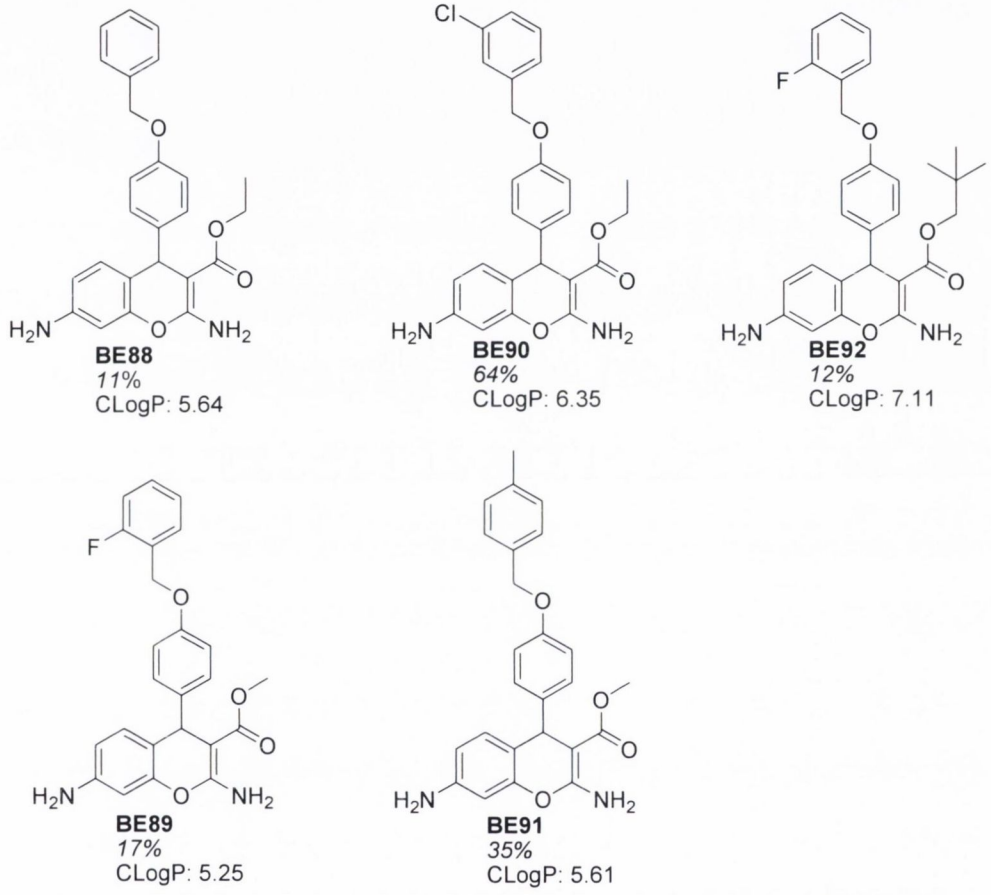

Figure 2. 25 2,7-Diamino-4-benzyloxyphenyl-4H-chromenes BE88-BE91

*CLogP calculated using Chemdraw Ultra version.

Figure 2.25 shows the structures of the five 2,7-diaminochromenes **BE88-BE91** synthesised for the series. Synthesis was achieved using 3-aminophenol in place of the previously used resorcinol for the Knoevenagel condensation reaction. Yields ranged from 11 to 64%. CLogP values ranged from 5.2 to 7.11 depending on the alkylcyano acetate ester chosen. It may be possible to modulate these values further with introduction of a phenolic hydroxy group on the 4-benzyloxyaryl ring.

2.8.2 Spectroscopic identification

Identification of each chromene compound in this series was achieved using Nuclear Magnetic Resonance (NMR) spectroscopy, Infared (IR) spectroscopy and Mass spectrometry(MS). The following figures 2.26 and 2.27 display the NMR spectra for compound **BE89.** Discussion of the NMR spectra of this compound is used as an example of the characteristic features in the identification of this series.

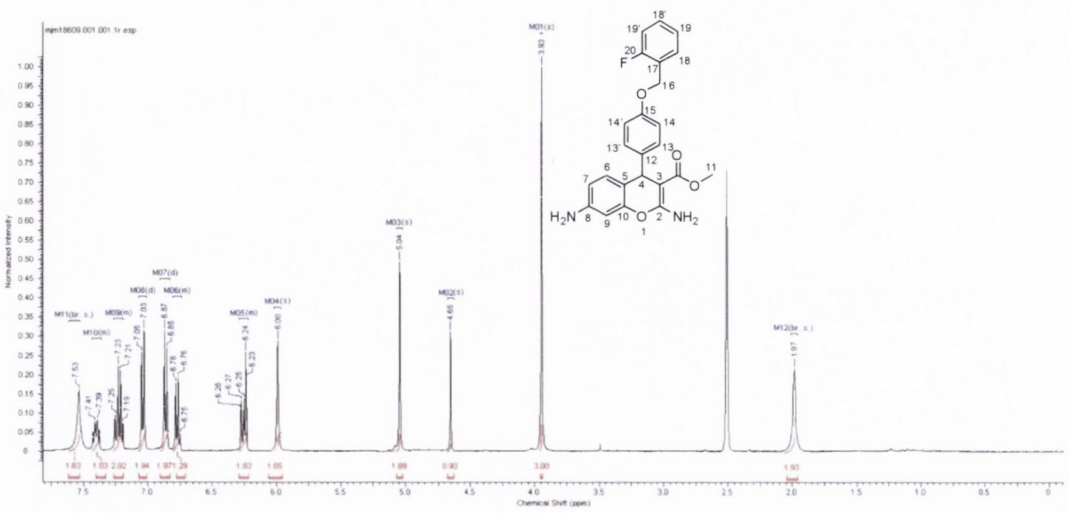

Figure 2. 26 ^{1}H NMR spectrum of BE89

In the ^{1}H NMR spectrum (in figure 2.26) for compound **BE89** displayed, a broad absorbance for one of the NH_2 group at C2 is identified at δ 1.97 integrating for 2 protons. At δ 3.93 a singlet signal is observed indicating the methyl ester at C11, and integrated for 3 protons. At δ 4.65 the chiral CH at C4 is seen as a singlet integrating for 1H. At δ 5.04 the OCH_2 at position C16 is seen as another singlet integrated to 2H. At δ 6.00 a doublet is observed, 1H, and integrated for J=7.51, is identified as Ar-H at the C9 position. Between δ 6.23 to 6.28 a multiplet is observed, integrating for 2H, and assigned to the Ar-H protons at C7. Between δ 6.75 to 6.78 is another multiplet, 1H, indicating the Ar-H at C6. A doublet is observed at δ 6.85 with a J coupling constant value of 8.41 Hz, integrating for 2H, and assigned to the Ar-H protons at C14 and C14′. At δ 7.03 another doublet is indicated, with a J coupling value of 8.53 Hz, and is integrated to 2H, indicating the Ar-H protons at C19, C19′ and C13 and C13′. Between δ 7.19 and 7.25 a multiplet is seen, integrating to 2H, for the Ar-H at C18 and C18′. At δ 7.39 another multiplet is identiifed, integrating for 1H, indicating the Ar-

H at C6. Finally at δ 7.53 a broad singlet peak is observed, integrated to 2H corresponding to the second NH_2 group at C8.

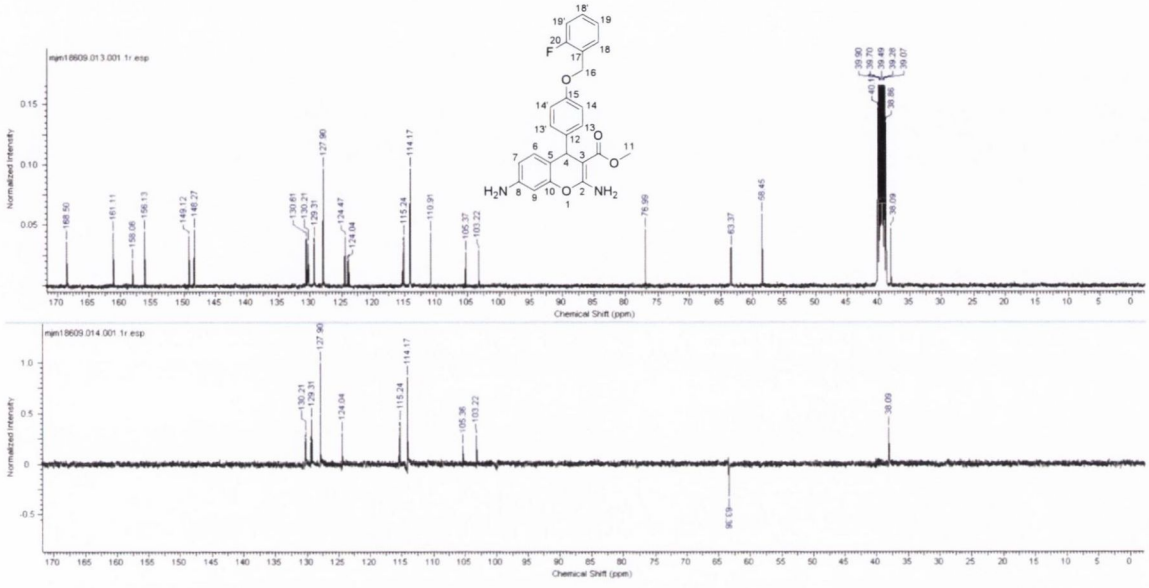

Figure 2. 27 ^{13}C NMR (upper) and DEPT-135 (lower) spectra for benzopyran compound BE89

In ^{13}C and DEPT-135 carbon NMR spectra in fig 2.27 for compound **BE89** the C4 chiral CH can be seen at 38.09 ppm in both the ^{13}C and the DEPT-135 spectra. The C11 methyl ester peak is seen at 58.45 ppm in the ^{13}C spectrum. The C16 OCH_2 is observed assigned to the signal at 63.37 ppm as a positive peak in the ^{13}C spectrum and is confirmed as a negative peak in the DEPT-135 spectrum. At 76.99 ppm the C3 carbon is observed. All of the aryl tertiary carbons(CH) occurred between 103 ppm to 130 ppm together with with two quaternary carbons occurring in this region and the remaining quaternary carbons observed as positive peaks in the ^{13}C spectrum from 103 ppm to 168 ppm; the CH at the C9 position was identified at 103.22 ppm, the signal at 105.37 ppm indicates the CH group at the C7 position, the signal at 110.91 ppm was assigned to the C at C5, while the CH at the C14 position was identified at ppm 114.17. The following signals were also assigned:at 115.24 ppm the CH at C19', at 124.04 ppm the CH at C19, at 124.47 ppm the C at the C17 position, at 127.90 ppm the CH at C18, at 129.31 ppm the CH at C13, C13' and C18', and at 130.21 ppm the CH at C12. The following quaternary signal were aso identified: at 130.61 ppm the C at C12, at 148.27 ppm the C-N at C8, at 149.12 ppm the C-O at position C10, at 156.13 ppm the signal indicates the Bn-C-O at C15, at 158.06 ppm the O-C-N at C2, at 161.11 ppm the C-F at C20 and at 168.50 ppm the C=O group is assigned.

In the IR spectrum for compound **BE89** the absorbances were as follows; 3494.05 and 3384.81 cm^{-1},(NH_2) ; 1668.37 cm^{-1}, (C=O) and 1630.31 and 1622.41 cm^{-1} for the C=C group absorptions..

The mass spec HRMS (EI) for **BE89,** was determined for $C_{24}H_{22}FN_2O_4$ [M^+ + H] which requires (m/e) 421.1564; the value found was 421.1564, (+0.1 ppm). The analysis confirmed the identity of the novel 2,7-diamino-4-(2-fluorobenzyloxyphenyl)-4*H*-chromene methylcarboxylate **BE89**.

2.9 Series 9: 4-Benzyloxyaryl chromenes with N,N-dimethylamino substituent group at C-7

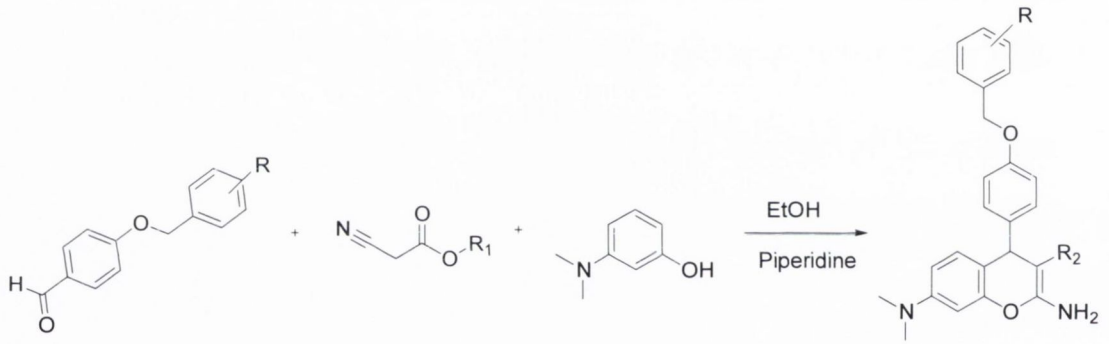

Scheme2. 19 General synthetic route for 7-dimethylamino-2-amino-4-benzyloxyphenyl-4H-chromenes BE93-98

Scheme 2.19 shows the synthetic route used for the 7-dimethylamino-2-amino-4-benzyloxyphenyl-4*H*-chromenes ***BE93-98***, performed using 3-dimethylaminophenol with structural variation on the benzyloxy position. The reaction produced 7-dimethylamino substituted chromenes in contrast to the 7-amino substituted compounds obtained in series 8. R_1 was varied with a selection of benzyloxy substitutions, along with a variety of esters R_2 on the C-3 position of the chromene ring. These products would allow a study of the effect of replacement of the C-7 OH and NH_2 of the previous series of compounds with a N,N-dimethylamino functional group. Yields ranged from 4 to 91%. CLogP values were between 7.2 to 11.3, and are observed to be higher than compared with the previous 2,7-diamino series 8, due to

the lipophilic structures of the esters used and also the tertiary amine at C-7, compared to the primary amine as in previous series 8. The different benzyloxy type substitutions were chosen to complement the compounds synthesised in series 8, and to afford a range of compounds for structure-activity studies

2.9.1 Results series 9

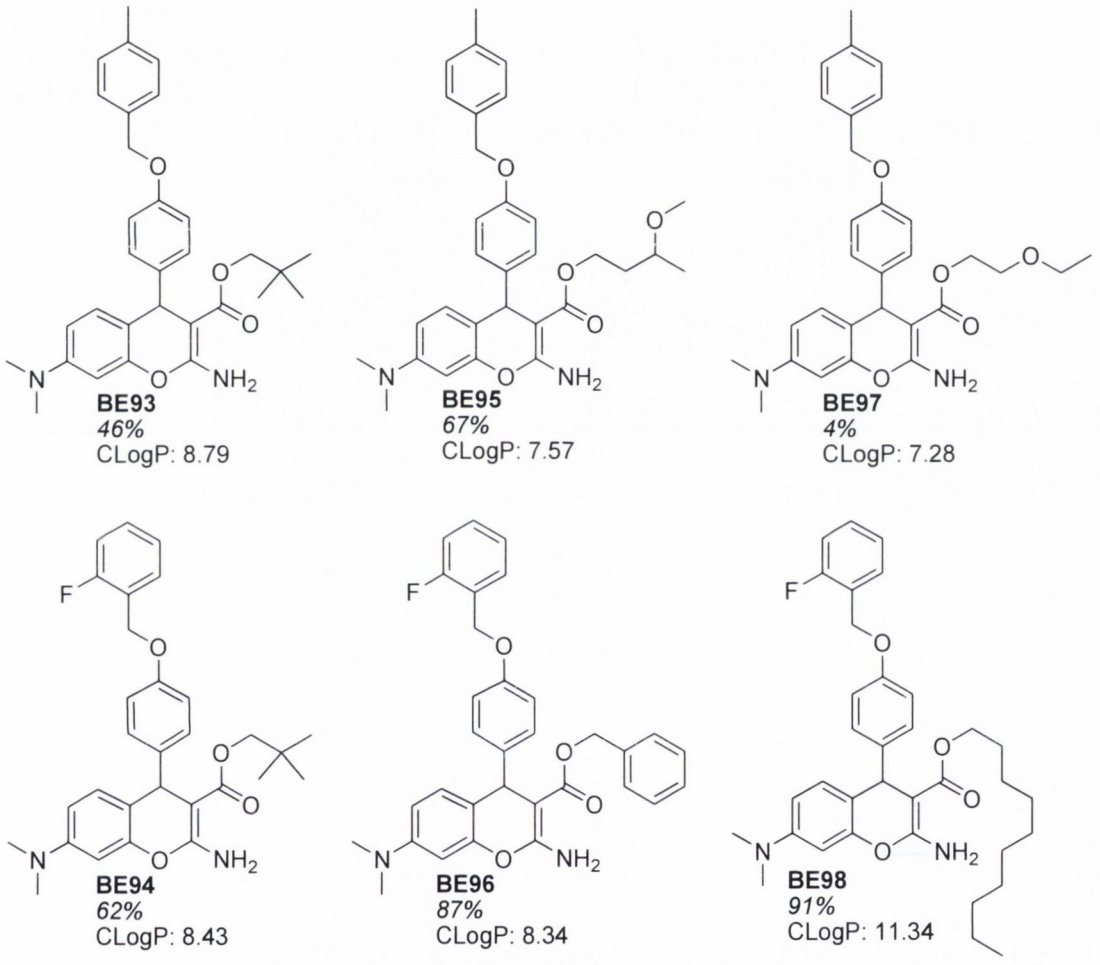

Figure 2. 28 Dimethylamino-4-(4-benzyloxyphenyl)-4H-chromenes BE93-BE98

*CLogP calculated using Chemdraw Ultra version.

The results of series 9 displayed in Figure 2. 28 are a series of six 7-N,N-dimethylamino-4-(4-benzyloxyphenyl)-4*H*-chromenes synthesised using the Knoevenagel condensation reaction; the general synthesis shown in scheme 2.19.

2.9.2 Spectroscopic identification

Identification of each chromene compound for series 9 was achieved using Nuclear Magnetic Resonance (NMR) spectroscopy, Infared (IR) spectroscopy, and Mass spectrometry(MS). The following figures 2.29 and 2.30 display the NMR spectra for compound **BE93.** Discussion of the NMR spectra of **BE93** is used as an example of the structural identification of each compound in this series.

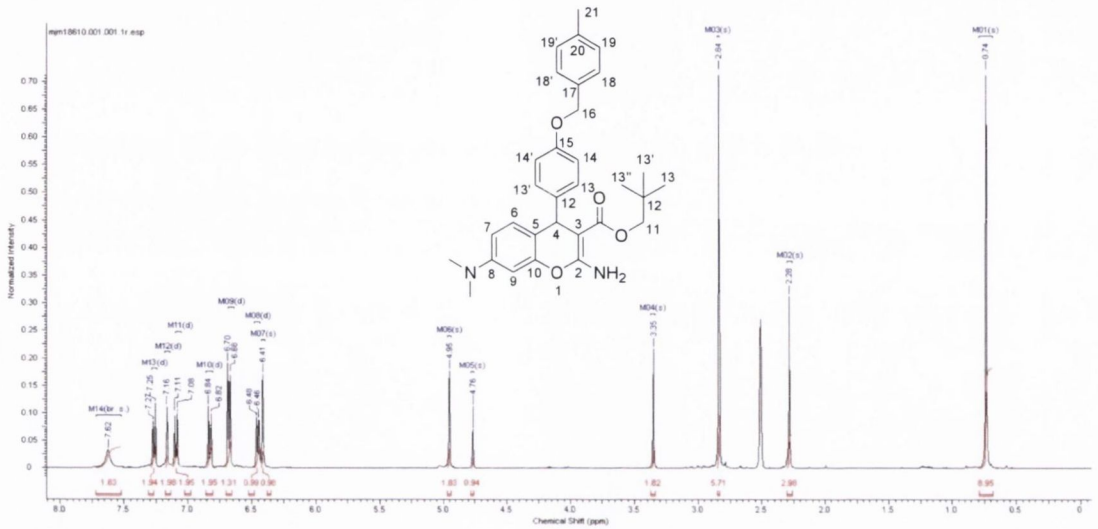

Figure 2. 29 ^{1}H NMR Spectrum for compound BE93

In the ^{1}H NMR spectrum displayed in figure 2.29 for compound **BE93**, a singlet absorbance for the three CH_3 groups C13, C13' and C13'' on the neopentyl ester chain were identified at δ 0.74 and is integrated for 9 protons. The methyl group on position C21 can be seen at δ 2.28 as a singlet integrated for 3H. The C8 N,N-dimethylamino group was identified as a singlet at δ 2.84 and integrated for 6H. At δ 3.35 a singlet was observed for the CH_2 group at position C11 adjacent to the ester, and is integrating for 2H. At δ 4.76 a singlet denoted the C4 chiral CH and integrates for 1 proton. The singlet at δ 4.95 and integrated to 2H, is assigned to the benzyloxy CH_2 group at the C16 position. At δ 6.41 a singlet signal is observed, integrated to 1H, indicating the Ar-H proton at C9. At δ 6.46 a doublet is seen, J=6.88 Hz, integrating for 1H, and assigned to the Ar-H at C7. Another doublet signal is observed at δ 6.68, J=7.42, integrating for 1H, for the Ar-H at C6. At δ 6.82 a doublet signal was observed with a coupling J constant of 7.14 Hz, and integrating for 2H, for the Ar-H protons at the C14 and C14' positions. At δ 7.08 a doublet absorbance can be observed, with a coupling constant value of J=7.04 Hz, and integrating for 2H, indicating the Ar-H protons at positions C13 and C13. At δ 7.16 another doublet was observed, J=8.03 Hz,

integrating for 2H, for the Ar-H protons at C19, C19'. A final doublet signal was observed at δ 7.25 with a *J* coupling value of 7.22 Hz, integrating for 2H, and assigned to the Ar-H protons C18 and C18' positions. Finally a broad singlet absorbance was observed at δ 7.62 and integrating for 2H, this indicate the NH_2 group protons at the C2 position.

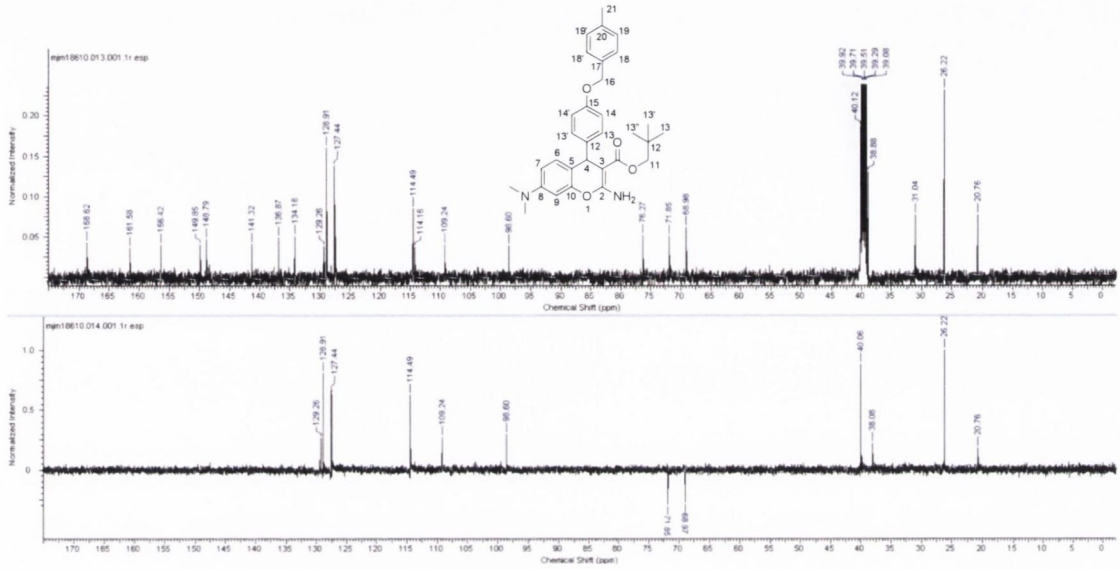

Figure 2. 30 ^{13}C NMR (upper) and DEPT 135 (lower) spectra for benzopyran BE93

In the ^{13}C and DEPT-135 carbon NMR spectra displayed in fig 2.30 for compound **BE93** the CH_3 group at position C21 was observed at 20.76 ppm in both the ^{13}C and the DEPT-135 spectra. The signal for the three methyl groups of C13, C13' and C13'' are observed at 26.22 ppm in both spectra. The absorbance of the quaternary C12 carbon attached to the three methyl groups on the ester chain can be seen at 31.04 ppm as a positive peak in the ^{13}C spectrum. The C4 chiral CH absorbance is observed at 38.88 ppm in both spectra. The dimethyl amino group carbons at C8 are identified at 40.12 ppm in both spectra. The C15 OCH_2 of the benzyloxy group is observed at 68.98 ppm as a positive peak in the ^{13}C and a negative peak in the DEPT-135 spectrum. The C11 OCH_2 group of the ester chain was observed at 71.85 ppm as a positive peak in the ^{13}C and confirmed as a negative peak in the DEPT-135 spectrum. The carbon of the C3 ester chain was observed at 76.27 ppm as a positive peak on the ^{13}C spectrum. There are 6 absorbances indicating the aryl hydrogens (CH) from 98 ppm to 129 ppm. There is one quaternary carbon identified at 114.16 ppm and the remaining quaternary carbon signals are seen from 134 ppm to 168 ppm. The following tertiary aromatic carbon signals are assigned as follows: at 98.60 ppm the CH group at position C9, at

109.24 ppm the CH of the C7 position, at 114.16 ppm the carbon of the C5 position, at 114.49 ppm the CH of C14 and C14', at 127.44 ppm the CH groups of C18 and C18', at 128.91 ppm the CH of positions C19, C19' and C13, C13', at 129.26 ppm the CH of C6. The following quaternary carbon signals were assigned: at 134.18 ppm the carbon of C12, at 136.87 ppm the C of C20 and at 141.32 ppm the carbon of C17. In addition the followoing quaternary signals were identified: at 148.79 ppm the C-N at C8, at 149.85 ppm the C-O of the C10 position, at 156.42 ppm the C-O of C15, at 161.58 ppm the O-C-N at C2, and finally the quaternary signal for the C=O group was assigned at 168.62 ppm

The characteristic IR spectrum absorbances for compound **BE93** were identified as follows; 3475.83 and 3263.98 cm^{-1},(NH_2) 1666.12 cm^{-1},(C=O) and 1634.48 and 1611.68 cm^{-1}.(C=C).

The mass spectrum HRMS (EI) for **BE93,** $C_{31}H_{37}N_2O_4$ [M^+ + H] requires (m/e) 501.2753, and the value found was 501.2774, (+4.1 ppm). This result confirmed the structure proposed for the novel 7-dimethylamino-2-amino-4-methylbenzyloxyphenyl-4H-chromene compound.

2.10 Series 10: 4-Arylchromene compounds synthesised with ester subsuituents introduced at C-7

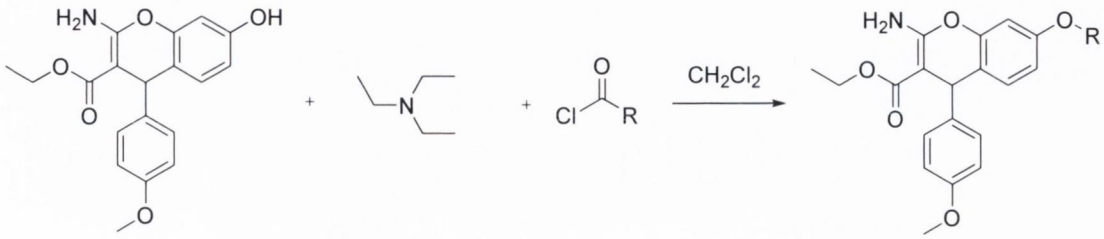

BE6 **BE99-BE111**

Scheme2. 20 General synthesis of 2-amino-4-methoxyphenyl-4H-chromenes with ester substituents at C-3 and C-7

A series of chromenes **BE99-BE111** with structural variations on the ester substituent at C-7 was also synthesised. This series of ester derivatives, 13 in total, were obtained by reaction of the chromene phenolic group at C-7 of compound **BE6** with an appropriate acid chloride (scheme 2.20). The chromene products were obtained using catalytic triethylamine and structurally varied acid chlorides in anhydrous solvent CH_2Cl_2 to yield the diester products **BE99-BE111**. These ester compounds were designed to investigate the effect of introduction of a potentially stericallly hindered substituent at C-7, rather than at C-3 as outlined in the previous series of compounds (e.g. see Series 6 chromenes) and monitor the potential effect on the ER LBP. Initial molecular modelling experiments and biochemical ER binding studies had indicated that exploring the introduction of lipophilic ester substituents at the C-7 position of chromene **BE6** would be beneficial for optimising ER LBP interactions. (Chapter 1 and Chapter 4).

2.10.1 Results series 10

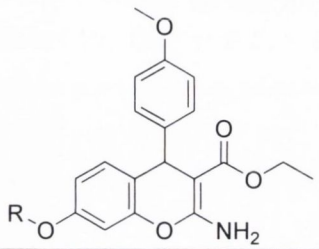

No.	R Group	% Yield	CLogP	No.	R Group	% Yield	CLogP
BE99		*52*	4.44	**BE106**	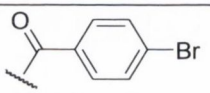	*76*	7.44
BE100	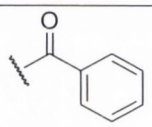	*20*	6.57	**BE107**	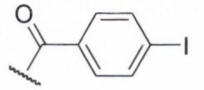	*86*	7.7
BE101	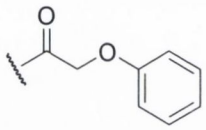	*23*	5.88	**BE108**	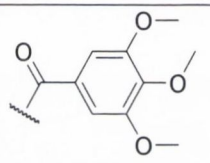	*44*	5.99
BE102	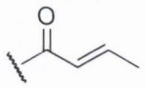	*73*	5.50	**BE109**	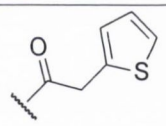	*51*	5.94
BE103	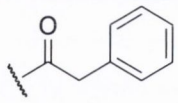	*88*	6.29	**BE110**	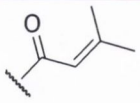	*27*	5.90
BE104	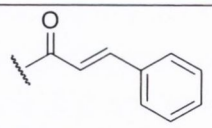	*89*	7.06	**BE111**	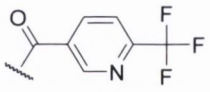	*50*	6.10
BE105	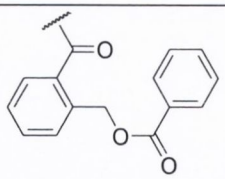	*39*	8.37				

Table 2. 11 Library of chromene compounds BE99-BE111 produced with structural variation in the ester substituent at C-7

*CLogP calculated using Chemdraw Ultra version.

Table 2.11 displays a wide variety of chromenes **BE99-BE111** with substituted esters at C-7. Synthesised products contain a second ester group at C-7 of the chromene product in addition to the ester at C-3 as in the previous series 1-9. Yields were in the range 20 to 89 %. CLogP values were higher in the series 10 when compared to the previous compounds in series1-9 due to the introduction of the additional lipophilic ester at C-7 in place of the hydrophilic polar C-7 OH, and in addition to the C-3 ethyl ester.

2.10.2 Synthesis of4*H*-chromene ester BE108

Scheme 2.21 shows the synthesis of the 4*H*-chromene ester **BE108**.

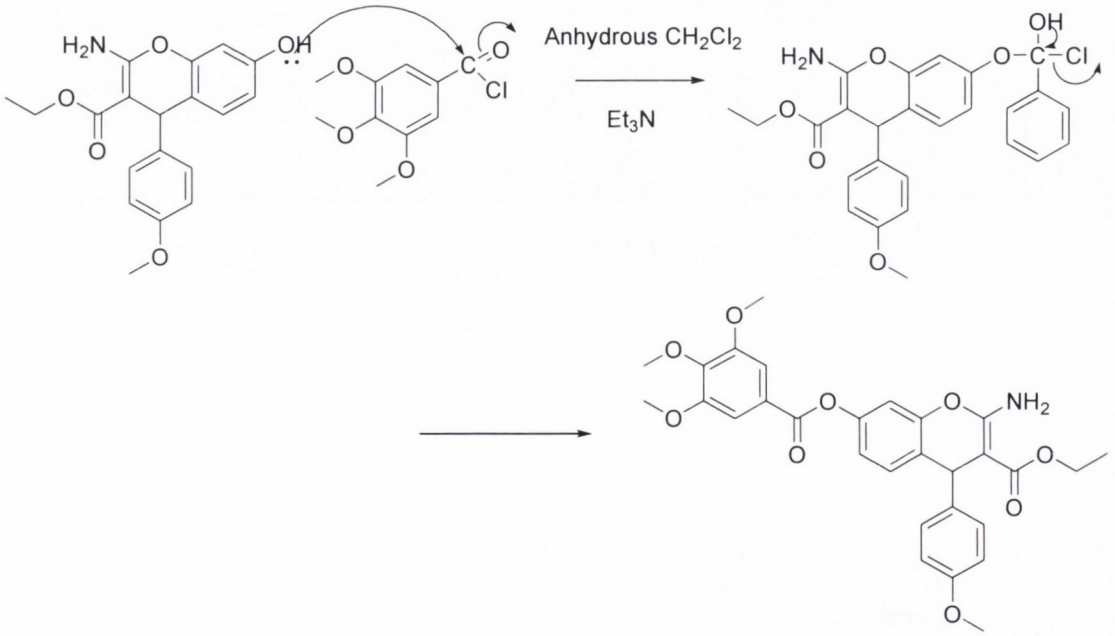

Scheme2. 21 Synthesis of compound BE108

2.10.3 Spectroscopic identification

Identification of each chromene compound was carried out using Nuclear Magnetic Resonance (NMR) spectroscopy, Infared (IR) spectroscopy, and Mass spectrometry(MS). The following figures 2.31 and 2.32 display the NMR spectra for compound ***BE108***. Discussion of the NMR spectra is provided as an example of the identification of each molecule in this series.

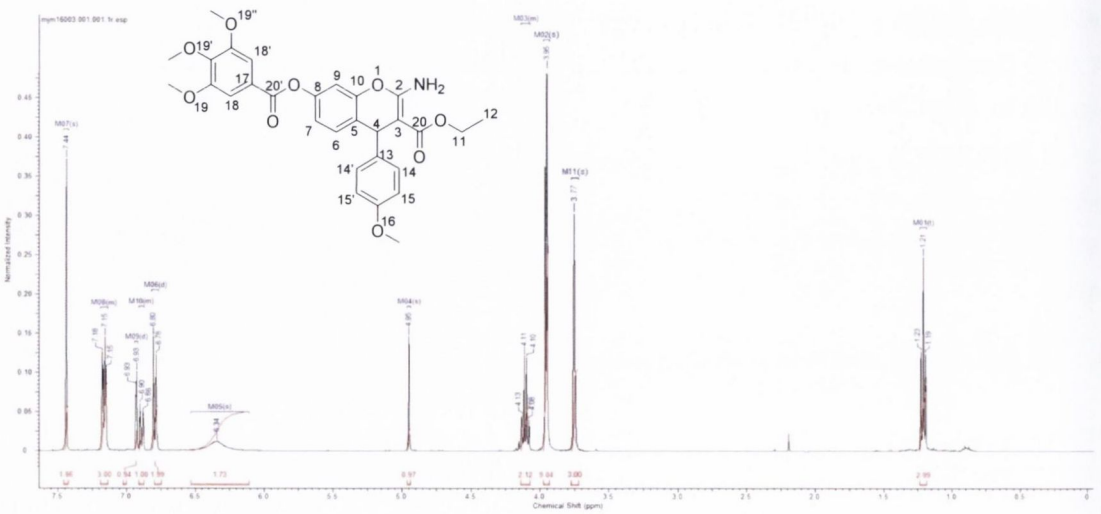

Figure 2. 31 ^{1}H NMR spectrum for BE108

The ^{1}H NMR spectrum for the 7-(3,4,5-trimethoxybenzoyloxy)chromene compound **BE108** is illustrated in figure 2.31. At δ 1.21 there is a triplet absorbance for the CH_3 group on the ester chain at the C12 position, and is integrating for 3 protons with a *J* coupling constant value of 7.28 Hz. At δ 3.77 a singlet absorbance can be observed, integrating for 3H, indicating the OCH_3 group of the C16 position. At δ 3.95 a singlet signal is observed, integrating for 9H protons for the three OCH_3 groups of the C19, C19′ and C19″ positions. At δ 4.10 a multiplet is observed for the OCH_2 group at C11 on ethyl ester chain, this integrating for 2 protons. At δ 4.95 a singlet absorbance was observed integrated to 1H, for the chiral CH at C4. A broad peak can be seen at δ 6.34 for the NH_2 group at C2, 2H. At δ 6.78 there is a doublet, *J*=8.12, integrating for 2H, which is assigned to the Ar-H protons at positions C9 and C7. At δ 6.86 to 6.90 there is a multiplet, integrating for 1H, for the Ar-H proton at C15. At δ 6.93 a doublet occurred, integrating for 1H, *J*=7.01, indicating the Ar-H at C15′. Between δ 7.15 to 7.18 a multiplet can be seen, integrating to 3H, for the Ar-H protons at positions C14 , C14′ and C6. Finally at δ 7.44 a singlet absorbance is seen, integrating for 2H protons, indicating the Ar-H protons at positions C18 and C18′.

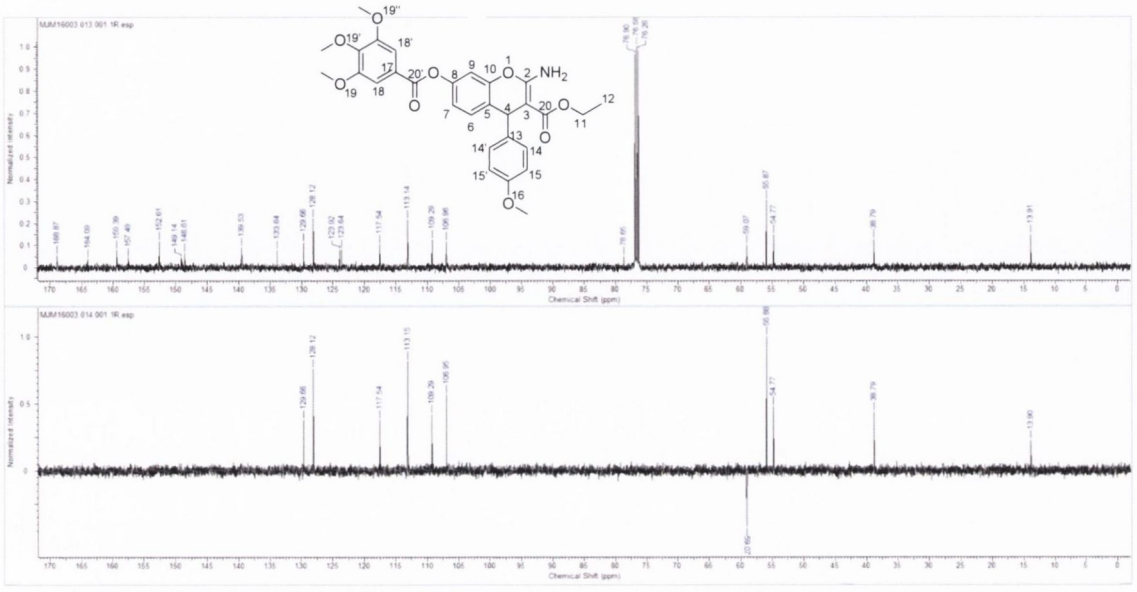

Figure 2. 32 ^{13}C NMR (upper) and DEPT 135 (lower) spectra for benzopyran BE108

In ^{13}C and DEPT-135 carbon NMR spectra in fig 2.32 for compound **BE108** the signal indicating the CH_3 group of position C12 on the ethyl ester chain was seen at 13.91 ppm confirmed in both spectra. The C4 chiral CH signal was seen at 38.79 ppm. At 54.77 ppm there is the signal assigned to C16 the methyl OCH_3, and at 55.87 ppm the signal for the trimethoxy groups at positions C19, C19′ and C19″ are observed. At 59. ppm the C11 CH_2 group occurred as a positive peak in the ^{13}C spectrum and a negative peak in the DEPT-135 spectrum. At 78.65 ppm the carbon at the C3 position was observed in the ^{13}C spectrum. From ppm 106 to 129 the aryl tertiary carbon (CH) signals can be seen. The remaining quaternary carbon signals are seen from 133 ppm ppm to 168 ppm. The tertiary aromatic carbon signals are identified as follows: at 106.96 ppm the CH at positions C18 and C18′, at 109.29 ppm the CH at C9, at 113.14 ppm the CH at C15 and C15′, and at 117.54 ppm the CH at C7. The following quaternary signals were assigned: at 123.64 ppm the carbon at the C5 position,and at 123.92 ppm the C at C17. The tertiary aromatic signals were also assigned: at 128.12 ppm the signal for the CHs at CH14 and CH14′ positions, and at 129.66 ppm the CH at C6. The remaining quaternary signals were also identified : at 133.64 ppm the C at C13, at 139.53 ppm the C-O at C19′, at 148.61 ppm the C-O at C8, at ppm 149.14 the C-O, at C19 and C19″, at 152.61 ppm the C-O at C10, at 157.49 ppm the C-OCH_3 at position C16, at 159.39 ppm the O-C-N at C2 position, at 164.09 ppm the C=O at the

C20' position, and finally at 168.87 ppm the signal was assigned to the C=O at the C20 position.

The IR spectrum absorbances for compound **BE108** were assigned as follows; 3495.88 and 3443.95 cm^{-1},(NH_2), 1680.87 and 1768.41 cm^{-1},(C=O) and 1649.29 and 1631.74 cm^{-1}(C=C).

The mass spectrum HRMS (EI) for compound **BE108,** with molecular formula $C_{29}H_{30}NO_9$ [M^+ + H] requires (m/e) 536.1921; the value found was 536.1927, (-1.1 ppm). The analysis confirmed the identity of the ethyl 7-(3,4,5-trimethoxybenzoyloxy)-2-amino-4-(4-methoxyphenyl)-4H-chromene-3-carboxylate compound **BE108**.

2.11 Series 11: *Bis* 4*H*-chromene compounds

A series of *bis* 4*H*-chromene compounds were synthesised from the phenolic chromene **BE6** using a series of bis acid chlorides to afford the novel bis 4*H*-chromene products **BE112 – BE115**.

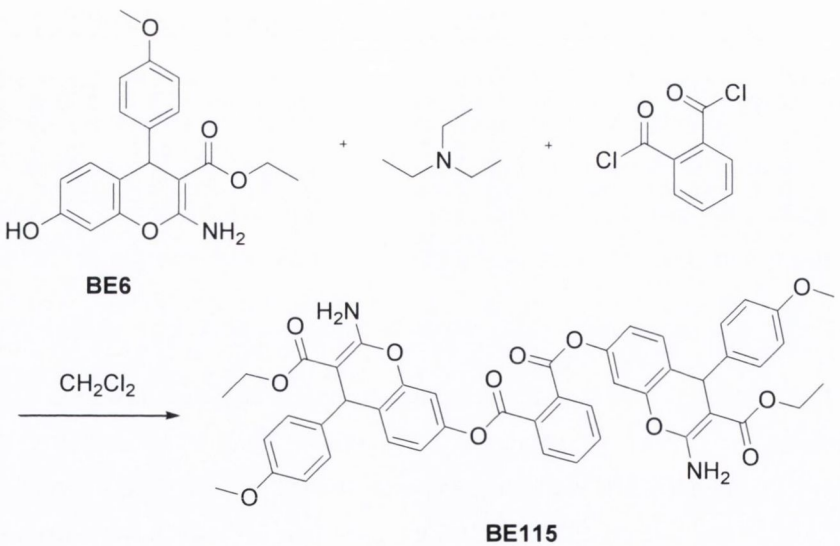

Scheme2. 22 Synthesis of bis-2-amino-4-methoxyphenyl-4H-chromene ester BE115

Synthetic route to novel *bis* (4*H*-chromen-7-yl)terephthalate and *bis* (4*H*-chromen-7-yl)phthalate esters

The synthesis of the *bis*chromene ester **BE115** is shown in reaction scheme 2.23. Starting phenolic chromene **BE6** was dissolved in anhydrous dichloromethane under a nitrogen atmosphere. The appropriate diacid chloride was then added and reaction was refluxed for 5 hours and monitored by TLC until no starting material remained. Mono ester product was not isolated. The reaction mechanism is indicated in scheme 2.23 and is initiated by reaction of the phenolic OH with the carbonyl of the acid chloride.

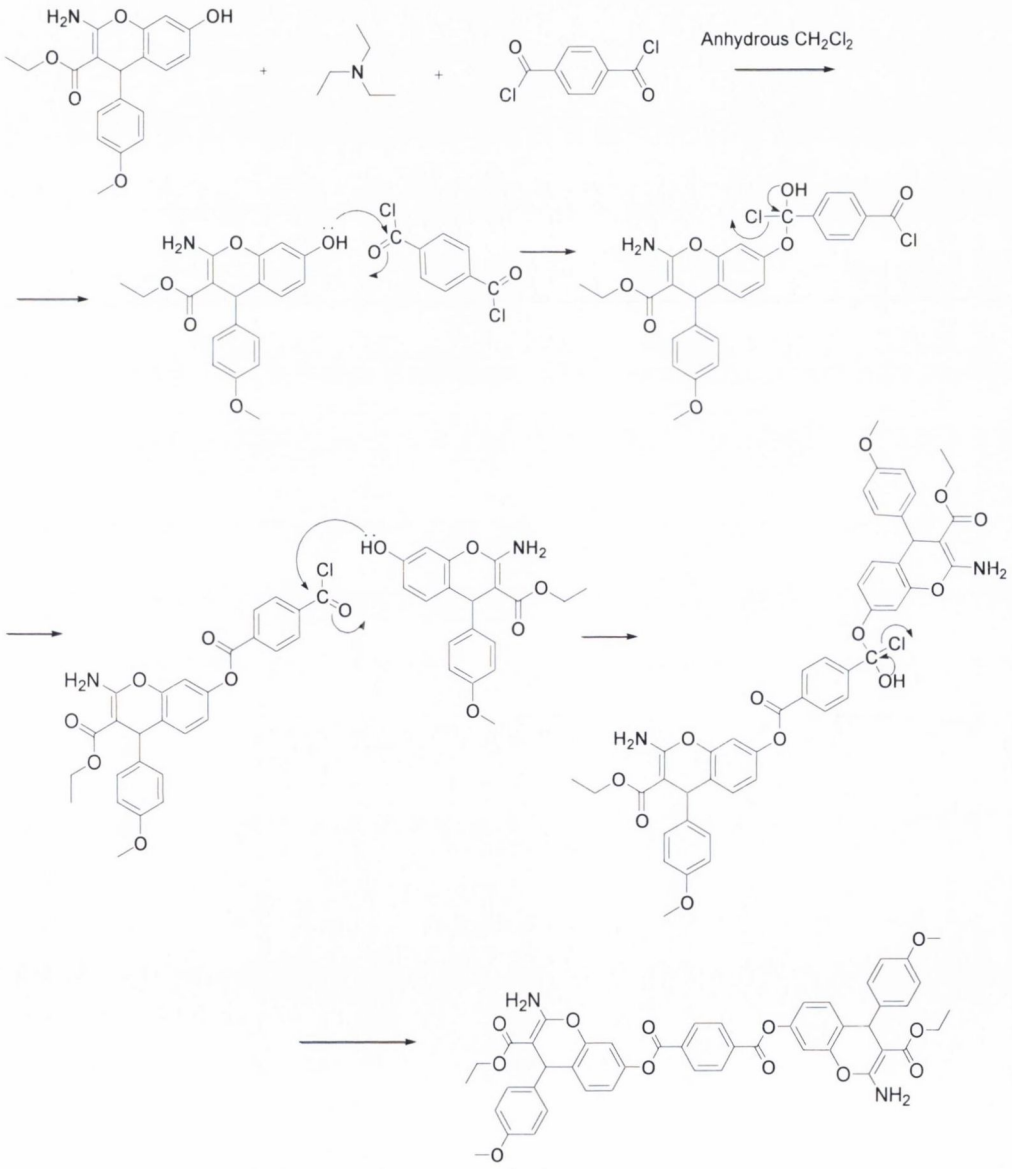

Scheme2. 23 Synthesis of diester BE113

2.11.1 Results series 11 *bis* chromenes

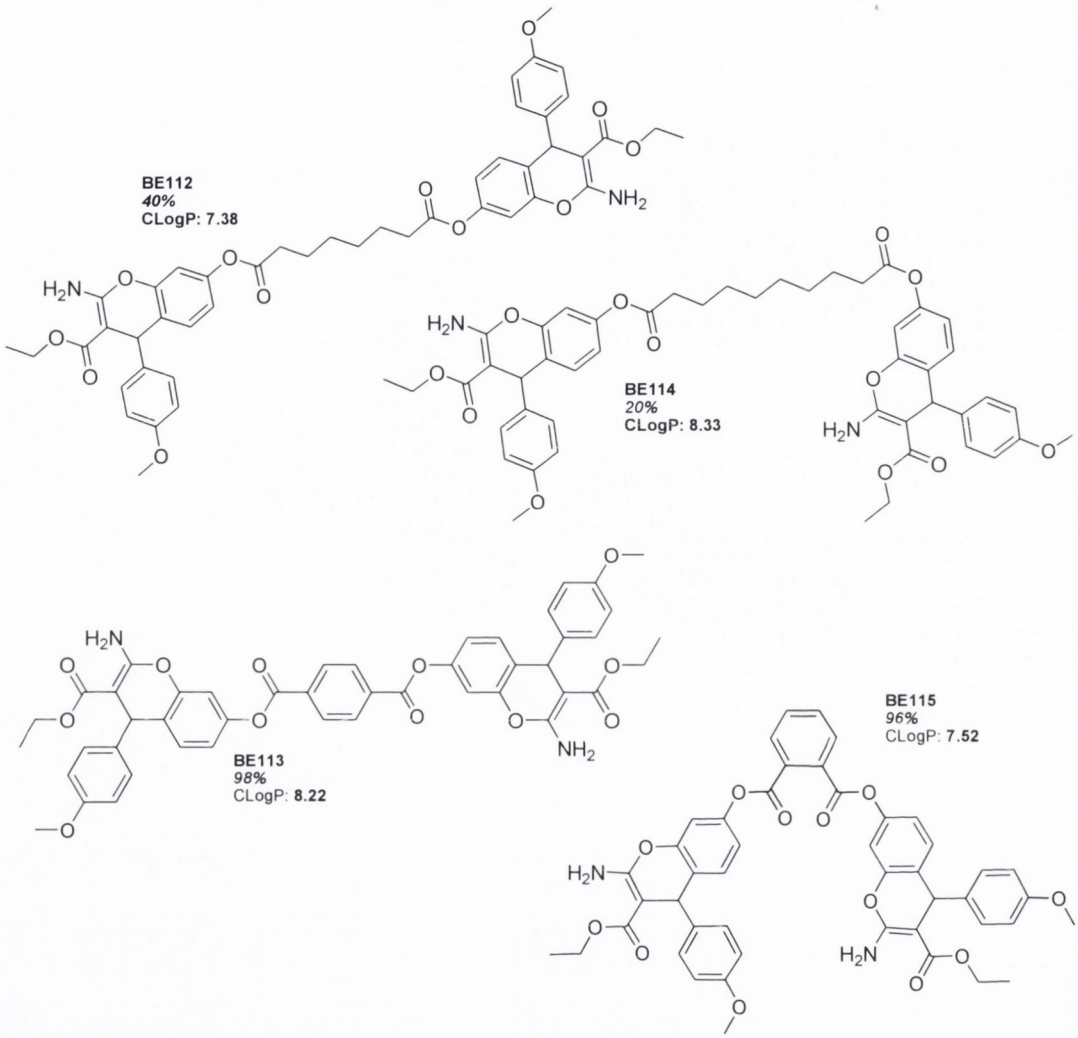

Figure 2. 33 Bis 4H-chromene compounds BE112-115

*CLogP calculated using Chemdraw Ultra version.

The *bis* chromenes prepared **(BE112 – BE115)** are displayed in figure 2.33. Four in total were produced in this series using phthaloyl, terephthaloyl, suberoyl and sebacoyl acid chlorides. The ability to synthesise *bis* chromenes using this reaction illustrates the possibility to obtain a extensive number of varied chromenes depending on the type of *bis* acid chloride used. Yields in series 11 were in the acceptable range of 20 to 98 percent. CLogP values ranged from 7.38 to 8.33 and were high, this was due to the large lipophilic non-polar structures produced and absence any of hydrophilic OH groups. The products contain two chromenes separated by a linking aliphatic or

aromatic functional group. The novel *bis* chromenes synthesised in this series would be of interest for *in vitro* biochemical evaluation and *in silico* molecular modelling as potential ligands targetting two potential ligand binding pockets in the estrogen receptor.

2.11.2 Spectroscopic Identification

Identification of each chromene compound was carried out using Nuclear Magnetic Resonance (NMR) spectroscopy, Infared (IR) and Mass spectrometry(MS). The following figures 2.34 and 2.35 display NMR spectra for compound **BE113.**

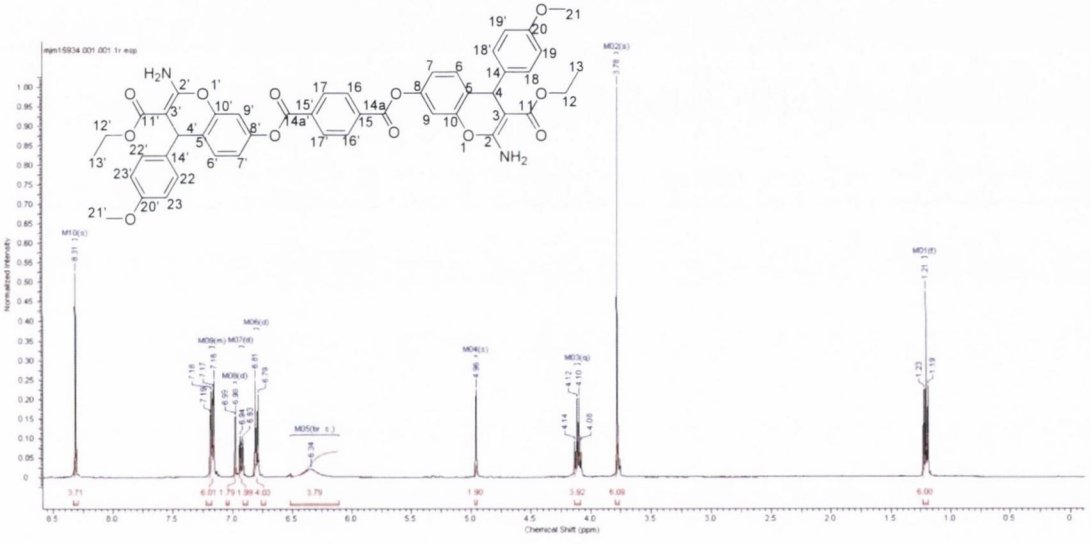

Figure 2. 34 ^{1}H NMR spectrum for BE113

In the ^{1}H NMR spectrum displayed in figure 2.34 for compound **BE113**, at δ 1.21 a triplet absorbance is assigned for the two CH_3 groups at C13 and C13′ on the ethyl ester and is integrated for 6 protons with a *J* coupling constant value of 7.02 Hz. At δ 3.78 there is a singlet absorbance, integrated for 6 protons, indicating the 2xOCH_3 groups at C21 and C21′. At δ 4.08 there is a quartet absorbance for the 2xCH_2 groups at C12 and C12′ and this signal is integrating for 4 protons. At δ 4.96 there is a singlet, 2H, corresponding to the 2xCH at C4 and C4′. At δ 6.34 a broad singlet is assigned to the absorbance for the 2xNH_2 groups. At δ 6.79 a doublet peak is seen, integrating for 4H protons and with a *J* coupling value of 8.12 Hz, assigned to the Ar-H groups at positions C9, C7 and C9′ and C7′. Between δ 6.93 to 6.94 a multiplet can be observed, integrating for 2H protons, indicating the Ar-H protons at C19 and C19′. At δ 6.98 a

doublet is observed, J=7.08 Hz, integrating for 2H, and is assigned to the Ar-H protons at C23 and C23′. Following this, a multiplet is seen between δ 7.16 to 7.19, integrating for 6H, for the Ar-H protons at C18, C18′ , C6, and C22, C22′ and C6′. Finally at δ 8.31, a singlet peak is observed integrating for 4 protons and this signal is assigned to the Ar-H protonss at positions C16, C16′ and C17, C17′.

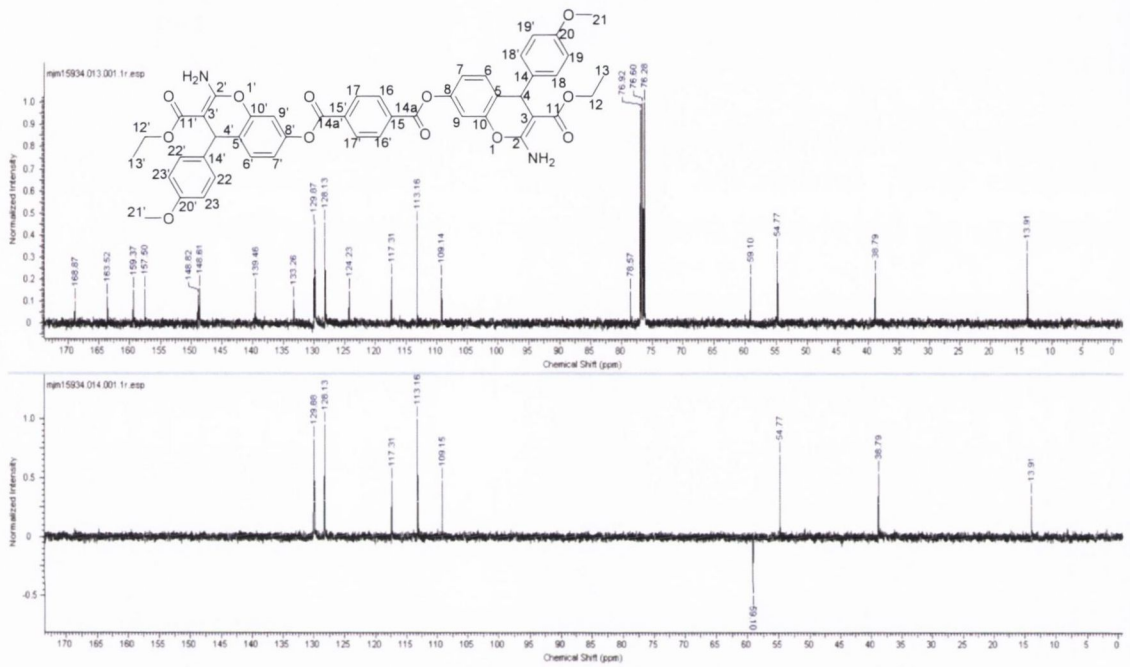

Figure 2. 35 ^{13}C NMR (upper) and DEPT 135 (lower) spectra for benzopyran diester BE113

In ^{13}C and DEPT-135 carbon NMR spectra in fig 2.35 for compound **BE113** the signal indicating the CH_3 groups at C13 and C13′ of the ethyl ester chain is seen at 13.91 ppm confirmed in both spectra. At 38.79 ppm there is a signal assigned to the CH at C4 and C4′. At 54.77 ppm the signal is observed for the OCH_3 at C21 and C21′. At 59.10 ppm the signals indicates the OCH_2 at C12 and C12′. At 78.57 ppm the signal is assigned to the carbon at C3 and C3′, while the signal at 109.14 ppm indicates the aryl CH at C9 and C9′ and the signal at113.16 ppm indicates the aryl CH at positions C19, C19′ and C23, C23′. At 117.31 ppm the signal is assigned to the aryl CH at C7 and C7′, and at 124.23 ppm the quaternary carbon signal is observed for positions C5 and C5′. The following tertiary carbon signals are identified: at 128.13 ppm there is the signal for aryl CH at C18, C18′, C6 and C22, C22′ and C6′. There is then a signal at 129.77 ppm assigned to the CH groups at C16, C16′ and C17, C17′.The following quaternary carbon (C) signals are identified:at 133.26 ppm the carbon at C14 and C14′ positions,

at 139.46 ppm there is a signal assigned to the carbon at C15 and C15', and at 148.61 ppm the C-O at C8 and C8'. The more upfield quaternary carbon signals are assigned as follows: at 148.82 ppm the signal is assigned to the C-O at positions C10 and C10', at 157.50ppm the signal is observed for the C-OCH_3 at C20 and C20', at 159.37 ppm there is the signal assigned to the O-C-N at C2 and C2'; at 163.52 ppm the carbonyl (C=O) groups of C14a and C14a' are indicated, and finally at 168.87 the carbonyl C=O groups at C11 and C11' positions are assigned.

The IR spectrum of **BE113**, the following absorbances were assigned; 3484.38 and 3380.59 cm^{-1},(NH_2); 1671.40, 1666.86 and 1661.83 cm^{-1},(C=O) and 1645.21 and 1636.53 cm^{-1}, (C=C).

In the mass spectrum HRMS (EI) for **BE113**, the molecular ion $C_{46}H_{41}N_2O_{12}$ [M^+ H] requires (m/e) 813.2659; and was found at 813.2659, (-0.1ppm). This result confirmed the structural identification of the *bis* chromene ester **BE113**.

2.12 Coumarin ring as a scaffold for design of Selective Estrogen Receptor Modulators (SERMS)

2.12.1 Introduction

Coumarins are natural or synthetic benzopyran derivatives that form a family of active compounds with a wide range of pharmacological properties. Coumarins (IUPAC name benzopyrone) can display anticoagulant activity, antipsoriasis activity, inhibitory activity on viral proteases, antibacterial/antitumoral activity, antioxidant activity, antiproliferative activity, estrogen-like effects or central nervous system modulating activities[102]. Coumarin has shown anti-tumour activity *in vivo*, and the therapeutic effect is thought to be due to its metabolites (e.g. 7-hydroxycoumarin, 4-hydroxycoumarin, (see fig 2.36)[148]. The discovery of coumarins with weak ER activity has potential benefit to clinical therapeutics as such derivatives may be developed to be used as therapeutic agents to prevent adverse effects associated with menopause, such as osteoporosis, cardiovascular risk (atherosclerosis), or cognitive deficiency[149].

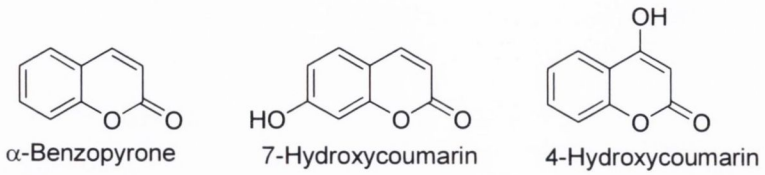

Fig 2.36 Basic coumarin structure (benzo-α-pyrone), active metabolites 7-hydroxycoumarin, and 4-hydroxycoumarin

4-Hydroxycoumarin preparation

Preparation of many of the coumarin derivatives can be carried out using the Pechmann condensation illustrated in scheme 2.24. With simple phenols, the conditions are harsh, although yields may still be good. Coumarins can also be synthesised using a Knoevenagel type condensation, which was the method chosen in this project as the synthesis can be performed quickly in milder conditions and relative ease and these methods are described in the following section.

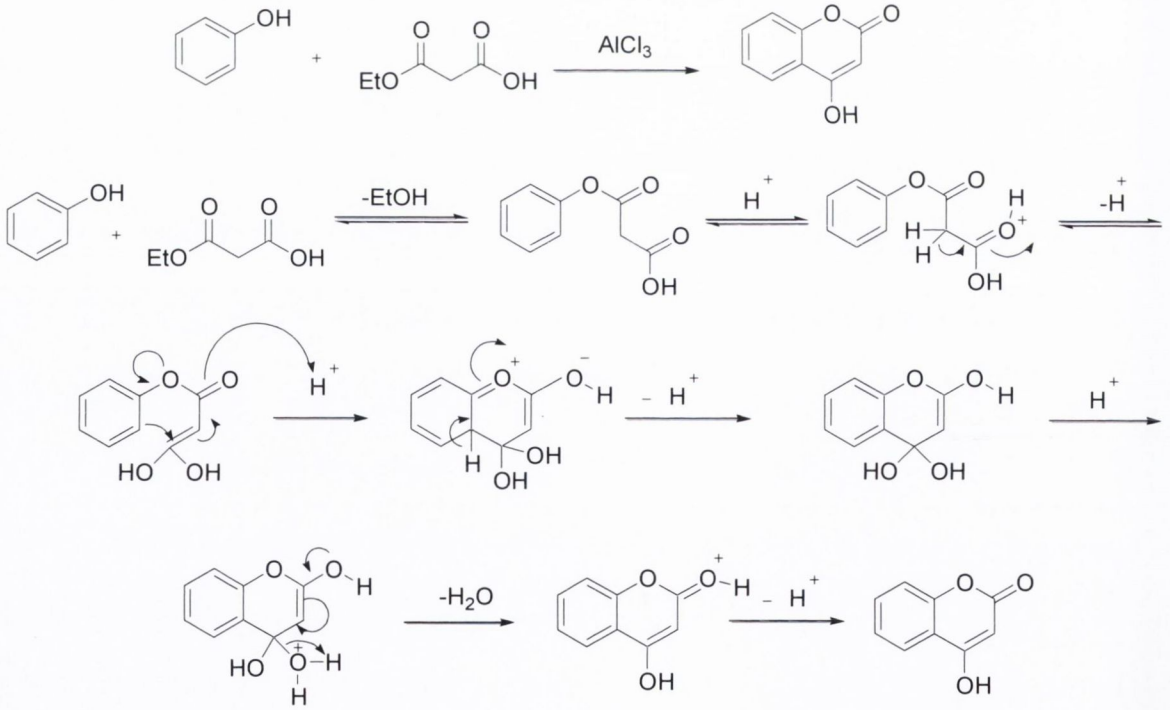

Scheme2. 24 Reaction mechanism for formation of 4-Hydroxycoumarin in the Pechmann condensation reaction

The reaction mechanism shown in scheme 2.24 for production of 4-hydroxycoumarin, is conducted with a strong Brønstedt acid such as methanesulfonic acid or a Lewis acid such as $AlCl_3$ or acetic acid. The acid catalyses transesterification as well as keto-enol tautomerisation. A Michael addition leads to the formation of the coumarin skeleton. This addition is followed by a rearomatisation, the subsequent acid-induced elimination of water gives the 4-hydroxycoumarin product [150].

Research undertaken [149, 151] related to 3-substituted coumarinic derivatives related to Coumestrol (see fig 2.37), showed the presence of estrogenic activity related to their structural analogy with the natural hormone estradiol (see fig 2.32). Furthermore, a study of the relationships between the structure of various 3-substituted coumarins and their relative binding affinities (RBAs) to steroid receptors and to their antiproliferative activity on human breast cancer MCF-7 cells, showed the importance of the substituents at positions 3 and 7 in the phenolic ring[149, 151]. Warfarin is a clinically available anticoagulant which incorporates the 4-hydroxycoumarin structure. It decreases blood coagulation by inhibiting vitamin K epoxide reductase, an enzyme that recycles oxidized vitamin K to its reduced form after it has participated in the carboxylation of several blood coagulation proteins (Fig 2.37), [152].

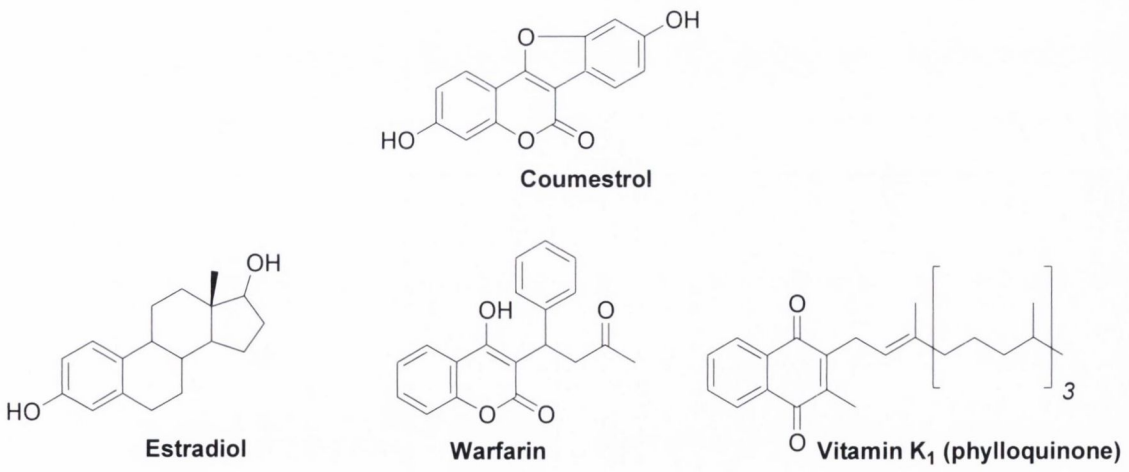

Fig 2.37 Coumestrol, Estradiol , Warfarin and Vitamin K_1 (phylloquinone).

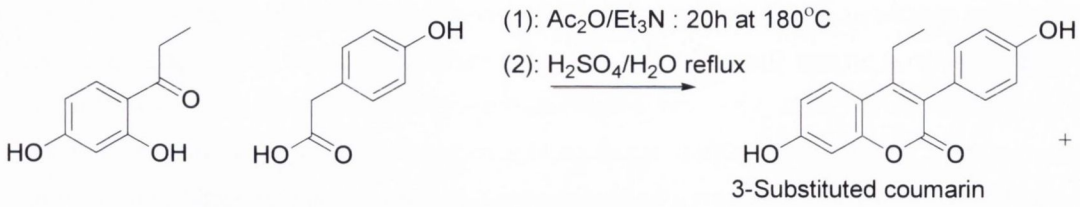

Scheme2. 25 Synthesis of 3-(4-hydroxyphenyl)-7-hydroxycoumarin

The synthesis of the 4-ethyl-3-(4-hydroxyphenyl)-7-hydroxycoumarin (fig 2.37) is achieved using the modified Perkin–Oglialoro reaction [153] by condensation of 2,4-dihydroxypropiophenone with conveniently substituted phenylacetic acids in the presence of triethylamine and acetic anhydride (see scheme 2.25). The reaction leads to a mixture of 7-acetoxy derivatives. After acid hydrolysis, the corresponding 7-hydroxycoumarin was obtained [154].

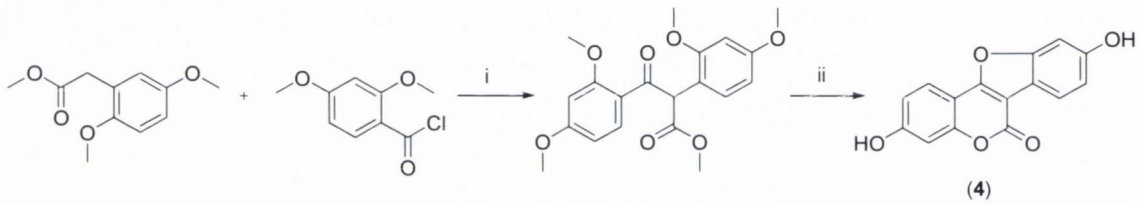

Scheme2. 26 Synthesis of Coumestrol (i) n-BuLi, i-Pr2NH, THF, -78 °C for 2 h then 0 °C for 3 h; (ii) 1M BBr3, CH2Cl2, rt, 72h

A convenient and simple two-step method for the synthesis of coumestrol (Scheme 2.26) has been reported, which involves a base catalysed condensation of phenyl acetate ester with benzoyl chloride, followed by demethylation and subsequent tandem intramolecular cyclisation [155].

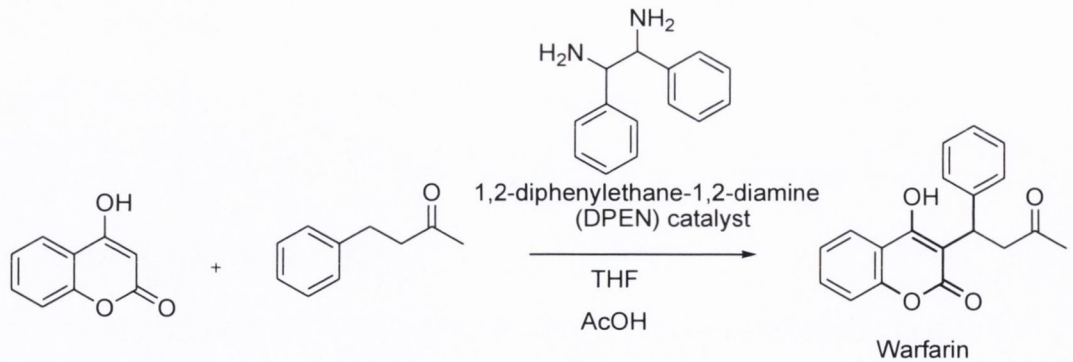

Scheme2. 27 Reaction scheme for synthesis of Warfarin

In scheme 2.27 the reaction scheme for preparation of warfarin is shown starting from 4-hydroxycoumarin and benzylacetone, using a 1,2-diphenylethane-1,2-diamine (DPEN) catalyst, in the presence of acetic acid and THF. The required 4-hydroxycoumarin can be prepared using a Pechman condensation as shown in Scheme 2.24.

1) 4-Phenyl-3-butene-2-one preparation

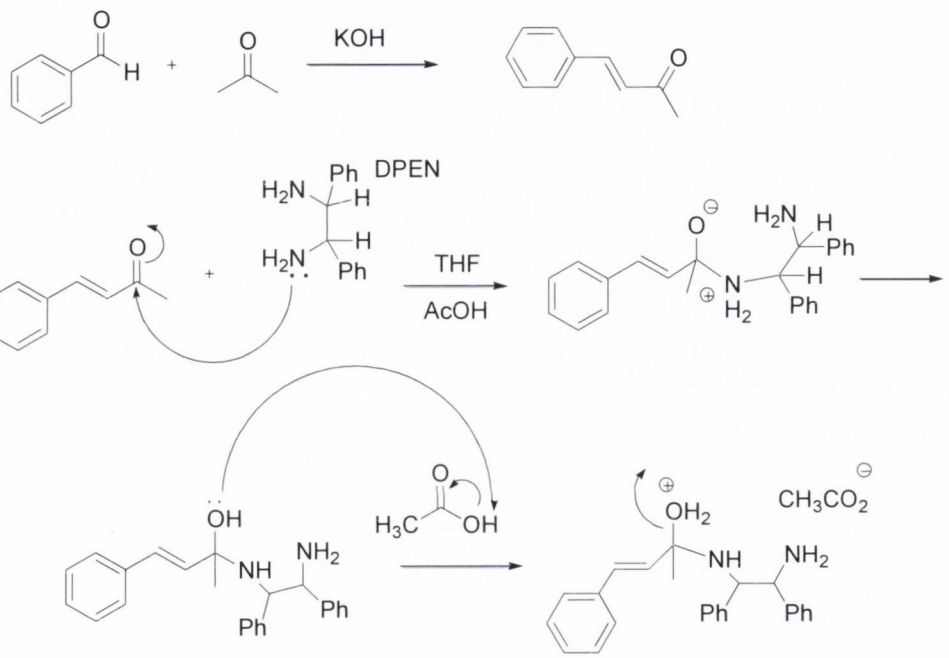

2) Formation of Schiff base

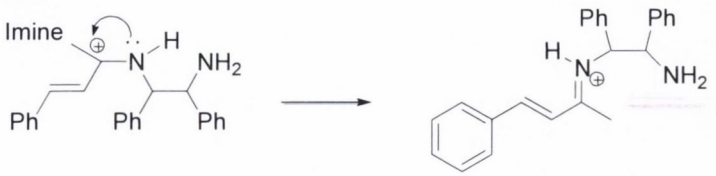

3) Cyclisation

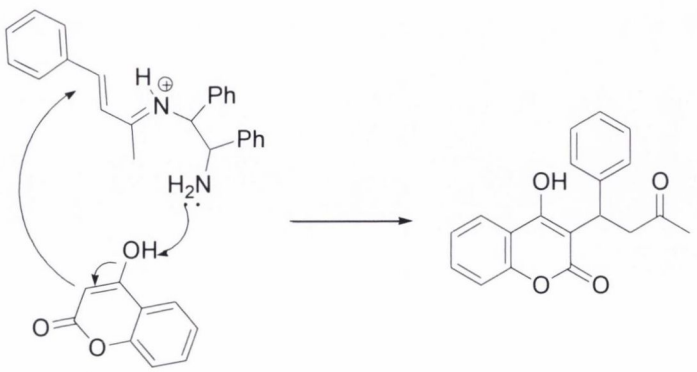

Scheme2. 28 Synthesis of Warfarin

In scheme 2.28 the synthesis of warfarin using the DPEN catalyst is illustrated[156]. The first step is synthesis of the ketone required for the production of warfarin, 4-phenyl-3-butene-2-one. The next step is the formation of the Schiff base, with the carbonyl reacting with the amino group of the DPEN catalyst to form the imine. The last step of the mechanism is the cyclisation of 4-hydroxycoumarin with the phenyl imine intermediate to produce warfarin [157].

This chapter reports synthetic methods for development of various novel coumarins as SERMs, and describes the development of a Knoevenagel type condensation reaction to afford substituted tricyclic coumarin containing ring systems. A library of the novel pyranoocoumarins are prepared with structural variations of the pyranocoumarin scaffold. The analytical identification techniques are described and the compounds are subsequently evaluated for biological activity (Chapter 3).

2.12.2 Series 12, Pyranocoumarin (pyrano[3,2-c]benzopyran-5-one) precursors: Benzylidene malononitrile intermediates

In the present work, in order to synthesise the required pyranocoumarin (pyrano[3,2-c]benzopyran-5-one) products with potential activity at the targeted estrogen receptor, the design and synthesis of the libraries required the use of Knoevenagel[116] type condensation reactions. A selection of benzylidene malononitrile intermediates were required on route to the synthesis of final coumarin products. The initial library for the malononitrile intermediates prepared is shown below in reaction scheme 2.29.

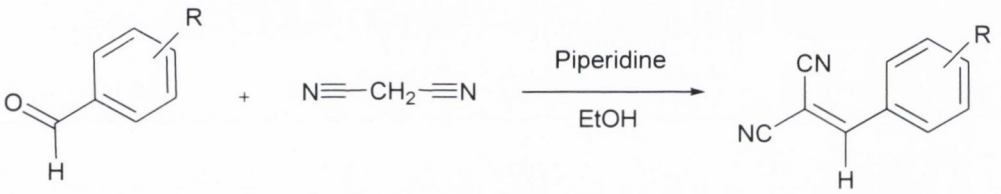

Scheme2. 29 Synthesis of benzylidene malononitrile intermediates

The benzylidene malononitrile intermediates were synthesised as illustrated in reaction scheme 2.29. The appropriate benzaldehyde was reacted with the malononitrile in ethanol. The reactions were catalysed by piperidine. By using a wide variety of easily available aldehydes the synthetic method allowed production of a substantial library of varied benzylidene intermediates, **BE116-BE129,** shown in table 2.12.

2.12.3 Results series 12 Synthesis of the library of malononitrile intermediates BE116-BE129

No.	Intermediate	% Yield	CLogP	No.	Intermediate	% Yield	CLogP
BE116	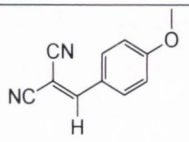	*75*	1.35	**BE123**	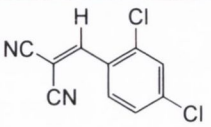	*28*	2.85
BE117	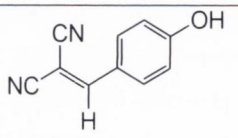	*44*	0.76	**BE124**	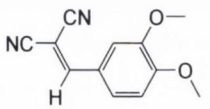	*73*	1.09
BE118	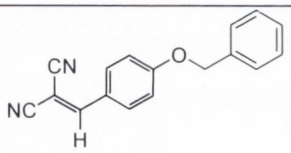	*69*	3.11	**BE125**	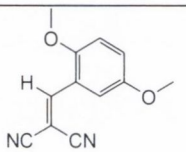	*42*	1.44
BE119	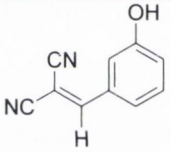	*96*	0.76	**BE126**	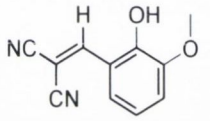	*64*	0.61
BE120	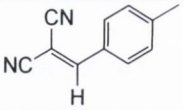	*95*	1.93	**BE127**	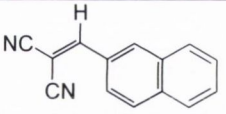	*91*	2.60
BE121	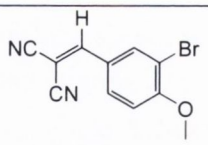	*98*	2.12	**BE128**	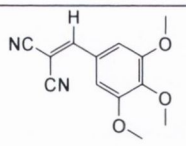	*70*	0.73
BE122	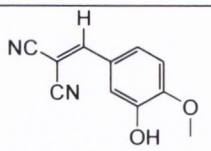	*90*	0.61	**BE129**	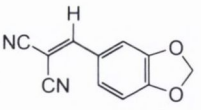	*90*	1.39

Table 2. 12 Benzylidene malononitrile intermediates BE116-BE129

*CLogP calculated using Chemdraw Ultra version.

Table 2.12 displays the library totalling 14 compounds produced featuring substitution on the aryl ring obtained by using a wide variety of benzaldehydes including 4-methyl benzaldehyde, and various methoxy, dioxane, bromo, hydroxyl, benzyloxy and chloro

substituted benzaldehydes. Yields ranged from 28 to 98%, with good CLogP values not greater than 5. However compounds **BE117**, **BE119**, **BE122**, **BE126 and BE128** recorded low CLogP values(ClogP <1) indicating the polar nature of these compounds. This facile method of synthesis allowed production of a substantial library of starting materials with potential for further synthesis of pyranocoumarin products.

2.12.4 Synthetic route to 2-(4-methoxybenzylidene)malononitrile

Scheme 2.30 demonstrates the synthesis of the library of benzylidene malononitriles using compound **BE116** as an example. This proposed mechanism for this Knoevenagel condensation reaction requires reaction of an aldehyde with malononitrile catalysed by piperidene as shown below.

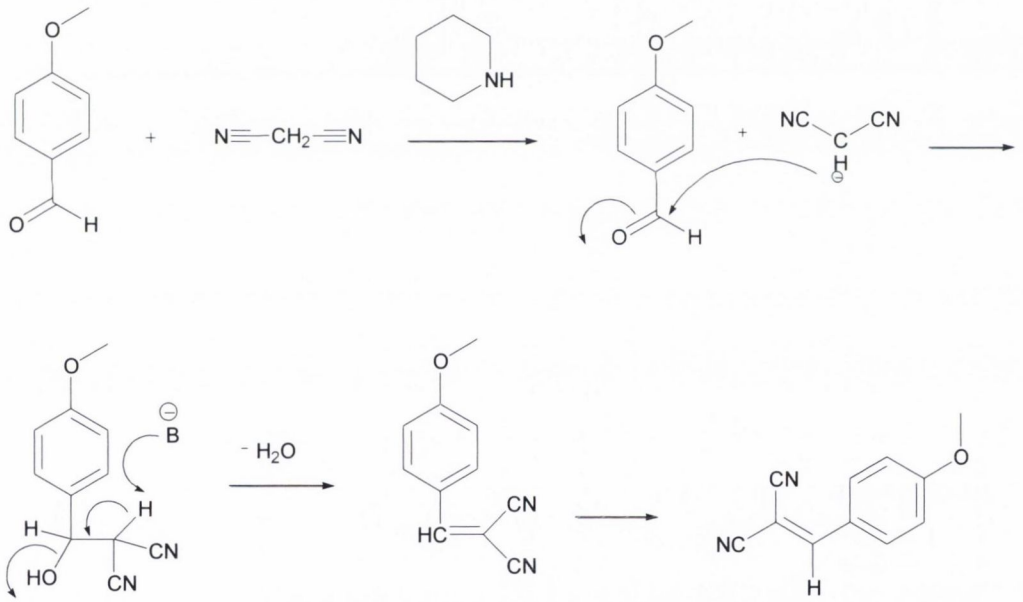

Scheme2. 30 Synthesis of intermediate BE116

2.12.5 Spectroscopic identification

Identification of the library of benzylidene malononitrile compounds **BE116-BE129** was performed using ^{1}H, ^{13}C and DEPT Nuclear Magnetic Resonance (NMR) Spectroscopy, Infared (IR) Spectroscopy, and High Resolution Mass Spectrometry (HRMS). The following figures 2.38 and 2.39 display NMR spectra for compound

BE116. Discussion of the NMR spectra for **BE116** is used as an example of the identification of each molecule in this series.

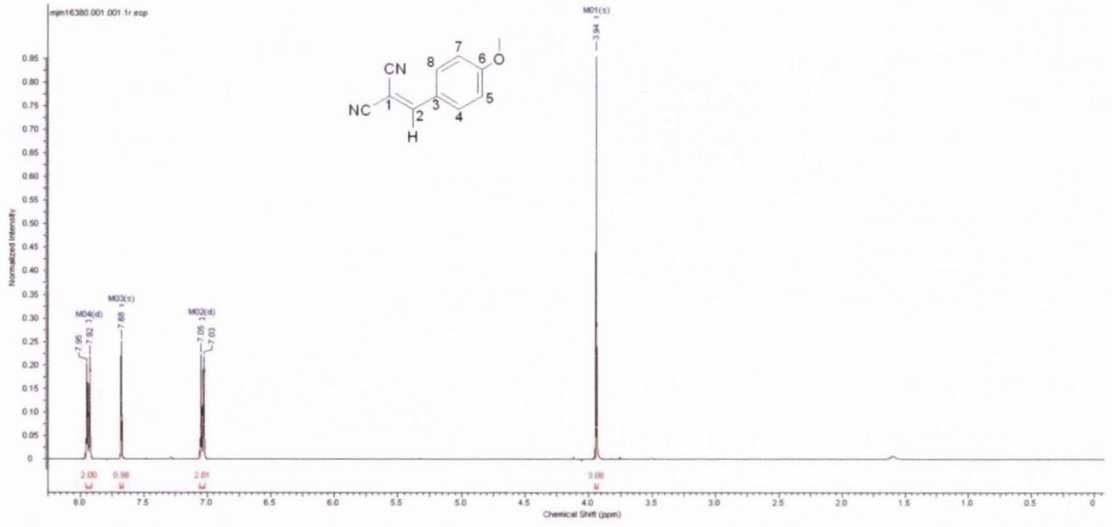

Figure 2. 38 ^{1}H NMR spectrum for benzylidene malonitrile BE116

In the proton NMR spectrum as seen in figure 2.38 for compound **BE116**, the methoxy group can be identified as a singlet absorbance, at δ 3.94, and integrates for 3 protons for the OCH_3 group at the C6 position. At δ 7.03 a doublet signal was observed for two aryl hydrogens at carbon positions C5 and C7, with a *J* coupling constant value of 7.04 Hz, and this signal integrated for 2H. At δ 7.68 there was a singlet for the hydrogen at C2 position, CH, integrated to 1 proton. Finally at δ 7.92 there was seen a doublet, with a coupling constant *J*=8.02 Hz, integrated to 2H, indicating the aryl protons at C4 and C8.

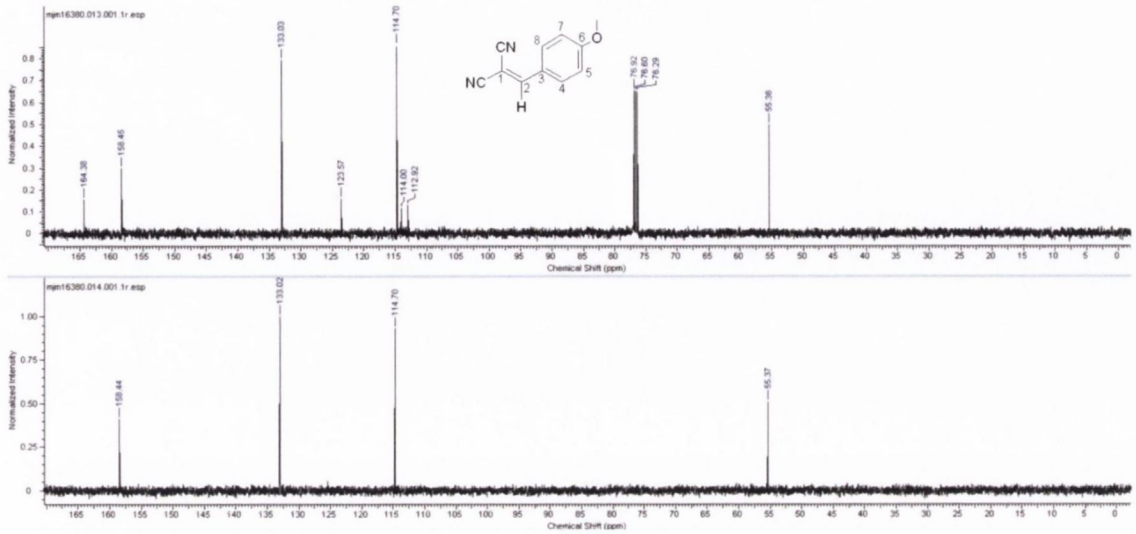

Figure 2. 39 ^{13}C NMR (upper) and DEPT 135 (lower) spectra for benzylidene malonitrile compound-BE116

In the ^{13}C and DEPT-135 spectra shown in figure 2.39 for compound **BE116**, the OCH_3 at C5 is indicated in the signal at ppm 55.38. Then at 76.29 ppm there is the carbon signal of the C=C double bond at position C1, seen as a positive absorbance in the ^{13}C spectrum. At 112.92 ppm and 114 ppm there are the two signals for each of the CN groups. At 114.70 ppm there is a signal indicating 2x aryl CH at C5 and C7, while at 123.57 ppm the carbon at position 3 of the phenyl ring is identified. At 133.03 ppm there is a signal assigned to the aryl CH at C4 and C8, and at 158.45 ppm there is a signal assigned for the CH of the double bond, C2. Finally at 164.38 ppm the signal indicating the C-6 quaternary carbon bearing the O-CH_3 is identified.

The IR spectrum absorbances for compound **BE116** were confirmed as follows; 3144.76 and 3036.41 cm^{-1}, (CH)**;** 2258.75 and 2242.62 cm^{-1}, (CN) and at 1674.51 and 1625.33 cm^{-1}(C=C) .

The mass spectrum HRMS (EI) for **BE116**, $C_{11}H_8N_2O$ [M^+] requires (m/e) 184.0637, value found 184.0636, (-0.5 ppm). The analysis confirmed the structure of the 2-(4-methoxybenzylidene)malononitrile for compound **BE116**.

2.13 Series 13, Pyranocoumarin (pyrano[3,2-c]benzopyran-5-one) synthesis

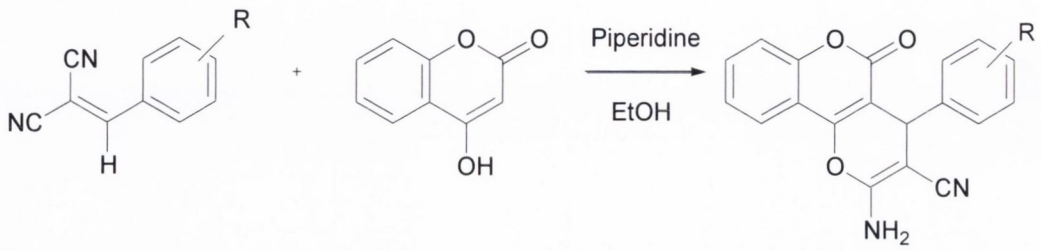

BE116-129 **BE130-139**

Scheme2. 31 Synthesis of pyranocoumarin compounds BE130-139

The general reaction scheme, seen in scheme 2.31, outlines the method used for the synthesis of the pyranocoumarin (pyrano[3,2-c]benzopyran-5-one) compounds **BE130-139** illustrated in figure 2.40. The appropriate benzylidene malononitrile was added with 4-hydroxy coumarin in solvent ethanol. The reaction was catalysed with base piperidene. The wide variety of previously prepared benzylidene malonitrile intermediate compounds **116-129** allowed synthesis of a library of novel pyranocoumarin compounds (see Figure 2.40).

2.13.1 Results series 13 Synthesis of the library of 4-arylpyrancoumarin (pyrano[3,2-c]benzopyran-5-one) products

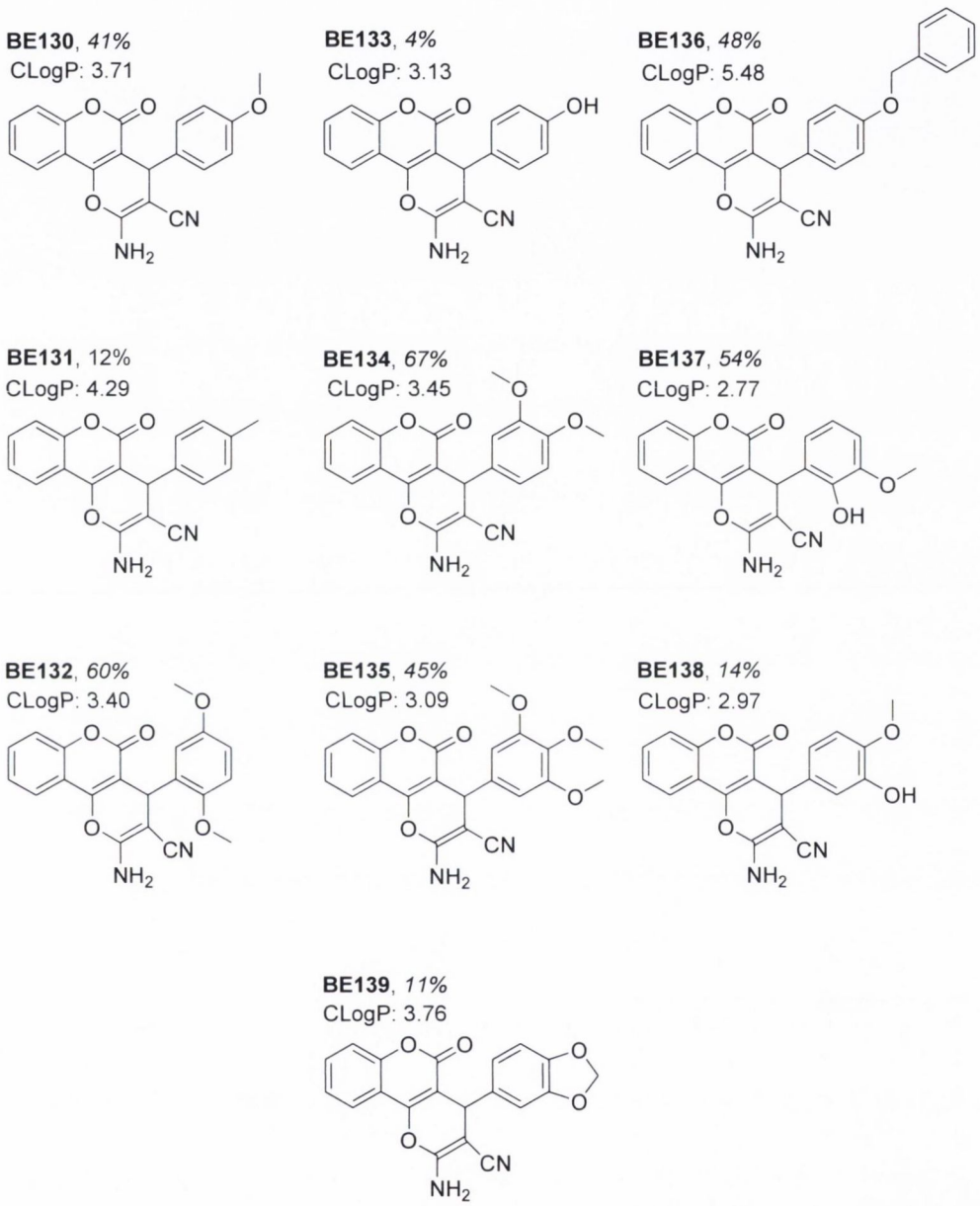

Figure 2. 36 Pyranocoumarins (pyrano[3,2-c]benzopyran-5-ones) BE130-139

*CLogP calculated using Chemdraw Ultra version.

The 4-arylpyranocoumarin compounds ***BE130-139*** displayed in figure 2.40 were produced using the reaction scheme shown in Scheme 2.31 . Ten pyranocoumarin products were obtained with a wide selection of substitutions on the aryl C-4 group.

Yields varied from 4 to 67%. CLogP values were in the range 2.7 – 5.4, were all within Lipinski's rule of 5, showing potential as druggable candidates for therapeutic SERMs [158].

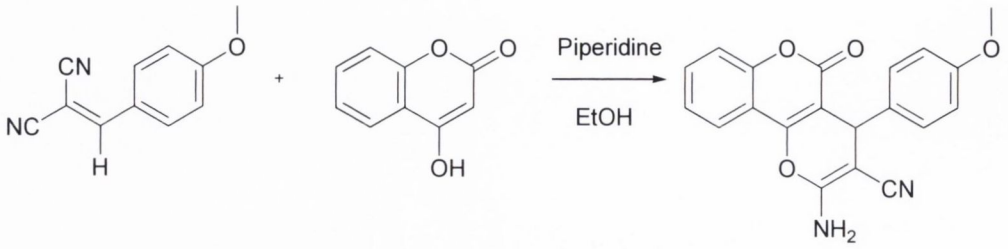

Scheme2. 32 Synthesis of pyranocoumarin product BE130

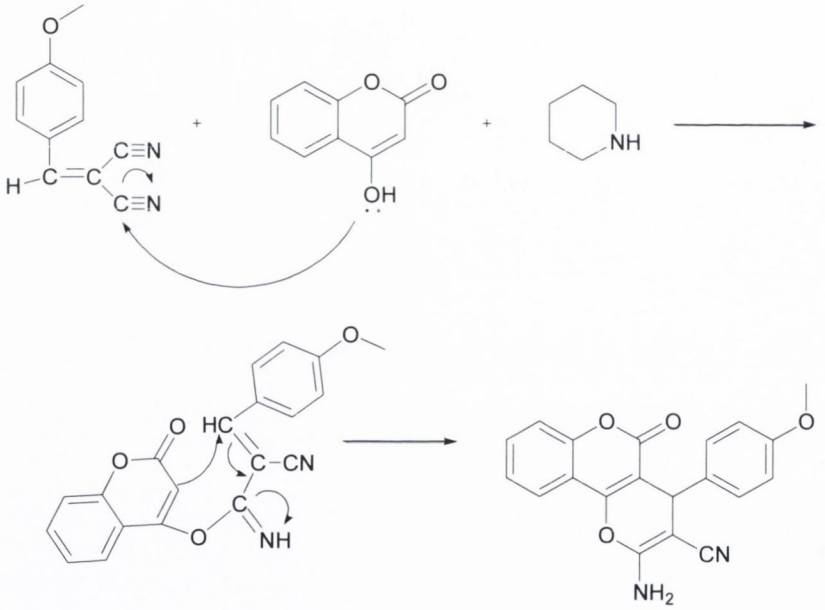

Scheme2. 33 Proposed reaction for synthesis of pyranocoumarin BE130

2.13.2 Synthetic route to *pyranocoumarin BE130*

Scheme 2.32 shows the reaction scheme for the synthesis of pyranocoumarin compound **BE130**. The proposed reaction mechanism is illustrated in scheme 2.33. This Knoevenagel condensation reaction is initiated by attack of the nucleophilic OH of the 4-hydroxycoumarin ring on the electrophilic CN of the benzylidene malonitrile

BE116, followed by a cyclisation of the C-3 of the 4-hydroxycoumarin on the benzylic carbon of the benzylidene malonitrile to afford the pyranocoumarin product **BE130**.

2.13.3 Spectroscopic identification

Analysis for identification of each pyranocoumarin compound in the series was achieved using Nuclear Magnetic Resonance (NMR) spectroscopy, Infared (IR) spectroscopy, and Mass spectrosctrometry(HRMS). The following figures 2.41 and 2.42 are NMR spectra for compound **BE130**. Discussion of the NMR spectra is used as an example of the identification of each compound in this series.

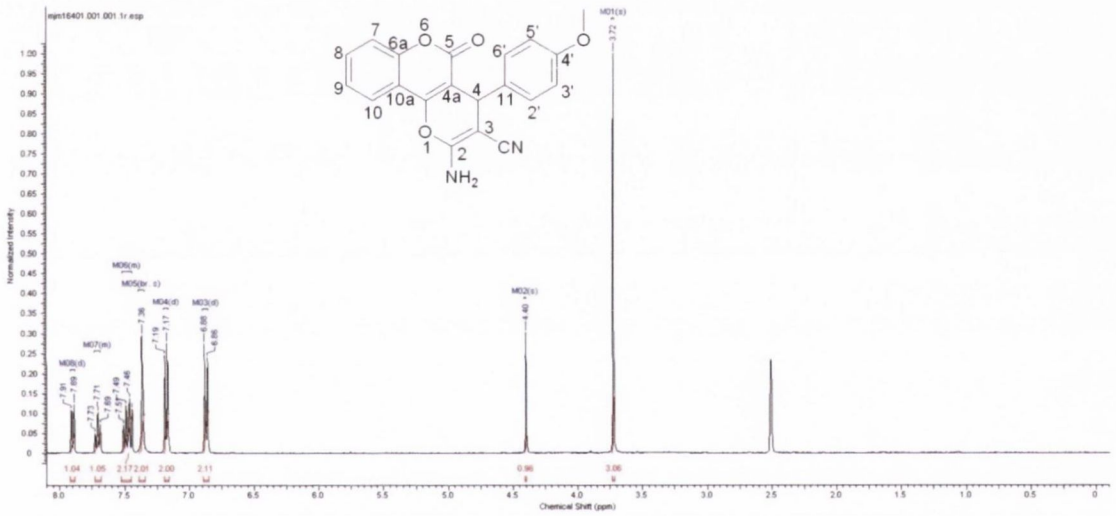

Figure 2.41 ^{1}H NMR spectrum for pyranocoumarin BE130

In the proton NMR spectrum as seen in figure 2.41 for compound **BE130**, the methoxy group at C4 can be seen as a singlet absorbance, at δ 3.72 integrating to 3H protons. At δ 4.40 a singlet is observed integrated to 1H, and is assigned to the chiral hydrogen CH at C4. At δ 6.86 there is a doublet absorbance, integrating to 2 protons, the *J* couple constant was valued at 7.24 Hz, indicating the two aryl protons at C3 and C5. At 7.17 there is a doublet signal, integrating for 2H, *J*=8.12 Hz, assigned to the 2xAr-H at positions C2 and C6. At δ 7.36 a broad singlet is assigned to the primary amine group protons, NH_2, integrated to 2H. Between δ 7.46 and 7.51 a multiplet was observed, integrated to 2H, and assigned to two aryl protons at C7 and C9. Another multiplet was seen between 7.69 and 7.73 indicating the aryl proton at C8 integrated to 1H. Lastly at δ 7.89 there is a doublet absorbance, 1H, *J* coupling constant value is 8.03 Hz, and this identified as the aryl proton at the C10 position.

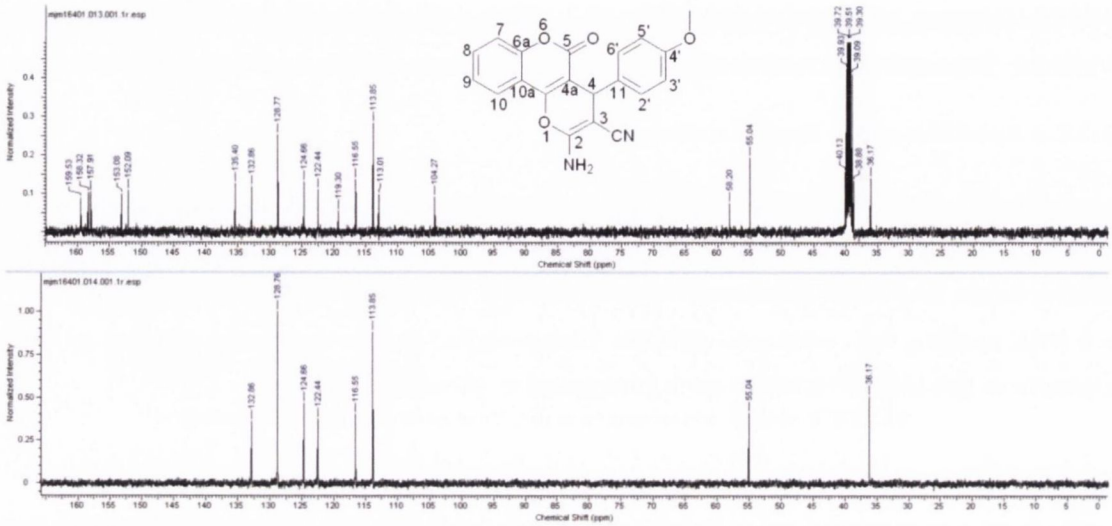

Figure 2.42 ^{13}C NMR (upper) and Dept 135 (lower) spectra for pyranocoumarin BE130

In the C^{13} and DEPT 135 spectrum shown in figure 2.42 for compound **BE130**, the chiral CH at C4 is observed as the signal at 36.17 ppm. The carbon C4' indicating the methoxy group was identified at 55.04 ppm. The signal for the C=C double bond of C3 appeared at 58.20 ppm. The next signal is observed at 104.27 ppm indicating the C=C of C4a position. The signal at 113.01 ppm is assigned to the aryl quaternary carbon of C10a. At 113.85 ppm is the signal for the two tertiary carbons CH at C3 and C5. At 116.55 ppm is the aryl CH at position C7 while at 119.30 ppm was the CN carbon located at C3. The following tertiary carbon (CH) signals were identified: at 122.44 ppm the signal for the CH of C9; at 124.66 ppm the CH at position C10; at 128.77 ppm the CH at C8 and at 132.86 ppm the two CH signals for the C2 and C6 positions were observed. The following quaternary carbon (C) signals were identified: at 135.40 ppm the signal indicating the carbon at C11, at 152.09 ppm C-O of the C6a position, at 153.08 ppm the signal indicating the carbon of the OCH_3 group at position C4' and at 157.91 ppm the signal indicating the O-C-N at C2 position was observed. The carbon signal at 158.32 ppm was assigned to the C-O at the C1 position, and finally at 159.53 ppm the quaternary carbon of the carbonyl C=O of the C5 position was identified.

The IR spectrum absorbances for compound **BE130** were assigned as follows; 3456.71 and 3359.63 cm^{-1} for for NH_2 group, 2258.75 cm^{-1} for the CN group, 1674.51 cm^{-1} for the C=O group and 1625.33 and 1611.48 cm^{-1} for the C=C and aryl rings.

The mass spectrum HRMS (EI) for **BE130** $C_{20}H_{15}N_2O_4$ [M^+ H] requires (m/e) 347.1032, value found 347.1022, (+2.9 ppm). This result confirmed the structure assigned to the 2-amino-4-(4-methoxyphenyl)-3-cyanopyrano[3,2-c]benzopyran compound **BE130**.

2.14 Series 14 Synthesis of the library of pyranoocoumarins (pyrano[3,2-c]benzopyran-5-ones) substituted with basic ether chains

There is much interest in the preparation, improvement and availability of antimetastatic drugs in clinical oncology therapy. Specifically in breast cancer therapy, estrogen targeting anticancer drugs which are effective in lowering estrogen levels are of great benefit to breast cancer patients. The design of antagonistic drugs that act on the ER is of great benefit, and molecular modelling studies have reported that design of structures with amine containing antagonistic type substituents (Tamoxifen) cause the inhibition of the helix-12 mechanism in the ER LBD, preventing the interaction of estrogen. (see chapter 1, ER alpha antagonism).

The objective of synthesising coumarin type compounds with longer amine-containing alkyl substituents is to mimic the bulky chains of clinically available pure antiestrogen Fulvestrant. In our efforts to introduce these longer amino alkyl chains, the production of pyranocoumarins with antagonistic basic ether chains on the molecular structure is investigated.

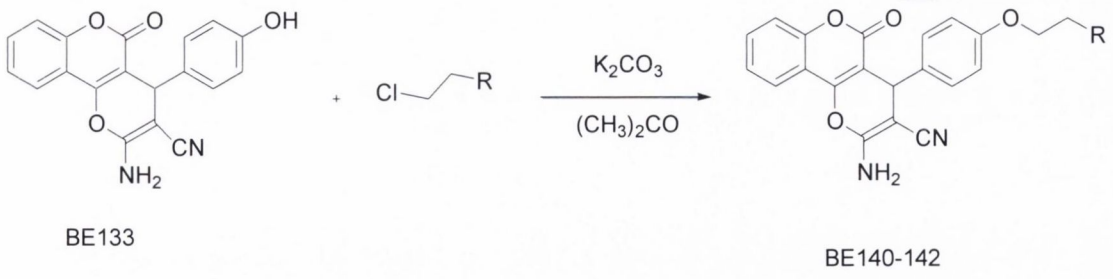

Scheme2. 34 Synthesis of pyranocoumarins products BE140-142 with basic ether substituent

In the general reaction scheme 2.34, the previously obtained pyranocoumarin **BE133** compound is reacted with an appropriate chloro-substituted alkylamine in the presence of potassium carbonate base and solvent acetone. Reaction mixture was refluxed for 8 h to obtain novel pyranocoumarins incorporating the antagonistic basic ether chain moiety.

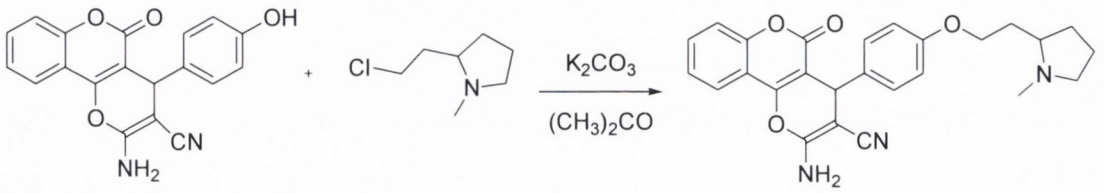

Scheme2. 35 Preparation of coumarin product BE140

Preparation of the novel 4-(4-(2-(1-methylpyrrolidin-2-yl)ethoxy)phenyl)-2-amino-4,5-dihydro-5-oxopyrano[3,2-c]chromene-3-carbonitrile **BE140** is illustrated scheme 2.35.

2.14.1 Results Series 14

BE140, *8%* CLogP: 4.78

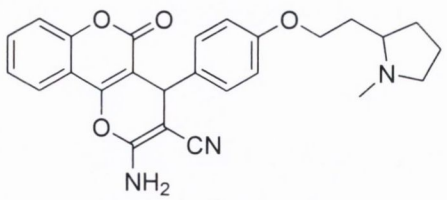

BE141, *36%* CLogP: 3.83



BE142, *20%* CLogP: 4.49

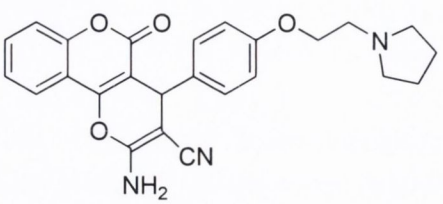

Figure 2. 43 Methylpyrrolidine, pyrrolidine and morpholine substituted pyranocoumarins

*CLogP calculated using Chemdraw Ultra version.

Figure 2.43 displays the antagonistic pyranocoumarins **BE140, BE141 and BE142** obtained. Yields were in the range 8 to 36% and optimisation of the yields can be possible by changing the solvent or using microwave methods. All CLogP values were within Lipinski's guidelines of CLogP <5 for optimum oral biovailability of drug molecules. The modest selection of pyranocoumarins displayed in Figure 2.43 serves as an example of the potential for further synthesis in this series as proposed ER targeting antagonistic agents.

2.14.2 Synthetic route to basic ether substituted pyranocoumarins

The alkylation reactions for the introduction of the substituted basic ether chain onto the pyranocoumarin structures **BE141 and BE142** are shown in scheme 2.36.

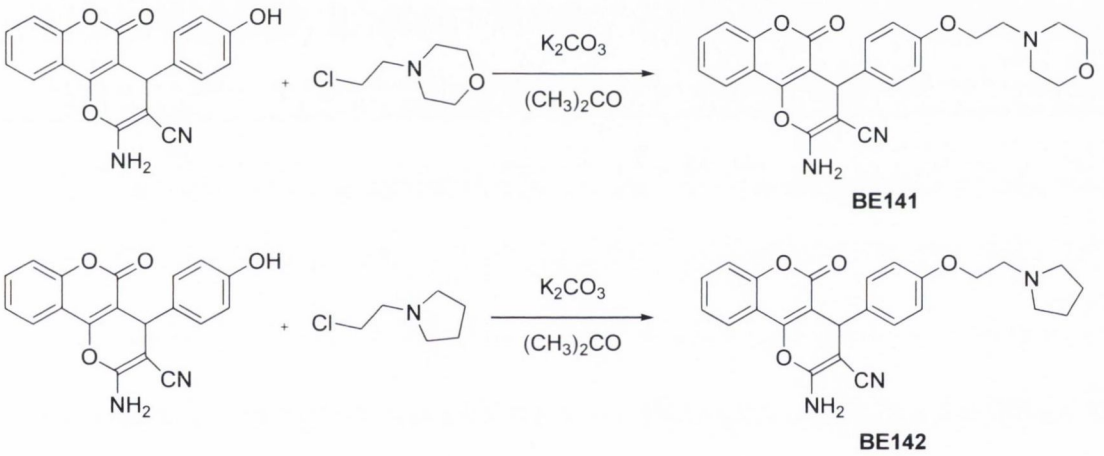

Scheme 2. 36 Synthesis of pyranocoumarin BE141 and BE142

2.14.3 Spectroscopic identification

Identification of each pyranocoumarin compound was accomplished using Nuclear Magnetic Resonance (NMR) spectroscopy, Infared (IR) spectroscopy, and Mass spectrometry(HRMS). The following figures 2.44 and 2.45 display ^{1}H and ^{13}C NMR spectra for compound BE140. Discussion of the NMR spectra is provided as an example of the identification of the compounds in this series.

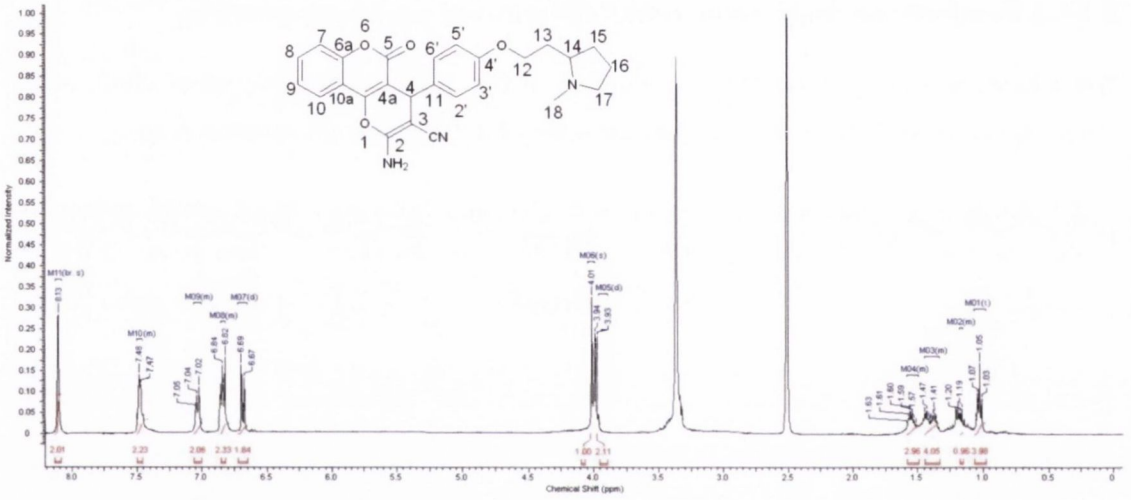

Figure 2. 44 ^{1}H NMR spectrum of pyranocoumarin BE140

In the proton NMR spectrum as seen in figure 2.44 for compound **BE140** at δ 1.03 there was a triplet peak for 2xCH_2 groups at position C15 and C16 on the five membered pyrrolidine ring, integrated to 4H. Between δ 1.19 and 1.20 there is a multiplet shown, integrated to 1H, and is assigned to the CH at the C14 position. From δ 1.41 to 1.47 there is another multiplet is observed, integrated to 4 protons, for 2xCH_2 groups at C13 and C17. Between δ 1.57 to 1.63 there is a multiplet, 3H, indicating the methyl group protons at position C18. At δ 3.93 a doublet can be seen, 2H, with a *J* coupling constant of 7.03 Hz, assigned to the CH_2 at position C16. At δ 4.01 a singlet absorbance is seen, integrated to 1H, and assigned to the single hydrogen at position C14. At δ 6.67 a doublet absorbance was seen, integrating to 2H, *J*=9.03 Hz, and was assigned to the Ar-H protons at the C12 position. At δ 6.82 to 6.84 there is a multiplet, integrating for 2H, indicating the Ar-H at C3'. Between δ 7.02 to 7.05 there is another multiplet, with an integration of 2 protons, assigned to the 2xAr-H, at positions C2' and C6'. At δ 7.47 to 7.48 there is a multiplet, integrated to

2H, which corresponds to the Ar-H proton at the C5′ position. Lastly at δ 8.13 there is a broad singlet absorbance for the NH_2 group integrated to 2H.

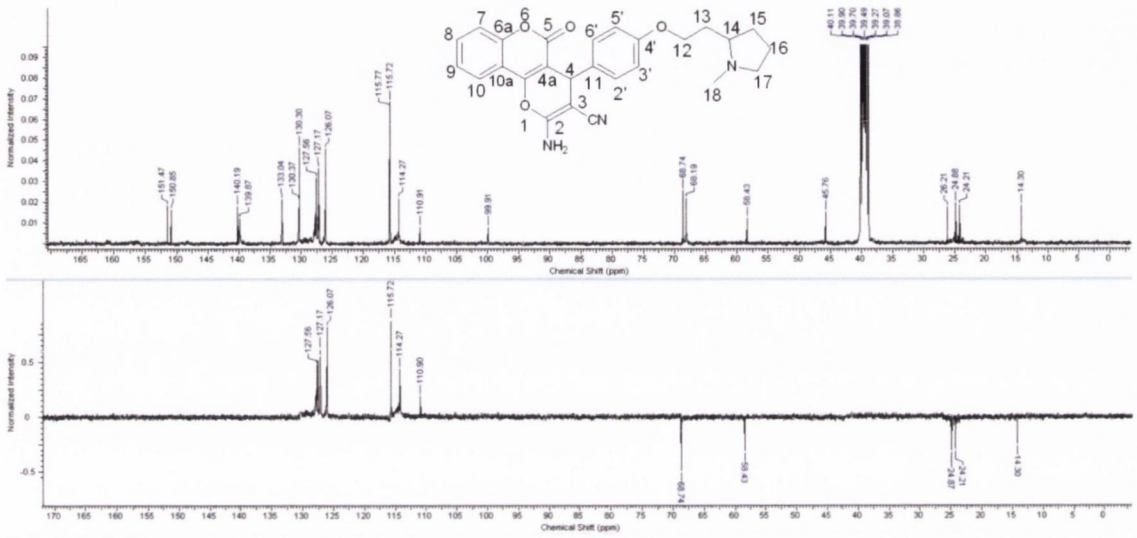

Figure 2. 45 ^{13}C NMR (upper) and Dept-135 (lower) spectra for pyranocoumarin BE140

In the ^{13}C and DEPT-135 spectrum shown in figure 2.45 for pyranocoumarin compound **BE140**, a CH_2 is seen as the first negative signal on the DEPT-135 spectrum at ppm 14.30 at C16. Further 2xCH_2 negative signals can be seen on the DEPT-135 spectrum at 24.21 ppm at C15, and δ ppm 24.88 C13. At ppm 26.20 there is indicated the signal for the chiral CH group at position C4. At 45.76 ppm there is a signal indicating the CH_3 group at position C18. An identical signal for both the C=C quaternary C at C3 and CH_2 group at C17 at 58.43 ppm is observed. At 68.19 ppm there is a signal indicating the tertiary carbon of the five membered ring at C14. At 68.74ppm there is a negative absorption seen on the DEPT-135 for the final CH_2 group at the C12 position. At ppm 99.91 the signal indicating the quaternary C=C at position C4a. The following tertiary carbon signals are identified: at 110.91 ppm the aryl CH at C3′ and C5′ positions; at 114.27 ppm the signal is assigned to the CH at position C7 and at 115.72 ppm the signal indicates the CH at C9. The CN signal at the C3 position is observed at 115.77 ppm, while the following tertiary carbon (CH) signals were identified: at 126.07 ppm the CH at C10, at 127.17 ppm the aryl CH at C8 position and at 127.56 ppm the CH at positions C2′ and C6′. The following quaternary signals were assigned: at 130.30 ppm there is observed the signal for the carbon at position C11; at 130.37 ppm the carbon

at C10a is assigned, at 133.04 ppm the C-O at C6a is indicated, at 139.87 ppm the C-O at C4' position is observed, at 140.19 ppm there is the signal assigned to the O-C-N at the C2 position, at 150.85 ppm there is the signal corresponding to the C-O adjacent to the C1 position, and finally at 151.47 ppm there is the signal assigned to the carbonyl C=O at the C5 position.

The characteristic IR spectrum absorbances for compound **BE140** were assigned as follows; 3531.67 and 3473.67 cm^{-1} for the NH_2 group, 2246.84 cm^{-1}, for the CN group, 1674.59 cm^{-1} for the C=O group and 1632.60 and 1620.62 cm^{-1} for the C=C group absorbances.

The mass spectrum HRMS (EI) result for **BE140,** $C_{26}H_{24}N_3O_4$ $[M^+ H]$ requires the molecular ion (m/e) 442.1767; the value observed was 442.1774, (-1.5 ppm). The analysis confirmed the structure assigned for this novel 2-amino-4-{4-[2-(1methylpyrrolidin-2-yl)ethoxy)phenyl)-2-amino-4,5-dihydro-5-oxopyrano[3,2-c]chromene-3-carbonitrile product **BE140**.

2.15 Conclusion

A series of novel benzopyran structures, previously identified as potential ER ligands from virtual HTS, has been synthesised. We have demonstrated a simple, versatile method of synthesizing the substituted 4*H*-chromenes by performing the Knoevenagel condensation reaction to afford 13 libraries, with 127 products in total. Completion of NMR characterisation of the libraries of chromene products was performed. X-Ray diffraction analysis has enabled the determination of the crystal structure of selected chromene compounds and the XRD characterisation studies have much benefit in exploring the ER modelling and potential ER binding of the structures to be investigated in Chapter 3.

Further synthesis and chemical modifications has been carried out on related coumarin derivatives. These compounds are obtained by reaction of 4-hydroxycoumarin in place of resorcinol in the synthetic sequence. From the libraries of varied chromene compounds, further chemical modifications has also been investigated on, OH, NH_2 and CN and ester substituent groups. Alternative synthetic methods for modification of the chromene scaffold structure has been examined. The effect on biochemical activity of modification to these functional group is of interest in understanding the mechanism of action of these compounds (see chapter 3).

Chapter 3 4*H*-Chromenes and pyranocoumarins: Biochemical activity and molecular modelling

3. Introduction: Biochemical activity of 4*H*-Chromenes

Drug molecules containing the benzopyran ring (IUPAC name chromene) and the coumarin ring (benzopyrone) scaffold have applications in the treatment of a diverse range of conditions. Products containing these heterocyclic rings are in use as treatments of bacterial infections and leukaemias they also have applications as anticoagulants, antitumor agents, anti-anaphylactics and are also reported for Alzheimer's disease, amyotrophic lateral sclerosis(motor neuron disease), Parkinson's disease, Huntington's disease and AIDS associated dementia [159], and are reported in clinical trials for the treatment of inflammation and inflammatory pain (COX-2 Inhibitor) [160]. In this thesis, a novel series of compounds based on the chromene and coumarin ring scaffolds are evaluated for biochemical activity. The results of antiproliferative activity on MCF-7 breast cancer cells and ER binding experiments of these analogues are presented. As already mentioned in chapter 1, breast cancer is classified as estrogen receptor positive or estrogen receptor negative, with the most primary incidences being estrogen receptor positive. All novel chromene/coumarin compounds were assessed in MCF-7 breast cancer cells (ER positive) and selected compounds were also assessed in LnCaP prostate cancer cell lines for their antiproliferative effects. For the most potent compounds an ER binding study was completed. Results obtained from the National Cancer Institute, Developmental Therapeutics Program (DTP) (which consists of a screening over a panel 60 different human tumor cell lines, representing leukemia, melanoma and cancers of the lung, colon, brain, ovary, breast, prostate, and kidney) is also presented for a select number of compounds synthesised.

3.1 Experimental details

Both MCF-7 (estrogen receptor positive) and LNCaP (human prostate cancer) cell lines were used for evaluation of antiproliferative activities for the chromene compounds. Both types of cells were obtained from the laboratories of Dr. Daniela Zisterer and Dr. David Lloyd, School of Biochemistry and Immunology, Trinity College Dublin.

3.1.1 MCF-7 human breast cancer cell lines

The MCF-7 cell line (*figure 3.1*) is a human breast cancer cell line derived from the breast of a 69-year old Caucasian female with adenocarcinoma, taken by pleural effusion[161]. The cells express the estrogen receptor and are adherent. They were used as evaluation of antiproliferative activities for chromene compounds. The cells are grown in Eagles Minimum Essential Medium (EMEM), supplemented with 1 % non-essential amino acid, 1 % (v/v) L-glutamine, 1 % (v/v) penicillin/streptomycin and 10 % (v/v) foetal bovine serum (FBS).

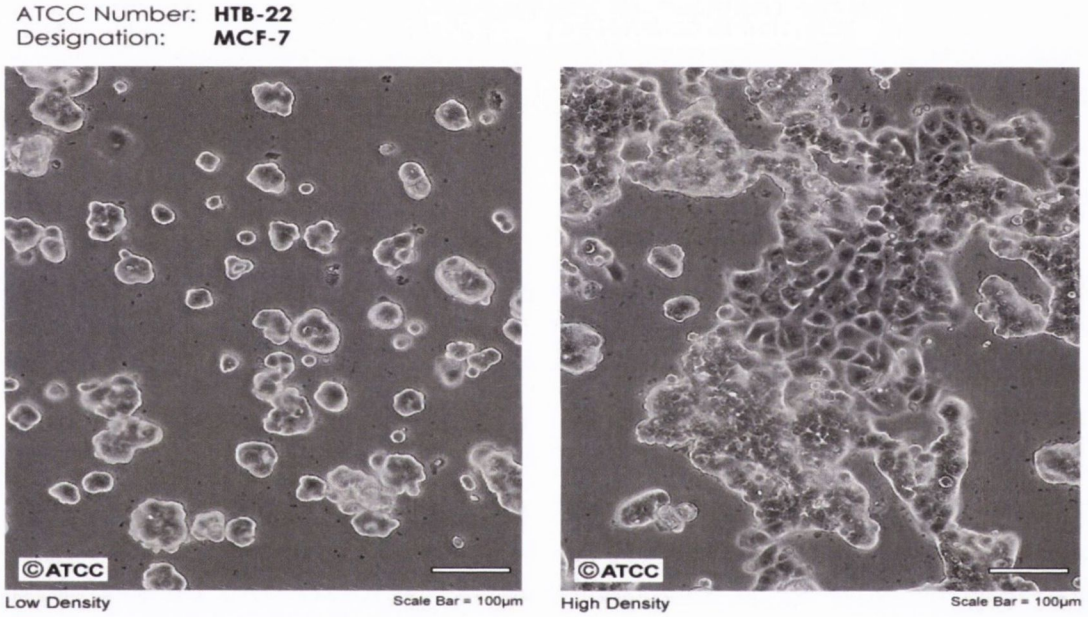

Figure 3. 1 Images of MCF-7 cells at low and high cell densities

3.1.2 LNCaP human prostate cancer cell lines

LNCaP cells were isolated from a needle aspiration biopsy of a lymph node metastatic lesion of human prostate cancer from a 50-year-old Caucasian male [162], (See figure 3.2 for LNCaP cells image). LNCaP cells are used as a model for androgen dependent prostate cancer; they respond to androgen and express AR target genes like PSA upon androgen regulation. They were used as evaluation of antiproliferative activities for selected chromene compounds. The cells are grown in RPMI media glutamax

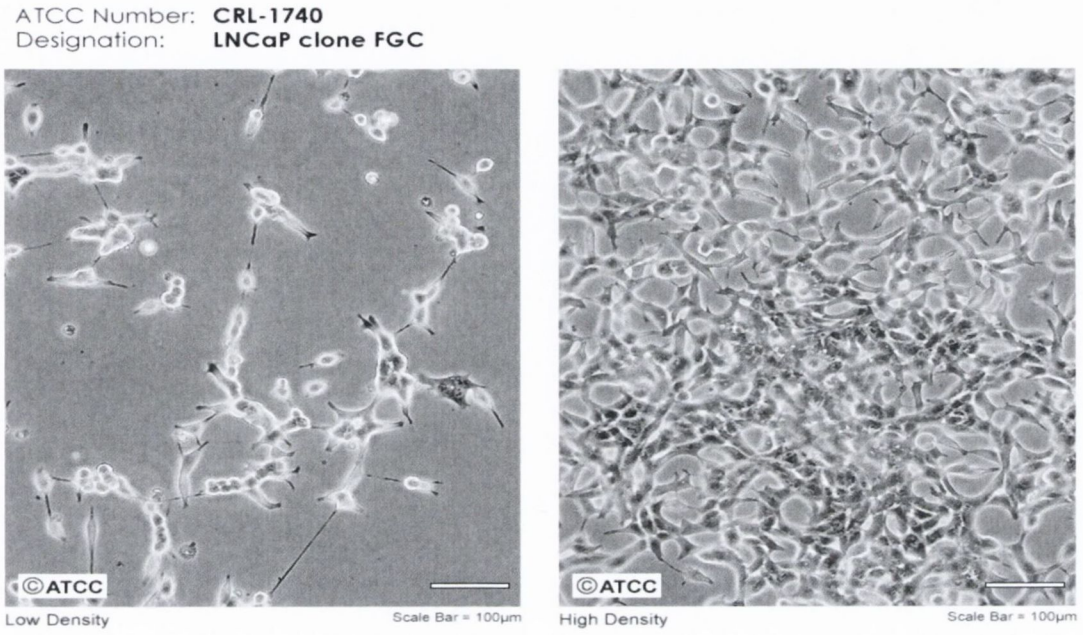

Figure 3. 2 Images of LNCaP cells at low and high cell densities

3.1.3 Storage and breaking out of cells

When cells are not in use, they are stored in a liquid nitrogen vapour phase environment at approximately -178 °C. When preserving cells, they are suspended in 10% dimethylsulfoxide (DMSO)/90% foetal bovine serum (FBS) in a cryotube, placed in a freezer at -78 °C overnight and transferred into liquid nitrogen after 24 hours. Cells that are required for anti-proliferation studies are thawed at 37 °C, diluted with complete growth medium and centrifuged at 1250rpm for 5 minutes. The supernatant containing DMSO is poured off, the cells are re-suspended in complete growth medium and are transferred into a 25 cm^2 culture flask. 10 mL of the appropriate complete growth medium is added to the flask and it is incubated at 5% CO_2/95% air and 37 °C until confluency is reached. The cells can then be transferred to a 75 cm^2 culture flask.

3.1.4 Growth and maintenance of cells

MCF-7 cells are grown in Minimum Essential Medium Eagle (MEM), supplemented with non-essential amino acids, FBS, L-glutamine and penicillin/streptomycin. LNCaP cells were grown in RPMI media with glutamax used for our cell culturing. It contains the reducing agent glutathione and high concentrations of vitamins. RPMI 1640 contains biotin, vitamin B_{12} and PABA which are not found in Eagle's, as well as additional supplementary components.

Cell culture flasks are stored in an incubator at 5% CO_2/95% air and at 37 °C. When cells reach confluency, they must be split to prevent cell death. To split the cells, the growth media is decanted and 3 mL of trypsin-EDTA solution 10X is added. When trypsinization is complete the cells are in suspension and are round in shape. Trypsin causes cellular damage and the time of exposure should be kept to a minimum. 10 mL of complete growth medium is added, the mixture is centrifuged at 1250 rpm for 5 minutes after which the supernatant, containing trypsin, is decanted. The pellet of cells remaining is re-suspended in 2 – 4 mL of complete growth media. Cells are counted as described in the next section and a fraction of the re-suspended cells are transferred to a culture flask with 13 – 15 mL of complete growth medium.

3.1.5 Counting cells

A haemocytometer is used to count cells. It is etched with 5 by 5 grid of squares, as depicted in *figure 3.3*. The cells in the four corner squares and in the centre square are counted. Cells touching the top and left hand sides of these squares are included in the count, but cells touching the bottom and right hand sides are excluded. The total number of cells counted in the five squares is multiplied by 5 to give the number of cells in the grid. This is equivalent to the number of cells by 10^4 per mL of medium. The process is repeated a second time and the average of the two values is used to calculate the number of cells per mL.

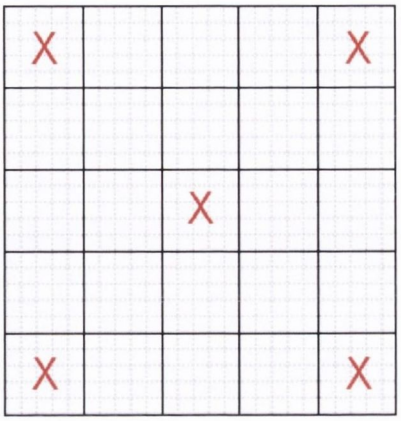

Figure 3. 3 A representative haemocytometer grid. Cells falling in the five squares marked with a red 'X' are counted

3.1.6 Dosing

From the stock solution (10 mM), a serial dilution was carried out to produce solutions of 5 mM, 2 mM, 1 mM, 200 µM, 100 µM, 50 µM. The solvent used for the dilution was 100 % DMSO, to ensure benzopyran compounds were fully dissolved and precipitation did not occur. Each well was dosed with 1 µM of test compound to give the final concentration ranging from 25 µM to 250 nM, and wells were dosed in triplicate (0.5 % DMSO final concentration in well). Each plate contained 1 row of wells with solvent only, and 1 row of wells with cells only for a blank standard, see figure 3.4. The cells were incubated for a further 72 hours before the assays were carried out.

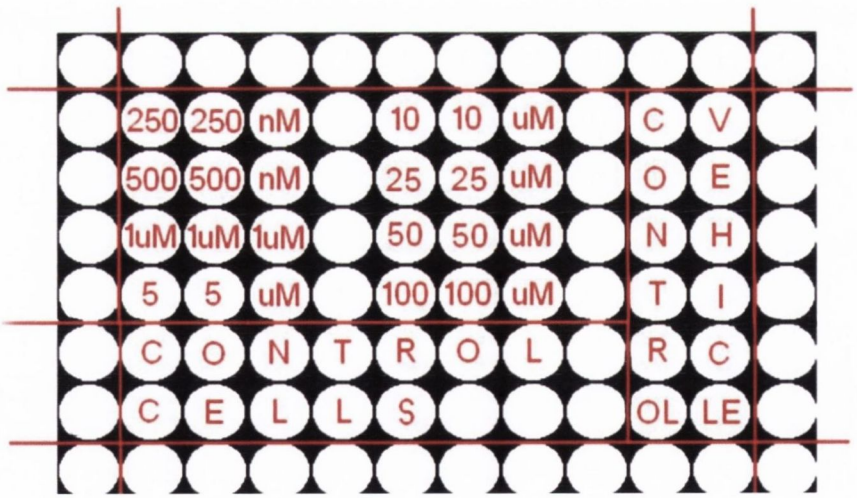

Figure 3. 4 A representative 96-well plate showing the pattern of dosing. The concentrations shown are the final concentration of the drug diluted in the well

3.1.7 Measurement of growth inhibitory effects: the alamarBlue assay

A dye known as alamarBlue® has been introduced for measurement of cell viability since 1993[163, 164]. As with the tetrazolium dyes, alamarBlue monitors the reducing environment of the cell. The internal environment of the proliferating cell is more reduced than that of a non-proliferating cell. As the dye is reduced, it changes from an oxidised indigo-blue, non-fluorescing state to a fluorescent pink reduced state (see figure 3.5). There are two ways to measure alamarBlue reduction, either by measuring the absorbance spectrophotometrically at 570 nm and 600 nm or by measuring the fluorescence, with excitation at 530 - 560 nm and emission at 590 nm. In an evaluation of the alamarBlue assay in 14 cell lines, it was determined that the optimal incubation period for MCF-7 cells was 4 hours. The major advantages of using alamarBlue is that it does not require solubilisation and it is non-toxic. AlamarBlue is now the agent of choice in the laboratory and was used for cytotoxicity studies in MCF-7 and LNCaP cells described in chapter 3. The chromene compounds were evaluated for antiproliferative activities in MCF-7 and LNCaP. The 96-well plates were treated with the compounds and were incubated at 5 % CO_2/95 % air at 37 °C. After 72 hours each well was treated with 20 μM of alamarBlue (prewarmed to 37 °C) and left to incubate in the dark for 4 h, followed by measuring the fluorescence at emission 590 nm and excitation 544 nm. The background fluorescence of the media without cells was deducted from each group, and the control untreated cells represented 100 % cell viability.

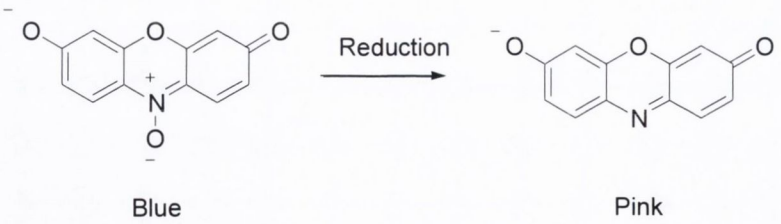

Figure 3. 5 Alamarblue as an indicator of cell viability

3.1.8 ER FRET ligand binding assay

The Lanthascreen® ER FRET assays were purchased from Invitrogen. The protocol follows the suggested method for preparation of buffers and compounds. Nuclear receptor buffer K was prepared by adding DTT to make a final concentration of DTT 5mM. This buffer was used for all other dilutions. A 'no ligand' control was used to show minimum binding. DMSO was added to make a final concentration of 2%. A positive control was also used, in this case estradiol. This served as the 'maximum ligand' control, where estradiol was at a final concentration of 2 μM in each well.
2X dilutions of each ligand were made in buffer. A stock solution of ligand was dissolved in DMSO. From this, 1 μL of 10 mM stock was added to 49 μL buffer. 10 μL of the 2X dilution was added into each well. To make a 4X (12 nM) dilution of Fluoromone ES2 using a stock concentration of 1800 nM, 6.7 μL of fluoromone was added to 993 μL of buffer. 5 μL of this mixture was added to each well.

3.2 Biochemical evaluation of chromene products for antiproliferative activity

Antiproliferative assays were carried out on all of the compounds synthesised using the ER positive MCF-7 breast cancer cells. Tamoxifen was chosen as a standard positive control drug. The IC_{50} value obtained after reviewing the sigmoidal curve obtained was taken as 6.9 μM (see fig 3.6), which was close to the value from literature of 8 μM in MCF-7 cells [165]. This confirmed the techniques performed were standardised, and with this clarification in the methods of bioevaluation, further antiproliferative evaluation could be then undertaken on the libraries of synthesised chromene products.

The ER binding properties of selected examples from the various compound libraries synthesised have also been obtained using a fluorescence polarisation method. Computational docking experiments were also performed with MOE software. The results from the *in vitro* binding experiments could be rationalised for some of the examples from the *in silico* modelling results.

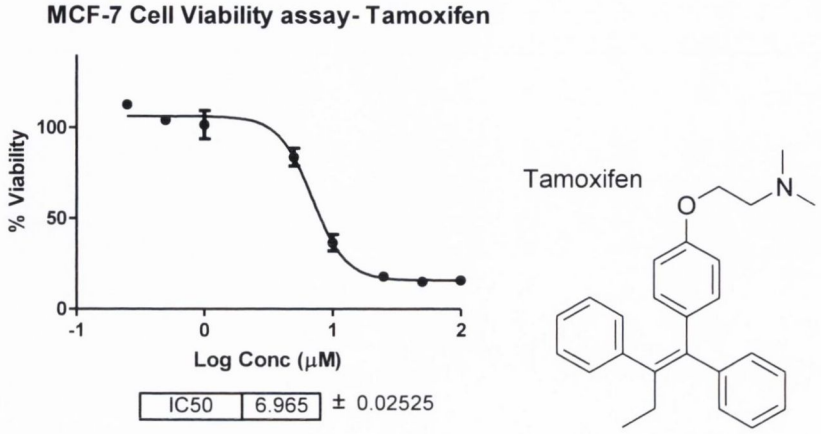

Figure 3. 6 Tamoxifen standard cell viability assay performed

The synthesised compounds from chapter 2 were evaluated by means of biochemical cell viability assay using MCF-7 cells and also by ER binding studies. The results from cytotoxicity study values for each compound is presented in the following antiproliferative tables for each of the compound libraries of chapter 2 as listed below. ER (α and β) binding results are displayed following the antiproliferative results in this chapter.

The clogP value is calculated for each of the compounds synthesised from ChemDraw, (see Table 3.1). The partition coefficient is a ratio of concentrations of un-ionized compound between two solutions. To measure the partition coefficient of an ionizable molecule, the pH of the aqueous phase is adjusted such that the predominant form of the compound is un-ionized. The logarithm of the ratio of the concentrations of the un-ionized solute in the two solvents(e.g. octanol and water) is called log P: The log P value is used as a measure of lipophilicity. The LogP is defined as the partition coefficient of the neutral molecule in octanol/water. However, SERM type compounds such as tamoxifen and raloxifene are not neutral at physiological pH: many contain a tertiary nitrogen which becomes positively charged on protonation. For the compounds. The polar surface area (PSA) of a molecule is defined as the surface sum over all polar atoms, such as oxygen and nitrogen. PSA is frequently used in structure-activity relationship studies of bioactive compounds as a measure of the ability of a drug to permeate cells. It is generally accepted that compounds with a polar surface area of greater than 140 $Å^2$ are likely to be poor at permeating cell membranes. For

molecules to penetrate the blood–brain barrier(BBB) and show activity act on receptors in the central nervous system, a PSA value of less than 60 $Å^2$ is usually required.

The discussion of the antiproliferative activity of the compound libraries synthesised is arranged as follows:

Series 1: 4-Aryl-4*H*-chromenes with varied aryl and benzyloxy substitutions.

Series 2: 4*H*-Chromenes synthesised using a 2 step method.

Series 3: 4*H*,6*H*-pyrano[3,2-g]chromene product

Series 4: Phenyl-4*H*-chromenes with C-3 ester substituents.

Series 5: 4-Hydroxyphenyl-4*H*-chromenes with ester substituents.

Series 6a and 6b: 4-Benzyloxyphenyl-4*H*-chromenes with various C-3 esters

Series 7: 3,4,5-Trimethoxyphenyl chromenes with variation on theC-3 ester

Series 8: 2,7-Diaminochromene compounds.

Series 9: 4-Benzyloxyarylchromenes with N,N-dimethylamino substituent at C-7.

Series 10: Chromenes with ester substituent at C-7,

Series 11: *bis* 4-aryl-4*H*-chromenes

Series 13: Pyranocoumarins (pyrano[3,2-c]benzopyran-5-ones)

Series 14: Pyranocoumarins (pyrano[3,2-c]benzopyran-5-ones) with substituted antagonistic type basic ether chains

3.2.1 Results series 1: 4-Aryl substituted 4*H*-chromenes with varied aryl and benzyloxy substitutions.; type1

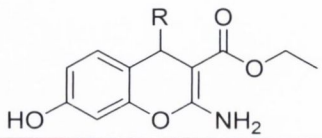

No.	R Group	IC_{50} µM	PSA Å²	CLogP	No.	R Group	IC_{50} µM	PSA Å²	CLogP
BE1	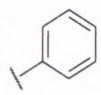	5.76	81.79	4.52	**BE7**	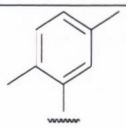	*5.00*	81.79	5.47
BE2	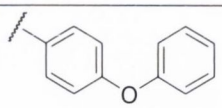	>100	91.02	6.62	**BE8**	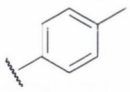	*2.50*	81.79	5.02
BE3	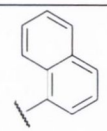	>100	81.79	5.69	**BE9**	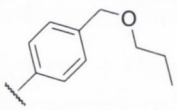	*1.74*	91.02	5.35
BE4	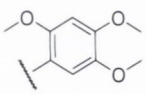	>100	109.49	3.77	**BE10**	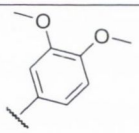	*>100*	100.25	4.18
BE5	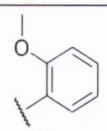	9.63	91.02	4.04	**BE11**	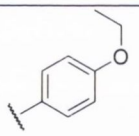	*>100*	91.02	4.97
BE6	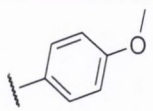	>100	91.02	4.44	**BE12**	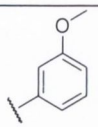	*>100*	91.02	4.44

Table 3. 1 Antiproliferative results of chromene compounds series 1 type I, with IC_{50} values(µM and TSA values (Å²)

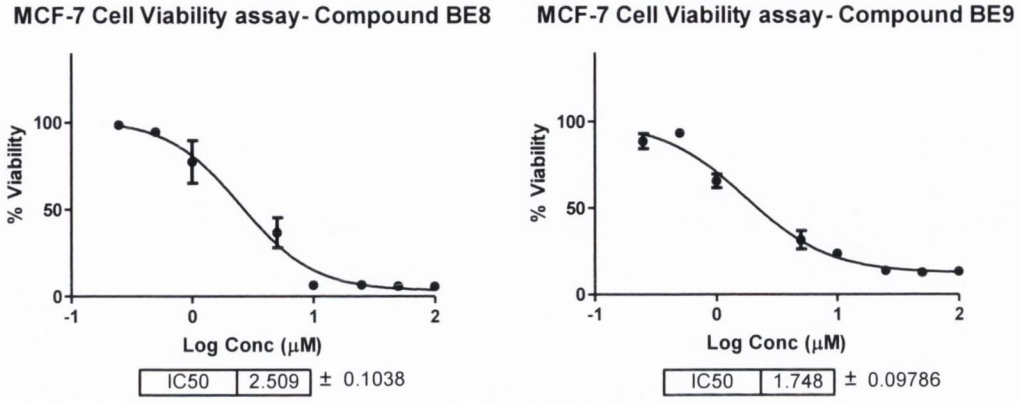

Figure 3.7 Cell viability assay for chromenes BE8 and BE9, (Series 1-Type I)

The results of the antiproliferative evaluation of chromenes **BE1 – BE12** with variation of substituents on C-4 aryl ring are shown in Table 3.1(Series 1-Type I). These examples include many substituents which are classified as electron donating substituents such as monomethoxyaryl (**BE5**, **BE6** and **BE12**), dimethoxyaryl (**BE10**), trimethoxyaryl (**BE4**), ethoxyaryl (**BE11**), methylaryl (**BE8**), dimethylaryl(**BE7**), phenoxyaryl (**BE2**) and propoxymethylaryl (**BE9)** together with the 4-phenyl prototype **BE1**. Some promising results can be seen, with 5 compounds from this series producing IC_{50} value of less than 10 μM. Compounds **BE8** and **BE9** showed the most potent activity with IC_{50} values of 2.5 μM and 1.74 μM respectively (fig 3.7). There was not a clear correlation between activity and either partition coefficient (cLogP) or Polar surface area(PSA) for this series. Introduction of multiple or bulky substitution on the 4-aryl ring of the chromene system as observed in compounds **BE2** (phenoxy), **BE3**(1-naphthyl), **BE4**(2,4,5-trimethoxy) and **BE10**(3,4-trimethoxy) can cause a dramatic loss in antiproliferative activity.

<u>Series 1</u>: 4-Aryl substituted 4H-chromenes with varied aryl and benzyloxy substitutions.; Type II

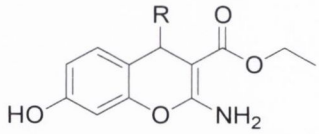

No.	R Group	IC_{50} µM	PSA Å²	CLogP	No.	R Group	IC_{50} µM	PSA Å²	CLogP
BE13	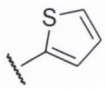	*>100*	81.79	4.16	**BE21**	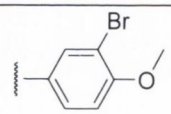	*7.5*	91.02	5.21
BE14	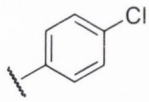	*3.13*	81.79	5.23	**BE22**	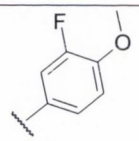	*11.09*	91.02	4.52
BE15	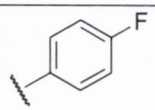	*5.00*	81.79	4.66	**BE23**	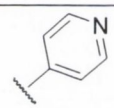	*28*	94.68	3.02
BE16	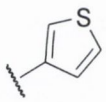	*8.20*	81.79	4.16	**BE24**	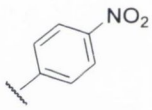	*12.98*	127.61	4.26
BE17	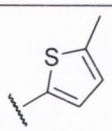	*>100*	81.79	4.66	**BE25**	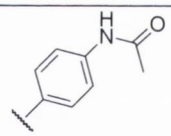	*49*	110.88	3.54
BE18	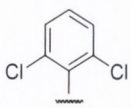	*>100*	81.79	5.94	**BE26**	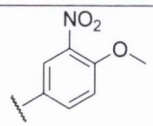	*>100*	136.84	4.20
BE19	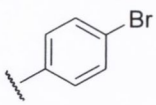	*7.44*	81.79	5.38	**BE27**	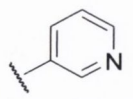	*>100*	94.68	3.02
BE20	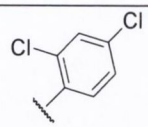	*2.42*	81.79	5.94	**BE28**	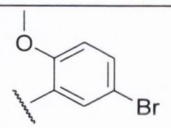	*29.92*	91.02	5.04

Table 3. 2 Antiproliferative results of chromene compounds series 1 type II, with IC_{50} values (µM), and PSA values (Å²)

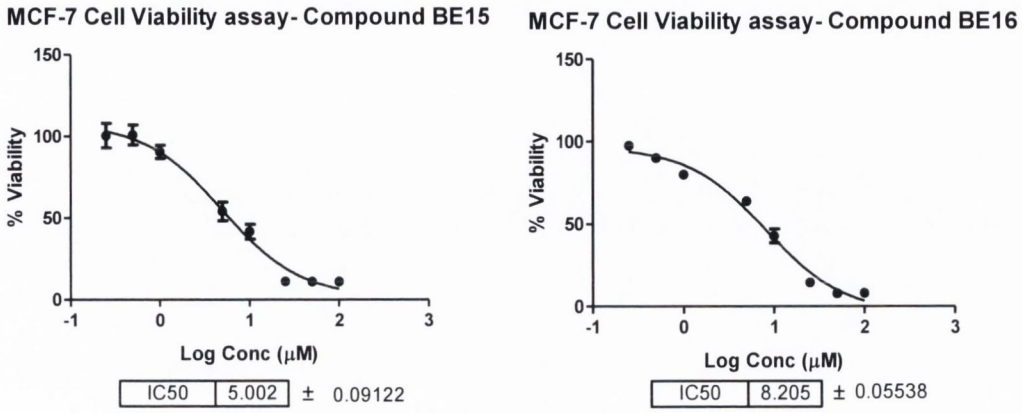

Figure 3. 8 Cell viability assay for compounds BE15 and BE16 showing IC_{50} results

Table 3.2 shows the results obtained for the series 1, Type II compounds, which featured the introduction of halogens (as in compounds **B14**, **B15**, **B19**, **B20**, **B21,** **BE22** and **BE28**), pyridines as in compounds **B23** and **B27,** thiophenes as in compounds **BE13**, **BE16** and **BE17** and nitro substituents such as compounds **BE24** and **BE26** onto the chromene scaffold. Improved antiproliferative values were observed with some of the candidates shown, see compounds **BE14**(IC_{50} = 3.13 μM) and **BE15**(IC_{50} = 5.00 μM) and **BE16**(IC_{50} = 8.20 μM), **BE19**(IC_{50} = 7.44 μM), **BE20** (IC_{50} = 2.05 μM) and **BE21**(IC_{50} = 7.50 μM), This selection had 6 novel compounds with IC_{50} values under the 10 μM limit, and another 5 chromenes with IC_{50} values higher, but nevertheless displaying IC_{50} values < 100 μM. The total polar surface(PSA) areas of each compound was less than 140 $Å^2$ and these compounds are candidates with potential to permeate cell membranes, however their clogP values could be lowered with introduction of additional phenolic or amino groups. The cell viability assay for compounds **BE15** and **BE16** are displayed in Figure 3.8.

3.2.2 Results series 2: 4*H*-Chromenes synthesised using a 2 step method.

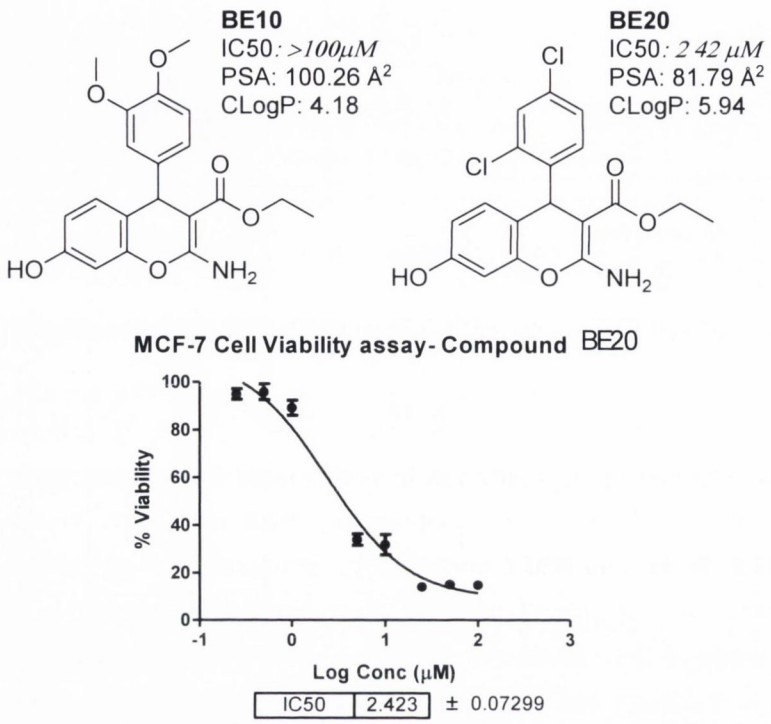

Figure 3. 9 Antiproliferative results of compound BE20, with dose-response curve for BE32 and IC_{50} value

Antiproliferative results for the 4*H*-chromene compounds **BE10** and **BE20** synthesised using the 2 step method can be observed in fig 3.9, **BE10** was demonstrated to show an IC_{50} value of >100 μM while the IC_{50} value for **BE20** is observed at 2.42 μM. PSA values were 100 and 81 Å respectively for compounds **BE10** and **BE20** and CLogP values are calculated as 4.18 and 5.94 respectively. The MCF-7 cell viability dose response curve for **BE20** is displayed in Figure 3.9 and the favourable IC_{50} value of 2.42 μM suggests that this compound has acceptable druggability values.

3.2.3 Results series 3: *4H,6H*-pyrano[3,2-g]chromene product BE33.

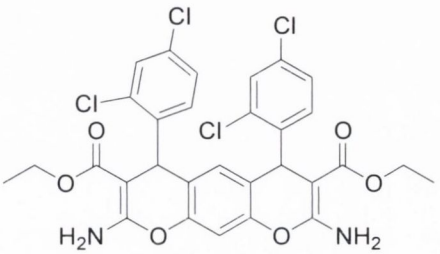

BE33
IC50:>*100μM*
PSA: 123.12Å^2
CLogP: 10.9

Figure 3. 10 Results of 4H,6H-pyrano[3,2-g]chromene compound BE33

The novel 4*H*,6*H*-pyrano[3,2-g]chromene product **BE33** (figure 3.10) did not show positive antiproliferative values when evaluated in MCF7 cells (IC_{50} > 100 μM). However further studies of some related pyranocoumarins and knowledge of how they may bind in the ER LBD, could prove beneficial for further design and varied synthesis of such fused structures. This adduct is much more lipophilic than the prototype chromene **BE1** and therefore results in a higher CLogP value (cLogP = 10.9), and also a higher PSA value of 123 Å^2, which may correlate with the lower antiproliferativ activity observed for **BE33**.

3.2.4 Results series 4: 3-Phenyl-4*H*-chromenes with C-3 ester substituents

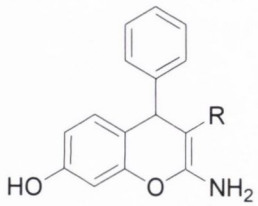

No.	R Group	IC_{50} µM	PSA Å²	CLogP	No.	R Group	IC_{50} µM	PSA Å²	ClogP
BE34		*>100*	79.27	2.91	**BE38**	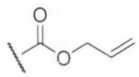	*7.95*	81.79	4.76
BE35		*23.12*	81.79	3.99	**BE39**	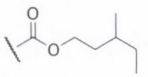	*>100*	81.79	6.50
BE36	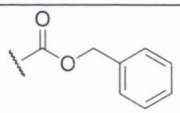	*6.60*	81.79	5.76	**BE40**	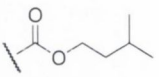	*11.15*	81.79	5.98
BE37	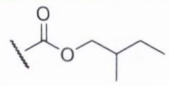	*3.04*	81.79	5.98					

Table 3. 3 ***Antiproliferative results of chromene compounds series 4 IC_{50} in (µM), PSA values (Å²)and CLogP values***

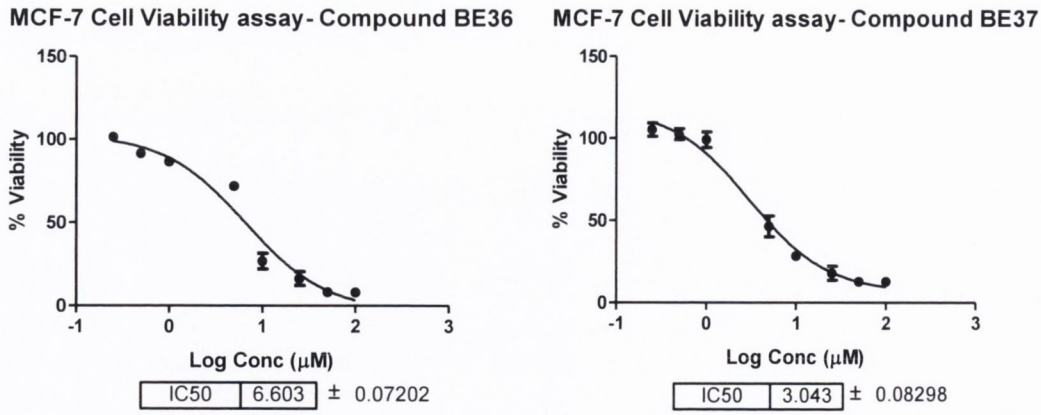

Table 3. 4 Cell viability assay and IC_{50} value for compounds BE36 and BE37

The 3-phenyl-4*H*-chromenes with C-3 ester substituents (Series 4, **BE34-BE40**) demonstrated very promising results as cytotoxic agents when evaluated in MCF-7 breast cancer cells. The IC_{50} values for the antiproliferative assays are presented in table 3.3. The most potent compounds in the series were identified as **BE36**, **BE37** and **BE38** showing IC_{50} values of 3.00 μM, 7.9 μM and 7.95 μM respectively The dose response curves for the two most potent compounds in the series, **BE36** and **BE37** are presented in Table 3.4. The CLogP and PSA values are shown also and were all consistent with the potential of these compounds as SERMs and potential clinical candidates.

3.2.5 Results series 5: 4-Hydroxyphenyl-4*H*-chromenes with ester substituents chain.

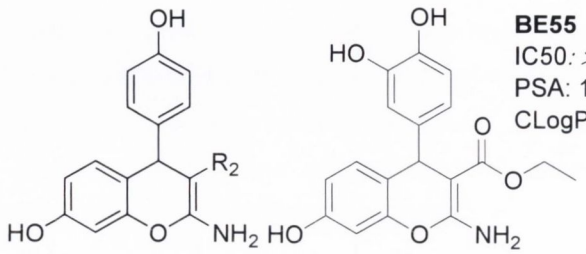

BE55
IC50*: >100μM*
PSA: 122.246 Å
CLogP: 3.2592

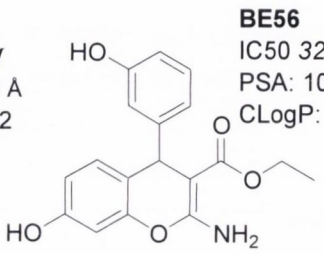

BE56
IC50 *32.50μM*
PSA: 102.018 Å
CLogP: 3.8562

No	R Group	IC_{50} μM	PSA Å²	CLogP	No	R_2 Group	IC_{50} μM	PSA Å²	CLogP
BE41	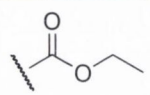	*>100*	102.02	3.85	**BE48**	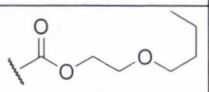	*>100*	111.25	4.73
BE42	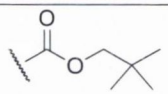	*>100*	102.02	5.18	**BE49**	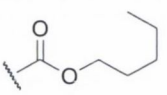	*39.20*	102.01	5.44
BE43	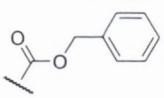	*37.55*	102.02	5.09	**BE50**	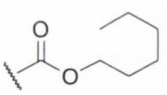	*52.53*	102.01	5.97
BE44	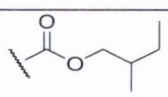	*>100*	102.02	5.31	**BE51**	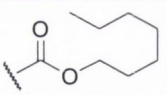	*60.64*	102.01	6.50
BE45	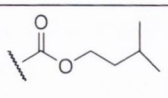	*43.73*	102.02	5.31	**BE52**	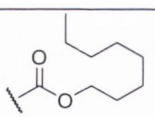	*17.99*	102.01	7.03
BE46	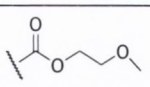	*>100*	111.25	3.28	**BE53**	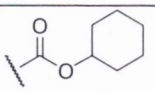	*>100*	102.01	5.35
BE47	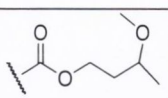	*>100*	111.25	3.96	**BE54**	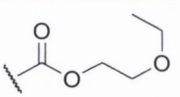	*>100*	111.25	3.67

Table 3. 5 Antiproliferative results of chromene compounds series 5 IC50 in (μM), PSA values (Å²)and CLogP values

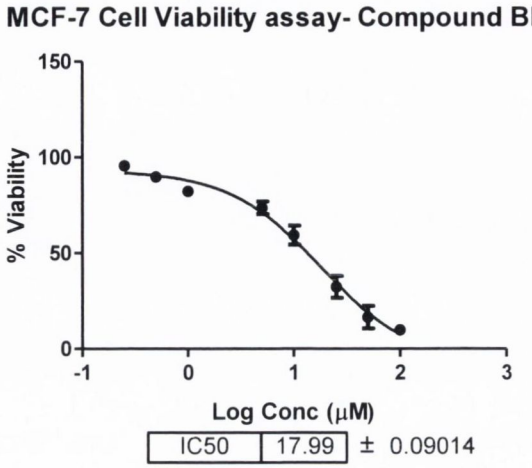

Figure 3. 11 Cell viability assay and IC_{50} value for compound BE52

The antiproliferative results for the 4-hydroxyphenyl-4*H*-chromenes with ester substituents chain, series 5 compounds, are dsplayed in table 3.5. These compounds showed higher IC_{50} values than anticipated in most cases, than the prototype examples in the previous series above. It is proposed that this effect may be due to the larger size and more lipophilic character of the molecules in series 5. The introduction of long aliphatic ester substituents onto the chromene as the C3 ester has brought about this effect, producing a lengthened bulky moiety on each chromene molecule. It was initially anticipated that this type of substituent would resemble the aliphatic substituent in the fulvestrant type antiestrogen and would result in an increase in anrtiproliferaticve activity observed in the estrogen receptor positive MCF-7 breast cancer cells. This result shows some correlation with higher PSA values, ranging from 102 to 111 $Å^2$. The most potent compound in the series, **BE52,** containing the *n*-octylester substituent at C-3 of the chromene ring was shown to have an acceptable antiproliferative IC_{50} value of 17.99 μM, see figure 3.11,

3.2.6 Results series 6: 4-Benzyloxyphenyl-4*H*-chromenes with various C-3 esters.

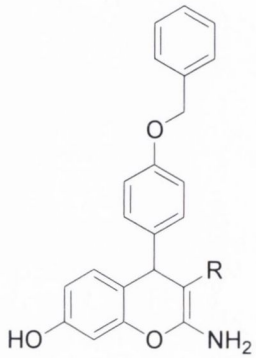

No	R Group	IC_{50} µM	PSA Å²	CLogP	No	R Group	IC_{50} µM	PSA Å²	CLogP
BE57	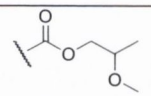	*1.76*	100.25	5.95	**BE64**	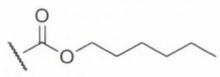	*5.05*	91.02	8.32
BE58	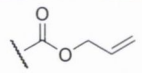	*1.49*	91.02	6.45	**BE65**	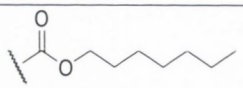	*2.03*	91.02	8.85
BE59	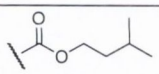	*11.67*	91.02	7.66	**BE66**	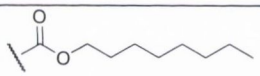	*4.93*	91.02	9.38
BE60	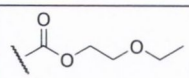	*>100*	100.25	6.03	**BE67**	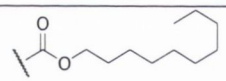	*4.11*	91.02	10.44
BE61	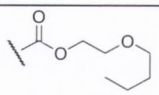	*>100*	100.25	7.08	**BE68**	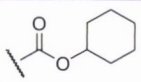	*2.07*	91.02	7.71
BE62	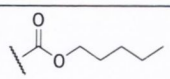	*2.31*	91.02	7.79	**BE69**	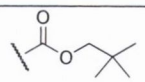	*4.40*	91.02	7.53
BE63	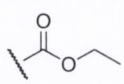	*4.5*	91.02	6.21					

Table 3. 6 Antiproliferative results of chromene compounds series 6a IC50 in (µM), PSA values (Å²)and CLogP values

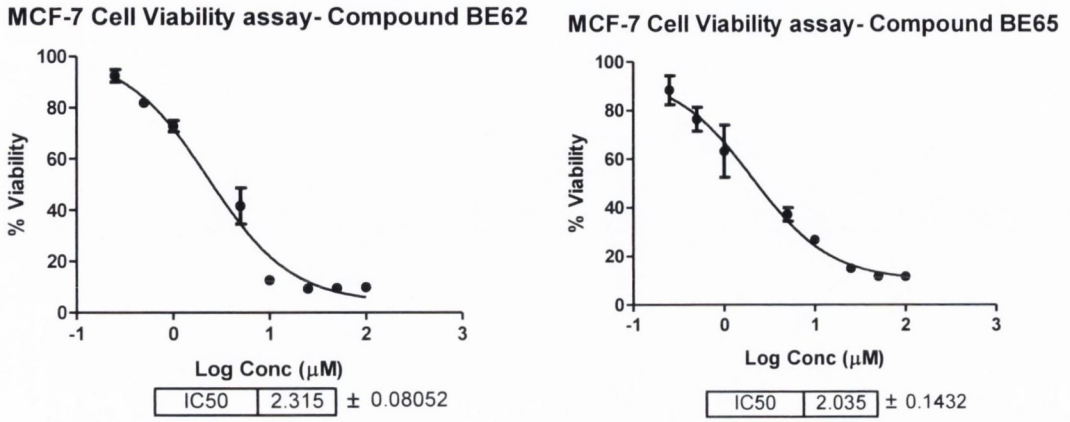

Figure 3. 12 Cell viability assays and IC_{50} values for compounds BE62 and BE65

The results from the antiproliferative evaluation of the 4-benzyloxyphenyl-4*H*-chromenes with various C-3 esters (series 6a compounds) are presented in table 3.6. It can be observed that many compounds in the series showed IC_{50} values ranging from 1.49 to 11.67 μM, with 3 of the compounds having IC_{50} values >100 μM. The most potent compound in the series was found to be **BE58**, having the allyl ester substituent at C-3 As shown in table 3.6, 10 compounds in total resulted in IC_{50} values under 10 μM, all of which are favourable cytotoxicity values. The PSA values are observed in the range 91 to 100 $Å^2$ and the CLogP values are in the range 5.95 to 10.44. These CLogP values are regarded as too high for druggability to meet the Lipinski rules for optimum properties for orally active drugs, (see section 3.7). This is due to the introduction of the lipophilic benzyloxyphenyl ether at C4, together with the lipophilic ester type substituent at C-3. Representative examples of dose response curves for two of the most potent compounds in the series e.g. compounds **BE62** and **BE65,** are presented in Figure 3.12, showing good IC_{50} values of 2.31 μM and 2.03 μM respectively. These results indicate that the series 6 chromenes, having the combination of the 4-benzyloxyphenyl substituent with the lipophilic ester functional group at C-3 provides the optimised chromene pharmacophore for antiproliferative activity. The more polar esters, **BE60** and **BE61** did not display activity in this assay.

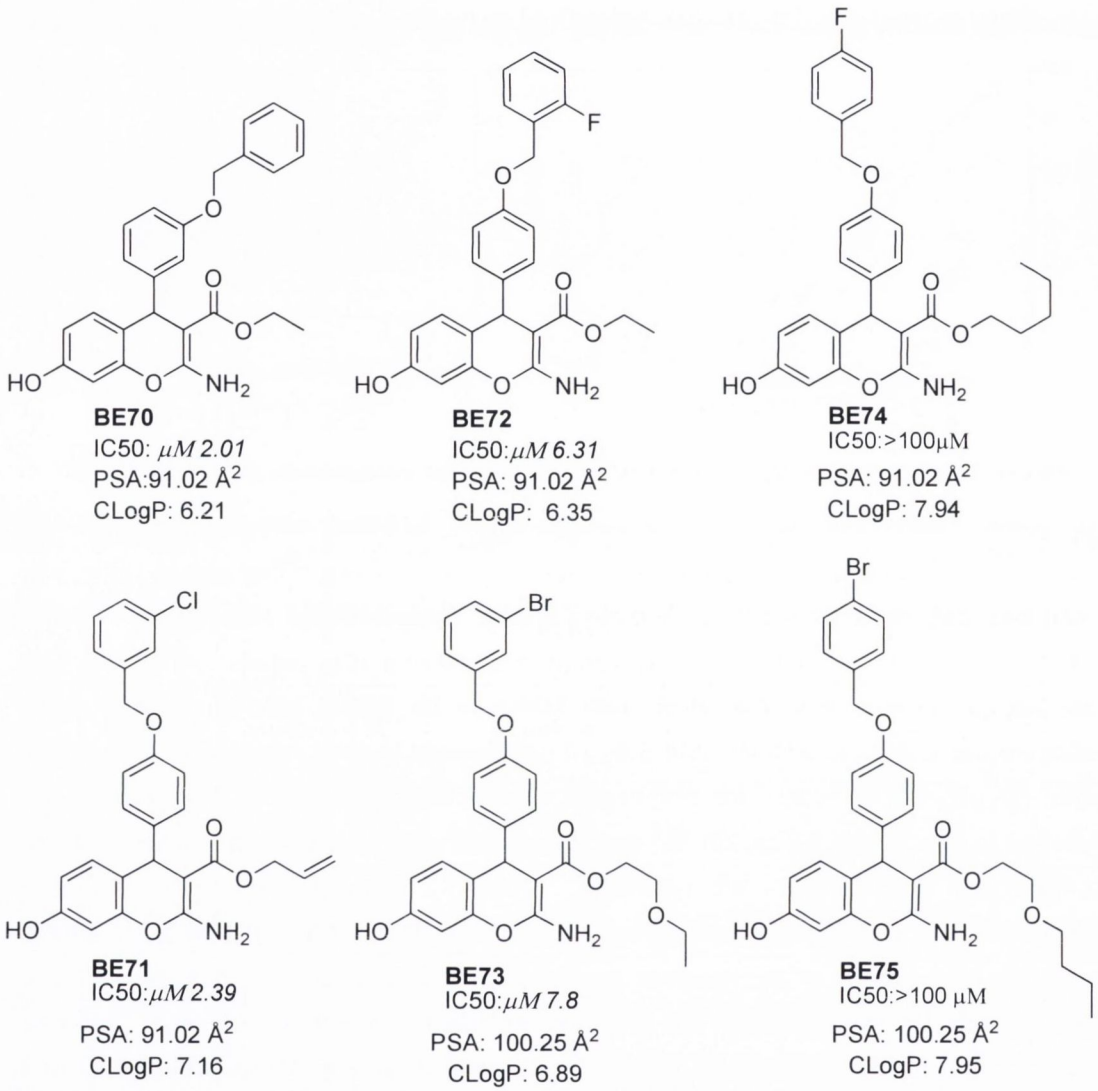

Figure 3. 13 Antiproliferative results of chromene compounds, series 6b, IC_{50} in (μM), PSA values (Å²)and CLogP values

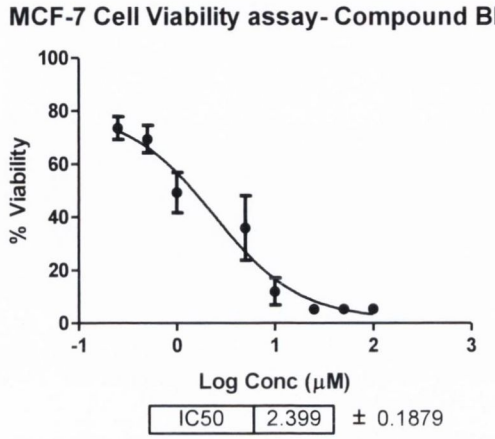

Figure 3. 14 Cell viability assay and IC_{50} value for compound BE71

A further series of 4-benzyloxyphenyl-4*H*-chromenes with various C-3 esters were now investigated. These compounds were analysed to determine if the inclusion of a halogen substituent on the benzyloxy aryl ring (as was indicated in the preliminary *in silico* screening) would influence the biochemical activity of the chromene products. The antiproliferative results obtained for the chromene compounds of series 6b are presented in Figure 3.13. In this series, the 4-benzyloxy ether substituent also contains the fluoro (**BE72** and **BE74),** bromo (**BE73** and **BE75**) and chloro (**BE71**) substituent groups; The 3-benzyloxy ether **BE70** is also included in this series. The IC_{50} values obtained are displayed in table 3.13, and are in the range 2.01 μM to 7.80 μM for the active compounds (**BE74** and **BE75** were inactive, (IC_{50} > 100 μM)). These results indicate that inclusion of a halogen on the benzyloxy aryl ring improved activity only in the case of compound **BE73** (IC_{50} = 7.8 μM) when compared with compound **BE60** (IC_{50} > 100 μM). A slight reduction in activity was observed for compounds **BE72** (IC_{50} = 6.31μM) and **BE71**(IC_{50} = 2.84 μM) when compared to compound **BE63** (IC_{50} = 4.50 μM). PSA values from 91 to 100 $Å^2$, are calculated for these compounds, which would predict good cell permeability. However, CLogP values from 6.21 μM to 7.95 μM are calculated, and were above the Lipinski limit of 5 which is unfortunate as IC_{50} antiproliferative values for compounds **BE70 – BE73** were mostly favourable. In this series, the two compounds **BE74** and **BE75** with the highest ClogP values (7.94 and 7.95 respectively) were inactive, (IC_{50} > 100 μM). Figure 3.14 displays the dose response curve for compound **BE71** with an IC_{50} value of 2.39 μM.

3.2.7 Results series 7: 3,4,5-Trimethoxyphenyl substituted chromenes with variation on the C-3 ester

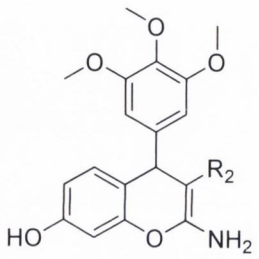

No	R Group	IC_{50} µM	PSA Å²	CLog P	No	R Group	IC_{50} µM	PSA Å²	CLog P
BE76	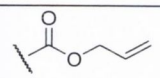	*>100*	109.49	4.06	**BE81**	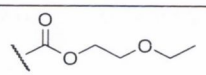	*>100*	118.72	3.64
BE77	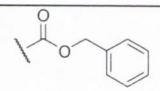	*>100*	109.49	5.06	**BE82**	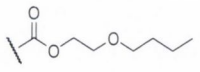	*>100*	118.72	4.70
BE78	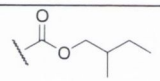	*65.84*	109.49	5.28	**BE83**	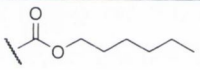	*>100*	109.49	5.93
BE79	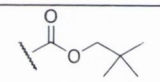	*15.24*	109.49	5.15	**BE84**	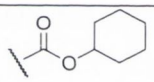	*>100*	109.49	5.32
BE80	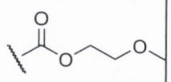	*>100*	109.49	3.25	**BE85**	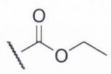	*>100*	109.49	3.82

Table 3. 7 Antiproliferative results of chromene compounds series 7 IC_{50} in (µM), PSA values (Å²)and CLogP values

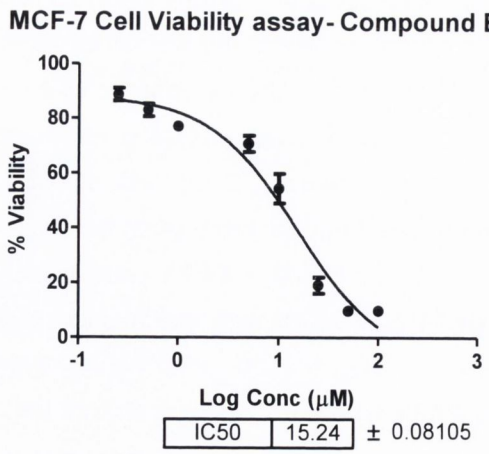

Figure 3. 15 Cell viability assay and IC_{50} value for compound BE79

A comprehensive library of 3,4,5-trimethoxyphenyl substituted chromenes with variation on the C-3 ester (**BE76-BE85**, series 7) was synthesised and evaluated to determine if the inclusion of the 3,4,5-trimethoxyphenyl motif in the chromene structure, known to be present in many tubulin targetting agents such as colchicine and combretastatin, could promote antiproliferative activity in these compounds. The results of this study are presented in table 3.7. It can be observed that the IC_{50} values are in the range from 15.24 μM to >100 micromolar. The antiproliferative IC_{50} values are not as favourable in this table comparing to the previous series of results with only two compounds **BE78** and **BE79** displaying values under 100 μM and none of the values were recorded under 10 μM. It is not clear why the loss in activity was observed for these products. When compared with the chromene structures of series 1(see Table 3.1), it is apparent that introduction of multiple or bulky substitution on the 4-aryl ring of the chromene system as observed in compounds **BE2** (phenoxy), **BE3**(1-naphthyl), **BE4**(2,4,5-trimethoxy) and **BE10**(3,4-trimethoxy) can cause a dramatic loss in antiproliferative activity. The total polar surface area values for these compounds are higher than calculated for the more active compounds in Series 1, (see Table 3.1) ranging from 109 – 118 $Å^2$, due to the introduction of the trimethoxyaryl substituent at C4. However the CLogP values were more favourable due to the introduction of this trimethoxyaryl substituent, and is calculated in the range 3.25 – 5.93. It is concluded that the introduction of the trimethoxyaryl moiety at C-4 of the chromene is not favourable for antiproliferative activity. A selected dose response sigmoidal curve is displayed in figure 3.15 for **BE79,** with a moderate IC_{50} value of 15.25 μM.

3.2.8 Results series 8: 2,7-Diaminochromene compounds

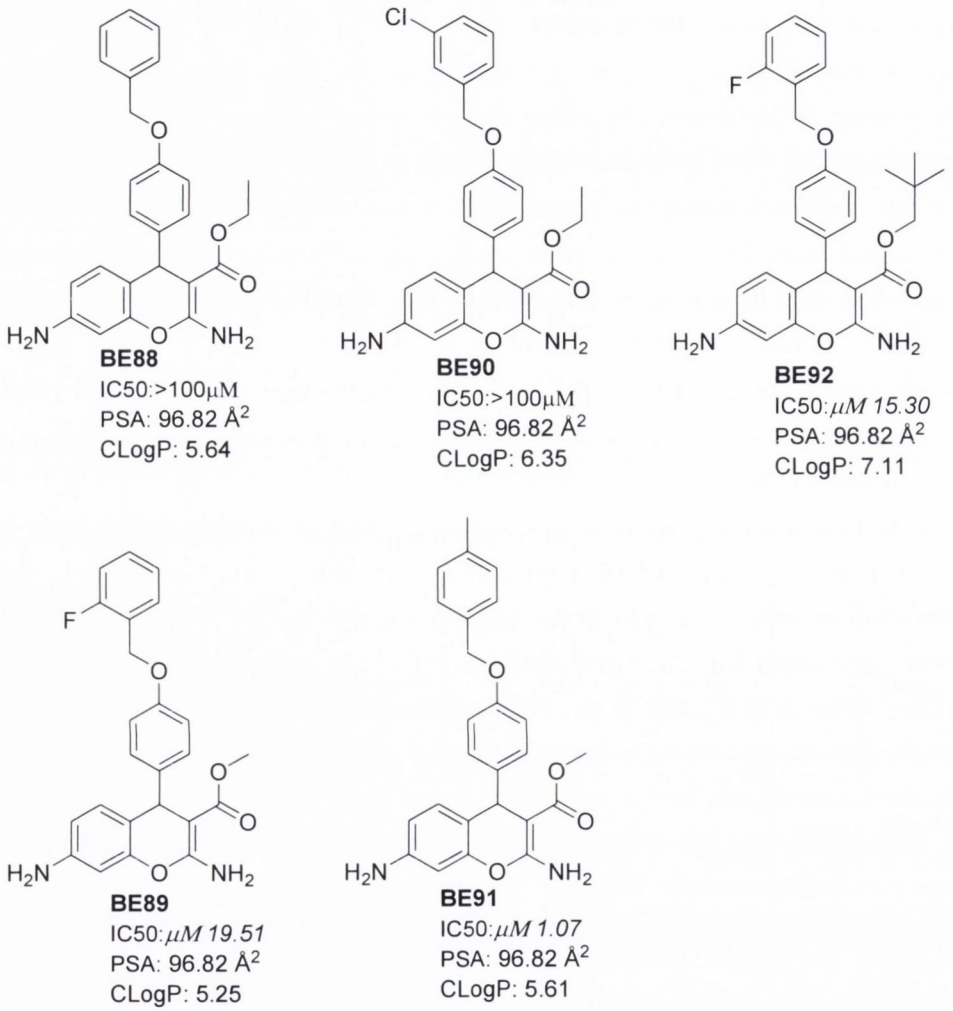

Figure 3. 16 Antiproliferative results of chromene compounds series 8 IC_{50} (μM),PSA values (Å²)and CLogP values

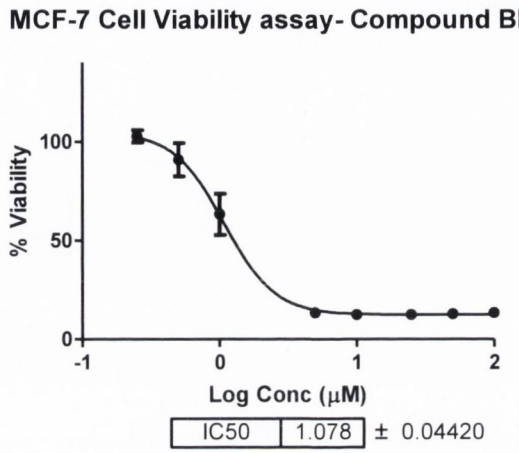

Figure 3. 17 Cell viability assay and IC_{50} value for compound BE91

The antiproliferative results for the series 8 compounds are displayed in Figure 3.16. Thse compounds were synthesised to explore the possible effect on the antiproliferative activity of the introduction of the replacement of the phenolic substituent at C-7 of the chromene by a primary amine. The results show that the IC_{50} values of the products are in the range of 1.07 to 19.51 μM, with two of the compounds **BE88** and **BE90** having IC_{50} values of >100 μM. Total polar surface area values are all calculated to be 96.82 Å. CLogP values are observed ranging from 5.25 to 7.11. The most potent compound in the series was identified as **BE91**, with IC_{50} value of 1.07 μM. The sigmoidal dose response curve of selected compound **BE91** is displayed in Figure 3.17. The introduction of the second amino group on the chromene at C-7 was not detrimental to the antiproliferative activity with three compounds from the group of five having antiproliferative activity under 20 μM, and compound **BE91** displaying one of the most potent activities in the entire series, (IC_{50} value of 1.07 μM). It is possible that for compound **BE91**, a combination of the effects of the 4-methylbenzyloxyaryl ether at C4, the methyl ester at C-3 and the primary amine at C-7 contribute to optimise the structural requirements for activity.

3.2.9 Results series 9: 4-Benzyloxyarylchromenes with N,N-dimethylamino substituent at C-7

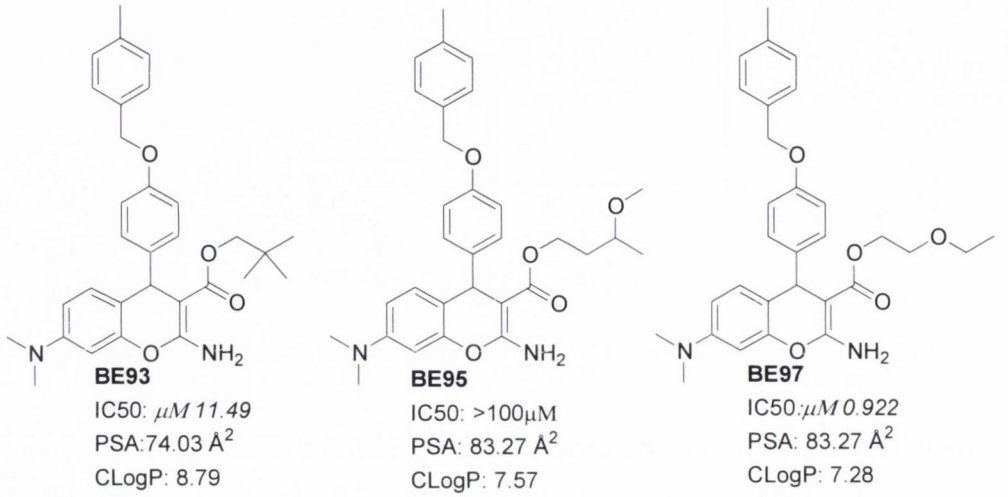

BE93
IC50: μM *11.49*
PSA:74.03 Å^2
CLogP: 8.79

BE95
IC50: >100μM
PSA: 83.27 Å^2
CLogP: 7.57

BE97
IC50:μM *0.922*
PSA: 83.27 Å^2
CLogP: 7.28

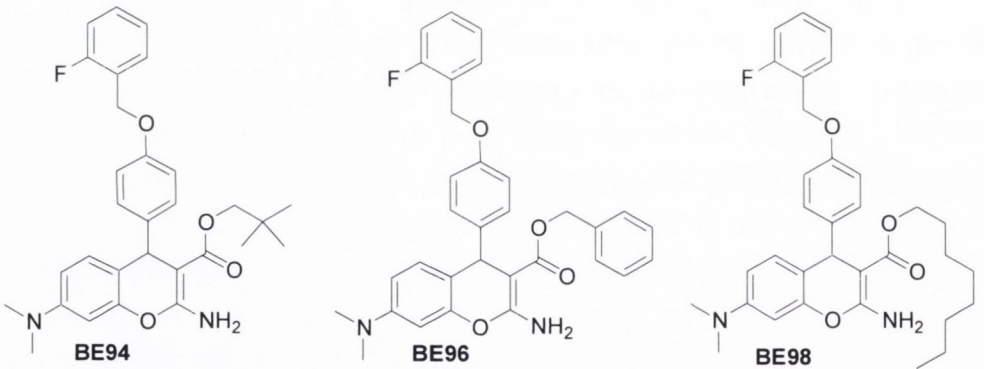

BE94
IC50: μM *11.25*
PSA:74.03 Å^2
CLogP: 8.43

BE96
IC50:μM *5.307*
PSA: 74.03 Å^2
CLogP: 8.35

BE98
IC50: >100μM
PSA: 74.03 Å^2
CLogP: 11.35

Figure 3. 18 Antiproliferative results of chromene compounds series 9 IC_{50} in (μM), PSA values (Å^2)and CLogP values

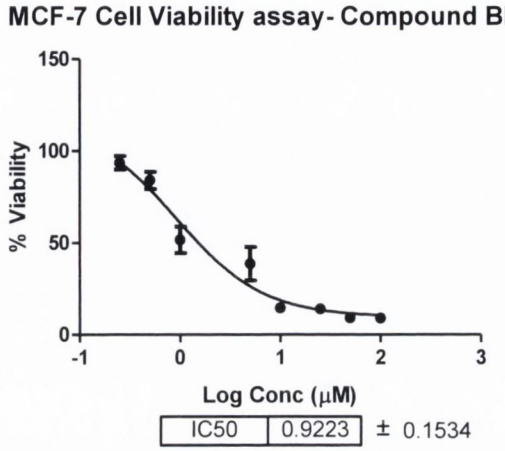

Figure 3. 19 Cell viability assay and IC_{50} value for compound BE97

To further exploit the effects of the introduction of an amine function at C-7 of the chromene, an additional library of compounds was synthesised which contain the N,N-dimethylamino substituent at C-7. The design of these compounds reflected the optimised benzyloxyaryl ether substituents identified from series 8. The novel 7-N,N-dimethylamino-4-benzyloxyaryl chromene compounds **BE93-BE98** were evaluated in a cytotoxicity study, and the antiproliferative IC_{50} values obtained are displayed in figure 3.18. The products displayed IC_{50} values ranging from 0.920 to 11.49 μM on four of the compounds, Two of the compounds, **BE95** and **BE98** were inactive with IC_{50} falling over 100 μM. Total polar surface area values calculated were in the range 74.03 to 83.27 $Å^2$, reflecting the lowering of the polar surface are as a consequence of the replacement of the primary amine by the tertiary amine. CLogP values as expected were however higher than in series 8 ranging from 7.57 to 11.35. The introduction of the N,N-dimethylamino group resulted in an increased cytotoxicity of some of the compounds when compared with the 7-amino analogs. Results for the MCF-7 cell viability assay dose response curve are shown for the most potent compound **BE97** and displays an IC_{50} value of 0.92 μM, see figure 3.19. The combination of the effects of the 4-methylbenzyloxyaryl ether at C4, the ethoxyethyl ester at C-3 and the N,N-dimethylamino substituent at C-7 contributes to optimise the structural requirements for activity. It is interesting that compound **BE97** was identified as the most potent compound in the entire library of products evaluated.

3.2.10 Results series 10: Chromenes with ester substituent at C-7

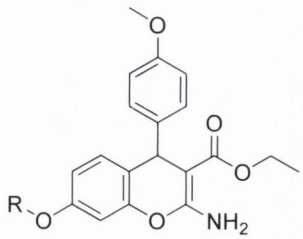

No.	R Group	IC_{50} µM	PSA Å²	CLogP	No.	R Group	IC_{50} µM	PSA Å²	CLogP
BE99		*>100*	97.10	4.44	**BE106**	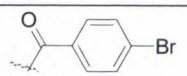	*>100*	97.10	7.44
BE100	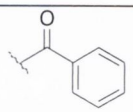	*18.81*	97.10	6.57	**BE107**	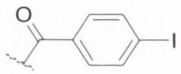	*>100*	97.10	7.70
BE101	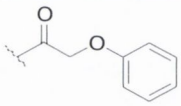	*>100*	106.33	5.88	**BE108**	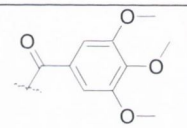	*>100*	124.80	5.99
BE102	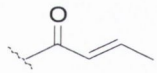	*13.59*	97.10	5.50	**BE109**	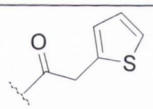	*>100*	97.10	5.94
BE103	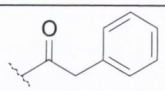	*>100*	97.10	6.29	**BE110**	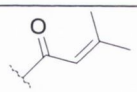	*>100*	97.10	5.90
BE104	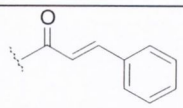	*>100*	97.10	7.06	**BE111**	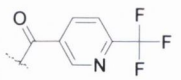	*>100*	109.99	6.10
BE105	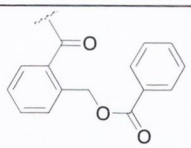	*>100*	123.40	8.37					

Table 3. 8 Antiproliferative results of chromene compounds series 10 IC_{50} in (µM), PSA values (Å²)and CLogP values

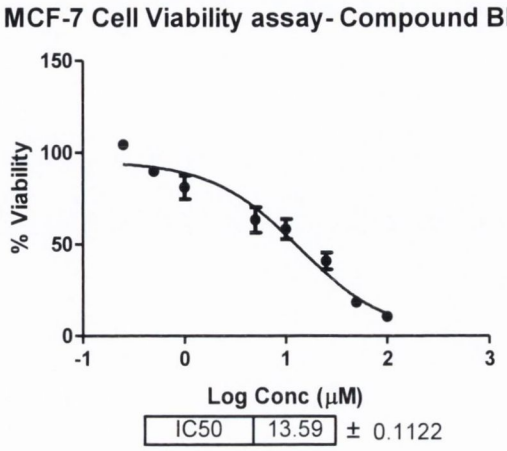

Figure 3. 20 Cell viability assay and IC_{50} value for compound BE102

The synthesis of a library of chromenes with various ester substituent at C-7, (**BE99-BE111**) was investigated to determine if esterification of the phenolic group at C-7 would contribute to the cytotoxic activity of the compounds. It was suggested from the initial *in silico* screening that the inclusion of a lipophilic ester substituent at C-7 of the chromene might mimic the [(4,4,5,5,5-pentafluoropentyl)sulfinyl]nonyl substituent located at C-9 of the steroid scaffold structure of the estrogen antagonist fulvestrant, which is known to cause disruption of agonist conformation of Helix 12 of the estrogen receptor. The results of the antiproliferative assay for series 10 compounds **BE99-BE111** are displayed in Table 3.9. surprisingly, only 2 of the compounds demonstrated moderate IC_{50} values, with **BE102** and **BE100** having IC_{50} values of 13.59 µM and 18.81 µM respectively. Interestingly, for these two compounds, the replacement of the phenol at C-7 of the chromene with an ester function resulted in a marked increase in the antiproliferative activity when compared to the parent compound **BE6** which had an IC_{50} > 100 µM. All other compounds in the series demonstrated antiproliferative results with IC_{50} over 100 µM. The total polar surface area values for the series ranged from 97 to 123 $Å^2$, while CLogP values ranged from 4.44 to 8.37. The MCF-7 dose response curve of **BE102** is displayed in figure 3.20 and shows an IC_{50} value of 13.59 µM.

3.2.11 Results series 11: *bis* 4-aryl-4*H*-chromenes

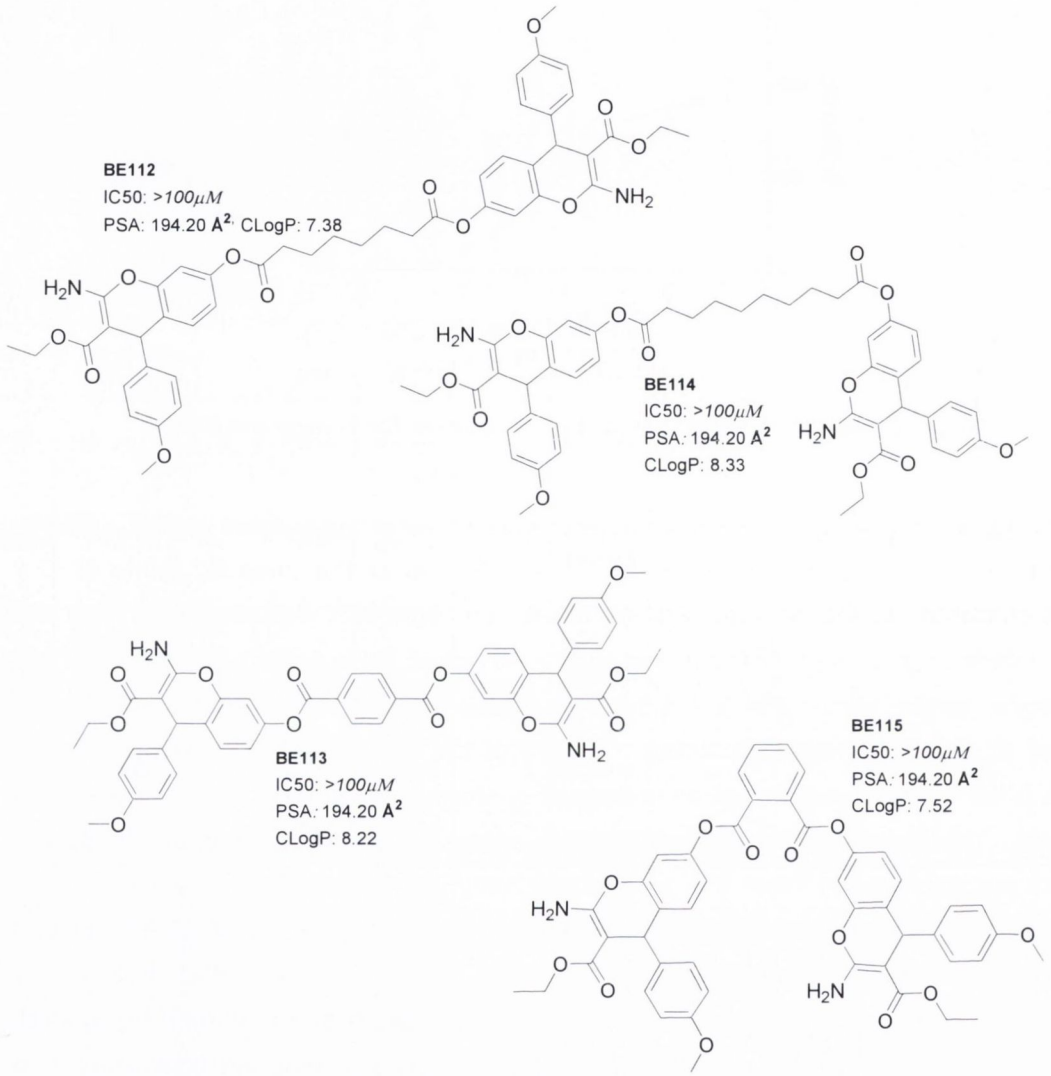

Figure 3. 21 Antiproliferative results of bischromene compounds series 11 IC_{50} in (μM), PSA values (Å²) and CLogP values

The synthesis of the *bis*-chromene compounds **BE112-BE115** was investigated to explore if a chromene based ligand containing two potential locations for interaction with the ligand binding domain of the estrogen receptor, would demonstrate useful antiproliferative activity. The results from the antiproliferative biochemical evaluation of the *bis*chromene compounds, **BE112-BE115,** series 11 is displayed in figure 3.21. The large molecules all were found to be inactive in the MCF-7 assay with IC_{50} values over 100 μM. The total polar surface area for all four compounds was calculated to be

194.20 $Å^2$, outside the range for cell penetration and the CLogP values were all found to be over the druggability limit of 5.

3.2.12 Results series 13: Pyranocoumarin (pyrano[3,2-c]benzopyran-5-one) products.

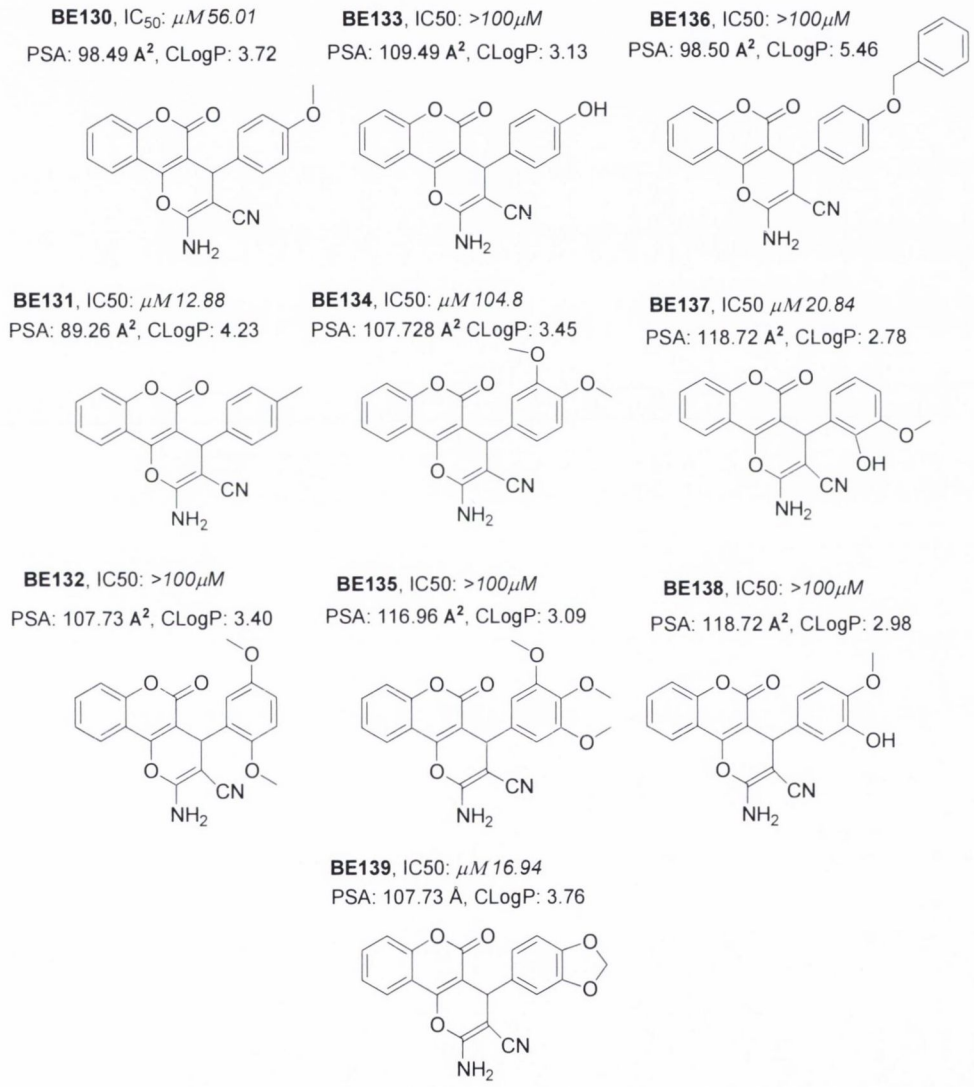

Figure 3. 22 Antiproliferative results of pyranocoumarin compounds series 11 IC_{50} in(μM), PSA values ($Å^2$)and CLogP values

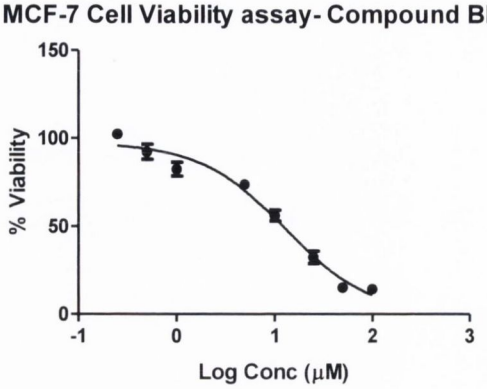

Figure 3. 23 Cell viability assay and IC_{50} value for compound BE131

The pyranocoumarin (pyrano[3,2-c]benzopyran-5-one) products synthesised (**BE130-139**) are displayed in Figure 3.22. These compounds are of interest as they incorporate the coumarin scaffold fused to a 4*H*-pyran. The biochemical evaluation for all the pyranocoumarins was performed similarly to the chromene products and the results are displayed in figure 3.22. The most potent compound in the series was identified as **BE131** with an IC_{50} value obtained with MCF-7 cells of 12.88 μM, indicating that fusion of the coumarin scaffold to the 4*H*-pyran ring system facilitates the antiproliferative mechanism of action. Interestingly the most active compound **BE131** contains the same 4-methylphenyl substituent on the 4*H*-pyran ring as the similarly substituted chromene compound **BE7**, which was one of the more active compound identified in Series 1 (see table 3.1). Other moderately active pyranocoumarin compounds in the series were identified as **BE139**(IC_{50} value = 56.01 μM) and **BE139**(IC_{50} value 16.94 μM) and **BE137**(IC_{50} value 20.84 μM) PSA results for this series are calculated ranging from 89 to 118 $Å^2$., while CLogP values are calculated to be between 2.78 to 5.46 and indicate that the compounds are druggable. The MCF-7 dose response curve of **BE131** is illustrated in figure 3.23 and displays an IC_{50} value of 12.88 μM.

3.2.13 Results series 14: Pyranocoumarins (pyrano[3,2-*c*]benzopyran-5-ones) with substituted antagonistic type basic ether chains

BE140, IC50: *10.75μM*

PSA: 101.73 Å, CLogP: 4.78

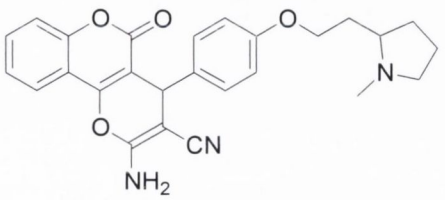

BE141, IC50: *>100μM*

PSA: 110.96 Å, CLogP: 3.83

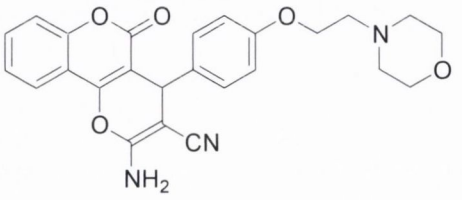

BE142, IC50: *>100μM*

PSA: 101.73 Å, CLogP: 4.49

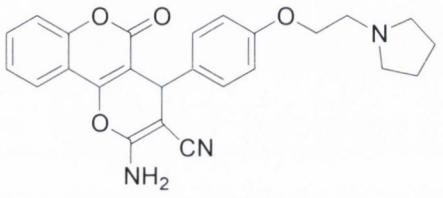

Figure 3. 24 Antiproliferative results of coumarin compounds series 14 IC_{50} in (μM), PSA values (Å^2)and CLogP values

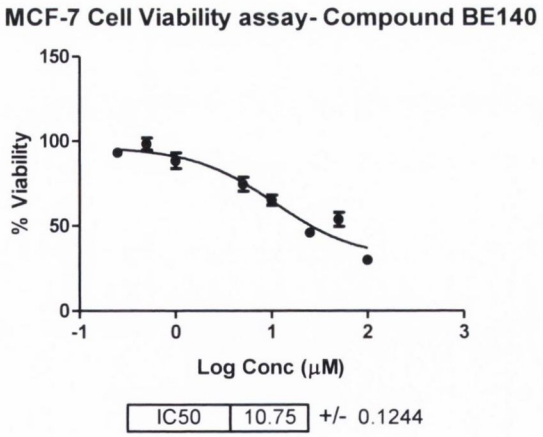

Figure 3. 25 Cell viability assay and IC_{50} value for compound BE140

A series of three pyranocoumarins (pyrano[3,2-c]benzopyran-5-ones), **BE140-BE142** were prepared containing a basic arylether substituent at C-4 to determine the effect on antiproliferative activity of the introduction of the basic arylether functionality, (see

figure 3.24). The basic arylether structural motif is frequently associated with antiestrogenic activity as in the structures of tamoxifen and raloxifene. The biochemical antiproliferative evaluation for the series 14 pyranocoumarins containing the antagonistic type substituent was performed in the MCF-7 cell line and the results of the IC_{50} determinations are presented in Figure 3.24. The most active compound was identified **BE140** with IC_{50} value of 10.75 μM. This result is very encouraging as the parent phenolic compound **BE135** was inactive with IC_{50} value > 100 μM, (see figure 3.22). This result supports the proposed mechanism of action of these compounds as targetting the estrogen receptor. This compound was therefore selected for estrogen receptor(ER) binding evaluation *in silico* and *in vitro*. The remaining two compounds **BE141** and **BE142** gave poor results in the antiproliferative assay, with IC_{50} value values >100 μM. The PSA values for these compounds are calculated as 101.73 $Å^2$ for **BE140** and **BE142** and 110.96 $Å^2$ for **BE141** and Clog P values are observed as 3.83 for **BE141**, 4.49 for **BE142** and 4.78 **BE140**. The dose response curve is displayed for **BE140** in figure 3.25.

3.3 Antiproliferative results of LNCaP Assays

Antiproliferative assays were carried out on a select number of compounds using the LNCaP androgen receptor human prostate cancer cell line **LNCaP**. As the compounds were synthesised to specifically target the estrogen receptor and with limited availability of time and resources, only 6 chromene compounds were selected for LNCaP toxicity studies, **BE6, BE17, BE18, BE23, BE69** and **BE92**. A general antiproliferative screen of LNCaP cells for the selected six compounds at 3 concentrations (50 μM, 10 μM and 500 nM) was initially conducted (Fig 3.26) to determine if the candidate compounds have potential for further full concentration range assays to obtain IC_{50} values for the compounds.

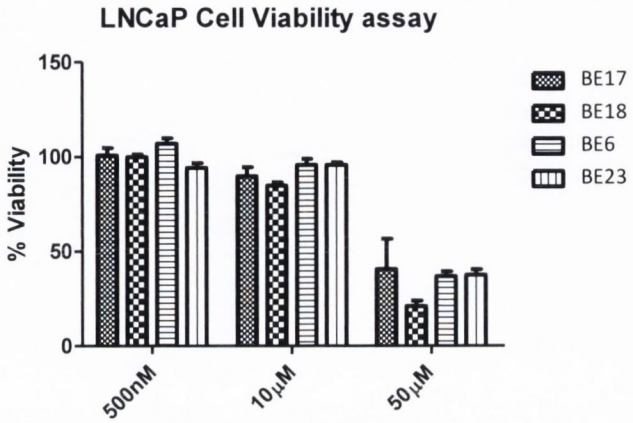

Figure 3. 26 LNCaP cell preliminary viability screening,

Of the 6 compounds selected for the initial LNCaP assays, 2 compounds (**BE69** and **BE92**) demonstrated favourable values as antiproliferative agents on LNCaPs (demonstrated < 50% viability at 10 μM) to allow the evaluation over the full 8 dose concentration range (100 μM -10 nM). Shown above are the dose response curves for **BE69**(IC_{50} = 1.154 μM) and **BE92** (IC_{50} = 7.310 μM) with IC_{50} values both under 10 μM (see figure 3.27). This suggests that these chromene containing compounds synthesised have potential use for development as prostate cancer cell line therapies as well as showing potential as estrogen receptor breast cancer therapeutics.

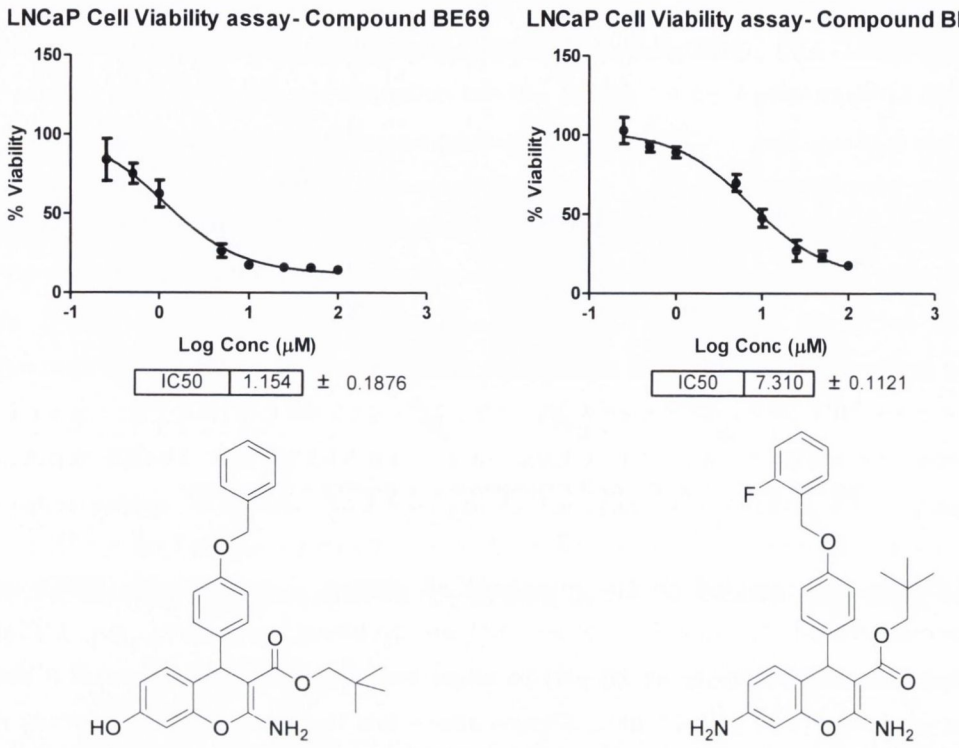

Figure 3. 27 LNCaP Dose-response curve and IC50 value for compounds BE69 and BE92

3.4 Molecular Modelling

A virtual screening was performed on selected compounds, mapping onto the estrogen receptor ligand binding domain. Molecular Operating Environment (MOE) software was employed to predict the ligand-protein interactions. X-Ray structures have been reported for the ERα LBD with agonist (estradiol) and antagonist (4-hydroxytamoxifen). The crystal structure of hERα LBD bound to the selective antagonist (OHT) was obtained from the protein database, PDB code 3ERT [125, 166]. A crystal structure was also obtained for the ERα LBD also with agonist (estradiol) and antagonist (Raloxifene). This crystal structure of hERα LBD bound to the selective antagonist (RAL) was also obtained from the protein database, PDB code 1ERR [167, 168]. ER antagonistic ligands, such as 4-hydroxytamoxifen and raloxifene, have molecular characteristics similar to estradiol such as the phenolic groups which partake in direct hydrogen bonding with the same key residues in the ER (i.e. Glu353, Arg394 and His524 in human ERα). In addition, ER antagonists ligands commonly contain a substituent amine ether which is too large to be accommodated in the binding cavity (agonist mode) which causes a displacement of the Helix-12 in the protein structure.

The docking studies were performed using MOE 2012.10 software. All parameters were kept at default unless stated otherwise. The initial and final energy of protein were calculated (in kcal/mol) by GizMOE using MMFF94X force field with conjugant gradient method. The docked ligands were drawn in MOE and conformers were not created as the ligands were not docked as rigid molecules. The docking protocol was set as 'Rigid Receptor' and a pharmacophore was used in most cases. The placement method used was Triangle Matcher with the rescoring function of London dG. This was subsequently refined using the refinement of Forcefield with a rescoring function of GBVI/WSA dG. The docking protocol was set to keep 30 docking poses only. The resulting docked compounds were then visualised using Discovery Studio Visualizer.

For the molecular modelling study, an initial pharmacophore was generated using MOE pharmacophore elucidator. The most significant features, including hydrophobic, hydrophilic, donor and acceptor features were examined. The results showing optimum activity in the *in silico* screening study were subsequently chosen for evaluation in the *in vitro* ER binding assays using Fluorescence polarisation and FRET assay methods.

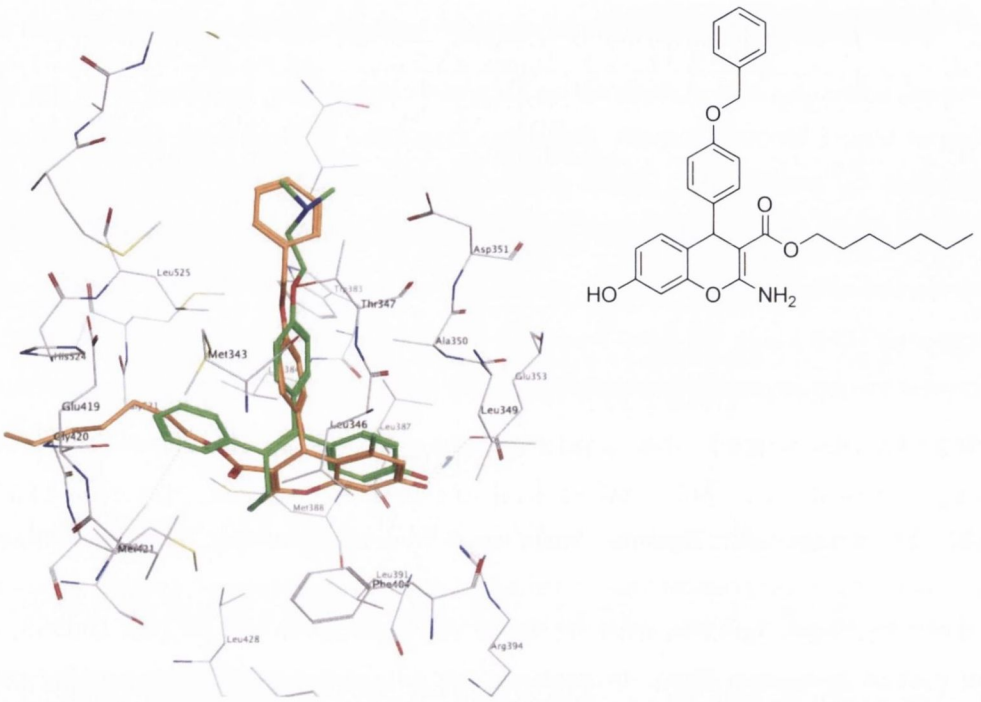

Figure 3. 28 Top-ranking docked conformation of BE65 (yellow) in ERα, 3ERT.pdb. overlapped with 4-hydroxytamoxifen (green)

Fig 3.28 displays the structure **BE65** overlapped with 4-hydroxytamoxifen(4-OHT) in the ER LBP(3ERT). It is observed that the structure of the compound **BE65** has a similar shape and overlaps well with 4-hydroxytamoxifen when the two molecules are superimposed. The hydroxyl groups of **BE65** occupies a similar position to the hydroxyl group of 4-hydroxytamoxifen (4OHT) with the benzyloxy group of **BE65** observed to overlap with the N,N-dimethylaminoalkyl ether substituent of 4OHT. The rigid chromene structure appears to provide a scaffold that can accommodate the steric and geometric requirements of the aromatic pharmacophores for ER binding.

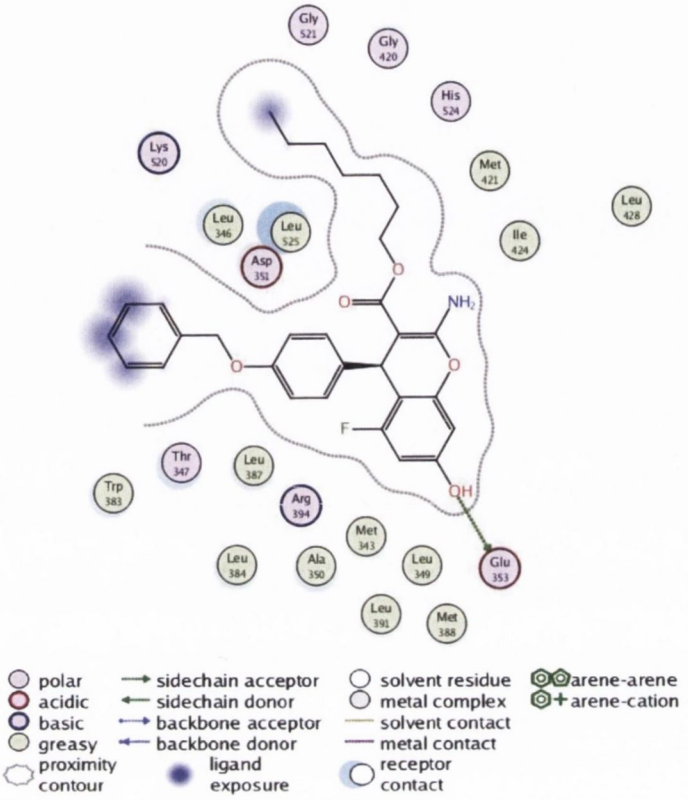

Figure 3. 29 2D representation of binding interactions of BE65 in the LBD ERα binding site (pdb 3ERT). 2-D rendering of ligand–protein interactions using LigX module of MOE used to create docked structure of BE65 in the LBD ERα binding site.

Further 2D analysis of the *in silico* docking study was carried out for the compound **BE65** docked in the ER with the hER α LBD in complex with 4OHT, see fig 3.29. Some side chain acceptor interaction can be observed for the hydroxyl group of compound **BE65** interacting with the carboxylate residue in Glu 353. The residue Asp351 is indicated in proximity to the ester carbonyl and the ether oxygen; however the expected donor-acceptor interactions are not observed. These results indicate that the **BE65** candidate compound demonstrates some potential as an ER binding ligand. A practical ER-α/ER-β TR-FRET (antagonist mode) assay was performed and showed the compound **BE65** had ER-β specific antagonist binding activity of 20 μM (see table 3.11).

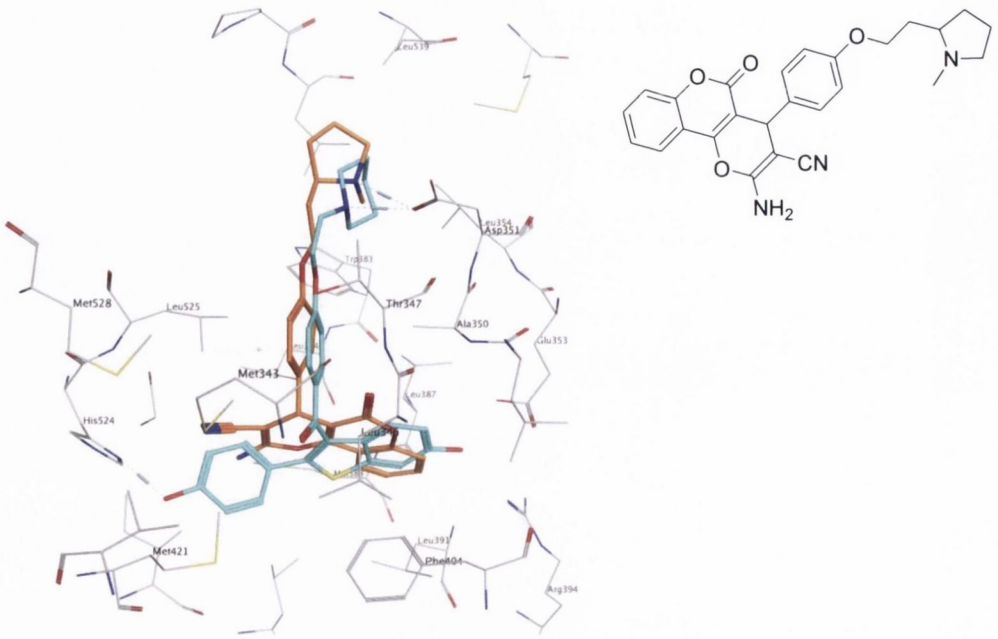

Figure 3. 30 Top-ranking docked conformation of B140 (yellow) in ERα, (1ERR.pdb). overlaid with Raloxifene(RAL) (blue)

The ER antagonistic modulation of clinical relevant compounds such as 4OHT (the active metabolite of tamoxifen) and RAL are known to be possible through key interactions with protein residues including Glu353, Arg394, His524, and Asp351. To modulate the ER helix-12 and demonstrate antagonistic activity, the bulky amino groups on these clinical candidates are know to interact with Asp351. Some compounds were chosen with similar amino bulky chains from the synthesized libraries in this thesis for preliminary molecular modelling analysis, to evaluate any potential ER activity, namely compounds **BE140** and **BE141.** Fig 3.30 shows the structure of **BE140** overlapped with Raloxifene (RAL) in the ERα LBP, (1ERR). Docking studies were carried out on two separate crystal structures which were available; hER α LBD in complex with 4-hydroxytamoxifen OHT (3ERT), and hER α LBD in complex with Raloxifene, RAL (1ERR), both obtained from the protein data bank. The result of the raloxifene study (1ERR) was chosen for this docking study as optimised docking interactions were observed when using this crystal structure.

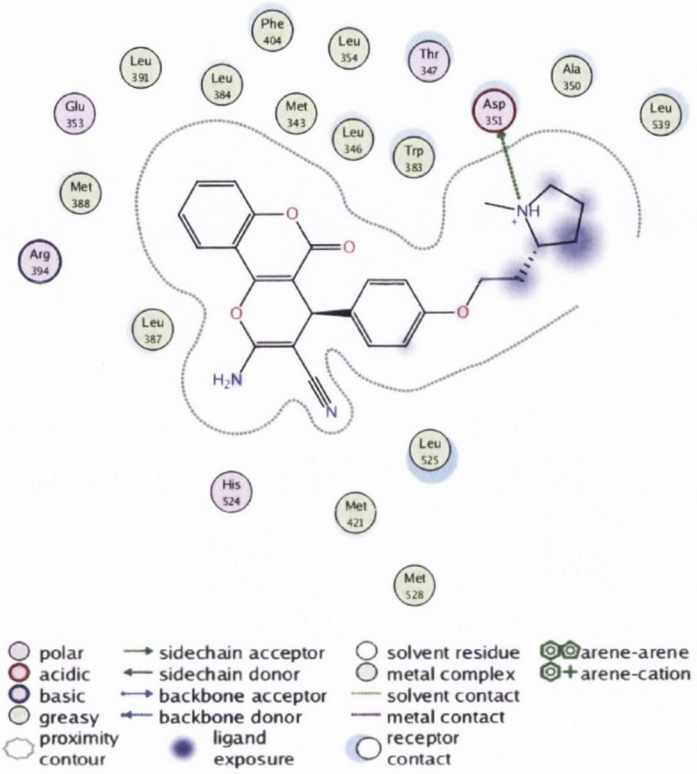

Figure 3. 31 2D representation of binding interactions of BE140 in the LBD ERα binding site (pdb 1ERR). 2-D rendering of ligand–protein interactions using LigX module of MOE used to create docked structure of BE140 in the LBD ERα binding site.

Fig 3.31 shows 2D representation of binding interactions of compound **BE140** in the hER α LBD in the complex crystallised with RAL(raloxifene), (1ERR). As expected, ionic interaction can be observed for the protonated amine which is positioned adjacent to the Asp351 residue.The interaction with protein residue Asp351 is known to be important in ER antagonistic profiling. This gave an indication for **BE140** as a potential candidate in ER therapeutics. Further practical binding studies showed that compound **BE140** gave good ER α binding values (see table 3.9 and table 3.10).

A structurally related compound **BE141** also having an aminoether group substituent antagonistic type chain also clearly displayed ionic type interaction with Asp351 in the hER α LBD in complex with TAM(3ERT), see fig 3.32,(2D representation of binding interactions).

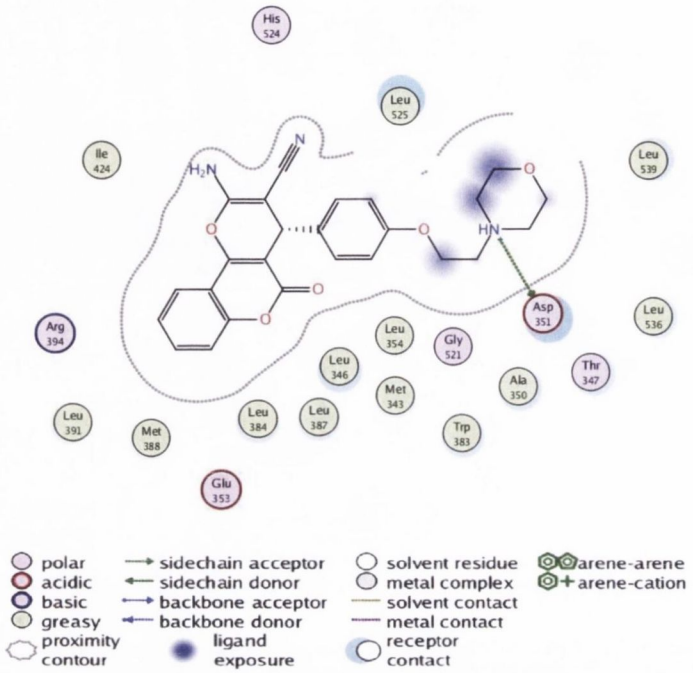

Figure 3. 32 2D representation of binding interactions of BE141 in the LBD ERα binding site (pdb 3ERT). 2-D rendering of ligand–protein interactions using LigX module of MOE used to create docked structure of BE140 in the LBD ERα binding site.

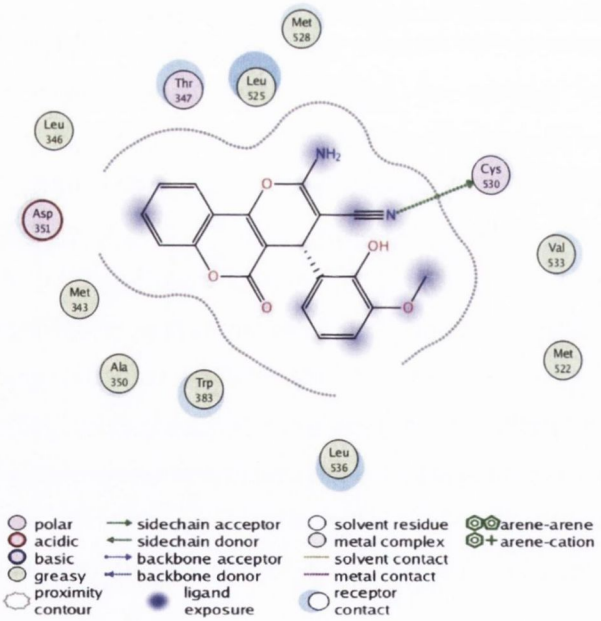

Figure 3. 33 2D representation of binding interactions of BE137 in the LBD ERα binding site (pdb 3ERT). 2-D rendering of ligand–protein interactions using LigX module of MOE used to create docked structure of BE137 in the LBD ERa binding site.

Fig 3.33 shows **BE137** pyranocoumarin compound the hER α LBD complex crystallised with 4OHT(4-hydroxytamoxifen), 3ERT. Docking in the antagonistic mode is predicted, although interactions with the key residue Asp351 are not indicated. However, some interesting additional interactions can be observed between the CN at C-3 of the chromene ring and Cys 530 residue.

3.5 ER binding assays

Methods to characterise binding to Estrogen Receptor Ligand Binding Domain

3.5.1 Time Resolved Fluorescence Resonance Energy Transfer (TR-FRET)

Fluorescence resonance energy transfer (FRET) is the distance dependent transfer of excitation energy from two fluorophores, a donor to an acceptor molecule. As the energy transfer occurs over 1-10 nm distance, comparable to the size of biological macromolecules, FRET is considered as a valuable tool to study proximity events occurring in biological systems, such as in protein-protein interactions [135]. As for any fluorescence based technique, the background fluorescence brought by the assay components or by the test compounds may be a problem in limiting the application of FRET in high throughput assays. To overcome the intrinsic fluorescence limitations, lanthanide chelates with longer fluorescence lifetimes have been used as donors combined with a delay in the signal measurement (typically with a 200 or 100 μs delay), which allows for the decay of background fluorescence from interfering systems (usually decaying within the 10 ns range for most commonly used organic dyes). This technique with improved sensitivity is referred to as time-resolved (TR) fluorescence resonance energy transfer (TR-FRET). In TR-FRET lanthanide chelates are used as donors, improving significantly the lifetime (between 200-1500 μs) and the assay sensitivity, overcoming the short lived background fluorescence interfering signals due to intrinsic fluorescence or light scattering. The fluorescence decay is exponential and proportional to the lifetime (τ_F) of individual fluorophores[135]. Figure 3.34 shows a TR-FRET schematic. In TR-FRET, after excitation, measurement of emission commences at a fixed time (typically between 100-400 μs) after the flash lamp pulse. The sample is then re-excited and a new measurement cycle begins[169].

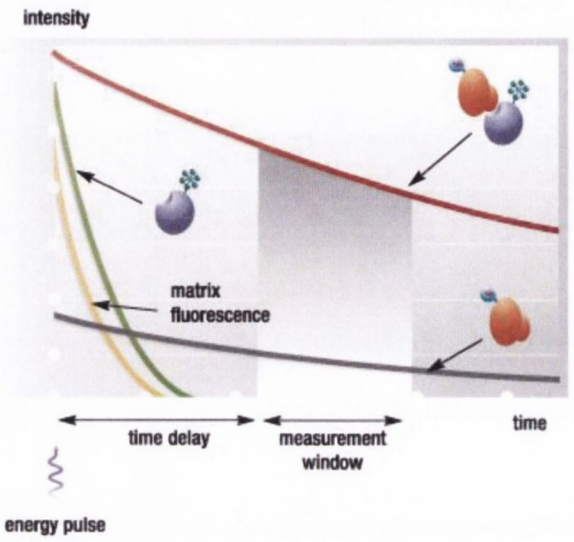

Figure 3. 34 Time-resolved measurement allows the signal to be cleared of background fluorescence; the energy pulse from the excitation source (flash lamp, laser) is immediately followed by a time delay, allowing interfering short-lived fluorescence to decay [170].

3.5.2 Fluorescence Polarization (FP)

The theory of fluorescence polarization was first developed by Perrin in 1926[171], who observed that when a small molecule is excited with plane polarized light the emitted light is largely depolarized because molecules tumble rapidly in solution during its fluorescence lifetime. The polarization value of a molecule is directly proportional to the molecule's rotational relaxation time. Rotational relaxation time depends on viscosity (η), absolute temperature (T), molecular volume (V) and the gas constant (R) according to the following equation 0.1:

$$Rotational\ Relaxation\ Time = \frac{3\eta V}{RT}$$

Equation 0.1

According to this equation, if viscosity and temperature are constant, then the polarization value is directly proportional to the molecular volume in terms of size. In the specific case outlined in this chapter, a specific change in the size of the molecule occurs in response to a binding event, such as the competition of a test compound for a fluorescently labelled proprietary ligand (Fluormone™) from the NR(nuclear receptor) LBD. The binding of the compound in the LBP, results in the dissociation of the

Fluormone-LBP complex, therefore in a decrease of the molecular size, and as a consequence, in a reduction in polarization value of the emitted light. Small molecules rotate quickly during the excited state so they have a low polarization value upon emission. Large molecules rotate little during the excited state and therefore they have high polarization value upon emission.

The polarization value, usually expressed in millipolarization units (mP) is a ratio of light intensities (I) emitted both in the horizontal and vertical planes, as described in this equation 0.2:

$$P = \frac{I_{2(vertical)} I_{2(horizontal)}}{I_{1(vertical)} I_{1(horizontal)}}$$

Equation 0.2

Sometimes the term polarization is used interchangeably with the term anisotropy. Anisotropy is associated and interrelated to polarization, also derived from ratio of vertical and horizontal intensities. Anisotropy values are usually preferred due to mathematical simplicity of the equations compared to those that describe polarization. Anisotropy is related to polarization according to the following equation 0.3:

$$\alpha = \frac{2P}{3 - P}$$

Equation 0.3

One of the biggest limitations of FP in its application to high throughput screening is the interference from intrinsic fluorescence of small organic compounds. Generally, conjugated bonds within the compound confer a fluorescent character, and the greater the degree of conjugation within a compound, the longer the wavelength at which it fluoresces [172]. Compound libraries used in HTS generally contain heterocyclic compounds and compounds with low levels of conjugation. In light of these observations, assays that are based on excitation at relatively short wavelengths (350 nm) that detect fluorescence in the green spectral region (450–495 nm), just like the assay described in this chapter, have a greater chance of false positives due to compound fluorescence [172, 173]. Thus, to overcome interference, fluorescence assays that employ red-shifted longer wavelength fluorescent probes have been developed[174].

A method to flag fluorescent compounds and false positive wells in HTS screens was provided by Turconi and colleagues [175] by calculating the total fluorescence intensity from a well and the observed anisotropy. With the same method, it is also possible to flag false negatives due to compounds present as aggregates and light scattering. In

this case, the fluorescence intensity will increase along with the polarization if the aggregation does not quench the fluorescence. Light scattering from particulates or precipitated compounds can also lead to high polarization values due to scattered light being infinitely polarized[175].

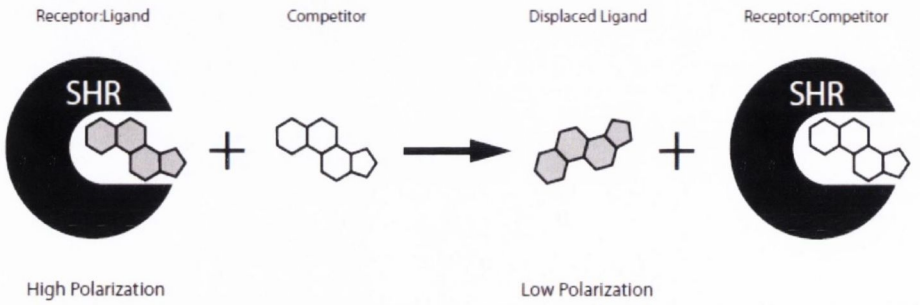

Figure 3. 35 PolarscreenTM fluorescence assay principle for ER

The Fig 3.35 displays the Polarscreen^{TM} fluorescence assay principle for ER. The complex between the fluormone and the LBD result in a high polarization value, due to increase in size, if the added test compound is competing for the LBD, then fluormone will be liberated into solution, resulting in a decrease in the polarization value.

In this chapter a fluorescence polarization assay commercially available from Invitrogen (PolarScreen^{TM}) is used, where fluorescence was detected in the green spectral region. In this assay a fluorescently labelled ligand (Fluoromone^{TM}) binds with high affinity to the LBD and it is included in the assay at a concentration close to its $K_{D,}$ to ensure around 80% saturation of the receptor and effective competition from the test compound

3.5.3 Estrogen receptor binding activity results

The ER binding activity (as IC_{50} values) for both ER isoforms (ERα and ERβ) are displayed for the selected compounds in Table 3.9 and Table 3.10 respectively. The compounds were selected for ER binding assay on the basis of the initial antiproliferaive screening in ER positive MCF-7 cells and also on review of the *in silico* docking results presented. Estradiol was used as the standard positive control in each experiment and demonstrated IC_{50} value for ER binding of 0.0023 μM(ERα) and 0.0021 μM(ERβ).

3.5.31 ERα binding assay results

Compound	IC_{50} μM ERα	Compound	IC_{50} μM ERα
BE1	*1.77*	**BE38**	*2.32*
BE5	*8.53*	**BE58**	*>100*
BE7	*2.58*	**BE62**	*53.91*
BE16	*1.69*	**BE63**	*40.32*
BE19	*>100*	**BE67**	*>100*
BE36	*0.59*	**BE140**	*13.47*
		Estradiol	*0.0023*

Table 3. 9 ERα binding results for selected compounds (IC50 μM)

Table 3.9 shows the ER alpha binding assay results for the 12 compounds screened with IC_{50} in μM and it is observed that 6 of the selected compounds have favourable IC_{50} binding values below 10 μM(compounds **BE1, BE5, BE7, BE16, BE36, BE38**). Compound **BE36** was the most potent compound in the series with IC_{50} value of 0.59 μM) Of the compounds identified from preliminary *in silico* evaluation, compound **BE140** was predicted to show potential binding activity *in vitro* as a potential ER modulator. The moderate value for compound **BE140** obtained in the *in vitro* FRET ERα binding experiment (IC_{50} 13.47 μM, table 3.09) is also in agreement with the ER docking prediction for ERα. Compound **BE140** was selective for ERα as the binding value observed for ERβ was > 100 μM indicating that this compound was selective in recognition of the ERα ligand binding domain.

3.5.32 ERβ binding assay results

Compound	IC_{50} μM ERβ	Compound	IC_{50} μM ERβ
BE1	0.19	**BE62**	>100
BE5	2.56	**BE63**	>100
BE7	1.00	**BE66**	>100
BE8	>100	**BE67**	>100
BE16	2.10	**BE68**	>100
BE19	>100	**BE70**	>100
BE21	>100	**BE71**	>100
BE36	1.52	**BE72**	>100
BE38	>100	**BE91**	7.22
BE58	>100	**BE140**	>100
		Estradiol	0.00210

Table 3. 10 ERβ binding results for selected compounds (IC50 μM)

Binding activity in table 3.10 for the ERβ isoform was determined for 20 compounds selected from the chromenes synthesised. The results from the ER binding FRET experiments identified 6 compounds (**BE1, BE5, BE7, BE16, BE36, BE91**), with IC_{50} values of less than 100 μM. The most potent compound identified was **BE1** with IC_{50} value of 0.19 μM. Examples of the dose response curves obtained for specific examples are illustrated below.

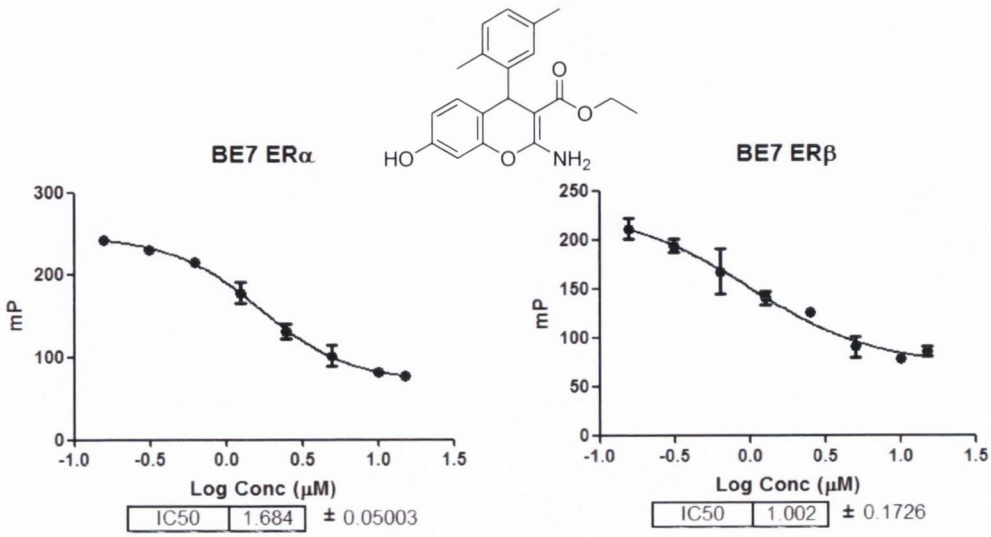

Figure 3. 36 ERα and ERβ binding results for compound BE7

The dose-response curves for compound **BE7** in the FRET ERα and ERβ assay is displayed in figure 3.36. An 8 point concentration curve was generated over the range 10 μM to 10 nM. Compound **BE7,** containing a 2,4-dimethylphenyl substituent at C-4 of the chromene ring demonstrated potent binding affinity for each receptor subtype with IC_{50} values of 1.68 μM and 1.00 μM for ERα and ERβ respectively.

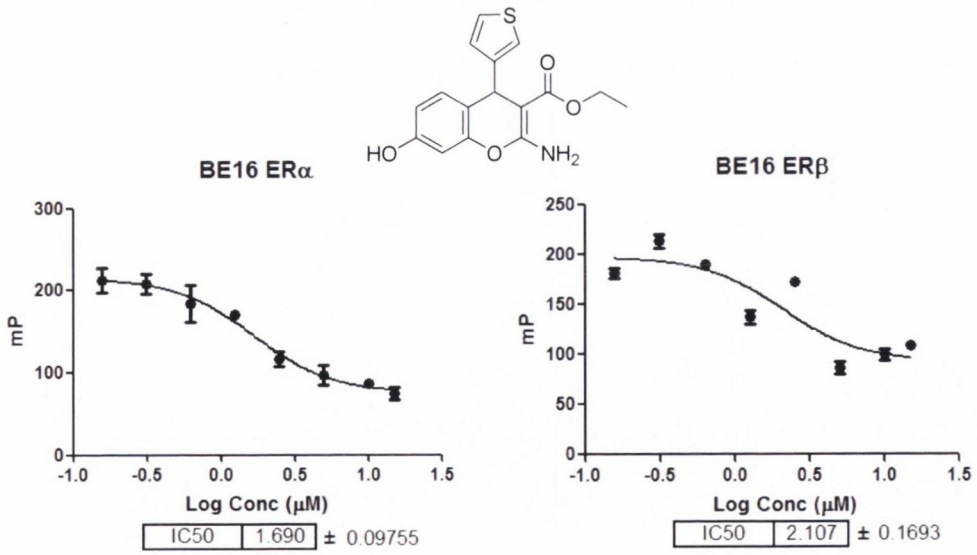

Figure 3. 37 ERα and ERβ binding results for compound BE16

Compound **BE16**, containing the 3-thienylsubstituent at C-4 of the chromene ring, showed good binding results on both ER alpha and ER beta receptors, as seen from the results in figure 3.37, with IC_{50} values of 1.69 μM and 2.10 μM for ERα and ERβ respectively, and some selectivity for the estrogen alpha receptor.

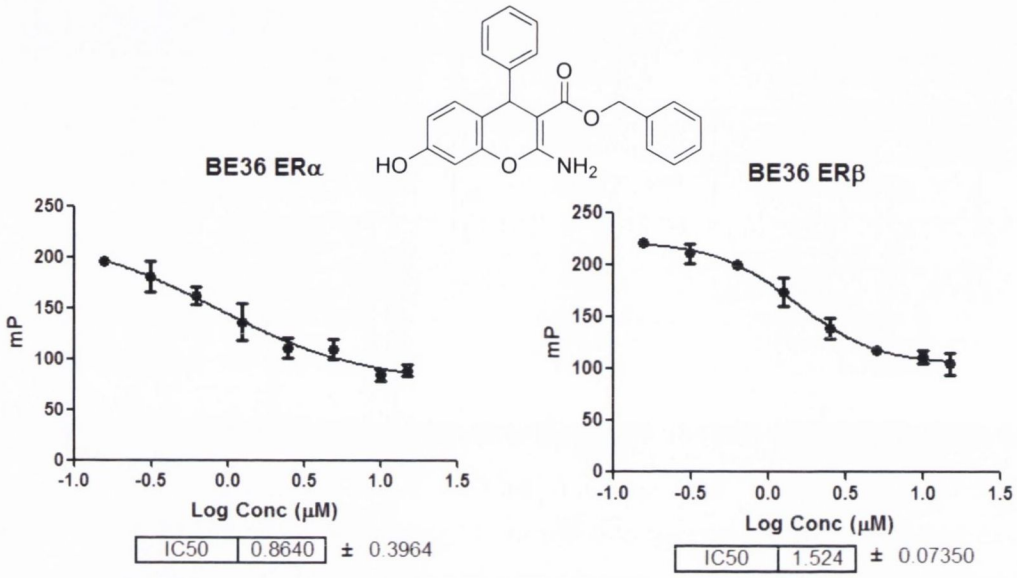

Figure 3. 38 ERα and ERβ binding results for compound BE36

Another favourable binding value was indicated in evaluation for **BE36**, see figure 3.38. The agonistic structure of **BE36** showed activity both on ER alpha and beta isoforms with with with IC_{50} values of 0.86 μM and 1.52 μM for ERα and ERβ respectively, and some selectivity for the estrogen alpha receptor.

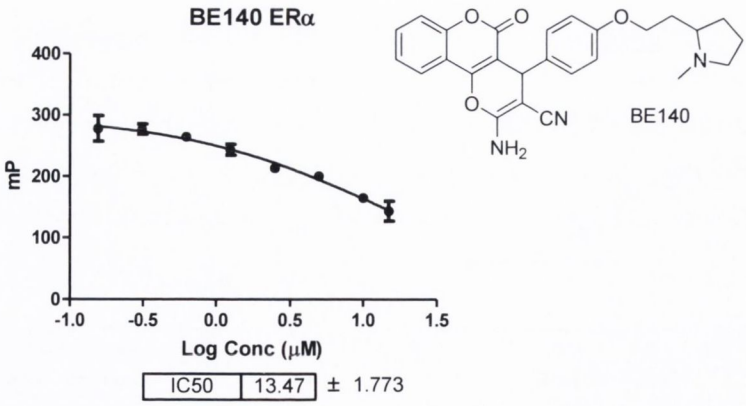

Figure 3. 39 BE140 ERα binding curve of compound BE140 .

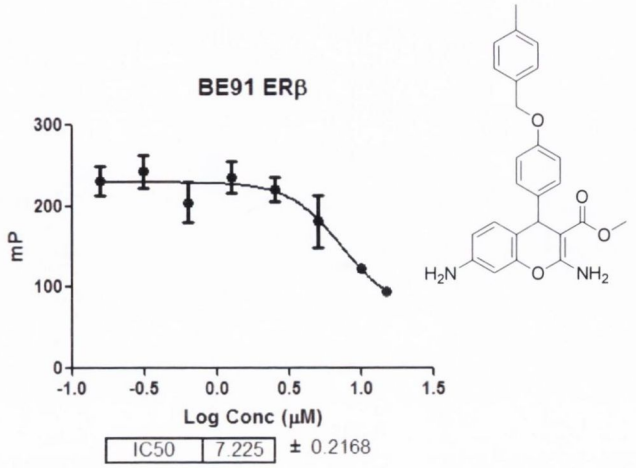

Figure 3. 40 ERβ binding result for compound BE91

On review of the ER binding values obtained for both ERα and ERβ isoforms, displayed in tables 3.9 and 3.10, it is observed that most of the compounds that gave acceptable activity values were active on both ER alpha and ER beta subtypes. However it is concluded from the data in both tables that some compounds such as **BE1**, **BE38** and **BE140** selectively bound to the ERα and compounds such as **BE1, BE5 and BE7** selectively bound to ERβ. Figures 3.39 and 3.40 show the selectivity displayed by the two compounds each binding selectively to either of the ER subtypes. **BE 140** can be seen with binding activity on the ER α (see figure 3.39, IC_{50} = 13.47 μM), however there was no activity observed on the ER beta isoform. The dose-response curve for **BE91** can be observed with IC_{50} value of 7.22 μM selectively bound to the ERβ, (see figure 3.40).

3.5.4 FRET ER binding assay in agonist and antagonist mode

Further FRET binding assays were carried out on three selected compounds, **BE1, BE14** and **BE65**. The assay was performed on ER-α/ER-β TR-FRET in antagonist mode, so the assay was evaluating specifically to identify any potential compounds with selective antagonist activity on the ER. The binding results for 3 of the selected compounds can be observed below in Figure 3.41. Tamoxifen was used as the ER antagonist standard positive control.

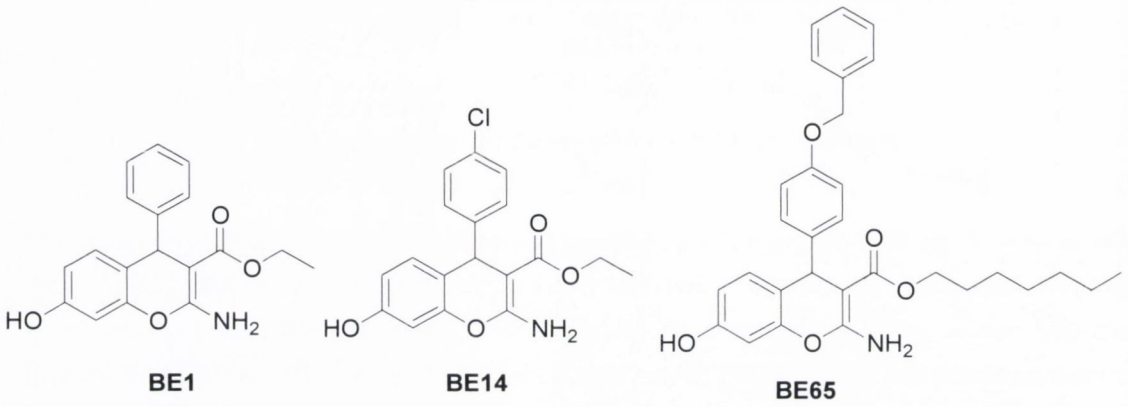

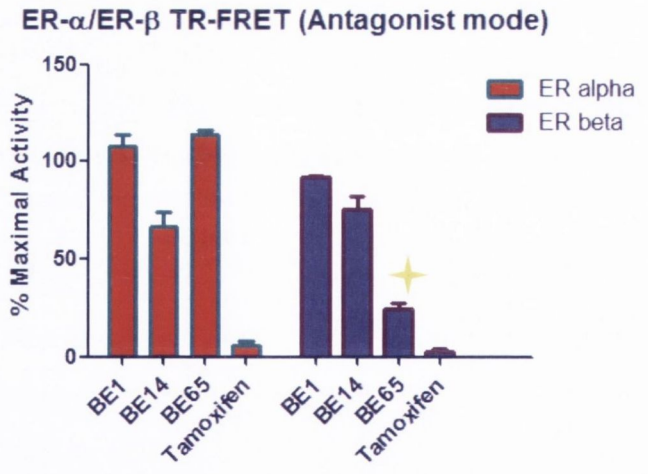

Figure 3. 41 ER-α/ER-β TR-FRET binding assay in antagonist mode

In the TR-FRET binding results displayed in the figure 3.41, it is observed that the compound **BE65** had binding values significantly (3-fold) more selective for ER-β over ER-α at 100 μM concentration. The assay performed in antagonist mode gives

significantly more information for the design and production of potentially useful anticancer ER therapies. In this case the results show that **BE65** is favouring specifically the ER-β receptor as an antagonistic candidate.

3.6 The NCI-60 human tumour cell line drug screen and the COMPARE algorithm

In the early 1980's, the US National Cancer Institute (NCI) developed an anticancer drug screen in the 1980's with a panel of cell lines from nine distinct tumour types: leukaemia, colon, lung, CNS, renal, melanoma, ovarian, breast and prostate. Cell lines that showed acceptable growth characteristics, such as adaptability to the standard cell culture medium, were chosen for the panel. At the time that the assay was conceived, practical endpoints such as the use of tetrazolium dyes had not been developed. A new tetrazolium dye assay, using the XTT dye, was developed. Subsequently a method that used sulphorhodamine B was selected for use in the screen. This assay employs a chemical fixation step at the end of drug treatment, enabling batch processing of plates in a time-independent manner. It can also differentiate cell kill from growth inhibiton. In 1998, a three-cell line pre-screen was introduced to increase the efficiency and throughput. This pre-screen was automated in 2001 to a high throughput format, using 384-well plates and alamarBlue dye to assay at endpoint. After pre-screening, one-dose testing is performed on the submitted samples and, based on the potency of the sample, it may progress to 5-dose testing in up to 60 cell lines.

The NCI60 screen is hugely useful as a research tool. *Figure 3.42* (a) shows that number of compounds screened each year is increasing steadily, with over 400,000 samples screened in 2007. *Figure 3.42* (b) provides a breakdown of the origin of submissions between 1999 and 2005, showing that 54% of samples were submitted by foreign (non-US) academics over this time period

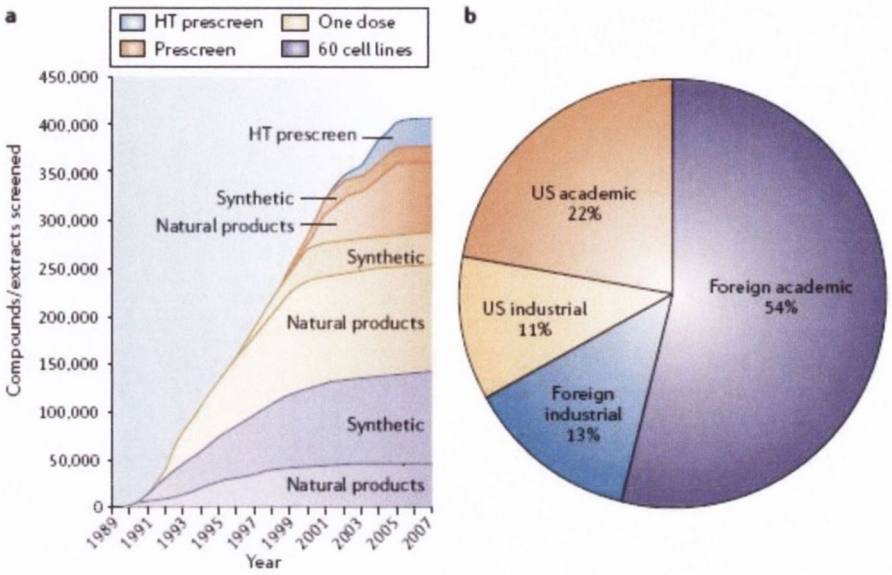

Figure 3. 42 (a) Number of samples screened by the NCI from 1989 – 2007; (b) source of samples between 1999 – 2005

3.6.1 Compounds submitted to NCI-DTP

As a follow up to in house evaluation, a group of 22 of the synthesised compounds was accepted for further evaluation by the National Cancer Institute(NCI) Developmental Therapeutics Program (DTP) in the United States for evaluation on 60 human tumour cell line screen [176]. The National Cancer Institute, Developmental Therapeutics Program (DTP) which operates a progressive, tiered *in vitro* and *in vivo* anti-cancer compound screening program for single pure compounds with the goal of identifying and evaluating novel chemical leads and biological mechanisms of action. Many of the compounds showed moderate to good activity in the 60 human tumour cell line screen in the initial 1 dose screen (10 μM). As an example, the result from the 1 dose screen for compound **BE65(767434)** is illustrated in Table 3.11 below. This compound showed particularly potent reslts against the following leukaemia cell lines, having low growth percentages in each case: C-CRF-CEM, (49.47%), HL60-TB (1.97%), K-562(8.83%), MOLT-4(28.82%), RPMI-8226(36.08%), SR(-3.65%).

Developmental Therapeutics Program

One Dose Mean Graph

NSC: D-767434 / 1	Conc: 1.00E-5 Molar	Test Date: Sep 24, 2012
Experiment ID: 1209OS49		Report Date: Feb 04, 2013

Panel/Cell Line	Growth Percent
Leukemia	
CCRF-CEM	49.47
HL-60(TB)	1.97
K-562	8.83
MOLT-4	28.82
RPMI-8226	36.08
SR	-3.65
Non-Small Cell Lung Cancer	
A549/ATCC	41.59
HOP-62	50.44
HOP-92	59.46
NCI-H226	84.70
NCI-H23	66.37
NCI-H322M	68.13
NCI-H460	33.46
NCI-H522	16.57
Colon Cancer	
COLO 205	53.72
HCC-2998	70.34
HCT-116	29.88
HCT-15	41.56
HT29	20.58
KM12	29.11
SW-620	31.28
CNS Cancer	
SF-268	62.35
SF-539	52.97
SNB-19	69.52
SNB-75	46.09
Melanoma	
LOX IMVI	51.83
MALME-3M	34.13
M14	28.81
MDA-MB-435	-48.74
SK-MEL-2	72.12
SK-MEL-28	65.56
SK-MEL-5	43.85
UACC-62	43.26
Ovarian Cancer	
IGROV1	54.46
OVCAR-3	61.53
OVCAR-4	87.20
OVCAR-5	92.34
OVCAR-8	73.51
NCI/ADR-RES	21.48
SK-OV-3	61.52
Renal Cancer	
786-0	56.43
A498	56.32
ACHN	69.99
CAKI-1	47.99
RXF 393	81.91
SN12C	73.02
TK-10	75.48
UO-31	67.96
Prostate Cancer	
PC-3	59.06
DU-145	84.71
Breast Cancer	
MCF7	49.15
MDA-MB-231/ATCC	61.11
HS 578T	60.66
BT-549	75.97
T-47D	61.35
MDA-MB-468	53.17
Mean	50.48
Delta	99.22
Range	141.08

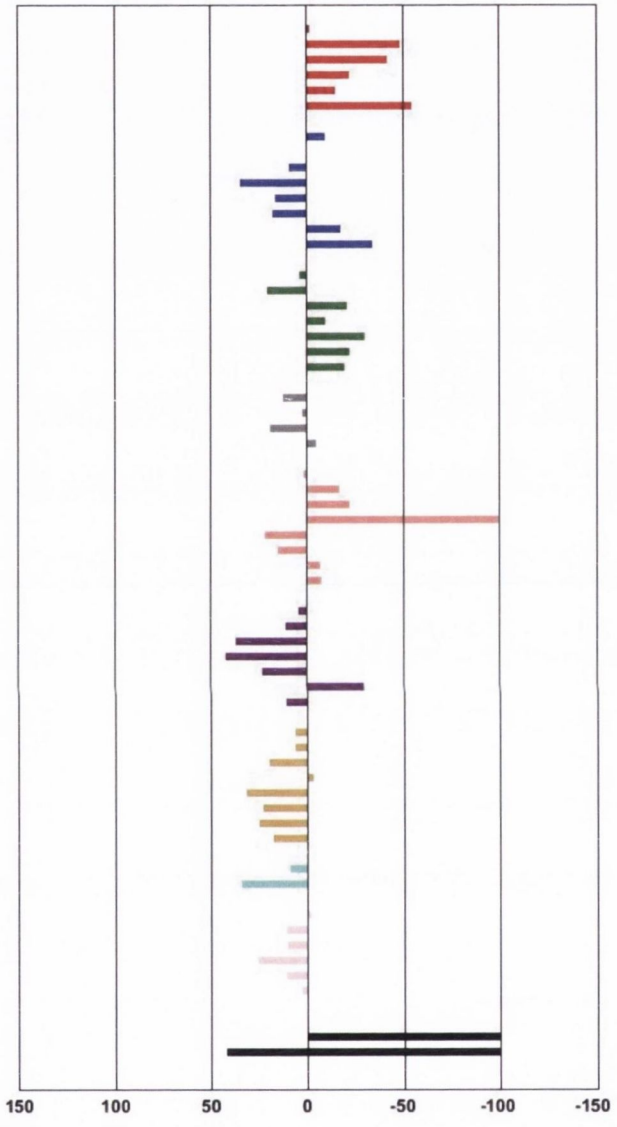

Table 3. 11 One Dose Screen (10 mM) result for compound BE65 (767434)

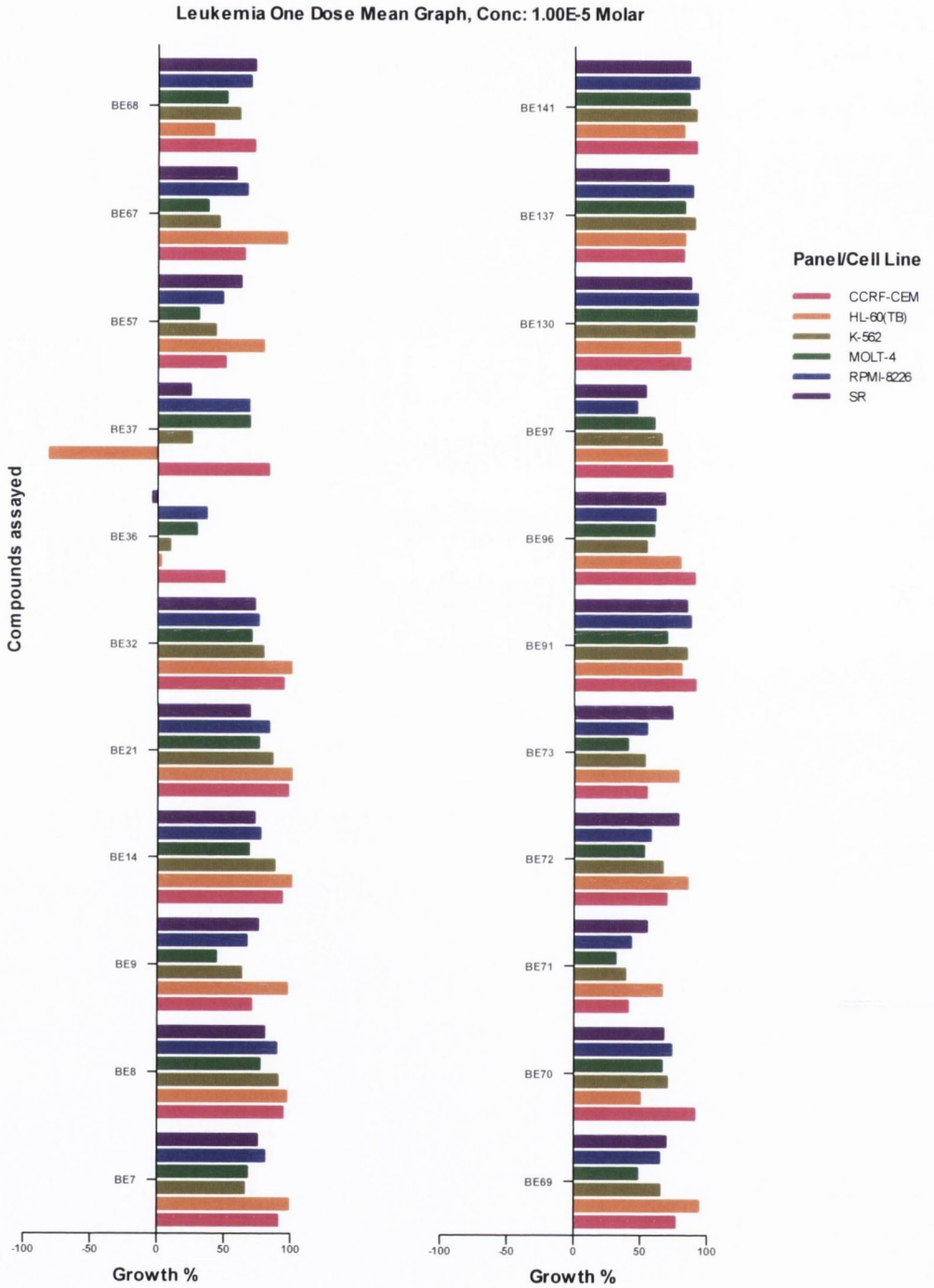

Table 3. 12 Leukaemia growth activity (%) on full panel of compounds screened

Many of the compounds evaluated also showed some selective activity in the panel leukaemia cell lines evaluated. The results obtained for the panel of compounds evaluated in the leukaemia cell lines is shown in Table 3.12. Compound **BE36** can be seen to be clearly the most potent, with compounds **BE37, BE57 and BE71** also displaying interesting positive activities. These structures could have potential for further development as anti-leukaemia agents.

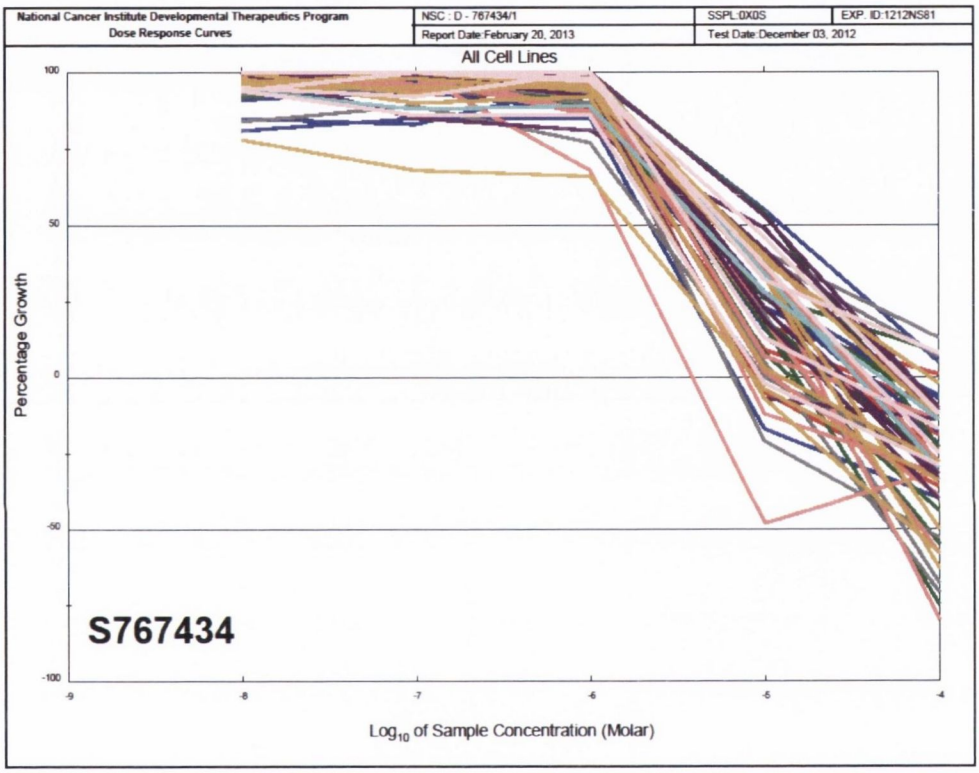

Figure 3. 43 5 dose NCI results for compound BE65 (Sample S767434) for 60 cell lines (Log10 of sample concentration plotted against percentage growth).

The result from the 5 dose NCI screen for compound **BE65** (Sample S767434) for the 60 cell lines (Log_{10} of sample concentration plotted against percentage growth) is displayed in Figure 3.43. The result shows that the compound displays good antiproliferative activity at micromolar levels in all cell lines evaluated.

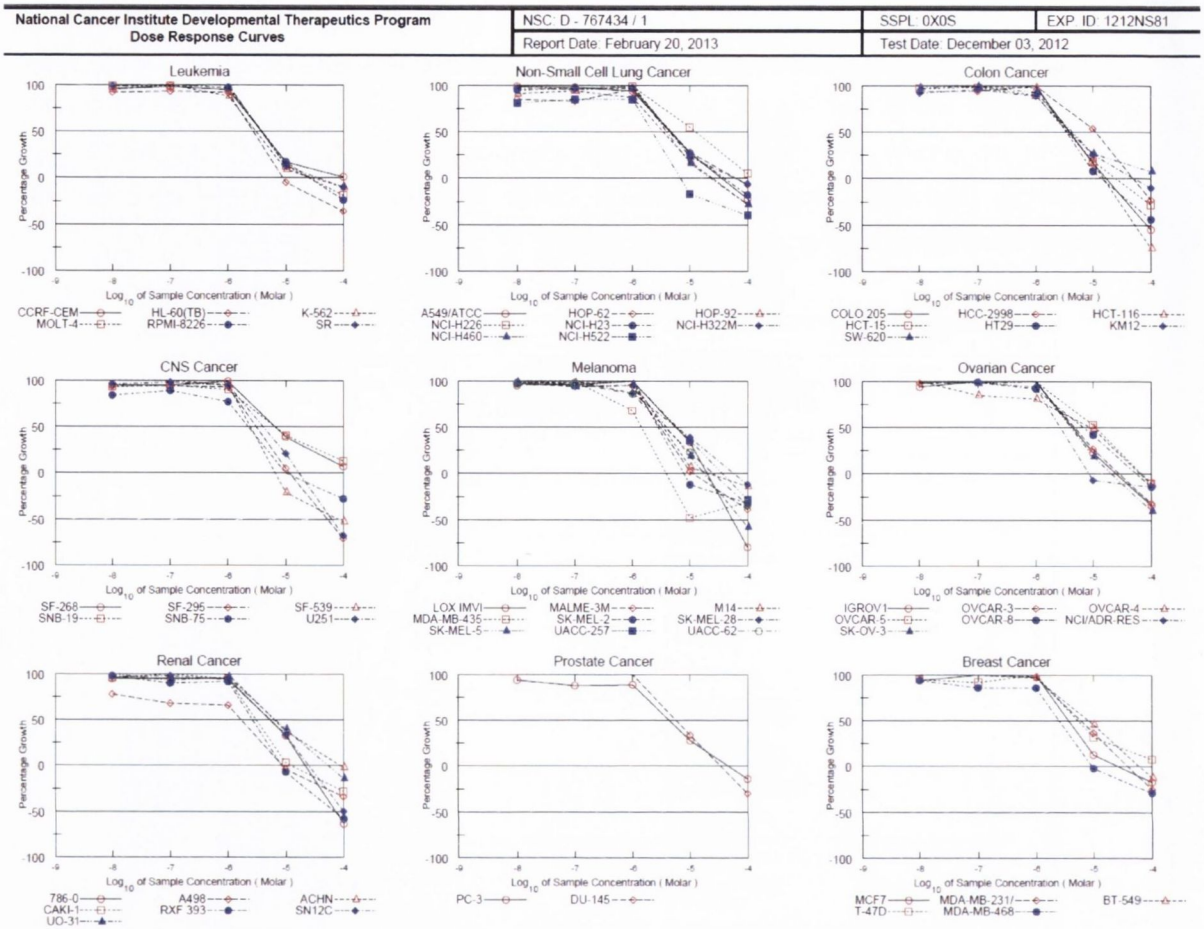

Figure 3. 44 Growth percentage results for compound BE36 on 9 cell lines

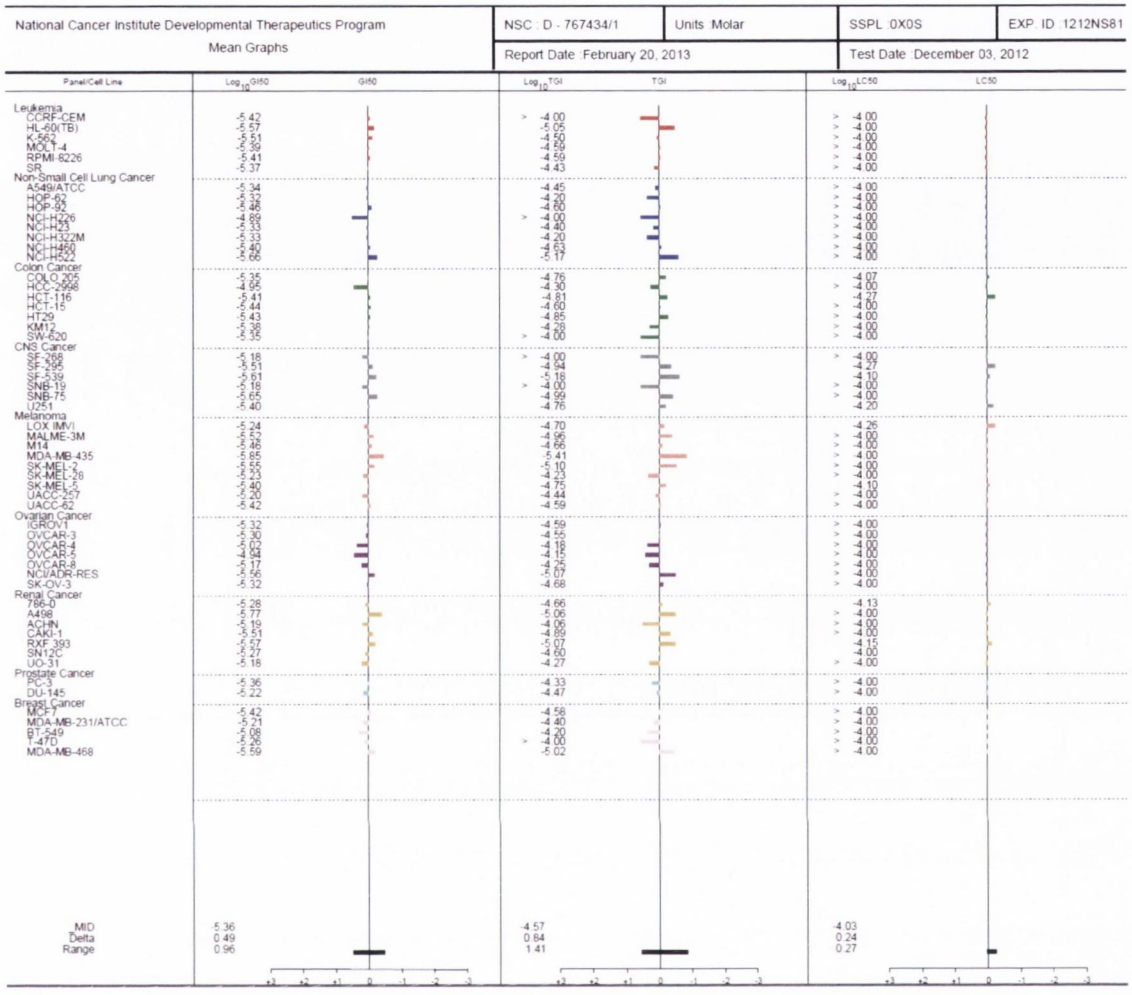

Figure 3. 45 Mean GI50, TGI and LC50 results for BE36 on 60 cell lines

Three endpoints (negative $\log_{10}$ of the concentration inhibiting the growth of 50% of the cells (GI_{50}), total growth inhibition (TGI) and negative $\log_{10}$ (concentration required to kill 50% of the cells (LC_{50}) are calculated from 5-log dose response curves for compounds tested in the National Cancer Institute (NCI) 60 human tumour cell line Screen. Figure 3.44 displays the results from the 9 tumour cell panels evaluated for compound BE36. The more sensitive cell lines for **BE36** are observed to be melanoma, non-small cell lung cancer, ovarian cancer, and CNS cancer [176]. A mean graph for **BE36** is shown in figure 3.45. The midline of each portion of the graph represents the mean for that endpoint, calculated across all 60 cell lines. This mean value is then subtracted from the value for each individual cell line and plotted. Cell lines more sensitive to **BE36** are visualised as bars deflecting to the right, while more resistant

cell lines have bars extending to the left of the mean. Compound **BE36** displayed mean log_{10}GI50 value of -5.36 (GI50 value 4.36 μM) over the panel of 60 cell lines tested. Compound **BE36** shows values here selective for melanoma, breast cancer, and renal cancer with seleced GI50 values of 3.09 μM for the leukaemia cell line HL-60, 3.80 μM for MCF-7 and 2.57 μM for MDA MB-468. The complete listing of the GI50, TGI and LC50 results for **BE36** on 60 cell lines are displayed in Figure 3. 46.

National Cancer Institute Developmental Therapeutics Program
In-Vitro Testing Results

NSC : D - 767434 / 1	Experiment ID : 1212NS81	Test Type : 08	Units : Molar
Report Date : May 11, 2013	Test Date : December 03, 2012	QNS :	MC :
COMI : BE180 (121336)	Stain Reagent : SRB Dual-Pass Related	SSPL : 0X0S	

			Log10 Concentration											
	Time		Mean Optical Densities					Percent Growth						
Panel/Cell Line	Zero	Ctrl	-8.0	-7.0	-6.0	-5.0	-4.0	-8.0	-7.0	-6.0	-5.0	-4.0	GI50	TGI	LC50
Leukemia															
CCRF-CEM	0.596	2.131	2.075	2.095	2.057	0.856	0.607	96	98	95	17	1	3.78E-6	> 1.00E-4	> 1.00E-4
HL-60(TB)	0.628	2.855	2.670	2.700	2.686	0.596	0.404	92	93	92	-5	-36	2.72E-6	8.87E-6	> 1.00E-4
K-562	0.230	1.447	1.388	1.455	1.305	0.345	0.208	95	101	88	9	-10	3.06E-6	3.14E-5	> 1.00E-4
MOLT-4	0.620	2.023	2.005	2.015	2.138	0.802	0.504	99	99	108	13	-19	4.08E-6	2.56E-5	> 1.00E-4
RPMI-8226	1.538	3.135	3.169	3.137	3.093	1.810	1.169	102	100	97	17	-24	3.89E-6	2.60E-5	> 1.00E-4
SR	0.256	0.711	0.707	0.729	0.774	0.315	0.231	99	104	114	13	-10	4.29E-6	3.70E-5	> 1.00E-4
Non-Small Cell Lung Cancer															
A549/ATCC	0.477	1.935	1.926	1.909	1.841	0.877	0.372	99	98	94	27	-22	4.56E-6	3.59E-5	> 1.00E-4
HOP-62	0.508	1.395	1.260	1.243	1.358	0.759	0.473	85	83	96	28	-7	4.77E-6	6.37E-5	> 1.00E-4
HOP-92	1.407	1.818	1.781	1.795	1.765	1.481	1.019	91	94	87	18	-28	3.44E-6	2.48E-5	> 1.00E-4
NCI-H226	0.992	2.451	2.445	2.373	2.441	1.800	1.070	100	95	99	55	5	1.28E-5	> 1.00E-4	> 1.00E-4
NCI-H23	0.899	2.594	2.504	2.548	2.535	1.354	0.736	95	97	97	27	-18	4.65E-6	3.95E-5	> 1.00E-4
NCI-H322M	0.925	1.628	1.607	1.601	1.667	1.088	0.872	97	96	105	23	-6	4.72E-6	6.34E-5	> 1.00E-4
NCI-H460	0.366	2.962	3.009	3.010	2.954	0.791	0.265	102	102	100	16	-28	3.95E-6	2.35E-5	> 1.00E-4
NCI-H522	0.807	1.444	1.324	1.351	1.351	0.668	0.482	81	85	85	-17	-40	2.21E-6	6.79E-6	> 1.00E-4
Colon Cancer															
COLO 205	0.405	1.318	1.404	1.322	1.432	0.559	0.184	109	100	113	17	-55	4.50E-6	1.72E-5	8.60E-5
HCC-2998	0.837	2.323	2.240	2.234	2.408	1.639	0.648	94	94	106	54	-23	1.13E-5	5.06E-5	> 1.00E-4
HCT-116	0.189	1.726	1.772	1.709	1.690	0.453	0.047	103	99	98	17	-75	3.91E-6	1.53E-5	5.32E-5
HCT-15	0.314	1.936	1.886	1.900	1.777	0.617	0.227	97	98	90	19	-28	3.65E-6	2.52E-5	> 1.00E-4
HT29	0.229	1.238	1.280	1.267	1.307	0.308	0.129	104	103	107	8	-44	3.75E-6	1.42E-5	> 1.00E-4
KM12	0.284	1.632	1.530	1.573	1.484	0.636	0.255	92	96	89	26	-10	4.17E-6	5.23E-5	> 1.00E-4
SW-620	0.320	2.270	2.222	2.255	2.142	0.844	0.467	98	99	93	27	8	4.49E-6	> 1.00E-4	> 1.00E-4
CNS Cancer															
SF-268	0.667	2.068	1.999	1.991	2.059	1.217	0.760	95	95	99	39	7	6.63E-6	> 1.00E-4	> 1.00E-4
SF-295	0.886	2.600	2.490	2.490	2.473	0.969	0.259	94	94	93	5	-71	3.06E-6	1.16E-5	5.31E-5
SF-539	0.911	2.277	2.305	2.297	2.215	0.719	0.427	102	101	95	-21	-53	2.45E-6	6.59E-6	7.96E-5
SNB-19	0.681	2.130	2.022	2.062	1.985	1.276	0.869	93	95	90	41	13	6.56E-6	> 1.00E-4	> 1.00E-4
SNB-75	0.893	1.713	1.584	1.626	1.525	0.896	0.643	84	89	77	.	-28	2.25E-6	1.03E-5	> 1.00E-4
U251	0.482	1.965	1.905	1.929	1.884	0.792	0.155	96	98	95	21	-68	4.02E-6	1.72E-5	6.28E-5
Melanoma															
LOX IMVI	0.291	1.449	1.412	1.400	1.466	0.680	0.059	97	96	101	34	-80	5.73E-6	1.98E-5	5.45E-5
MALME-3M	0.757	1.436	1.416	1.393	1.403	0.768	0.463	97	94	95	2	-39	3.04E-6	1.10E-5	> 1.00E-4
M14	0.505	1.891	1.868	1.857	1.893	0.603	0.436	98	98	100	7	-14	3.46E-6	2.18E-5	> 1.00E-4
MDA-MB-435	0.532	2.240	2.329	2.276	1.686	0.278	0.365	105	102	68	-48	-31	1.42E-6	3.85E-6	> 1.00E-4
SK-MEL-2	1.121	2.122	2.099	2.165	2.132	0.989	0.766	98	104	101	-12	-32	2.83E-6	7.86E-6	> 1.00E-4
SK-MEL-28	0.662	1.581	1.609	1.612	1.463	1.018	0.586	103	103	87	39	-12	5.85E-6	5.89E-5	> 1.00E-4
SK-MEL-5	0.876	3.281	3.256	3.140	3.191	1.329	0.371	99	94	96	19	-58	3.96E-6	1.76E-5	7.94E-5
UACC-257	0.834	1.536	1.585	1.507	1.597	1.085	0.597	107	96	109	36	-28	6.37E-6	3.61E-5	> 1.00E-4
UACC-62	0.734	2.668	2.566	2.628	2.402	1.185	0.483	95	98	86	23	-34	3.77E-6	2.54E-5	> 1.00E-4
Ovarian Cancer															
IGROV1	0.670	1.464	1.413	1.489	1.516	0.853	0.445	94	103	107	23	-34	4.75E-6	2.55E-5	> 1.00E-4
OVCAR-3	0.600	1.873	1.843	1.867	1.933	0.938	0.406	98	99	105	27	-32	5.01E-6	2.82E-5	> 1.00E-4
OVCAR-4	0.621	1.052	1.064	0.986	0.970	0.834	0.552	103	85	81	49	-11	9.59E-6	6.55E-5	> 1.00E-4
OVCAR-5	0.624	1.446	1.444	1.449	1.471	1.064	0.565	100	100	103	53	-10	1.14E-5	7.06E-5	> 1.00E-4
OVCAR-8	0.590	2.036	2.062	2.026	1.927	1.192	0.509	102	99	92	42	-14	6.83E-6	5.63E-5	> 1.00E-4
NCI/ADR-RES	0.815	2.435	2.464	2.422	2.345	0.755	0.704	102	99	94	-7	-14	2.73E-6	8.47E-6	> 1.00E-4
SK-OV-3	0.634	1.269	1.306	1.259	1.373	0.754	0.383	106	98	116	19	-40	4.80E-6	2.10E-5	> 1.00E-4
Renal Cancer															
786-0	0.833	2.560	2.478	2.466	2.479	1.397	0.310	95	95	95	33	-63	5.29E-6	2.20E-5	7.34E-5
A498	1.722	2.326	2.196	2.136	2.121	1.652	1.133	78	68	66	-4	-34	1.69E-6	8.75E-6	> 1.00E-4
ACHN	0.338	1.464	1.487	1.500	1.465	0.767	0.330	102	103	100	38	-2	6.43E-6	8.74E-5	> 1.00E-4
CAKI-1	1.171	2.756	2.688	2.774	2.683	1.225	0.844	96	101	95	3	-28	3.11E-6	1.28E-5	> 1.00E-4
RXF 393	0.960	1.712	1.695	1.634	1.650	0.898	0.407	98	90	92	-7	-58	2.66E-6	8.59E-6	7.10E-5
SN12C	0.730	2.695	2.636	2.653	2.574	1.396	0.365	97	98	94	34	-50	5.38E-6	2.53E-5	9.98E-5
UO-31	0.865	1.946	1.980	1.867	1.916	1.297	0.741	103	93	97	40	-14	6.67E-6	5.43E-5	> 1.00E-4
Prostate Cancer															
PC-3	0.664	1.706	1.645	1.585	1.595	0.956	0.572	94	88	89	28	-14	4.38E-6	4.67E-5	> 1.00E-4
DU-145	0.407	1.437	1.433	1.439	1.500	0.755	0.285	100	100	106	34	-30	5.97E-6	3.38E-5	> 1.00E-4
Breast Cancer															
MCF7	0.614	2.718	2.603	2.736	2.728	0.882	0.508	94	101	100	13	-17	3.76E-6	2.66E-5	> 1.00E-4
MDA-MB-231/ATCC	0.680	1.494	1.509	1.546	1.481	0.981	0.513	102	106	98	37	-25	6.13E-6	3.99E-5	> 1.00E-4
BT-549	1.169	2.281	2.283	2.356	2.246	1.678	1.034	100	107	97	46	-12	8.27E-6	6.28E-5	> 1.00E-4
T-47D	0.598	1.534	1.485	1.460	1.538	0.902	0.669	95	92	100	32	8	5.52E-6	> 1.00E-4	> 1.00E-4
MDA-MB-468	1.003	2.283	2.209	2.100	2.102	0.982	0.712	94	86	86	-2	-29	2.56E-6	9.47E-6	> 1.00E-4

Figure 3. 46 GI50, TGI and LC50 results for BE36 on 60 cell lines

3.6.2 COMPARE algorithm

The NCI have developed a COMPARE algorithm that allows the antiproliferative profiles of compounds evaluated using the NCI screen to be compared and correlated. The program evaluates patterns of cytotoxicity among the cell lines in the screen and provides a numerical evaluation of the degree of similarity between the patterns obtained with any two agents. Compounds with a similar mechanism of antiproliferative effect, e.g. tubulin binding compounds, often shown the same differential antiproliferative profile across cell lines. High correlation values may indicate compounds with a similar mechanism of action, such as anti-tubulin agents or ER antagonists.

The COMPARE algorithm was used to compare the differential antiproliferative activities of chromene **BE36** to compounds with known mechanisms of action in the NCI Standard Agent Database. All three measures of activity (GI_{50}, TGI and LC_{50}) were used and the analysis showed correlations to vinblastine, maytansine and rhizoxin, all of which affect microtubule polymerisation (see table 3.13) and also to tamoxifen which is known to target the ER. There is no evidence that the COMPARE algorithm distinguishes between different tubulin-based mechanisms of action. *In vitro* ER-binding studies have confirmed that **BE36** is acting as an ER targetting agent (section 3.5.3).

Rank	Compound	*r*	*Target*
	Based on GI_{50} mean graph		
1	**S-trityl-L-cysteine**	**0.576**	**antimitotic**
2	**Rhizoxin (hiConc:-4.3)**	**0.543**	**antimitotic**
3	**batracylin**	**0.455**	**topoisomerases I and II**
4	**Rhizoxin(hiConc:-4.0)**	**0.402**	**antimitotic**
5	**Maytansine(hiConc:-4.0)**	**0.377**	**antimitotic**
6	**tamoxifen**	**0.376**	**ER antagonist**
7	**Maytansine(hiConc:-3.6)**	**0.371**	**antimitotic**
8	**asaley**	**0.370**	**DNA alkylation**
9	**gallium nitrate**	**0.368**	**hypercalcemia**
10	**Rhizoxin(hiConc:-9.0)**	**0.353**	**antimitotic**
11	**Maytansine(hiConc:-9.0)**	**0.35**	**antimitotic**
12	**tamoxifen**	**0.349**	**ER antagonist**

	Based on TGI mean graph		
1	rhizoxin	0.475	antimitotic
2	S-trityl-L-cysteine	0.448	antimitotic
3	batracylin	0.441	topoisomeraseI,II
4	hexamethylenebisacetamide	0.394	apoptosis
5	gallium nitrate	0.365	hypercalcemia
6	Mitotane	0.361	steroid metabolism
7	N-(phosphonacetyl)-L-aspartic acid	0.357	L-aspartate transcarbamoylase
8	maytansine	0.325	antimitotic
9	asaley	0.325	DNA alkylation
10	vinblastine sulphate (hiConc:-4.0)	0.317	antimitotic
11	vinblastine sulphate (hiConc:-4.0)	0.314	antimitotic
12	tamoxifen	0.304	ER antagonist
	Based on LC_{50} mean graph		
1	N-(phosphonacetyl)-L-aspartic acid(hiConc:-4.0)	0.471	L-aspartate transcarbamoylase
2	mitindomide	0.430	DNA topoisomerase II
3	N-(phosphonacetyl)-L-aspartic acid (hiConc:-4.0)	0.398	L-aspartate transcarbamoylase
4	emofolin sodium	0.386	antifolate
5	DUP785 (brequinar)	0.364	pyrimidine synthesis
6	chlorozotocin	0.353	DNA alkylation
7	cyanomorpholino-ADR(CMA)	0.352	DNA topoisomerase
8	dichloroallyl lawsone	0.349	antimitotic
9	S-trityl-L-cysteine	0.333	Antimitotic
10	AT-125 (acivicin)	0.331	Antimetabolite
11	PCNU	0.329	DNA alkylation
12	tetrocarcin A sodium salt	0.327	Apoptosis

Table 3. 13 Standard COMPARE Analysis of chromene BE36.

The target set was the standard agent database and the target set endpoints were selected to be equal to the seed end points. Standard COMPARE analysis was performed. Correlation values (*r*) are Pearson correlation coefficients. Rhizoxin, maytansine and vinblastine sulfate appear at different concentrations as it has been tested by the NCI at multiple concentration ranges

3.7 Conclusions

The full range of structurally varied novel benzopyran and pyranocoumarin compounds, arranged in thirteen different categories, was designed and synthesised. Spectroscopic characterisation confirmed the identity of all synthetic products and HPLC recorded high percentage purity of products. The novel compounds contain the 4-aryl-4*H*-chromene scaffold which was initially identified from target specific vHTS to have ERα binding affinities. Activity against the MCF-7 human breast cancer cell line was demonstrated for many examples of the various structural types evaluated with IC_{50} values at the low micromolar level. Activity in the androgen receptor positive human prostate cancer cell line LNCaP was also demonstrated for two examples, **BE69** and **BE92** at the low micromolar level. One of the most interesting compounds to emerge from this study was identified as **BE36**, which displayed antiproliferative activity against MCF-7 human breast cancer cells (IC_{50} = 6.60 μM). This compound was also shown to be active against a range of human cancer cell lines e.g. ovarian, leukaemia, lung, colon, renal, prostate, melanoma and CNS at the low micromolar level. The estrogen receptor binding values for compound **BE36** were determined as IC_{50} = 0.59(ERα) and IC_{50} =1.52(ERβ). Compound **BE91** with its diamino substitute and **BE97** with its dimethyl amino group were both evaluated by the NCI and both were shown to be active molecules. Both compounds on the one dose testing assays were shown to have good cytotoxicity values on the MCF-7 human breast cancer cell line. In the cell viability assays compound **BE91** had an IC_{50} of 1.078 μM and **BE97** had an IC_{50} value of 0.92 μM, indicating the NH_2 groups are an improvement on the previously substituted phenolic group. **BE91** had a binding value of 7.22 μM on the ERβ isoform. Calculated Lipinski properties for **BE91** were an acceptable CLogP value of 5.61, however for compound **BE97** the CLogP value was 7.28, and is seen to be higher due to the lipophilic dimethyl group and bulky non-polar ester side chain.

As an example, the potential lead compound **BE36** was evaluated for "druggability" properties. The Lipinski's rules describe molecular properties important for a drug's

pharmacokinetics in the human body, including their absorption, distribution, metabolism, and excretion. However, the rule does not predict if a compound is pharmacologically active. The rule is important for drug development where a pharmacologically active lead structure is optimized step-wise to provide increased activity and selectivity, as well as preserving and enhancing drug-like properties. Lipinski's rule says that, in general, an orally active drug has no more than one violation of the following criteria:

- Not more than 5 hydrogen bond donors (nitrogen or oxygen atoms with one or more hydrogen atoms)
- Not more than 10 hydrogen bond acceptors (nitrogen or oxygen atoms)
- A molecular mass not greater than 500 Daltons
- An octanol-water partition coefficient log *P* not greater than 5

Extensions are:

- Polar surface area ≤140Å^2
- Rotatable bonds ≤ 10

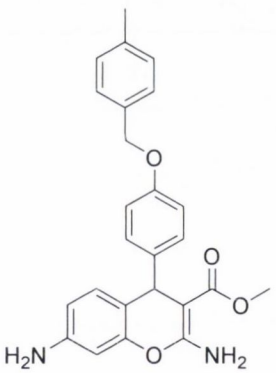

BE91

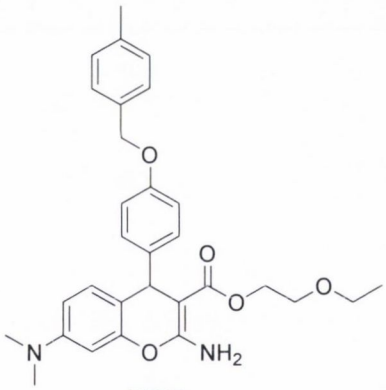

BE97

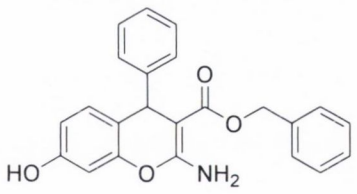

BE36

In the case of compound **BE36**, the molecular weight is calculated as 373.13, with 5 hydrogen bond acceptors, three OH/NH bond donators, five rotatable bonds, and the cLogP value of 5,76 therefore one violation of the Lipinski rules. Many of the active compounds investigated in this study have calculated LogP value of greater than 5, therefore violate one of the Lipinski rules and may be classified as too lipophilic to be considered for development for oral drug delivery.

The molecular modelling evaluations performed on the novel chromene products synthesized are useful in predicting how they will potentially bind in the ER alpha and ER beta receptors. Further structure-activity studies may be useful to optimise the potential of these structures as novel Selective Estrogen Receptor Modulators(SERMs) and lead to the design of more potent antiproliferative and ER binding compounds.

Chapter 4 Synthesis of novel non-ligand binding pocket androgen receptor antagonists

4.1 Introduction

The Androgen Receptor (AR) is a relevant target in drug discovery involved in a variety of pathological processes such as androgen insensitivity syndrome (AIS), spinal bulbar muscular atrophy (SBMA) and prostate cancer [177]. Specifically, in prostate cancer, androgens and androgen signalling through AR are required for both prostate development as well as cancer initiation and progression[178, 179].

The AR is a member of the highly homologous family of steroidal nuclear receptors (NRs) that regulate transcription of target genes in a ligand dependent fashion[180]. NRs are composed of a modular structure including an N-terminal domain (NTD), a DNA binding domain (DBD) and a ligand binding domain (LBD) which encloses a central ligand binding pocket (LBP) where natural hormones bind[181]. These hormones include testosterone and dihydrotestosterone in the specific case of AR. The mechanism of activation of AR involves the binding of the natural androgens testosterone and dihydrotestosterone to the ligand binding domain (LBD). The LBD is highly structurally conserved throughout the NR superfamily as was discussed in the case of the estrogen receptor, (see Chapter 1). It contains 12 α-helices that are folded into a typical three-layer helix sandwich, enclosing a hydrophobic region, constituting the ligand binding pocket (LBP). When the ligand binds to the LBP, helix 12 undergoes a conformational change generating a secondary hydrophobic region called Activation Function 2 (AF-2) on the surface of the protein suitable for the recruitment of coactivators and correpressors [182]. More than 165 coactivators are known to interact with the AR alone[183]. The ligand-dependent AR:coactivator interaction modulates the transcriptional activity of AR, and deregulations at this interface - such as coregulator overexpression or acquired mutations are frequently associated with prostate cancer[134, 184].

Traditionally, the mainstay for prostate cancer treatment has been androgen deprivation therapy (ADT)[185], typically achieved through chemical castration and mostly employing concurrent LBP directed intervention ('LBP' antiandrogens). These therapeutics bind to AR in the LBP, mimicking androgen's mode of action, but blocking the receptor's dynamic formation of the AF-2 co-regulator through their incorporation of specific bulky substituents that prevent the 'closure' of helix 12. A major drawback of this therapy is the development of drug resistance. Castration Resistant Prostate Cancer (CRPC) is frequently metastatic and almost invariably fatal. Recent studies have concentrated on this progression from an androgen-dependent and therapy-responsive stage to an androgen-independent, therapy-resistant stage[186]. One of

the postulated molecular mechanisms of resistance to therapy relates to the intrinsic agonistic activity of the 'LBP' antiandrogens, which increase the transactivation potential of AR[187]. Due to these unfavourable limitations, recent efforts have concentrated on designing compounds that could overcome drug resistance in CRPC[188, 189]. 'True' LBP antiandrogens like RD-162[133], MDV-3100[122, 190], BMS-641988[191, 192] and the newly discovered ARN-509[193] are noteworthy among this class of inhibitors. An alternative approach is the design of non-LBP antiandrogens that could circumvent LBP related shortcomings. Recently, non-LBP strategies directly disrupting the interaction between the protein and its coactivator at AF-2 or at allosteric regulatory surfaces have been reported for AR[194, 195] and some other members of the family of nuclear receptors[196]. The viability of the non-LBP approach has also been documented for AR [197-200] where the interaction with coactivators has been blocked by peptide antagonists[201, 202] or small molecules[194, 199, 203, 204].

This chapter reports the synthesis of biologically active members of the 3-hydroxy-N'-((naphthalen-2-yl)methylene)naphthalene-2-carbohydrazide family as novel androgen receptor (AR) antagonists and their potential application in prostate cancer therapeutics[121]. Antiandrogens in a therapeutic setting typically performed by displacing the natural hormones from the LBP, but acquired drug resistance after prolonged use is a difficulty which impairs their application in advanced stages of prostate cancer. The *N*-acylhydrazone compounds that have been recently reported[121] use an alternative non-LBP mediated mechanism which target AR association with coactivators. Coactivators are essential for AR activity as a transcription factor, and the direct disruption of this interaction can potentially overcome therapeutic liabilities of solely targeting the LBP. All of these compounds share the presence of an *N*-acylhydrazone linker, which can exist in the *E/Z* isomeric forms. The first systematic studies of the *E/Z* isomerism of hydrazones were carried out by Karabatsos[205-207].

The simpler hydrazones (**A**, N-NH_2) were studied by Minabe[208], by Lemal[209], and by Alkorta[210]. *N,N*-dimethyl derivatives (**B**) were studied by Elguero[211] and by Lu[212]. *N*-aryl derivatives, usually *N*-phenyl **C**, are the most common hydrazones[205-207, 213-215] while *N*-acylhydrazones **D** are also reported [216-219]. The crystal structure of an example of the structural type **E** shows two hydrogen bonds (HB), N–H···O and O–H···N present in its structure[220] (Figure 4.1)

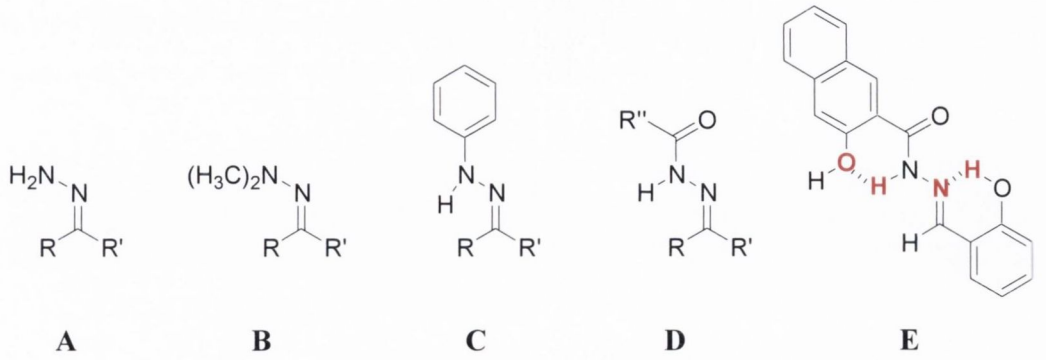

Figure 4. 1 Hydrazone Types A to E

In the present work, an investigation of the synthesis, NMR and X-Ray characterization and conformational analysis of a series of *N*-acylhydrazones was carried out. The compounds chosen for the initial study are representative examples of active ligands of the AR non-LBP type e.g the 3-hydroxy-*N'*-(naphthalen-2-ylmethylene)-2-naphthohydrazide (**5**) and some related systems (**7-9**)(figure 4.2). Biological and qualitative SAR analysis of these compounds as well as some related analogues has been also included in this study.

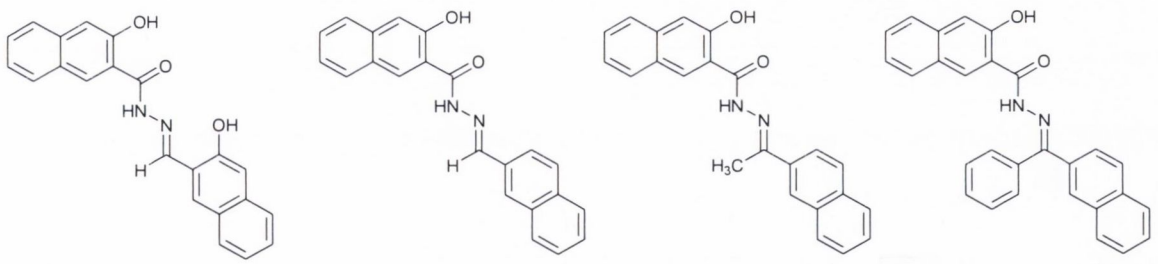

Figure 4. 2 Compounds studied in this work

This class of compound has previously been reported as androgen receptor (AR)-coactivator disruptors for potential application in prostate cancer therapy[121]. The presence of *E/Z* isomerism around the imine linker group (hydrazide) is important to define from a biochemical mechanistic point of view. A theoretical study of the *E/Z* isomerism in a series of 3-hydroxy-*N'*-((naphthalen-2-yl)methylene)naphthalene-2-

carbohydrazide (Figure 4.3) indicated that the *E* geometry and conformation as illustrated was preferred for the compounds[221]



(*Z*)-Isomer **(*E*)-Isomer**

Figure 4. 3 E/Z isomerism in 3-hydroxy-N'-(naphthalen-2-ylmethylene)-2-naphthohydrazide derivatives

4.2. Synthesis of 3-hydroxy-N'-((naphthalen-2yl)methylene)naphthalene-2-carbohydrazide derivatives

The full panel of N-acylhydrazone compounds **1-45** chosen for the study is illustrated in Figures 4.11 (Panel 1) and Figure 4.13 (Panel 2). For the initial biochemical screening experiments, a number of these compounds were purchased from the commercial sources e.g. Specs (http://www.specs.net). For the first study, a series of 3-hydroxy-N'-((naphthalen-2-yl)methylene)naphthalene-2-carbohydrazides (**2,3,6-9**) analogues and the closely related *N'*-benzylidene-3-hydroxy-2-naphthohydrazide (**27**) were synthesised following a standard synthetic route (Scheme 4.1). Starting from the commercially available 3-hydroxy-2-naphthoic acid (**I**), an esterification was performed in the presence of hydrochloric acid to afford the corresponding methyl 3-hydroxynaphthalene-2-carboxylate intermediate (**II**). Treatment of **II** with hydrazine hydrate afforded the hydrazide **III**. Condensation of **III** with the appropriate aldehyde or ketone (**IV**) afforded the products (**V**) in good yields. Systems **2,3,6,7** and **8** were isolated as a single isomer, subsequently characterized by ^{1}H NMR as the *E* isomer. Compound **9**, however, resulted as an inseparable mixture of *E/Z* isomers (see structure **V**) consistent with theoretical predictions.

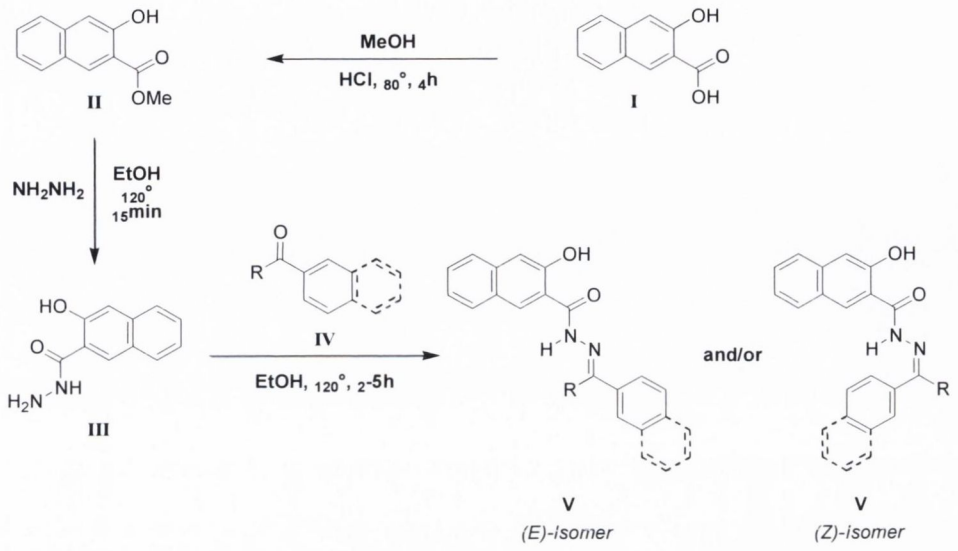

Scheme 4. 1 General synthetic pathway of 3-hydroxy-N'-(naphthalen-2-ylmethylene)-2-aromatic hydrazides derivatives 2,3,6-9(R = H, CH_3, Ph)(Panel 1)

4.3. NMR spectroscopic characterization

The combination of different NMR spectroscopic methodologies has been employed for the unequivocal characterization of the compounds studied in this work. As an example, the ^{1}H and ^{13}C NMR spectra of compound **7** are displayed in Figure 4.4 and Figure 4.5 respectively.

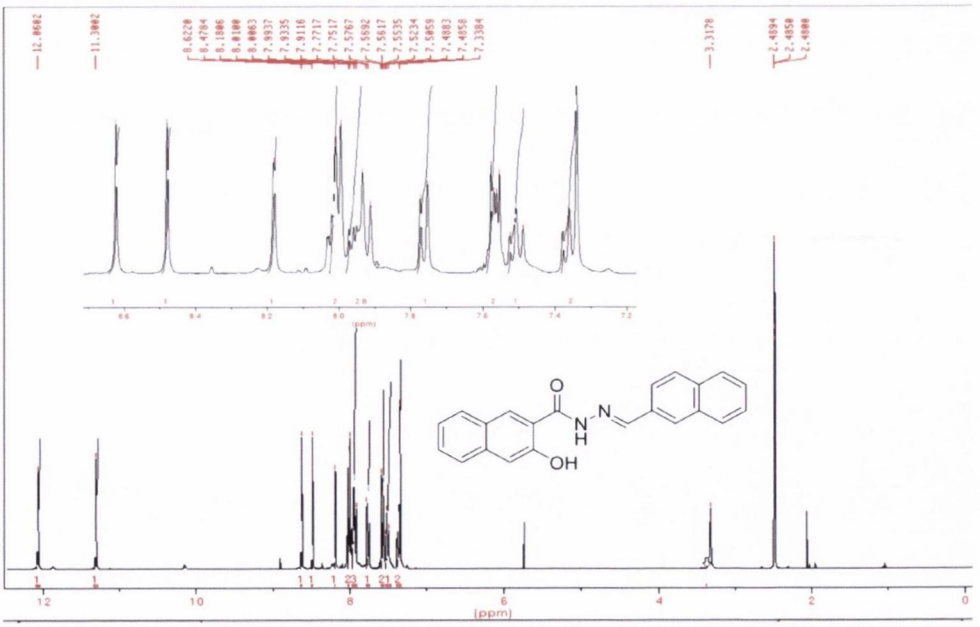

Figure 4. 4 ^{1}H NMR spectrum of compound 7

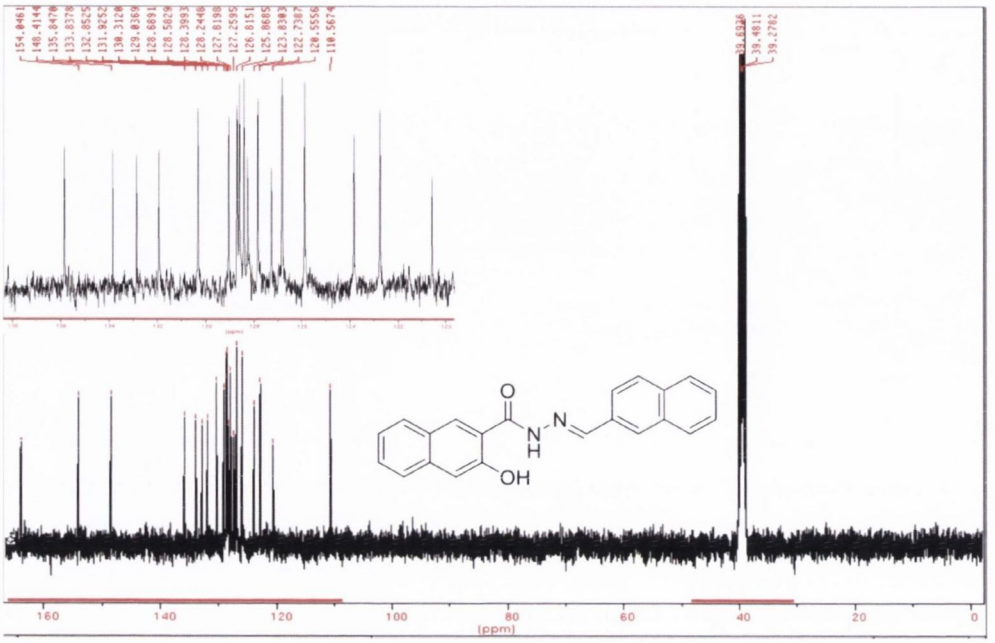

Figure 4. 5 ^{13}C NMR spectrum of compound 7

Figure 4.6 shows the ^{1}H NMR spectroscopic signals within the range of 7.0 to 12.4 ppm corresponding to the series **7, 8** and **9**. This region includes all the aromatic hydrogen atoms as well as NH/OH hydrogen atoms present in these compounds. Two important conclusions are evident:

1. The spectra of compounds **7** [R^1=H] and **8** [R^1=CH_3] correspond to an isolated isomer, conversely compound **9** [R^1=Ph] presents duplicated signals for all protons – indicating, as predicted, a mixture of isomers.

2. OH hydrogen atoms are strongly displaced downfield with chemical shift values above 10.0 ppm clearly indicating their participation in an intramolecular hydrogen bond with the lone pairs of the carbonyl oxygen atom.

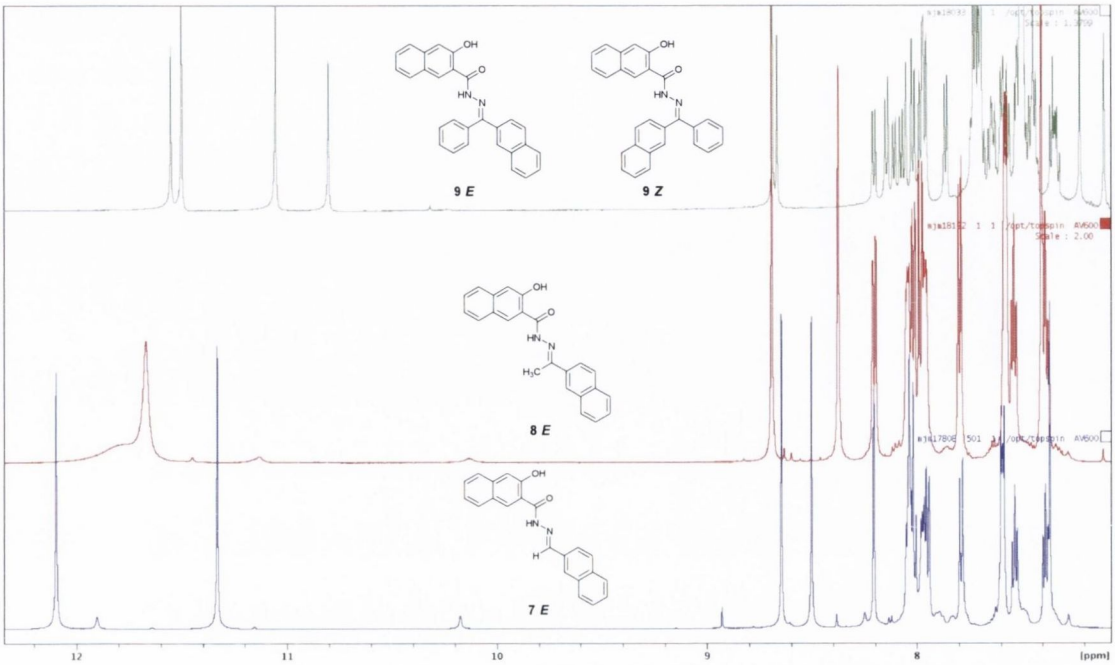

Figure 4. 6 ^{1}H NMR spectra of compounds 7, 8 and 9

Figure 4.7 illustrates the most significant intramolecular interactions which were probed by NMR and employed for the correct assignment of the experimentally obtained isomers for compounds **7** and **8**. In NOE experiments, irradiation of hydrogens corresponding to the R^2 groups H (8.64ppm) and CH_3 (2.52ppm) resulted in the perturbation of the signals of NH at 12.09 and 11.68 for **7** and **8** respectively, demonstrating the *E* character of the isolated isomers (a hypothetical *Z* isomer could not show this NOE interaction due to the greater distance between the involved groups), (see Figure 4.7).

It can be concluded that the *E*-isomer is formed under the described synthetic conditions for this family of compounds. The Z-isomer is formed only when the steric hindrance of the second imine substituent is sufficiently high as in the case of compound **9** in this case as a balanced mixture with the corresponding E-isomer.

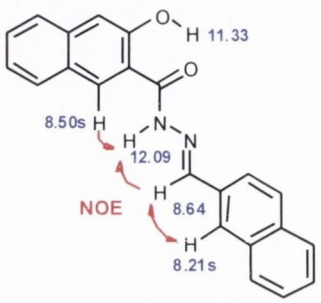

7 *E-Isomer*

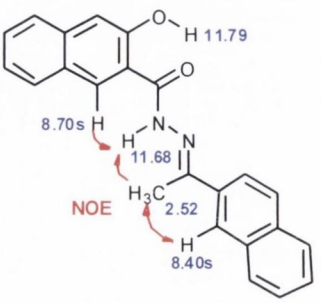

8 *E-Isomer*

Figure 4. 7 Relevant spectroscopic data used for NMR structure elucidation

4.4. X-ray analysis

Confirmation of the NMR experimental data was achieved with the X-ray crystal analysis. Slow recrystallization of compound **7** from methanol provided the crystal structure of the (*E*)-3-hydroxy-N'-((naphthalen-2-yl)methylene)-naphthalene-2-carbohydrazide as an isolated *E* isomer (Figure 4.8). The specific orientation of the naphthalene ring A in the newly obtained structure (**7**) is consistent with the crystal structures of some related compounds previously deposited in the Cambridge Structural Database [222-225]. See crystal data in table 4.1. for the crystallographic Data of Compound **7**, (Cambridge Database Deposition number: CCDC 864271).

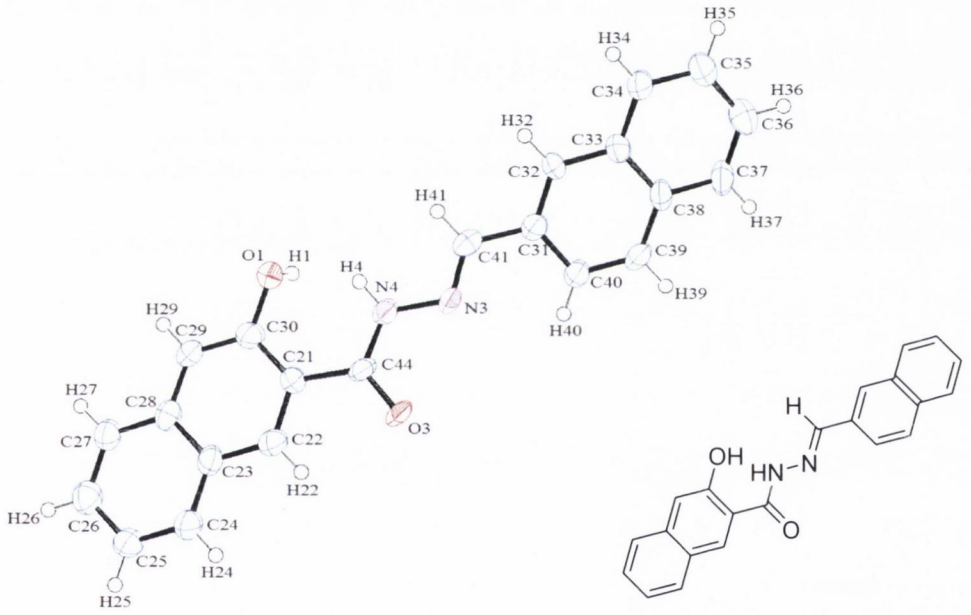

Figure 4. 8 ORTEP representation of the crystal structure of compounds 7, with the thermal ellipsoids at 50% probability

Identification code	shelxl	
Empirical formula	C44 H32 N4 O4	
Formula weight	680.74	
Temperature	150(2) K	
Wavelength	0.71073 Å	
Crystal system	Monoclinic	
Space group	P2(1)/c	
Unit cell dimensions	a = 15.352(3) Å	α= 90°.
	b = 6.4600(13) Å	β= 91.48(3)°.
	c = 8.4600(17) Å	γ = 90°.
Volume	838.7(3) $Å^3$	
Z	1	
Density (calculated)	1.348 Mg/m^3	
Absorption coefficient	0.088 mm^{-1}	
F(000)	356	
Crystal size	0.30 x 0.20 x 0.10 mm^3	
Theta range for data collection	3.15 to 31.09°.	
Index ranges	-21<=h<=22, -9<=k<=8, -9<=l<=10	
Reflections collected	11508	
Independent reflections	4183 [R(int) = 0.0654]	
Completeness to theta = 25.00°	85.1 %	
Absorption correction	None	
Max. and min. transmission	1.0000 and 0.5919	
Refinement method	Full-matrix least-squares on F2	
Data / restraints / parameters	4183 / 2 / 235	
Goodness-of-fit on F2	3.202	
Final R indices [I>2sigma(I)]	R1 = 0.1867, wR2 = 0.4857	
R indices (all data)	R1 = 0.1971, wR2 = 0.4944	
Largest diff. peak and hole	0.814 and -0.705 $e.Å^{-3}$	

Table 4. 1 Crystal data and structure refinement for compound 7

4.5. Biochemical study

The biochemical study was carried out by Dr. Laura Caboni, School of Biochemistry and Immunology, Trinity College Dublin. The results for ten different diarylhydrazide compounds of the initial panel were initially evaluated [226] (Figure 4.9, figure 4.10), including those conformationally studied in this work (**5, 7-9**), for their ability to displace AR:coactivator interaction using TR-FRET techniques. The structures of the full panel of compounds synthesized and evaluated in this initial study is presented in Figure 4.11

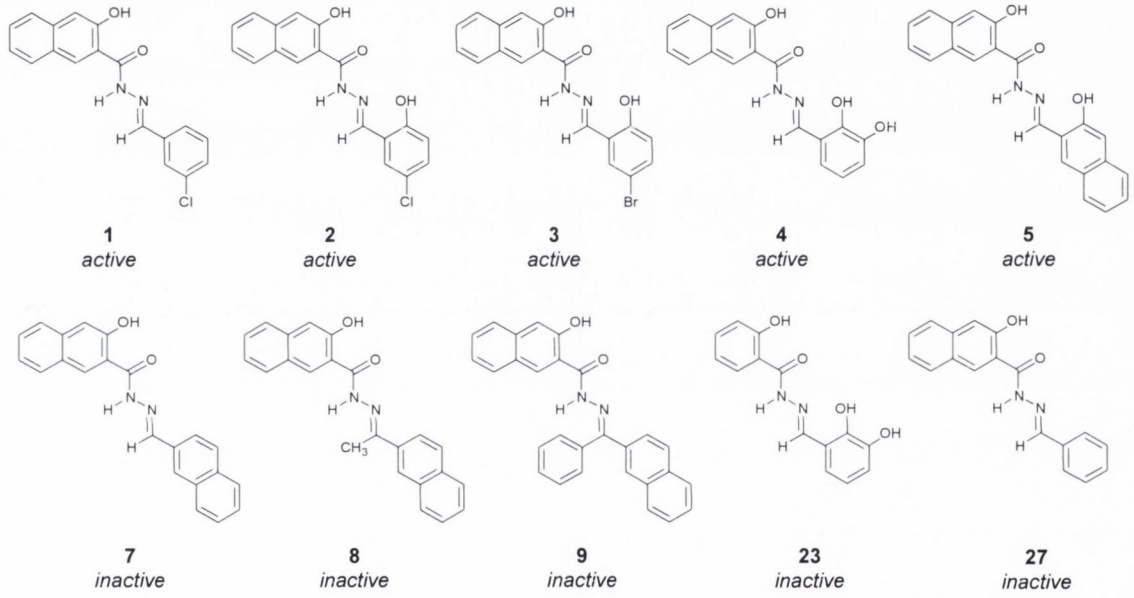

Figure 4. 9 Series of diarylhydrazides assayed on AR TR-FRET

TR-FRET technique measures the recruitment of a fluorescent (Fl) labelled co-activator (of the AR specific FxxLF type: acceptor) to a Terbium (Tb) labelled GST tagged AR-LBD (donor). The technique is dependent on the distance between the donor/acceptor pair[227]. In the case of an agonist bound LBD, the Fl labelled coactivator is associated with LBD, so when Tb is excited at 340nm, energy is transferred to Fl resulting in an increase in TR-FRET signal. In the presence of an antagonist, Fl coactivator is not bound to the LBD; therefore energy cannot be successfully transferred from Tb to Fl resulting in a decrease of TR-FRET signal.

Data is presented as a percentage maximum of activity as described previously[228] and the binding data of the tested compounds is presented in Figure 4.10.

a)

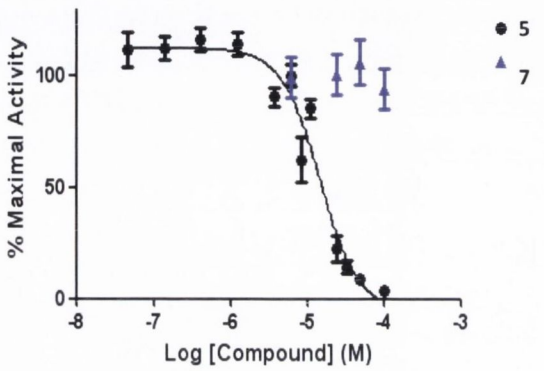

b)

Compounds	IC_{50}
1	42.7 ± 3.5 µM
2	10.3 ± 1.4 µM
3	11.7 ± 3.1 µM
4	40.8 ± 2.5 µM
5	15.8 ± 5.5 µM
7	NA >100 µM
8	NA >100 µM
9	NA >100 µM
23	NA >100 µM
27	NA >100 µM

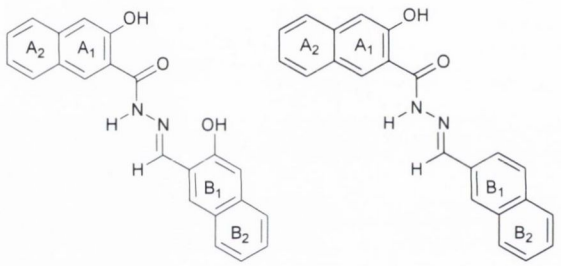

5
active

7
inactive

Figure 4. 10 Dose response curve and IC50 values for hydrazides (5) and (7)

Figure 4.10 **a)** displays the Dose response curve for compounds (**5**) and (**7**). Compounds were tested using a maximum concentration of 100 µM in the presence of a concentration of DHT (endogenous agonist) equal to its EC_{80} concentration (see experimental section). Data points are presented as standard error of mean (SEM) of at least two independent experiments in triplicate. Data was fitted using the dose-response curve (variable slope) available from GraphPad Prism. **b)** Diarylhydrazides activity towards AR-LBD. Values are presented as IC_{50} ±SEM of at least two independent experiments where each well was included as triplicate.

4.6 Qualitative SAR analysis

Derived from the biological evaluation of targeted modifications of the diarylhydrazide scaffold some initial qualitative SAR conclusions can be proposed:

i. The OH group on naphthalene ring B seems important for activity when comparing **5/7, 4/27** and **2/1** pairs of analogues. If not present it abolishes (**4** and **27**) or diminishes (**1**) the activity.

ii. Naphthalene ring **A2** seems to be required when comparing **4/23** pair since the substitution of naphthalene by a benzene ring abolishes the activity (**23**).

iii. Compounds **5**, **2** and **3** are equipotent, demonstrating that the presence of naphthalene ring B2 (**5**) or a hydrophobic group like chlorine (**2**) or bromine (**3**) increase the activity on AR.

In summary, compounds **1-5** were characterised as non-LBP 'true' antiandrogens with an IC_{50} in the low micromolar range (10-50 μM). Compounds **6-25** did not display antiandrogen activity. A systematic computational structure-activity relationship study was now required to better understand the preferred molecular conformation of the compounds binding to AR. It is important to note that diarylhydrazides were identified as non-LBP binders; therefore they do not bind in an enclosed pocket. The proposed mechanism of action is a functional disruption of AR interaction with coactivators on the surface of AR protein. The activity of ten structurally varied diarylhydrazides analogues, including those synthesised in this work, as non-ligand binding pocket antagonists of the androgen receptor has been performed using TR-FRET. Initial SAR evaluation highlighted the importance of naphthalene ring placement for compound binding. Further design, synthesis and evaluation of a second series of non-LBP AR binding analogues is discussed in the following section.

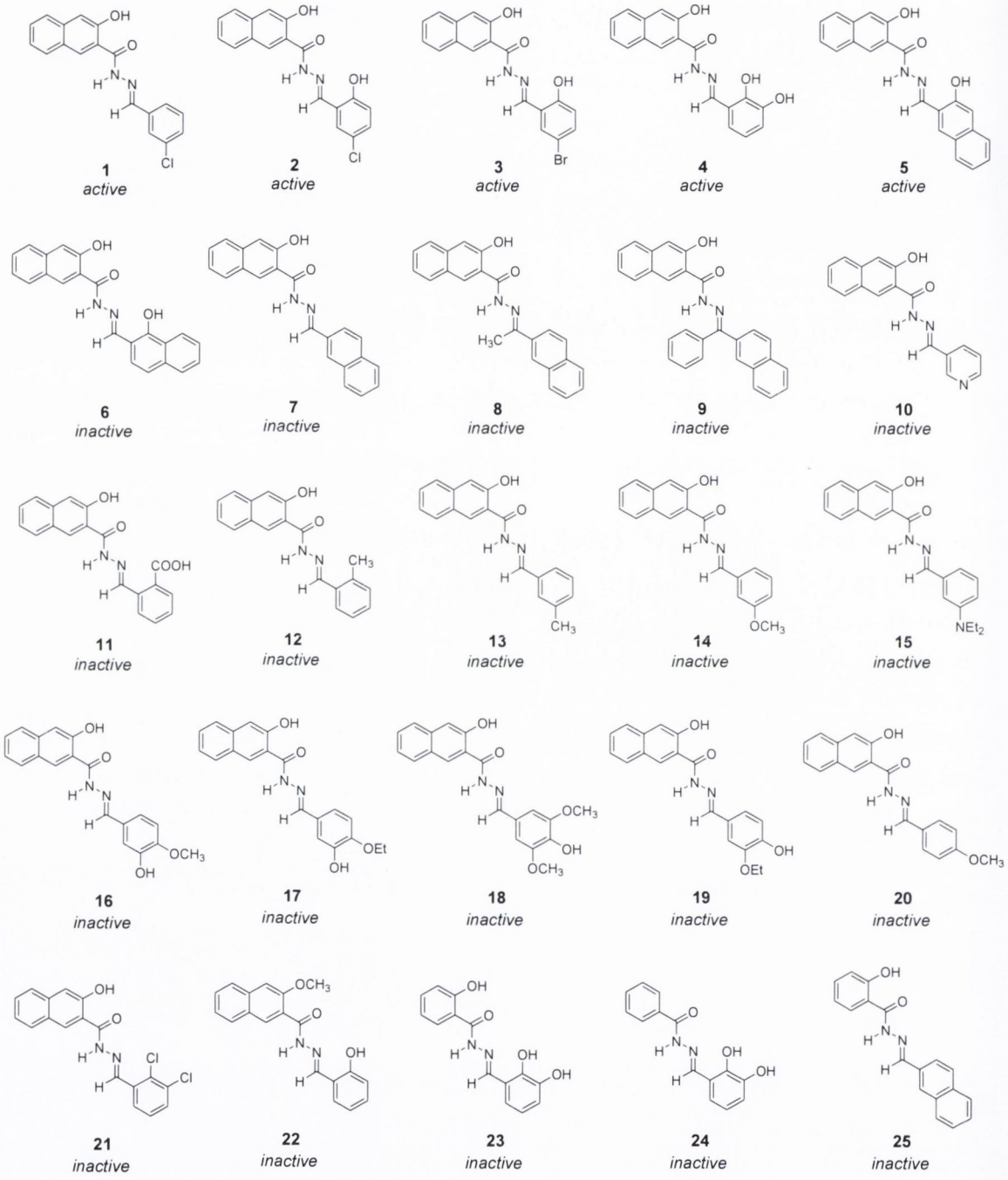

Figure 4. 11 Diarylhydrazides: Selection of Analogues as AR Antagonists (Panel 1).

4.7 Structural Basis of AR-Antagonism by Diarylhydrazides.

From the selection of diarylhydrazides evaluated from Panel 1, five derivatives were identified and characterised as non-LBP AR-antagonists (**1**-**5**). However, this data shows that small differences in the substitution patterns on the main scaffold produce dramatic effects on the activity. Building on these initial observations, a second generation of derivatives was designed.

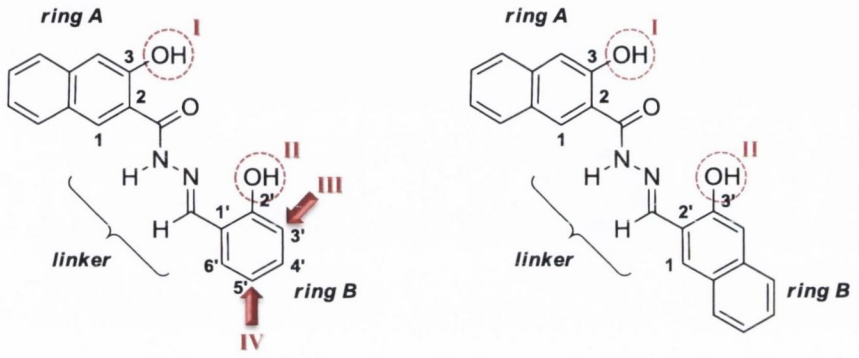

Figure 4. 12 Diarylhydrazides: General Structure and SAR Guidelines. I. Significance of OH group in the C3 position of ring A; II. Significance of OH group in the C2'/C3' position of ring B (for phenyl/naphthyl analogues respectively); III. Substitution effects at the C3' position of ring B and IV. Effect of substituents at position C5' of ring B.

An initial SAR analysis (Fig 4.12) of our compounds illustrated in Panel 1, see Figure 4.11, provided us with the following key points that guided the synthesis of new candidates: a) *Naphthyl vs. Phenyl Functionality at Rings A and B:* Solely the naphthyl decoration at ring A provides active ligands. Substitution with a phenyl ring (**4** vs. **23**) abolishes the activity. Conversely, both phenyl (**1-4**) and naphthyl (**5**) functionality at the ring B position lead to active ligands; b) *OH Substitution on Ring A:* Most of the active compounds identified, bear an OH group at the C3 position of naphthyl ring A. Methylation at this position (**22**) eliminates the AR antagonistic activity, suggesting that the hydrogen of the hydroxyl group could be essential for activity and c) *OH Substitution on Ring B:* Almost all of the active compounds (**2**-**5**) have a hydroxyl group on ring B located *ortho* to the linker (C2' or C3' for phenyl and naphthyl rings respectively), removal of this OH group abolishes the activity (**5** vs. **7**). Moreover, none of the other substituents evaluated at this position (CH_3, Cl and COOH) provided active ligands (**11**, **12** and **21**). The results also suggest that the contributory effect of the OH group occurs specifically when it occupies the C2' position (phenyl ring), since

derivatives hydroxylated in other positions (C3′ and C4′) were not active (**16-19**). A further series of compounds in Panel 2 (**26-45**), illustrated in Figure 4.13, were chosen for study to allow the structure-activity relationships of this series to be further developed. These compounds specifically feature substitutions in the naphthyl ring B at positions C3′ and C5 (See figure 4.12).

4.8. Synthesis of Diarylhydrazides (Panel 2).

New (*E*)-*N*′-benzylidene-2-naphthohydrazide analogues **26-32, 35-38, 40-42, 48** from (Panel 2) were synthesized following the standard procedure previously reported and illustrated in Scheme 4.2, [221]. Esterification of 3-hydroxy-2-naphthoic acid (**I**) in the presence of hydrochloric acid, treatment of the resulting ester intermediate **II** with hydrazine hydrate producing hydrazide **III**, and condensation of **III** with the appropriate aldehyde to afford the products (**IV**) in good yields. The products were charactrised by ^{1}H and ^{13}C NMR spectroscopy. As an example, the ^{1}H and ^{13}C NMR spectra for compound **37** are displayed in Figure 4.14 Under these conditions, the *E*-isomer of the C=N is obtained almost quantitatively.

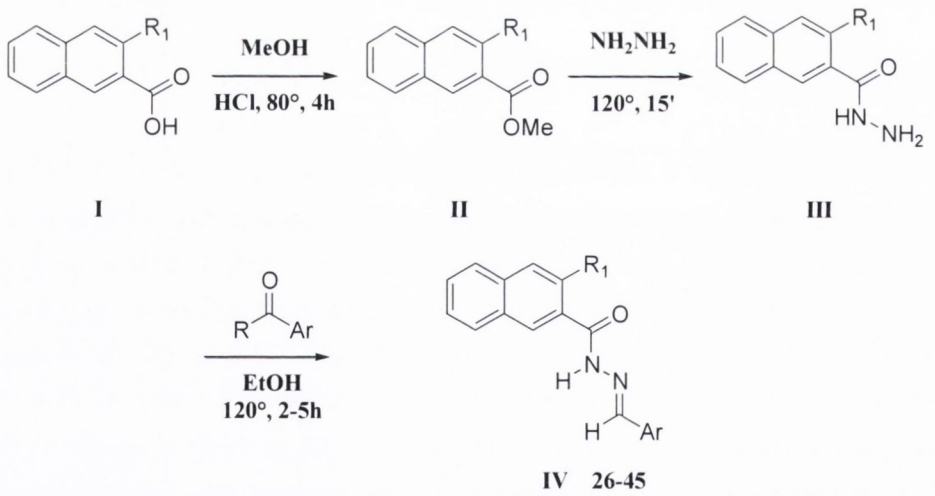

Scheme 4. 2 Synthesis of Diarylhydrazides 26-45, (Panel 2).

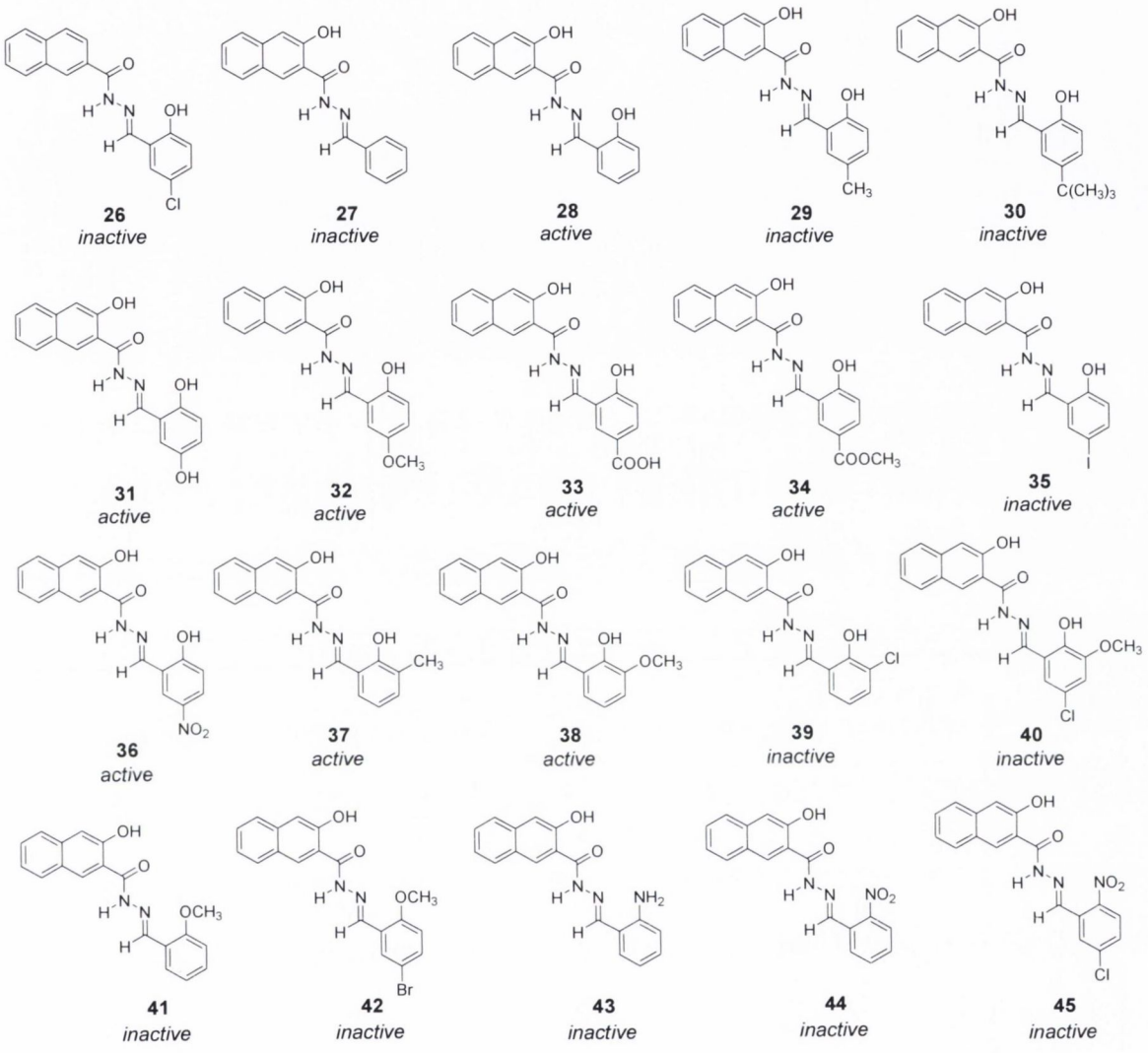

Figure 4. 13 Diarylhydrazides 26-45 (Panel 2)

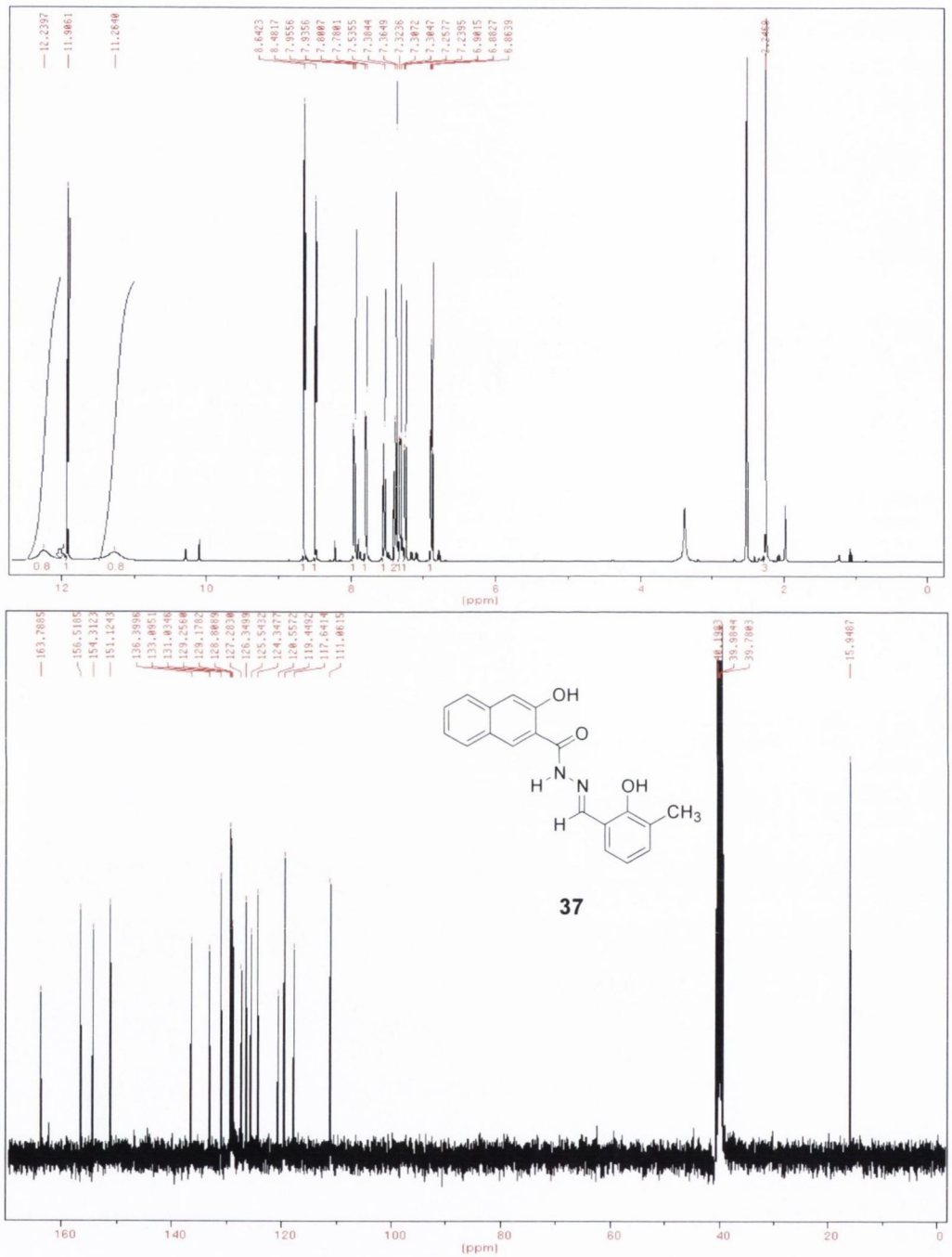

Figure 4. 14 ^{1}H and ^{13}C NMR spectra of compound 37

4.9 X-ray analysis

Confirmation of the NMR experimental data was achieved with the X-ray crystal analysis. Slow recrystallization of compound **42** from methanol provided the crystal structure of the (*E*)-N'-(5-bromo-2-methoxybenzylidene)-3-hydroxynaphthalene-2-carbohydrazide(**42**) as an isolated *E* isomer (Figure 4.15). The related crystal data is displayed in Table 4.2

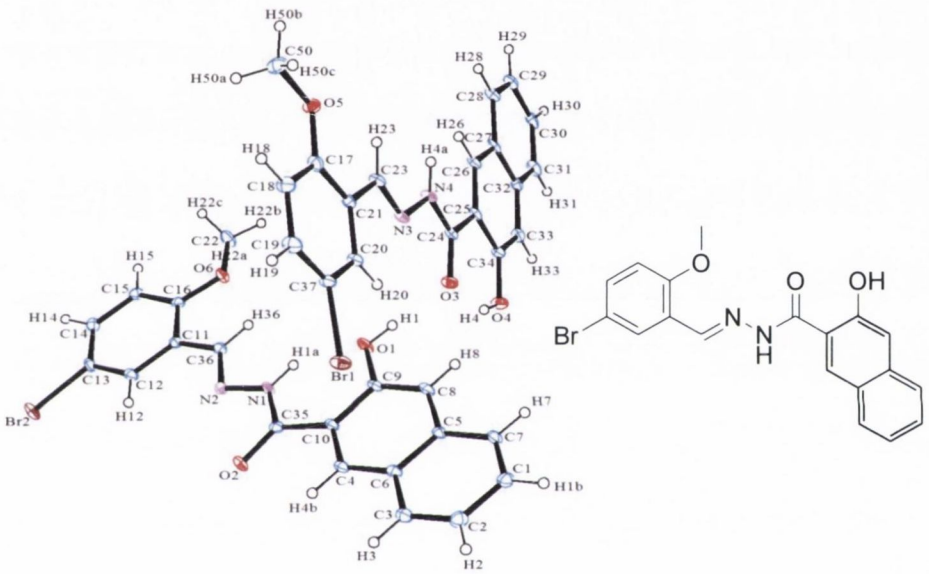

Figure 4. 15 Ortep representation of the X-ray structure of compound 42, ellipsoids set at 50% probability.

Identification code	shelxl	
Empirical formula	C152 H120 Br8 N16 O24	
Formula weight	*3193.92*	
Temperature	150(2) K	
Wavelength	0.71073 Å	
Crystal system	Monoclinic	
Space group	P2(1)/c	
Unit cell dimensions	a = 8.7298(17) Å	α= 90°.
	b = 19.876(4) Å	β= 100.90(3)°
	c = 19.544(4) Å	γ = 90°.
Volume	3330.0(12) $Å^3$	
Z	1	
Density (calculated)	1.593 Mg/m^3	
Absorption coefficient	2.490 mm^{-1}	
F(000)	1616	
Crystal size	1.50 x 0.60 x 0.20 mm^3	
Theta range for data collection	1.47 to 25.00°	
Index ranges	--8<=h<=10, -23<=k<=23, -23<=l<=23	
Reflections collected	23028	
Independent reflections	5612 [R(int) = 0.0537]	
Completeness to theta = 25.00°	95.5 %	
Absorption correction	Sadabs	
Max. and min. transmission	1.0000 and 0.5919	
Refinement method	Full-matrix least-squares on F2	
Data / restraints / parameters	5612 / 0 / 456	
Goodness-of-fit on F2	1.197	
Final R indices [I>2sigma(I)]	R1 = 0.0476, wR2 = 0.1535	
R indices (all data)	R1 = 0.0612, wR2 = 0.2134	
Largest diff. peak and hole	1.137 and -1.349 $e.Å^{-3}$	

Table 4. 2 Crystal data and structure refinement for 42

4.10 Biochemical Evaluation of AR Modulation.

Measurement of AR Antagonistic Activity - AR TR-FRET Assays. The biochemical study was carried out by Dr. Laura Caboni, School of Biochemistry and Immunology, Trinity College Dublin. Diarylhydrazides **26-45** were evaluated in AR TR-FRET experiments to determine their activity as AR antagonists. This technique evaluates the ability of the compounds to inhibit the recruitment of the fluorescently labelled D11-FXXLF coactivator peptide in the presence of an agonist (DHT) at a concentration equal to the EC_{80}. Results of these assays are presented in Table 4.3. For those compounds that showed antagonist activity (**28**, **31**-**34** and **36**-**38**), IC_{50} values were determined from 12-point dose–response curves (Figure 4.16). Compounds **37** and **38** were identified as the most potent hydrazides, with IC_{50} values of 13.2 and 12.2 μM respectively.

Comp.	TR-FRET	$IC_{50}(\mu M)^1$	**Comp.**	TR-FRET	$IC_{50}(\mu M)^1$
26	inactive	---	**36**	active	33.4 ± 4.7
27	inactive	---	**37**	active	13.2 ± 2.8
28	active	55.2 ± 19.2	**38**	active	12.2 ± 0.5
29	inactive	---	**39**	inactive	---
30	inactive	---	**40**	inactive	---
31	active	39.9 ± 16.9	**35**	inactive	---
32	active	53.0 ± 13.5	**42**	inactive	---
33	active	43.5 ± 3.7	**43**	inactive	---
34	active	60.7 ± 20.0	**44**	inactive	---
35	inactive	---	**45**	inactive	---

[1] *All assays were performed in triplicate, the values represents the average of the three assays. Compounds with IC_{50} >100 μM were considered inactive (NA= Not Active).*

Table 4. 3 Quantification of the AR-Antagonism of Diarylhydrazides by AR TR-FRET Assays

Determination of Non-LBP Mechanism of Action - AR FP Assays: Since the TR-FRET assay cannot differentiate between direct disruptors of coactivator binding (non-LBP antagonists), and classical AR modulators (LBP antagonists) acting at the ligand binding pocket, active compounds were tested for their ability to displace a

fluorescently labelled AR ligand from the AR LBP. Compounds were assayed at a single point concentration (50 μM) using Cyproterone Acetate (CPA) as a reference, a known AR LBP antagonist. As illustrated in Figure 4.16 (b), none of the compounds tested showed significant inhibition of the AR-LBD:*Fluormone* complex, indicating a non-LBP based mechanism.

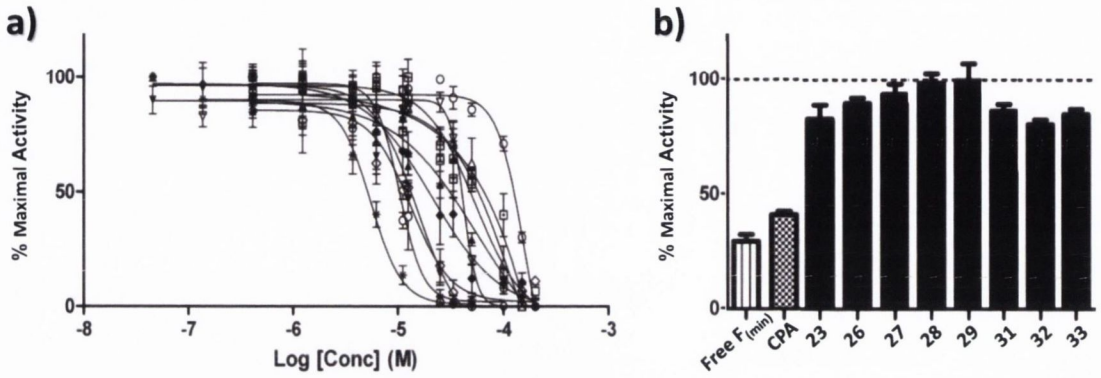

Figure 4. 16 Biological Characterization of Active Ligands (28, 31-34 and 36-38).

a) TR-FRET dose response curves: compounds were tested in a TR-FRET assay across a concentration range from 45 nM to 100 μM, where applicable in the presence of a concentration of DHT = EC_{80} in AR-LBD wt. Data points represent the mean of two independent experiments performed in triplicate. Error bars represent the standard error of the mean (SEM) for n = 6 values. Data was fitted using Log antagonist concentration vs. response (variable slope) with GraphPad Prism 5.

b) FP data: Fluorescence polarization data is plotted as % Maximal Activity represented by the AR-LBD and fluorophore complex (0% inhibition). Minimum control value represents free fluorophore (Free F) in solution (100% inhibition). Error bars represent the SEM for n = 6 values.

4.11 Structure Activity Relationship Study (Panel 2)

The Structure Activity Relationship Study of Panel 2 was carried out in collaboration with Dr. Laura Caboni and Dr. Fernando Blanco, School of Biochemistry and Immunology, Trinity College Dublin. Analysis of the biological results provided interesting SAR patterns that are summarized below. The following discussion is focused uniquely on phenyl ring B derivatives.

No Interchangeability of Aromatic Ends. Despite the apparent symmetry of these hydrazide compounds the two ends are not interchangeable. The same replacement performed on ring A and B - substitution of a naphthyl group by a phenyl one - produces the opposite effect in the activity. While in the case of B the antagonist character is maintained on this substitution (**5** and **28**), in A the activity is abolished (**4** vs. **23**). This suggests that the ligands adopt a consistent conformation in the binding site.

Requirement for OH in the C3 Position of Naphthyl Ring A. The results confirm unambiguously the important role played by the hydroxyl function. Both removal (**2** *vs.* **26**) and methylation (**28** *vs.* **22**) of this group lead to the elimination of antagonistic effects. The key factor seems to be the presence of the hydrogen available to participate in hydrogen bond interactions with specific residues in the binding pocket.

Relevance of OH in the C2' Position of Phenyl Ring B. The new examples investigated in this study with Panel 2 compounds highlight the importance of the hydroxyl group on ring B *ortho* to the linker. With only one exception (**1**), all active compounds contain this substituent (**2**-**5**, **28**, **31**-**34**, **36**-**38**). Similarly to what was observed with ring A, methylation of this group results in loss of activity (**28** *vs.* **41** and **3** *vs.* **42**). This hydroxyl could be involved in hydrogen bonding interactions with the pocket or contribute to conferring rigidity to the ligands through interactions with the linker-hydrazone nitrogen's lone-pair of electrons.

Substitution Effects at Position C2' of Phenyl Ring B - 2'-substituted series: In addition to OH, six different functionalities on C2' with different electronic profiles were studied (CO_2H, CH_3, Cl, OCH_3, NO_2 and NH_2), none of which were active (**11**, **12**, **21**, **41**-**45**). This result indicates the necessity for the OH substituent in this position. However, the unexpected lack of activity of the amino derivative (**43**) is noteworthy, since it is a classical bioisostere of OH.

Substitution Effects at Position C3' of Phenyl Ring B - 2'-Hydroxy-3'-Substituted Series: The functionalization of C3' shows that compounds **37** and **38** (2'-hydroxy-3'-methyl- and 2'-hydroxy-3'-methoxyderivatives) are active within a similar range (IC_{50} = 12.3 and 13.2 μM respectively), improving significantly the IC_{50} value of the 3'-unsubstituted analogue **28** (IC_{50} = 55.2 μM); Compound **39** (2'-hydroxy-3'-chloroderivative) is inactive.

Substitution Effects at Position C5' of Phenyl Ring B - 2'-Hydroxy-5'-Substituted Series: The functionalization of C5' is the feature that we have explored most

extensively. Due to its synthetic feasibility; there is a greater amount of commercially available aldehydes for the synthetic study with this position substituted than any other. Eleven derivatives have been synthesized and evaluated with the following substituents: H (**27**), CH_3 (**29**), tBu (**30**), OH (**31**), OCH_3 (**32**), CO_2H (**33**), CO_2CH_3 (**34**), Cl (**26**), Br (**3**), I (**35**) and NO_2 (**36**). Inductive electron-withdrawing groups (OH, OCH_3, CO_2H, CO_2CH_3, Cl, Br and NO_2) provide active analogues and electron-donating ones (CH_3 and ^tBu) abolish the activity. It can be concluded that the electronic profile of the substituent at C5′ determines the activity of the compounds.

Methylation of Hydroxyl Groups: It has been demonstrated that OH groups at positions C3 and C2′ are essential for AR activity. Considering that the hydroxyl and methoxy functions share a similar electronic profile the fact that the methoxy group eliminates the antagonist character can only be explained by steric effects or because the hydrogen donor hydrogen of the OH is essential for binding activity. Methoxylation of other positions C3′ (**4** and **38**) and C5′ (**31** and **32**) does not affect compound's activity, indicating that these ligands interact through a well-defined bioactive conformation.

A new family of antiandrogen ligands has been developed which interact with the AR disrupting the binding of coactivators. In the absence of confirmation by structural studies, there is sufficient evidence to consider that diarylhydrazides could bind, as designed, in the AF-2 region. To support the proposed binding site, docking and molecular dynamics simulations study was investigated.

4.12 Molecular Modelling study of Diarylhydrazides into AR AF-2.

The Molecular Modelling Study was carried out by Dr. Laura Caboni, School of Biochemistry and Immunology, Trinity College Dublin. The interaction of coactivators within the AF-2 groove occurs *via* the so-called 'Nuclear Receptor Box'[35] a short peptide motif of 5 amino acids. In general, most of the NRs accommodate coactivators with an LxxLL motif, where *L* represents a leucine and *x* represents any amino acid. AR, however, has a specific preference towards phenylalanine-enriched motifs like FxxLF. The AF-2 interface is divided into three hydrophobic subpockets: S1, S2 and S3, (Figure 4.18), and the amino acid sequence of each region is established. The following structures were specifically chosen to carry out the study (Figure 4.17): Compound **28** was selected as the active compound of reference, subsequently **27**, **46** and **47** were

selected to check the effect of removal of OH groups, and **22** and **41** were chosen to evaluate the effect of methoxylation on critical positions C3 and C2'.

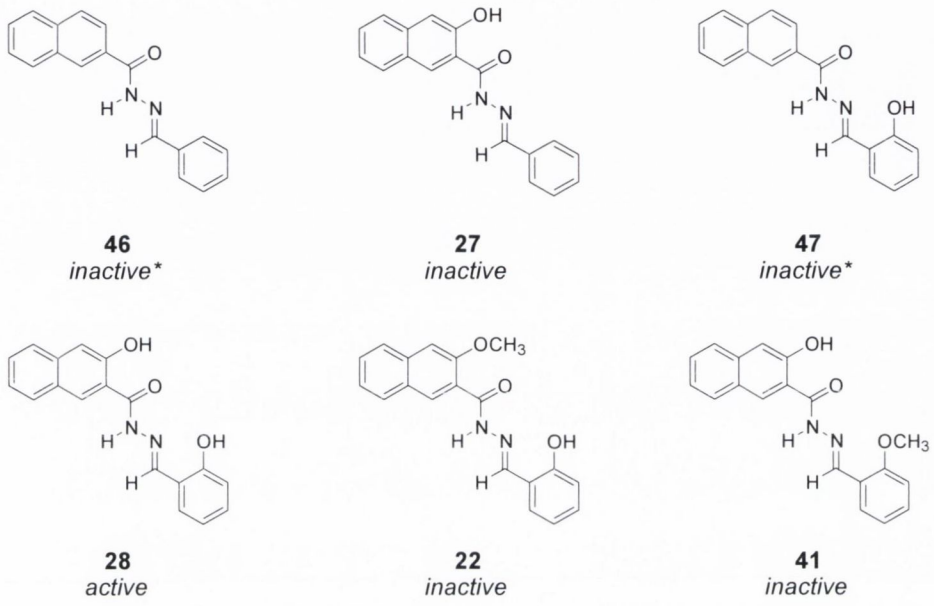

Figure 4. 17 Structures selected for Molecular Modeling.

The induced fit docking of compound **28** and the related analogues **46**, **27**, **47**, **22** and **41** with AR AF-2 is displayed in Figure 4.18. The role of OH Groups in the bioactive conformation and the consequences of methoxylation were examined. One of the most significant conclusions of the structure-activity study for compounds **26-45** was the essential role played by the OH groups on positions C2 and C2' in contributing antagonist character to these ligands. The proposed bioactive conformation **P1(Pose 1)** would rationalize this observation since both groups are relevant for its particular interaction with the AF-2 site. Figure 4.18 shows the *before* and *after* geometries of the simulated Pose 1(**P1)** conformation for compounds **46**, **27**, **47**, **28**, **22** and **41** after 40 ns of production dynamics. The results highlight the role of the hydroxyl groups in conferring activity to this class of ligands. OH containing derivatives **27** and **28** remain in the pocket throughout the entire production period and monohydroxylated derivative **47** is partially maintained in the pocket thanks to the strength of the binding of the phenyl moiety with S3. The non hydroxylated derivative **46**, however, is not able to maintain its position in the site. The introduction of methoxy groups in analogues **22** and **41** resullt in expulsion from the site due to both the disruption of the interacting points and the introduction of steric clashes caused the

methoxy moiety. All of these results are in good agreement with the reported SAR observations and strongly support the designation of **P1** as the bioactive conformation of our compounds. Based on all of this evidence, the design of new candidates must incorporate the functionalization of key positions in the diarylhydrazide skeleton which increase the ability of this class of ligand to bind strongly to the AF-2 region.

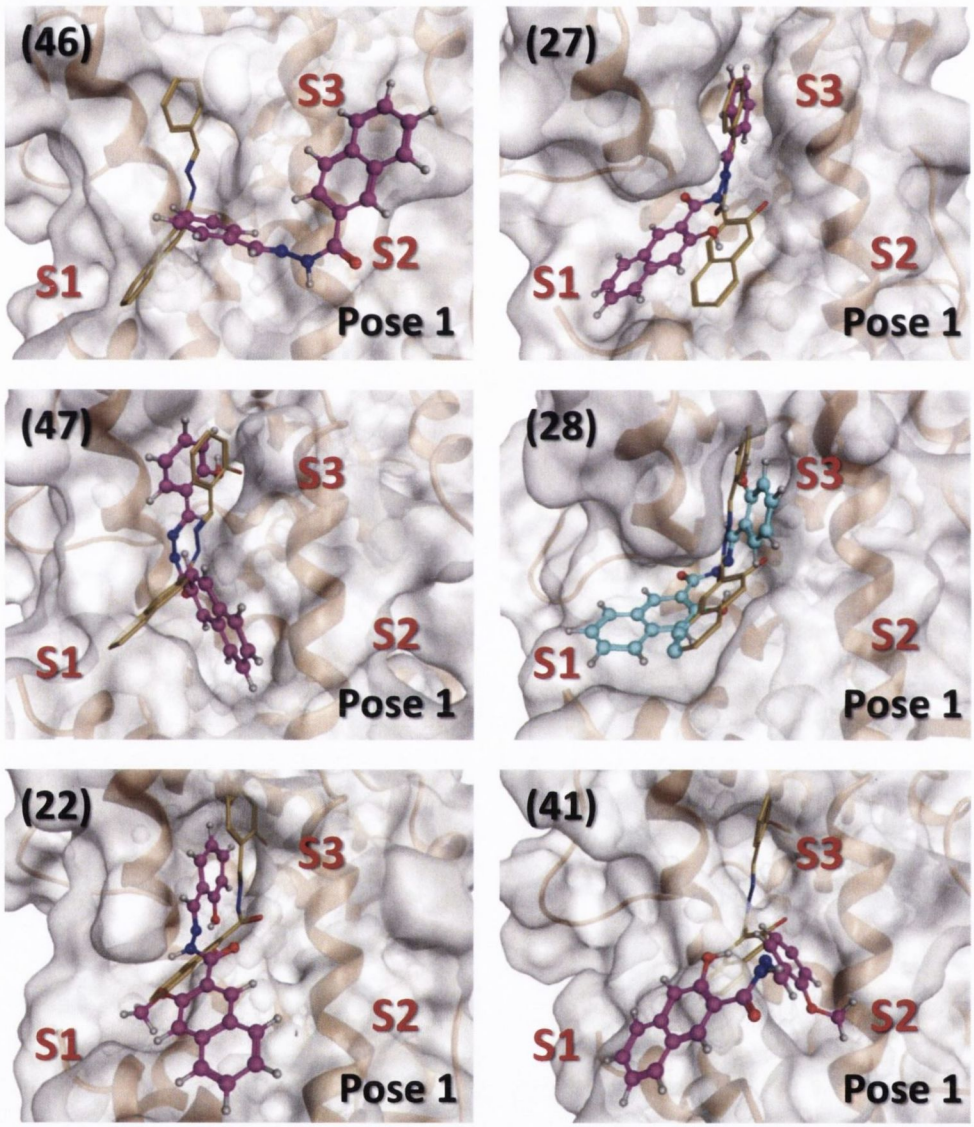

Figure 4. 18 Role of Hydroxylation and Methoxylation: Effect on Bioactive Conformation P1 (MD Study). Before and after conformations over the 40 ns of production dynamics are represented in yellow and magenta respectively. Images were generated by MOE [54]

4.13 Conclusions

A new series of diarylhydrazides has been synthesized and evaluated for AR antagonist activity. Of the 45 compounds evaluated in Panel 1 and Panel 2, thirteen examples have shown antiandrogen activity by a proven non-LBP mechanism of action, confirming the diarylhydrazide class of molecules as a promising alternative to traditional therapeutics for the treatment of Castration Resistant Prostate Cancer. The structures of these hydrazides have been established by ^{1}H and ^{13}C NMR spectroscopy and also by X-Ray diffraction analysis. Structure activity relationships have identified the significant role played by the phenolic hydroxyl substituents at the critical positions C-3 and C-3' within the diarylhydrazide scaffold, and the negative effects which are observed by their removal or methylation. From these SAR observations a deeper understanding of the main parameters that determine the effectiveness of these compounds as AR antagonists have been provided.

In the absence of a ligand-cocrystal structure, a combined study of docking and molecular dynamics has been performed, which afford insights into the potential binding mode of these active ligands to the AF-2 site. These results strongly support the main conclusions deduced from the SAR analysis and provide a bioactive conformation as a basis for the design of new candidates.

5.1 Chemistry Experimental Section

Melting points were measured on a Gallenkamp apparatus. Infra-red (IR) spectra were recorded on a Perkin Elmer FT-IR Paragon 1000 spectrometer. ^{1}H, ^{13}C and ^{19}F nuclear magnetic resonance (NMR) spectra were recorded at 27°C on a Brucker DPX 400 spectrometer (400.13MHz, ^{1}H; 100.61MHz, ^{13}C; 376.47MHz, ^{19}F) in either $CDCl_3$, CD_3OD, or DMSO-d6 (internal standard tetramethylsilane (TMS)). For $CDCl_3$, ^{1}H-NMR spectra were assigned relative to the TMS peak at 7.26 δ and ^{13}C-NMR spectra were assigned relative to the middle $CDCl_3$ triplet at 77.16 ppm. For CD_3OD, ^{1}H and ^{13}C-NMR spectra were assigned relative to the center peaks of the CD_3OD multiplets at 3.31 δ and 49.00 ppm respectively. For DMSO-d6, ^{1}H-NMR spectra were assigned relative to the TMS peak at 2.50 δ and ^{13}C-NMR spectra are assigned relative to the middle DMSO singlet at 39.52 ppm. ^{19}F-NMR spectra were not calibrated. Coupling constants are reported in Hertz. For ^{1}H-NMR assignments, chemical shifts are reported: shift value (number of protons, description of absorption, coupling constant(s) where applicable). ^{13}C spectra were also obtained using distortionless enhancement by polarization transfer (DEPT). With this technique the signals of CH and CH_3 carbon atoms appear normal (positive mode) and the signals of CH_2 carbon atoms appear negative. Electrospray ionisation mass spectrometry (ESI-MS) was performed in the positive ion mode on a liquid chromatography time-of-flight mass spectrometer (Micromass LCT, Waters Ltd., Manchester, UK). The samples were introduced into the ion source by an LC system (Waters Alliance 2795, Waters Corporation, USA) in acetonitrile: water (60:40 %v/v) at 200 µL/min. The capillary voltage of the mass spectrometer was at 3 kV. The sample cone (de-clustering) voltage was set at 40V. For exact mass determination, the instrument was externally calibrated for the mass range m/z 100 to m/z 1000. A lock (reference) mass (m/z 556.2771) was used. Mass measurement accuracies of < ±5 ppm were obtained. Low resolution mass spectra (LRMS) were acquired on a Hewlett-Packard 5973 MSD GC-MS system in electron impact (EI) mode. Elemental analyses were performed on an Exetor Analytical CE4400 CHN analyser in the microanalysis laboratory, Department of Chemistry, University College Dublin. Thin layer chromatography was performed on silica gel Merck F-254 plates. Flash column chromatography was carried out on Merck Kieselgel 60 (particle size 0.040-0.063mm), Aldrich aluminium oxide, (activated, neutral, Brockmann I, 50 mesh) or Aldrich aluminium oxide, (activated, acidic, Brockmann I, 50 mesh). The HPLC instrument used for (compound) purity testing was a Waters binary pump model number 1525 with 2487 UV detector, inline degasser, and 717 autosampler. The column used for the

HPLC analysis was Hypersil Gold PFP $C_{18,}$ 1.9µm, (150×4.6 mm). Eluent was Acetonitrile: 1% TFA H_2O (70:30) isocratic.

5.2 Synthesis of Chromenes using one-pot *piperidine*-catalyzed *Knoevenagel* condensations

General Procedure

The appropriate benzaldehyde (1 equiv., 10 mmol) was placed in a round bottomed flask. The appropriate alkyl cyanoacetate or malononitrile (10 mmol) and resorcinol (10 mmol) were added. Ethanol (30 mL) was added and reaction mixture was warmed to dissolve all the reactants. After cooling to room temperature, 0.5 mL of piperidine was added dropwise and the reaction was refluxed for 5 h. Afterwards solvent was removed and product was purified by recrystallisation in ethanol. Purity was checked *via* TLC to yield products in yields ranging from 2-98%.

BE1 Synthesis of 2-Amino-7-hydroxy-4-phenyl-4*H*-chromene-3-carboxylic acid ethyl ester

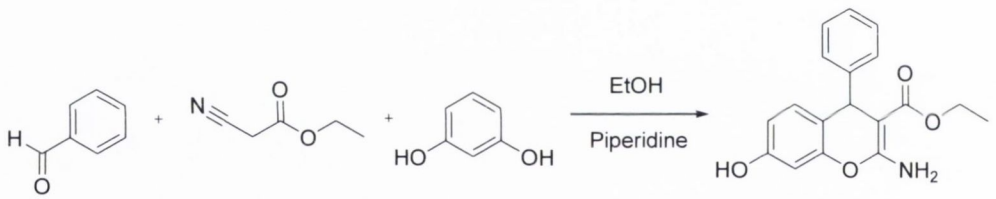

Yield: 1.37 g, 44 %, white powder (Recrystallisation, EtOH) **HPLC Purity:** 93%

MP: 233-235°C **Lit. Ref:** [229] **Lit. MP:** 233-234 °C

IRϑ_{max} (KBr): 3422.60 (OH), 3306.2, 3240.39 (NH_2), 1660.22 (C=O), 1626.11 (C=C), 1605.22 (C=C), 1519.09, 1462.47, 1409.54, 1368.86 cm^{-1}.

^{1}H NMR (400 MHz, DMSO-d6): δ ppm 1.11 (t, 3H, *J*=7.04 Hz, CH_3), 2.05 (s (br), 2H, NH_2), 4.00 (q, 2H, *J*=7.02 Hz, OCH_2), 4.80 (s, 1H, CH), 6.48 - 6.49 (m, 2H, Ar-H), 6.88 (d, 2H, *J*=6.52 Hz, Ar-H), 7.05 (d, 2H, *J*=8.02 Hz, Ar-H), 7.18 - 7.20 (m, 2H, Ar-H) , OH not observed.

^{13}C NMR (100 MHz, DMSO-d6): δ ppm 14.24 (CH_3), 39.90 (CH), 58.52 (CH_2), 76.50 (C), 102.03 (CH), 112.08 (CH), 116.71 (C), 125.69 (CH), 126.95 (CH), 128.11 (CH), 129.80 (CH), 148.64 (C), 149.04 (C-O), 156.71 (C-OH), 161.00 (O-C-N), 168.37 (C=O).

HRMS (ESI): $C_{18}H_{17}NNaO_4$ [M^+ +Na] requires (m/e) 334.1055, found 334.1047 (-2.5ppm)

BE2 Synthesis of ethyl 2-amino-7-hydroxy-4-(4-phenoxyphenyl)-4H-chromene-3-carboxylate

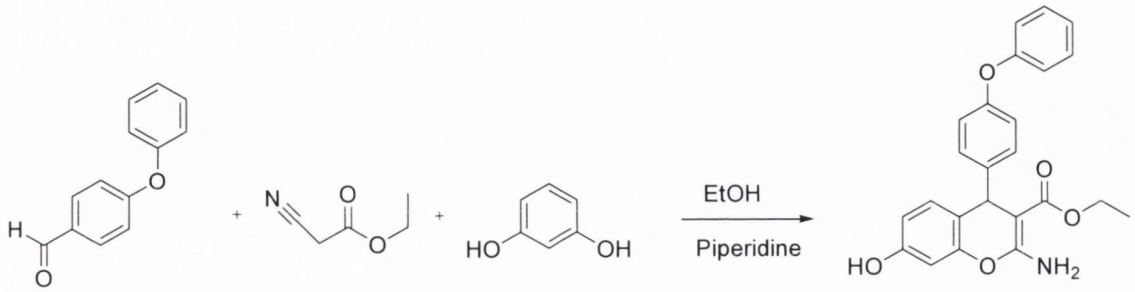

Yield: 1.32 g, 33 %, cream powder (Recrystallisation, EtOH) **HPLC Purity:** 96%

MP: 272-276°C

IRϑ_{max} (KBr): 3480.76 (OH), 3414.57, 3387.63 (NH_2), 1676.55 (C=O), 1649.70 (C=C), 1631.85 (C=C), 1597.34, 1584.52, 1537.47 cm^{-1}

^{1}H NMR (400 MHz, DMSO): δ ppm 1.06 (t, 3H, *J*=7.03 Hz, CH_3), δ 3.98 (q, 2H, *J*=7.02 Hz, OCH_2), δ 4.80 (s, 1H, CH), δ 6.44 (d, 1H, *J*=7.42 Hz, Ar-H), δ 6.51 (m, 1H, Ar-H), δ 6.86 (d, 2H, *J*=8.54 Hz, Ar-H), δ 6.94 (d, 2H, *J*=8.03 Hz, Ar-H), δ 7.01 (d, 1H, *J*=8.54 Hz, Ar-H), δ 7.07 - 7.11 (m, 1H, Ar-H), δ 7.14 (d, 2H, *J*=7.04 Hz, Ar-H), δ 7.32 - 7.36 (m, 2H, Ar-H), δ 7.61 (s (br), 2H, NH_2), δ 9.63 (s (br), 1H, OH)

^{13}C NMR (100 MHz, DMSO): δ ppm 14.72 (CH_3), 39.34 (CH), δ 58.99 (CH_2), δ 76.98 (C), δ 102.50 (CH), δ 112.55 (CH), δ 117.18 (C), δ δ 126.16 (CH), δ 127.41 (CH), δ 128.58 (CH), δ 130.28 (CH), δ 139.50 (C), δ 149.11 (C-O), δ 149.52 (C-OH), δ 157.18 (Bnz-C-O), δ 161.47 (O-C-N), δ 168.81 (C=O)

HRMS (ESI): $C_{24}H_{21}NO_5$ [M^+ Na] requires (m/e) 426.1317, found 426.1326, (2.0ppm)

BE3 Synthesis of Ethyl 2-amino-7-hydroxy-4-(naphthalen-1-yl)-4*H*-chromene-3-carboxylate

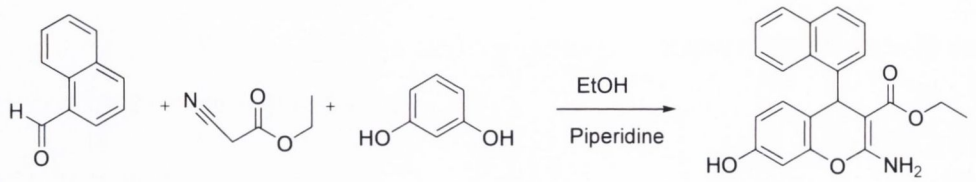

Yield: 1.12 g, 31 %, yellow powder (Recrystallisation, EtOH) **HPLC Purity:** 97%

MP: 266-268°C

IRϑ_{max} (KBr): 3484.58 (OH), 3417.94, 3397.63 (NH_2), 1680.84 (C=O), 1640.83 (C=C), 1632.86 (C=C), 1589.28, 1549.84, 1459.74 cm^{-1}

^{1}H NMR (400 MHz, DMSO): δ ppm 0.63 (t, 3H, *J*=7.04 Hz, CH_3), δ 3.81 (q, 2H, *J*=7.22, OCH_2), δ 4.56 (s, 1H, CH), δ 6.34 (d, 1H, *J*=8.56 Hz, Ar-H), δ 6.46 (d, 1H, *J*=8.04 Hz, Ar-H), δ 7.23 (d, 1H, *J*=7.08 Hz, Ar-H), δ 7.36 (d, 1H, *J*=7.78 Hz, Ar-H), δ 7.48 (d, 1H, *J*=7.52 Hz, Ar-H), δ 7.60 - 7.66 (m, 4H, Ar-H), 7.89 (d, 1H, *J*=8.04 Hz, Ar-H), δ 8.11 (s (br), 1H, OH), NH_2 not observed.

^{13}C NMR (100 MHz, DMSO): δ ppm 13.79 (CH_3), δ 38.86 (CH), δ 58.36 (CH_2), δ 76.97 (C), δ 102.19 (CH), δ 111.97 (CH), δ 116.96 (C), δ 123.73 (CH), δ 125.32 (CH), δ 125.45 (CH), δ 125.81 (CH), δ 128.44 (CH), δ 128.99 (CH), δ 132.36 (C), δ 133.33 (C), δ 148.56 (C-O), δ 156.68 (C-OH), δ 160.90 (O-C-N), δ 168.50 (C=O)

HRMS (ESI): $C_{22}H_{19}NO_4$ [M^+ +Na] requires (m/e) 384.1212, found 384.1222, (2.7ppm)

BE4 2-Amino-4(2,4,5-Trimethoxyphenyl)-7-hydroxy-4*H*-chromene-3-carboxylic acid ethyl ester

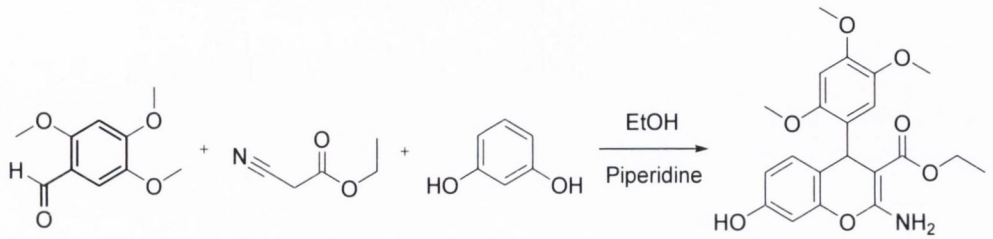

Yield: 1.56 g, 39 %, yellow crystals (Recrystallisation, EtOH) **HPLC Purity:** 88%

MP: 205°C

IRϑ_{max} (KBr): 3405.20 (OH), 3382.51, 3323.74 (NH_2), 1658.84 (C=O), 1617.85 (C=C), 1613.16 (C=C), 1585.73, 1524.51 cm^{-1}

^{1}H NMR (400 MHz, DMSO-d6): δ ppm 1.01 (t, 3H, *J*=7.26 Hz, CH_3), 3.60 (s, 3H, OCH_3), 3.72 (s, 6H, 2xOCH_3), 3.93 (q, 2H, *J*=7.04 Hz, OCH_2), 5.03 (s, 1H, CH), 6.37 (d, 1H, *J*=8.52 Hz, Ar-H), 6.41 (d, 1H, *J*=8.28 Hz, Ar-H), 6.59 (d, 2H, *J*=6.52 Hz, Ar-H), 6.80 - 6.88 (m, 1H, Ar-H), 7.12 (s (br), 1H, OH), NH_2 not observed

^{13}C NMR (100 MHz, DMSO-d6): δ ppm 14.06 (CH_3), 32.96 (CH), 55.70 (CH_3), 56.21 (CH_3), 56.38 (CH_3), 58. 36 (CH_2), 75.30 (C), 99.16 (CH), 101.72 (CH), 111.66 (C), 113.42 (CH), 116.75 (C), 128.48 (CH), 129.24 (CH), 142.32 (C-OCH_3), 147.75 (C-OCH_3), 149.10 (C-OCH_3), 150.59 (C-O), 156.35 (C-OH), 161.41 (O-C-N), 168.58 (C=O)

HRMS (ESI): $C_{21}H_{23}NNaO_7$ [M^+ +Na] requires (m/e) 424.1372, found 424.1360 (-2.9ppm)

BE5 Synthesis of 2-Amino-4(2-methoxyphenyl)-7-hydroxy-4*H*-chromene-3-carboxylic acid ethyl ester

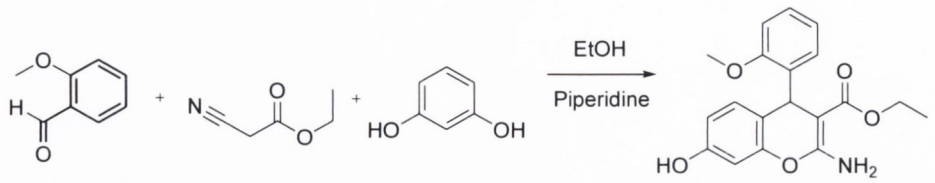

Yield: 0.58 g, 17 %, white powder (Recrystallisation, EtOH) **HPLC Purity:** 86%

MP: 189-194°C **Lit. Ref**: [230]

IRϑ_{max} (KBr): 3401.26 (OH), 3314.38, 3285.26 (NH_2), 1684.32 (C=O), 1660.34 (C=C), 1630.69 (C=C), 1612.36, 1554.49, 1484.96 cm^{-1}

^{1}H NMR (400 MHz, DMSO): δ ppm 1.04 (t, 3H, *J*=7.02 Hz, CH_3), 3.82 (s, 3H, OCH_3), 3.93 (q, 2H, *J*=7.02 Hz, OCH_2), 5.26 (s, 1H, CH), 6.42 (d, 2H, *J*=7.26 Hz, Ar-H), 6.79 (d, 1H, *J*=7.28 Hz, Ar-H), 6.87 (d, 1H, *J*=8.42 Hz, Ar-H), 7.00 (d, 1H, *J*=8.2 Hz, Ar-H), 7.06 - 7.14 (m, 2H, Ar-H), 7.21 (s (br), 1H, OH), 7.64 (s (br), 2H, NH_2)

^{13}C NMR (100 MHz, DMSO): δ ppm 14.39 (CH_3), 33.95 (CH), 40.09 (CH_3), 58.66 (CH_2), 78.00 (C), 101.73 (CH), 112.09 (CH), 116.95 (C), 122.58 (CH), 123.46 (C), 127.69 (CH), 129.73 (CH), 144.35 (C-O), 153.49 (C-OH), 157.03 (C-OCH_3), 161.21 (O-C-N), 168.11 (C=O)

HRMS (ESI): $C_{19}H_{20}NO_5$ [M^+ +H] requires (m/e) 342.1341, found 342.1351 (2.8 ppm)

BE6 Synthesis of 2-Amino-4-(4-methoxyphenyl)-7-hydroxy-4*H*-chromene-3-carboxylic acid ethyl ester

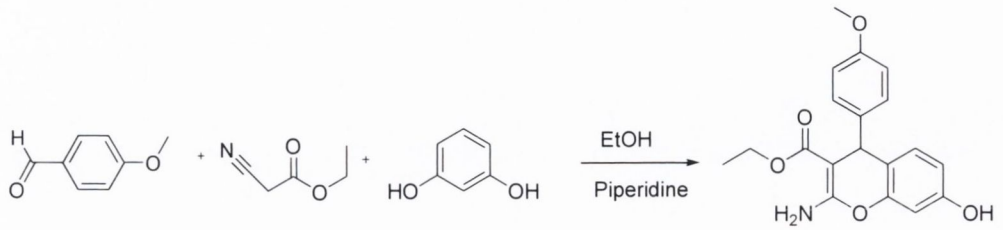

Yield: 2.11 g, 62 %, brown crystals (Recrystallisation, EtOH) **HPLC Purity:** 96%

MP: 176-178°C **Lit. Ref.**[231]**Lit. MP:** 178 °C

IRϑ_{max} (KBr): 3544.15 (OH), 3417.33, 3376.26 (NH_2), 1660.08 (C=O), 1632.51 (C=C), 1611.50 (C=C), 1597.65, 1534.73, 1482.95 cm^{-1}

^{1}H NMR (400 MHz, DMSO): δ ppm 1.07 (t, 3H, *J*=7.42 Hz, CH_3), δ 3.69 (s, 3H, OCH_3), δ 3.94 (q, 2H, *J*=6.76 Hz, OCH_2), δ 4.73 (s, 1H, CH), δ 6.42 - 6.48 (m, 2H, Ar-H), δ 6.77 (d, 2H, *J*=8.52 Hz, Ar-H), δ 6.95 (d, 1H, *J*=8.52 Hz, Ar-H), δ 7.02 (d, 2H, *J*=7 Hz, Ar-H), 7.21 (s (br), 1H, OH), NH_2 not observed

^{13}C NMR (100 MHz, DMSO): δ ppm 14.31 (CH_3), δ 39.27 (CH), δ 54.91 (OCH_3), δ 58.52 (CH_2), δ 76.81 (C), δ 101.98 (CH), δ 112.06 (CH), δ 113.45 (CH), δ 117.08 (C), δ 127.86 (CH), δ 129.76 (CH), δ 140.85 (C), δ 149.03 (C-O), δ 156.63 (C-OH), δ 157.26 (OCH_3), δ 160.91 (O-C-N), δ 168.41 (C=O)

HRMS (ESI): $C_{19}H_{19}NO_5$ [M^+ +H] requires (m/e) 342.1341, found 342.1352, (+3.4 ppm)

BE7 Synthesis of 2-Amino-4-(2,5-dimethylphenyl)-4-methoxyphenyl)-7-hydroxy-4*H*-chromene-3-carboxylic acid ethyl ester

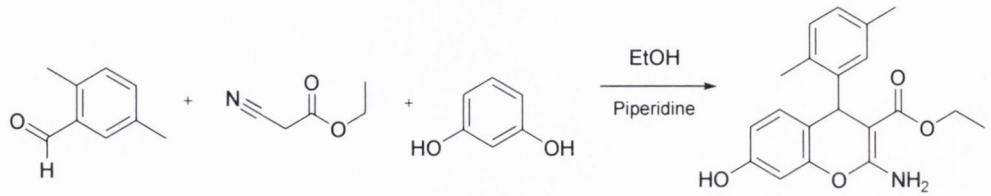

Yield: 1.01 g, 32 %, white powder (Recrystallisation, EtOH) **HPLC Purity:** 93%

MP: 214-215°C

IRϑ_{max} (KBr): 3526.66 (OH), 3442.08, 3276.92 (NH_2), 1667.44 (C=O), 1632.09 (C=C), 1614.37 (C=C), 1611.36, 1582.17, 1539.21 cm^{-1}

^{1}H NMR (400 MHz, DMSO-d6): δ ppm 1.11 (t, 3H, *J*=7.04 Hz, CH_3), δ 2.15 (s, 3H, CH_3), 2.76 (s, 3H, CH_3), 3.95 (q, 2H, *J*=7.02 Hz, OCH_2), δ 5.10 (s, 1H, CH), δ 6.45 (d, 2H, *J*=8 Hz, Ar-H, δ 6.68 - 6.94 (m, 3H, Ar-H), δ 7.85 (d, 1H, *J*=7.53 Hz, Ar-H), δ 8.06 (s (br), 1H OH), NH_2 not observed.

^{13}C NMR (100 MHz, DMSO-d6): δ ppm 14.12 (CH_3), δ 18.93 (CH_3), δ 20.79 (CH_3), δ 34.57 (CH), δ 58.59 (CH_2), δ 76.60 (C), δ 102.06 (CH), δ 112.12 (CH), δ 116.83 (C), δ 126.20 (CH), δ 128.57 (CH), δ 129.40 (CH), δ 129.92 (CH), δ 130.66 (C), δ 134.65 (C), δ 148.65 (C-O), δ 156.57 (C-OH), δ 160.80 (O-C-N), 168.51 (C=O)

HRMS (ESI): $C_{20}H_{21}NO_4$ [M^+ +Na] requires (m/e) 340.1549, found 340.1559 (3.0 ppm)

BE8 Synthesis of 2-Amino-4-*p*-tolyl-7-hydroxy-4*H*-chromene-3-carboxylic acid ethyl ester

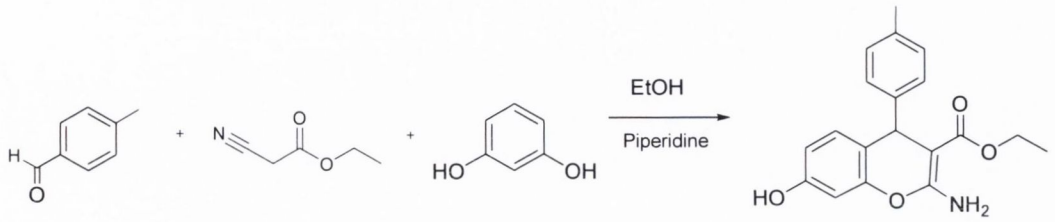

Yield: 0.94 g, 29 %, white powder (Recrystallisation, EtOH) **HPLC Purity:** 89%

MP: 218-223°C

IRϑ_{max} (KBr): 3487.12 (OH), 3419.84, 3406.54 (NH_2), 1660.82 (C=O), 1641.36, 1629.57 (C=C), 1577.31, 1545.84, 1494.72 cm^{-1}

^{1}H NMR (400 MHz, DMSO-d6): δ ppm 1.06 (t, 3H, *J*=7.28 Hz, CH_3), δ 2.19 (s, 3H, CH_3), δ 3.95 (q, 2H, *J*=7.22 Hz, OCH_2), δ 4.74 (s, 1H, CH), δ 5.21 (s (br), 1H, OH), δ 6.42 - 6.51 (m, 2H, Ar-H), δ 6.93 (d, 1H, *J*=8.04 Hz, Ar-H), δ 7.01 (d, 4H, *J*=9.04 Hz, Ar-H), NH_2 not observed.

^{13}C NMR (100 MHz, DMSO-d6): δ ppm 14.28 (CH_3), δ 20.53 (CH_3), δ 38.56 (CH), δ 58.53 (CH_2), δ 76.62 (C), δ 101.99 (CH), δ 112.03 (CH), δ 116.95 (C), δ 126.82 (CH), δ 128.66 (CH), δ 129.76 (CH), δ 134.58 (C-CH_3), δ 145.70 (C), δ 149.03 (C-O), δ 156.63 (C-OH), δ 160.95 (O-C-N), δ 168.38 (C=O)

HRMS (ESI): $C_{19}H_{19}NO_4$ M^+ +H requires (m/e) 326.1392, found 326.1388, (-1.3 ppm)

BE9 Synthesis of 2-Amino-4-(4-Butoxyphenyl)-7-hydroxy-4*H*-chromene-3-carboxylic acid ethyl ester

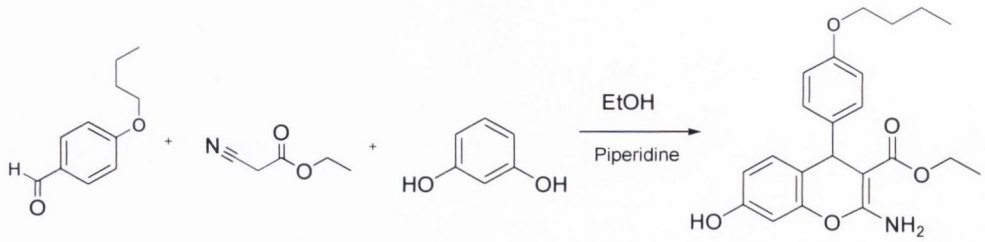

Yield: 1.53 g, 44 %, brown crystals (Recrystallisation, EtOH) **HPLC Purity:** 78%

MP: 237-241°C

IRϑ_{max} (KBr): 3488.26 (OH), 3417.01, 3328.56 (NH_2), 1684.24 (C=O), 1663,75 (C=C), 1636.23 (C=C), 1567.24, 1530.21, 1485.70 cm^{-1}

^{1}H NMR (400 MHz, DMSO-d6): δ ppm 0.91 (t, 3H, *J*=7.52 Hz, CH_3), δ 1.07 (t, 3H, *J*=7.02 Hz, CH_3), δ 1.38 - 1.45 (m, 2H, CH_2), δ 1.81 (m, 2H, CH_2), δ 2.83 (s (br), 2H, NH_2) δ 3.84 (q, 2H, *J*=6.28 Hz, OCH_2), 4.17 - 4.19 (m, 2H, OCH_2), δ 4.72 (s, 1H, CH), δ 6.42 - 6.51 (m, 2H, Ar-H), δ 6.74 (d, 2H, *J*=8.56 Hz, Ar-H), δ 6.93 (d, 1H, *J*=8.52 Hz, Ar-H), δ 7.00 (d, 2H, *J*=8.56 Hz, Ar-H), δ 7.21 (s (br), 1H, OH)

^{13}C NMR (100 MHz, DMSO-d6): δ ppm 13.67 (CH_3), δ 14.30 (CH_3), δ 18.74 (CH_2), δ 30.78 (CH_2), δ 38.78 (CH), δ 58.51 (CH_2), δ 66.91 (CH_2), δ 76.81 (C), δ 101.97 (CH), δ 112.04 (CH), δ 113.94 (C), δ 116.12 (CH), δ 127.83 (CH), δ 129.74 (CH), δ 139.02 (C), δ 156.59 (C-O), δ 156.71 (C-OH), δ 160.91 (O-C-N), δ 168.40 (C=O)

HRMS (ESI): $C_{22}H_{25}NO_5$ [M^+ +H] requires (m/e) 348.1811, found 349.1806, (-1.3 ppm)

BE10 Ethyl 2-amino-7-hydroxy-4-(3,4-dimethoxyphenyl)-4*H*- chromene-3-carboxylate

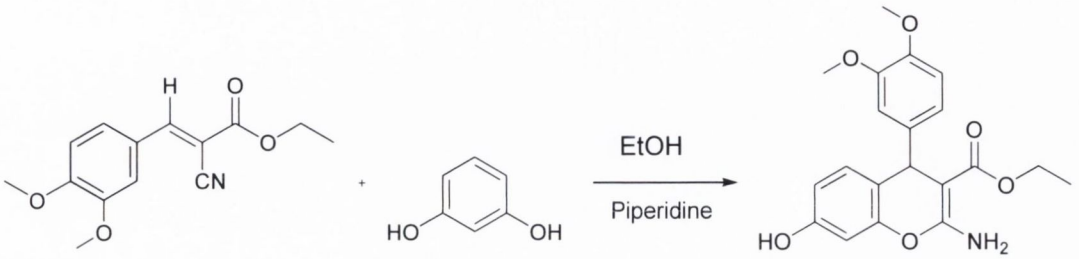

Yield: 0.07 g, 2 %, yellow crystals (Recrystallisation, EtOH) **HPLC Purity:** 96%

MP: 284-288°C

IRϑ_{max} (KBr): 3488.34 (OH), 3431.11, 3412.48 (NH_2), 1681.40 (C=C), 1642.76 (C=C), 1629.45 (C=O), 1562.75 cm^{-1}

^{1}H NMR (400 MHz, DMSO): δ ppm 1.09 (t, 3H, *J*=7.04 Hz, CH_3), δ 3.66 (s, 3H, OCH_3), δ3.71 (s, 3H, OCH_3), δ 3.95 (q, 2H, *J*=7.04 Hz, OCH_2), δ 4.73 (s, 1H, CH), δ 6.42 (s, 1H, Ar-H), δ 6.46 (dd, 1H, *J*=2.48, *J*=7.02 Hz, Ar-H), δ 6.55 (d, 1H, *J*=9.04 Hz, Ar-H), δ 6.77 (d, 2H, *J*=9.04 Hz, Ar-H), δ 6.99 (d, 1H, *J*=8.52 Hz, Ar-H), δ 7.55 (s (br), 2H, NH_2), δ 9.57 (s (br), 1H, OH)

^{13}C NMR (100 MHz, DMSO): δ ppm 14.36 (CH_3), δ 38.45 (CH), δ 55.40 (CH_3), δ 58.53 (CH_2), δ 76.72 (C), δ 101.97 (CH), δ 110.23 (CH), δ 111.15 (CH), δ 111.86 (C), δ 117.04 (CH), δ 118.64 (CH), δ 129.73 (CH), δ 141.44 (C), δ 146.83 (OCH_3), δ 148.19 (OCH_3), δ 149.03 (C-O), δ 156.60 (C-O), δ 160.97 (O-C-N), δ 168.43 (C=O)

HRMS (ESI): $C_{20}H_{21}NNaO_6$ [M^+ +Na] requires (m/e) 394.1267, found 394.1262, (-1.2ppm)

BE11 Synthesis of 2-Amino-4-(4-ethoxyphenyl)-7-hydroxy-4*H*-chromene-3-carboxylic acid ethyl ester

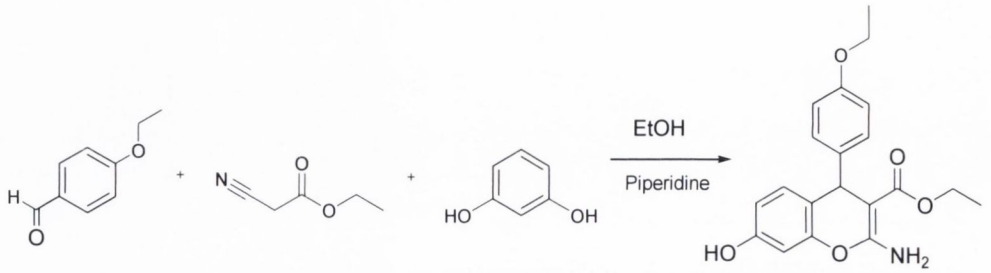

Yield: 0.78 g, 22 %, yellow crystals(Recrystallisation, EtOH) **HPLC Purity:** 94%

MP: 258-263°C

IRϑ_{max} (KBr): 3563.54 (OH), 3431.59, 3419.15 (NH_2), 1660.91 (C=O), 1634.86 (C=C), 1613.89 (C=C), 1583.43, 1568,42, 1458.83 cm^{-1}

^{1}H NMR (400 MHz, DMSO-d6): δ ppm 1.05 (t, 3H, *J*=7.04 Hz, CH_3), δ 1.25 (t, 3H, *J*=7.02 Hz, CH_3), δ 3.93 - 4.18 (m, 4H, 2xOCH_2), δ 4.72 (s, 1H, CH), δ 6.42 - 6.50 (m, 2H, Ar-H), δ 6.73 (d, 2H, *J*=9.04 Hz, Ar-H), δ 6.94 (d, 2H, *J*=8.04 Hz, Ar-H), δ 7.01 (d, 1H, *J*=8.12 Hz, Ar-H), OH not observed, NH_2 not observed.

^{13}C NMR (100 MHz, DMSO-d6): δ ppm 14.31 (CH_3), δ 14.68 (CH_3) δ 38.09 (CH), δ 58.51 (CH_2), δ 62.79 (CH_2), δ 76.81 (C), δ 101.97 (CH), δ 112.04 (CH), δ 113.91 (CH), δ 117.13 (C), δ 127.84 (CH), δ 129.76 (CH), δ 140.71 (C), δ 149.02 (C-OEt), δ 156.53 (C-OH), δ 160.91 (O-C-N), δ 168.40 (C=O)

HRMS (ESI): $C_{20}H_{21}NO_5$ [M^+ +H] requires (m/e) 356.1498, found 356.1488, (-2.8 ppm)

BE12 Synthesis of 2-Amino-4-(3-methoxyphenyl)-7-hydroxy-4*H*-chromene-3-carboxylic acid ethyl ester

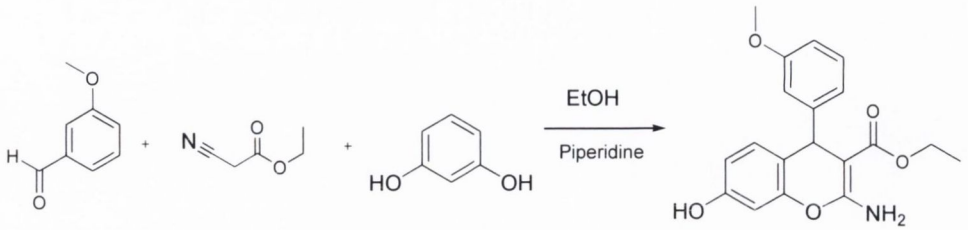

Yield: 2.73 g, 80 %, brown crystals(Recrystallisation, EtOH) **HPLC Purity:** 76%

MP: 272-278°C

IRϑ_{max} (KBr): 3508.26 (OH), 3417.01, 3368.38 (NH_2), 1675.68 (C=O), 1630.17 (C=C), 1628.43 (C=C), 1587.21, 1510.87 cm^{-1}

^{1}H NMR (400 MHz, DMSO-d6): δ ppm 1.19 (t, 3H, *J*=7.28 Hz, CH_3), δ 3.76 (s, 3H, OCH_3), δ 4.06 (q, 2H, *J*=7.04 Hz, OCH_2), δ 4.85 (s, 1H, CH), δ 6.52 (d, 2H, *J*=7.52 Hz, Ar-H), δ 6.77 (d, 3H, *J*=8.54 Hz, Ar-H), δ 6.92 (d, 1H, *J*=8.04 Hz, Ar-H), δ 7.13 (s, 1H, Ar-H), 7.87 (s (br), 1H, OH), NH_2 not observed.

^{13}C NMR (100 MHz, DMSO-d6): δ ppm 13.88 (CH_3) δ 39.30 (CH), δ 54.65 (CH_3), δ 59.06 (CH_2), δ 78.40 (C), δ 102.43 (CH), δ 110.32 (CH), δ 111.86 (C), δ 113.22 (CH), δ 117.51 (CH), δ 119.61 (CH), δ 128.63 (CH), δ 129.56 (CH), δ 143.82 (C), δ 151.82 (C-O), δ 154.93 (C-OH), δ 158.91 (O-C-N), δ 159.89 (C-OCH_3), δ 169.16 (C=O)

HRMS (ESI): $C_{19}H_{20}NO_5$ [M^+ +H] requires (m/e) 342.1341, found 342.1331, (-3.1 ppm)

BE13 Synthesis of 2-Amino-4(thophen-2-yl)-7-hydroxy-4H-chromene-3-carboxylic acid ethyl ester

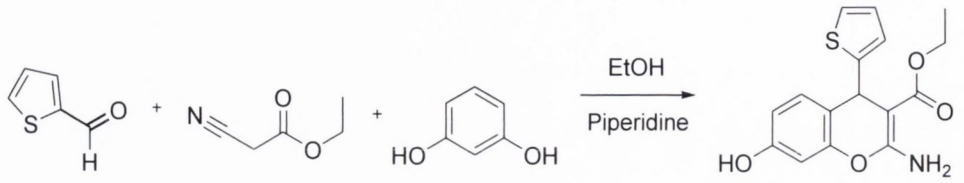

Yield: 1.20 g, 38 %, yellow powder (Recrystallisation, EtOH) **HPLC Purity:** 89%

MP: 215-218°C

IRϑ_{max} (KBr): 3409.98 (OH), 3301.85, 3249.73 (NH_2), 1657.00 (C=O), 1632.96 (C=C), 1618.91 (C=C), 1595.63, 1546.78 cm^{-1}

^{1}H NMR (400 MHz, DMSO-d6): δ ppm 1.13 (t, 3H, *J*=7.02 Hz, CH_3), 4.17 (q, 2H, *J*=7.12 Hz, OCH_2), δ 5.12 (s, 1H, CH), 6.43 (d, 1H, *J*=6.52 Hz, Ar-H), 6.55 – 6.59 (m, 1H, Ar-H), 6.72 (d, 1H, *J*=6.52 Hz, Ar-H), 6.81 (d, 1H, *J*=7.4 Hz, Ar-H), 7.13 (d, 1H, *J*=8.52 Hz, Ar-H), 7.18 (d, 1H, *J*=6.54 Hz, Ar-H), 7.24 (s (br), 1H OH), NH_2 not observed.

^{13}C NMR (100 MHz, DMSO-d6): δ ppm 14.23 (CH_3), δ 34.23 (CH), δ 58.73 (CH_2), δ 76.91 (C), δ 102.07 (CH), δ 113.13 (C), δ 115.29 (CH), δ 122.84 (CH), δ 124.62 (CH), δ 126.58 (CH), δ 129.64 (CH), δ 149.27 (C), δ 153.54 (C-O), δ 158.04 (C-OH), δ 163.56 (O-C-N), δ 169.76 (C=O)

HRMS (ESI): $C_{16}H_{16}NO_4S$ [M^+ +H] requires (m/e) 318.0800, found 318.0807 (+2.2 ppm)

BE14 Synthesis of 2-Amino-4-(4-Chlorophenyl)-7-hydroxy-4*H*-chromene-3-carboxylic acid ethyl ester

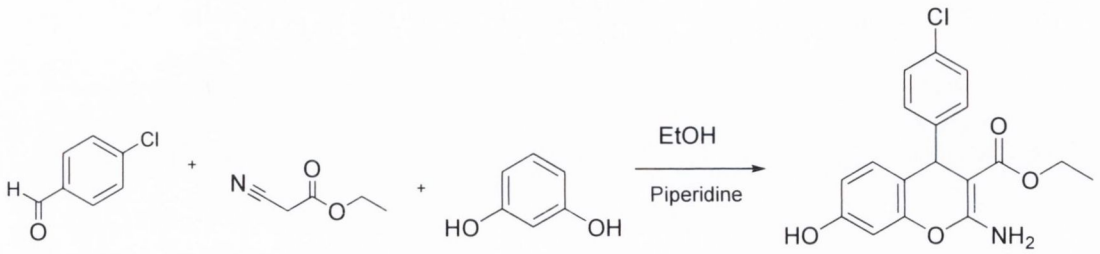

Yield: 1.55 g, 45 %, white powder (Recrystallisation, EtOH) **HPLC Purity:** 86%

MP: 231-236°C **Lit.Ref**.[232]

IRϑ_{max} (KBr): 3572.72 (OH), 3416.43, 3317.84 (NH_2), 1689.64 (C=O), 1659.58 (C=C), 1620.64 (C=C), 1582.94, 1567.62 cm^{-1}

^{1}H NMR (400 MHz, DMSO-d6): δ ppm 1.04 (t, 3H, *J*=7.04 Hz, CH_3), δ 3.95 (q, 2H, *J*=6.8 Hz, OCH_2), δ 4.80 (s, 1H, CH), δ 6.44 - 6.50 (m, 2H, Ar-H), δ 6.95 (d, 1H, *J*=8.56 Hz, Ar-H), δ 7.14 (d, 2H, *J*=7.24 Hz, Ar-H), δ 7.26 (d, 2H, *J*=8.52 Hz, Ar-H), 8.04 (s (br), 2H, NH_2), OH not observed

^{13}C NMR (100 MHz, DMSO-d6): δ ppm 14.27 (CH_3), δ 38.37 (CH), δ 58.58 (CH_2), δ 76.07 (C), δ 102.08 (CH), δ 112.20 (CH), δ 116.06 (C), δ 128.07 (CH), δ 128.82 (CH), δ 129.85 (CH), δ 130.19 (C), δ 147.67 (C), δ 148.95 (C-O), δ 156.87 (C-OH), δ 160.95 (O-C-N), δ 168.19 (C=O)

HRMS (ESI): $C_{18}H_{16}{}^{35}ClNO_4$ [M^+ +H] requires (m/e) 346.0846, found 346.0850, (+1.1 ppm)

BE15 Synthesis of 2-Amino-4-(4-fluorophenyl)-7-hydroxy-4*H*-chromene-3-carboxylic acid ethyl ester

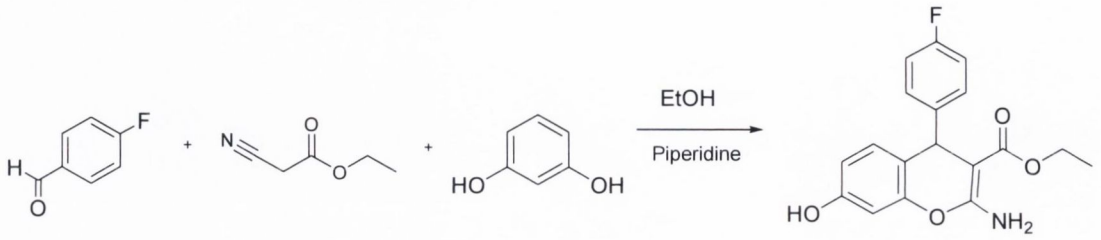

Yield: 1.08 g, 33 %, yellow powder(Recrystallisation, EtOH) **HPLC Purity:** 89%

MP: 280-286°C **Lit.Ref:** [233]

IRϑ_{max} (KBr): 3497.86 (OH), 3416.06, 3394.75 (NH_2), 1698.54 (C=O), 1660.12 (C=C), 1597.88 (C=C), 1561.47, 1526.31 cm^{-1}

^{1}H NMR (400 MHz, DMSO-d6): δ ppm 1.04 (t, 3H, *J*=7.02 Hz, CH_3), 4.01 (q, 2H, *J*=7.48, OCH_2), 4.81 (s, 1H, CH), 6.41 - 6.50 (m, 2H, Ar-H), 6.95 (d, 1H, *J*=8.56 Hz, Ar-H), 7.00 (d, 2H, *J*=8.78 Hz, Ar-H), 7.14 - 7.21 (m, 2H, Ar-H), OH not observed, NH_2 not observed.

^{13}C NMR (100 MHz, DMSO-d6): δ ppm 14.26 (CH_3), δ 38.21 (CH), δ 58.54 (CH_2), δ 76.40 (C), δ 102.05 (CH), δ 112.17 (CH), δ 114.64 (CH), δ 116.44 (C), δ 128.63 (CH), δ 129.84 (CH), δ 144.85 (C), δ 148.96 (C-O), δ 156.78 (C-OH), δ 160.11 (C-F), δ 160.93 (O-C-N), δ 168.25 (C=O)

HRMS (ESI): $C_{18}H_{16}FNO_4$ M^+ +H requires (m/e) 330.1142, found 330.1157, (+4.7 ppm)

BE16 Synthesis of 2-Amino-4-(thiophen-3-yl)-7-hydroxy-4*H*-chromene-3-carboxylic acid ethyl ester

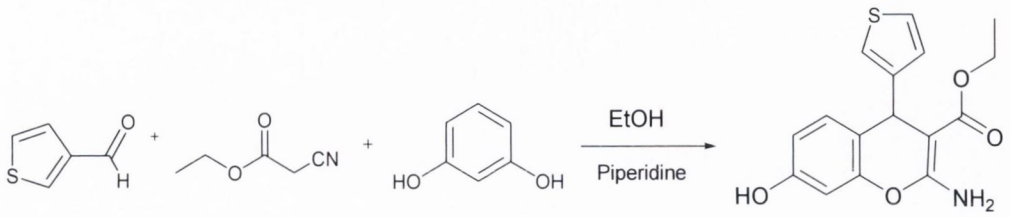

Yield: 0.85 g, 27 %, yellow crystals(Recrystallisation, EtOH) **HPLC Purity:** 79%

MP: 278 - 282°C

IRϑ_{max} (KBr): 3593.28 (OH), 3417.01 (NH_2), 3347.98 (NH_2), 1661.46 (C=O), 1629.40 (C=C), 1618.47 (C=C), 1573.37, 1521.84 cm^{-1}

^{1}H NMR (400 MHz, DMSO-d6): δ ppm 1.11 (t, 3H, *J*=7.02 Hz, CH_3), δ 4.02 (q, 2H, *J*=7.02 Hz, OCH_2) δ 4.91 (s, 1H, CH), δ 6.43 (d, 1H, *J*=7 Hz, Ar-H), δ 6.50 (d, 1H, *J*=8.52 Hz, Ar-H), δ 6.80 (d, 1H, *J*=7.02 Hz, Ar-H), δ 6.96 (d, 1H, *J*=6.88 Hz, Ar-H), δ 7.06 (d, 1H, *J*=8 Hz, Ar-H), δ 7.30 (d, 1H, *J*=7.12 Hz, Ar-H), 7.41 (s (br), 1H, OH), 7.89 (s (br), 2H, NH_2)

^{13}C NMR (100 MHz, DMSO-d6): δ ppm 14.40 (CH_3), δ 34.09 (CH), δ 58.54 (CH_2), δ 76.42 (C), δ 102.11 (CH), δ 111.99 (CH), δ 116.48 (C), δ 119.33 (CH), δ 125.85 (CH), δ 126.93 (CH), δ 129.63 (CH), δ 148.99 (C), δ 149.40 (C-O), δ 156.77 (C-OH), δ 161.18 (O-C-N), δ 168.29 (C=O)

HRMS (ESI): $C_{16}H_{15}NO_4S$ [M^+ +H] requires (m/e) 318.0800, found 318.0797 (-1.0 ppm)

BE17 Synthesis of 2-Amino-4-(5-methylthiophen-2-yl)-7-hydroxy-4*H*-chromene-3-carboxylic acid ethyl ester

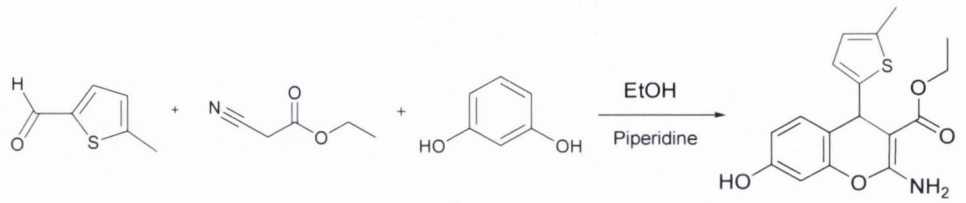

Yield: 0.33 g, 10 %, yellow powder(Recrystallisation, EtOH) **HPLC Purity:** 98%

MP: 189-194°C

IRϑ_{max} (KBr): 3634.56 (OH), 3414.36, 3285.28 (NH_2), 1660.89 (C=O), 1635.79 (C=C), 1617.45 (C=C), 1583.63, 1556.31 cm^{-1}

^{1}H NMR (400 MHz, MeOD): δ ppm 1.23 (t, 3H, *J*=7.14 Hz, CH_3), 2.33 (s, 3H, CH_3), 4.13 (q, 2H, *J*=6.98, OCH_2), 5.06 (s, 1H, CH), 6.45 - 6.52 (m, 3H, Ar-H), 6.54 - 6.60 (m, 1H, Ar-H), 7.05 (d, 1H, *J*=8.52 Hz, Ar-H), OH not observed, NH_2 not observed.

^{13}C NMR (100 MHz, MeOD): δ ppm 13.04 (CH_3), 13.85 (CH_3), 34.70 (CH), 58.25 (CH_2), 77.57 (C), 102.07 (CH), 111.64 (CH), 116.88 (C), 121.93 (CH), 123.79 (CH), 129.42 (CH), 135.83 (C-CH_3), 137.13 (C), 149.66 (C-O), 150.95 (C-OH), 156.89 (O-C-N), 169.57 (C=O)

HRMS (ESI): $C_{17}H_{17}NO_4S$ [M^+ +H] requires (m/e) 332.0957, found 332.0966, (+2.8 ppm)

BE18 Synthesis of 2-Amino-4-(2,6-dichlorophenyl)-7-hydroxy-4*H*-chromene-3-carboxylic acid ethyl ester

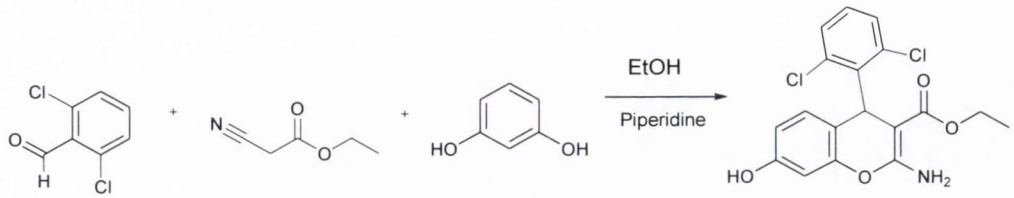

Yield: 1.92 g, 51 %, brown powder(Recrystallisation, EtOH) **HPLC Purity:** 100%

MP: 203-205°C

IRϑ_{max} (KBr): 3510.60 (OH), 3424.55, 3382.62 (NH_2), 1673.71 (C=O), 1632.86 (C=C), 1616.38 (C=C), 1587.54, 1535.85 cm^{-1}

^{1}H NMR (400 MHz, DMSO): δ ppm 0.94 (t, 3H, *J*=7.14 Hz, CH_3), 3.86 (q, 2H, *J*=7.04 Hz, OCH_2), 5.77 (s, 1H, CH), 6.38 (d, 1H, *J*=7.04 Hz, Ar-H), 6.45 (d, 1H, *J*=8.12 Hz, Ar-H), 7.14 - 7.21 (m, 3H, Ar-H), 7.39 - 7.46 (m, 1H, Ar-H), OH not observed, NH_2 not observed.

^{13}C NMR (100 MHz, DMSO): δ ppm 14.33 (CH_3), 19.03 (CH), 58.85 (CH_2), 73.01 (C), 102.12 (CH), 106.63 (CH), 112.53 (C), 128.55 (CH), 128.77 (CH), 129.23 (CH), 130.70 (CH), 134.83 (C-Cl), 135.72 (C), 141.49 (C), 149.77 (C-O), 157.73 (C-OH), 161.88 (O-C-N), 168.72 (C=O)

HRMS (ESI): $C_{18}H_{15}{}^{35}Cl_2NO_4$ [M^+ +H] requires (m/e) 378.0300, found 378.0296, (-1.0 ppm)

BE19 Synthesis of 2-Amino-4-(4-Bromophenyl)-7-hydroxy-4*H*-chromene-3-carboxylic acid ethyl ester

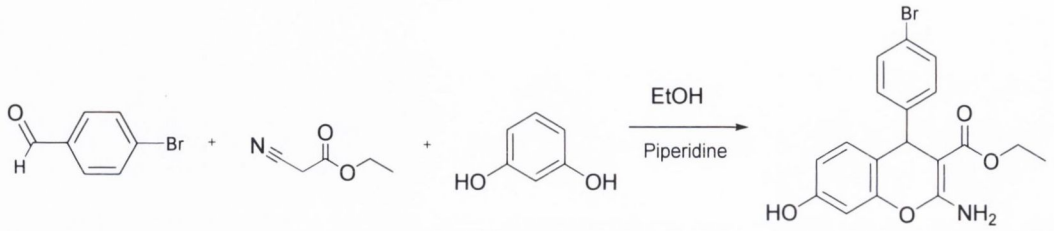

Yield: 1.63 g, 42 %, yellow powder(Recrystallisation, EtOH) **HPLC Purity:** 83%

MP: 243-248°C

IRϑ_{max} (KBr): 3532.42 (OH), 3415.61, 3327.74 (NH_2), 1660.03 (C=O), 1629.77 (C=C), 1611.29 (C=C), 1579.75, 1541.59 cm^{-1}

^{1}H NMR (400 MHz, DMSO-d6): δ ppm 1.05 (t, 3H, *J*=7 Hz, CH_3), 3.91 (q, 2H, *J*=7.02 Hz, OCH_2), δ 4.79 (s, 1H, CH), δ 6.43 - 6.59 (m, 2H, Ar-H), δ 6.95 (d, 1H, *J*=8.04 Hz, Ar-H), δ 7.09 (d, 2H, *J*=8.52 Hz, Ar-H), δ 7.39 (d, 2H, *J*=8.56 Hz, Ar-H), 7.87 (s (br), 1H, OH), 8.04 (s (br), 2H, NH_2)

^{13}C NMR (100 MHz, DMSO-d6): δ ppm 14.27 (CH_3), δ 38.45 (CH), δ 58.60 (CH_2), δ 76.00 (C), δ 102.08 (CH), δ 112.20 (CH), δ 115.99 (C), δ 118.66 (C-Br), δ 129.24 (CH), δ 129.85 (CH), δ 130.98 (CH), δ 148.08 (C), δ 148.94 (C-O), δ 156.88 (C-OH), δ 160.95 (O-C-N), δ 168.18 (C=O)

HRMS (ESI): $C_{18}H_{15}{}^{79}BrNO_4$ [M^- -H] requires (m/e) 388.0184, found 388.0177, (-1.9 ppm)

BE20 Ethyl 2-amino-4-(2,4-dichlorophenyl)-7-hydroxy-4*H*-chromene-3-carboxylate

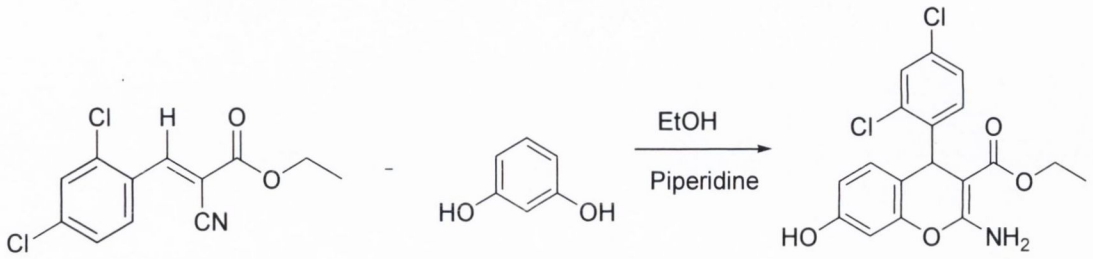

Yield: 3.32 g, 88 %, white powder (Recrystallisation, EtOH) **HPLC Purity:** 93%

MP: 198 -202°C **Lit. Ref.**: [234] **Lit. MP:** 201 - 202 °C

IRϑ_{max} (KBr): 3583.69 (OH), 3475,26, 3417.48 (NH_2), 1691.37 (C=C), 1645.68 (C=C), 1586.26 (C=O), 1575.48, 1437.28, 1449.57 cm^{-1}

^{1}H NMR (400 MHz, DMSO-d6): δ ppm 1.13 (t, 3H, *J*=7.42 Hz, CH_3), 4.04 (q, 2H, *J*=6.98 Hz, OCH_2), 4.68 (s, 1H, CH), 5.29 (s (br), 1H, OH), 6.36 (s, 1H, Ar-H), 6.41 – 6.49 (m, 1H, Ar-H), 6.81 – 6.89 (m, 1H, Ar-H), 6.95 (s, 1H, Ar-H), 7.09 – 7.13 (m, 1H, Ar-H), 7.17 (m, 2H, Ar-H), NH_2 not observed.

^{13}C NMR (100 MHz, DMSO-d6): δ ppm 11.62 (CH_3), 30.34 (CH), 60.97 (CH_2), 79.57 (C), 106.28 (CH), 115.43 (CH), 117.16 (C), 127.37 (CH), 130.08 (CH), 130.81 (CH), 133.25 (C-Cl), 136.96 (C-Cl), 147.37 (C), 152.46 (C-O), 156.37 (C-OH), 161.36 (O-C-N), 169.41 (C=O)

HRMS (ESI): $C_{18}H_{15}{}^{37}Cl_2NO_4$ [M^- -H] requires (m/e) 379.0378, found 379.0374, (+1 ppm)

BE21 Synthesis of 2-Amino-4-(3-bromo-4-methoxyphenyl)-7-hydroxy-4*H*-chromene-3-carboxylic acid ethyl ester

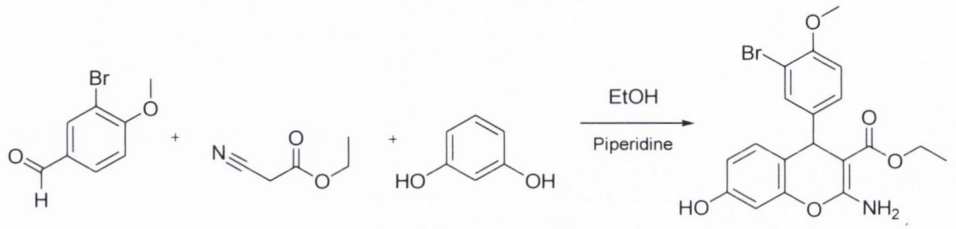

Yield: 1.26 g, 30 %, yellow powder (Recrystallisation, EtOH) **HPLC Purity:** 80%

MP: 194-198°C

IRϑ_{max} (KBr): 3602.38 (OH), 3416.08, 3317.34 (NH_2), 1658.41 (C=O), 1632.98 (C=C), 1605.27 (C=C), 1558.37, 1523.27 cm^{-1}

^{1}H NMR (400 MHz, DMSO-d6): δ ppm 1.08 (t, 3H, *J*=7.02 Hz, CH_3), δ 3.73 (s, 3H, OCH_3), δ 3.92 - 3.96 (q, 2H, *J*=7.12 Hz, OCH_2), δ 4.73 (s, 1H, CH), δ 6.41 (s, 1H, Ar-H), δ 6.95 (d, 2H, *J*=8.02 Hz, Ar-H), δ 7.05 – 7.10 (m, 1H, Ar-H), δ 7.26 (d, 1H, *J*=7.24 Hz, Ar-H), δ 7.59 (s, 1H, Ar-H), δ 8.12 (s (br), 1H, OH), NH_2 not observed.

^{13}C NMR (100 MHz, DMSO-d6): δ ppm 14.76 (CH_3), δ 38.25 (CH), δ 56.55 (OCH_3), δ 59.08 (CH_2), δ 76.80 (C), δ 102.50 (CH), δ 110.42 (CH), δ 112.70 (C-Br), δ 116.76 (CH), δ 127.83 (CH), δ 130.36 (CH), δ 131.70 (CH), δ 143.00 (C), δ 149.45 (C-O), δ 153.84 (C-OCH_3), δ 157.30 (C-OH), δ 161.34 (O-C-N), δ 168.68 (C=O)

HRMS (ESI): C19H18^{79}BrNO5 [M^+ +H] requires (m/e) 420.0447, found 420.0447 (0.1 ppm)

BE22 Synthesis of 2-Amino-4-(3-fluoro-4-methoxyphenyl)-7-hydroxy-4*H*-chromene-3-carboxylic acid ethyl ester

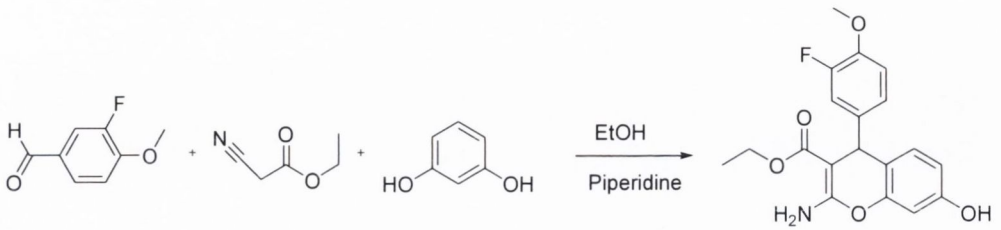

Yield: 1.51 g, 42 %, yellow crystals (Recrystallisation, EtOH) **HPLC Purity:** 97%

MP: 211-215°C

IRϑ_{max} (KBr): 3534.62 (OH), 3417.14, 3389.62 (NH_2), 1660.02 (C=O), 1631.21 (C=C), 1628.66 (C=C), 1587.54, 1569.63, 1525.85 cm^{-1}

^{1}H NMR (400 MHz, DMSO): δ ppm 1.07 (t, 3H, *J*=7.02 Hz, CH_3), δ 3.75 (s, 3H, OCH_3), δ 3.97 (q, 2H, *J*=7.04 Hz, OCH_2), δ 4.76 (s, 1H, CH), δ 6.43 (d, 1H, *J*=7.52 Hz, Ar-H), δ 6.48 (d, 2H, *J*=7.28, Hz, Ar-H), δ 6.86 - 6.94 (m, 2H, Ar-H, δ 6.98 - 7.05 (m, 1H, Ar-H), δ 7.12 (s (br), 1H, OH), δ 7.68 (s, (br), 2H, NH_2)

^{13}C NMR (100 MHz, DMSO): δ ppm 14.30 (CH_3), δ 37.97 (CH), δ 55.89 (CH_3), δ 58.56 (CH_2), δ 76.22 (C), δ 102.03 (CH), δ 112.17 (CH), δ 113.62 (C), δ 114.39 (CH), δ 116.39 (CH), δ 122.64 (CH), δ 129.80 (OCH_3), δ 141.82 (C-F), δ 148.97 (C-OH), δ 156.79 (C-OCH_3), δ 160.97 (O-C-N), δ 168.26 (C=O)

HRMS (ESI): $C_{19}H_{18}FNO_5$ [M^+ +H] requires (m/e) 360.1247, found 360.1246, (-0.4 ppm)

BE23 Synthesis of 2-Amino-4-(pyridin-4-yl)-7-hydroxy-4*H*-chromene-3-carboxylic acid ethyl ester

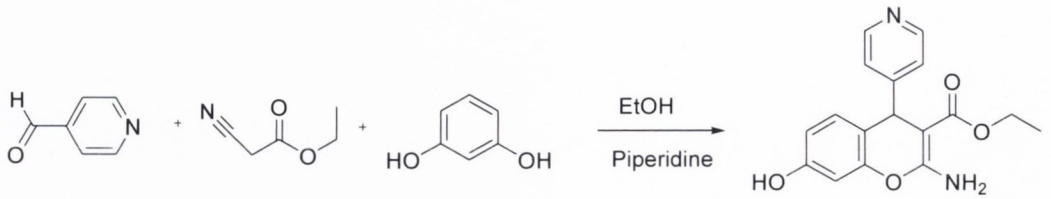

Yield: 0.87 g, 28 %, yellow powder (Recrystallisation, EtOH) **HPLC Purity:** 95%

MP: 242-245°C **Lit. Ref**: [235]

IRϑ_{max} (KBr): 3304.11 (OH), 3421.09, 3376.35 (NH_2), 1693.14 (C=O), 1642.51 (C=C), 1630.36 (C=C), 1582.68, 1563.47, 1481.63 cm^{-1}

^{1}H NMR (400 MHz, DMSO): δ ppm 1.02 (t, 3H, *J*=7.02 Hz, CH_3), δ 3.94 (q, 2H, *J*=7.42 Hz, OCH_2), δ 4.82 (s, 1H, CH), δ 6.45 - 6.54 (m, 2H, Ar-H), δ 6.99 (d, 1H, *J*=8.56 Hz, Ar-H), δ 7.14 (d, 2H, *J*=6.52 Hz, Ar-H), 7.07 (s (br), 2H, NH_2), δ 8.38 (d, 2H, *J*=6.84 Hz, Ar-H), δ 8.69 (s (br), 1H, OH).

^{13}C NMR (100 MHz, DMSO): δ ppm 14.22 (CH_3), δ 38.47 (CH), δ 58.63 (OCH_2), δ 75.00 (C), δ 102.20 (CH), δ 112.30 (C), δ 114.91 (CH), δ 122.34 (CH), δ 129.87 (CH), δ 149.04 (C), δ 149.51 (CH), δ 156.80 (C-O), δ 157.17 (C-OH), δ 161.16 (O-C-N), δ 168.05 (C=O)

HRMS (ESI): $C_{17}H_{16}N_2O_4$ [M^+ +H] requires (m/e) 313.1188, found 313.1196, (+2.5 ppm)

BE24 Synthesis of 2-Amino-4-(4-Nitrophenyl)-7-hydroxy-4*H*-chromene-3-carboxylic acid ethyl ester

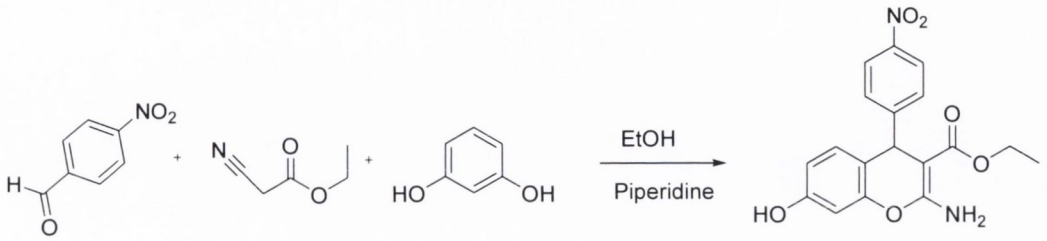

Yield: 0.25 g, 7 %, red crystals (Recrystallisation, EtOH) **HPLC Purity:** 94%

MP: 253°C **Lit. Ref**: [236]

IRϑ_{max} (KBr): 3598.45 (OH), 3410.23, 3379.64 (NH_2), 1662.67 (C=O), 1629.84 (C=C), 1628.56 (C=C), 1567.83, 1526.63 cm^{-1}

^{1}H NMR (400 MHz, $CDCl_3$): δ ppm 1.20 (t, 3H, *J*=7.02 Hz, CH_3), δ 4.06 (q, 2H, *J*=8.02, OCH_2), δ 5.06 (s, 1H, CH), δ 6.55 (d, 2H, *J*=7.52 Hz, Ar-H), δ 6.96 (d, 1H, *J*=8.04 Hz, Ar-H), δ 7.47 (d, 2H, *J*=8.56 Hz, Ar-H), δ 8.14 (d, 2H, *J*=8.56 Hz, Ar-H), δ 8.41 (s (br), 1H, OH), NH_2 not observed

^{13}C NMR (100 MHz, $CDCl_3$): δ ppm 13.34 (CH_3), δ 39.67 (CH), δ 60.15 (CH_2), δ 76.12 (C), δ 102.27 (CH), δ 112.02 (CH), δ 115.36 (C), δ 123.05 (CH), δ 129.66 (CH), δ 146.11 (CH), δ 149.14 (C-NO_2), δ 149.67 (C), δ 156.37 (C-O), δ 157.52 (C-OH), δ 161.50 (O-C-N), δ 169.20 (C=O)

HRMS (ESI): $C_{18}H_{18}N_2O_6$ [M^+ +H] requires (m/e) 357.1087, found 357.1073, (-3.8ppm)

BE25 Synthesis of 2-Amino-4-(4-acetamidophenyl)-7-hydroxy-4*H*-chromene-3-carboxylic acid ethyl ester

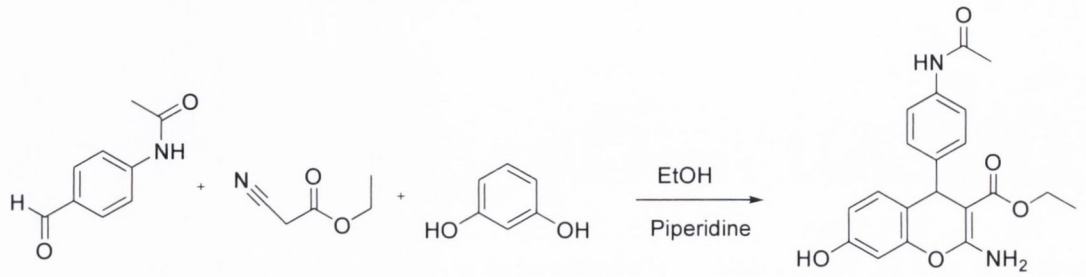

Yield: 1.80 g, 49 %, white powder (Recrystallisation, EtOH) **HPLC Purity:** 98%

MP: 236-241°C

IRϑ_{max} (KBr): 3565.52 (OH), 3414.36, 3354.98 (NH_2), 1660.32 (C=O), 1644.34 (C=C), 1639.75 (C=C), 1594.86, 1563.64, 1537.42 cm^{-1}

^{1}H NMR (400 MHz, DMSO): δ ppm 1.06 (t, 3H, *J*=7.08 Hz, CH_3), δ 1.99 (s, 3H, CH_3), δ 3.94 (q, 2H, *J*=7.32 Hz, OCH_2), δ 4.73 (s, 1H, CH), δ 6.40 - 6.48 (m, 2H, Ar-H), δ 6.94 (d, 1H, *J*=8.12 Hz, Ar-H), δ 7.04 (d, 2H, *J*=8.24 Hz, Ar-H), δ 7.38 (d, 2H, *J*=8.28 Hz, Ar-H), δ 7.59 (s (br), 2H, NH_2), δ 8.60 (s (br), 1H, NH), δ 8.82 (s (br), 1H, OH).

^{13}C NMR (100 MHz, DMSO): δ ppm 14.77 (CH_3), δ 24.33 (CH_3), δ 38.87 (CH), δ 58.99 (CH_2), δ 76.99 (C), δ 102.47 (CH), δ 112.52 (CH), δ 117.29 (C), δ 119.42 (CH), δ 127.56 (CH), δ 128.26 (CH), δ 137.48 (C), δ 149.46 (C-O), δ 157.11 (C-OH), δ 161.37 (O-C-N), δ 168.46 (C=O), δ 168.86 (C=O)

HRMS (ESI): $C_{20}H_{20}N_2O_5$ [M^+ +Na] requires (m/e) 391.1270, found 391.1288, (4.6ppm)

BE26 Synthesis of 2-Amino-4-(4-Methoxy-3-Nitrophenyl)-7-hydroxy-4*H*-chromene-3-carboxylic acid ethyl ester

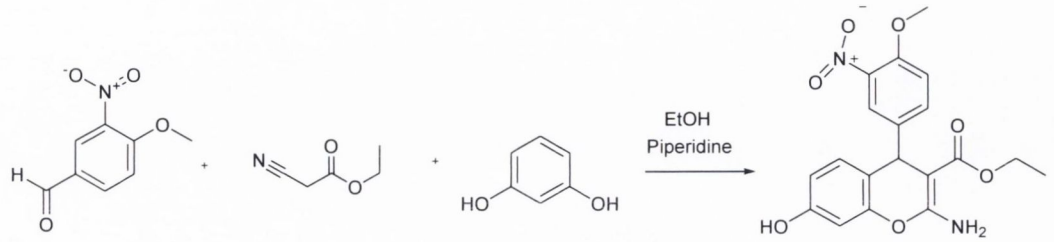

Yield: 3.78 g, 98 %, brown crystals(Recrystallisation, EtOH) **HPLC Purity:** 91%

MP: 295-298°C

IRϑ_{max} (KBr): 3502.34 (OH), 3440.74, 3372.84 (NH_2), 1689.39 (C=O), 1665.37 (C=C), 1622.54 (C=C), 1574.34, 1326.85 (NO_2) cm^{-1}

^{1}H NMR (400 MHz, DMSO-d6): δ ppm 1.19 (t, 3H, *J*=7.02 Hz, CH_3), δ 3.72 (s, 3H, OCH_3), δ 4.02 (q, 2H, *J*=7.04 Hz, OCH_2), δ 4.76 (s, 1H, CH), δ 6.43 (d, 1H, *J*=6.26 Hz, Ar-H), δ 6.67 (d, 1H, *J*=8.54 Hz, Ar-H), δ 6.79 - 6.82 (m, 2H, Ar-H), δ 7.22 (s, 1H, Ar-H), δ 7.89 (s, 1H, Ar-H), δ 7.97 (s (br), 2H, NH_2), OH not observed.

^{13}C NMR (100 MHz, DMSO-d6): δ ppm 14.26 (CH_3), 39.88 (CH), δ 55.61 (OCH_3), δ 60.72 (CH_2), δ 80.12 (C), δ 104.57 (CH), δ 110.32 (CH), δ 113.70 (C), δ 115.54 (CH), δ 124.37 (CH), δ 130.96 (CH), δ 131.70 (C), δ 133.70 (C-NO_2), δ 134.84 (CH), δ 154.64 (C-OCH_3), δ 168.68 (C-OH), 169.74 (O-C-N), δ 171.84 (C=O)

HRMS (ESI): $C_{19}H_{18}N_2O_7$ [M^+ +Na] requires (m/e) 409.1012, found 409.1020, (2.0 ppm)

BE27 Synthesis of 2-Amino-4-(pyridine-3-yl)-7-hydroxy-4*H*-chromene-3-carboxylic acid ethyl ester

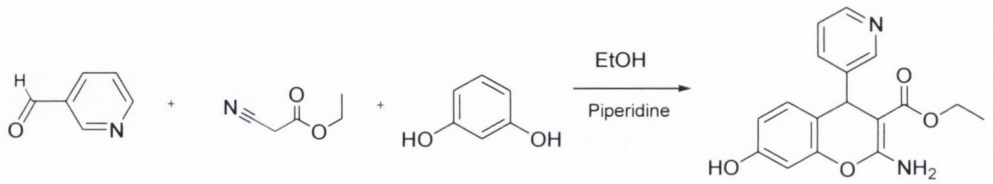

Yield: 1.65 g, 53 %, white powder (Recrystallisation, EtOH) **HPLC Purity:** 85%

MP: 263-269°C

IRϑ_{max} (KBr): 3510.29 (OH), 3477.99, 3424.95 (NH_2), 1672.70 (C=O), 1645.81 (C=C), 1621.87 (C=C), 1567.03, 1516.47 cm^{-1}

^{1}H NMR (400 MHz, DMSO-d6): δ ppm 1.03 (t, 3H, *J*=7 Hz, CH_3), δ 3.97 (q, 2H, *J*=7.02 Hz, OCH_2), δ 4.84 (s, 1H, CH), δ 6.47 - 6.50 (m, 1H, Ar-H), δ 7.22 – 7.28 (m, 1H, Ar-H), δ 7.42 - 7.47 (m, 1H, Ar-H), δ 7.68 (d, 2H, *J*=8.04 Hz, Ar-H), δ 8.30 - 8.36 (m, 1H, Ar-H), δ 8.47 (d, 1H, *J*=7.26 Hz, Ar-H), NH_2 not observed, OH not observed.

^{13}C NMR (100 MHz, DMSO-d6): δ ppm 14.22 (CH_3), δ 36.56 (CH), δ 58.61 (CH_2), δ 75.63 (C), δ 102.13 (CH), δ 112.33 (C), δ 115.56 (CH), δ 123.55 (CH), δ 129.98 (CH), δ 134.46 (C), δ 143.83 (CH), δ 147.07 (CH), δ 148.45 (CH), δ 149.04 (C-O), δ 157.01 (C-OH), δ 161.01 (O-C-N), δ 168.06 (C=O)

HRMS (ESI): $C_{17}H_{16}N_2O_4$ [M^+ +H] requires (m/e) 313.1188, found 313.1176 (-3.9 ppm)

BE28 Synthesis of 2-Amino-4-(5-bromo-2-methoxyphenyl)-7-hydroxy-4*H*-chromene-3-carboxylic acid ethyl ester

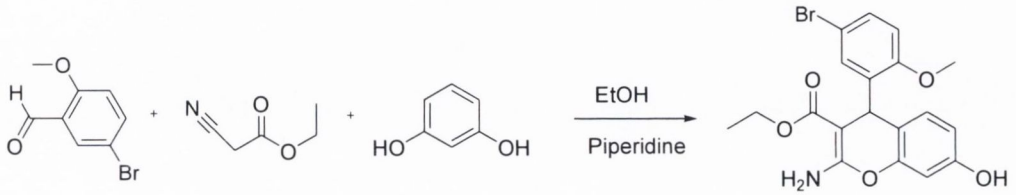

Yield: 2.30 g, 55 %, yellow crystals (Recrystallisation, EtOH) **HPLC Purity:** 90%

MP: 228-232°C

IRϑ_{max} (KBr): 3518.43 (OH), 3432.48, 3386.37 (NH_2), 1672.48 (C=O), 1623.89 (C=C), 1614.71 (C=C), 1596.65, 1562.41, 1512.75 cm^{-1}

^{1}H NMR (400 MHz, DMSO-d6): δ ppm 098 (t, 3H, *J*=7.02 Hz, CH_3), δ 3.77 (s, 3H, OCH_3), δ 3.88 (q, 2H, *J*=7.52 Hz, OCH_2), δ 5.16 (s, 1H, CH), δ 6.40 - 6.47 (m, 2H, Ar-H), δ 6.89 (d, 1H, *J*=8.52 Hz, Ar-H), δ 6.95 (d, 1H, *J*=8.56 Hz, Ar-H), δ 7.07 (d, 1H, *J*=6.48 Hz, Ar-H), δ 7.24 (d, 1H, *J*=6.8 Hz, Ar-H), 7.45 (s (br), 1H, OH), 7.68 (s (br), 2H, NH_2)

^{13}C NMR (100 MHz, DMSO-d6): δ ppm 14.04 (CH_3), δ 32.69 (CH), δ 55.92 (OCH_3), δ 58.45 (CH_2), δ 74.72 (C), δ 101.92 (CH), δ 111.75 (CH), δ 111.94 (C), δ 113.74 (C), δ 115.63 (CH), δ 129.17 (C), δ 129.48 (CH), δ 130.52 (CH), δ 139.34 (CH), δ 149.06 (C), δ 155.46 (C-OCH_3), δ 156.76 (C-OH), δ 161.43 (O-C-N), δ 168.23 (C=O)

HRMS (ESI): $C_{19}H_{18}{}^{81}BrNO_5$ [M^+ +H] requires (m/e) 420.0447, found 420.0435, (-2.8 ppm)

BE29 Synthesis of (E)-ethyl 2-cyano-3-(3,4-dimethoxyphenyl)acrylate

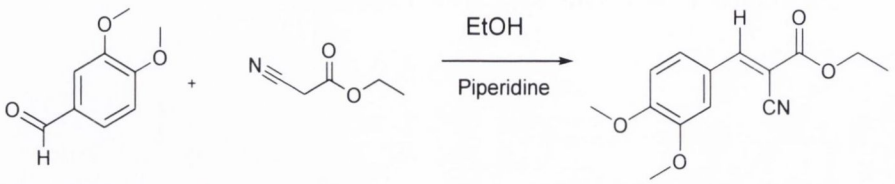

Yield: 0.34 g, 13 %, yellow crystals (Recrystallisation, EtOH)

MP: 160°C **Lit. Ref**.[237] **Lit. MP**: 157 °C

IRϑ_{max} (KBr): 2244.68 (CN), 1673.71 (C=C), 1643.64 (C=O), 1563.74, 1473.48 cm^{-1}

^{1}H NMR (400 MHz, DMSO): δ 0.94 (t, 3H, *J*=7.14 Hz, CH_3), 3.72 (s, 6H, 2xOCH_3), 3.86 (q, 2H, *J*=7.04, CH_2), 6.38 (d, 1H, *J*=2.28, Ar-H), 6.45 – 6.51 (m, 1H, Ar-H), 7.18 - 7.27 (m, 1H, Ar-H), 8.46 (d, 1H, *J*=6.98, CH)

^{13}C NMR (100 MHz, DMSO): δ 14.33 (CH_3), 58.85 (OCH_3), 62.03 (CH_2), 78.01 (C), 106.63 (CH), 112.53 (CN), 120.75 (CH), 128.77 (C), 148.70 (C-OCH_3), 149.77 (C-OCH_3), 157.73 (CH), 168.72 (C=O)

HRMS (ESI): $C_{14}H_{16}NO_4$ [M^+ +H] requires (m/e) 262.1079, found 262.1086, (-2.67 ppm)

BE31 Synthesis of intermediate, (E)-ethyl 3-(2,4-dichlorophenyl)-2-cyanoacrylate

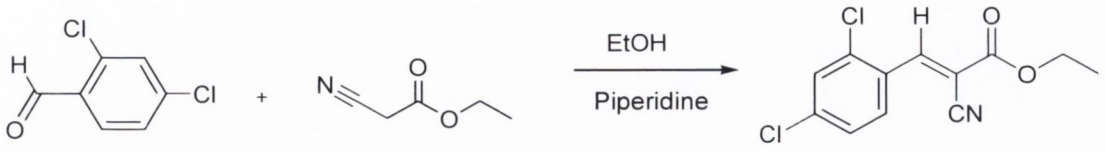

Yield: 1.74 g, 65 %, brown powder (Recrystallisation, EtOH)

MP: 72-79°C **Lit. Ref.**: [238] **Lit. MP:** 72 °C

IRϑ_{max} (KBr): 3084.63 (CH), 2256.72 (CN), 1684.59 (C=C), 1661.49 (C=C), 1626.59 (C=O), 1563.48, 800.71 (C-Cl) cm^{-1}

^{1}H NMR (400 MHz, DMSO-d6): δ 1.19 (t, 3H, *J*=7.04, CH_3), 4.20 (q, 2H, *J*=6.78, CH_2), 7.09 – 7.14 (m, 2H, Ar-H), 7.18 - 7.23 (m, 1H, Ar-H), 8.56 (s, 1H, CH)

^{13}C NMR (100 MHz, DMSO-d6): δ 14.09 (CH_3), 60.27 (CH_2), 86.58 (C), 114.71 (CN), 126.97 (CH), 129.35 (CH), δ 130.92 (CH), 132.37 (C), 133.48 (C-Cl), 134.83 (C-Cl) 154.67 (CH), 167.97 (C=O)

HRMS (ESI): $C_{12}H_9{}^{37}Cl_2NO_2$ [M^+] requires (m/e) 269.0010, found 269.0014, (-1.4 ppm)

BE33 3,7-diethyl 2,8-Diamino-4,6-*bis*(2,4-dichlorophenyl)-4*H*,6*H*-pyrano[3,2-g]chromene-3,7-dicarboxylate

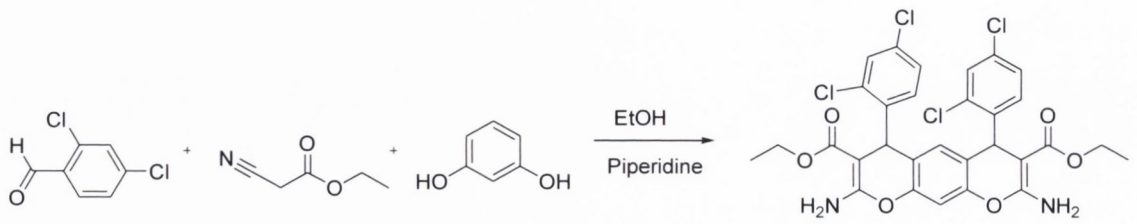

Yield: 0.13 g, 2 %, yellow crystals (Recrystallisation, EtOH) **HPLC Purity:** 99%

MP: 260-268°C

IRϑ_{max} (KBr): 3481.93, 3416.35 (NH_2), 1683.33 (C=O), 1634.97 (C=C), 1624.62 (C=C), 1551.39, 1498.62 cm^{-1}

^{1}H NMR (400 MHz, DMSO-d6): δ ppm 0.94 (t, 6H, *J*=7.02 Hz, 2xCH_3), 3.83 (q, 4H, *J*=6.76 Hz, 2xOCH_2), 5.33 (s, 2H, 2xCH), 6.69 (s, 1H, Ar-H), 6.90 (d, 2H, *J*=8.56 Hz, Ar-H), 7.06 - 7.11 (m, 3H, Ar-H), 7.38 (s, 2H, Ar-H), 7.73 (s (br), 4H, 2xNH_2).

^{13}C NMR (100 MHz, DMSO-d6): δ ppm 13.95 (CH_3), 34.90 (CH), 58.72 (CH_2), 74.40 (C), 103.15 (CH), 120.96 (C), 127.64 (CH), 128.06 (CH), 130.45 (CH), 130.95 (C-Cl), 131.87 (C-Cl), 144.46 (C), 147.18 (C-O), 160.77 (O-C-N), 167.82 (C=O)

HRMS (ESI): $C_{30}H_{24}{}^{37}Cl_4N_2O_6$ [M^- -H] requires (m/e) 647.0310, found 647.0313, (+0.4 ppm)

BE34 Synthesis of 2-(2-amino-7-hydroxy-4-phenyl-4*H*-chromen-3-yl)acetonitrile

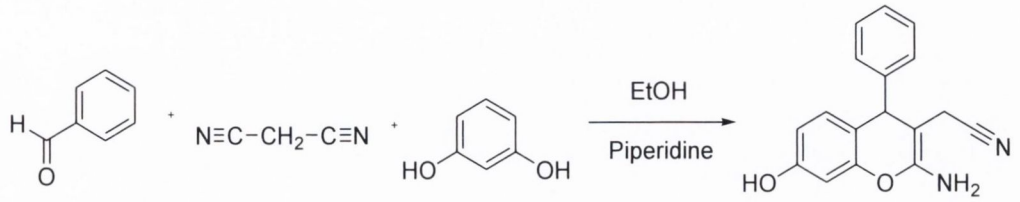

Yield: 2.19 g, 83 %, pale yellow powder(Recrystallisation, EtOH) **HPLC Purity:** 90%

MP: 269-278°C **Lit. Ref:**[229] **Lit. MP:** 241-242 °C

IRϑ_{max} (KBr): 3336.05 (OH), 3218.99, 3294.63 (NH_2), 2183.42 (CN), 1638.46 (C=C), 1624.90 (C=C), 1584.95, 1484.84 cm^{-1}

^{1}H NMR (400 MHz, DMSO-d6): δ ppm 1.45-1.50 (s (br), 2H, NH_2), 2.65 (s (br), 1H, OH), 3.11 (s, 2H, CH_2), 4.61 (s, 1H, CH), 6.40 (d, 1H, *J*=7.28 Hz, Ar-H), 6.47 (d, 1H, *J*=6.04 Hz, Ar-H), 6.78 (d, 1H, *J*=8.52 Hz, Ar-H), 7.15 - 7.17 (m, 3H, Ar-H), 7.28 - 7.30 (d, 2H, *J*=7.56 Hz, Ar-H)

^{13}C NMR (100 MHz, DMSO-d6): δ ppm 16.87 (CH_2), 46.50 (CH), 77.58 (C), 102.64 (CH), 112.16 (CH), 114.04 (C), 121.16 (CN), 127.09 (CH), 127.84 (CH), 129.05 (CH), 130.36 (CH), 146.87 (C), 149.32 (C-O), 157.76 (C-OH), 160.72 (O-C-N)

HRMS (ESI): $C_{16}H_{12}N_2NaO_2$ [M^+ +Na] requires (m/e) 287.0796, found 287.0794 (-0.9 ppm)

BE35 Synthesis of 2-Amino-7-hydroxy-4-phenyl-4*H*-chromene-3-carboxylic-acid methyl ester

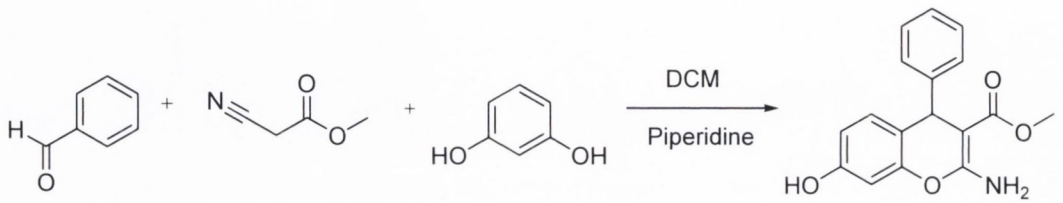

Yield: 0.35 g, 12 %, yellow powder (Recrystallisation, MeOH) **HPLC Purity:** 98%

MP: 277-280°C **Lit. Ref**:[239]

IRϑ_{max} (KBr): 3418.27 (OH), 3378.45, 3227.45 (NH_2), 1669.51 (C=O), 1634.81 (C=C), 1629.69 (C=C), 1547.84, 1438.47 cm^{-1}

^{1}H NMR (400 MHz, DMSO-d6): δ ppm 3.50 (s, 3H, CH_3), 4.81 (s, 1H, CH), 6.44 (d, 1H, *J*=7.52 Hz, Ar-H), 6.47 - 6.50 (m, 1H, Ar-H), 7.00 (d, 1H, *J*=8.28 Hz, Ar-H), 7.07 - 7.11 (m, 1H, Ar-H), 7.15 - 7.16 (m, 2H, Ar-H), 7.17 - 7.22 (m, 2H, Ar-H), 7.63 (s (br), 2H, NH_2), 9.62 (s (br), 1H, OH)

^{13}C NMR (100 MHz, DMSO-d6): δ ppm 39.96 (CH), 50.87 (CH_3), 76.77 (C), 102.54 (CH), 112.55 (CH), 117.42 (C), 126.24 (CH), 127.20 (CH), 128.72 (CH), 130.13 (CH), 148.94 (C), 149.57 (C-O), 157.19 (C-OH), 161.72 (O-C-N), 169.13 (C=O)

HRMS (ESI): $C_{17}H_{15}NNaO_4$ [M^+ +Na] requires (m/e) 320.0899, found 320.0900 (+0.4 ppm)

BE36 Benzyl 2-amino-7-hydroxy-4-phenyl-4*H*-chromene-3-carboxylate

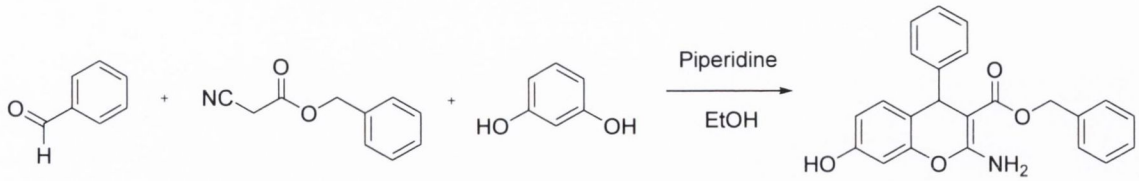

Yield: 0.96 g, 26 %, pale yellow powder(Recrystallisation,EtOH) **HPLC Purity:** 81 %

MP: 252-257°C

IRϑ_{max} (KBr): 3586.32 (OH), 3448.34, 3385.32 (NH_2), 1657.36 (C=O), 1640.24 (C=C), 1623.95 (C=C), 1587.52, 1557.14 cm^{-1}

^{1}H NMR (400 MHz, DMSO-d_6) δ ppm 4.80 (s, 1H, CH), 5.41 (dd, 2H, *J*=2.12, *J*=7.03 Hz, OCH_2), 6.43 - 6.51 (m, 1H, Ar-H), 6.98 (d, *J*=8.28 Hz, 2H, Ar-H), 7.07 - 7.12 (m, 2H, Ar-H), 7.13 - 7.18 (m, 5 H, Ar-H), 7.19 - 7.25 (m, 3 H, Ar-H), 7.60 (s (br), 2 H, NH_2), 8.61 (s (br), 1 H, OH).

^{13}C NMR (101 MHz, DMSO-d_6) δ ppm 39.72 (CH), 58.98 (CH_2), 77.02 (C), 102.52 (CH), 112.56 (CH), 117.20 (C), 126.16 (CH), 127.41 (CH), 128.57 (CH), 129.37 (CH), 130.27 (CH), 140.31 (C), 149.11 (C), 149.53 (C-O), 157.19 (C-OH), 161.48 (O-C-N), 168.82 (C=O)

HRMS (ESI): $C_{23}H_{20}NO_4$ [M^+ H] requires (m/e) 374.1392, found 374.1379, (-3.4 ppm)

BE37 2-Methylbutyl 2-amino-7-hydroxy-4-phenyl-4*H*-chromene-3-carboxylate

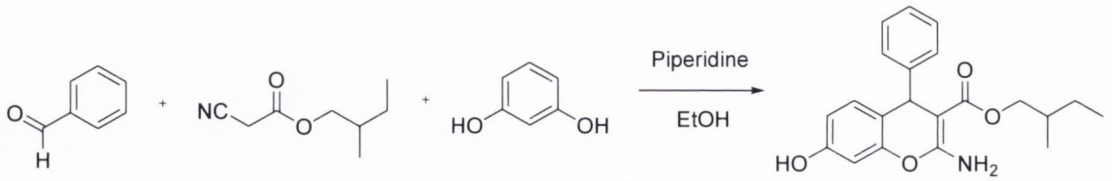

Yield: 3.25 g, 92 %, brown powder (Recrystallisation, EtOH) **HPLC Purity:** 87 %

MP: 245-247°C

IRϑ_{max} (KBr): 3478.73 (OH), 3423.58, 3397.49 (NH_2), 1660.86 (C=O), 1640.41 (C=C), 1632.87 (C=C), 1554.27, 1459.71 cm^{-1}

^{1}H NMR (400 MHz, MeOH) δ ppm 1.12 (t, *J*=7.28 Hz, 6H, 2xCH_3), 1.31 - 1.68 (m, 1H, CH), 3.27 - 3.37 (m, 2H, OCH_2), 3.96 - 4.08 (m, 2H, CH_2), 4.82 (s, 1H, CH), 5.92 (s, 1H, Ar-H), 6.48 (d, 2H, *J*=7.08 Hz, Ar-H), 6.91 (d, 1H, *J*=8.04 Hz, Ar-H), 7.13 - 7.24 (m, 4H, Ar-H), OH not observed, NH_2 not observed.

^{13}C NMR (101 MHz, MeOH) δ ppm 11.58 (CH_3), 15.87 (CH_3), 26.27 (CH_2), 34.78 (CH), 38.82 (C), 57.15 (CH_2), 76.23 (C), 101.81 (CH), 110.63 (CH), 116.12 (C), 126.22 (CH), 127.22 (CH), 127.32 (CH), 129.08 (CH), 129.10 (C), 148.14 (C-O), 148.17 (C-OH), 148.76 (O-C-N), 166.13 (C=O)

HRMS (ESI): $C_{21}H_{24}NO_4$ [M^+ H] requires (m/e) 354.1705, found 354.1710, (-1.4 ppm)

BE38 Allyl 2-amino-7-hydroxy-4-phenyl-4*H*-chromene-3-carboxylate

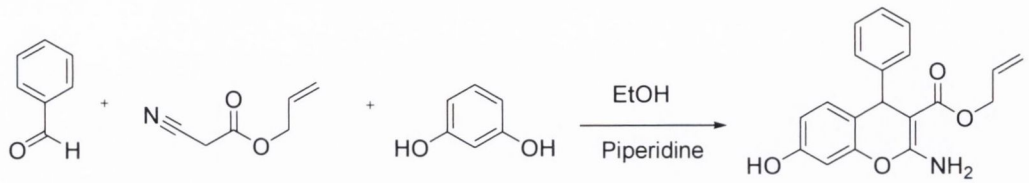

Yield: 1.06 g, 33 %, brown solid (Recrystallisation, EtOH) **HPLC Purity:** 89 %

MP: 126-228 °C

IRϑ_{max} (KBr): 3547.61 (OH), 3472.48, 3423.15 (NH_2), 1760.46 (C=C), 1664.51 (C=C), 1604.98 (C=O), 1574.85, 1536.51, 1529.58 cm-1

^{1}H NMR (400 MHz, DMSO-d_6): δ ppm 4.71 (s, H, CH), δ 4.32 (d, *J*=6.98 H, OCH_2), δ 4.38 - 4.44 (m, 2H, -C=CH_2), δ 5.89 - 5.96 (m, 1H, CH), δ 6.20 (s, 1H, Ar-H) δ 6.31 (d, 1H, *J*=6.98 Hz, Ar-H), δ 6.69 - 6.74 (m, 1H, *J*=7.13 H, Ar-H), δ 7.74 - 7.81 (m, 5H, Ar-H), δ 8.09 (s (br), 2H, NH_2) δ 8.34 (s (br), 1H, OH)

^{13}C NMR (101 MHz, DMSO-d_6): δ ppm 39.75 (CH), δ 67.91 (CH_2), δ 83.21 (C), δ 106.39 (CH), δ 112.71 (CH), δ 114.36 (C), δ 118.62 (CH_2), δ 120.78 (CH), δ 125.01 (CH), δ 127.42 (CH), δ 128.03 (CH), δ 135.71 (CH), δ 141.67 (C), δ 152.93 (C-O), δ 154.24 (C-OH), δ 157.41 (O-C-N),δ 167.31 (C=O)

HRMS (ESI): $C_{19}H_{17}NNaO_4$ [M^+ +Na] requires (m/e) 346.1055, found 346.1062 (+2.0 ppm)

BE39 3-Methylpentyl-2-amino-7-hydroxy-4-phenyl-4*H*-chromene-3-carboxylate

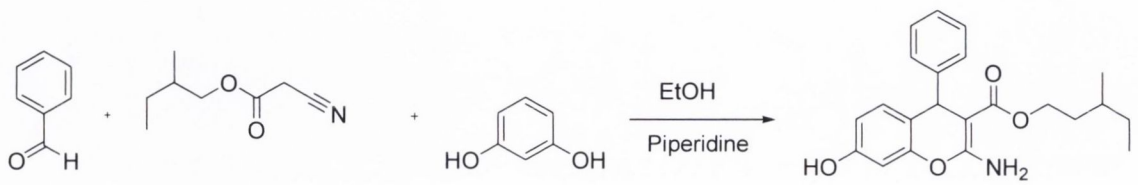

Yield: 1.47 g, 40 %, light brown solid (Recrystallisation, EtOH) **HPLC Purity:** 100 %

MP: 148-154 °C

IRϑ_{max} (KBr): 3491.64 (OH), 3432.18, 3411.73 (NH_2), 1755.89 (C=C), 1648.62 (C=C), 1634.42 (C=O), 1588.42, 1547.22, 1486.52 cm-1.

^{1}H NMR (400 MHz, DMSO-d_6): δ ppm 1.01 (t, 3H, *J*=6.98 Hz, CH_3), δ 1.21 (d, 3H, *J*=7.13 Hz, CH_3), δ 1.26 - 1.34 (m, 2H, CH_2), δ 1.52 - 1.61 (m, 1H, CH), δ 1.66 – 1.69 (m, H, CH_2) δ 4.31 (q, *J*=7.81 2H, CH_2), δ 4.82 (s, 1H, CH), δ 6.12 (s, 1H, Ar-H), δ 6.19 - 6.27 (m, 1H, Ar-H), δ 6.29 - 6.35 (m, 1H, Ar-H), δ 7.38 (d, 1H, *J*=8.10 Hz, Ar-H), δ 7.45 (m, 4H, Ar-CH), δ 7.75 (s (br), 2H, NH_2) δ 8.28 (s (br), 1H, OH)

^{13}C NMR (101 MHz, DMSO-d_6): δ ppm 13.05 (CH_3), δ 14.05 (CH_3), δ 30.29 (CH_2), δ 36.32 (CH), δ 39.31 (CH_2), δ 40.25 (CH), δ 63.28 (CH_2), δ 79.41 (C), δ 105.92 (CH), δ 110.53 (CH), δ 113.75 (C), δ 128.71 (CH), δ129.72 (CH), δ 129.93 (CH), δ 130.04 (CH), δ 140.41 (C), δ 154.36 (C-O), 156.82 (C-OH), δ 160.71 (O-C-N), δ 168.94 (C=O)

HRMS (ESI): $C_{22}H_{26}NO_4$ [M^+ +H] requires (m/e) 368.1862, found 368.1875 (-3.53 ppm)

BE40 Isopentyl-2-amino-7-hydroxy-4-phenyl-4*H*-chromene-3-carboxylate

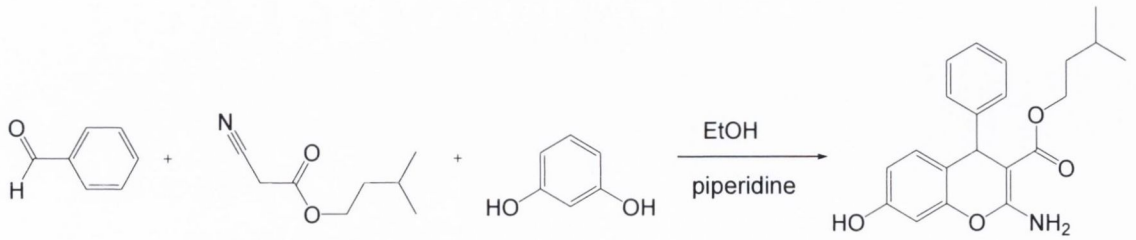

Yield: 1.13 g, 32 %, light brown solid (Recrystallisation, EtOH) **HPLC Purity:** 85 %

MP: 154 – 156 °C

IRϑ_{max} (KBr): 3596.71 (OH), 3472.58, 3428.47 (NH_2), 1755.66 (C=C), 1654.41 (C=C), 1671.2 (C=O), 1574.85, 1475.84 cm-1

^{1}H NMR (400 MHz, DMSO-d_6): δ ppm 1.34 (d, 6H, *J*=7.54, 2xCH_3), δ 1.52 – 1.56 (m, 2H, CH_2), δ 1.63 – 1.68 (m, 1H, CH), δ 5.12 - 5.18 (m, 2H, OCH_2), δ 5.21 (s, 1H, CH) δ 6.03 (s, 1H, Ar-H), δ 6.41 (d, 1H, *J*=6.18 H, Ar-H), δ 6.78 – 6.83 (m, 1H, Ar-H), 7.08 - 7.18 (m, 2H, Ar-H), δ 7.53 - 7.61 (m, 3H, Ar-CH), δ 8.51 (s (br), 2H, NH_2), δ 8.12 (s (br), 1H, OH)

^{13}C NMR (101 MHz, DMSO-d_6): δ ppm 24.57 (CH_3), δ 26.19 (CH), δ 38.33 (CH_2), δ 38.79 (CH), δ 64.2 (CH_2), δ 80.10 (C), δ 107.01 (CH), δ 111.42 (CH), δ 117.31 (C), δ 115.86 (CH), δ 126.51 (CH), δ 129.51 (CH), δ 133.67 (CH), δ 141.04 (C), δ 157.11 (C-O), δ 158.95 (C-OH), δ 160.71 (O-C-N), δ 168.94 (C=O).

HRMS (ESI): $C_{21}H_{23}NNaO_4$ [M^+ +Na] requires (m/e) 376.1525, found 376.1532 (-1.86 ppm)

BE41 Ethyl 2-amino-7-hydroxy-4-(4-hydroxyphenyl)-4*H*-chromene-3-carboxylate

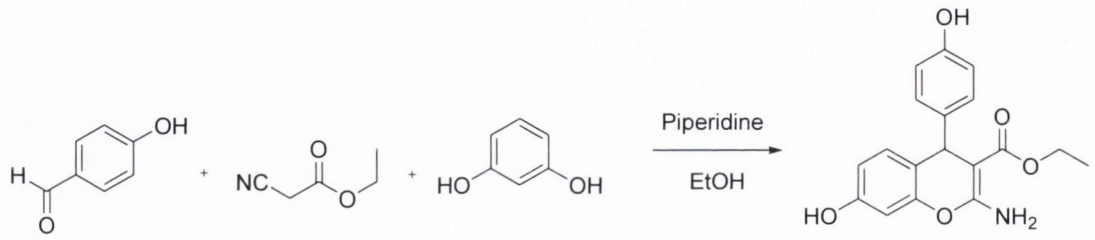

Yield: 1.04 g, 32 %, dark brown solid (Flash Column; CH_2Cl_2 - MeOH 15%)

HPLC Purity: 85 % **MP:** 228-230°C **Lit. Ref**. [240]

IRϑ_{max} (KBr): 3614.49, 3595.36, (OH), 3485.10, 3357.31 (NH_2), 1659.71 (C=O), 1629.41 (C=C), 1630.48 (C=C), 1591.36, 1538.14 cm^{-1}

^{1}H NMR (400 MHz, DMSO-d_6) δ ppm 0.98 (t, 3H, *J*=7.2, CH_3), 4.28 - 4.47 (m, 2H, OCH_2), 4.68 (s, 1H, CH), 6.13 - 6.23 (m, 3H, Ar-H), 6.61 - 6.68 (m, 2H, Ar-H), 6.85 - 6.99 (m, 2H, Ar-H), 8.14 (s (br), 1H, OH), 9.15 (s (br), 2H, NH_2)

^{13}C NMR (101 MHz, DMSO-d_6) δ ppm 14.31 (CH_3), 56.03 (CH), 58.49 (CH_2), 76.97 (C), 101.96 (CH), 102.44 (CH), 106.17 (CH), 114.75 (C), 127.81 (CH), 129.70 (CH), 132.74 (C), 152.56 (C-O), 154.93 (C-OH), 155.24 (C-OH), 158.44 (O-C-N), 160.88 (C=O)

HRMS (ESI): $C_{18}H_{17}NNaO_5$ [M^+ Na] requires (m/e) 350.1004, found 350.0997, (-1.9 ppm)

BE42 Neopentyl 2-amino-7-hydroxy-4-(4-hydroxyphenyl)-4*H*-chromene-3-carboxylate

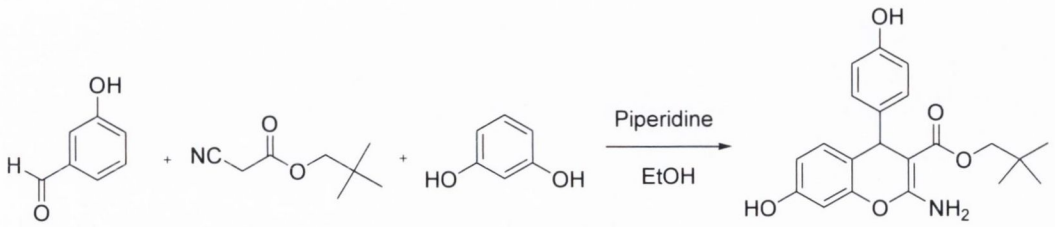

Yield: 2.39 g, 65 %, black solid (Flash Column, Hexane - EtOAc, 1.5:1)

HPLC Purity: 89 %, **MP:** 256-262°C

IRϑ_{max} (KBr): 3414.71 (OH), 3418.48, 3389.35 (NH_2), 1687.86 (C=O), 1678.54 (C=O), 1661.85 (C=C), 1640.65 (C=C), 1610.53, 1557.93, 1546.34, 1479.73 cm^{-1}

^{1}H NMR (400 MHz, DMSO-d_6) δ ppm 0.74 (s, 9H, 3xCH_3), 3.94 (s, 2H, OCH_2), 4.79 (s, 1H, CH), 6.40 - 6.49 (m, 1H, Ar-H), 6.85 (d, 2H, *J*=8.02 Hz, Ar-H), 7.05 (d, 2H, *J*=8.80 Hz, Ar-H), 7.11 (d, 2H, *J*=7.46 Hz, Ar-H), 7.35 - 7.39 (s, 1H, Ar-H), 7.54 (s (br), 2H, NH_2), 7.61 (s (br), 1H, OH)

^{13}C NMR (101 MHz, DMSO-d_6) δ ppm 26.21 (CH_3), 31.04 (C), 38.16 (CH), 76.09 (C), 76.91 (CH_2), 102.00 (CH), 112.06 (CH), 114.52 (C), 117.20 (CH), 127.51 (CH), 127.62 (CH), 127.69 (CH), 129.75 (C), 154.88 (C-O), 157.35 (C-OH), 158.38 (C-OH), 161.20 (O-C-N), 167.91 (C=O)

HRMS (ESI): $C_{21}H_{22}NO_5$ [M^- H] requires (m/e) 368.1498, found 368.1519, (-5.7 ppm)

BE43 Benzyl 2-amino-7-hydroxy-4-(4-hydroxyphenyl)-4*H*-chromene-3-carboxylate

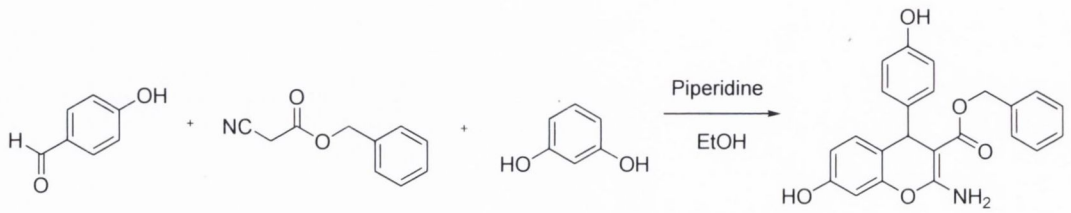

Yield: 0.12 g, 3 %, brown solid (Flash Column, Hexane - EtOAc, 1:2)

HPLC Purity: 95% **MP:** 226-229°C

IRϑ_{max} (KBr): 3498.58 (OH), 3417.94, 3397.63 (NH_2), 1660.83 (C=O), 1640.84 (C=C), 1632.16 (C=C), 1594.37, 1509.26, 1459.18 cm^{-1}

^{1}H NMR (400 MHz, DMSO-d_6) δ ppm 3.95 (s, 1H, CH), 4.68 (s, 2H, OCH_2), 6.16 - 6.22 (m, 1H, Ar-H), 6.42 (s, 1H, Ar-H), 6.46 (d, 1H, *J*=8.01 Hz, Ar-H), 6.48 (s, 1H, Ar-H), 6.56 - 6.59 (m, 1H, Ar-H), 6.60 (d, 1H, *J*=6.54 Hz, Ar-H), 6.91 - 6.96 (m, 2H, Ar-H), 7.53 (s, 1 H, Ar-H), 7.97 - 8.05 (m, 1H, Ar-H), 8.25 (s, 2 H, Ar-H), 9.10 (s (br), 2H, NH_2), 9.16 (s (br), 1 H, OH), 9.57 (s (br), 1 H, OH)

^{13}C NMR (101 MHz, DMSO-d_6) δ ppm 39.67 (CH), 68.41 (CH_2), 80.18 (C), 105.13 (CH), 110.45 (CH), 113.64 (C), 115.4 (CH), 127.25 (CH), 129.48 (CH), 130.21 (CH), 133.47 (C), 140.37 (C), 155.97 (C-O), 156.31 (C-OH), 157.37 (C-OH), 161.93 (O-C-N), 167.83 (C=O)

HRMS (ESI): $C_{23}H_{19}NNaO_5$ [M^+ H] requires (m/e) 412.1161, found 412.1182, (5 ppm)

BE44 2-Methylbutyl 2-amino-7-hydroxy-4-(4-hydroxyphenyl)-4*H*-chromene-3-carboxylate

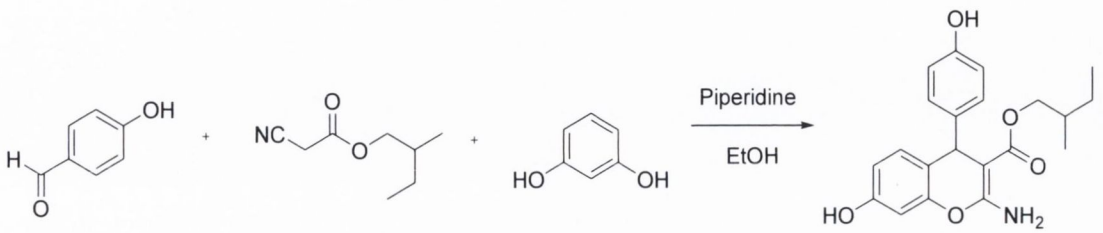

Yield: 1.64 g, 42 %, light brown solid (Flash Column, Hexane - EtOAc, 1.5:1)

HPLC Purity: 94% **MP:** 234-238°C

IRϑ_{max} (KBr): 3538.84 (OH), 3492.50, 3370.36 (NH_2), 1684.49 (C=O), 1657.95 (C=C), 1654.15 (C=C), 1613.68, 1492.45, 1473.72 cm^{-1}

^{1}H NMR (400 MHz, DMSO-d_6) δ ppm 0.97 - 1.07 (m, 6H, 2xCH_3), 1.97 - 2.10 (m, 2 H, CH_2), 2.28 - 2.37 (m, 1H, CH), 3.95 - 4.14 (m, 2H, CH_2), 4.67 (s, 1 H, CH), 6.41 (d, 1H, *J*=8.01 Hz, Ar-H), 6.47 (d, 2H, *J*=8.28 Hz, Ar-H), 6.59 (d, 2H, *J*=8.03 Hz, Ar-H), 6.88 - 6.99 (m, 2 H, Ar-H), 7.53 (s (br), 1 H, OH), 9.10 (s (br), 1 H, OH), 9.57 (s (br), 2 H, NH_2)

^{13}C NMR (101 MHz, DMSO-d_6) δ ppm 11.65 (CH_3), 15.42 (CH_3), 28.59 (CH_2), 34.11 (CH), 39.93 (CH), 71.83 (CH_2), 79.26 (C), 106.17 (CH), 110.65 (CH), 113.52 (C), 116.18 (CH), 129.61 (CH), 130.48 (CH), 133.15 (C), 154.71 (C-O), 155.39 (C-OH), 156.31 (C-OH), 164.82 (O-C-N), 168.72 (C=O)

HRMS (ESI): $C_{21}H_{23}NNaO_5$ M^+ H requires (m/e) 392.1474, found 392.1477, (+0.7 ppm)

BE45 Isopentyl 2-amino-7-hydroxy-4-(4-hydroxyphenyl)-4*H*-chromene-3-carboxylate

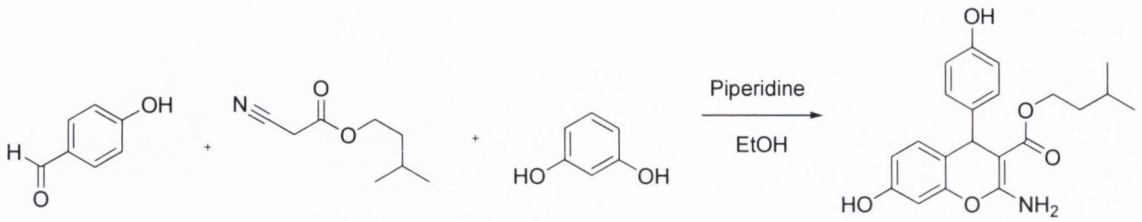

Yield: 0.15 g, 4 %, dark brown powder (Flash Column, CH_2Cl_2 - MeOH 10%)

HPLC Purity: 89% **MP:** 221-226°C

IRϑ_{max} (KBr): 3474.73 (OH), 3410.67, 3375.84 (NH_2), 1672.74 (C=O), 1655.95 (C=C), 1628.58 (C=C), 1571.03, 1452.94 cm^{-1}

^{1}H NMR (400 MHz, DMSO-d_6) δ ppm 0.78 (d, 6H, *J*=6.53 Hz, 2xCH_3), 1.29 - 1.32 (m, 2H, CH_2), 3.35 – 3.40 (m, 1H, CH), 4.29 – 4.32 (m, 2H, OCH_2), 4.66 (s, 1H, CH), 6.19 (s, 1 H, Ar-H), 6.40 (d, 1 H, *J*=7.04 Hz, Ar-H), 6.43 - 6.46 (m, 1 H, Ar-H), 6.46 (s, 1 H, Ar-H), 6.58 (d, 2 H, *J*=8.03 Hz, Ar-H), 6.94 (d, 1 H, *J*=8.28 Hz, Ar-H), 7.54 (s (br), 1H, OH), 8.01 (s (br), 1H, OH), 8.57 (s (br), 2 H, NH_2)

^{13}C NMR (101 MHz, DMSO-d_6) δ ppm 22.83 (CH_3), 25.48 (CH), 38.72 (CH_2), 39.83 (CH), 61.83 (CH_2), 80.38 (C), 107.29 (CH), 110.91 (CH), 114.67 (C), 116.47 (CH), 129.17 (CH), 130.56 (CH), 134.37 (C), 152.82 (C-O), 153.44 (C-OH), 155.28 (C-OH), 166.47 (O-C-N), 167.72 (C=O)

HRMS (ESI): $C_{21}H_{23}NNaO_5$ [M^+ Na] requires (m/e) 392.1474, found 392.1471, (-0.7 ppm)

BE46 2-Methoxyethyl 2-amino-7-hydroxy-4-(4-hydroxyphenyl)-4*H*-chromene-3-carboxylate

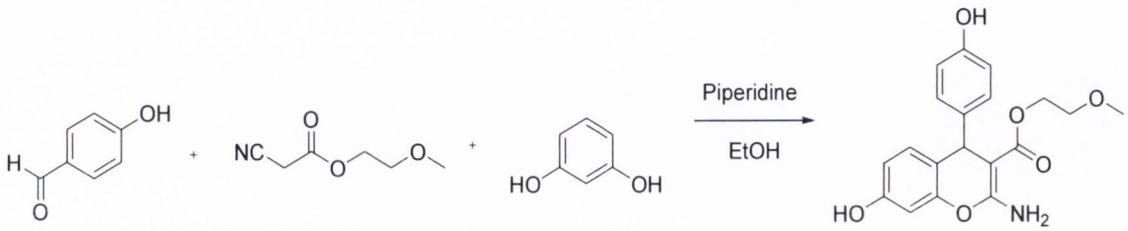

Yield: 1.50 g, 42 %, brown resin (Flash Column, CH_2Cl_2 - MeOH 10%)

HPLC Purity: 93% **MP:** na

IRϑ_{max} (KBr): 3558.83 (OH), 3468.58, 3412.85 (NH_2), 1680.59 (C=O), 1661.75 (C=C), 1623.01 (C=C), 1576.84, 1522.04 cm^{-1}

^{1}H NMR (400 MHz, DMSO-d_6) δ ppm 2.29 (s, 3 H, CH_3), 3.52 - 3.59 (m, 2H, CH_2), 3.77 (s (br), 2H, NH_2), 4.01 (q, 2H, *J*=7.12, CH_2), 4.32 (s, 1H, CH), 6.17 - 6.21 (m, 1 H, Ar-H), 6.92 (d, 2 H, *J*=8.53 Hz, Ar-H), 7.99 (d, 2 H, *J*=7.50 Hz, Ar-H), 8.23 (s, 2 H, Ar-H), OH not observed.

^{13}C NMR (101 MHz, DMSO-d_6) δ ppm 38.70 (CH), 47.51 (CH_3), 46.36 (CH_2), 61.88 (CH_2), 79.01 (C), 102.44 (CH), 106.16 (CH), 115.43 (C), 116.61 (CH), 129.07 (CH), 130.31 (CH), 134.08 (C), 154.66 (C-O), 155.93 (C-OH), 156.62 (C-OH), 158.57 (O-C-N), 162.75 (C=O)

HRMS (ESI): $C_{19}H_{20}NO_6$ [M^+ H] requires (m/e) 358.1291, found 358.1287, (-1.1 ppm)

BE47 3-Methoxybutyl 2-amino-7-hydroxy-4-(4-hydroxyphenyl)-4*H*-chromene-3-carboxylate

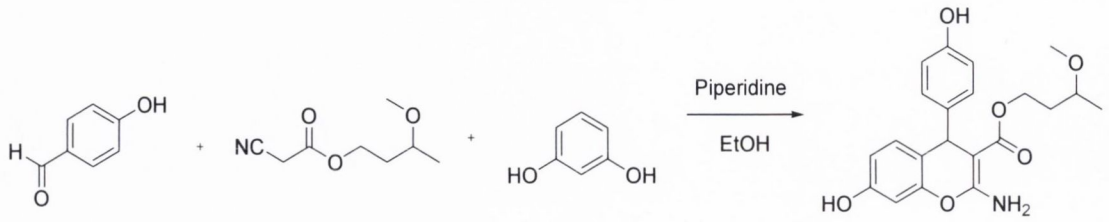

Yield: 0.34 g, 9 %, brown resin (Flash Column, CH_2Cl_2 - MeOH 10%)

HPLC Purity: 89 % **MP:** na

IRϑ_{max} (KBr): 3529.41, 3481.79 (OH), 3450.82, 3367.34 (NH_2), 1682.39 (C=O), 1678.60 (C=O), 1668.18, 1612.94 (C=C), 1549.45, 1459.74 cm^{-1}

^{1}H NMR (400 MHz, DMSO-d_6) δ ppm 1.06 (d, 3H, *J*=6.02 Hz, CH_3), 1.28 - 1.35 (m, 2 H, CH_2), 3.12 – 3.18 (m, 1 H, CH), 3.20 (s, 3H, CH_3), 3.44 (q, 2 H, *J*=7.02 Hz, CH_2), 4.25 (s, 1 H, CH), 6.52 (d, 2 H, *J*=6.78 Hz, Ar-H), 6.61 (d, *J*=8.03 Hz, 2 H, Ar-H), 6.71 (d, *J*=8.53 Hz, 2 H, Ar-H), 6.94 (s (br), 1 H, OH), 7.90 - 7.96 (m, 1 H, Ar-H), 9.18 (s (br), 2H, NH_2)

^{13}C NMR (101 MHz, DMSO-d_6) δ ppm 19.01 (CH_3), 37.94 (CH_2), 38.85 (CH), 55.27 (CH_3), 57.50 (CH_2), 61.56 (CH), 73.34 (C), 102.59 (CH), 103.24 (CH), 114.67 (C), 117.47 (CH), 128.52 (CH), 131.83 (CH), 134.38 (C), 151.90 (C-O), 154.49 (C-OH), 155.07 (C-OH), 156.30 (O-C-N), 157.50 (C=O)

HRMS (ESI): $C_{21}H_{23}NNaO_6$ [M^+ Na] requires (m/e) 408.1423, found 408.1415, (-1.9 ppm)

BE48 2-Butoxyethyl 2-amino-7-hydroxy-4-(4-hydroxyphenyl)-4*H*-chromene-3-carboxylate

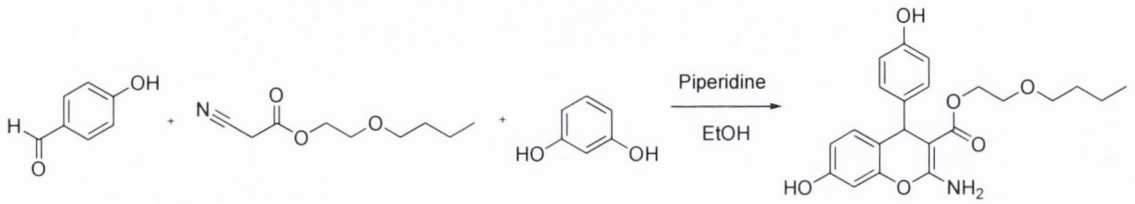

Yield: 3.27 g, 82 %, light brown solid (Flash Column, Hexane - EtOAc, 1.5:1)

HPLC Purity: 84 % **MP:** 231-234°C

IRϑ_{max} (KBr): 3551.06, 3497.26 (OH), 3429.73, 3321.67 (NH_2), 1698.31 (C=O), 1683.21 (C=C), 1645.95 (C=C), 1581.84, 1545.74 cm^{-1}

^{1}H NMR (400 MHz, DMSO-d_6) δ ppm 1.14 (t, 3 H, *J*=7.12 Hz, CH_3), 1.28 - 1.35 (m, 2 H, CH_2), 1.39 - 1.46 (m, 2H, CH_2), 3.36 - 3.41 (m, 2 H, CH_2), 3.67 - 3.72 (m, 2H, CH_2), 4.31 – 4.36 (m, 2 H, CH_2), 4.72 (s, 1 H, CH), 6.26 (d, 1 H, *J*=8.02, Hz, Ar-H), 6.16 - 6.21 (m, 1H, Ar-H), 6.58 (d, 2 H, *J*=7.02 Hz, Ar-H), 6.91 (d, 2 H, *J*=8.14 Hz, Ar-H), 8.23 (d, 1 H, *J*=7.04 Hz, Ar-H), 8.76 (br. s, 1 H, OH), NH_2 not observed.

^{13}C NMR (101 MHz, DMSO-d_6) δ ppm 14.28 (CH_3), 19.73 (CH_2), 32.67 (CH_2), 39.85 (CH), 61.74 (CH_2), 63.62 (CH_2), 69.63 (CH_2), 78.78 (C), 106.52 (CH), 110.94 (CH), 113.37 (C), 116.62 (CH), 129.39 (CH), 130.28 (CH), 133.38 (C), 153.48 (C-O), 154.75 (C-OH), 156.91 (C-OH), 162.14 (O-C-N), 167.38 (C=O)

HRMS (ESI): $C_{22}H_{25}NNaO_6$ [M^+ Na] requires (m/e) 422.1579, found 422.1567, (2.8 ppm)

BE49 Pentyl 2-amino-7-hydroxy-4-(4-hydroxyphenyl)-4*H*-chromene-3-carboxylate

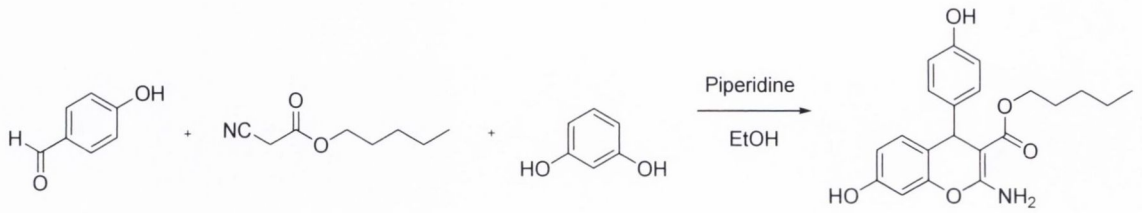

Yield: 3.39 g, 92 %, brown powder (Flash Column, CH_2Cl_2 - MeOH 10%)

HPLC Purity: 78 % **MP:** 237-241°C

IRϑ_{max} (KBr): 3493.84 (OH), 3485.11, 3365.74 (NH_2), 1672.94 (C=O), 1647.74 (C=C), 1628.43 (C=C), 1536.58, 1473.07 cm^{-1}

^{1}H NMR (400 MHz, DMSO-d_6) δ ppm 0.81 (t, 3H, *J*=7.03 Hz, CH_3), 1.07 - 1.11 (m, 2H, CH_2), 1.15 - 1.20 (m, 2H, CH_2), 1.26 - 1.31 (m, 2H, CH_2), 3.95 – 4.02 (m, 2 H, CH_2), 4.67 (s, 1 H, CH), 6.41 (d, 2 H, *J*=7.14 Hz, Ar-H), 6.46 (d, 2 H, *J*=8.03 Hz, Ar-H), 6.59 (d, 1 H, *J*=8.53 Hz, Ar-H), 6.87 - 6.96 (m, 2H, Ar-H), 7.53 (s (br), 2 H, NH_2), 8.98 (s (br), 1 H, OH)

^{13}C NMR (101 MHz, DMSO-d_6) δ ppm 14.31 (CH_3), 21.86 (CH_2), 38.08 (CH_2), 38.85 (CH_2), 40.10 (CH), 58.49 (CH_2), 76.99 (C), 101.96 (CH), 111.99 (CH), 114.75 (C), 117.37 (CH), 127.81 (CH), 129.70 (CH), 139.16 (C), 149.06 (C-O), 155.25 (C-OH), 156.82 (C-OH), 160.99 (O-C-N), 168.45 (C=O)

HRMS (ESI): $C_{21}H_{24}NO_5$ [M^+ H] requires (m/e) 370.1655, found 370.1672, (4.5 ppm)

BE50 Hexyl 2-amino-7-hydroxy-4-(4-hydroxyphenyl)-4*H*-chromene-3-carboxylate

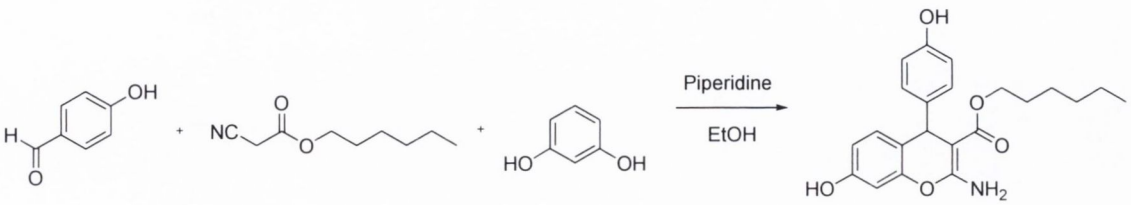

Yield: 0.60 g, 15 %, brown solid (Flash Column, CH_2Cl_2 - MeOH 10%)

HPLC Purity: 86 % **MP:** 255-264°C

IRϑ_{max} (KBr): 3562.94 (OH), 3476.59, 3348.72 (NH_2), 1678.35 (C=O), 1656.94 (C=C), 1633.85 (C=C), 1624.87, 1584.60, 1469.42 cm^{-1}

^{1}H NMR (400 MHz, DMSO-d_6) δ ppm 0.85 (t, 3H, *J*=7.03 Hz, CH_3), 1.07 - 1.12 (m, 6 H, 2xCH_2), 1.29 - 1.34 (m, 2H, CH_2), 3.94 – 3.99 (m, 2H, CH_2), 4.67 (s, 1 H, CH), 6.41 (s (br), 2 H, NH_2), 6.46 (d, 2 H, *J*=8.03 Hz, Ar-H), 6.59 (d, 2 H, *J*=8.03 Hz, Ar-H), 6.89 - 6.96 (m, 1 H, Ar-H), 7.54 (s (br), 1 H, OH), 7.99 (d, 1 H, *J*=8.53 Hz, Ar-H), 8.22 (s, 1 H, Ar-H), 8.94 (s (br), 1 H, OH)

^{13}C NMR (101 MHz, DMSO-d_6) δ ppm 14.08 (CH_3), 14.31 (CH_2), 38.09 (CH_2), 38.84 (CH_2), 39.05 (CH_2), 40.09 (CH), 58.49 (CH_2), 76.99 (C), 101.96 (CH), 111.99 (CH), 114.76 (C), 116.71 (CH), 117.37 (CH), 127.81 (CH), 129.73 (CH), 134.13 (C), 149.04 (C-O), 155.25 (C-OH), 156.50 (C-OH), 160.89 (O-C-N), 168.45 (C=O)

HRMS (ESI): $C_{22}H_{25}NNaO_5$ [M^+ H] requires (m/e) 406.1630, found 406.1633, (0.7 ppm)

BE51 Heptyl 2-amino-7-hydroxy-4-(4-hydroxyphenyl)-4*H*-chromene-3-carboxylate

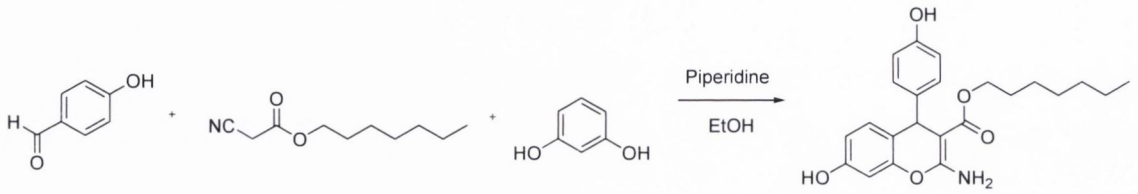

Yield: 0.50 g, 12 %, light brown powder (Flash Column, CH_2Cl_2 - MeOH 10%)

HPLC Purity: 87 % **MP:** 249-253°C

IRϑ_{max} (KBr): 3462.76 (OH), 3431.74, 3386.48 (NH_2), 1664.42 (C=O), 1638.54 (C=C), 1637.38 (C=C), 1568.62, 1464.27 cm^{-1}

^{1}H NMR (400 MHz, DMSO-d_6) δ ppm 0.86 (t, 3H, *J*=7 Hz, CH_3), 1.07 - 1.14 (m, 8H, 4xCH_2), 1.27-1.32 (m, 2 H, CH_2), 3.95 (q, 2H, *J*=7.03 Hz, CH_2), 4.67 (s, 1H, CH), 6.41 (d, 1H, *J*=7.04 Hz, Ar-H), 6.46 (s, 2H, Ar-H), 6.59 (d, 3H, *J*=8.02 Hz, Ar-H), 6.93 (s, 1 H, Ar-H), 7.53 (s (br), 1 H, OH), 9.11 (s (br), 2H, NH_2), 9.57 (s (br), 1 H, OH)

^{13}C NMR (101 MHz, DMSO-d_6) δ ppm 14.32 (CH_3), 29.23 (CH_2), 31.09 (CH_2), 38.08 (CH_2), 38.85 (CH_2), 40.10 (CH), 68.49 (CH_2), 78.53 (C), 101.92 (CH), 112.01 (CH), 114.75 (C), 117.35 (CH), 127.81 (CH), 129.72 (CH), 139.09 (C), 149.07 (C-O), 155.26 (C-OH), 156.55 (C-OH), 160.76 (O-C-N), 168.37 (C=O)

HRMS (ESI): $C_{23}H_{27}NNaO_5$ [M^+ H] requires (m/e) 420.1787, found 420.1803, (3.8 ppm)

BE52 Octyl 2-amino-7-hydroxy-4-(4-hydroxyphenyl)-4*H*-chromene-3-carboxylate

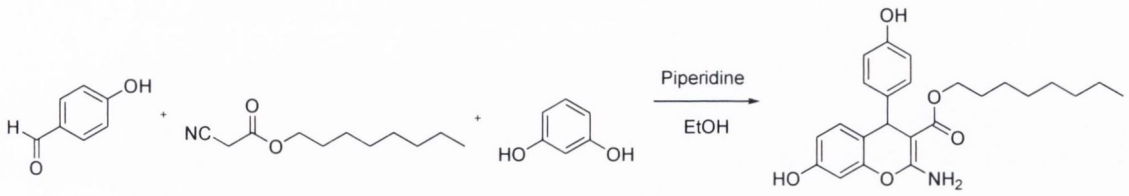

Yield: 1.51 g, 36 %, light brown solid (Flash Column, CH_2Cl_2 - MeOH 10%)

HPLC Purity: 96 % **MP:** 267-269°C

IRϑ_{max} (KBr): 3674.20 (OH), 3460.32, 3364.64 (NH_2), 1689.63 (C=O), 1658.17 (C=C), 1643.61 (C=C), 1567.86, 1505.14 cm^{-1}

^{1}H NMR (400 MHz, DMSO-d_6) δ ppm 0.86 (t, 3 H, *J*=7.02 Hz, CH_3), 1.07 - 1.13 (m, 8H, *J*=7.03 Hz, 4xCH_2), 1.23 - 1.32 (m, 2H, CH_2), 3.90 - 3.95 (m, 2H, CH_2), 4.29 (q, 2H, *J*=7.03 Hz, CH_2), 4.67 (s, 1 H, CH), 6.41 (s, 2H, Ar-H), 6.46 (d, 2 H, *J*=8.03 Hz, Ar-H), 6.59 (d, 2 H, *J*=8.03 Hz, Ar-H), 6.92 (d, 1 H, *J*=7.53 Hz, Ar-H), 7.53 (s (br), 2H, NH_2), 7.99 (s (br), 1 H, OH), 8.22 (s (br), 1 H, OH)

^{13}C NMR (101 MHz, DMSO-d_6) δ ppm 14.10 (CH_3), 14.35 (CH_2), 22.05 (CH_2), 25.26 (CH_2), 28.55 (CH_2), 31.19 (CH_2), 38.06 (CH), 58.46 (CH_2), 61.85 (CH_2), 76.97 (C), 101.83 (CH), 111.93 (CH), 114.75 (C), 116.43 (CH), 117.55 (CH), 127.81 (CH), 129.87 (CH), 134.04 (C), 148.98 (C-O), 154.61 (C-OH), 155.20 (C-OH), 156.45 (O-C-N), 160.87 (C=O)

HRMS (ESI): $C_{24}H_{29}NNaO_5$ [M^+ Na] requires (m/e) 434.1943, found 434.1930, (-2.9 ppm)

BE53 Cyclohexyl 2-amino-7-hydroxy-4-(4-hydroxyphenyl)-4*H*-chromene-3-carboxylate

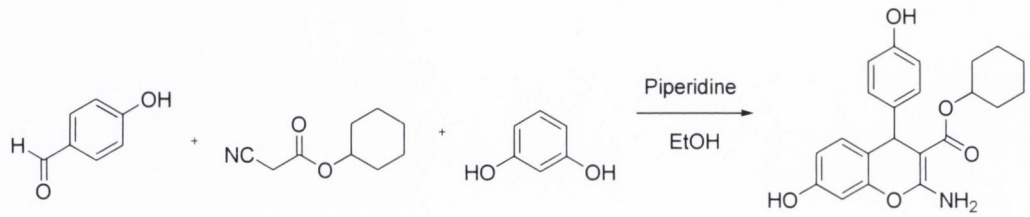

Yield: 0.27 g, 7%, light brown solid (Recrystallisation, EtOH)

HPLC Purity: 95 % **MP:** 240-245°C

IRϑ_{max} (KBr): 3584.58 (OH), 3417.96, 3397.63 (NH_2), 1672.38 (C=O), 1660.83 (C=C), 1632.34 (C=C), 1549.84, 1523.74 cm^{-1}

^{1}H NMR (400 MHz, DMSO-d_6) δ ppm 1.09 - 1.12 (m, 6H, 3xCH_2), 1.19 - 1.33 (m, 2H, CH_2), 2.03 - 2.09 (m, 2H, CH_2), 3.95 (s, 1H, CH), 4.67 (s, 1H, CH), 6.41 (d, 1 H, *J*=8.01 Hz, Ar-H), 6.47 (s, 1 H, Ar-H), 6.59 (d, 2 H, *J*=8.53 Hz, Ar-H), 6.69 (d, 2H, *J*=8.03 Hz, Ar-H), 6.88 - 6.95 (m, 1 H, Ar-H), 7.07 (s (br), 1 H, OH), 7.53 (s (br), 2 H, NH_2)

^{13}C NMR (101 MHz, DMSO-d_6) δ ppm 25.66 (CH_2), 30.74 (CH_2), 34.55 (CH_2), 43.81 (CH), 67.70 (CH), 68.84 (C), 111.98 (CH), 114.75 (CH), 115.15 (C), 117.57 (CH), 118.98 (CH), 127.80 (CH), 129.87 (CH), 133.41 (C), 153.72 (C-O), 155.61 (C-OH), 156.83 (C-OH), 162.54 (O-C-N), 166.07 (C=O)

HRMS (ESI): $C_{22}H_{23}NNaO_5$ [M^+ Na] requires (m/e) 404.1474, found 404.1437, (9 ppm)

BE54 2-Ethoxyethyl 2-amino-7-hydroxy-4-(4-hydroxyphenyl)-4*H*-chromene-3-carboxylate

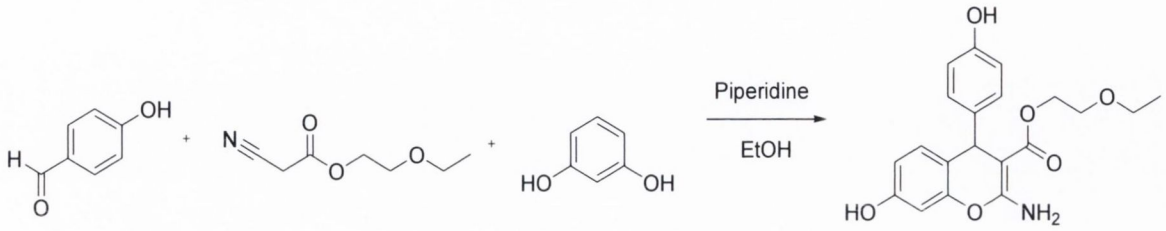

Yield: 0.40 g, 11%, green powder (Flash Column, CH_2Cl_2 - MeOH 10%)

HPLC Purity: 92 % **MP:** 245-247°C

IRϑ_{max} (KBr): 3529.04, 3499.62 (OH), 3439.26, 3409.61 (NH_2), 1667.07 (C=O), 1632.53 (C=C), 1624.48 (C=C), 1584.83, 1512.52 cm^{-1}

^{1}H NMR (400 MHz, DMSO-d_6) δ ppm 1.07 (t, 3H, *J*=7.03 Hz, CH_3), 1.29 - 1.34 (m, 2H, CH_2), 3.95 (q, 2H, *J*=7.04 Hz, CH_2), 4.29 - 4.34 (m, 2H, CH_2), 4.67 (s, 1H, CH), 6.46 (d, 1H, *J*=8.28, Ar-H), 6.59 (d, 2H, *J*=8.53 Hz, Ar-H), 6.92 (m, 4H, Ar-H), 7.53 (s (br), 2H, NH_2), 8.01 (s (br), 1H, OH), 8.24 (s (br), 1H, OH)

^{13}C NMR (101 MHz, DMSO-d_6) δ ppm 14.32 (CH_3), 38.08 (CH), 58.49 (CH_2), 61.92 (CH_2), 67.43 (CH_2), 76.98 (C), 101.95 (CH), 111.99 (CH), 114.75 (C), 117.37 (CH), 127.81 (CH), 129.72 (CH), 134.06 (C), 154.64 (C-O), 155.24 (C-OH), 156.49 (C-OH), 160.88 (O-C-N), 168.44 (C=O)

HRMS (ESI): $C_{20}H_{21}NNaO_6$ [M^+ Na] requires (m/e) 394.1267, found 394.1258, (-2.2 ppm)

BE55 Ethyl 2-amino-7-hydroxy-4-(3,4-dihydroxyphenyl)-4*H*-chromene-3-carboxylate

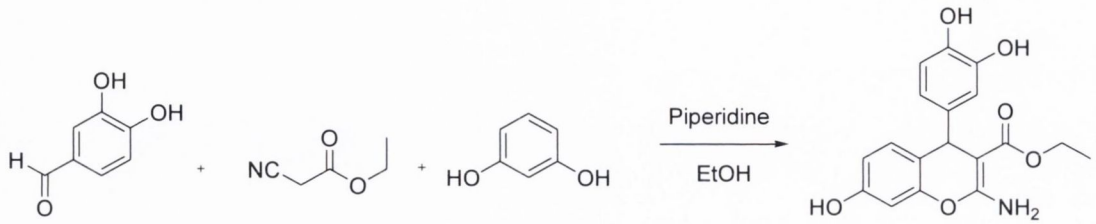

Yield: 1.44 g, 42%, brown solid (Flash Column; CH_2Cl_2 – EtOAc, 9:1)

HPLC Purity: 93 % **MP:** 236-240°C

IR ϑ_{max} (KBr): 3562.46, 3484.58 (OH), 3417.94, 3370.63 (NH_2), 1672.84 (C=O), 1663.63 (C=C), 1663.16 (C=C), 1583.64, 1549.84, 1422.68 cm^{-1}

^{1}H NMR (400 MHz, DMSO-d_6) δ ppm 1.28 (t, 3H *J*=7.03 Hz, CH_3), 4.08 (s, 1H, CH), 4.27 (q, 2H, *J*=7.02, OCH_2), 6.16 - 6.21 (m, 1H, Ar-H), 6.83 (s, 1H, Ar-H), 6.90 - 7.02 (m, 1H, Ar-H), 7.38 (d, 2H *J*=8.53 Hz, Ar-H), 7.65 (s, 1H, Ar-H), 8.09 (s (br), 1H, OH), 8.49 (s (br), 1H, OH), NH_2 not observed.

^{13}C NMR (101 MHz, DMSO-d_6) δ ppm 14.09 (CH_3), 40.08 (CH), 61.72 (CH_2), 79.43 (C), 94.89 (CH), 102.45 (CH), 106.17 (CH), 115.60 (C), 116.00 (CH), 116.96 (CH), 122.05 (CH), 127.79 (C), 129.69 (C-OH), 146.14 (C-OH), 153.94 (C-O), 154.70 (C-OH), 158.44 (O-C-N), 162.95 (C=O)

HRMS (ESI): $C_{18}H_{17}NNaO_6$ [M^+ Na] requires (m/e) 366.0954, found 366.0958, (-1 ppm)

BE56 Ethyl 2-amino-7-hydroxy-4-(3-hydroxyphenyl)-4*H*-chromene-3-carboxylate

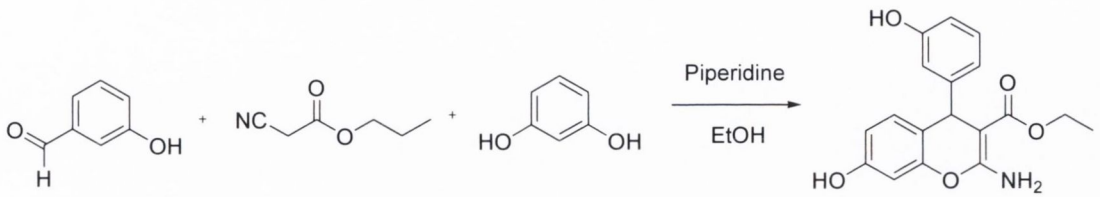

Yield: 1.05 g, 32 %, yellow powder (Flash Column; CH_2Cl_2 - MeOH 5%)

HPLC Purity: 94 % **MP:** 262-268°C **Lit. Ref**. [241]

IRϑ_{max} (KBr): 3573.48, 3531.95 (OH), 3452.17, 3337.51 (NH_2), 1676.48 (C=O), 1638.26 (C=C), 1624.53 (C=C), 1612.94, 1568.38, 1478.42 cm^{-1}

^{1}H NMR (400 MHz, DMSO-d_6) δ ppm 1.07 (t, 3H, *J*=6.78 Hz, CH_3), 2.45 (s (br), 1 H, OH), 3.97 (q, 2H, *J*=7.42 Hz, OCH_2), 4.70 (s, 1H, CH), 6.39 - 6.55 (m, 2H, Ar-H), 6.62 (d, 2H, *J*=7.53 Hz, Ar-H), 6.91 - 7.04 (m, 2H, Ar-H), 7.59 (s, 1H, Ar-H), 9.19 (s (br), 2H, NH_2), 9.61 (s (br), 1 H, OH).

^{13}C NMR (101 MHz, DMSO-d_6) δ ppm 14.29 (CH_3), 40.09 (CH), 58.54 (CH_2), 76.54 (C), 102.01 (CH), 112.00 (CH), 112.75 (C), 113.73 (CH), 116.85 (CH), 117.76 (CH), 128.93 (CH), 129.71 (CH), 149.08 (C), 150.04 (C-O), 156.68 (C-OH), 157.16 (C-OH), 161.01 (O-C-N), 168.41 (C=O)

HRMS (ESI): $C_{18}H_{17}NNaO_5$ [M^+ Na] requires (m/e) 350.1004, found 350.1006, (-0.5 ppm)

BE57 2-Methoxypropyl-2-amino-4-(4-(benzyloxy)phenyl)-7-hydroxy-4*H*-chromene-3-carboxylate

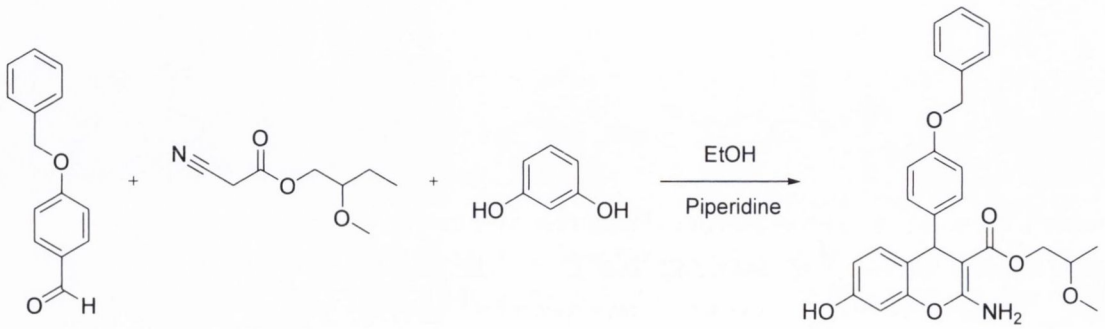

Yield: 2.90 g, 63 %, grey solid (Recrystallisation, EtOH) **HPLC Purity:** 88 %

MP: 178-185 °C

IRϑ_{max} (KBr): 3594.41 (OH), 3471.99, 3372.79 (NH_2), 1672.61 (C=O), 1657.72 (C=C), 1622.37 (C=C), 1583.61, 1497.33 cm^{-1}

^{1}H NMR (400 MHz, DMSO-d_6) δ ppm 1.06 (d, 3H, *J*=7.04 Hz, CH_3), δ 3.35 (s, 3H, CH_3), δ 3.61 (s, 1H, CH), δ 4.33 (d, 2H, *J*=8.06 Hz, CH_2), 4.74 (s, 1H, CH), δ 5.10 (s, 2H, CH_2), δ 6.19 (s, 1H, Ar-CH), δ 6.42 (d, 1H, *J*=8.45, Ar-H), δ 6.78 - 6.84 (m, 2H, Ar-H), δ 7.05 - 7.11 (m, 5H, Ar-H), δ 7.57 (d, *J*=8.04, 2H, Ar-H) δ 7.91 (s (br), 2H, NH_2), δ 8.0 (s (br), 1H, OH)

^{13}C NMR (101 MHz, DMSO-d_6) δ ppm 14.31 (CH_3), δ 38.09 (CH), δ 58.32 (CH_3), δ 69.1 (CH_2), δ 71.47 (CH_2), δ 76.77 (CH), δ 79.01 (C), δ 101.98 (CH), δ 106.17 (CH), δ 112.06 (C) , δ 114.32 (CH), δ 117.62 (CH), δ 127.63 (CH), δ 127.88 (CH), δ 128.38 (CH), δ 129.79 (CH), δ 137.2 (C), δ 141.09 (C), δ 149.07 (C-O), δ 156.4 (C-OH), δ 156.6 (Bnz-C-O), δ 160.92 (O-C-N), δ 168.39 (C=O)

HRMS (ESI): $C_{27}H_{27}NO_6$ [M^+] requires (m/e) 461.1838, found 461.1823. (+ 3.25 ppm)

BE58 Allyl 2-amino-4-(4-(benzyloxy)phenyl)-7-hydroxy-4*H*-chromene-3-carboxylate

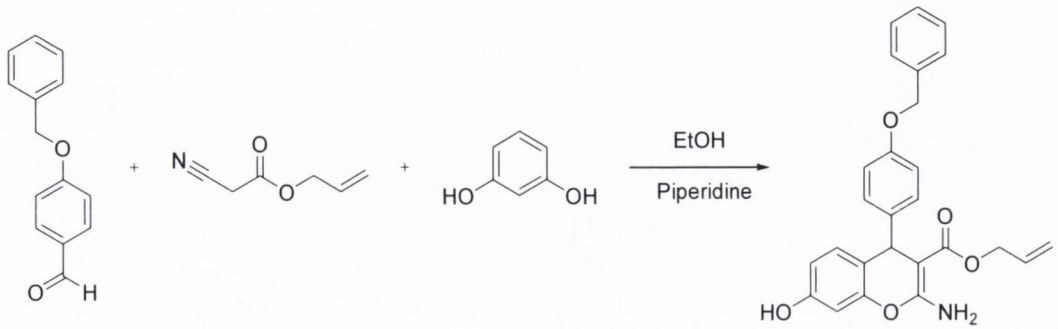

Yield: 1.63 g, 38 %, yellow solid (Recrystallisation, EtOH)

HPLC Purity: 90 % **MP:** 182-183°C

IRϑ_{max} (KBr): 3571.93 (OH), 3469.82, 3420.92 (NH_2), 1673.48 (C=O), 1643.21 (C=C), 1627.42 (C=C), 1530.64, 1474.84 cm^{-1}

^{1}H NMR (400 MHz, DMSO-d_6) δ ppm 1.68 (s (br), 2H, NH_2), δ 4.07 (s, 1H, CH), δ 4.34 - 4.40 (m, 2H, CH_2), δ 5.08 (s, 2H, CH_2), δ 5.14 - 5.24 (m, 2H, CH) δ 5.56 - 5.89 (m, 1H, CH), δ 6.08 (s, 1H, Ar-H), δ 6.34 (s 2H, Ar-H), δ 7.07 (d, 2H, *J*=6.38 Hz, Ar-H), δ 7.28 (s, 2H, Ar-H), δ 7.43 - 7.51 (m, 5H, Ar-H), δ 8.18 (s (br), 1H, OH), NH_2 not observed.

^{13}C NMR (101 MHz, DMSO-d_6) δ ppm 40.25 (CH), δ 62.51 (CH_2), δ 70.52 (CH_2), δ 76.73 (C), δ 105.30 (CH), δ 107.2 (CH), δ 110.3 (C), δ 115.61 (CH), δ 116.42 (CH_2), δ 127.53 (CH), δ 127.95 (CH), δ 128.71 (CH), 129.56 (CH), δ 132.84 (C), δ 133.67 (CH), δ 138.63 (C), δ 141.04 (C-O), δ 153.76 (C-OH), δ 154.89 (Bnz-C-O), δ 158.41 (O-C-N), δ 162.94 (C=O)

HRMS (ESI): $C_{26}H_{22}NO_5$ [M^- - H] requires (m/e) 428.1576, found, 428.1511. (+0.95 ppm)

BE59 3-Methoxybuty-2-amino-4-(4-(benzyloxy)phenyl)-7-hydroxy-4*H*-chromene-3-carboxylate

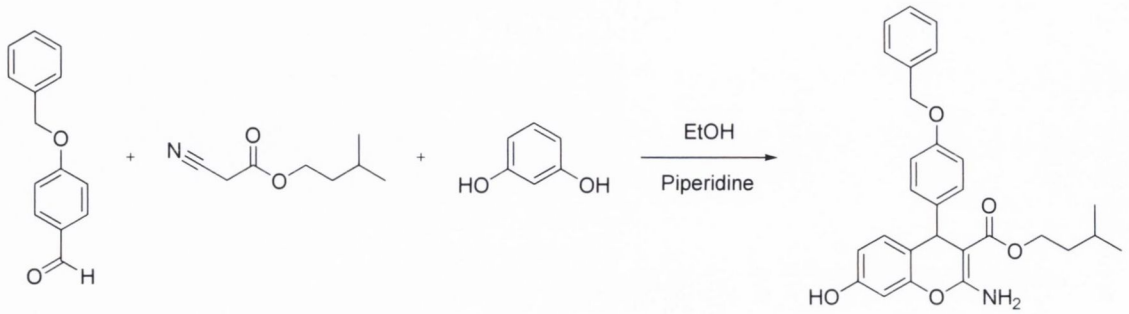

Yield: 1.51 g, 33 %, light brown solid (Recrystallisation, EtOH)

HPLC Purity: 92 % **MP:** 170-172°C

IRϑ_{max} (KBr): 3571.94 (OH), 3420.15, 3219.73 (NH_2), 1676.78 (C=O), 1634.63 (C=C), 1628.64 (C=C), 1503.24, 1462.09 cm^{-1}

^{1}H NMR (400 MHz, DMSO-d_6) δ ppm 1.11 (d, 6H, J=7.04 Hz, 2xCH_3), δ 1.56 - 1.67 (m, 1H, CH), δ 2.36 – 2.41 (m, 2H, CH_2), δ 3.89 - 3.94 (m, 2H, CH_2), δ 4.73 (s, 1H, CH), δ 5.20 (s, 2H, CH_2), δ 6.11 (s, 1H, OH), δ 6.45 (d, 2H, *J*=8.56 Ar-H), δ 6.72 - 6.84 (m, 2H, Ar-H), 7.06 (d, 1H, *J*=8.04 Hz, Ar-H), δ 7.32 – 7.36 (m, 5H, Ar-H), δ 7.49 (s (br), 2H, Ar-H), NH_2 not observed.

^{13}C NMR (101 MHz, DMSO-d_6) δ ppm 14.31 (CH_3), 22.54 (CH), δ 38.09 (CH_2), 40.13 (CH), δ 58.53 (CH_2), δ 69.11 (CH_2), δ 76.78 (C), δ 101.98 (CH), δ 112.05 (CH), δ 114.32 (C), δ 117.06 (CH), δ 127.62 (CH), δ 127.75 (CH), δ 127.87 (CH), δ 127.9 (CH), δ 128 (CH), δ 128.10 (CH), δ 128.38 (CH), δ 129.7 (CH), δ 129.74 (CH), δ 132.85 (C), δ 141.76 (C), δ 149.02 (C-O), δ 154.65 (C-OH), δ 156.60 (Bnz-C-O), δ 160.91 (O-C-N), δ 168.39 (C=O)

HRMS (ESI): $C_{28}H_{29}NNaO_5$ [M^+ + Na] requires (m/e) 482.1943, found 482.1946 (-0.6 ppm)

BE60 3-Methoxybutyl-2-amino-4-(4-(benzyloxy)phenyl)-7-hydroxy-4*H*-chromene-3-carboxylate

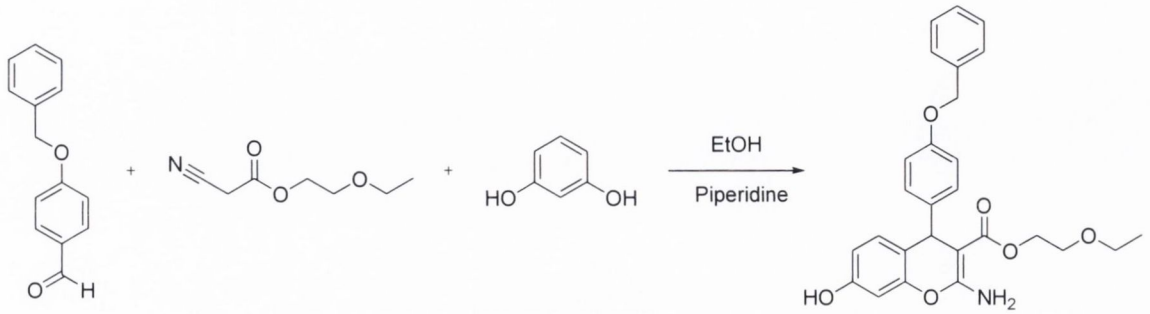

Yield: 1.47 g, 32 %, yellow solid (Recrystallisation, EtOH)

HPLC Purity: 95 % **MP:** 183-187°C

IRϑ_{max} (KBr): 3581.97 (OH), 3476.40, 3420.98 (NH_2), 1658.47 (C=O), 1631.73 (C=C), 1618.56 (C=C), 1583.13 1567.63, 1531.74 cm^{-1}

^{1}H NMR (400 MHz, DMSO-d_6) δ ppm 1.06 (t, 3H, *J*=7.03 Hz, CH_3), δ 1.30 (s (br), 2H, NH_2), δ 3.36 – 3.42 (m, 2H, CH_2), δ 3.94 - 4.04 (m, 2H, CH_2), δ 4.28 – 4.32 (m, 2H, CH_2), δ 4.73 (s, 1H, CH), δ 5.19 (s, 2H, CH_2), δ 6.43 (s, 2H, Ar-H), δ 6.48 (d, 4H, *J*=7.56, Ar-H), δ 6.67 - 6.84 (m, 1H, Ar-H), δ 6.91 - 6.98 (m, 3H, 6.94, Ar-H), δ 7.19 (s, 2H, Ar-H), δ 9.59 (s (br), 1H, OH)

^{13}C NMR (101, DMSO-d_6) δ ppm 20.12 (CH_3), δ 35.09 (CH), δ 40.53 (CH_2), δ 59.11 (CH_2), δ 62.81 (CH_2), δ 70.18 (CH_2), δ 78.12 (C), δ 110.46 (CH), δ 117.62 (C), δ 122.98 (CH), δ 127.57 (CH), δ 128.9 (CH), δ 131.51 (CH), δ 132.90 (CH), δ 135.38 (CH), δ 136.98 (C), δ 141.54 (C), δ 145.72 (C-O), δ 153.46 (C-OH), δ 158.81 (Bnz-C-O), δ 168.39 (O-C-N), δ 170.56 (C=O)

HRMS (ESI): $C_{27}H_{27}NNaO_6$ [M^+ +Na] requires (m/e) 484.1738 found, 484.1739 (+2.22 ppm)

BE61 2-Butoxyethyl-2-amino-4-(4-(benzyloxy)phenyl)-7-hydroxy-4*H*-chromene-3-carboxylate

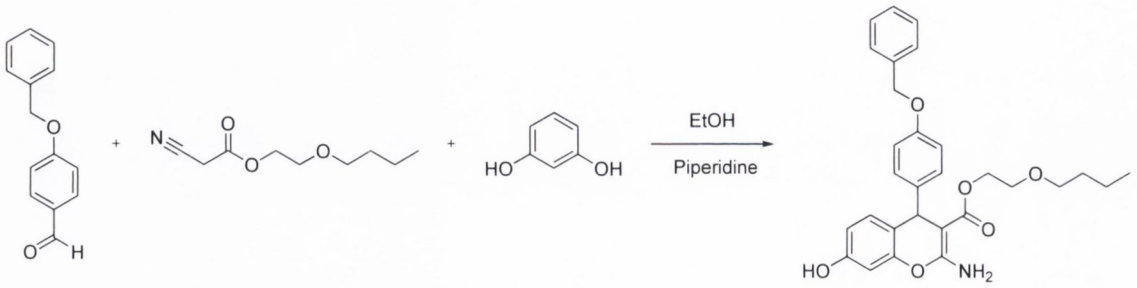

Yield: 1.95 g, 40 %, yellow solid (Recrystallisation, EtOH)

HPLC Purity: 94 % **MP:** 180-185°C

IRϑ_{max} (KBr): 3598.62 (OH), 3485.61, 3423.52 (NH_2), 1673.47 (C=O), 1656.54 (C=C), 1614.27 (C=C), 1559.54, 1519.40, 1493.97 cm^{-1}

^{1}H NMR (400 MHz, DMSO-d_6) δ ppm 1.1 (t, 3H, *J*=7.12 Hz, CH_3), δ 1.43 - 1.49 (m, 2H, CH_2), δ 3.75 - 3.81 (m, 2H, CH_2), δ 4.12 - 4.15 (m, 2H, CH_2), δ 4.38 - 4.43 (m, 2H, CH_2), δ 4.71 (s, 1H, CH), δ 4.84 (s, 2H, CH_2), δ 5.15 - 5.21 (m, 2H, CH_2), δ 6.30 (s, 2H, Ar-H), δ 6.52 (s, 1H, Ar-H), δ 6.61 (s, 1H, Ar-H), δ 6.67 - 6.76 (m, 2H, Ar-H), δ 6.83 (s, 1H, Ar-H), δ 6.85 - 6.92 (m, 5H, Ar-H), δ 8.01 (s (br), 2H, NH_2), δ 8.12 (s (br), H, OH)

^{13}C NMR (101 MHz, DMSO-d_6) δ ppm 13.43 (CH_3), δ 18.91 (CH_2), δ 29.27 (CH_2), δ 38.44 (CH), δ 42.62 (CH_2), δ 53.99 (CH_2), δ 59.06 (CH_2), δ 79.89 (C), δ 102.37 (CH), δ 103.68 (CH), δ 114.42 (C), δ 121.87 (CH), δ 127.92 (CH), δ 128.67 (CH), δ 129.74 (CH), δ 136.28 (C), δ 141.86 (C), δ 148.38 (C-O), δ 151.7 (C-OH), δ 154.74 (Bnz-C-O), δ 156.02 (O-C-N), δ 164.41 (C=O)

HRMS (ESI): $C_{29}H_{31}NNaO_6$ [M^+ +Na] requires (m/e) 512.2049, found 512.2057 (-1.56 ppm)

BE62 Pentyl-2-amino-4-(4-(benzyloxy)phenyl)-7-hydroxy-4*H*-chromene-3-carboxylate

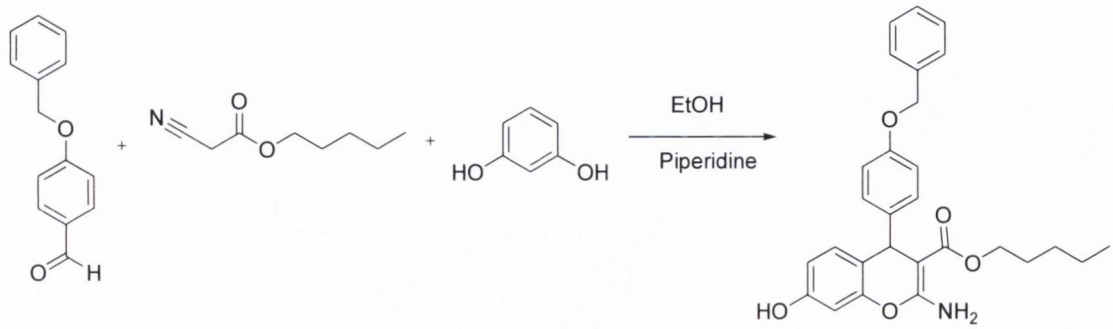

Yield: 1.88 g, 41 %, yellow powder (Recrystallisation, EtOH)

HPLC Purity: 99 % **MP:** 170-176°C

IRϑ_{max} (KBr): 3541.83 (OH), 3486.72, 3425.71 (NH_2), 1683.71 (C=O), 1664.96, 1642.59 (C=C), 1562.58, 1511.48, 1477.28 cm^{-1}

^{1}H NMR (400 MHz, DMSO-d_6) δ ppm 0.98 (t, 3H, *J*=8.01 Hz, CH_3), δ 1.48 – 1.56 (m, 2H, CH_2), δ 1.71 – 1.76 (m, 2H, CH_2), δ 3.42 – 3.49 (m, 2H, CH_2), δ 4.71 - 4.80 (m, 2H, CH_2), δ 5.01 (s, 2H, CH), δ 5.35 (s, 2H, OCH_2), δ 6.11 - 6.19 (m, 2H, Ar-H), δ 6.52 (m, 3H, Ar-H), δ 7.69 (m 2H, Ar-H), δ 8.01 - 8.11 (m, 5H, Ar-H), δ 8.89 (s (br), 2H, NH_2), δ 9.12 (s (br), H, OH)

^{13}C NMR (101 MHz, DMSO-d_6) δ ppm 13.43 (CH_3), δ 18.93 (CH_2), δ 29.27 (CH_2), δ 38.44 (CH), δ 42.62 (CH_2), δ 53.99 (CH_2), δ 69.89 (CH_2), δ 79.84 (C), δ 102.37 (CH), δ 103.68 (CH), δ 114.42 (C), δ 121.87 (CH), δ d 127.9 (CH), δ 128 (CH), δ 129.36 (CH), δ 136.28 (C), δ 148.38 (C), δ 151.7 (C-OH), δ 154.74 (Bnz-C-O), δ 156.02 (O-C-N), δ 164.41 (C=O)

HRMS (ESI): $C_{28}H_{28}NO_5$ [M^- -H] requires (m/e) 458.2045 found at 458.2024 (+4.5 ppm)

BE63 Synthesis of 2-Amino-4(4-benzyloxy-phenyl)-7-hydroxy-4*H*-chromene-3-carboxylic acid ethyl ester

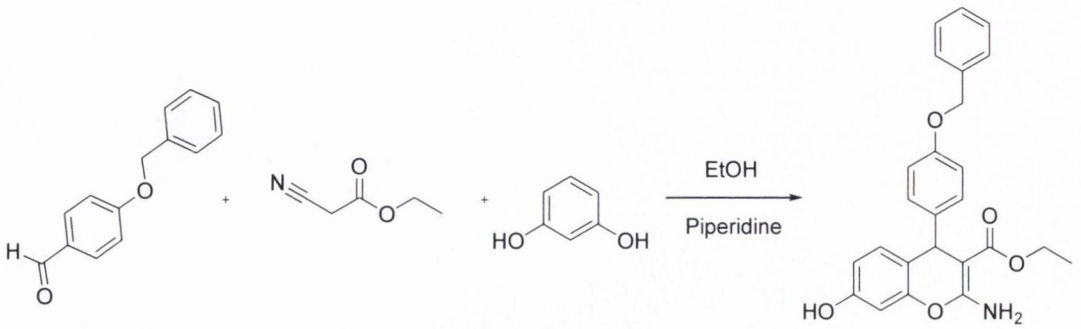

Yield: 1.54 g, 37 %, yellow powder (Recrystallisation, EtOH)

HPLC Purity: 91% **MP:** 192-194°C

IRϑ_{max} (KBr): 3421.76 (OH), 3304.84, 3248.32 (NH_2), 1659.05 (C=O), 1610.67 (C=C), 1598.45 (C=C), 1503.32, 1454.01, 1311.69 cm^{-1}.

^{1}H NMR (400 MHz, DMSO-d6): δ ppm 1.1 (t, 3H, *J*=7 Hz, CH_3), 2.07 (s (br), 2H, NH_2), 3.96 (q, 2H, *J*=7.04 Hz, OCH_2), 4.75 (s, 1H, CH), 5.01 (s, 2H, OCH_2), 6.43 (d, 1H, *J*=6.52 Hz, Ar-H), 6.47 (d, 1H, *J*=8.04 Hz, Ar-H),4 (d, 1H, *J*=8.52 Hz, Ar-H), 6.94 (d, 2H, *J*=8.52 Hz, Ar-H), 7.23 (d, 2H, *J*=8 *Hz*, Ar-H), 7.31 (d, 1H, *J*=7.04 Hz, Ar-H), 7.34 - 7.39 (m, 2H, Ar-H), 7.42 (d, 1H, *J*=6.76 Hz, Ar-H), OH not observed.

^{13}C NMR (100 MHz, DMSO-d6): δ ppm 14.78 (CH_3), 38.58 (CH), 58.19 (CH_2), 69.58 (CH_2), 77.56 (C), 102.46 (CH), 112.53 (CH), 114.80 (C), 117.53 (CH), 128.08 (CH), 128.35 (CH), 128.85 (CH), 130.24 (CH), 137.68 (C), 141.58 (C), 149.51 (C-O), 156.89 (C-OH), 157.09 (Bnz-C-O), 161.39 (O-C-N), 168.87 (C=O).

HRMS (ESI): $C_{25}H_{23}NNaO_5$ [M^+ +Na] requires (m/e) 440.1474, found 440.1463 (-2.5 ppm)

BE64 Hexyl 2-amino-4-(4-(benzyloxy)phenyl)-7-hydroxy-4*H*-chromene-3-carboxylate

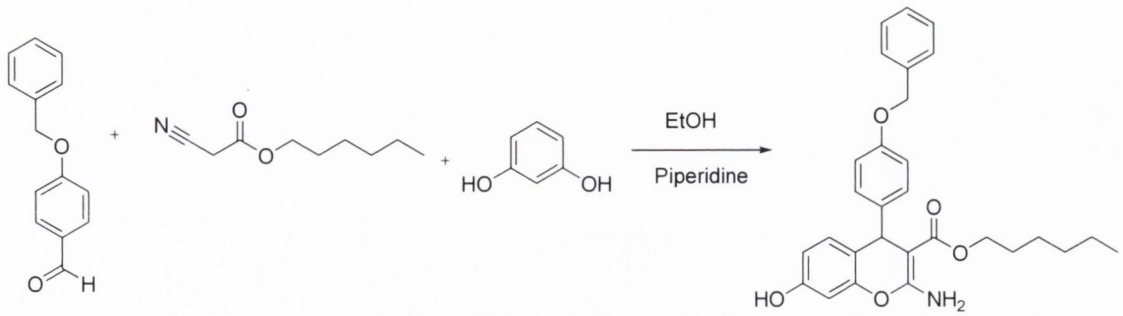

Yield: 1.61 g, 34 %, light brown powder (Recrystallisation, EtOH)

HPLC Purity: 95 % **MP:** 174-179°C

IRϑ_{max} (KBr): 3562.05 (OH), 3468.46, 3422.15 (NH_2), 1669.48 (C=O), 1651.62, 1624.73 (C=C), 1563.95, 1525.79 cm^{-1}

^{1}H NMR (400 MHz, DMSO-d_6) δ ppm 1.08 (t, 3H, *J*=7.05 Hz, CH_3), δ 1.20 (t, *J*=6.85 Hz, 2H, CH_2), δ 2.61 – 2.68 (m, 6H, 3xCH_2), δ 3.94 (d, *J*=8.2 Hz, 2H, CH_2), δ 4.73 (s, H, CH), δ 5.16 (s, 2H, CH_2), δ 6.42 (d, 2H, *J*=8.24 Hz, Ar-H), δ 6.68 (d, 2H, *J*=8.57 Hz, Ar-H), δ 6.84 (s, 1H, Ar-H), δ 7.03 (d, 2H, *J*=7.11 Hz, Ar-H), δ 7.34 - 7.38 (m, 5H, Ar-H), δ 8.23 (s (br), 2H, NH_2), δ 8.51 (s (br), 1H, OH)

^{13}C NMR (101 MHz, DMSO-d_6) δ ppm 14.31 (CH_3), δ 21.01 (CH_2), δ 27.07 (CH_2), δ 28.44 (CH_2), δ 31.01 (CH_2), δ 38.10 (CH), δ 57.47 (CH_2), δ 69.11 (CH_2), δ 76.77 (C), δ 101.98 (CH), δ 112.05 (CH), δ 114.32 (C), δ 116.45 (CH), δ 127.62, (CH), δ 128.38 (CH), δ 129.77 (CH), δ 130.64 (CH), δ 137.23 (C), δ 143.37 (C), δ 149.74 (C-O), δ 156.41 (C-OH), δ 156.62 (Bnz-C-O), δ 160.91 (O-C-N), δ 168.39 (C=O)

HRMS (ESI): $C_{29}H_{30}NO_5$ [M^--H] requires (m/e) 472.2124, found 472.2138 (-2.96 ppm)

BE65 Heptyl-2-amino-4-(4-(benzyloxy)phenyl)-7-hydroxy-4*H*-chromene-3-carboxylate

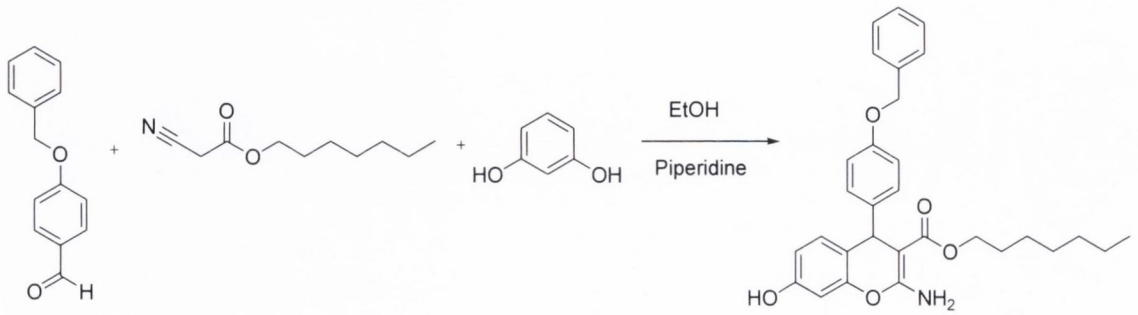

Yield: 1.80 g, 37 %, light brown solid (Recrystallisation, EtOH)

HPLC Purity: 94 % **MP:** 176-180°C

IRϑ_{max} (KBr): 3582.65 (OH), 3472.84, 3421.37 (NH_2), 1684.37 (C=O), 1660.86 1628.63 (C=C), 1594.32, 1561.64, 1501.02 cm^{-1}

^{1}H NMR (400 MHz, DMSO-d_6) δ ppm 0.96 (t, 3H, *J*=6.25 Hz, CH_3), δ 1.38 - 1.45 (m, 8H, 4xCH_2), δ 1.87 (d, 2H, *J*=7.31 Hz, CH_2), δ 4.18 - 4.23 (m, 2H, CH_2), δ 4.80 (s, 1H, CH), δ 5.19 (s, 2H, CH_2), δ 6.11 (s, 1H, Ar-H), δ 6.24 (d, 1H, *J*=7.24 Hz, Ar-H), δ 6.58 - 6 64 (m, 2H, Ar-H), δ 6.74 (s, 1H, Ar-H), δ 7.10 - 7.17 (m, 2H, Ar-H), δ 7.19 - 7.26 (m, 5H, Ar-H), δ 8.83 (s (br), 2H, NH_2), δ 9.01 (s (br), H, OH)

^{13}C NMR (101 MHz, DMSO-d_6) δ ppm 14.36 (CH_3), δ 22.09 (CH_2), δ 25.35 (CH_2), δ 29.56 (CH_2), δ 31.19 (CH_2), δ 37.56 (CH), δ 58.53 (CH_2), δ 62.51 (CH_2), δ 70.48 (C), δ 104.36 (CH), δ 113.57 (CH), δ 114.32 (C), δ 117.06, (CH), δ 127.38 (CH), δ 127.63 (CH), δ 127.75 (CH), δ 129.95 (CH), δ 136.37 (C), δ 141.74 (C), δ 149.41 (C-O), δ 156.42 (C-OH), δ 157.30 (Bnz-C-O), δ 164.93 (O-C-N), δ 167.83 (C=O)

HRMS (ESI): $C_{30}H_{33}NNaO_5$ [M^+ +Na] requires (m/e) 510.2256 found at 510.2254 (+0.3 ppm)

BE66 Octyl-2-amino-4-(4-(benzyloxy)phenyl)-7-hydroxy-4*H*-chromene-3-carboxylate

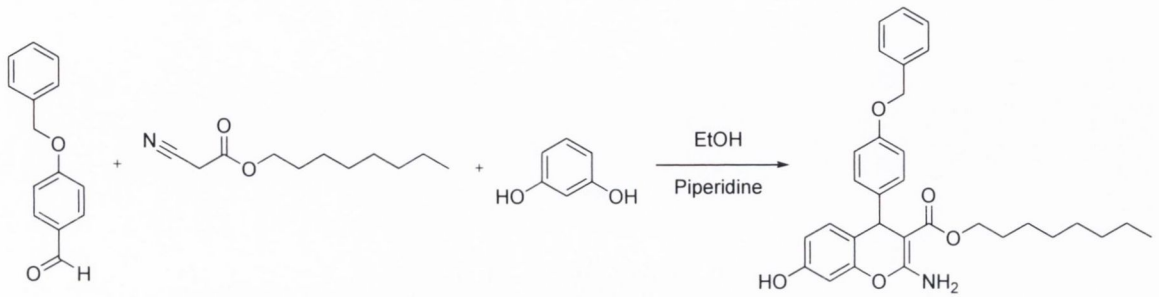

Yield: 2.25 g, 45 %, brown solid (Recrystallisation, EtOH)

HPLC Purity: 90 % **MP:** 164-166 °C

IRϑ_{max} (KBr): 3494.62 (OH), 3421.14, 3338.74 (NH_2), 1684.35 (C=O), 1670.72, 1648.28 (C=C), 1593.74, 1540.01, 1512.57 cm^{-1}.

^{1}H NMR (400 MHz, DMSO-d_6): δ ppm 0.98 (t, 3H, *J*=7.22 Hz, CH_3), δ 1.35 – 1.41 (m, 8H, 4xCH_2), δ 1.92 (d, 4H, *J*=7.02 Hz, 2xCH_2), δ 4.14 - 4.21 (m, 2H, CH_2), δ 4.81 (s, 1H, CH), δ 5.18 (s, 2H, CH_2), δ 6.02 (d, 2H, *J*=6.79 Hz, Ar-H), δ 6.68 – 6.72 (m, 2H, Ar-H), δ 6.86 (s, 1H, Ar-H), δ 7.18 - 7.21 (m, 2H, Ar-H), δ 7.25 – 7.32 (m, 5H, Ar-H), δ 8.24 (s (br), 2H, NH_2), OH not observed.

^{13}C NMR (101 MHz, DMSO-d_6): δ ppm 16.21 (CH_3), δ 20.65 (CH_2), δ 23.41 (CH_2), δ 25.73 (CH_2), δ 28.19 (CH_2), δ 31.63 (CH_2), δ 39.66 (CH), δ 65.91 (CH_2), δ 68.71 (CH_2), δ 79.51 (C), δ 107.28 (CH), δ 110.01 (CH), δ 112.54 2 (C), δ 116.92 (CH), δ 126.63 (CH), δ 127.51 (CH), 129.61 (CH), δ 130.87 (CH), δ 132.85 (C), δ 141.74 (C), δ 154.17 (C-O), δ 159.61 (C-OH), δ 160.42 (Bnz-C-O), δ 161.13 (O-C-N), δ 173.29 (C=O)

HRMS (ESI): $C_{31}H_{35}NNaO_5$ [M^+ +Na] requires (m/e) 524.2413 found at 524.2419 (-1.14 ppm)

BE67 Decyl-2-amino-4-(4-(benzyloxy)phenyl)-7-hydroxy-4*H*-chromene-3-carboxylate.

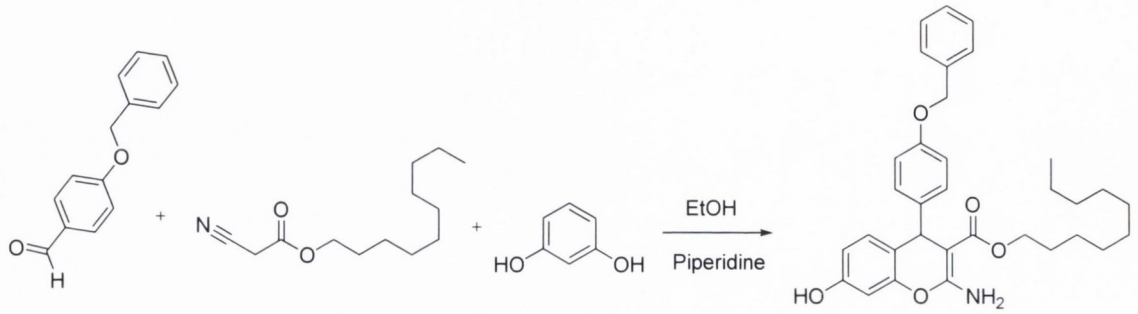

Yield: 2.96 g, 56 %, light brown powder (Recrystallisation, EtOH)

HPLC Purity: 91 % **MP:** 186-189°C

IRϑ_{max} (KBr): 3541.95 (OH), 3442.68, 3415.42 (NH_2), 1683.57 (C=O), 1658.45 (C=C), 1606.32 (C=C), 1587.35, 1567.52, 1532.58 cm-1

^{1}H NMR (400 MHz, DMSO-d_6): δ ppm 1.01 (t, 3H, *J*=7.42 Hz, CH_3), δ 1.32 - 1.41 (m, 12H, 6xCH_2), δ 1.46 (d, 2H, *J*=8.45 Hz, CH_2), δ 1.58 (t, 2H, *J*=6.76 Hz, CH_2), δ 4.61 (q, 2H, *J*=6.91, CH_2) δ 5.03 (s, 1H, CH), δ 5.28 (s, 2H, CH_2), δ 6.31 (d, 1H, *J*=7.38, Ar-H), δ 6.27 - 6.34 (m, 1H, Ar-H), δ 6.78 - 6.86 (m, 2H, Ar-H), δ 7.25 - 7.31 (m, 1H, Ar-H), δ 7.38 - 7.46 (m, 2H, Ar-H), δ 7.61 - 7.71 (m, 5H, Ar-H), δ 7.95 (s (br), 2H, NH_2) δ 8.18 (s (br), 1H, OH)

^{13}C NMR (101 MHz, DMSO-d_6): δ ppm 14.25 (CH_3), δ 22.51 (CH_2), δ 25.52 (CH_2), δ 29.46 (CH_2), δ 30.83 (CH_2), δ 31.37 (CH_2), δ 40.2 (CH), δ 66.78 (CH_2), δ 75.01 (CH_2), δ 79.42 (C), δ 106.76 (CH), 109,88 (CH), 110,21 (C), δ 114.67 (CH), δ 127.53 (CH), δ 127.95 (CH), δ 128.71 (CH), δ 129.63 (CH), δ 133.67 (C), δ 140.04 (C), 156.04 (C-O), δ 157.41 (C-OH), 158.04 (Bnz-C-O), δ 160.41 (O-C-N), δ 168.94 (C=O).

HRMS (ESI): $C_{33}H_{39}NNaO_5$ [M^+ +Na] requires (m/e) 552.2726, found 552.2727 (-0.1 ppm)

BE68 Cyclohexyl 2-amino-4-(4-(benzyloxy)phenyl)-7-hydroxy-4*H*-chromene-3-carboxylate

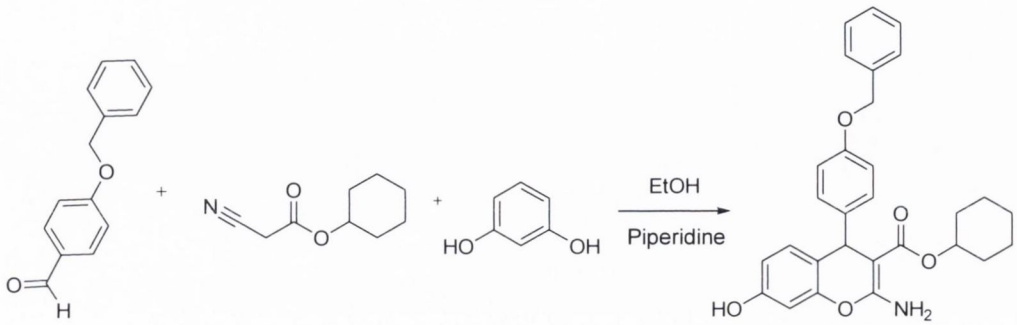

Yield: 2.35 g, 50 %, light brown powder (Recrystallisation, EtOH)

HPLC Purity: 84 % **MP:** 150-154 ° C

IRϑ_{max} (KBr): 3548.31 (OH), 3491.93, 3417.25 (NH_2), 1760.17 (C=C), 1649.74(C=C), 1620.10 (C=O), 1573.95, 1552.84, 1521.69 cm-1

^{1}H NMR (400 MHz, DMSO-d_6): δ ppm 1.38 - 1.47 (m, 6H, 3xCH_2), δ 1.50-1.56 (m, 4H, 2xCH_2), δ 4.37 - 4.28 (m, 1H, CH), δ 4.76 (s, 1H, CH) δ 5.31 (s, 2H, CH_2), δ 6.18 (s, 1H, Ar-H), δ 6.25 (d, 1H, *J*=6.28, Ar-H), δ 6.37 (d, 2H, J=7.31, Ar-H), δ 6.78 (s, 1H, Ar-H), δ 7.02 - 7.13 (m, 2H, Ar-H), δ 7.38 - 7.57 (m, 5H, Ar-CH), δ 7.84 (s (br) 2H, NH_2) δ 8.79 (s (br), 1H, OH)

^{13}C NMR (101 MHz, DMSO-d_6): δ ppm 23.25 (CH_2), δ 28.41 (CH_2), δ 32.18 (CH_2) , δ 40.83 (CH), δ 71.37 (CH_2), δ 74.92 (CH), δ 78.77 (C), δ 105.53 (CH), δ 110.95 (CH), δ δ 113.67 (C), δ 114.23 (CH), δ 127.79 (CH), δ 129.48 (CH), δ 130.15 (CH), δ 131.71 (CH), δ δ 133.31 (C), δ 141.64 (C), 154.41 (C-O), δ 154.98, (C-OH), 157.04 (Bnz-C-O), δ 160.79 (O-C-N), δ 175.52 (C=O)

HRMS (ESI): $C_{29}H_{29}NNaO_5$ [M^+ +Na] requires (m/e) 494.2045, found 494.2035 (+2.02 ppm)

BE69 Ethyl 2-amino-7-hydroxy-4-(3,4-dihydroxyphenyl)-4*H*-chromene-3-carboxylate

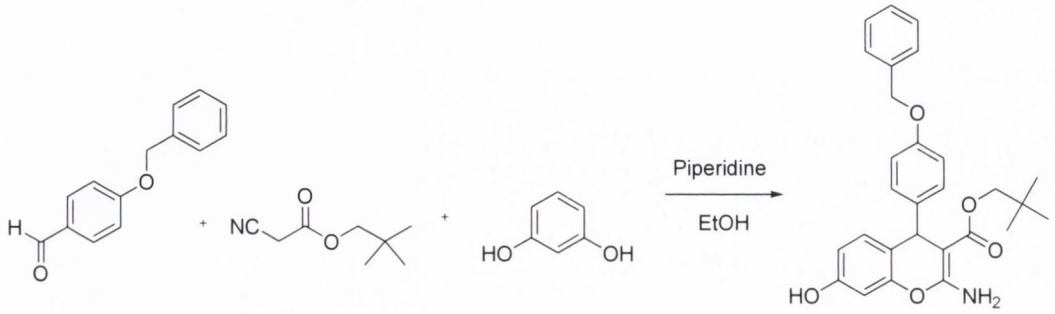

Yield: 0.59 g, 13 %, yellow powder (Recrystallisation, EtOH)

HPLC Purity: 92 % **MP:** 248-254°C

IRϑ_{max} (KBr): 3483.73 (OH), 3465.83, 3386.24 (NH_2), 1685.80 (C=O), 1669.72 (C=C), 1636.22 (C=C), 1614.37, 1521.93, 1483.63 cm^{-1}

^{1}H NMR (400 MHz, DMSO-d_6) δ ppm 0.74 (s, 9H, 3xCH_3), 3.94 (s, 2H, OCH_2), 4.79 (s, 1 H, CH), 5.01 (s, 2H, OCH_2), 6.40 - 6.49 (m, 3 H, Ar-H), 6.84 (d, 2H, *J*=8.04 Hz, Ar-H), 7.05 (d, 3H, *J*=8.80 Hz, Ar-H), 7.10 (d, 3H, *J*=7.24 Hz, Ar-H), 7.35 (s, 1 H, Ar-H), 7.54 (s (br), 1H, OH), 7.61 (s (br), 2 H, NH_2)

^{13}C NMR (101 MHz, DMSO-d_6) δ ppm 26.21 (CH_3), 31.04 (C), 38.16 (CH), 69.09 (CH_2), 71.88 (CH_2), 76.09 (C), 102.00 (CH), 112.06 (CH), 114.32 (C), 114.52 (CH), 117.20 (CH), 127.51 (CH), 129.62 (CH), 130.12 (CH), 132.69 (C), 141.48 (C), 155.88 (C-O), 156.35 (C-OH), 158.38 (Bnz-C-O), 160.20 (O-C-N), 164.91 (C=O)

HRMS (ESI): $C_{28}H_{30}NO_5$ [M^+ H] requires (m/e) 460.2124, found 460.2114, (+2.17 ppm)

BE70 Synthesis of 2-Amino-4(3-Benzyloxy-phenyl)-7-hydroxy-4*H*-chromene-3-carboxylic acid ethyl ester

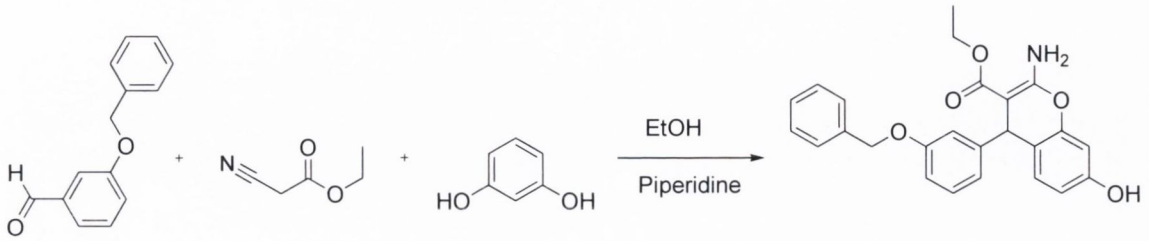

Yield: 1.42 g, 34 %, yellow powder (Recrystallisation, EtOH)

HPLC Purity: 85% **MP:** 211-213°C

IRϑ_{max} (KBr): 3525.58 (OH), 3442.95, 3385.65 (NH_2), 1664.84 (C=O), 1632.78 1614.27 (C=C), 1582.45, 1538.65 cm^{-1}

^{1}H NMR (400 MHz, DMSO-d6): δ ppm 1.04 (t, 3H, *J*=7.02 Hz, CH_3), 3.95 (q, 2H, *J*=6.76 Hz, OCH_2), 4.76 (s, 1H, CH), 5.02 (dd, 2H, *J*=2.14, *J*=8.02 Hz, OCH_2), 6.39 - 6.43 (m, 2H, Ar-H), 6.71 - 6.82 (m, 3H, Ar-H), 6.97 (d, 1H, *J*=8.52 Hz, Ar-H), 7.12 (d, 1H, *J*=8.04 Hz, Ar-H), 7.37 - 7.86 (m, 5H, Ar-H), 7.56 (s (br), 2H, NH_2), OH not observed

^{13}C NMR (100 MHz, DMSO-d6): δ ppm 14.29 (CH_3), 30.70 (C), 58.53 (CH_2), 69.03 (CH_2), 76.32 (C), 102.04 (CH), 111.45 (CH), 112.06 (CH), 113.90 (C), 116.59 (CH), 119.38 (CH), 127.77 (CH), 128.39 (CH), 129.20 (CH), 129.74 (CH), 149.03 (C), 150.24 (C-O), 156.75 (C-OH), 158.16 (O-C-N), 161.06 (Bnz-C-O), 168.33 (C=O)

HRMS (ESI): $C_{25}H_{23}NNaO_5$ [M^+ +Na] requires (m/e) 440.1474, found 440.1475 (+0.2 ppm)

BE71 Allyl 4-(4-(3-Chlorobenzyloxy) phenyl)-2-amino-7-hydroxy-4*H* chromene-3-carboxylate

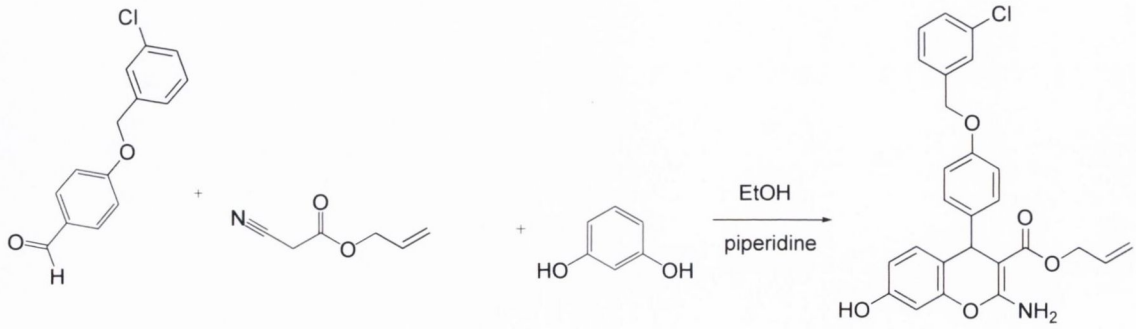

Yield: 0.65 g, 14 %, yellow solid (Flash Column, CH_2Cl_2 - MeOH 10%)

HPLC Purity: 99 % **MP:** 142°C

IRϑ_{max} (KBr): 3562.65 (OH), 3416.32 (NH_2), 3304.09 (NH_2), 1660.17 (C=O), 1629.46, 1628.45 (C=C), 1610.47, 1570.53, 777.23 (C-Cl) cm^{-1}.

^{1}H NMR (400 MHz, DMSO-d_6): δ ppm 3.94 (s, 1H, CH) δ 4.68 - 4.73 (m, 2H, CH_2), δ 5.03 (s, 2H, -C=CH_2), δ 5.34 – 5.39 (m, 2H, CH_2), δ 5.58 - 5.62 (m, 2H, CH), δ 6.45 (d, 2H, *J*=7.26, Ar-H), δ 6.85 – 6.91 (m, 1H, Ar-H), δ 6.95 (d, 2H, *J*=8.52 Hz, Ar-H), δ 7.32 - 7.38 (m, 3H, Ar-H) δ 7.47 – 7.56 (s, 3H, Ar-H) δ 7.61 (s (br), 2H, NH_2) δ 9.59 (s (br), 1H, OH)

^{13}C NMR (101 MHz, DMSO-d_6): δ ppm 39.89 (CH), δ 76.32 (CH_2), δ 76.0 (CH_2), δ 80.14 (C), δ 104.19 (CH), δ 114.44 (CH), δ 113.83 (C), δ 115.18 (CH), δ 116.72 (-C=CH_2), δ 124.12 (CH), δ 125.83 (CH), δ 127.37 (CH), δ 128.89 (CH), δ 129.91 (CH), δ 130.26 (C), δ 131.34 (CH), δ 133.89 (C-Cl), δ 142.13 (C), δ 156.34 (C-O), δ 158.97 (C-OH), δ 161.31 (Bnz-C-O), δ 163.38 (O-C-N), δ 168.58 (C=O)

HRMS (ESI): $C_{26}H_{22}{}^{37}ClNO_5$ [M^- +Na] requires (m/e) 486.1186, found 486.0884

BE72 Ethyl 4-(4-(2-Fluorobenzyloxy) phenyl)-2-amino-7-hydroxy-4*H*-chromene-3- carboxylate

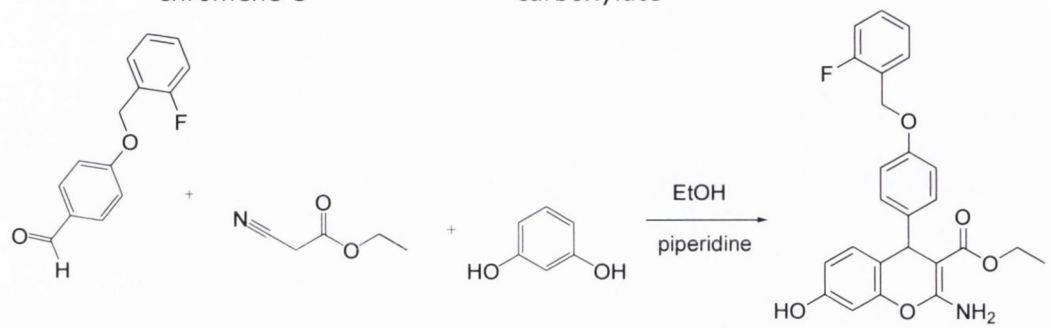

Yield: 2.52 g, 58 %, brown solid (Flash Column; CH_2Cl_2 - MeOH 10%)

HPLC Purity: 97 % **MP:** 148°C

IRϑ_{max} (KBr): 3581.63 (OH), 3421.38 (NH_2), 3299.51 (NH_2), 1665.23 (C=O), 1642.85, 1639.48 (C=C), 1563.85, 1532.95, 1158.7 (C-F) cm^{-1}.

^{1}H NMR (400 MHz, DMSO-d_6): δ ppm 1.07 (t, 3H, *J*=6.42 Hz, CH_3), δ 3.95 (q, 2H, *J*=7.04 Hz, OCH_2), δ 4.74 (s, 1H, CH), δ 5.04 (s, 2H, CH_2), δ 6.18 – 6.22 (m, 1H, Ar-H), δ 6.42 (s, 1H, Ar-H), δ 6.47 (d, 1H, *J*=8.52 Hz, Ar-H), δ 6.83 - 6.92 (m, 2H, Ar-H) δ 7.05 (d, 2H, *J*=7.04 Hz, Ar-H) δ 7.25 – 7.31 (m, 2H, Ar-H) δ 7.41 – 7.46 (m, 1H, Ar-H), δ 7.51 (d, 1H, *J*=7.54 Hz, Ar-H), δ 7.57 (s (br), 2H, NH_2), δ 9.59 (s (br), 1H, OH)

^{13}C NMR (101 MHz, DMSO-d_6): δ ppm 14.31 (CH_3), δ 39.49 (CH), δ 58.53 (Bnz-OCH_2), δ 63.37 (OCH_2), δ 76.74 (C), δ 101.99 (CH), δ 102.44 (CH), δ 112.06 (C), δ 114.24 (CH), δ 115.24 (CH), δ 124.01 (CH), δ 127.93 (C), δ 128.47 (CH), δ 129.7 (CH), δ 130.63 (CH), δ 131.33 (C), δ 149.02 (C-O), δ 156.23 (C-OH), δ 156.61 (Bnz-C-O), δ 158.44 (C-F), δ 160.91 (O-C-N), δ 168.38 (C=O)

HRMS (ESI): $C_{25}H_{21}FNO_5$ [M^- -H] requires (m/e) 434.1482, found 434.1407

BE73 2-Ethoxyethyl 4-(4-(3-bromobenzyloxy) phenyl)-2-amino-7-hydroxy-4*H*-chromene 3-carboxylate

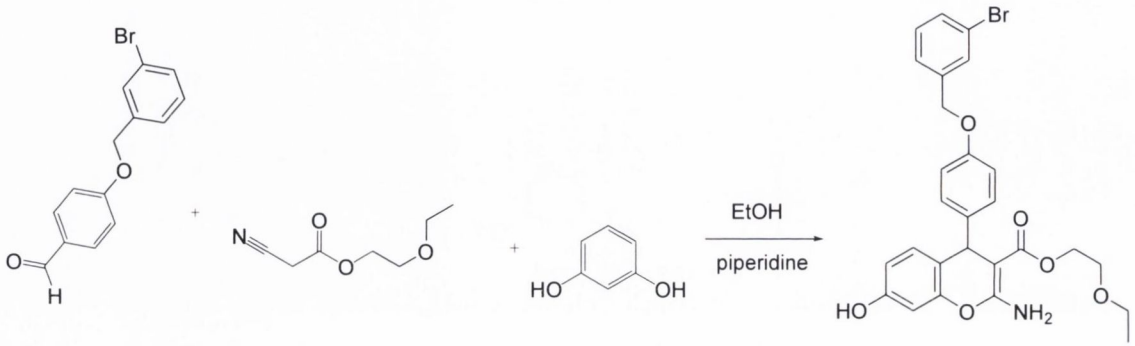

Yield: 1.13 g, 21 %, light brown solid (Flash Column, CH_2Cl_2 - MeOH 10%)

HPLC Purity: 93 % **MP:** 105- 107 °C

IRϑ_{max} (KBr): 3580.42 (OH), 3418.31 (NH_2), 3303.27 (NH_2), 1659.36 (C=O), 1631.52, 1628.46 (C=C), 1589.46, 1548.31, 774.64 (C-Br) cm^{-1}

^{1}H NMR (400 MHz, DMSO-d_6): δ ppm 1.05 (t, 3H, *J*=7.26 Hz, CH_3) δ 2.36 – 2.42 (m, 2H, CH_2), δ 3.89 - 3.94 (m, 2H, CH_2), δ 4.03 (q, 2H, *J*=7.04 Hz, CH_2), δ 4.73 (s, 1H, CH), δ 5.02 (s, 2H, CH_2), δ 6.19 (s, 1H, Ar-H), δ 6.42 (d, 2H, *J*=6.48 Hz, Ar-H), δ 6.85 (d, 1H, *J*=8.56 Hz, Ar-H), δ 6.95 (d, 2H, *J*=8.52 Hz, Ar-H), δ 7.04 – 7.11 (m, 2H, Ar-H) δ 7.34 (d, 1H, *J*=7.04 Hz, Ar-H) δ 7.43 (s, 1H, Ar-H), δ 7.51 (d, 1H, *J*=8.04 Hz, Ar-H), δ 7.61 (s (br), 2H, NH_2), δ 8.59 (s (br), 1H, OH)

^{13}C NMR (101 MHz, DMSO-d_6): δ ppm 14.15 (CH_3), δ 39.49 (CH), δ 58.53 (CH_2), δ 59.77 (CH_2), δ 68.13 (CH_2), δ 69.51 (CH_2), δ 76.74 (C), δ 101.99 (CH), δ 102.45 (CH), δ 112.06 (C), δ 114.36 (CH), δ 117.01 (C-Br), δ 121.65 (CH), δ 126.49 (CH), δ 127.94 (CH), δ 129.69 (CH), δ 130.56 (CH), δ 133.09 (C), δ 141.32 (C), δ 149.01 (C-O), δ 156.15 (C-OH), δ 158.44 (C-O), δ 160.9 (O-C-N), δ 168.38 (C=O)

HRMS (ESI): $C_{27}H_{26}{}^{81}BrNO_6$ [M^+ + H] requires (m/e) 540.0943, found 540.0051

BE74 Pentyl 4-(4-(4-Fluorobenzyloxy) phenyl)-2-amino-7-hydroxy-4*H*-chromene-3- carboxylate

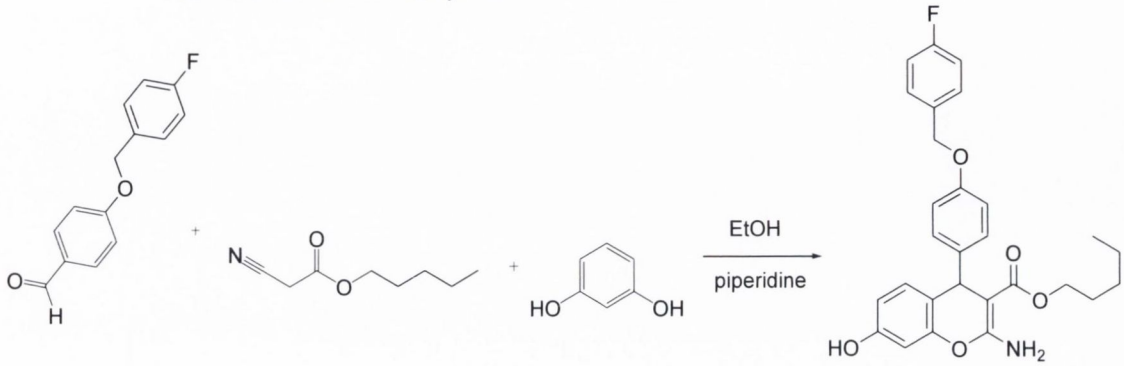

Yield: 0.24 g, 5 %, light brown solid (Flash Column; CH_2Cl_2 - MeOH 10%)

HPLC Purity: 99 % **MP:** 146 °C

IRϑ_{max} (KBr): 3521.47 (OH), 3420.45 (NH_2), 3301.61 (NH_2), 1656.23 (C=O), 1626.42, 1618.41 (C=C), 1568.32, 1159.7 (C-F) cm^{-1}.

^{1}H NMR (400 MHz, DMSO-d_6): δ ppm 1.05 (t, 3H, *J*=7.0 Hz, CH_3) δ 1.32 – 1.38 (m, 4H, 2xCH_2), δ 1.45 – 1.51 (m, 2H, *J*=7.52 Hz, CH_2), δ 4.01 (q, 2H, *J*=6.62 Hz, CH_2), δ 4.75 (s, 1H, CH), δ 4.94 (s, 2H, OCH_2), δ 6.79 - 6.86 (m, 2H, Ar-H), δ 7.01 - 7.06 (m, 2H, Ar-H), δ 7.09 - 7.18 (m, 4H, Ar-H), δ 7.24 - 7.37 (m, 2H, Ar-H), δ 7.55 (s (br), 2H, NH_2), 8.08 (s (br), 1H, OH)

^{13}C NMR (101 MHz, DMSO-d_6): δ ppm 13.83 (CH_3), δ 18.84 (CH_2), δ 30.70 (CH_2), δ 31.35 (CH_2), δ 40.01 (CH), δ 60.24 (CH_2), δ 69.97 (CH_2), δ 76.74 (C), δ 102.45 (CH), δ 106.17 (CH), δ 112.06 (C), δ 114.36 (CH), δ 117.02 (CH), δ 127.90 (CH), δ 129.41 (CH), δ 129.78 (CH), δ 131.31 (C), δ 136.70 (C), δ 149.02 (C-O), δ 156.19 (C-OH), δ 156.61 (Bnz-C-O), δ 158.45 (O-C-N), δ 160.91 (C-F), δ 168.38 (C=O)

HRMS (ESI): $C_{28}H_{28}FNO_5$ [M^- -H] requires (m/e) 476.1951, found 476.1932

BE75 2-Butoxyethyl 4-(4-(4-bromobenzyloxy)phenyl)-2-amino-7-hydroxy-4*H*-chromene-3-carboxylate

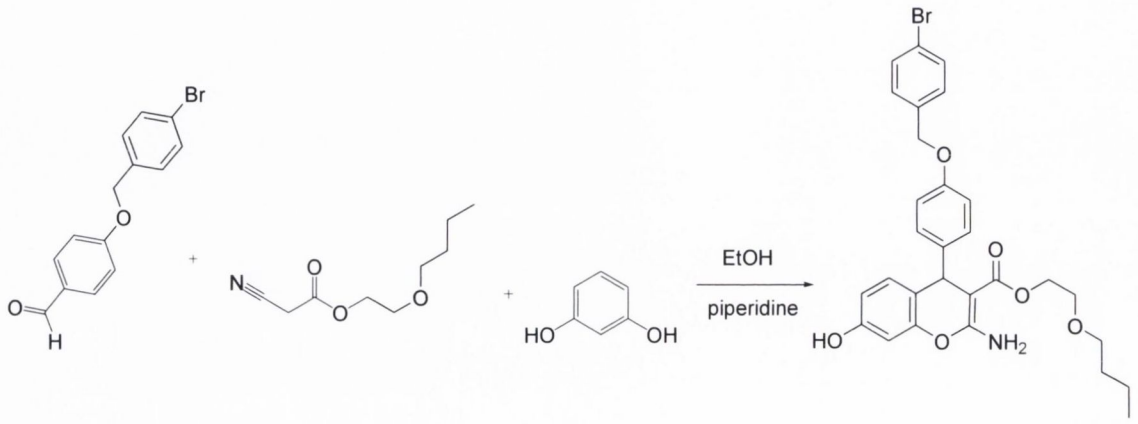

Yield: 0.68 g, 12 %, light brown solid (Flash Column, CH_2Cl_2 - MeOH 10%)

HPLC Purity: 98 % **MP:** 144- 147°C

IRϑ_{max} (KBr): 3575.98 (OH), 3412.77 (NH_2), 3299.51 (NH_2), 1659.06 (C=O), 1630.74 1610.02 (C=C), 753.04 (C-Br) cm^{-1}

^{1}H NMR (400 MHz, DMSO-d_6): δ ppm 0.87 (t, 3H, *J*=7.04 Hz, CH_3), δ 1.05 – 1.11 (m, 2H, CH_2), δ 2.09 (s, 2H, CH_2), δ 2.51 (s, 2H, CH_2), δ 3.36 (s, 2H, CH_2), δ 3.94 – 3.99 (m, 2H, CH_2), δ 4.73 (s, 1H, CH), δ 4.99 (s, 2H, CH_2), δ 6.18 (d, 2H, *J*=7.16 Hz, Ar-H), δ 6.42 (d, 1H, *J*=7.02 Hz, Ar-H), δ 6.46 (d, 2H, *J*=8.52 Hz, Ar-H), δ 6.84 (d, 2H, *J*=7.24 Hz, Ar-H), δ 6.94 (d, 2H, *J*=8.56 Hz, Ar-H), δ 7.04 (d, 2H, *J*=7.12 Hz, Ar-H), δ 7.57 (s (br), 2H, NH_2), δ 9.59 (s (br), 1H, OH)

^{13}C NMR (101 MHz, DMSO-d_6): δ ppm 14.31 (CH_3), δ 18.85 (CH_2), δ 31.36 (CH_2) δ 39.49 (CH), δ 58.53 (CH_2), δ 60.24 (CH_2), δ 68.29 (CH_2), δ 69.98 (CH_2) δ 76.75 (C), δ 102.46 (CH), δ 106.17 (CH), δ 112.06 (C), δ 114.36 (CH), δ 120.08 (C-Br), δ 127.91 (CH), δ 129.71 (CH), δ 131.31 (CH), δ 136.71 (C), δ 141.25 (C), δ 156.19 (C-O), δ 157.56 (C-OH), δ 158.45 (Bnz-C-O), δ 160.91 (O-C-N), δ 168.38 (C=O)

HRMS (ESI): $C_{29}H_{30}{}^{81}BrNO_6$ [M^+ +OH] requires (m/e) 584.1256, found 584.1796

BE76 Allyl 2-amino-7-hydroxy-4-(3,4,5-trimethoxyphenyl)-4*H*-chromene-3-carboxylate

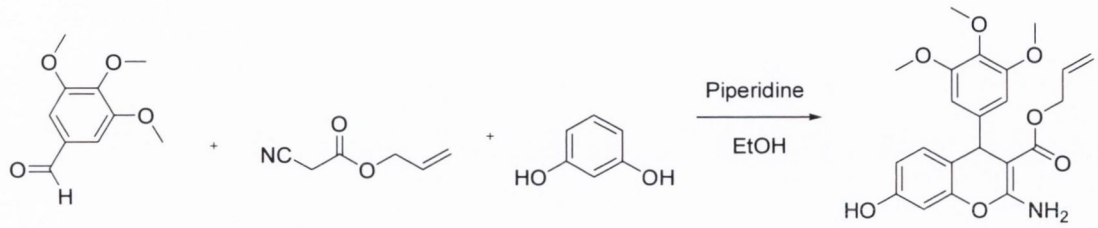

Yield: 1.90 g, 46 %, light brown solid (Recrystallisation, EtOH)

HPLC Purity: 100 % **MP:** 214-218°C

IRϑ_{max} (KBr): 3560.58 (OH), 3464.12, 3379.72 (NH_2), 1671.47 (C=O), 1645.91 (C=C), 1636.49 (C=C), 1628.93 (C=C), 1582.59, 1551.75, 1435.82 cm^{-1}

^{1}H NMR (400 MHz, DMSO-d_6) δ ppm 3.58 (s, 3H, OCH_3), 3.68 (s, 6H, 2xOCH_3), 3.97 (m, 2H, OCH_2), 4.72 (s, 1H, CH), 5.27 - 5.32 (m, 3H, CH-CH_2), 6.42 - 6.44 (m, 3H, Ar-H), 6.44 – 6.49 (m, 1 H, Ar-H), 7.04 (d, 1H, *J*=8.53 Hz, Ar-H), 7.59 (s (br), 2H, NH_2), OH not observed

^{13}C NMR (101 MHz, DMSO-d_6) δ ppm 39.17 (CH), 56.62 (OCH_3), 56.72 (OCH_3), 58.56 (CH_2), 76.37 (C), 102.03 (CH), 104.08 (CH), 112.09 (CH_2), 116.59 (C), 129.75 (CH), 132.23 (CH), 135.61 (C), 144.46 (C-OCH_3), 149.06 (C-OCH_3), 152.53 (C-O), 156.73 (C-OH), 161.08 (O-C-N), 168.39 (C=O)

HRMS (ESI): $C_{22}H_{23}NNaO_7$ [M^+ Na] requires (m/e) 436.1372, found 436.1382, (+2.2 ppm)

BE77 Benzyl 2-amino-7-hydroxy-4-(3,4,5-trimethoxyphenyl)-4*H*-chromene-3-carboxylate

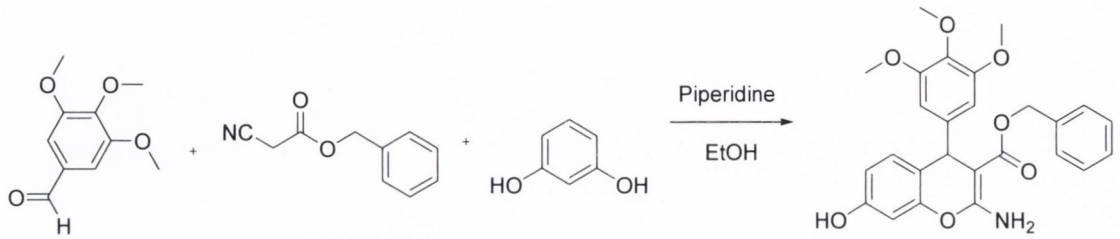

Yield: 1.48 g, 32 %, light brown solid (Recrystallisation, EtOH)

HPLC Purity: 97 % **MP:** 238-245°C

IRϑ_{max} (KBr): 3597.71 (OH), 3476.94, 3356.44 (NH_2), 1686.39 (C=O), 1663.59 (C=C), 1645.65 (C=C), 1583.59, 1542.51, 1438.97 cm^{-1}

^{1}H NMR (400 MHz, DMSO-d_6) δ ppm 3.56 (s, 3 H, OCH_3), 3.65 (s, 6 H, 2xOCH_3), 3.98 (m, 2H, OCH_2), 4.75 (s, 1H, CH), 6.42 (s, 2H, Ar-H), 6.44 (d, 2H, *J*=7.01 Hz, Ar-H), 6.47 - 6.49 (m, 1H, Ar-H), 6.50 - 6.52 (m, 1H, Ar-H), 7.05 (d, 4 H, *J*=8.53 Hz, Ar-H), 7.59 (s (br), 1H, OH), 9.63 (s (br), 2H, NH_2)

^{13}C NMR (101 MHz, DMSO-d_6) δ ppm 40.34 (CH), 55.70 (OCH_3), 58.58 (OCH_3), 59.90 (CH_2), 76.29 (C), 102.00 (CH), 104.08 (CH), 112.14 (C), 116.64 (CH), 127.83 (CH), 129.69 (CH), 130.59 (CH), 133.37 (C), 135.50 (C-O), 144.54 (C), 149.05 (C-OCH_3), 152.53 (C-O), 156.72 (C-OH), 160.80 (O-C-N), 168.37 (C=O)

HRMS (ESI): $C_{26}H_{26}NO_7$ [M^+ H] requires (m/e) 464.1709, found 464.1705, (-0.8 ppm)

BE78 2-Methylbutyl 2-amino-7-hydroxy-4-(3,4,5-trimethoxyphenyl)-4*H*-chromene-3- carboxylate

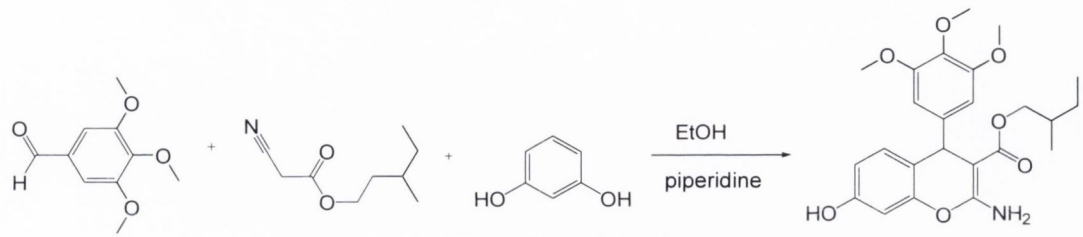

Yield: 2.48 g, 56 %, yellow powder (Recrystallisation, EtOH)

HPLC Purity: 98 % **MP:** 195-200 °C

IRϑ_{max} (KBr): 3583.55 (OH), 3405.99 (NH_2), 3211.67 (NH_2), 1684.21 (C=C), 1674.95 (C=C), 1605.48 (C=O), 1560.83, 1537.48 cm^{-1}

^{1}H NMR (400 MHz, DMSO-d_6): δ ppm 1.09 (t, 3H, *J*=7.16 Hz, CH_3), δ 1.51 - 1.59 (m, 3H, CH_3), δ 1.69 – 1.73 (m, 2H, CH_2), δ 2.26 – 2.32 (m, 1H, CH), δ 3.58 (s, 3H, OCH_3), δ 3.68 (s, 6H, 2xOCH_3), δ 3.98 – 4.05 (m, 2H, CH_2), δ 4.75 (s, 1H, CH), δ 6.43 (d, 3H, *J*=7.12 Hz, Ar-H), δ 6.49 (d, 1H, *J*=7.22 Hz, Ar-H), δ 7.05 (d, 1H, *J*=8.52 Hz, Ar-H), δ 7.57 (s (br), 2H, NH_2), δ 8.46 (s (br), 1H, OH)

^{13}C NMR (101 MHz, DMSO-d_6): δ ppm 11.28 (CH_3), δ 14.84 (CH_3), δ 26.73 (CH_2), δ 34.63 (CH), δ 40.38 (CH), δ 56.78 (OCH_3), δ 57.55 (OCH_3), δ 58.68 (CH_2), δ 78.35 (C), δ 101.57 (CH), δ 104.05 (CH), δ 113.59 (C), δ 131.82 (CH), δ 135.56 (C), δ 137.37 (C-OCH_3), δ 151.47 (C-OCH_3), δ 153.28 (C-O), δ 157.62 (C-OH), δ 162.57 (O-C-N), δ 167.27 (C=O)

HRMS (ESI): $C_{24}H_{29}NNaO_7$ [M^- -Na] requires (m/e) 420.1944, found 420.1938 (1.42 ppm)

BE79 Neopentyl 2-amino-7-hydroxy-4-(3,4,5-trimethoxyphenyl)-4*H*-chromene-3 carboxylate

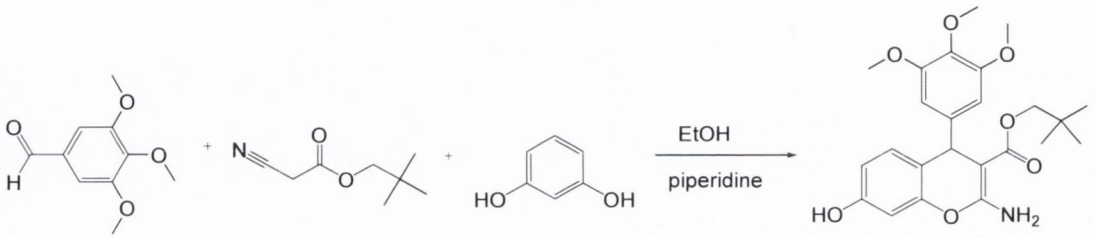

Yield: 1.11 g, 25 %, white crystals (Recrystallisation, EtOH)

HPLC Purity: 87 % **MP:** 201-206°C

IRϑ_{max} (KBr): 3590.74 (OH), 3420.29 (NH_2), 3295.93 (NH_2), 1670.22 (C=C), 1671.84 (C=C), 1625.25 (C=O), 1538.66, 1463.82 cm^{-1}

^{1}H NMR (400 MHz, DMSO-d_6): δ ppm 0.76 (s, 9H, 3xCH_3), δ 3.55 (s, 3H, OCH_3), δ 3.69 (s, 6H, 2xOCH_3), δ 3.78 (s, 2H, CH_2), δ 4.89 (s, 1H, CH), δ 6.42 (s, 1H, Ar-H), δ 6.57 - 6.68 (m, 3H, Ar-H), δ 7.24 (d, 1H, *J*=8.52 Hz, Ar-H) δ 7.68 (s (br), 2H, NH_2) δ 8.63 (s (br), 1H, OH)

^{13}C NMR (101 MHz, DMSO-d_6): δ ppm 26.57 (OCH_3), δ 31.52 (C), δ 39.97 (CH), δ 56.18 (OCH_3), δ 72.32 (C), δ 76.05 (CH_2), δ 102.46 (CH), δ 104.43 (CH), δ 112.45 (C), δ 130.28 (CH), δ 136.26 (C), δ 139.13 (C-OCH_3), δ 149.04 (C-OCH_3), δ 153.15 (C-O), δ 157.16 (C-OH), δ 161.91 (O-C-N), δ 169.03 (C=O)

HRMS (ESI): $C_{24}H_{30}NO_7$ [M^+ +H] requires (m/e) 444.2022, found 444.2039 (-3.82 ppm)

BE80 2-Methoxyethyl 2-amino-7-hydroxy-4-(3,4,5-trimethoxyphenyl)-4*H*-chromene-3-carboxylate

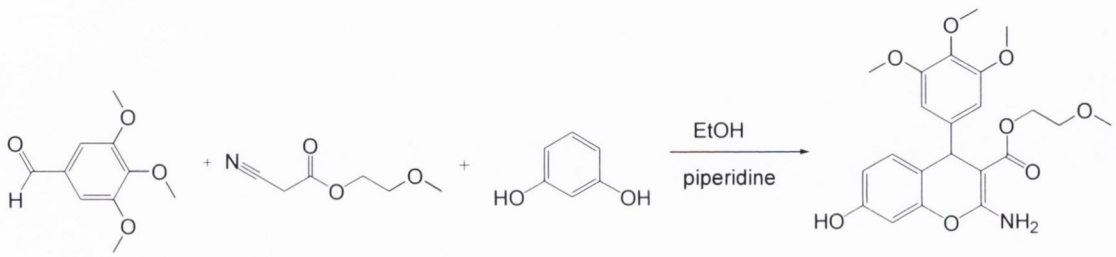

Yield: 1.77 g, 41 %, yellow powder (Recrystallisation, EtOH)

HPLC Purity: 95 % **MP:** 211-229°C

IRϑ_{max} (KBr): 3582.69 (OH), 3406.06 (NH_2), 3210.93 (NH_2), 1679.29 (C=C), 1629.71 (C=C), 1589.63 (C=O), 1562.47, 1520.94, 1471.96 cm^{-1}

^{1}H NMR (400 MHz, DMSO-d_6): δ ppm 3.11 - 3.16 (m, 3H, CH_3), δ 3.36 – 3.40 (m, 2H, CH_2), δ 3.59 (s, 3H, OCH_3), δ 3.65 (s, 6H, 2xOCH_3), δ 3.97 (q, 2H, *J*=6.78 Hz, CH_2), δ 4.75 (s, 1H, CH), δ 6.43 (d, 3H, *J*=7.52 Hz, Ar-H), δ 6.49 (d, 1H, *J*=8 Hz, Ar-H) δ 7.05 (d, 1H , *J*=8.52 Hz, Ar-H) δ 7.59 (s (br), 2H, NH_2) δ 8.63 (s (br), 1H, OH)

^{13}C NMR (101 MHz, DMSO-d_6): δ ppm 39.14 (CH), δ 56.19 (OCH_3), δ 59.02 (CH_3), δ 60.37 (CH_2), δ 65.75 (CH_2), δ 76.87 (C), δ 102.51 (CH), δ 104.61 (CH), δ 112.56 (C), δ 130.21 (CH), δ 136.11 (C), δ 144.91 (C-OCH_3), δ 149.54 (C-OCH_3), δ 153.01 (C-O), δ 157.21 (C-OH), δ 161.56 (O-C-N), δ 168.86 (C=O)

HRMS (ESI): $C_{22}H_{24}NO_8$ [M^- -H] requires (m/e) 430.1502, found 430.1520 (-4.28 ppm)

BE81 2-Ethoxyethyl 2-amino-7-hydroxy-4-(3,4,5-trimethoxyphenyl)-4*H*-chromene-3- carboxylate

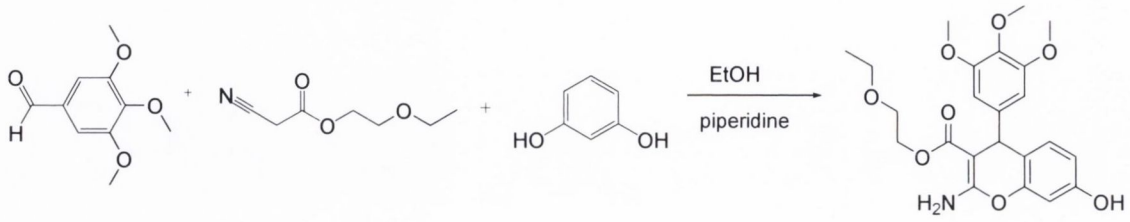

Yield: 1.87 g, 42 %, yellow powder (Recrystallisation, EtOH)

HPLC Purity: 100 % **MP:** 212-228 °C

IRϑ_{max} (KBr): 3517.59 (OH), 3405.8 (NH_2), 3200.34 (NH_2), 1679.4 (C=C), 1657.21 (C=C), 1629.8 (C=O), 1568.48 cm^{-1}.

^{1}H NMR (400 MHz, DMSO-d_6): δ ppm 1.09 (t, 3H, *J*=7.14 Hz, CH_3), δ 3.34 – 3.40 (d, 4H, *J*=7.24 Hz, 2xCH_2), δ 3.58 (s, 3H, OCH_3), δ 3.69 (s, 6H, 2xOCH_3), δ 3.99 (q, 2H, *J*=7.63 Hz, CH_2), δ 4.76 (s, 1H, CH), δ 6.44 (d, 3H, *J*=8.02 Hz, Ar-H), δ 6.51 (d, 1H, *J*= 7.62 Hz, Ar-H), δ 7.06 (d, 1H, *J*= 8.52 Hz, Ar-H), δ 7.58 (s (br), 2H, NH_2), δ 8.62 (s (br), 1H, OH)

^{13}C NMR (101 MHz, DMSO-d_6): δ ppm 14.57 (CH_3), δ 40.01 (CH), δ 56.21 (OCH_3), δ 59.02 (CH_2), δ 60.37 (CH_2), 65.35 (CH_2), δ 76.86 (C), δ 102.51 (CH), δ 104.61 (CH), δ 112.56 (C), δ 130.21 (CH), δ 134.48 (C), δ 136.12 (C-OCH_3), δ 149.55 (C-OCH_3), δ 153.01 (C-O), δ 157.21 (C-OH), δ 161.55 (O-C-N), δ 168.86 (C=O)

HRMS (ESI): $C_{23}H_{28}NO_8$ [M^+ +H] requires (m/e) 446.1815, found 446.1819 (0.89 ppm)

BE82 2-Butoxyethyl 2-amino-7-hydroxy-4-(3,4,5-trimethoxyphenyl)-4*H*-chromene-3- carboxylate

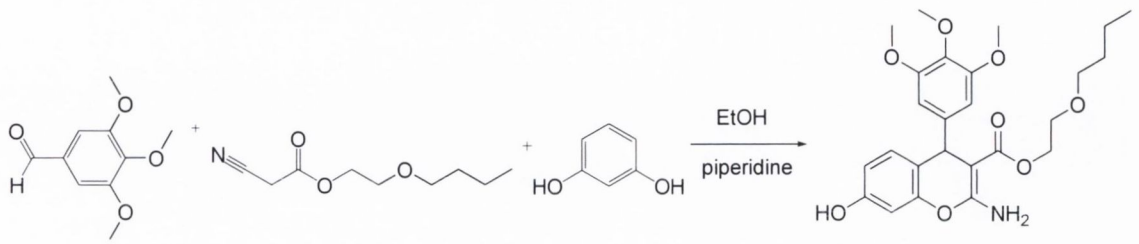

Yield: 1.65 g, 35 %, yellow powder (Recrystallisation, EtOH)

HPLC Purity: 94 % **MP:** 217 -219°C

IRϑ_{max} (KBr): 3591.68 (OH), 3426.69 (NH_2), 3200.3 (NH_2), 1681.64 (C=C), 1664.55 (C=C), 1631.44 (C=O), 1576.51 cm^{-1}

^{1}H NMR (400 MHz, DMSO-d_6): δ ppm 0.98 (t, 3H, *J*=7.22 Hz, CH_3), δ 1.36 - 1.42 (m, 4H, 2xCH_2), δ 3.57 - 3.67 (m, 2H, CH_2), δ 3-81 - 3.87 (m, 2H, CH_2), δ 4.06 (s, 9H, 3xOCH_3), δ 4.24 – 4.31 (m, 2H, CH_2), δ 4.74 (s, 1H, CH), δ 6.04 (d, 2H, *J*=7.2 Hz, Ar-H), δ 6.53 (d, 1H, *J*=8.56 Hz, Ar-H), δ 6.87 (d, 1H, *J*=7.41 Hz, Ar-H), δ 6.97 (d, 1H, *J*=8.03 Hz, Ar-H), δ 7.52 (s (br), 2H, NH_2), δ 8.27 (s (br), 1H, OH)

^{13}C NMR (101 MHz, DMSO-d_6): δ ppm 14.49 (CH_3), δ 19.87 (CH_2), δ 31.2 (CH_2), δ 39.19 (CH), δ 56.88 (OCH_3), δ 64.38 (CH_2), δ 67.05 (CH_2), δ 72.34 (CH_2), δ 80.73 (C), δ 105.53 (CH), δ 111.87 (CH), δ 114.65 (C), δ 130.37 (CH), δ 132.43 (C), δ 135.14 (C-OCH_3), δ 147.83 (C-OCH_3), δ 149.45 (C-O), δ 154.31 (C-OH), δ 156.63 (O-C-N), δ 168.38 (C=O)

HRMS (ESI): $C_{25}H_{30}NO_8$ [M^- -H] requires (m/e) 472.2049, found 472.2048 (2.11 ppm)

BE83 Hexyl 2-amino-7-hydroxy-4-(3,4,5-trimethoxyphenyl)-4*H*-chromene-3-carboxylate

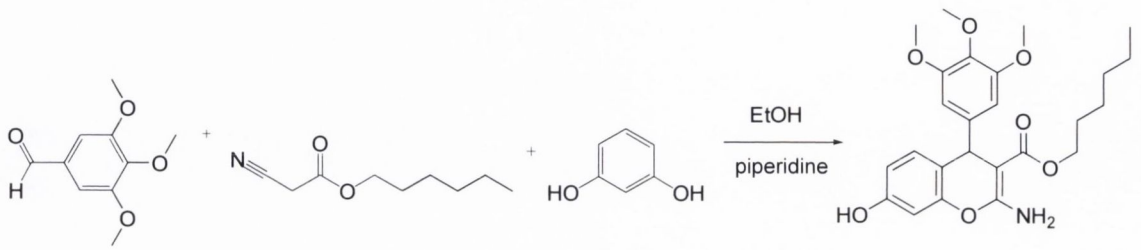

Yield: 0.82 g, 18 %, yellow powder (Recrystallisation, EtOH)

HPLC Purity: 92 % **MP:** 208 – 212 °C

IRϑ_{max} (KBr): 3571.84 (OH), 3406.22 (NH_2), 3213.58 (NH_2), 1680.23 (C=C), 1681.75 (C=C), 1630.0 (C=O), 1579.64, 1458.72 cm^{-1}

^{1}H NMR (400 MHz, DMSO-d_6): δ ppm 1.12 (t, 3H, *J*=7.41 Hz, CH_3), δ 1.33-143 (m, 6H, 3xOCH_2), δ 1.56 (s, 2H, CH_2), δ 3.58 (s, 3H, OCH_3), δ 3.69 (s, 6H, 2xOCH_3), δ 4.11 – 4.19 (m, 2H, CH_2), δ 4.72 (s, 1H, CH), δ 6.44 (d, 2H, *J*=7.4 Hz, Ar-H), δ 6.55 (s, 1H, Ar-H), δ 6.87 (s, 1H, Ar-H), δ 6.93 (d, 1H, *J*=8.46 Hz, Ar-H), δ 7.78 (s (br), 2H, NH_2), δ 8.27 (s (br), 1H, OH)

^{13}C NMR (100MHz, DMSO-d6): δ 14.63 (CH_3), δ 22.80 (CH_2), δ 24.76 (CH_2), δ 29.3 (CH_2), δ 31.45 (CH_2) δ 39.58 (CH), δ 56.88 (OCH_3), δ 67.05 (CH_2), δ 79.08 (C), δ 105.69 (CH), δ 111.76 (CH), δ 113.48 (C), δ 129.24 (CH), δ 132.84 (C), δ 136.74 (C-OCH_3), δ 151.67 (C-OCH_3), δ 154.31 (C-O), δ 158.51 (C-OH), δ 161.89 (O-C-N), δ 167.35 (C=O)

HRMS (ESI): $C_{25}H_{32}NO_7$ [M^+ + H] requires (m/e) 458.2179, found 458.2183 (0.87 ppm)

BE84 Cyclohexyl 2-amino-7-hydroxy-4-(3,4,5-trimethoxyphenyl)-4*H*-chromene-3-carboxylate

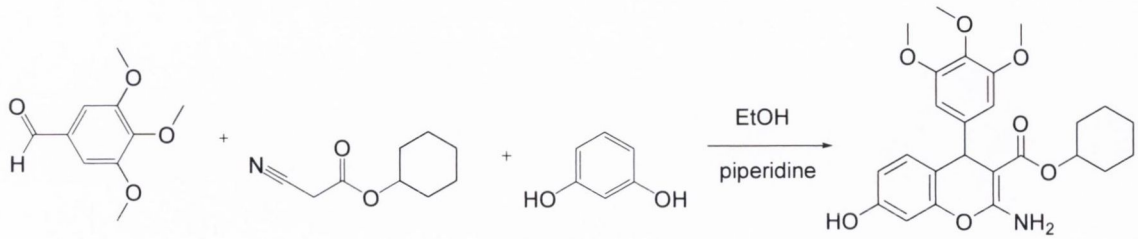

Yield: 3.64 g, 80 %, white powder (Recrystallisation, EtOH)

HPLC Purity: 84 % **MP:** 221 – 223°C

IRϑ_{max} (KBr): 3530.11 (OH), 3417.25 (NH_2), 3341.73 (NH_2), 1684.83 (C=C), 1674.95 (C=C), 1652.48 (C=O), 1630.19, 1608.36, 1560.45 cm^{-1}

^{1}H NMR (400 MHz, DMSO-d_6): δ ppm 1.18 - 1.45 (m, 10H, 5xCH_2), 3.89 (s, 9H, 3xOCH_3), 3.98 (s, 1H, CH), 4.74 (s, 1H, CH), 6.06 (d, 2H, *J*=2.2 Hz, Ar-H), 6.15 (s, 1H, Ar-H), 6.27 (s, 1H, Ar-H), 6.73 (d, 1H, *J*=6.46 Hz, Ar-H), 8.48 (s (br), 2H, NH_2), 8.32 (s (br), 1H, OH)

^{13}C NMR (101 MHz, DMSO-d_6): δ ppm 22.63 (CH_2), 27.80 (CH_2), 32.89 (CH_2), 40.04 (CH), 57.28 (OCH_3), 75.05 (CH), 79.08 (C), 105.69 (CH), δ 111.76 (CH), 113.48 (C), 129.24 (CH), 132.75 (C), 138.74 (C-OCH_3), 151.67 (C-OCH_3), 154.31 (C-O), 158.51 (C-OH), 161.89 (O-C-N), 167.35 (C=O)

HRMS (ESI): $C_{25}H_{30}NO_7$ [M^+ + H] requires (m/e) 456.2022, found 456.2043 (-4.6 ppm)

BE85 Synthesis of 2-Amino-4-(3,4,5-Trimethoxy-phenyl)-7-hydroxy-4*H*-chromene-3-carboxylic acid ethyl ester

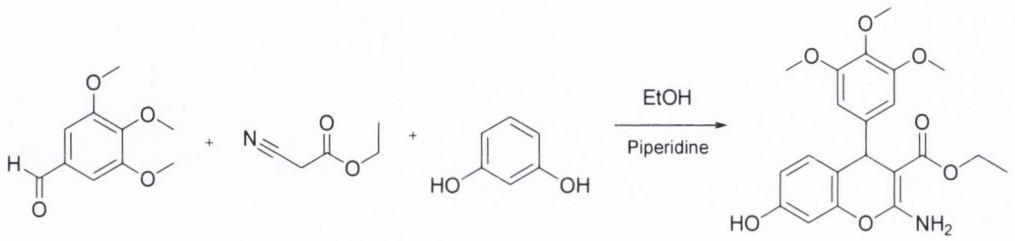

Yield: 1.48 g, 39 %, cream powder (Recrystallisation, EtOH)

HPLC Purity: 96% **MP:** 229 - 231°C **Lit. Ref**: [242] **Lit.MP:** 215-217 °C

IRϑ_{max} (KBr): 3412.94 (OH), 3306.67, 3283.07 (NH_2), 1680.35 (C=O), 1658.35 (C=C), 1630.32 (C=C), 1586.36, 1533.84 cm^{-1}

^{1}H NMR (400 MHz, DMSO-d6): δ ppm 1.09 (t, 3H, *J*=7.16 Hz, CH_3), δ 3.58 (s, 3H, OCH_3), δ 3.69 (s, 6H, 2xOCH_3), δ 3.98 (q, 2H, *J*=7.52 Hz, OCH_2), δ 4.76 (s, 1H, CH), δ 6.43 (d, 2H, *J*=6.78 Hz, Ar-H), δ 6.49 - 6.54 (m, 2H, Ar-H), δ 7.05 (d, 1H, *J*=8.52 Hz, Ar-H), OH not observed, NH_2 not observed.

^{13}C NMR (100 MHz, DMSO-d6): δ ppm 14.81 (CH_3), δ 40.16 (C), δ 56.16 (CH_3), δ 59.03 (CH_3), δ 60.36 (CH_2), δ 76.83 (C), δ 102.49 (CH), δ 104.55 (CH), δ 112.55 (CH), δ 117.05 (C), δ 130.21 (CH), δ 134.75 (C), δ 136.05 (C), δ 144.93 (C-OCH_3), δ 149.53 (C-OCH_3), δ 153.00 (C-O), δ 157.20 (C-OH), δ 161.55 (O-C-N), δ 168.86 (C=O)

HRMS (ESI): $C_{21}H_{23}NO_7$ [M^+ +Na] requires (m/e) 402.1553, found 402.1566 (+3.3 ppm)

BE86 Benzyl 2-amino-4-(2,4-dichlorophenyl)-7-hydroxy-4*H*-chromene-3-carboxylate

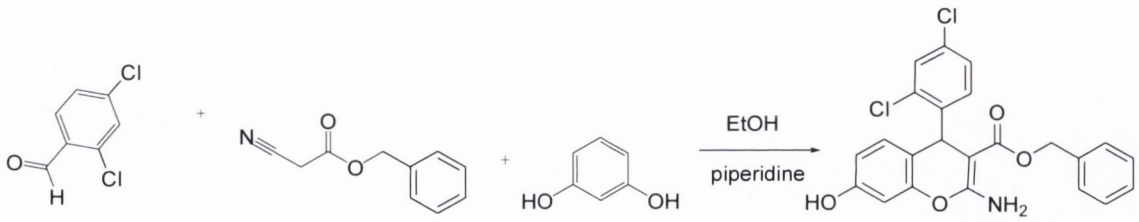

Yield: 2.16 g, 49 %, light brown solid (Flash Column, CH_2Cl_2 - MeOH 10%)

HPLC Purity: 85 % **MP:** 128-130°C

IRϑ_{max} (KBr): 3560.52 (OH), 3350.37 (NH_2), 3142.11 (NH_2), 1662.83 (C=O), 1622.48, 1608.10 (C=C) cm^{-1}.

^{1}H NMR (400 MHz, DMSO-d_6): δ ppm δ 4.74 (s, 1H, CH), 5.24 (dd, 2H, *J*=2.24, 7.28 Hz, CH_2), δ 6.22 (m, 2H, Ar-H), δ 6.46 (d, 1H, *J*=7.02 Hz, Ar-H), δ 6.58 (d, 1H, *J*=6.14 Hz, Ar-H), δ 6.84 (d, 2H, *J*=8.52 Hz, Ar-H), δ 7.24 - 7.33 (m, 5H, Ar-H), δ 7.98 (s (br), 2H, NH_2), δ 8.21 (s (br), 1H, OH)

^{13}C NMR (101 MHz, DMSO-d_6): δ ppm 31.37 (CH), δ 67.83 (CH_2), δ 80.06 (C), δ 104.64 (CH), δ 110.36 (CH), δ 113.58 (C), δ 126.89 (CH), δ 127.53 (CH), δ 129.07 (CH), δ 130.14 (CH), δ 131.38 (CH), δ 132.17 (C-Cl), δ 133.75 (C-Cl), δ 141.21 (C), δ 148.71 (C), δ 154.67 (C-O), δ 157.93 (C-OH), δ 158.23 (O-C-N), δ 163.89 (C=O)

HRMS (ESI): $C_{23}H_{17}{}^{37}Cl_2NO_4$ [M^- -H] requires (m/e) 440.05346, found 440.0551

BE87 2-Methylbutyl 2-amino-4-(2,4-dichlorophenyl)-7-hydroxy-4*H*-chromene-3-carboxylate

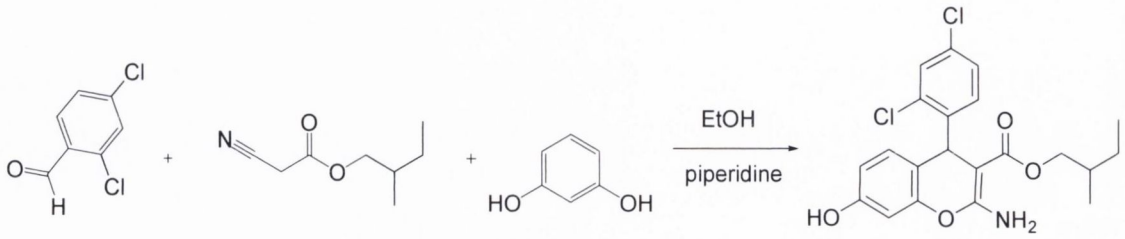

Yield: 2.52 g, 60 %, light brown solid (Flash Column, CH_2Cl_2 - MeOH 10%)

HPLC Purity: 95 % **MP:** 134-137 °C

IRϑ_{max} (KBr): 3537.61 (OH), 3412.83 (NH_2), 3128.31 (NH_2), 1655.13 (C=O), 1620.14 (C=C), 1611.54 (C=C), 1574.83, 1513.94 cm^{-1}

^{1}H NMR (400 MHz, DMSO-d_6): δ ppm 1.01 - 1.08 (m, 3H, CH_3), δ 1.10 - 1.14 (m, 3H, CH_3) δ 1.38 - 1.46 (m, 2H, CH_2), δ 2.68 - 2.73 (m, 1H, CH), δ 3.89 (s, 2H, CH_2), δ 4.76 (s, 1H, CH), δ 6.67 (d, 2H, *J*=7.02 Hz, Ar-H), δ 6.87 - 6.96 (m, 1H, Ar-H), δ 7.14 - 7.19 (m, 2H, Ar-H), δ 7.22 (d, 1H, *J*=8.64 Hz, Ar-H), δ 7.81 (s (br), 2H, NH_2), δ 8.27 (s (br), 1H, OH)

^{13}C NMR (101 MHz, DMSO-d_6): δ ppm 11.32 (CH_3), δ 16.4 (CH_3), δ 26.59 (CH_2), δ 30.02 (CH), δ 34.14 (CH), δ 73.76 (CH_2), δ 79.61 (C), δ 105.86 (CH), δ 111.62 (CH), δ 114.43 (C), δ 127.74 (CH), δ 130.18 (CH), δ 131.32 (CH), δ 132.84 (C-Cl), δ 134.53 (C-Cl), δ 148.35 (C), δ 151.21 (C-O), δ 158.91 (C-OH), δ 164.71 (O-C-N), δ 169.90 (C=O)

HRMS (ESI): $C_{21}H_{21}{}^{37}Cl_2NO_4$ [M^- -H] requires (m/e) 420.08476, found 420.0819

5.3 Synthesis of Diamino-chromenes using one-pot *piperidine*-catalyzed *Knoevenagel* condensation reactions

General Procedure

The appropriate Benzyloxybenzaldehyde (1 equiv., 2 mmol) was placed in a round bottomed flask, with appropriate alkyl cyanoacetate (1 equiv., 2 mmol). Addition of 3-aminophenol (1 equiv., 2 mmol) then followed. Ethanol (20 mL) was added and reaction mixture was warmed to dissolve all the reactants. After cooling to room temperature, 0.2 mL of piperidine was added dropwise and the reaction was refluxed for 5 h. Afterwards solvent was removed *in vacuo* and product was purified by flash column chromatography over silica gel. Purity was checked *via* TLC to yield various products and yields ranging from 11-91%.

BE88 Ethyl 2-amino-4-(4-(benzyloxy)phenyl)-7-hydroxy-4*H*-chromene-3-carboxylate

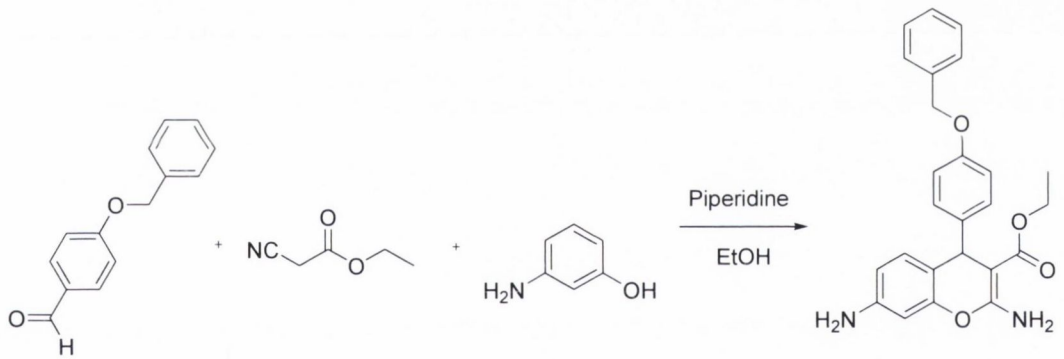

Yield: 0.92 g, 11%, brown powder (Flash Column, CH_2Cl_2)

HPLC Purity: 97 % **MP:** 258-259°C **Lit. Ref**: [243]

IRϑ_{max} (KBr): 3421.89, 3354.83 (NH_2), 1665.41 (C=O), 1632.31 (C=C), 1629.52 (C=C), 1554.85, 1468.93 cm^{-1}

^{1}H NMR (400 MHz, DMSO-d_6) δ ppm 1.06 (t, 3H, *J*=7.03 Hz, CH_3), 3.96 (q, 2H, *J*=7.28 Hz, OCH_2), 4.65 (s, 1H, CH), 5.20 (s, 2H, OCH_2), 6.84 (d, 2H, *J*=8.03 Hz, Ar-H), 6.99 - 7.09 (m, 2H, Ar-H), 7.19 - 7.26 (m, 3H, Ar-H), 7.36 - 7.43 (m, 3H, Ar-H), 7.48 - 7.55 (m, 2H, Ar-H), 7.25 (s (br), 2H, NH_2), 7.56 (s (br), 2H, NH_2).

^{13}C NMR (101 MHz, DMSO-d_6) δ ppm 23.18 (CH_3), 38.09 (CH), 58.51 (CH_2), 69.45 (CH_2), 82.91 (C), 100.33 (CH), 110.90 (C), 113.57 (CH), 114.44 (CH), 125.61 (CH), 127.61 (CH), 127.95 (CH), 128.38 (CH), 129.30 (CH), 130.30 (CH), 132.63 (C),

134.84 (C-Cl), 142.84 (C), 144.23 (C-N), 154.37 (C-O), 158.73 (Bnz-C-O), 159.55 (O-C-N), 161.09 (C=O)

HRMS (ESI): $C_{25}H_{25}N_2O_4$ M^+ H requires (m/e) 417.1814, found 417.1833, (4.5 ppm)

BE89 Methyl 4-(4-(2-fluorobenzyloxy)phenyl)-2,7-diamino-4*H*-chromene-3-carboxylate

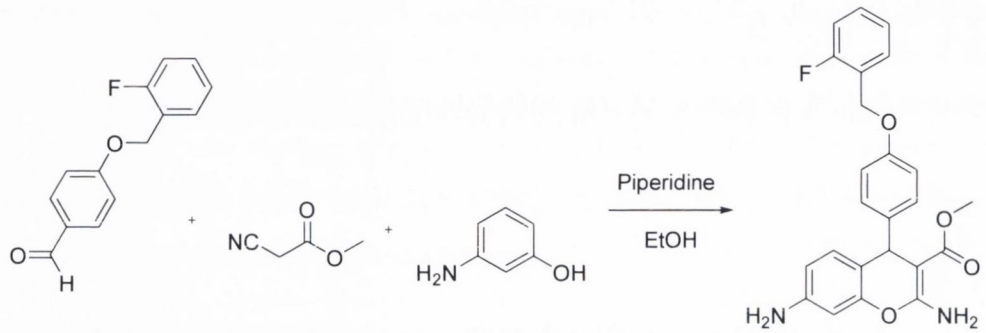

Yield: 0.14 g, 17 %, brown solid (Flash Column, CH_2Cl_2 - MeOH 10%)

HPLC Purity: 83 % **MP:** 208-211°C

IRϑ_{max} (KBr): 3494.05, 3384.81 (NH_2), 1668.37 (C=O), 1630.31 (C=C), 1622.41 (C=C), 1589.41, 1547.26, 1431.48 cm^{-1}

^{1}H NMR (400 MHz, DMSO-d_6) δ ppm 1.97 (s (br), 2H, NH_2), 3.93 (s, 3H, CH_3), 4.65 (s, 1H, CH), 5.04 (s, 2H, CH_2), 6.00 (d, 1H, *J*=7.51 Hz, Ar-H), 6.23 - 6.28 (m, 2H, Ar-H), 6.75 - 6.78 (m, 1H, Ar-H), 6.85 (d, 2H, *J*=8.41 Hz, Ar-H), 7.03 (d, 2H, *J*=8.53 Hz, Ar-H), 7.19 - 7.25 (m, 2H, Ar-H), 7.39 – 7.41 (m, 1H, Ar-H), 7.53 (s (br), 2H, NH_2)

^{13}C NMR (101 MHz, DMSO-d_6) δ ppm 38.09 (CH), 58.45 (CH_3), 63.39 (CH_2), 76.99 (C), 103.22 (CH), 105.37 (CH), 110.91 (C), 114.17 (CH), 115.24 (CH), 124.04 (CH), 124.47 (C), 127.90 (CH), 129.31 (CH), 130.21 (CH), 130.61 (C), 148.27 (C-N), 149.12 (C-O), 156.13 (Bnz-C-O), 158.06 (O-C-N), 161.11 (C-F), 168.50 (C=O)

HRMS (ESI): $C_{24}H_{22}FN_2O_4$ [M^+ H] requires (m/e) 421.1564, found 421.1564, (+0.1 ppm)

BE90 Ethyl 4-(4-(3-chlorobenzyloxy)phenyl)-2,7-diamino-4*H*-chromene-3-carboxylate

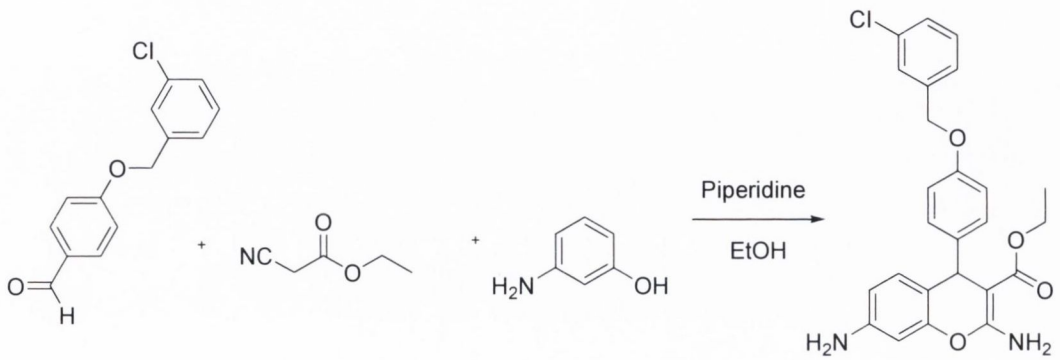

Yield: 0.58 g, 64 %, light brown solid (Flash Column, CH_2Cl_2 - MeOH 10%)

HPLC Purity: 100 % **MP:** 182-185°C

IRϑ_{max} (KBr): 3476.61, 3347.48 (NH_2), 1663.46 (C=O), 1643.18 (C=C), 1638.67 (C=C), 1579.37, 1529.04 cm^{-1}

^{1}H NMR (400 MHz, DMSO-d_6) δ ppm 1.31 (t, 3H, *J*=7.12 Hz, CH_3), 4.19 (q, 2H, *J*=8.24 Hz, OCH_2), 4.72 (s, 1H, CH), 5.18 (s, 2H, Bnz-OCH_2), 5.84 - 5.87 (m, 1H, Ar-H), 5.94 (s, 1H, Ar-H), 6.52 - 6.65 (m, 2H, Ar-H), 6.85 (d, 1H, *J*=7.21 Hz, Ar-H), 7.13 (d, 2H, *J*=8.02 Hz, Ar-H), 7.28 - 7.35 (m, 4H, Ar-H), 7.74 (s (br), 2H, NH_2).

^{13}C NMR (101 MHz, DMSO-d_6) δ ppm 14.93 (CH_3), 39.19 (CH), 60.14 (CH_2), 69.78 (CH_2), 80.62 (C), 102.26 (CH), 110.47 (C), 111.49 (CH), 114.93 (CH), 125.48 (CH), 127.13 (CH), 127.73 (CH), 129.38 (CH), 130.62 (CH), 132.74 (C), 136.44 (C), 142.45 (C), 145.56 (C-N), 156.58 (C-O), 159.58 (C-O), 162.85 (O-C-N), 165.37 (C=O)

HRMS (ESI): $C_{25}H_{24}{}^{37}ClN_2O_4$ [M^+ H] requires (m/e) 451.1425, found 451.1426, (+0.2 ppm)

BE91 Methyl 2,7-diamino-4-{4-[(4-methylphenyl)methoxy]phenyl}-4*H*-chromene 3-carboxylate

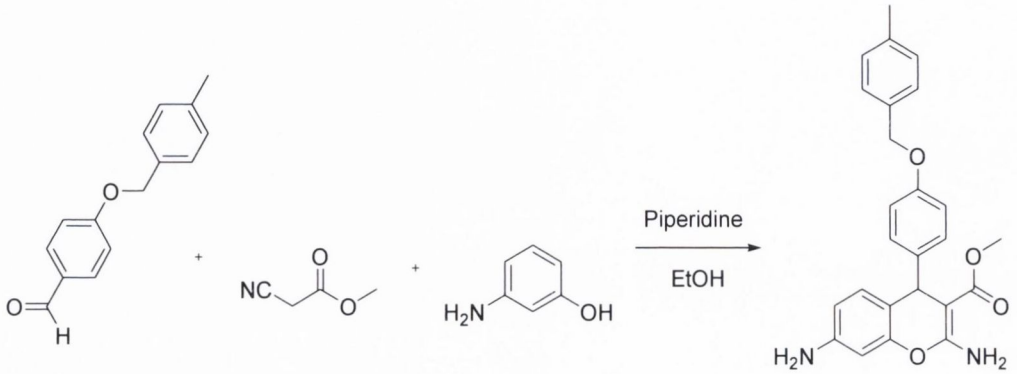

Yield: 0.3 g, 36 %, orange resin (Flash Column, CH_2Cl_2 - MeOH 10%)

HPLC Purity: 87 % **MP:** na

IRϑ_{max} (KBr): 3471.42, 3394.16 (NH_2), 1658.26 (C=O), 1635.41 (C=C), 1629.48 (C=C), 15832.47, 1562.95, 1423.53 cm^{-1}

^{1}H NMR (400 MHz, DMSO-d_6) δ ppm 1.07 (s, 3H, CH_3), 3.95 (s, 3H, CH_3), 4.68 (s, 1H, CH), 4.95 (s, 2H, CH_2), 5.17 (s (br), 2H, NH_2), 6.23 - 6.32 (m, 2H, Ar-H), 6.76 - 6.87 (m, 3H, Ar-H), 7.04 (d, 2H, *J*=8.03 Hz, Ar-H), 7.17 (d, 2H, *J*=7.53 Hz, Ar-H), 7.29 (d, 2H *J*=8.03 Hz, Ar-H), 7.56 (s (br), 2H, NH_2)

^{13}C NMR (101 MHz, DMSO-d_6) δ ppm 20.76 (CH_3), 38.14 (CH), 58.47 (CH_3), 69.02 (CH_2), 77.09 (C), 99.98 (CH), 110.95 (CH), 113.62 (C), 114.24 (CH), 127.70 (CH), 127.86 (CH), 128.94 (CH), 129.33 (CH), 134.17 (C), 136.95 (C), 141.51 (C), 148.26 (C-N), 149.16 (C-O), 156.33 (Bnz-C-O), 161.13 (O-C-N), 168.55 (C=O)

HRMS (ESI): $C_{26}H_{27}N_2O_4$ [M^+ CH_3] requires (m/e) 431.1971, found 431.1968, (-0.6 ppm)

BE92 Neopentyl 4-(4-(2-fluorobenzyloxy)phenyl)-2,7-diamino-4*H*-chromene-3-carboxylate

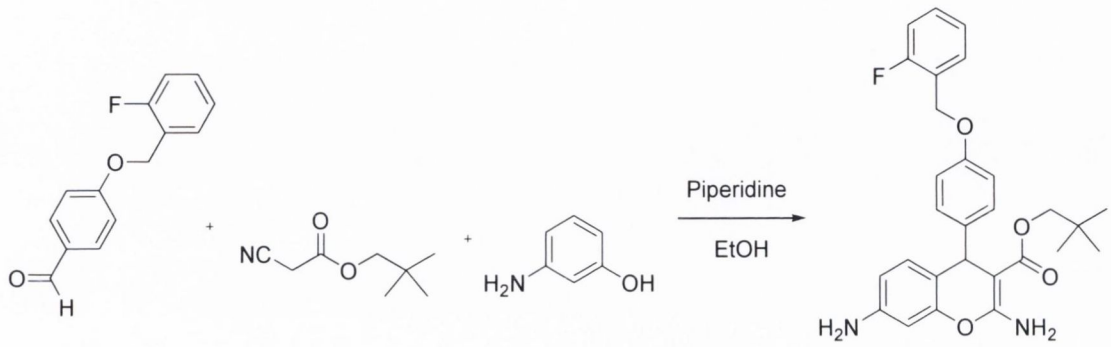

Yield: 0.11 g, 12 %, yellow solid (Flash Column, CH_2Cl_2 - MeOH 10%)

HPLC Purity: 86 % **MP:** 216-221°C

IRϑ_{max} (KBr): 3471.74, 3372.48 (NH_2), 1672.15 (C=O), 1648.31 (C=C), 1636.72 (C=C), 1583.18, 1484.59 cm^{-1}

^{1}H NMR (400 MHz, DMSO-d_6) δ ppm 0.74 (s, 9H, 3xCH_3), 3.97 (d, 2H, *J*=7.03 Hz, CH_2), 4.70 (s, 1H, CH), 5.04 (s, 2H, CH_2), 6.21 (d, 1H, *J*=8.04 Hz, Ar-H), 6.22 - 6.28 (m, 1H, Ar-H), 6.75 - 6.79 (m, 1H, Ar-H), 6.84 - 6.90 (m, 2H, Ar-H), 7.04 (d, 2H, *J*=8.02 Hz, Ar-H), 7.10 (d, 2H, *J*=8.42 Hz, Ar-H), 7.37 - 7.42 (m, 2H, Ar-H), 7.47 (s (br), 2H, NH_2), 7.64 (s (br), 2H, NH_2)

^{13}C NMR (101 MHz, DMSO-d_6) δ ppm 26.22 (CH_3), 31.04 (C), 38.19 (CH), 63.36 (CH_2), 71.82 (C), 76.28 (CH_2), 99.90 (CH), 110.90 (C), 113.63 (CH), 114.17 (CH), 115.43 (CH), 124.47 (CH), 127.53 (C), 128.71 (CH), 129.22 (CH), 130.27 (CH), 132.61 (C), 141.80 (C-N), 148.77 (C-O), 156.13 (Bnz-C-O), 159.22 (C-F), 161.63 (O-C-N), 168.63 (C=O)

HRMS (ESI): $C_{28}H_{30}FN_2O_4$ [M^+ H] requires (m/e) 477.2189, found 477.2168, (-4.4 ppm)

BE93 2,2-dimethylpropyl 2-amino-7-(dimethylamino)-4-{4-[(4-methylphenyl)methoxy]phenyl}-4H-chromene-3-carboxylate

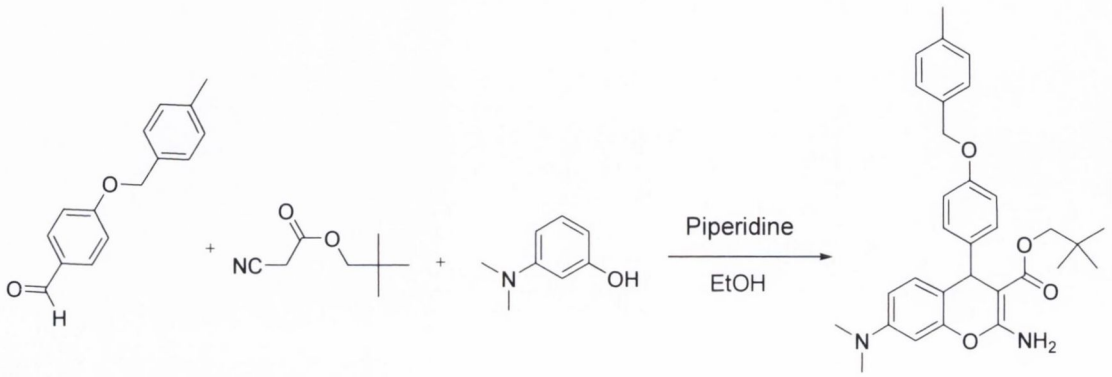

Yield: 0.46 g, 46 %, brown resin (Flash Column, CH_2Cl_2 - MeOH 10%)

HPLC Purity: 98 % **MP:** na

IRϑ_{max} (KBr): 3475.83, 3263.98 (NH_2), 1666.12 (C=O), 1634.48 (C=C), 1611.68 (C=C), 1575.49, 1547.26 cm^{-1}

^{1}H NMR (400 MHz, DMSO-d_6) δ ppm 0.74 (s, 9H, 3xCH_3), 2.28 (s, 3H, CH_3), 2.84 (s, 6H, 2xCH_3), 3.35 (s, 2H, CH_2), 4.76 (s, 1H, CH), 4.95 (s, 2H, CH_2), 6.41 (s, 1H, Ar-H), 6.46 (d, 1H, *J*=6.88 Hz, Ar-H), 6.68 (d, 1H, *J*=7.42 Hz, Ar-H), 6.82 (d, 2H, *J*=7.14 Hz, Ar-H), 7.08 (d, 2H, *J*=7.04 Hz, Ar-H), 7.16 (d, 2H, *J*=8.03 Hz, Ar-H), 7.25 (d, 2H, *J*=7.22 Hz, Ar-H), 7.62 (s (br), 2 H, NH_2)

^{13}C NMR (101 MHz, DMSO-d_6) δ ppm 20.76 (CH_3), 26.22 (3xCH_3), 31.04 (C), 38.88 (CH), 40.12 (2xCH_3), 68.98 (CH_2), 71.85 (CH_2), 76.27 (C), 98.60 (CH), 109.24 (CH), 114.16 (C), 114.49 (CH), 127.44 (CH), 128.91 (CH), 129.26 (CH), 134.18 (C), 136.87 (C), 141.32 (C), 148.79 (C-N), 149.85 (C-O), 156.42 (C-O), 161.58 (O-C-N), 168.62 (C=O)

HRMS (ESI): $C_{31}H_{37}N_2O_4$ [M^+ H] requires (m/e) 501.2753, found 501.2774, (+4.1 ppm)

BE94 Neopentyl 4-(4-(2-fluorobenzyloxy)phenyl)-2-amino-7-(dimethylamino)-4*H*-chromene-3-carboxylate

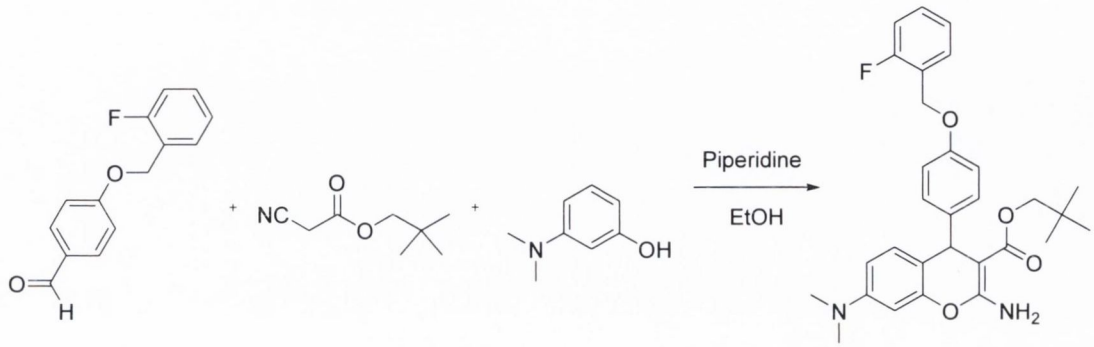

Yield: 0.62 g, 62 %, brown solid (Flash Column, CH_2Cl_2 - MeOH 10%)

HPLC Purity: 92 % **MP:** 179-183°C

IRϑ_{max} (KBr): 3419.04, 3315.93 (NH_2), 1662.41 (C=O), 1631.29 (C=C), 1624.01 (C=C), 1613.68, 1469.59 cm^{-1}

^{1}H NMR (400 MHz, DMSO-d_6) δ ppm 0.74 (s, 9H, 3xCH_3), 2.83 (s, 6H, 2xCH_3), 3.69 (s, 2H, CH_2), 4.79 (s, 1H, CH), 5.04 (s, 2H, CH_2), 6.13 (s., 2 H, Ar-H), 6.26 (s, 1H, Ar-H), 6.39 - 6.46 (m, 1H, Ar-H), 6.86 (s, 2H, Ar-H), 7.00 - 7.08 (m, 1H, Ar-H), 7.11 - 7.20 (m, 3 H, Ar-H), 7.39 - 7.46 (m, 1H, Ar-H), 7.59 (s (br), 2 H, NH_2)

^{13}C NMR (101 MHz, DMSO-d_6) δ ppm 26.21 (3xCH_3), 31.02 (C), 38.15 (CH), 40.09 (2xCH_3), 68.36 (CH_2), 71.88 (C), 76.28 (CH_2), 98.62 (CH), 99.54 (CH), 103.67 (C), 109.22 (CH), 114.13 (CH), 114.40 (CH), 114.49 (CH), 115.15 (CH), 127.53 (CH), 129.37 (CH), 129.65 (CH), 129.74 (CH), 148.81 (C), 149.84 (C-N), 151.81 (C-O), 156.29 (C-O), 158.13 (C-F), 161.60 (O-C-N), 168.66 (C=O)

HRMS (ESI): $C_{30}H_{34}FN_2O_4$ [M^+ H] requires (m/e) 505.2503, found 505.2516, (+2.5 ppm)

BE95 3-Methoxybutyl 2-amino-7-(dimethylamino)-4-{4-[(4 methylphenyl)methoxy]phenyl}-4*H*-chromene-3-carboxylate

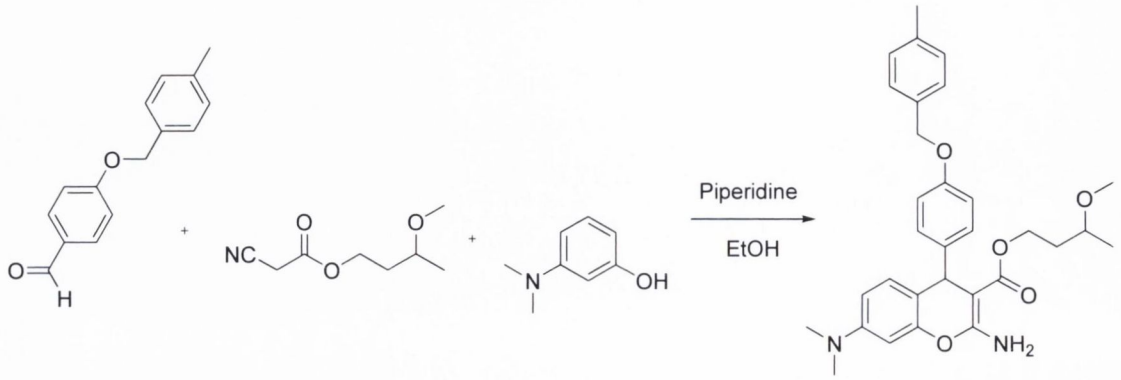

Yield: 0.69 g, 67 %, brown resin (Flash Column, CH_2Cl_2)

HPLC Purity: 93 % **MP:** na

IRϑ_{max} (KBr): 3482.77, 3379.39 (NH_2), 1671.45 (C=O), 1634.73 (C=C), 1622.85 (C=C), 1575.62, 1438.34 cm^{-1}

^{1}H NMR (400 MHz, DMSO-d_6) δ ppm 1.08 (d, 3H, *J*=7.12 Hz, CH_3), 1.56 - 1.60 (m, 2 H, CH_2), 2.28 (s, 3H, CH_3), 2.83 (s, 6H, 2xCH_3), 2.84 (s, 3H, CH_3), 3.05 - 3.11 (m, 1H, CH), 3.97 (q, 2H, *J*=7.00 Hz, CH_2), 4.74 (s, 1H, CH), 4.94 (s, 2H, CH_2), 6.10 - 6.20 (m, 2H, Ar-H), 6.29 (s, 1H, Ar-H), 6.40 - 6.45 (m, 1H, Ar-H), 6.81 - 6.86 (m, 2H, Ar-H), 6.95 (d, 2H, *J*=8.03 Hz, Ar-H), 7.02 - 7.08 (m, 1H, Ar-H), 7.16 (d, 1H, *J*=7.53 Hz, Ar-H), 7.28 (d, 1H, *J*=7.03 Hz, Ar-H), 7.59 (s (br), 2 H, NH_2)

^{13}C NMR (101 MHz, DMSO-d_6) δ ppm 14.29 (3xCH_3), 20.75 (CH_3), 38.07 (CH_2), 39.05 (CH), 40.09 (2xCH_3), 58.51 (CH_3), 69.00 (CH_2), 72.73 (CH_2), 77.03 (CH), 78.57 (C), 103.68 (CH), 103.77 (CH), 109.26 (C), 114.01 (CH), 114.26 (CH), 127.68 (CH), 127.88 (CH), 128.93 (CH), 129.49 (CH), 130.48 (C), 134.16 (C), 136.93 (C), 151.82 (C-N), 156.37 (C-O), 158.14 (C-O), 161.09 (O-C-N), 168.54 (C=O)

HRMS (ESI): $C_{31}H_{36}N_2NaO_5$ [M^+ Na] requires (m/e) 539.2522, found 539.2532, (-1.8 ppm)

BE96 Benzyl 4-(4-(2-fluorobenzyloxy)phenyl)-2-amino-7-(dimethylamino)-4*H*-chromene-3-carboxylate

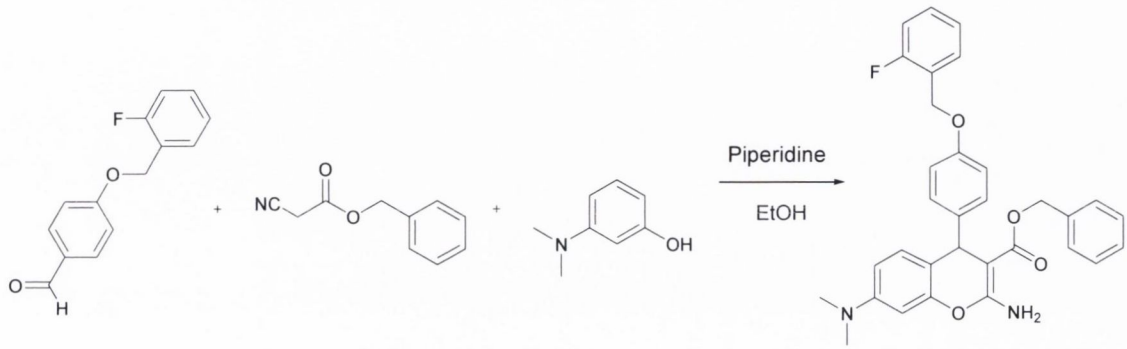

Yield: 0.91 g, 87 %, brown resin (Flash Column, CH_2Cl_2)

HPLC Purity: 93 % **MP:** na

IRϑ_{max} (KBr): 3461.91, 3383.45 (NH_2), 1665.21 (C=O), 1638.26 (C=C), 1621.60 (C=C), 1569.42, 1510.66, 1486.72 cm^{-1}

^{1}H NMR (400 MHz, DMSO-d_6) δ ppm 3.36 (s, 6H, 2xCH_3), 3.95 (dd, 2H, *J*=7.24 Hz, 2.06 Hz, OCH_2), 4.50 (s, 1H, CH), 5.04 (s, 2H, OCH_2), 6.81 - 6.86 (m, 3H, *J*=8.53 Hz, Ar-H), 6.91 - 6.97 (m, 2H, Ar-H), 7.05 (d, 2H, *J*=8.03 Hz, Ar-H), 7.22 (d, 1H, *J*=7.53 Hz, Ar-H), 7.29 - 7.35 (m, 3 H, Ar-H), 7.47 - 7.59 (m, 5H, Ar-H), NH_2 not observed

^{13}C NMR (101 MHz, DMSO-d_6) δ ppm 38.07 (CH), 40.84 (2xCH_3), 58.57 (CH_2), 62.75 (CH_2), 76.88 (C), 98.58 (CH), 109.35 (CH), 114.22 (C), 115.24 (CH), 115.45 (CH), 123.88 (CH), 126.40 (CH), 126.62 (CH), 127.92 (CH), 128.04 (CH), 129.40 (CH), 130.31 (s, 1 C), 130.67 (C), 142.50 (C), 149.15 (C-N), 149.78 (C-O), 156.16 (O-C-N), 161.09 (C-F), 168.51 (C=O)

HRMS (ESI): $C_{32}H_{29}FN_2NaO_4$ [M^+ Na] requires (m/e) 547.2009, found 547.2007, (0.3 ppm)

BE97 2-Ethoxyethyl 2-amino-7-(dimethylamino)-4-{4-[(4 methylphenyl) methoxy]phenyl}-4*H*-chromene-3-carboxylate

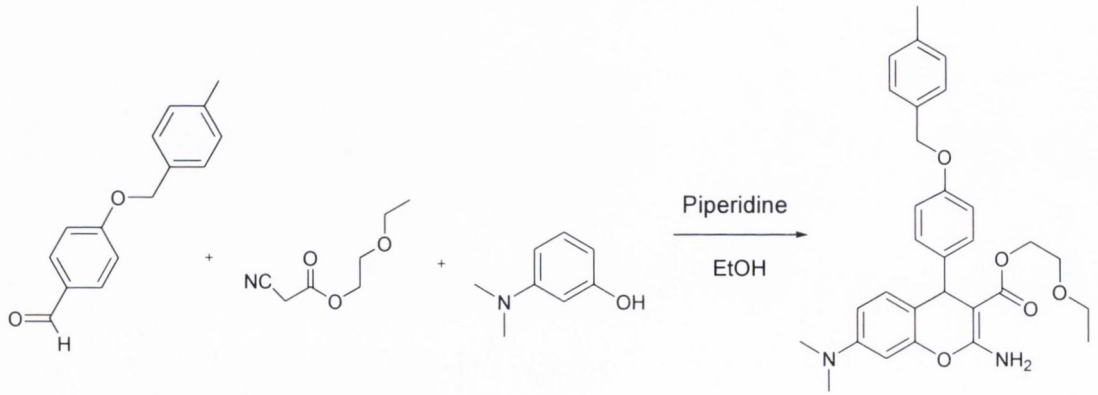

Yield: 0.04 g, 4 %, light brown solid (Flash Column, CH_2Cl_2)

HPLC Purity: 95 % **MP:** 186-192°C

IRϑ_{max} (KBr): 3483.55, 3346.62 (NH_2), 1660.14 (C=O), 1632.62 (C=C), 1614.62 (C=C), 1581.57, 1537.40, 1469.08 cm^{-1}

^{1}H NMR (400 MHz, DMSO-d_6) δ ppm 1.12 - 1.20 (m, 3H, CH_3), 2.32 (s, 6H, 2xCH_3), 2.79 (s, 3H, CH_3), 3.11 – 3.16 (m, 2H, CH_2), 3.90 - 3.97 (m, 2H, CH_2), 4.01 - 4.08 (m, 2H, CH_2), 4.93 - 5.00 (m, 1H, CH), 5.16 (s, 2H, CH_2), 6.79 - 6.86 (m, 2H, Ar-H), 7.16 - 7.20 (m, 2H, Ar-H), 7.24 (d, 2H, *J*=7.53 Hz, Ar-H), 7.32 (d, 3H, *J*=7.03 Hz, Ar-H), 7.40 (d, 1H, *J*=8.03 Hz, Ar-H), 7.48 (d, *J*=8.03 Hz, 1H, Ar-H), NH_2 not observed.

^{13}C NMR (101 MHz, DMSO-d_6) δ ppm 14.31 (CH_3), 20.94 (CH_3), 34.90 (CH), 40.30 (2xCH_3), 60.52 (CH_2), 68.98 (CH_2), 69.39 (CH_2), 89.51 (C), 96.87 (CH), 107.13 (CH), 110.78 (C), 114.92 (CH), 117.82 (CH), 127.70 (CH), 128.09 (CH), 128.93 (CH), 129.07 (CH), 130.40 (CH), 132.86 (C), 137.43 (C), 138.16 (C), 149.70 (C-N), 154.26 (C-O), 155.43 (C-O), 164.62 (O-C-N), 167.62 (C=O)

HRMS (ESI): $C_{30}H_{38}N_3O_5$ [M^+ NH_4] requires (m/e) 520.2811, found 520.2808, (-0.5 ppm)

BE98 Decyl 4-(4-(2-fluorobenzyloxy)phenyl)-2-amino-7-(dimethylamino)-4*H*-chromene-3-carboxylate

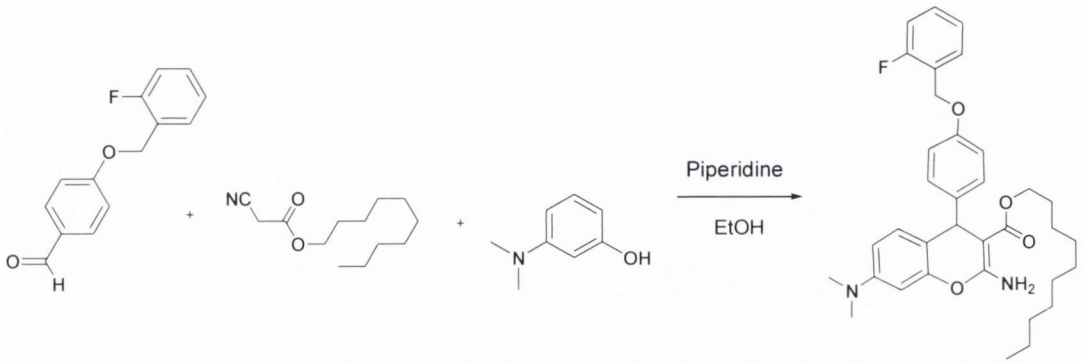

Yield: 1.04 g, 91 %, light brown solid (Flash Column, CH_2Cl_2)

HPLC Purity: 100 % **MP:** 197-201°C

IRϑ_{max} (KBr): 3468.05, 3461.64 (NH_2), 1668.19 (C=O), 1643.53 (C=C), 1628.76 (C=C), 1567.46, 1535.34, 1502.47 cm^{-1}

^{1}H NMR (400 MHz, DMSO-d_6) δ ppm 0.89 - 0.97 (m, 3H, CH_3), 1.34 - 1.39 (m, 14H, 7xCH_2), 1.84 – 1.91 (m, 2H, CH_2), 2.89 (s, 6H, 2xCH_3), 4.17 (s, 2H, CH_2), 4.73 (s, 1H, CH), 5.21 (s, 2H, CH_2), 6.19 (s, 1H, Ar-H), 6.21 - 6.29 (m, 1H, Ar-H), 6.42 (d, 2H, *J*=7.12 Hz, Ar-H), 6.82 - 6.88 (m, 3H, Ar-H), 7.08 - 7.16 (m, 1H, Ar-H), 7.26 (d, 2H, *J*=7.02 Hz, Ar-H), 7.39-7.46 (m, 1 H, Ar-H), 7.67 (s (br), 2H, NH_2)

^{13}C NMR (101 MHz, DMSO-d_6) δ ppm 15.14 (CH_3), 21.64 (CH_2), 22.64 (CH_2), 25.86 (CH_2), 29.17 (CH_2), 29.68 (CH_2), 30.43 (CH), 40.57 (2xCH_3), 61.79 (CH_2), 65.43 (CH_2), 79.47 (C), 100.14 (CH), 109.61 (CH), 110.49 (C), 114.58 (CH), 115.67 (CH), 124.76 (CH), 127.28 (C), 129.83 (CH), 129.79 (CH), 132.37 (C), 147.58 (C-N), 152.93 (C-O), 157.38 (C-O), 159.37 (C-F), 160.38 (O-C-N), 166.49 (C=O)

HRMS (ESI): $C_{35}H_{43}FN_2NaO_4$ [M^- Na] requires (m/e) 551.2209, found 551.2241, (+5 ppm)

Esterification of benzopyrans

General Procedure

To a solution of chromene [BE6] (1 equiv., 1 mmol) in anhydrous CH_2Cl_2 (20 mL) was added Et_3N (3 equiv., 3 mmol), followed by addition of the appropriate acid chloride (1 equiv., 1 mmol). The reaction mixture was stirred under a N_2 atmosphere at room temperature for 3 hours. After the solution was washed with H_2O (20ml) and organic layer was dried with Na_2SO_4 and concentrated *in vacuo* to provide a solid. This was purified *via* flash chromatography on silica gel (Hexane – EtOAc, or CH_2Cl_2 - MeOH, solvent systems of varied ratios) to afford products with yields ranging from 20-98%.

BE99 Synthesis of Ethyl 7-acetoxy-2-amino-4-(4-methoxyphenyl)-4*H*-chromene-3-carboxylic acid ethyl ester

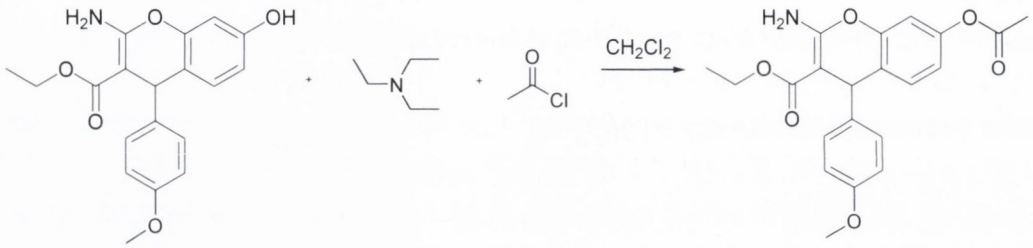

Yield: 0.20 g, 52 %, white solid (Flash Column; Hexane, EtOAc, 2:1)

HPLC Purity: 99% **MP**: 272 - 276°C

IRϑ_{max} (KBr): 3460.60 (NH_2), 3322.31 (NH_2), 1669.44 (C=O), 1661.29 (C=O), 1627.56 (C=C), 1621.57 (C=C), 1567.53, 1535.24, 1493.48 cm^{-1}

^{1}H NMR (400 MHz, $CDCl_3$): δ 1.19 (t, 3H, *J*=6.84 Hz, CH_3), δ 2.29 (s, 3H, CH_3), δ 3.76 (s, 3H, OCH_3), δ 4.07 (q, 2H, *J*=6.84 Hz, CH_2), δ 4.90 (s, 1H, CH), δ 6.68 - 6.75 (m, 3H, Ar-H), δ 6.81 (d, 1H, *J*=7.92 Hz, Ar-H), δ 7.15 - 7.21 (m, 3H, Ar-H), 8.21 (s (br), 2H, NH_2).

^{13}C NMR (100 MHz, $CDCl_3$): δ 13.88 (CH_3), δ 20.67 (CH_3), δ 38.74 (CH), δ 54.75 (OCH_3), δ 59.05 (CH_2), δ 78.56 (C), δ 109.08 (CH), δ 113.11 (CH), δ 116.37 (CH), δ 117.35 (C), δ 128.11 (CH), δ 129.56 (CH), δ 139.50 (C), δ 148.47 (C-O), δ 148.82 (C-O), δ 157.45 (C-O), δ 159.39 (OCH_3), δ 163.58 (O-C-N), δ 168.77 (C=O), δ 168.88 (C=O)

HRMS (ESI): $C_{21}H_{21}NNaO_6$ [M^+ +N] requires (m/e) 406.1266, found 406.1252, (-3.4 ppm)

BE100 Synthesis of Ethyl 2-amino-7-(benzoyloxy)-3,4-dihydro-4-(4 methoxyphenyl)-4*H*- chromene-3-carboxylic acid ethyl ester

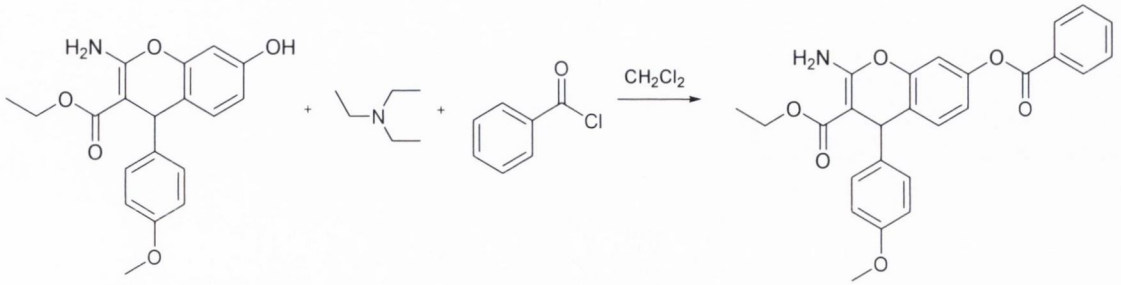

Yield: 0.09 g, 20 %, white solid (Flash Column; Hexane, EtOAc, 2:1)

HPLC Purity: 98% **MP:** 260 - 267°C

IRϑ_{max} (KBr): 3361.43 (NH_2), 1661.95 (C=O), 1659.52 (C=O), 1630.28 (C=C), 1624.74 (C=C), 1610.97, 1564.76, 1528.43 cm^{-1}

^{1}H NMR (400 MHz, DMSO-d6): δ 1.30 (t, 3H, *J*=7.02 Hz, CH_3), δ 3.68 (s, 3H, OCH_3), 3.99 (q, 2H, *J*=7.28 Hz, CH_2), 4.91 (s, 1H, CH), 6.80 (d, 2H, *J*=8.52 Hz, Ar-H), 7.06 (d, 3H, *J*=8.24 Hz, Ar-H), 7.29 (d, 1H, *J*=8.52 Hz, Ar-H), 7.91 – 8.12 (m, 6H, Ar-H), NH_2 not observed.

^{13}C NMR (100 MHz, DMSO-d6): δ 14.15 (CH_3), 45.19 (CH), 54.94 (CH_3), 60.73 (CH_2), 76.29 (C), 109.70 (CH), 113.66 (CH), 114.47 (CH), 118.15 (C), 127.93 (CH), 128.42 (CH), 128.97 (CH), 131.71 (C), 132.44 (C),133.25 (CH), 148.68 (C-O), 149.33 (C-O), 157.51 (C-OCH_3), 160.74 (O-C-N), 164.41 (C=O), 167.61 (C=O)

HRMS (ESI): $C_{26}H_{24}NO_6$ [M^+ +H] requires (m/e) 446.1604, found 446.1587, (-3.8 ppm)

BE101 Synthesis of ethyl 7-(2-phenoxyacetoyloxy)-2-amino-4-(4-methoxyphenyl)-4*H*-chromene-3-carboxylate

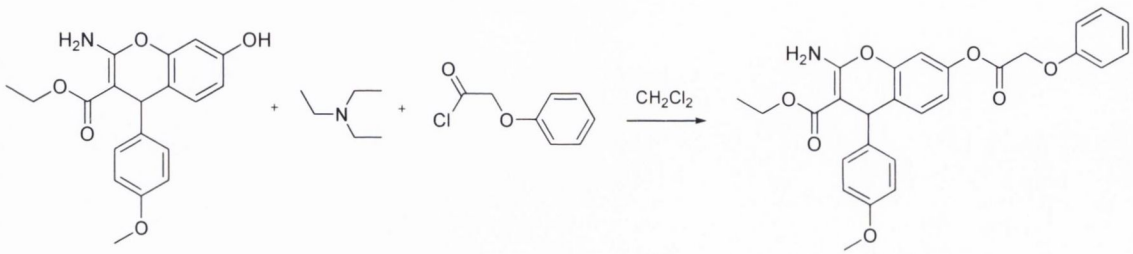

Yield: 0.11 g, 23 %, clear solid (Flash Column; Hexane, EtOAc, 2:1)

HPLC Purity: 100% **MP:** 217 - 220°C

IRϑ_{max} (KBr): 3467.14 (NH_2), 1668.97 (C=O), 1663.89 (C=O), 1633.97 (C=C), 1624.67 (C=C), 1564.87, 1531.48 cm^{-1}

^{1}H NMR (400 MHz, DMSO-d6): δ 1.21 (t, 3H, *J*=7.02 Hz, CH_3), 3,34 (q, 2H, *J*=7.22 Hz, CH_2), 3.94 - 4.10 (m, 1H, CH), 4.16 (s, 2H, CH_2), 6.42 - 6.51 (m, 1H, Ar-H), 6.75 (d, 2H, *J*=8.52 Hz, Ar-H), 6.91 - 7.04 (m, 6H, Ar-H), 7.18 - 7.27 (m, 2H, Ar-H), 7.56 (s, 1H, Ar-H), 8.12 (s (br), 2H, NH_2)

^{13}C NMR (100 MHz, DMSO-d6): δ 14.31 (CH_3), 38.09 (CH), 54.91 (OCH_3), 60.61 (CH_2), 64.50 (CH_2), 76.79 (C), 112.04 (CH), 113.45 (CH), 114.45 (CH), 117.10 (C), 121.16 (CH), 127.85 (CH), 129.37 (CH), 131.74 (C), 156.98 (C-O), 157.57 (C-O), 158.97 (C-OCH_3), 160.90 (O-C-N), 161.25 (C-O), 168.77 (C=O), 177 (C=O)

HRMS (ESI): $C_{27}H_{25}NNaO_7$ [M^+ +Na] requires (m/e) 498.1529, found 498.1515, (-2.8 ppm)

BE102 Synthesis of ethyl 7-((E)-but-2-enoyloxy)-2-amino-4-(4-methoxyphenyl) -4*H*-chromene-3-carboxylate

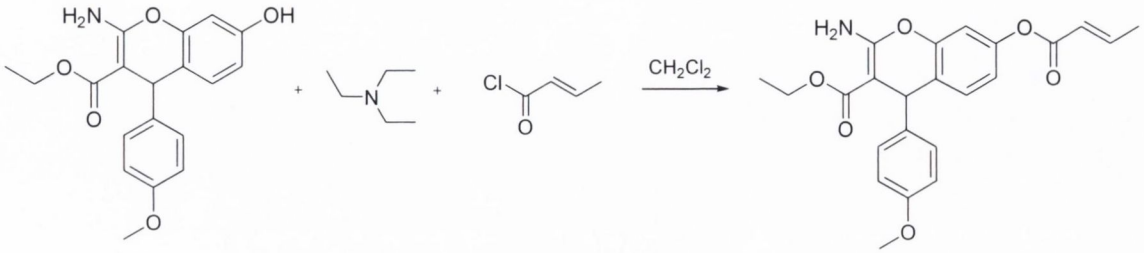

Yield: 0.29 g, 73 %, brown solid (Flash Column; Hexane, EtOAc, 1:1)

HPLC Purity: 94 % **MP:** 231 - 235°C

IRϑ_{max} (KBr): 3387.82 (NH_2), 1663.97 (C=O) 1659.85 (C=O), 1632.74 (C=C), 1628.88 (C=C), 1563.77, 1538.92, 1492.68 cm^{-1}

^{1}H NMR (400 MHz, $CDCL_3$): δ 1.21 (t, 3H, *J*=7.26 Hz, CH_3), 1.97 (d, 3H, *J*=6.52 Hz, CH_3), 3.76 (s, 3H, OCH_3), 4.08 (q, 2H, *J*=7.02 Hz, CH_2), 4.91 (s, 1H, CH), 6.77 (d, 3H, *J*=8.04 Hz, Ar-H), 6.84 (d, 1H, *J*=2.04 Hz, Ar-H), 7.09 - 7.18 (m, 3H, Ar-H), 7.88 (s (br), 2H, NH_2)

^{13}C NMR (100 MHz, $CDCL_3$): δ 13.90 (CH_3), 17.83 (CH_3), 38.75 (CH), 54.76 (OCH_3), 59.04 (CH_2), 78.91 (C), 109.15 (CH), 113.10 (CH), 117.45 (C), 121.35 (CH), 129.51 (CH), 136.57 (C), 145.67 (C), 146.97 (C-O), 148.46 (C-O), 157.43 (C-OCH_3), 159.44 (O-C-N), 164.11 (C=O), 168.91 (C=O)

HRMS (ESI): $C_{23}H_{23}NO_6$ [M^+ +Na] requires (m/e) 432.1423, found 432.1421, (-0.5ppm)

BE103 Synthesis of ethyl 7-(2-phenylacetoyloxy)-2-amino-4-(4 methoxyphenyl)-4*H*-chromene-3-carboxylate

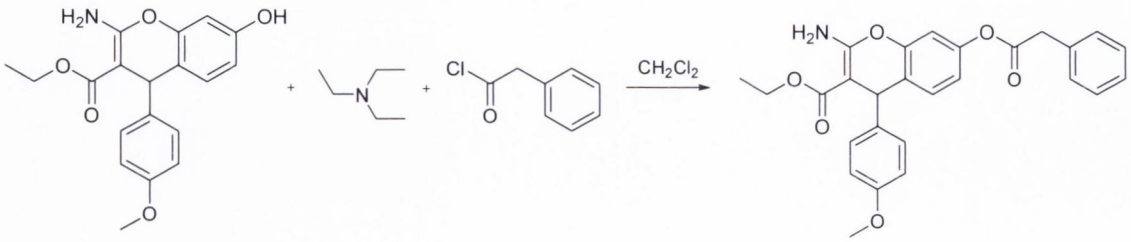

Yield: 0.40 g, 88 %, orange solid (Flash Column; Hexane, EtOAc, 1:1)

HPLC Purity: 91% **MP:** 243 - 248°C

IRϑ_{max} (KBr): 3472.46, 3388.47 (NH_2), 1664.50 (C=O), 1657.84 (C=O), 1639.83 (C=C), 1627.59 (C=C), 1618.47, 1591.46, 1557.41, 1543.72 cm^{-1}

^{1}H NMR (400 MHz, $CDCL_3$): δ 1.21 (t, 3H, *J*=7.02 Hz, CH_3), 3.76 (s, 2H, CH_2), 3.85 (s, 3H, CH_3), 4.06 (q, 2H, *J*=7.02 Hz, CH_2), 4.90 (s, 1H, CH_2), 6.73-7.80 (m, 4H, Ar-H), 7.06 - 7.12 (m, 3H, Ar-H), 7.28 (s, 1H, Ar-H), 7.38 (d, 4H, *J*=4.32 Hz, Ar-H)

^{13}C NMR (100 MHz, $CDCL_3$): δ 13.89 (CH_3), 38.72 (CH), 40.93 (CH_2), 54.75 (CH_3), 59.06 (CH_2), 78.58 (C), δ 111.49 (CH), 113.11 (C), 116.35 (CH), 117.23 (CH), 126.97 (CH), 128.09 (CH), 128.31 (CH), 129.06 (CH), 132.79 (C), 134.86 (C), 139.49 (C-O), 148.89 (C-O), 157.45 (C-OCH_3), 159.35 (O-C-N), 168.87 (C=O), 169.30 (C=O)

HRMS (ESI): $C_{27}H_{25}NO_6$ [M^+ +Na] requires (m/e) 482.1580, found 432.1573, (-1.4ppm)

BE104 Synthesis of ethyl 2-amino-7-(cinnamoyloxy)-4-(4-methoxyphenyl)-4*H*-chromene-3-carboxylate

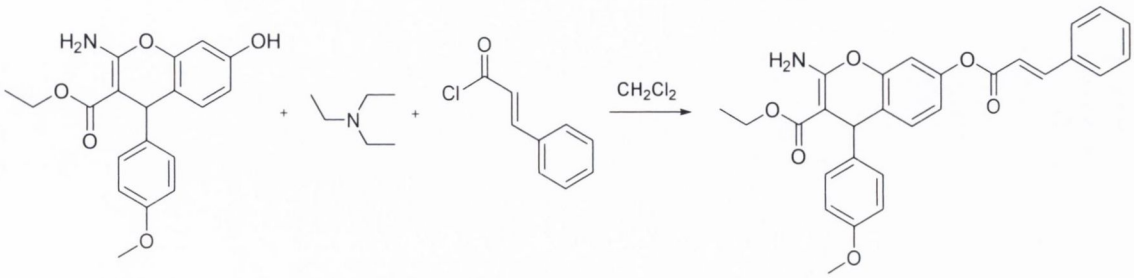

Yield: 0.42 g, 89 %, white powder (Flash Column; Hexane, EtOAc, 1:2)

HPLC Purity: 90% **MP:** 255 - 263°C

IRϑ_{max} (KBr): 3459.63 (NH_2), 3378.86 (NH_2), 1662.47 (C=O), 1660.68 (C=O), 1631.44 (C=C), 1629.92 (C=C), 1586.72, 1534.57, 1433.96 cm^{-1}

^{1}H NMR (400 MHz, $CDCL_3$): δ 1.20 (t, 3H, *J*=7.04 Hz, CH_3), 3.77 (s, 3H, CH_3), 4.05 – 4.11 (m, 2H, *J*=7.02 Hz, CH_2), 4.93 (s, 1H, CH), 6.06 (s, 1H, Ar-H), 6.64 (s, 1H, Ar-H), 6.78 (d, 2H, *J*=7.12 Hz, Ar-H), 6.84 (d, 1H, *J*=8.24 Hz, Ar-H), 6.91 (d, 1H, Ar-H), 7.12 - 7.18 (m, 3H, Ar-H), 7.44 (d, 3H, *J*=6.88 Hz, Ar-H), 7.56 – 7.62 (m, 2H, CH), NH_2 not observed

^{13}C NMR (100 MHz, $CDCL_3$): δ 13.90 (CH_3), 38.78 (CH), 54.77 (CH_3), 59.05 (CH_2), 78.61 (C), 109.15 (CH), 113.13 (CH), 114.73 (CH), 116.51 (CH), 117.43 (C), 127.89 (CH), 128.13 (CH), 129.57 (CH), 130.37 (CH), 133.59 (C), 139.55 (C), 146.46 (CH), 148.51 (C-O), 148.98 (C-O), 157.46 (C-OCH_3), 159.43 (O-C-N), 164.67 (C=O), 168.90 (C=O)

HRMS (ESI): $C_{28}H_{25}NO_6$ [M^+ +Na] requires (m/e) 494.1580, found 494.1584, (0.9ppm)

BE105 Ethyl 7-(2-((benzoyloxy)methyl)benzoyloxy)-2-amino-4-(4-methoxyphenyl)-4*H*-chromene-3-carboxylate

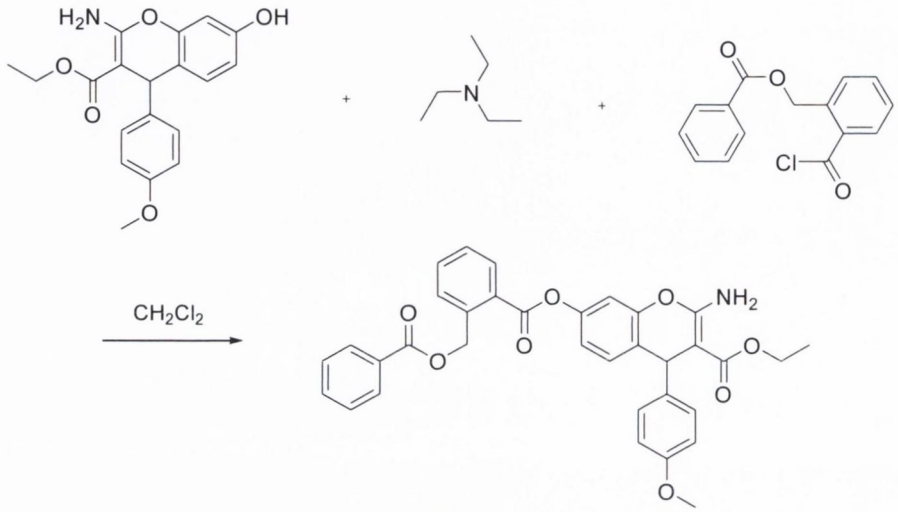

Yield: 0.22 g, 39 %, light brown powder (Flash Column; Hexane, EtOAc, 1:3)

HPLC Purity: 87% **MP:** 236 - 241 °C

IRϑ_{max} (KBr): 3496.53, 3453.57 (NH_2), 1655.18 (C=O), 1652.39 (C=O), 1640.74, 1619.74 (C=C), 1598.54 cm^{-1}

^{1}H NMR (400 MHz, CHLOROFORM-*d*) δ ppm 1.21 (t, 3H, *J*=6.78 Hz, CH_3), 3.78 (s, 3 H, OCH_3), 4.11 (q, 2H, *J*=7.28 Hz, CH_2), 4.94 (s, 1H, CH), 5.85 (s, 2 H, CH_2), 6.32 (s (br), 2 H, NH_2), 6.81 (s, 2 H, Ar-H), 6.89 (d, 2H, *J*=8.53 Hz, Ar-H), 6.94 (s, 1 H, Ar-H), 7.11 - 7.19 (m, 2 H, Ar-H), 7.29 (s, 2 H, Ar-H), 7.45 - 7.53 (m, 2H, Ar-H), 8.13 (d, 3H, *J*=7.53 Hz, Ar-H), 8.25 (s, 2H, Ar-H)

^{13}C NMR (101 MHz, CHLOROFORM-*d*) δ ppm 13.83 (CH_3), 38.77 (CH), 54.77 (OCH_3), 59.08 (CH_2), 64.44 (CH_2), 78.59 (C), 109.29 (CH), 113.15 (CH), 116.25 (CH), 117.48 (C), 127.07 (CH), 127.53 (CH), 127.82 (CH), 128.03 (CH), 128.14 (C), 129.30 (CH), 129.69 (CH), 130.97 (CH), 132.70 (C), 132.91 (CH), 139.51 (C), 148.57 (C-O), 148.84 (C-O), 157.48 (C-OCH_3), 159.38 (O-C-N), 164.46 (C=O), 165.69 (C=O), 168.90 (C=O)

HRMS (ESI): $C_{34}H_{30}NO_8$ [M^+ H] requires (m/e) 580.1971, found 580.1978, (-1.2 ppm)

BE106 Synthesis of ethyl 7-(4-bromobenzoyloxy)-2-amino-4-(4-methoxyphenyl)-4*H*-chromene-3-carboxylate

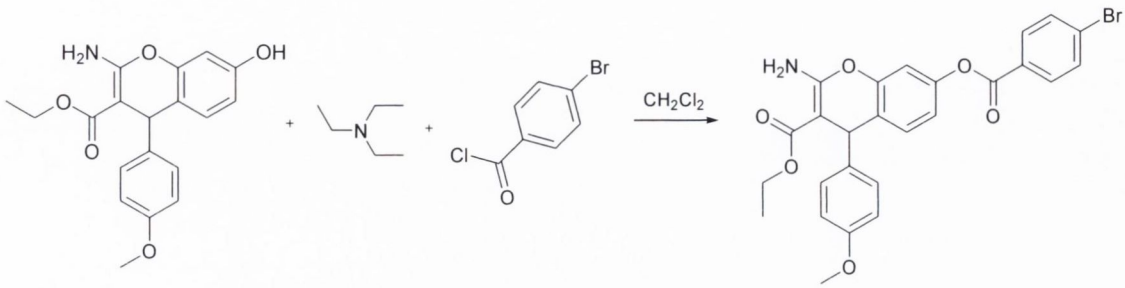

Yield: 0.39 g, 76 %, yellow crystals (Flash Column; Hexane, EtOAc, 2:1)

HPLC Purity: 93% **MP:** 255 - 261°C

IRϑ_{max} (KBr): 3459.63 (NH_2), 3381.56 (NH_2), 1673.46 (C=O), 1662.98 (C=O), 1639.31 (C=C), 1630.38 (C=C), 1592.58, 1567.94, 1497.41 cm^{-1}

^{1}H NMR (400 MHz, $CDCL_3$): δ 1.18 (t, 3H, *J*=7.02 Hz, CH_3), 3.77 (s, 3H, OCH_3), 4.11 (q, 2H, *J*=7.04 Hz, CH_2), 4.94 (s, 1H, CH), 6.32 (s, 2H, NH_2), 6.78 (d, 2H, *J*=7.26 Hz, Ar-H), 6.87 (d, 1H, *J*=7.12 Hz, Ar-H), 6.94 (d, 1H, *J*=6.76 Hz, Ar-H), 7.14 (d, 3H, *J*=8.04 Hz, Ar-H), 7.66 (d, 2H, *J*=8.44 Hz, Ar-H), 8.03 (d, 2H, *J*=7.24 Hz, Ar-H)

^{13}C NMR (100 MHz, $CDCL_3$): δ 18.90 (CH_3), 38.78 (CH), 54.77 (OCH_3), 59.08 (CH_2), 78.59 (C), 109.18 (CH), 113.15 (CH), 116.57 (CH), 117.37 (C), 124.06 (C-Br), 127.71 (C), 129.58 (CH), 131.21 (CH), 131.55 (C), 148.58 (C-O), 148.89 (C-O), 157.48 (C-OCH_3), 159.36 (O-C-N), 163.77 (C=O), 168.86 (C=O)

HRMS (ESI): $C_{26}H_{23}{}^{81}BrNO_6$ [M^+ H] requires (m/e) 524.0709, found 524.0764, (1.5 ppm)

BE107 Synthesis of ethyl 7-(4-iodobenzoyloxy)-2-amino-4-(4-methoxyphenyl)-4*H*-chromene-3-carboxylate

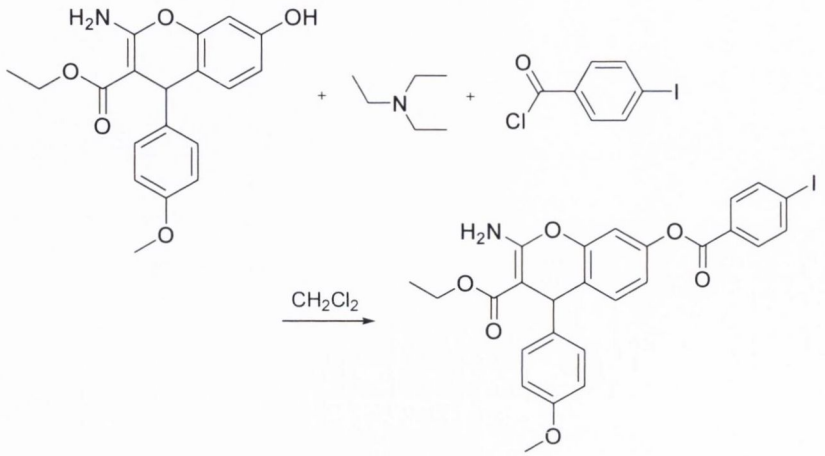

Yield: 0.49 g, 86%, white powder (Flash Column; Hexane, EtOAc, 2:1)

HPLC Purity: 95% **MP:** 258 - 267°C

IRϑ_{max} (KBr): 3368.50 (NH_2), 3356.64 (NH_2), 1655.50 (C=O), 1652.94 (C=O), 1630.88 (C=C), 1629.21 (C=C), 1576.45 cm^{-1}

^{1}H NMR (400 MHz, $CDCL_3$): δ 1.18 (t, 3H, *J*=7.04 Hz, CH_3), 3.77 (s, 3H, OCH_3), 4.09 (q, 2H, *J*=7.02 Hz, OCH_2), 4.94 (s, 1H, CH), 6.78 (d, 2H, *J*=8.12 Hz, Ar-H), 6.87 (d, 1H, *J*=7.14 Hz, Ar-H), 6.93 (d, 1H, *J*=6.82 Hz, Ar-H), 7.13 – 7.18 (m, 3H, Ar-H), 7.88 -7.93 (m, 4H, Ar-H)

^{13}C NMR (100 MHz, $CDCL_3$): δ 13.91 (CH_3), 38.78 (CH), 54.77 (OCH_3), 59.08 (OCH_2), 78.59 (C), 101.37 (C-I), 109.17 (CH), 113.15 (CH), δ 117.14 (CH), δ 117.37 (C), δ 124.06 (C), δ 124.85 (C), δ 129.70 (CH), 132.06 (C), δ 137.56 (CH), δ 148.58 (C-O), δ 153.27 (C-O), δ 157.48 (C-OCH_3), δ 159.37 (O-C-N), δ 164.02 (C=O), δ 168.87 (C=O)

HRMS (ESI): $C_{26}H_{22}{}^{127}INNaO_6$ [M^+ Na] requires (m/e) 594.0389, found 594.0378, (-1.8ppm)

BE108 Ethyl 7-(3,4,5-trimethoxybenzoyloxy)-2-amino-4-(4-methoxyphenyl)-4*H*-chromene-3-carboxylate

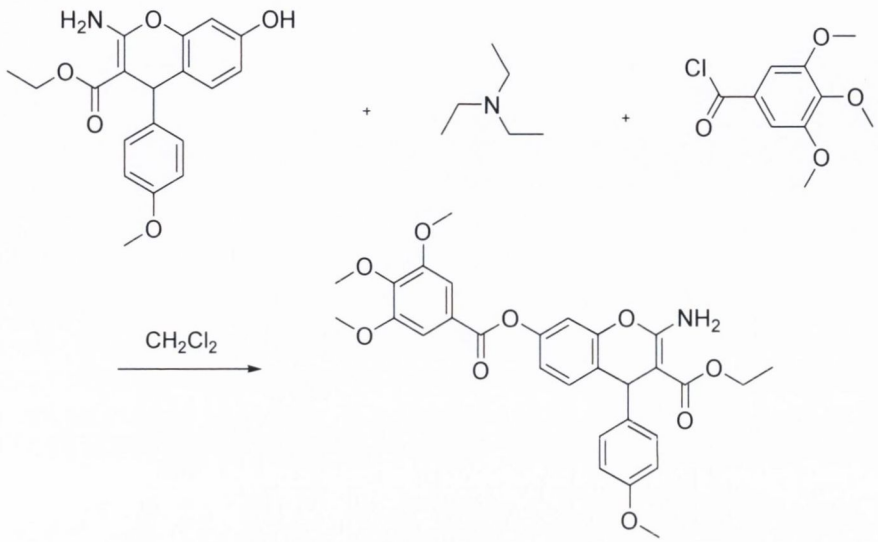

Yield: 0.23 g, 44 %, pale yellow powder (Flash Column; Hexane, EtOAc, 3:1)

HPLC Purity: 89% **MP:** 265-272°C

IRϑ_{max} (KBr): 3495.88, 3443.95 (NH_2), 1680.87 (C=O), 1668.41 (C=O), 1639.29 (C=C), 1631.74 (C=C), 1579.84, 1537.59, 1461.46 cm^{-1}

^{1}H NMR (400 MHz, CHLOROFORM-*d*) δ ppm 1.18 (t, 3H, *J*=7.28 Hz, CH_3), 3.77 (s, 3H, OCH_3), 3.95 (s, 9H, 3xOCH_3), 4.10 (m, 2H, CH_2), 4.95 (s, 1H, CH), 6.34 (s (br), 2H, NH_2) 6.78 (d, 2H, *J*=8.12 Hz, Ar-H), 6.86 - 6.90 (m, 1H, Ar-H), 6.93 (d, 1H, *J*=7.01 Hz, Ar-H), 7.15 – 7.18 (m, 3H, Ar-H), 7.44 (s, 2H, Ar-H)

^{13}C NMR (101 MHz, CHLOROFORM-*d*) δ ppm 13.91 (CH_3), 38.79 (CH), 54.77 (CH_3), 55.87 (CH_3), 59.07 (CH_2), 78.65 (C), 106.96 (CH), 109.29 (CH), 113.14 (CH), 117.54 (C), 123.64 (C), 123.92 (CH), 128.12 (CH), 129.66 (CH), 133.64 (C), 139.53 (C-O), 148.61 (C-O), 149.14 (C-O), 152.61 (C-O), 157.49 (C-OCH_3), 159.39 (O-C-N), 164.09 (C=O), 168.87 (C=O)

HRMS (ESI): $C_{29}H_{30}NO_9$ [M^+ H] requires (m/e) 536.1921, found 536.1927, (-1.1 ppm)

5.4 Coupling reaction of Ethyl 2-amino-7-hydroxy-4-(4-methoxyphenyl)-4H-chromene-3-carboxylate with 3,4,5-Trimethoxybenzoic acid

A mixture of 3,4,5-Trimethoxybenzoic acid (1 equiv., 1 mmol, [212 mg], DCC [2 equiv., 2 mmol, [412 mg]), and HOBt (2 equiv., 2 mmol, [270 mg]), were suspended in 20 mL of anhydrous THF and stirred for 10 mins under a nitrogen atmosphere. Ethyl 2-amino-7-hydroxy-4-(4-methoxyphenyl)-4H-chromene-3-carboxylate (2 equiv., 2mmol, [638 mg]), was then dissolved in 10mL of anhydrous THF and slowly added to the mixture *via* syringe. The reaction was allowed stir for 36 hours after TLC check and verified, mix was washed with H_2O and dried using Na_2SO_4 and evaporated to dryness under vacuum.

BE108b Ethyl 7-(3,4,5-trimethoxybenzoyloxy)-2-amino-4-(4-methoxyphenyl)-4*H*-chromene-3-carboxylate

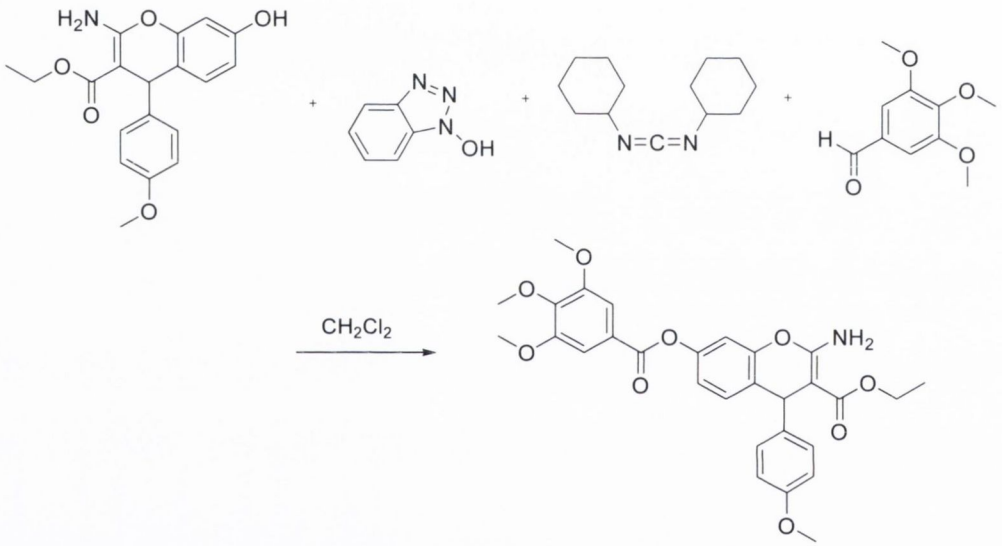

Yield: 0.29 g, 56 %, yellow powder (Flash Column; Hexane, EtOAc, 3:1)

HPLC Purity: 92% **MP:** 236 - 238°C

IRϑ_{max} (KBr): 3457.84, 3348.10 (NH_2), 1658.49 (C=O), 1654.11 (C=O), 1632.58 (C=C), 1627.53 (C=C), 1545.95, 1592.64, 1453.96 cm^{-1}

^{1}H NMR (400 MHz, CHLOROFORM-*d*) δ ppm 1.11 (t, 3 H, *J*=7.14, CH_3), 3.98 (s, 12 H, 4xOCH_3), 4.12 (q, 2H, *J*=7.12 Hz, CH_2), 4.84 (s, 1H, CH), 6.86 - 6.93 (m, 3H, Ar-H), 7.21 (d, 2H, *J*=7.22 Hz, Ar-H), 7.27 - 7.33 (m, 2H, Ar-H), 7.44 - 7.50 (m, 2H, Ar-H), 7.68 (s (br), 2H, NH_2)

^{13}C NMR (101 MHz, CHLOROFORM-*d*) δ ppm 16.01 (CH_3), 42.68 (CH), 54.97 (CH_3), 56.01 (CH_3), 60.73 (CH_2), 76.28 (C), 107.09 (CH), 107.96 (CH), 113.75 (CH), 118.62 (C), 124.29 (CH), 127.91 (CH), 129.36 (CH), 132,52 (C), 142.25 (C-O), 144.27 (C-O),

145.01 (C-O), 150.83 (C-O), 153.69 (C-OCH_3), 154.62 (O-C-N), 163.73 (C=O), 166.42 (C=O)

HRMS (ESI): $C_{29}H_{29}NNaO_9$ [M^+ Na] requires (m/e) 558.1740, found 558.1750, (-1.8 ppm)

BE109 Ethyl 7-(2-(thiophen-2-yl)acetoyloxy)-2-amino-4-(4-methoxyphenyl)-4*H*-chromene-3-carboxylate

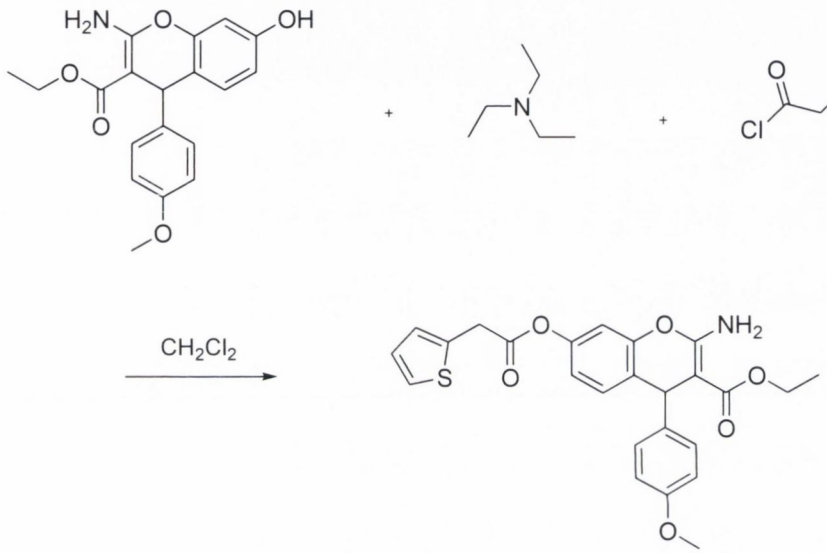

Yield: 0.23 g, 51 %, brown oil (Flash Column; Hexane, EtOAc, 3:1)

HPLC Purity: 91% **MP:** oil

IRϑ_{max} (KBr): 3539.29, 3493.75 (NH_2), 1676.59 (C=O), 1654.71 (C=O), 1634.40 (C=C), 1628.20 (C=C), 1615.74 (C=C), 1563.85, 1496.76 cm^{-1}

^{1}H NMR (400 MHz, CHLOROFORM-*d*) δ ppm 1.20 (t, 3H, *J*=7.21 Hz, CH_3), 3.76 (s, 3 H, OCH_3), 4.08 (s, 2H, CH_2), 4.17 (q, 2H, *J*=7.14 Hz, CH_2), 4.91 (s, 1H, CH), 6.30 (s (br), 2 H, NH_2), 6.78 (d, 2 H, *J*=6.78 Hz, Ar-H), 6.83 (d, 1 H, *J*=7.51 Hz, Ar-H), 7.00 - 7.07 (m, 3 H, Ar-H), 7.13 – 7.18 (m, 2H, Ar-H), 7.28 (s, 2 H, Ar-H)

^{13}C NMR (101 MHz, CHLOROFORM-*d*) δ ppm 13.89 (CH_3), 35.08 (CH_2), 38.73 (CH) 54.75 (CH_3), 59.06 (CH_2), 78.57 (C), 108.93 (CH), 113.12 (CH), 115.73 (CH), 117.16 (C), 124.96 (CH), 126.52 (CH), 128.10 (CH), 129.58 (CH), 133.65 (C), 136.69 (C), 148.36 (C-O), 148.78 (C-O), 157.46 (C-OCH_3), 159.33 (O-C-N), 168.19 (C=O), 168.85 (C=O)

HRMS (ESI): $C_{25}H_{23}NNaO_6S$ [M^+ Na] requires (m/e) 488.1144, found 488.1155, (-2.2 ppm)

BE110 Ethyl 7-(3-methylbut-2-enoyloxy)-2-amino-4-(4-methoxyphenyl)-4*H*-chromene-3-carboxylate

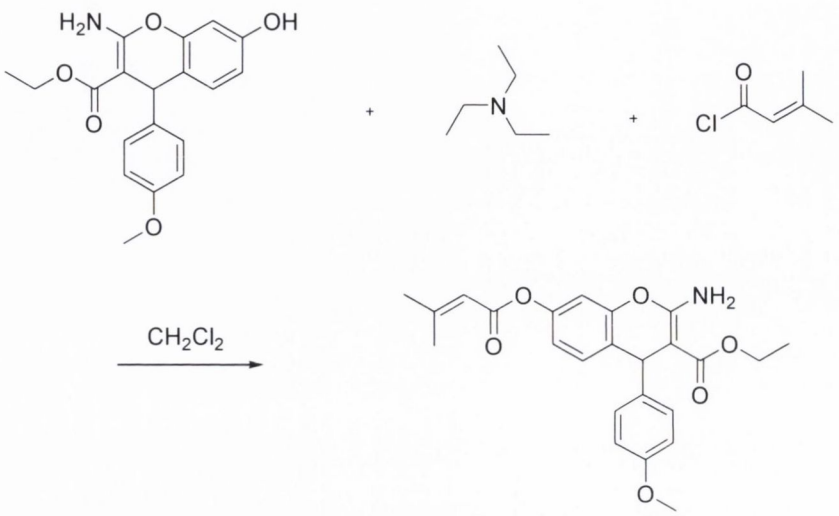

Yield: 0.11 g, 27 %, orange resin (Flash Column; Hexane, EtOAc, 3:1)

HPLC Purity: 89% **MP:** na

IRϑ_{max} (KBr): 3531.90, 3497.52 (NH_2), 1669.82 (C=O), 1660.65 (C=O), 1640.62 (C=C), 1631.29 (C=C), 1589.56 cm^{-1}

^{1}H NMR (400 MHz, CHLOROFORM-*d*) δ ppm 1.19 (t, 3 H, *J*=7.02 Hz, CH_3), 2.02 (s, 6H, 2xCH_3), 3.77 (s, 3H, OCH_3), 4.09 (q, 2 H, *J*=7.03 Hz, CH_2), 4.91 (s, 1H, CH), 5.88 (s, 1H, CH), 6.78 (d, 2H, *J*=8.53 Hz, Ar-H), 6.83 (m, 2H, Ar-H), 7.10 (s, 1H, Ar-H), 7.14 (d, 2H, *J*=9.03 Hz, Ar-H)

^{13}C NMR (101 MHz, CHLOROFORM-*d*) δ ppm 13.89 (CH_3), 20.08 (CH_3), 27.25 (CH_3), 38.74 (CH), 54.75 (OCH_3), 59.02 (OCH_2), 80.14 (C), 109.28 (CH), 113.09 (CH), 114.47 (CH), 116.94 (CH), 117.64 (C), 128.11 (CH), 129.43 (CH), 139.61 (C), 148.45 (C-O), 148.91 (C-O), 157.41 (C-OCH_3), 159.45 (C=C), 160.08 (O-C-N), 164.13 (C=O), 168.92 (C=O)

HRMS (ESI): $C_{24}H_{26}NO_6$ [M^+ H] requires (m/e) 424.1760, found 424.1767, (-1.6 ppm)

BE111 3-(Ethoxycarbonyl)-2-amino-4-(4-methoxyphenyl)-4*H*-chromen-7-yl 6-(trifluoromethyl)pyridine-3-carboxylate

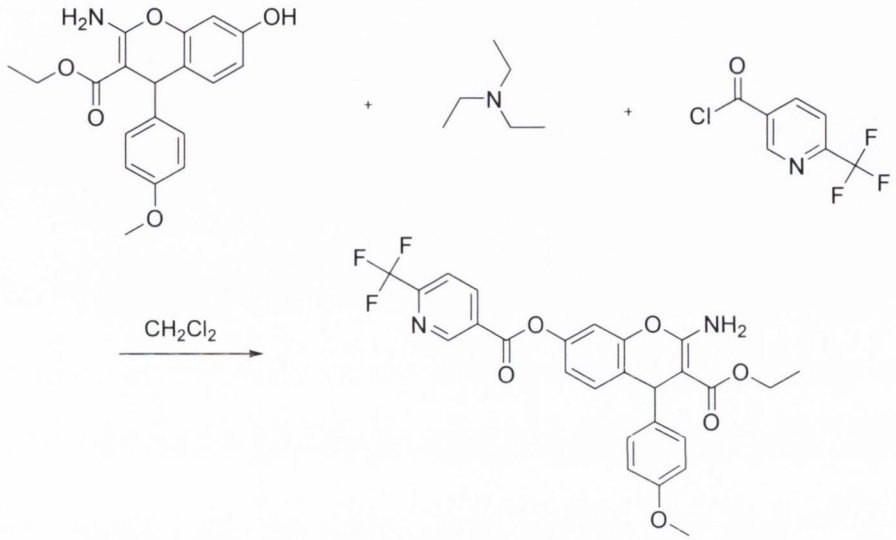

Yield: 0.25 g, 50 %, brown resin (Flash Column; Hexane, EtOAc, 2:1)

HPLC Purity: 90% **MP:** na

IRϑ_{max} (KBr): 3576.32, 3512.84 (NH_2), 1666.74 (C=O), 1652.83 (C=O), 1640.09 (C=C), 1630.48 (C=C), 1578.52 (C=C), 1521.01 cm^{-1}

^{1}H NMR (400 MHz, CHLOROFORM-*d*) δ ppm 1.21 (t, 3H, *J*=7.03 Hz, CH_3), 3.77 (s, 3H, OCH_3), 4.12 (q, 2H, *J*=7.41 Hz, CH_2), 4.96 (s, 1H, CH), 6.35 (s (br), 2H, NH_2), 6.80 (d, 2H, *J*=8.26 Hz, Ar-H), 7.12 - 7.23 (m, 3H, Ar-H), 7.29 (s, 1H, Ar-H), 7.89 (s, 1 H, Ar-H), 8.18 – 8.21 (m, 2H, Ar-H), 9.02 (s, 1H, Ar-H)

^{13}C NMR (101 MHz, CHLOROFORM-*d*) δ ppm 13.89 (CH_3), 38.79 (CH), 54.76 (CH_3), 59.13 (CH_2), 78.54 (C), 109.02 (CH), 113.18 (CH), 117.10 (CH), 119.97 (C), 124.42 (CH), 124.79 (C), 125.31 (C-F), 128.11 (CH), 129.90 (CH), 138.91 (C), 139.35 (CH), 147.31 (C-F), 149.61 (C-O), 151.58 (C=N-), 153.67 (C-O), 158.62 (C-OCH_3), 160.96 (O-C-N), 165.54 (C=O), 167.28 (C=O)

HRMS (ESI): $C_{26}H_{22}F_3N_2O_6$ [M^+ H] requires (m/e) 515.143, found 515.1438, (-1.5 ppm)

BE112 Bis[2-amino-3-(ethoxycarbonyl)-4-(4-methoxyphenyl)-4*H*-chromen-7-yl] octanedioate

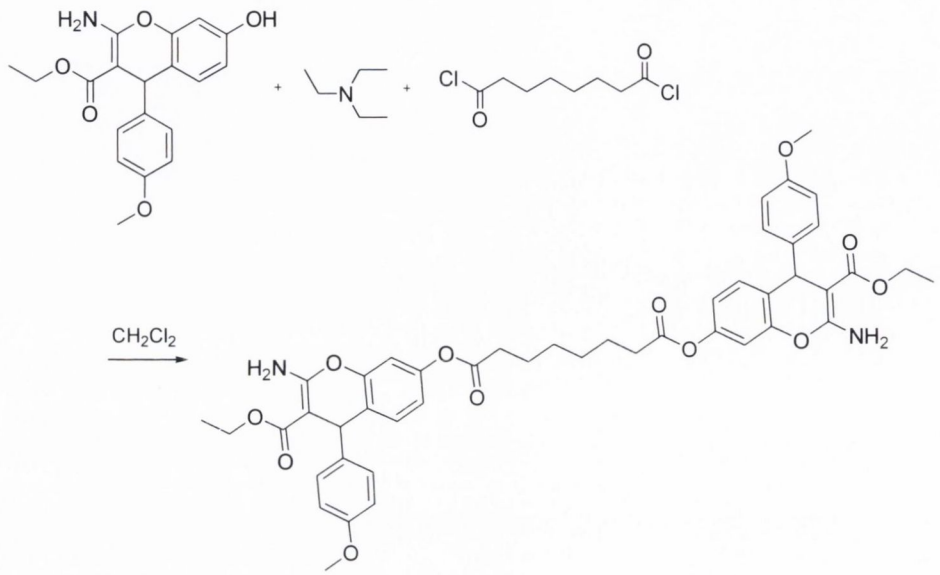

Yield: 0.32 g, 40 %, clear brown oil (Flash Column; Hexane, EtOAc, 2:1)

HPLC Purity: 98% **MP:** oil

IRϑ_{max} (KBr): 3493.60 (NH_2), 3380.38 (NH_2), 1658.45 (C=O), 1655.22 (C=O), 1631.54 (C=C), 1624.21, 1621.74 (C=C), 1583.28, 1538.77, 1474.89 cm^{-1}

^{1}H NMR (400 MHz, $CDCL_3$): δ 1.17 (t, 6H, *J*=7.04 Hz, 2xCH_3), δ 1.74 - 1.82 (m, 4H, 2xCH_2), 2.38 (t, 4H, *J*=7.52 Hz, 2xCH_2), 2.63 (t, 4H, *J*=7.52 Hz, 2xCH_2), 3.76 (s, 6H, 2xCH_3), 4.05 (q, 4H, *J*=7.04 Hz, 2xCH_2), 4.90 (s, 2H, 2xCH), 6.33 (s, 4H, 2xNH_2), 6.76 (d, 6H, *J*=7.26 Hz, Ar-H), 7.10-7.16 (m, 6H, Ar-H), δ 7.28 – 7.33 (m, 2H, Ar-H)

^{13}C NMR (100 MHz, $CDCL_3$): δ 13.80 (CH_3), 23.99 (CH_2), 28.19 (CH_2), 33.35 (CH_2), 38.72 (CH), 54.75 (OCH_3), 59.07 (CH_2), 78.54 (C), 109.07 (CH), 113.11 (CH), 116.79 (CH), 117.35 (C), 128.10 (CH), 129.52 (CH), 139.52 (C), 148.47 (C-O), 148.88 (C-O), 157.43 (C-OCH_3), 159.44 (O-C-N), 168.91 (C=O), 171.46 (C=O)

HRMS (ESI): $C_{46}H_{48}N_2NaO_{12}$ [M^+ Na] requires (m/e) 843.3105, found 843.3132, (+3.2 ppm)

BE113 Synthesis of bis(3-(ethoxycarbonyl)-2-amino-4-(4 methoxyphenyl)-4*H*-chromen-7-yl) terephthalate

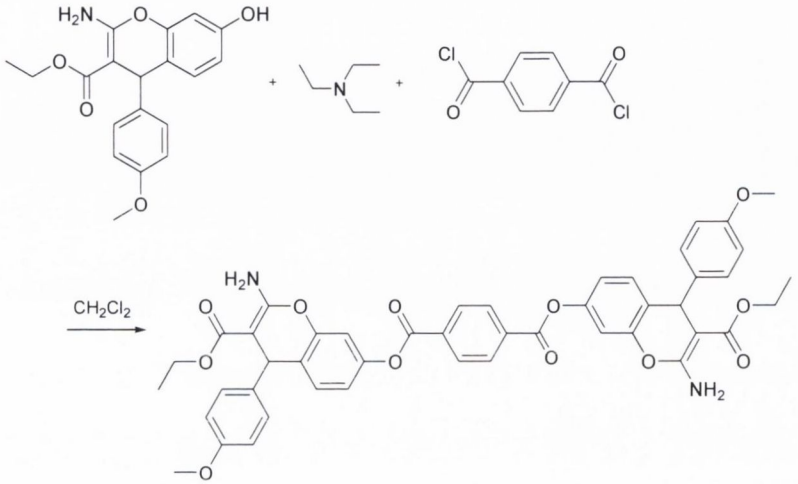

Yield: 0.79 g, 98 %, white powder (Flash Column; Hexane, EtOAc, 3:1)

HPLC Purity: 95 % **MP:** 276 - 289°C

IRϑ_{max} (KBr): 3484.38 (NH_2), 3380.59 (NH_2), 1671.40 (C=O), 1666.86 (C=O), 1645.21 (C=C), 1636.53 (C=C), 1574.86, 1476.43 cm^{-1}

^{1}H NMR (400 MHz, $CDCL_3$): δ 1.21 (t, 6H, *J*=7.02 Hz, 2xCH_3), 3.78 (s, 6H, 2xOCH_3), 4.08 (q, 4H, *J*=7.02 Hz, 2xCH_2), 4.96 (s, 2H, 2xCH), 6.34 (s (br), 4H, 2xNH_2), 6.79 (d, 4H, *J*=8.12 Hz, Ar-H), 6.93 - 6.94 (m, 2H, Ar-H), 6.98 (d, 2H, *J*=7.08 Hz, Ar-H), 7.16 - 7.19 (m, 6H, Ar-H), 8.31 (s, 4H, Ar-H)

^{13}C NMR (100 MHz, $CDCL_3$): δ 13.91 (CH_3), 38.79 (CH), 54.77 (OCH_3), 59.10 (OCH_2), 78.57 (C), 109.14 (CH), 113.16 (CH), 117.31 (CH), 124.23 (C), 128.13 (CH), 129.77 (CH), 133.26 (C), 139.46 (C), 148.61 (C-O), 148.82 (C-O), 157.50 (C-OCH_3), 159.37 (O-C-N), 163.52 (C=O), 168.87 (C=O)

HRMS (ESI): $C_{46}H_{41}N_2O_{12}$ [M^+ H] requires (m/e) 813.2659, found 813.2659, (-0.1ppm)

BE114 Bis[2-amino-3-(ethoxycarbonyl)-4-(4-methoxyphenyl)-4*H*-chromen-7-yl] decanedioate

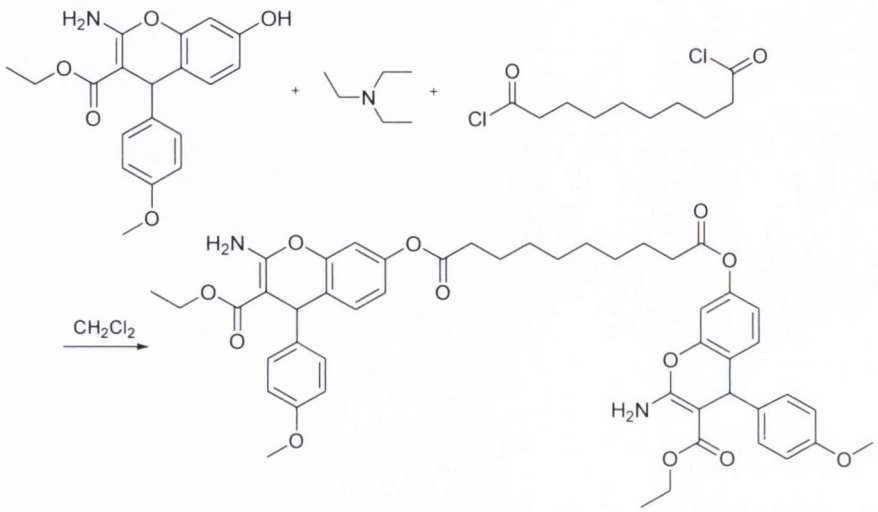

Yield: 0.16 g, 20 %, pale brown oil (Flash Column; Hexane, EtOAc, 3:1)

HPLC Purity: 97% **MP:** oil

IRϑ_{max} (KBr): 3579.11 (NH_2), 3378.85 (NH_2), 1664.41 (C=O), 1655.62 (C=O), 1630.48 (C=O), 1627.59 (C=C), 1622.87 (C=C), 1488.63, 1420.10 cm^{-1}

^{1}H NMR (400 MHz, $CDCL_3$): δ 1.17 (t, 6H, *J*=7.04 Hz, 2xCH_3), 1.39 - 1.46 (m, 12H, 6xCH_2), 2.55 (t, 4H, *J*=7.52 Hz, 2xCH_2), 3.76 (s, 6H, 2xOCH_3), 4.06 (q, 4H, 7.02 Hz, 2xOCH_2), 4.90 (s, 2H, 2xCH), 6.31 (s, 4H, 2xNH_2), 6.74-6.82 (m, 8H, Ar-H), 7.08-7.20 (m, 6H, Ar-H)

^{13}C NMR (100 MHz, $CDCL_3$): δ 13.89 (CH_3), 24.37 (CH_2), 28.49 (CH_2), 28.56 (CH_2), 33.85 (CH_2), 38.73 (CH), 54.75 (OCH_3), 59.04 (OCH_2), 79.90 (C), 109.07 (CH), 113.10 (CH), 117.12 (CH), 117.36 (C), 123.68 (CH), 128.10 (CH), 139.53 (C), 148.90 (C-O), 153.32 (C-O), 157.44, (C-OCH_3), 159.40 (O-C-N), 168.88 (C=O), 171.57 (C=O)

HRMS (ESI): $C_{48}H_{52}N_2NaO_{12}$ [M^+ Na] requires (m/e) 871.3418, found 871.3433, (1.7ppm)

BE115 Synthesis of bis(3-(ethoxycarbonyl)-2-amino-4-(4-methoxyphenyl)-4*H*-chromen-7-yl) phthalate

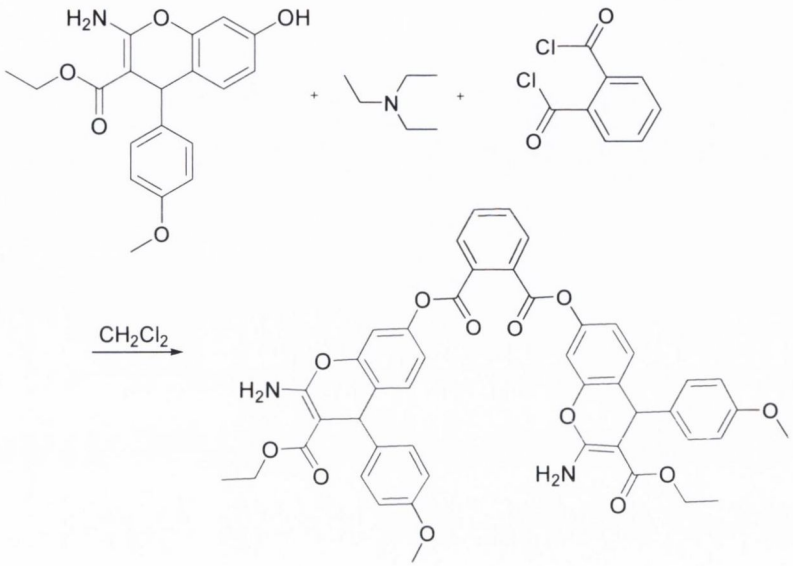

Yield: 0.77 g, 96 %, yellow solid (Flash Column; Hexane, EtOAc, 3:1)

HPLC Purity: 96% **MP:** 267 - 274°C

IRϑ_{max} (KBr): 3484.34, 3394.64 (NH_2), 1670.83 (C=O), 1665.51 (C=O), 1642.31 (C=C), 1538.75 (C=C), 1559.45, 1526.89 cm^{-1}

^{1}H NMR (400 MHz, CDCL$_3$): δ 1.18 (t, 6H, *J*=7.02 Hz, 2xCH_3), 3.77 (s, 6H, 2xOCH_3), 4.10 (q, 4H, *J*=7.04 Hz, 2xOCH_2), 4.92 (s, 2H, 2xCH), 6.64 - 6.76 (m, 4H, Ar-H), 6.88 (d, 2H, *J*=8.12 Hz, Ar-H), 6.94 (d, 2H, *J*=7.29 Hz, Ar-H), 7.11 - 7.20 (m, 6H, Ar-H), 7.70 – 7.79 (m, 2H, Ar-H), 7.90 - 7.97 (m, 2H, Ar-H)

^{13}C NMR (100 MHz, CDCL$_3$): δ 13.91 (CH_3), 38.78 (CH), 54.76 (CH_3), 59.07 (CH_2), 78.02 (C), 109.12 (CH), 113.14 (CH), 117.28 (C), 128.12 (CH), 129.09 (CH), 129.69 (CH), 130.96 (C), 131.49 (CH), 139.48 (C), 148.56 (C-O), 148.82 (C-O), 157.47 (C-OCH_3), 159.41 (O-C-N), 165.11 (C=O), 168.86 (C=O)

HRMS (ESI): $C_{46}H_{41}N_2O_{12}$ M^+ H requires (m/e) 813. 2659, found 813.2645, (-1.7ppm)

Synthesis of acrylate intermediates.

General Procedure

The appropriate benzaldehyde (1 equiv., 10 mmol.), was placed in a round bottom flask and the appropriate cyanoacetate was added (1 equiv., 10 mmol). Ethanol (30 mL) was added and the reaction mixture was then heated to dissolve all reactants. Piperidine (0.5 mL) was than added dropwise and the reation was refluxed for 5 hours. Progress was checked *via* TLC until no starting material remained. Afterwards, solvent was removed *in vacuo* and product was purified by recrystallization in ethanol.

Synthesis of benzopyrans from acrylate intermediates.

General Procedure

The appropriate acrylate intermediate (1 equiv., 1 mmol.), was placed in a round bottom flask and the resorcinol was added (1 equiv., 1 mmol). Ethanol (10 mL) was then added and reaction mix was heated to dissolve all reactants. Piperidine (0.05 mL) was then added dropwise with stirring, and the reation was left to reflux for 8 hours. Progress was checked *via* TLC until no starting material remained. Afterwards, solvent was removed and product was recrystallised in ethanol.

5.5 Synthesis of benzyloxyaldehydes

General Procedure

4-Hydroxybenzaldehyde (1 equiv., 20 mmol) was reacted with the appropriate benzyl bromide (1 equiv., 20 mmol) in a round bottom flask with base catalyst K_2CO_3 (0.66 equiv.). Solvent used was acetonitrile (30 mL), and reaction was stirred under N_2 for 6 to 8 h. Progress was checked *via* TLC. Purification was carried out by removal of the inorganic salts by filtration, then the filtrate was washed with ethyl acetate / H_2O x3. Solvent was removed *in vacuo* and product was purified by flash column chromatography over silica gel.

4-(2-Fluorobenzyloxy)benzaldehyde

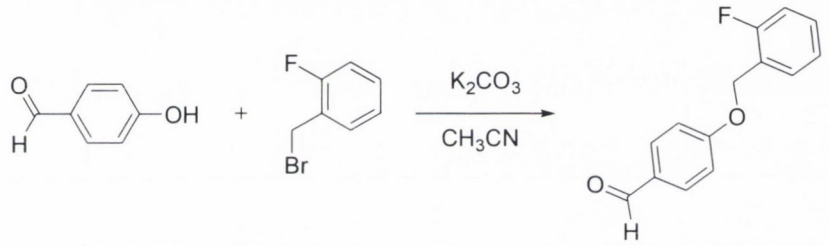

Yield: 3.49 g, 76 %, white powder (Flash Column; Hexane, EtOAc, 3:1)

MP: 53-55°C **Lit. Ref**: [244] **Lit. MP**: 54°C

IRϑ_{max} (KBr): 3148.46 (CH), 3094.63 (CH), 1743.62 (C=C), 1694.57 (C=C), 1631.76 (C=O), 1564.96, 1285.84 (C-F) cm^{-1}

^{1}H NMR (400 MHz, DMSO-d_6): δ ppm 5.21 (s, 2H, OCH_2), 7.17 (d, 2H, *J*=8.24 Hz, Ar-H), 7.19 - 7.22 (m, 2H, Ar-H), 7.68 (d, 2H, *J*=2.14 Hz, Ar-H), 7.86 (s, 2H, Ar-H), 9.84 (s, 1H, CHO)

^{13}C NMR (101 MHz, DMSO-d_6): δ ppm 67.93 (CH_2), 113.23 (CH), 114.90 (CH), 124.15 (CH), 125.69 (C), 128.63 (CH), 129.37 (CH), 131.82 (CH), 160.05 (C-F), 164.45 (C-O), 189.12 (C=O)

HRMS (ESI): $C_{14}H_{12}FO_2$ [M^+ + H] requires (m/e) 231.0821, found 231.0831, (-4.32 ppm)

4-(4-Fluorobenzyloxy)benzaldehyde

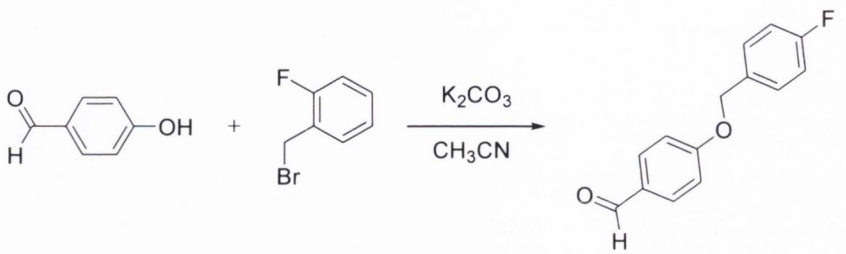

Yield: 1.88 g, 41 %, white powder (Flash Column; Hexane, EtOAc, 3:1)

HPLC Purity: 94 % **MP:** 108°C **Lit. Ref.**:[245]

IRϑ_{max} (KBr): 2860.4 (CH), 1680.36 (C=C), 1637.62 (C=C), 1611.84 (C=O), 1583.56, 1541.38, 1125.51 (C-F) cm^{-1}

^{1}H NMR (400 MHz, DMSO-d_6): δ ppm 5.20 (s, 2H, OCH_2), δ 7.16 - 7.19 (m, 2H, Ar-H), δ 7.21 - 7.29 (m, 2H, Ar-H), δ 7.52 (d, 2H, *J*=3.28, Ar-H), δ 7.82 - 7.88 (m, 2H, Ar-H), δ 9.89 (s, 1H, CHO)

^{13}C NMR (101 MHz, DMSO-d_6): δ ppm 69.33 (CH_2), δ 114.86 (CH), δ 115.54 (CH), δ 127.21 (CH), δ 129.70 (C), δ 131.93 (CH), δ 131.82 (C), δ 158.92 (C-F), δ 167.41 (C-O), δ 190.13 (C=O)

HRMS (ESI): $C_{14}H_{12}FO_2$ [M^+ + H] requires (m/e) 231.0821, found 231.0810, (4.76 ppm)

4-[(4-methylphenyl)methoxy]benzaldehyde

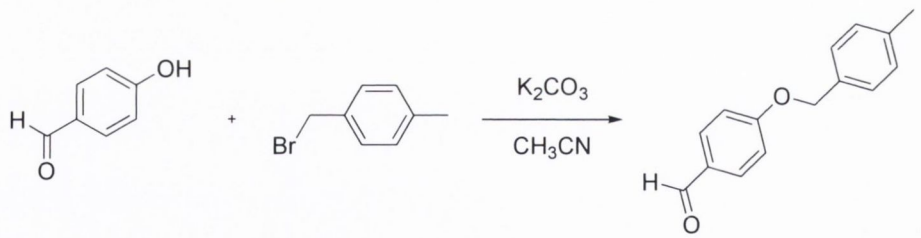

Yield: 3.16 g, 70 %, white solid (Flash Column; Hexane, EtOAc, 3:1)

MP: 154-159°C **Lit. Ref.** [245]

IRϑ_{max} (KBr): 3158.23 (CH), 1769.63 (C=C), 1651.73 (C=C), 1469.22 (C=O), 1628.63 (C-O), 1564.83, 1538.52, 1358.73 cm^{-1}

^{1}H NMR (400 MHz, DMSO-d_6): δ ppm 2.41 (s, 3H, CH_3), 5.19 (s, 2H, OCH_2), δ 6.96 – 7.10 (m, 4H, Ar-H), δ 7.14 (s, 2H, Ar-H), δ 7.62 (s, 2H, Ar-H), δ 9.68 (s, 1H, CHO)

^{13}C NMR (101 MHz, DMSO-d_6): δ ppm 25.64 (CH_3), δ 72.85 (CH_2), δ 114.84 (CH), δ 127.41 (CH), δ 129.48 (CH), δ 136.24 (C-CH_3), δ 138.61 (C), δ 166.15 (C-O), δ 187.83 (C=O)

HRMS (ESI): $C_{15}H_{15}O_2$ [M^+ H] requires (m/e) 227.1072, found 227.1078, (+2.6 ppm)

4-(3-Chlorobenzyloxy)benzaldehyde

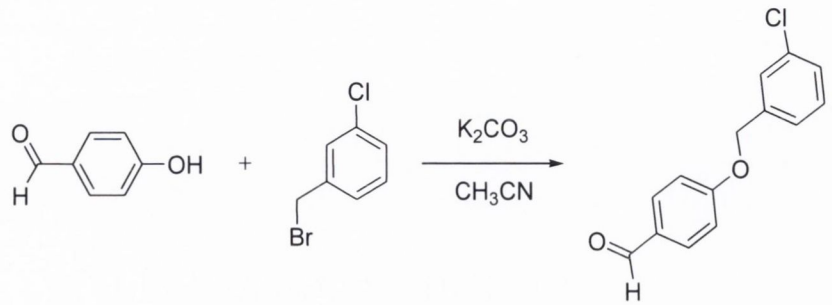

Yield: 3.05 g, 62 %, white powder (Flash Column; Hexane, EtOAc, 2:1)

MP: 92-101 °C **Lit. Ref**. [246] **Lit. MP**: 89-91 °C

IRϑ_{max} (KBr): 2917.83 (CH), 1688.29 (C=C), 1648.51 (C=O), 1594.73, 1535.17, 1262.36 (C-O), 770.19 (C-Cl), cm^{-1}

^{1}H NMR (400 MHz, DMSO-d_6): δ ppm 5.25 (s, 2H, OCH_2), δ 7.09 - 7.15 (m, 1H, Ar-H), δ 7.21 (d, 1H, *J*=8.56 Hz, Ar-H), δ 7.37 - 7.42 (m, 3H, Ar-H), δ 7.55 (s, 1H, Ar-H), δ 7.89 (s, 2H, Ar-H), δ 9.87 (s, 1H, CHO)

^{13}C NMR (101 MHz, DMSO-d_6): δ ppm 68.67 (CH_2), δ 114.62 (CH), δ 122.19 (CH), δ 126.30 (CH), δ 127.43 (CH), δ 128.01 (C), δ 130.44 (CH), δ 131.37 (CH), δ 134.57 (C-Cl), δ 142.54 (C), δ 163.01 (C-O), δ 191.34 (C=O)

HRMS (ESI): $C_{14}H_{12}{}^{35}ClO_2$ $[M^+ + H]$ requires (m/e) 247.0526, found 247.0517 (+3.6 ppm)

4-(3-Bromobenzyloxy)benzaldehyde

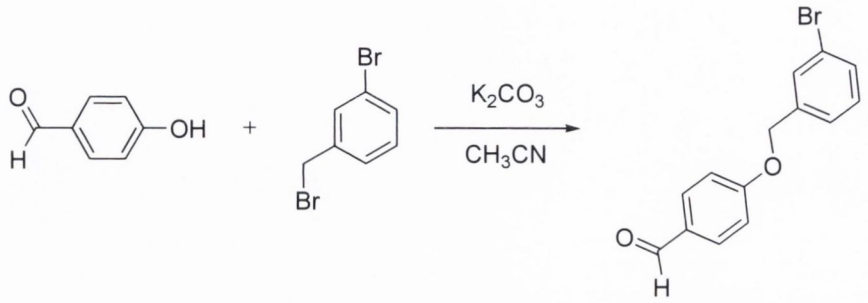

Yield: 3.78 g, 65 %, yellow powder (Flash Column; Hexane, EtOAc, 3:1)

MP: 66-69°C **Lit. Ref**. [247] **Lit. MP**: 65-69 °C

IRϑ_{max} (KBr): 2730.08 (CH), 1685.32 (C=C), 1664.39 (C=O), 1542.84, 1267.81 (C-O), 677.49 (C-Cl) cm^{-1}.

^{1}H NMR (400 MHz, DMSO-d_6): δ ppm 5.25 (s, 2H, OCH_2), δ 7.20 – 7.24 (m, 2H, Ar-H), δ 7.37 (d, 1H, *J*=7.52 Hz, Ar-H), δ 7.42 - 7.47 (m, 2H, Ar-H), δ 7.69 (s, 1H, Ar-H), δ 7.87 (d, 2H, *J*=9.04 Hz, Ar-H), δ 9.87 (s, 1H, CHO)

^{13}C NMR (101 MHz, DMSO-d_6): δ ppm 68.62 (CH_2), δ 115.30 (CH), δ 121.75 (C-Br), δ 127.78 (CH), δ 129.91 (CH), δ 130.39 (CH), δ 130.91 (CH), δ 131.83 (CH), δ 139.15 (C), δ 163.01 (C-O), δ 191.34 (C=O)

HRMS (ESI): $C_{14}H_{11}BrO_2$ [M^+] requires (m/e) 291.0020, found 291.0011 (3.09 ppm)

4-(4-Bromobenzyloxy)benzaldehyde

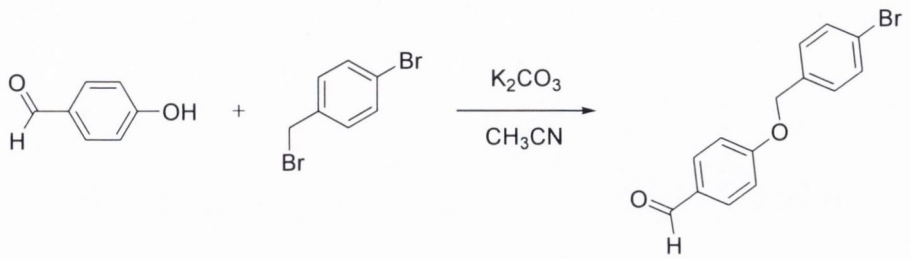

Yield: 3.77 g, 65 %, yellow powder (Flash Column; Hexane, EtOAc, 3:1)

MP: 94°C **Lit. Ref**. [248] **Lit. MP**: 88-92 °C

IRϑ_{max} (KBr): 2795.86 (CH), 1696.26 (C=C), 1672.67 (C=O), 1563.31, 1254.49 (C-O), 603.66 (C-Br) cm^{-1}

^{1}H NMR (400 MHz, DMSO-d_6): δ ppm 5.22 (s, 2H, OCH_2), δ 7.2 (d, 2H, *J*=8.40 Hz, Ar-H), δ 7.43 (d, 2H, *J*=8.52 Hz, Ar-H), δ 7.61 (d, 2H, *J*=8.52 Hz, Ar-H), δ 7.88 (d, 2H, *J*=9.04 Hz, Ar-H), δ 9.87 (s, 1H, CHO)

^{13}C NMR (101 MHz, DMSO-d_6): δ ppm 68.81 (CH_2), δ 115.30 (CH), δ 121.23 (C-Br), δ 126.98 (CH), δ 129.86 (CH), δ 131.46 (CH), δ 139.15 (C), δ 163.01 (O-C-N), δ 191.33 (C=O)

HRMS (ESI): $C_{14}H_{12}{}^{79}BrO_2$ [M^+ + H] requires (m/e) 291.0021, found 291.0022 (-0.34 ppm)

5.6 Synthesis of Benzyloxy-benzopyrans, using one-pot piperidine-catalyzed Knoevenagel condensations

General Procedure

The appropriate benzyloxybenzaldehyde (1 equiv., 2 mmol) was placed in a round bottomed flask. The appropriate alkyl cyanoacetate (2 mmol) and resorcinol (2 mmol) were added. Ethanol (15 mL) was added and reaction mixture was warmed to dissolve all the reactants. After cooling to room temperature, 0.2 mL of piperidine was added dropwise and the reaction was refluxed for 6 h, and progress was monitorerd *via* TLC until no further starting material remained. Afterwards solvent was removed *in vacuo* and product was purified by recrystallisation in EtOH, or by flash column chromatography over silica gel. Synthesised products had yields ranging from 5-58%.

5.7 Synthesis of Dimethylamino-chromenes using one-pot piperidine-catalyzed Knoevenagel condensations

General Procedure

The appropriate Benzyloxybenzaldehyde (1 equiv., 2 mmol) was placed in a round bottomed flask, with appropriate alkyl cyanoacetate (1 equiv., 2 mmol). Addition of 3-dimethylamino phenol (1 equiv., 2 mmol) then followed. Ethanol (20 mL) was added and reaction mixture was warmed to dissolve all the reactants. After cooling to room temperature, 0.2 mL of piperidine was added dropwise and the reaction was refluxed for 5 h. Afterwards solvent was removed *in vacuo* and product was purified by flash column chromatography over silica gel. Purity was checked *via* TLC to yield various products and yields ranging from 4 - 91%.

5.8 Synthesis of Benzylidene intermediates using malononitrile intermediates.

General Procedure

The appropriate benzaldehyde (1 equiv, 10 mmol) was added in a round bottom flask with malononitrile (1 equiv., 10 mmols). Base piperidine (0.5 mL) was added dropwise, and either refluxing in EtOH or stirring at RT in MeOH enabled the synthesis of benzylidene solids with favourable yields. Reaction time varied from 6 to 12 h, progress was checked *via* TLC until no starting material remained. Resulting precipitates were filtered off or purified with flash column chromatography.

BE116 2-(4-Methoxybenzylidene)malononitrile

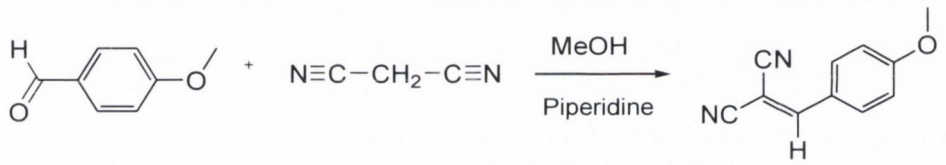

Yield: 1.38 g, 75 %, yellow powder (Recrystallisation, MeOH)

MP: 115-119°C **Lit. Ref**: [249] **Lit. MP**: 116-118 °C

IRϑ_{max} (KBr): 3144.76, 3036.41 (CH), 2258.75 (CN), 2242.62 (CN), 1634.51 (C=C), 1625.33 (C=C), 1594.26, 1541.95 cm^{-1}

^{1}H NMR (400 MHz, CHLOROFORM-*d*) δ ppm 3.94 (s, 3H, OCH_3), 7.03 (d, 2H, *J*=7.04 Hz, Ar-H), 7.68 (s, 1H, CH), 7.92 (d, 2H, *J*=8.02 Hz, Ar-H)

^{13}C NMR (101 MHz, CHLOROFORM-*d*) δ ppm 55.38 (CH_3), 76.29 (C=C), 112.92 (CN), 114.00 (CN), 114.70 (CH), 123.57 (C), 133.03 (CH), 158.45 (CH), 164.38 (C-OCH_3)

HRMS (ESI): $C_{11}H_8N_2O$ [M^+] requires (m/e) 184.0637, found 184.0636, (-0.5 ppm)

BE117 2-(4-Hydroxybenzylidene)malononitrile

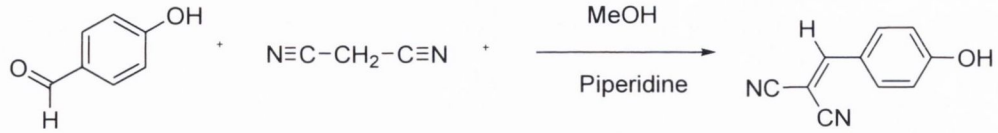

Yield: 0.75 g, 44 %, yellow powder (Recrystallisation, MeOH)

MP: 183-189°C **Lit. Ref**: [250] **Lit. MP**: 188-189 °C

IRϑ_{max} (KBr): 3131.58, 3069.76 (CH), 2260.14 (CN), 2247.58 (CN), 1683.62 (C=C), 1667.50 (C=C), 1542.10 cm^{-1}

^{1}H NMR (400 MHz, CHLOROFORM-*d*) δ ppm 5.18 (s (br), 1H, OH), 6.80 (d, 2H, *J*=8.03 Hz, Ar-H), 7.75 (s, 1H), 7.83 (d, 2H, *J*=7.12 Hz)

^{1}H NMR (100 MHz, CHLOROFORM -*d*) δ ppm 68.74 (C=C), 113.47 (CN), 113.75 (CN), 114.91 (CH), 135.03 (CH), 138.74 (C), 161.26 (CH), 162.47 (C-OH)

HRMS (ESI): $C_{10}H_5N_2O$ [M^- H] requires (m/e) 169.0402, found 169.0402, (0.1 ppm)

BE118 2-(4-(benzyloxy)benzylidene)malononitrile

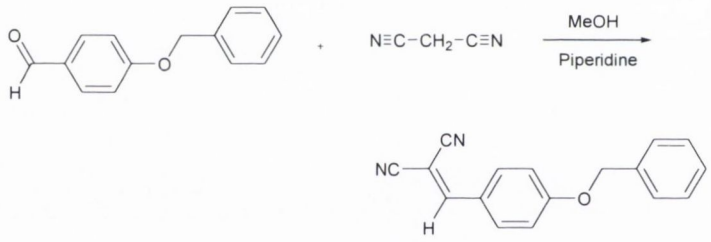

Yield: 1.79 g, 69 %, pale yellow powder (Recrystallisation, MeOH)

MP: 152-155°C **Lit. Ref**: [251] **Lit. MP**: 156 °C

IRϑ_{max} (KBr): 3151.33, 3127.55 (CH), 2349.82 (CN), 2252.76 (CN), 1661.79 (C=C), 1642.56 (C=C), 1559.20 cm^{-1}

^{1}H NMR (400 MHz, CHLOROFORM-*d*) δ ppm 5.20 (s, 2H, CH_2), 7.08 - 7.13 (m, 2H, Ar-H), 7.44 (d, 5H, *J*=8.24 Hz, Ar-H), 7.67 (s, 1H, Ar-H), 7.93 (d, 1H, *J*=7.22 Hz, CH)

^{13}C NMR (101 MHz, CHLOROFORM-*d*) δ ppm 70.07 (C=C), 78.24 (CH_2), 112.88 (CN), 113.12 (CN), 113.97 (CH), 127.08 (CH), 127.77 (CH), 128.56 (C), 133.03 (CH), 134.97 (C), 158.40 (CH), 163.47 (C-O)

HRMS (ESI): $C_{17}H_{13}N_2O$ [M^+ H] requires (m/e) 261.1028, found 261.1038, (-3.8 ppm)

BE119 2-(3-Hydroxybenzylidene)malononitrile

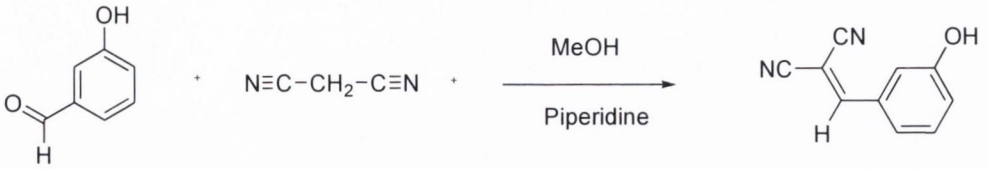

Yield: 1.63 g, 96 %, pale brown solid (Flash Column, CH_2Cl_2, MeOH 10%)

MP: 153-159°C **Lit. Ref**: [252] **Lit. MP**: 157-158 °C

IRϑ_{max} (KBr): 3528.74 (OH), 3148.22, 3116.74 (CH), 2254.90 (CN), 2244.83 (CN), 1662.87 (C=C), 1617.64 (C=C), 1549.65 cm^{-1}

^{1}H NMR (400 MHz, DMSO-d_6) δ ppm 5.11 (s (br), 1H, OH), 6.80 (d, 1H, *J*=6.52 Hz, Ar-H), 6.87 - 6.90 (m, 2H, Ar-H), 7.06 (s, 1H, Ar-H), 7.82 (s, 1H, CH)

^{13}C NMR (101 MHz, DMSO-d_6) δ ppm 65.62 (C=C), 110.96 (CH), 112.38 (CN), 113.05 (CN), 113.56 (CH), 115.79 (CH), 133.03 (CH), 138.74 (C), 160.37 (CH), 162.64 (C-OH)

HRMS (ESI): $C_{10}H_5N_2O$ [M$^-$ H] requires (m/e) 169.0402, found 169.0408, (3.6 ppm)

BE120 2-[(4-Methylphenyl)methylidene]propanedinitrile

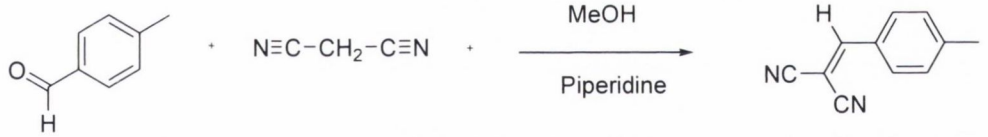

Yield: 1.59 g, 95 %, pale brown solid (Recrystallisation, MeOH)

MP: 138-141°C **Lit. Ref**: [253] **Lit. MP**: 137-139 °C

IRϑ_{max} (KBr): 3098.46 (CH), 2249.53 (CN), 2245.11 (CN), 1673.83 (C=C), 1617.62 (C=C), 1565.81 cm^{-1}

^{1}H NMR (400 MHz, DMSO-d_6) δ ppm 2.41 (s, 3H, CH_3), 7.45 (d, 2H, *J*=8.03 Hz, Ar-H), 7.87 (d, 2H, *J*=8.53 Hz, Ar-H), 8.49 (s, 1H, CH)

^{13}C NMR (101 MHz, DMSO-d_6) δ ppm 21.48 (CH_3), 79.92 (C=C), 113.36 (CN), 114.58 (CN), 128.75 (CH), 129.87 (CH), 145.70 (C), 145.22 (C-CH_3), 161.30 (CH)

HRMS (ESI): $C_{11}H_9N_2$ [M$^+$ H] requires (m/e) 169.0766, found 169.0774, (-4.7 ppm)

BE121 2-(3-bromo-4-methoxybenzylidene)malononitrile

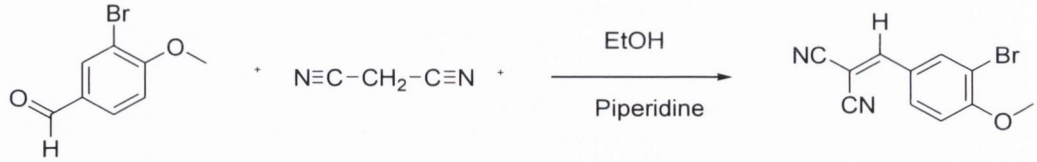

Yield: 2.55 g, 98 %, light beige solid (Recrystallisation, EtOH)

MP: 174-182°C **Lit. Ref**. [251] **Lit. MP**: 156 °C

IRϑ_{max} (KBr): 3194.73 (CH), 2249.60 (CN), 2256.17 (CN), 1675.17 (C=C), 1646.63 (C=C) 1547.67, 647.02 (C-Br) cm^{-1}

^{1}H NMR (400 MHz, CHLOROFORM-*d*) δ ppm 4.04 (s, 3H, OCH_3), 7.04 (d, *J*=8.53 Hz, 1H, Ar-H), 7.63 (s, 1H, Ar-H), 8.01 (d, 1H, *J*=8.32 Hz, Ar-H), 8.09 (d, 1H, *J*=7.28 Hz, CH)

^{13}C NMR (101 MHz, CHLOROFORM-*d*) δ ppm 56.39 (CH_3), 79.97 (C), 111.72 (C-Br), 112.37 (CN), 112.56 (CN), 113.46, (CH) 124.46 (CH), 131.42 (C), 156.97 (CH), 158.46 (C-OCH_3), 160.34 (CH)

HRMS (ESI): $C_{11}H_7{}^{79}BrN_2NaO$ [M^- Na] requires (m/e) 238.9715, found 238.9711, (1.6 ppm)

BE122 2-(3-Hydroxy-4-methoxybenzylidene)malononitrile

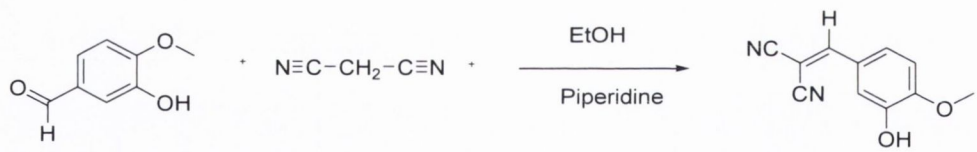

Yield: 2.19 g, 90 %, bright yellow powder (Recrystallisation, EtOH)

MP: 248 - 251°C **Lit. Ref**. [254] **Lit. MP**: 250 °C

IRϑ_{max} (KBr): 3561.84 (OH), 3156.68, 3120.84 (CH), 2255.26 (CN), 2241.68 (CN), 1668.93 (C=C), 1646.74 (C=C), 1592.38, 1576.48 cm^{-1}

^{1}H NMR (400 MHz, DMSO-d_6) δ ppm 3.37 (s, 3 H, OCH_3), 5.87 (s (br), 1 H, OH), 7.16 – 7.22 (m, 2 H, Ar-H), 7.54 (s, 1 H, Ar-H), 8.29 (s, 1 H, CH)

^{13}C NMR (101 MHz, DMSO-d_6) δ ppm 55.97 (OCH_3), 76.19 (C=C), 112.18 (CH), 113.42 (CN), 113.93 (CN), 115.01 (CH), 115.23 (CH), 126.31 (C), 146.95 (C-OH), 153.85 (C-OCH_3), 160.69 (CH)

HRMS (ESI): $C_{13}H_{13}N_2O_3$ [M^+ H] requires (m/e) 245.0926, found 245.0936, (-4.0 ppm)

BE123 2-(2,4-Dichlorobenzylidene)malononitrile

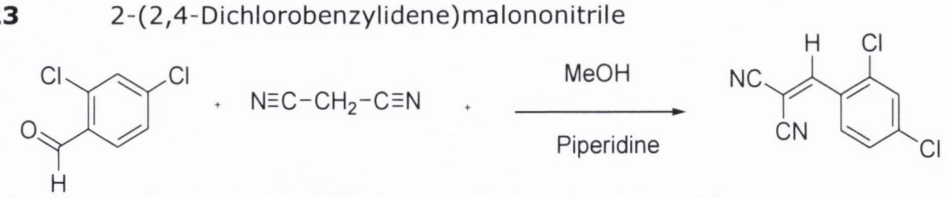

Yield: 0.62 g, 28 %, pale yellow powder (Recrystallisation, MeOH)

MP: 159-162°C **Lit. Ref**: [255] **Lit. MP**: 154-155 °C

IRϑ_{max} (KBr): 3276.61, 3051.98 (CH), 2262.71 (CN), 2256.84 (CN), 1685.67 (C=C), 1634.83 (C=C) 1582.05, 1462.98 cm^{-1}

^{1}H NMR (400 MHz, DMSO-d_6) δ ppm 7.29 (d, 1H, *J*=8.01 Hz, Ar-H), 7.44 (s, 1 H, Ar-H), 7.45 (d, 1 H, *J*=7.12 Hz, Ar-H), 8.21 (s, 1 H, CH)

^{13}C NMR (101 MHz, DMSO-d_6) δ ppm 69.16 (C=C), 113.24 (CN), 114.73 (CN), 128.39 (CH), 129.84 (CH), 130.38 (CH), 130.97 (C), 132.76 (C-Cl), 142.85 (C-Cl), 160.39 (CH)

HRMS (ESI): $C_{10}H_3{}^{35}Cl_2N_2$ [M$^-$ H] requires (m/e) 220.9669, found 220.9673, (-1.9 ppm)

BE124 2-(3,4-Dimethoxybenzylidene)malononitrile

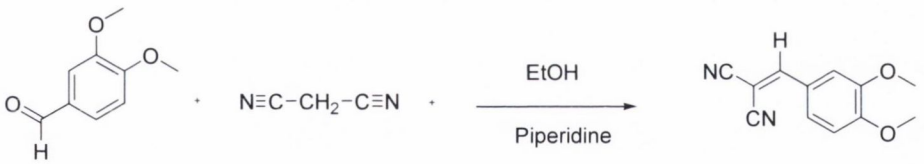

Yield: 1.56 g, 73 %, pale yellow powder (Recrystallisation, EtOH)

MP: 146-152°C **Lit. Ref**: [256] **Lit. MP**: 149-152 °C

IRϑ_{max} (KBr): 3150.56, 3121.74 (CH), 2255.43 (CN), 2247.66 (CN), 1657.43 (C=C), 1634.41 (C=C), 1574.25, 1542.39 cm^{-1}

^{1}H NMR (400 MHz, DMSO-d_6) δ ppm 3.96 (s, 6 H, 2xOCH_3), 6.99 (d, *J*=7.02 Hz, 2H, Ar-H), 7.67 (s, 2H, Ar-H), 7.70 (s, 1H, CH)

^{13}C NMR (101 MHz, DMSO-d_6) δ ppm 55.63 (OCH_3), 55.89 (OCH_3), 77.97 (C=C), 110.63 (CH), 113.14 (CN), 113.68 (CN), 115.97 (CH), 121.83 (CH), 127.79 (C), 149.08 (C-O), 154.41 (C-O), 158.71 (CH)

HRMS (ESI): $C_{12}H_{10}N_2NaO_2$ [M$^+$ Na] requires (m/e) 237.0640, found 237.0632, (-3.4 ppm)

BE125 2-(2,5-Dimethoxybenzylidene)malononitrile

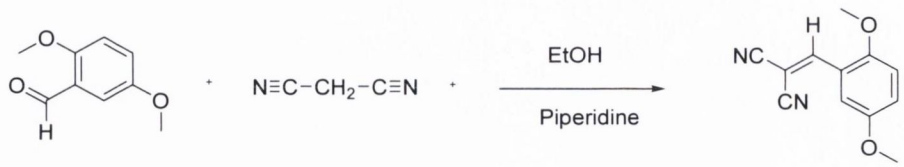

Yield: 0.89 g, 42 %, bright yellow powder (Recrystallisation, EtOH)

MP: 110-116°C **Lit. Ref**.[257] **Lit. MP**: 110 °C

IRϑ_{max} (KBr): 3146.13, 3069.61 (CH), 2252.17 (CN), 2241.89 (CN), 1670.83 (C=C), 1616.47 (C=C), 1585.91, 1484.76 cm^{-1}

^{1}H NMR (400 MHz, CHLOROFORM-*d*) δ ppm 3.84 (s, 3H, OCH_3), 3.91 (s, 3H, OCH_3), 6.95 (d, 1H, *J*=9.03 Hz, Ar-H), 7.19 (d, 1H, *J*=7.06 Hz, Ar-H), 7.76 (d, 1H, *J*=7.02 Hz, Ar-H), 8.32 (s, 1H, CH)

^{13}C NMR (101 MHz, CHLOROFORM-*d*) δ ppm 55.42 (OCH_3), 55.88 (OCH_3), 80.51 (C=C), 110.67 (CH), 112.48 (CN), 113.12 (CN), 113.92 (CH), 117.46 (CH), 119.68 (C), 153.00 (C-OCH_3), 153.33 (C-OCH_3), 153.71 (CH)

HRMS (ESI): $C_{12}H_9N_2O_2$ [M$^-$ H] requires (m/e) 213.0664, found 213.0659, (-2.4 ppm)

BE126 2-(2-Hydroxy-3-methoxybenzylidene)malononitrile

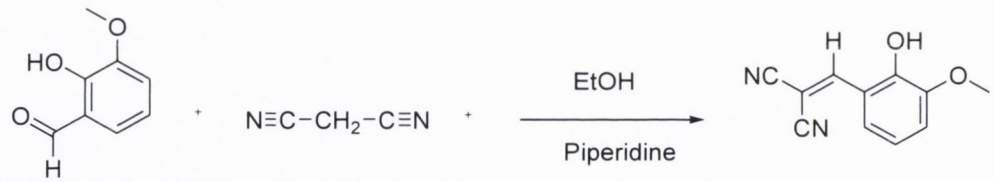

Yield: 1.28 g, 64 %, pale yellow powder (Recrystallisation, EtOH)

MP: 146-154°C **Lit. Ref**.[258]

IRϑ_{max} (KBr): 3582.18 (OH), 3152.60 (CH), 2248.18 (CN), 1675.83 (C=C), 1648.30 (C=C), 1561.78 cm^{-1}

^{1}H NMR (400 MHz, DMSO-d_6) δ ppm 3.35 (s, 3H, OCH_3), 5.07 (s (br), 1H, OH), 7.09 - 7.16 (m, 1 H, Ar-H), 7.32 (d, 1 H, *J*=7.14 Hz, Ar-H), 8.29 - 8.34 (m, 1H, Ar-H), 8.94 (s, 1 H, CH)

^{13}C NMR (101 MHz, DMSO-d_6) δ ppm 55.98 (OCH_3), 56.58 (C=C), 113.29 (CN), 114.23 (CN), 116.73 (CH), 117.73 (C), 120.60 (CH), 124.16 (CH), 146.03 (C-OH), 147.08 (C-OCH_3), 151.09 (CH)

HRMS (ESI): $C_{11}H_9N_2O_2$ [M$^+$ H] requires (m/e) 201.0664, found 201.0673, (4.5 ppm)

BE127 2-((Naphthalen-2-yl)methylene)malononitrile

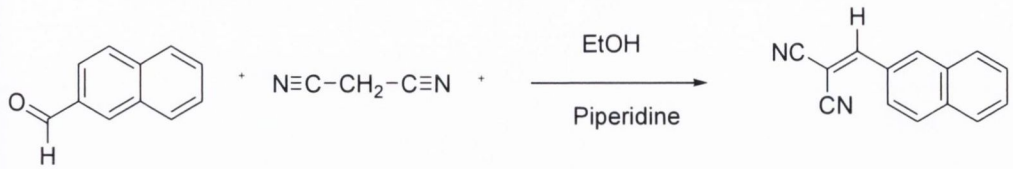

Yield: 1.85 g, 91 %, bright yellow powder (Recrystallisation, EtOH)

MP: 136-139°C **Lit. Ref**. [259] **Lit. MP**: 140.2 - 140.8 °C

IRϑ_{max} (KBr): 3142.58, 3087.64 (CH), 2250.16 (CN), 2246.41 (CN), 1684.38, 1617.49 (C=C), 1595.38, 1546.72 cm^{-1}

^{1}H NMR (400 MHz, CHLOROFORM-*d*) δ ppm 7.62 - 7.74 (m, 3H, Ar-H), 7.91 - 7.99 (m, 2H, Ar-H), 8.15 (d, 1H, *J*=7.28 Hz, Ar-H), 8.31 (d, 1H, *J*=6.87 Hz, Ar-H), 8.68 (s, 1 H, CH)

^{13}C NMR (101 MHz, CHLOROFORM-*d*) δ ppm 84.69 (C=C), 113.29 (CN), 113.81 (CN), 121.85 (CH), 124.96 (CH), 126.86 (CH), 127.05 (CH), 128.09 (CH), 133.08 (C), 133.37 (C), 134.51 (C), 157.30 (CH)

HRMS (ESI): $C_{14}H_7N_2$ [M^- H] requires (m/e) 203.0609, found 203.0606, (-1.6 ppm)

BE128 2-(3,4,5-Trimethoxybenzylidene)malononitrile

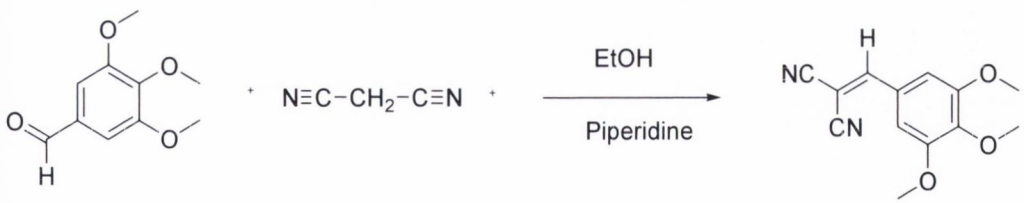

Yield: 1.70 g, 70 %, bright yellow powder (Recrystallisation, EtOH)

MP: 163-167°C **Lit. Ref**. [260] **Lit. MP**: 149-150 °C

IRϑ_{max} (KBr): 3178.95, 3130.84 (CH), 2243.94 (CN), 2232.47 (CN), 1641.73 (C=C), 1628.63 (C=C), 1561.69, 1530.73 cm^{-1}

^{1}H NMR (400 MHz, CHLOROFORM-*d*) δ ppm 3.93 (s, 6H, 2xOCH_3), 4.00 (s, 3 H, OCH_3), 7.21 (s, 2 H, Ar-H), 7.68 (s, 1 H, Ar-H), 8.19 (s, 1H, CH)

^{13}C NMR (101 MHz, CHLOROFORM-*d*) δ ppm 55.90 (OCH_3), 60.82 (OCH_3), 80.09 (C=C), 107.81 (CH), 112.77 (CN), 113.57 (CN), 125.50 (C), 143.49 (C-OCH_3), 152.89 (C-OCH_3), 159.02 (CH)

HRMS (ESI): $C_{13}H_{13}N_2O_3$ [M^+ H] requires (m/e) 245.0926, found 245.0925, (0.4 ppm)

BE129 2-((benzo[d][1,3]dioxol-5-yl)methylene)malononitrile



Yield: 1.78 g, 90 %, pale yellow powder (Recrystallisation, EtOH)

MP: 197 - 201°C **Lit. Ref**. [261] **Lit. MP**: 200-201 °C

IRϑ_{max} (KBr): 3144.76, 3036.41 (CH), 2258.75 (CN), 2242.62 (CN), 1694.51 (C=C), 1625.33 (C=C), 1578.36, 1541.95 cm^{-1}

^{1}H NMR (400 MHz, DMSO-d_6) δ ppm 6.23 (s, 2 H, OCH_2O), 7.19 (d, 1 H, *J*=8.80 Hz, Ar-H), 7.48 - 7.52 (m, 1 H, Ar-H), 7.54 (s, 1 H, Ar-H), 8.37 (CH)

^{13}C NMR (101 MHz, DMSO-d_6) δ ppm 77.46 (C=C), 102.91 (CH_2), 107.68 (CH), 109.29 (CN), 113.78 (CN), 114.68 (CH), 125.60 (CH), 129.94 (C), 148.30 (C-O), 152.99 (C-O), 160.36 (CH)

HRMS (ESI): $C_{11}H_7N_2O_2$ [M^+ H] requires (m/e) 199.0507, found 199.0509, (-1.0 ppm)

5.9 Coumarin Products

General procedure

The appropriate benzylidene malononitile intermediate (1 equiv., 10 mmol) was added to 4-hydroxy coumarin (1 equiv., 10 mmol) and brought to solution in ethanol (30 mL). Piperidine (0.5 mL) was added dropwise with stirring and reaction mixture was refluxed for 5 hours. Progress was checked *via* TLC until no starting material remained. Afterwards solvent was removed and product was recrystallized from EtOH.

BE130 2-Amino-4-(4-methoxyphenyl)-3-methylpyrano[3,2-c]chromen-5(4*H*)-one

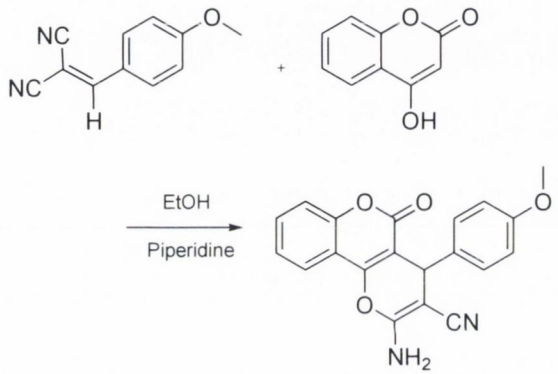

Yield: 1.42 g, 41 %, white powder (Recrystallisation, EtOH)

HPLC Purity: 96% **MP:** 236-242°C **Lit. Ref**. [262] **Lit. MP**: 241-243 °C

IRϑ_{max} (KBr): 3456.71, 3359.63 (NH_2), 3036.41 (CH), 2258.75 (CN), 1674.51 (C=O), 1625.33, 1611.48 (C=C), 1576.38, 1541.95 cm^{-1}

^{1}H NMR (400 MHz, CHLOROFORM-*d*) δ ppm 3.72 (s, 3H, OCH_3), 4.40 (s, 1H, CH), 6.86 (d, 2H, *J*=7.24 Hz, Ar-H), 7.17 (d, 2H, *J*=8.12 Hz, Ar-H), 7.36 (s (br), 2H, NH_2), 7.46 - 7.51 (m, 2H, Ar-H), 7.69 - 7.73 (m, 1H, Ar-H), 7.89 (d, 1H, *J*=8.03 Hz, Ar-H)

^{13}C NMR (101 MHz, CHLOROFORM-*d*) δ ppm 36.17 (CH), 55.04 (OCH_3), 58.20 (C=C), 104.27 (C=C), 113.01 (C), 113.85 (CH), 116.55 (CH), 119.30 (CN), 122.44 (CH), 124.66 (CH), 128.77 (CH), 132.86 (CH), 135.40 (C), 152.09 (C-O), 153.08 (C-OCH_3), 157.91 (O-C-N), 158.32 (C-O), 159.53 (C=O)

HRMS (ESI): $C_{20}H_{15}N_2O_4$ [M^+ H] requires (m/e) 347.1032, found 347.1022, (+2.9 ppm)

BE131 2-Amino-4,5-dihydro-5-oxo-4-p-tolylpyrano[3,2-c]chromene-3-carbonitrile

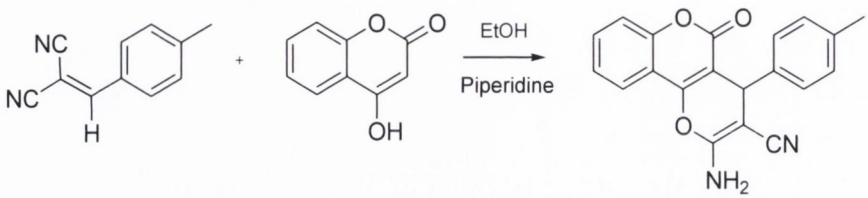

Yield: 0.39 g, 12 %, light brown solid (Recrystallisation, EtOH)

HPLC Purity: 95% **MP:** 246-252°C **Lit. Ref**. [263] **Lit. MP**: 259-260 °C

IRϑ_{max} (KBr): 3469.10, 3374.83 (NH_2), 3057.82 (CH), 2241.34 (CN), 1692.46 (C=O), 1668.60, 1631.73 (C=C) 1584.03, 1528.37, 1476.52 cm^{-1}

^{1}H NMR (400 MHz, DMSO-d_6) δ ppm 2.39 (s, 3H, CH_3), 4.05 (s, 1H, CH), 6.93 (d, 4H, *J*=8.04 Hz, Ar-H), 7.17 – 7.26 (m, 1H, Ar-H), 7.37 - 7.50 (m, 2H, Ar-H), 7.62 - 7.76 (m, 1H, Ar-H), 7.88 (s (br), 2H, NH_2)

^{13}C NMR (101 MHz, DMSO-d_6) δ ppm 14.09 (CH_3), 36.18 (CH), 58.19 (C=C), 104.25 (C=C), 112.15 (CN), 114.67 (C), 116.56 (CH), 118.70 (CH), 122.45 (CH), 124.67 (CH), 127.81 (CH), 135.64 (C-CH_3), 137.10 (C), 153.13 (C-O), 157.29 (O-C-N), 157.77 (C-O), 159.55 (C=O)

HRMS (ESI): $C_{20}H_{13}N_2O_3$ [M^- H] requires (m/e) 329.0926, found 329.0921, (-1.6 ppm)

BE132 2-Amino-4,5-dihydro-4-(2,5-dimethoxyphenyl)-5-oxopyrano[3,2-c]chromene-3-carbonitrile

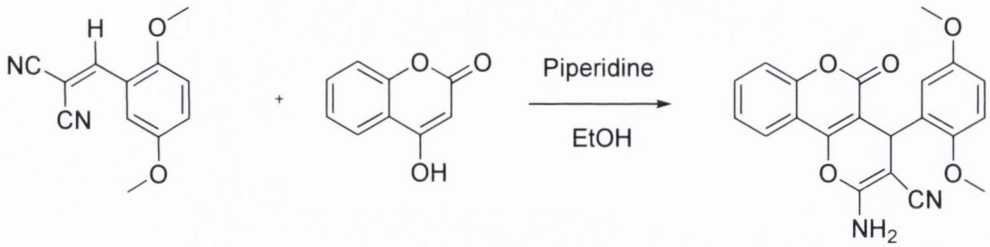

Yield: 2.25 g, 60 %, white powder (Recrystallisation, EtOH)

HPLC Purity: 92 % **MP:** 242-248°C **Lit. Ref**. [264] **Lit. MP**: 247-248 °C

IRϑ_{max} (KBr): 3584.11 (NH_2), 3125.39 (CH), 2250.46 (CN), 1693.57 (C=O), 1676.51, 1663.65 (C=C), 1586.49, 1568.73 cm^{-1}

^{1}H NMR (400 MHz, DMSO-d_6) δ ppm 3.66 (d, 6H, *J*=7.52 Hz, 2xOCH_3), 4.65 (s, 1H, CH), 6.67 (d, 1H, *J*=8.01 Hz, Ar-H), 6.77 - 6.82 (m, 1H, Ar-H), 6.92 (d, 1H, *J*=7.08 Hz, Ar-H), 7.29 (s (br), 2 H, NH_2), 7.48 (d, 2H, *J*=6.84 Hz, Ar-H), 7-64 - 7.70 (m, 1H, Ar-H), 7.91 (d, 1H, *J*=7.53 Hz, Ar-H)

^{13}C NMR (101 MHz, DMSO-d_6) δ ppm 22.21 (CH), 55.28 (OCH_3), 56.41 (OCH_3), 56.62 (C=C), 103.09 (C=C), 112.13 (CH), 113.03 (CH), 115.75 (CH), 116.56 (CN), 119.37 (C), 122.30 (CH), 124.66 (C), 129.59 (CH), 131.92 (CH), 132.76 (CH), 151.48 (C-O), 152.08 (C-OCH_3), 153.11 (C-OCH_3), 153.93 (O-C-N), 158.53 (C-O), 159.55 (C=O)

HRMS (ESI): $C_{21}H_{15}N_2O_5$ [M$^-$ H] requires (m/e) 375.0981, found 375.0982, (0.3ppm)

BE133 2-Amino-4,5-dihydro-4-(4-hydroxyphenyl)-5-oxopyrano[3,2-c]chromene-3-carbonitrile

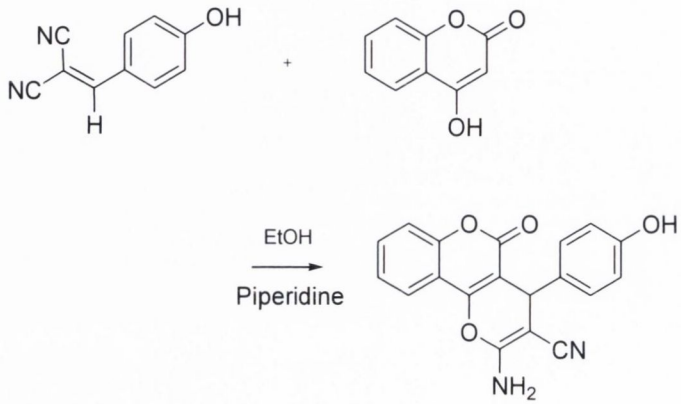

Yield: 0.14 g, 4 %, pale yellow powder (Recrystallisation, EtOH)

HPLC Purity: 99% **MP:** 258 - 266°C **Lit. Ref**. [265] **Lit. MP**: 266-267 °C

IRϑ_{max} (KBr): 3517.63 (OH), 4385.62 (NH_2), 3056.84 (CH), 2242.53 (CN), 1685.67 (C=O), 1664.63, 1627.41 (C=C), 1587.63, 1536.62 cm^{-1}

^{1}H NMR (400 MHz, CHLOROFORM-*d*) δ ppm 4.32 (s, 1H, CH), 6.67 (d, 2H, *J*=8.03 Hz, Ar-H), 7.03 (d, 2H, *J*=8.53 Hz, Ar-H), 7.33 (s (br), 2H, NH_2), 7.43 - 7.49 (m, 2H, Ar-H), 7.70 (t, 1H, *J*=7.12 Hz, Ar-H), 7.87 (d, 1 H, *J*=8.03 Hz, Ar-H), 9.34 (s (br), 1H, OH)

^{13}C NMR (101 MHz, CHLOROFORM-*d*) δ ppm 36.15 (CH), 58.37 (C=C), 104.51 (C=C), 113.03 (CH), 115.18 (C), 116.55 (CN), 117.63 (CH), 119.37 (CH), 122.41 (CH), 124.65 (CH), 128.68 (CH), 132.81 (C), 151.29 (C-O), 152.97 (C-OH), 156.47 (O-C-N), 157.90 (C-O), 159.54 (C=O)

HRMS (ESI): $C_{19}H_{12}N_2NaO_4$ [M^+ H] requires (m/e) 355.0695, found 355.0705, (2.9 ppm)

BE134 2-Amino-4,5-dihydro-4-(3,4-dimethoxyphenyl)-5-oxopyrano[3,2-c]chromene-3-carbonitrile

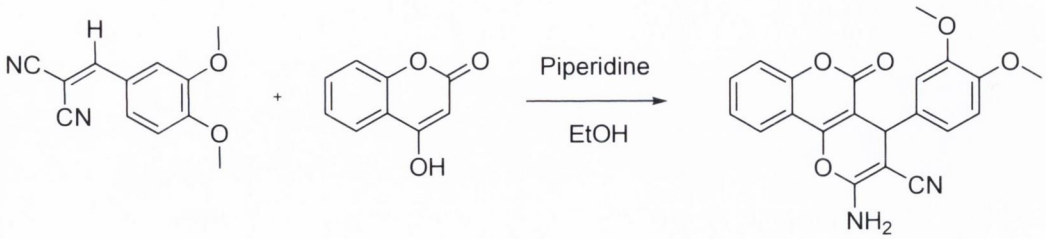

Yield: 1.80 g, 48 %, pale white solid (Recrystallisation, EtOH)

HPLC Purity: 97 % **MP:** 228-232°C **Lit. Ref**.: [266] **Lit. MP**: 233-235 °C

IRϑ_{max} (KBr): 3459.21, 3325.17 (NH_2), 3032.68 (CH), 2246.19 (CN), 1687.84 (C=O), 1659.83, 1628.35 (C=C), 1595.41, 1564.83 cm^{-1}

^{1}H NMR (400 MHz, DMSO-d_6) δ ppm 3.78 (s, 6H, 2xOCH_3), 4.41 (s, 1H, CH), 6.69 - 6.75 (m, 1H, Ar-H), 6.82 - 6.94 (m, 2H, Ar-H), 7.38 (s (br), 2H, NH_2), 7.49 (d, 2H, *J*=6.78 Hz, Ar-H), 7.67 - 7.74 (m, 1H, Ar-H), 7.90 (d, 1H, *J*=7.53 Hz, Ar-H)

^{13}C NMR (101 MHz, DMSO-d_6) δ ppm 36.50 (CH), 55.47 (OCH_3), 58.09 (C=C), 104.11 (C=C), 111.57 (CH), 111.82 (CH), 113.05 (C), 116.56 (CN), 119.33 (CH), 119.66 (CH), 122.46 (CH), 124.64 (CH), 132.85 (CH), 135.83 (C), 147.92 (C-OCH_3), 148.49 (C-OCH_3), 152.10 (C-O), 153.16 (O-C-N), 157.91 (C-O), 159.59 (C=O)

HRMS (ESI): $C_{21}H_{16}N_2NaO_5$ [M^+ Na] requires (m/e) 399.0957, found 399.0956, (-0.2 ppm)

BE135 2-Amino-4,5-dihydro-4-(3,4,5-trimethoxyphenyl)-5-oxopyrano[3,2-c]chromene-3-carbonitrile

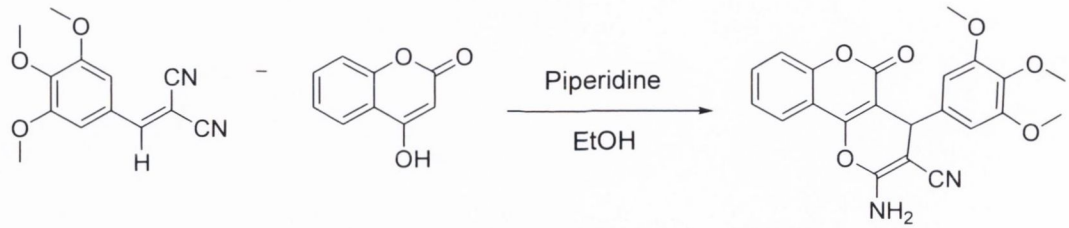

Yield: 1.82 g, 45 %, light cream solid (Recrystallisation, EtOH)

HPLC Purity: 98 % **MP:** 266-271°C **Lit. Ref**. [267]

IRϑ_{max} (KBr): 3582.30, 3464.14 (NH_2), 3047.61 (CH), 2255.61 (CN), 1696.36 (C=O), 1663.82 (C=C), 1640.67 (C=C), 1584.38, 1540.16 cm^{-1}

^{1}H NMR (400 MHz, DMSO-d_6) δ ppm 3.64 (s, 9H,3xOCH_3), 4.44 (s, 1H, CH), 6.53 (s, 2H, Ar-H), 7.40 (s (br), 2 H, NH_2), 7.45 - 7.51 (m, 2H, Ar-H), 7.68 - 7.74 (m, 1H, Ar-H), 7.90 (d, 1H, *J*=7.53 Hz, Ar-H)

^{13}C NMR (101 MHz, DMSO-d_6) δ ppm 37.20 (CH), 55.87 (OCH_3), 56.02 (OCH_3), 59.90 (C=C), 103.64 (C=C), 104.90 (CH), 116.58 (CN), 118.00 (C), 122.53 (CH), 124.62 (CH), 132.89 (CH), 136.54 (CH), 139.01 (C-OCH_3), 152.18 (C-O), 152.82 (C-OCH_3), 153.21 (O-C-N), 157.98 (C-O), 159.64 (C=O)

HRMS (ESI): $C_{22}H_{18}N_2NaO_6$ [M^+ Na] requires (m/e) 429.1063, found 429.1066, (-0.6 ppm)

BE136 2-Amino-4-(4-(benzyloxy)phenyl)-4,5-dihydro-5-oxopyrano[3,2-c]chromene-3-carbonitrile

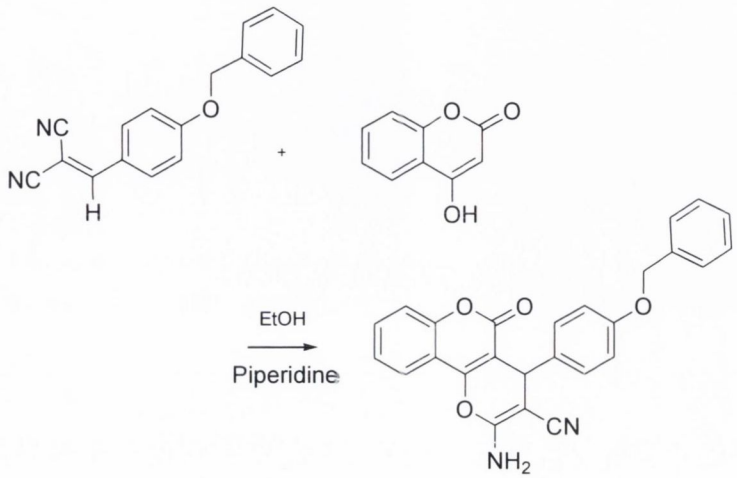

Yield: 2.13 g, 48 %, yellow powder (Recrystallisation, EtOH)

HPLC Purity: 96% **MP:** 242-245°C **Lit. Ref.** [267]

IRϑ_{max} (KBr): 3561.52, 3474.63 (NH_2), 3079.15 (CH), 2248.82 (CN), 1683.86 (C=O), 1663.58, 1639.62 (C=C), 1585.63, 1547.69 cm^{-1}

^{1}H NMR (400 MHz, DMSO-d_6) δ ppm ^{1}H NMR ppm 4.39 (s, 1H, CH), 5.05 (s, 2H, CH_2), 6.93 (d, 2H, *J*=9.03 Hz, Ar-H), 7.17 (d, 1H, *J*=8.12 Hz, Ar-H), 7.37 - 7.50 (m, 7H, Ar-H), 7.62 - 7.76 (m, 2H, Ar-H), 7.88 (d, 1H, *J*=8.03 Hz, Ar-H), NH_2 not observed.

^{13}C NMR (101 MHz, DMSO-d_6) δ ppm 36.18 (CH), 58.19 (C=C), 69.24 (CH_2), 104.25 (C=C), 112.15 (CH), 114.67 (C), 116.56 (CN), 118.70 (CH), 122.45 (CH), 124.67 (CH), 127.66 (CH), 127.81 (CH), 128.42 (CH), 128.78 (CH), 132.87 (CH), 135.64 (C), 137.10 (C), 152.11 (C-O), 153.13 (C-O), 157.29 (O-C-N), 157.77 (C-O), 159.55 (C=O)

HRMS (ESI): $C_{26}H_{18}N_2NaO_4$ [M^+ H] requires (m/e) 445.1164, found 445.1179, (-3 3 ppm)

BE137 2-Amino-4,5-dihydro-4-(2-hydroxy-3-methoxyphenyl)-5-oxopyrano[3,2-c]chromene-3-carbonitrile

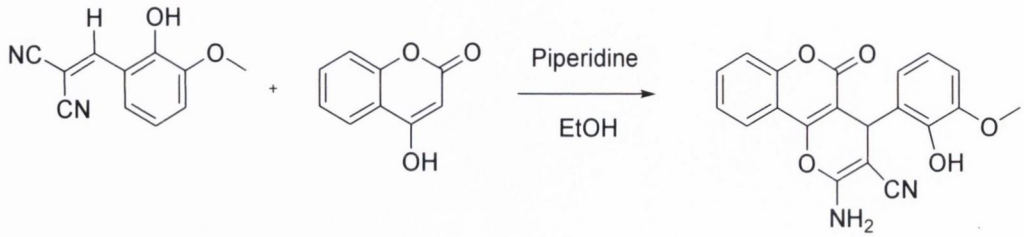

Yield: 0.14 g, 4 %, brown solid (Recrystallisation, EtOH)

HPLC Purity: 85 % **MP:** 221-228°C

IR ϑ_{max} (KBr): 3528.74 (OH), 3460.73, 3352.72 (NH_2), 3157.72 (CH), 2242.58 (CN), 1683.08 (C=O), 1664.84, 1623.68 (C=C) 1592.71, 1562.38 cm^{-1}

^{1}H NMR (400 MHz, DMSO-d_6) δ ppm 3.01 (s (br), 1 H, OH), 3.38 (s (br), 2 H, NH_2), 3.87 (s, 3 H, OCH_3), 4.44 (s., 1 H, CH), 6.78 (d, 1H, *J*=7.53 Hz, Ar-H), 6.85 - 6.98 (m, 2 H, Ar-H), 7.09 (d, 2H, *J*=8.53 Hz, Ar-H), 7.78 - 7.86 (m, 2 H, Ar-H)

^{13}C NMR (101 MHz, DMSO-d_6) δ ppm 14.26 (CH), 55.74 (OCH_3), 63.22 (C=C), 84.31 (C=C), 84.56 (CH), 112.95 (CH), 114.77 (CN), 115.23 (C), 119.14 (CH), 120.70 (CH), 121.71 (CH), 122.45 (C), 127.86 (CH), 128.53 (CH), 128.86 (CH), 142.84 (C-OH), 143.15 (C-O), 147.68 (C-OCH_3), 159.02 (O-C-N), 160.91 (C-O), 165.09 (C=O)

HRMS (ESI): $C_{20}H_{13}N_2O_5$ [M^- H] requires (m/e) 361.0824, found 361.0807, (-4.8 ppm)

BE138 2-Amino-4,5-dihydro-4-(3-hydroxy-4-methoxyphenyl)-5-oxopyrano[3,2-c]chromene-3-carbonitrile

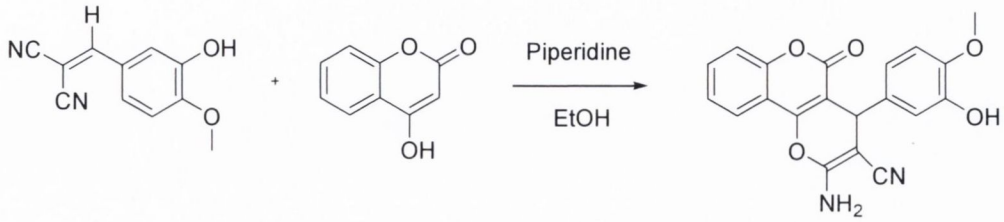

Yield: 0.50 g, 14 %, brown solid (Recrystallisation, EtOH)

HPLC Purity: 91 % **MP:** 256-262°C **Lit. Ref.**: [267]

IRϑ_{max} (KBr): 3595.73 (OH), 3415.85, 3384.18 (NH_2), 3148.73 (CH), 2244.76 (CN), 1695.26 (C=O), 1662.96, 1647.53 (C=C) 1598.87, 1551.84, 1458.97 cm^{-1}

^{1}H NMR (400 MHz, CHLOROFORM-*d*) δ ppm 3.96 (s, 3H, OCH_3), 4.00 (s, 1H, CH), 6.96 (s, 1 H, Ar-H), 6.98 (s (br), 2 H, NH_2), 7.03 (d, 1H, *J*=7.24 Hz, Ar-H), 7.05 (d, 2H, *J*=8.02 Hz, Ar-H), 7.09 (d, 2H, *J*=7.28 Hz, Ar-H), 7.28 (s, 1H, Ar-H)

^{13}C NMR (101 MHz, CHLOROFORM-*d*) δ ppm 48.80 (CH), 55.48 (OCH_3), 59.99 (C=C), 81.11 (C=C), 114.75 (CH), 116.31 (CN), 117.42 (C), 120.70 (CH), 121.38 (CH), 123.63 (CH), 127.30 (CH), 128.82 (CH), 132.14 (C), 145.19 (C-OH), 147.88 (C-OCH_3), 148.53 (C-O), 158.99 (O-C-N), 160.49 (C-O), 161.46 (C=O)

HRMS (ESI): $C_{20}H_{14}N_2NaO_5$ [M^+ Na] requires (m/e) 385.0800, found 385.0807, (-1.8 ppm)

BE139 2-Amino-4-(benzo[d][1,3]dioxol-6-yl)-4,5-dihydro-5-oxopyrano[3,2-c]chromene-3-carbonitrile

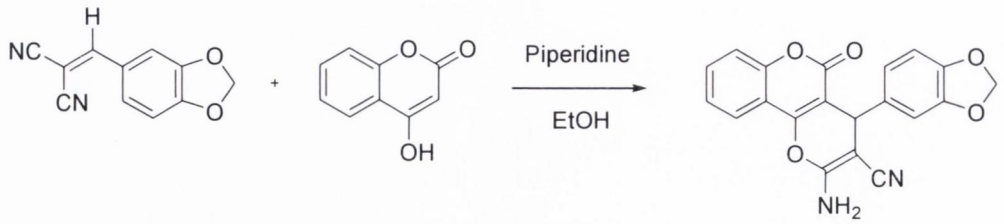

Yield: 0.39 g, 11 %, brown resin (Recrystallisation, EtOH)

HPLC Purity: 86 % **MP:** na°C **Lit. Ref**. [266] **Lit. MP**: 245-247 °C

IRϑ_{max} (KBr): 3523.80, 3475.52 (NH_2), 3053.62 (CH), 2248.31 (CN), 1686.84 (C=O), 1669.74, 1627.48 (C=C), 1568.42, 1537.38 cm^{-1}

^{1}H NMR (400 MHz, CHLOROFORM-*d*) δ ppm 3.82 (s, 1H, CH), 6.07 (s, 2H, OCH_2O), 6.93 (s, 1H, Ar-H), 6.95 (s, 1H, Ar-H), 6.97 (d, 1H, *J*=7.12 Hz, Ar-H), 7.00 - 7.01 (m, 1H, Ar-H), 7.03 (d, 2H, *J*=7.42 Hz, Ar-H), 7.28 (s, 1H, Ar-H), NH_2 not observed.

^{13}C NMR (101 MHz, CHLOROFORM-*d*) δ ppm 25.54 (CH), 48.94 (C=C), 83.08 (CH_2O), 101.28 (C=C), 108.28 (CH), 108.75 (CH), 116.06 (CN), 117.23 (C), 121.71 (CH), 122.89 (CH), 124.56 (CH), 127.72 (CH), 128.62 (CH), 135.69 (C), 147.50 (C-O), 149.18 (C-O), 150.48 (C-O), 158.82 (O-C-N), 159.86 (C-O), 161.55 (C=O)

HRMS (ESI): $C_{20}H_{12}N_2NaO_5$ [M^+ Na] requires (m/e) 383.0644, found 383.0658, (3.65 ppm)

5.10 Alkylation of Coumarins

General procedure

2-Amino-4,5-dihydro-4-(4-hydroxyphenyl)-5-oxopyrano[3,2-c]chromene-3-carbonitrile (1 equiv., 0.9 mmol, [300mg]) was dissolved in acetone in a round bottom flask. An excess of K_2CO_3 [400 mg] was added with stirring. The appropriate N,N-dialkylaminoethyl chloride hydrochloride was added and the reaction mix was heated to reflux for 18 – 48 h. Progress was checked *via* TLC. Afterwards the inorganic salts were removed with filtration, solvent was removed *in vacuo* and residue was dissolved in CH_2Cl_2 and washed twice with water. The organic phase was dried with $MgSO_4$ and the solvent was removed *in vacuo*. The remaining residue was purified *via* flash column: (CH_2Cl_2 – MeOH 10%)

BE140 4-(4-(2-(1-Methylpyrrolidin-2-yl)ethoxy)phenyl)-2-amino-4,5-dihydro-5-oxopyrano[3,2-c]chromene-3-carbonitrile

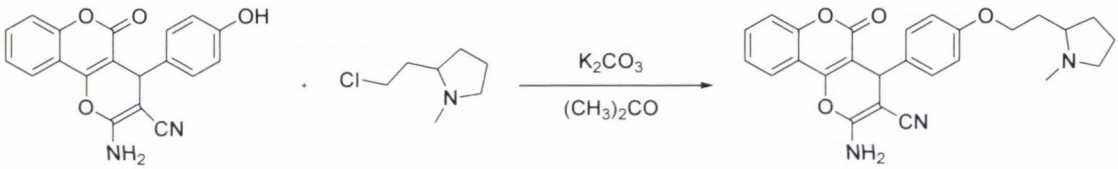

Yield: 0.032 g, 8 %, brown resin (Flash Column, CH_2Cl_2 – MeOH 10%)

HPLC Purity: 86 % **MP:** na

IRϑ_{max} (KBr): 3531.67, 3473.67 (NH_2), 3049.83 (CH), 2246.84 (CN), 1666.38 (C=O), 1632.60, 1620.62 (C=C), 1589.47 1552.85 cm^{-1}

^{1}H NMR (400 MHz, DMSO-d_6) δ ppm 1.03 (t, 4H, *J*=7.70 Hz, 2xCH_2), 1.19 - 1.20 (m, 1H, CH), 1.41 - 1.47 (m, 4H, 2xCH_2), 1.57 - 1.63 (m, 3H, CH_3), 3.93 (d, 2H, *J*=7.03 Hz, CH_2), 4.01 (s, 1H, CH), 6.67 (d, 2H, *J*=9.03 Hz, Ar-H), 6.82 - 6.84 (m, 2H, Ar-H), 7.02 – 7.05 (m, 2H, Ar-H), 7.47 – 7.48 (m, 2H, Ar-H), 8.13 (s (br), 2H, NH_2)

^{13}C NMR (101 MHz, DMSO-d_6) δ ppm 14.27 (CH_2), 24.24 (CH_2), 24.88 (CH_2), 26.20 (CH), 45.78 (CH_3), 56.46(C=C), 58.37 (CH_2), 68.15 (C), 68.74 (CH_2), 99.83 (C=C), 110.89 (CH), 113.39 (CN), 114.24 (C), 115.72 (CH), 115.77 (CH), 126.06 (CH), 127.14 (CH), 127.57 (CH), 130.28 (C), 133.05 (C-O), 139.88 (C-O), 140.18 (O-C-N), 150.85 (C-O), 151.46 (C=O)

HRMS (ESI): $C_{26}H_{24}N_3O_4$ [M^+ H] requires (m/e) 442.1767, found 442.1774, (-1.5 ppm)

BE141 4-(4-(2-Morpholinoethoxy)phenyl)-2-amino-4,5-dihydro-5-oxopyrano[3,2-c]chromene-3-carbonitrile

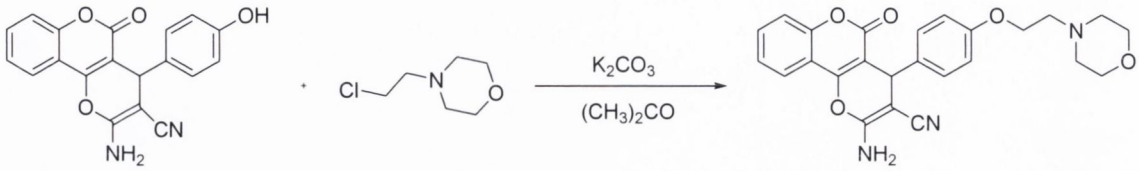

Yield: 0.14 g, 36 %, brown resin (Flash Column, CH_2Cl_2 – MeOH 10%)

HPLC Purity: 81 % **MP:** na

IRϑ_{max} (KBr): 3570.72, (NH_2), 3047.40 (CH), 2238.47 (CN), 1672.62 (C=O), 1641.49, 1634.67 (C=C), 1593.57, 1563.71 cm^{-1}

^{1}H NMR (400 MHz, DMSO-d_6) δ ppm 2.09 (s, 4H, 2xCH_2), 2.59 - 2.67 (m, 2H, CH_2), 3.62 (d, 4H, *J*=7.10 Hz, 2xCH_2), 3.75 - 3.78 (m, 1H, CH), 3.88 - 3.91 (m, 2H, CH_2), 6.85 - 7.06 (m, 2H, Ar-H), 7.13 - 7.27 (m, 2H, Ar-H), 7.35 - 7.48 (m, 2H, Ar-H), 7.74 - 7.86 (m, 2H, Ar-H), 8.12 (s (br), 2H, NH_2)

^{13}C NMR (101 MHz, DMSO-d_6) δ ppm 30.71 (CH), 53.00 (CH_2), 53.08 (CH_2), 53.59 (C=C), 65.63 (CH_2), 65.74 (CH_2), 113.50 (C=C), 115.13 (CH), 116.44 (CN), 117.43 (C), 119.42 (CH), 124.38 (CH), 128.44 (CH), 128.85 (CH), 130.01 (C), 131.96 (C-O), 132.09 (C-O), 152.08 (O-C-N), 152.46 (C-O), 152.76 (C=O)

HRMS (ESI): $C_{25}H_{23}N_3O_5$ [M^+] requires (m/e) 445.1738, found 445.1771, (+7 ppm)

BE142 4-(4-(2-(pyrrolidin-1-yl)ethoxy)phenyl)-2-amino-4,5-dihydro-5-oxopyrano[3,2-c]chromene-3-carbonitrile

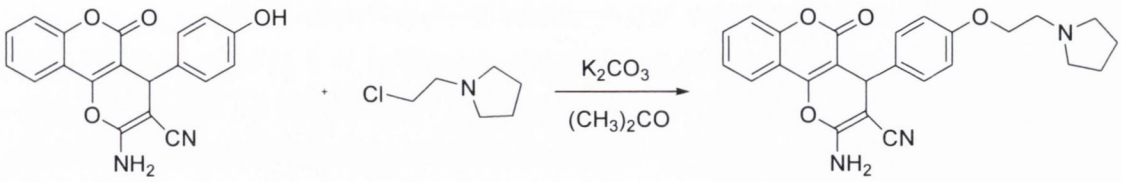

Yield: 0.077 g, 20 %, brown resin (Flash Column, CH_2Cl_2 – MeOH 10%)

HPLC Purity: 90 % **MP:** na

IRϑ_{max} (KBr): 3456.11 (NH_2), 3042.61 (CH), 2246.67 (CN), 1665.32 (C=O), 1640.52, 1610.42 (C=C), 1585.26, 1534.58 cm^{-1}

^{1}H NMR (400 MHz, DMSO-d_6) δ ppm 1.59 – 1.92 (m, 4H, 2xCH_2), 2.41 – 2.48 (m, 2H, CH_2), 3.21 (d, 4H, *J*=7.21, 2xCH_2), 3.64 - 3.72 (m, 2H, CH_2), 3.82 - 3.88 (CH), 6.94 - 7.14 (m, 1H, Ar-H), 7.32 (s, 2H, Ar-H), 7.35 - 7.48 (m, 2H, Ar-H), 7.66 - 7.74 (m, 3H, Ar-H), NH_2 not observed.

^{13}C NMR (101 MHz, DMSO-d_6) δ ppm 26.37 (CH_2), 39.82 (CH), 52.75 (CH_2), 54.65 (CH_2), 54.37 (C=C), 63.68 (CH_2), 111.78 (C=C), 114.47 (CH), 117.37 (CN), 118.46 (C), 121.38 (CH), 125.68 (CH), 126.89 (CH), 128.91 (CH), 129.03 (CH), 131.45 (C), 133.74 (C-O), 134.68 (C-O), 151.47 (O-C-N), 154.93 (C-O), 156.59 (C=O)

HRMS (ESI): $C_{25}H_{24}N_3O_4$ [M^+ H] requires (m/e) 430.1750, found 430.1767, (-3.9 ppm)

5.11 Synthesis of Naphthohydrazides

General Procedure **Step 1**- *Methyl 3-hydroxynaphthalene-2-carboxylate.*
3-Hydroxy-2-naphthoic acid, (3.76 g, 20 mmol) was added to a solution of MeOH (20 mL) and HCl 37% (20 mL). The reaction mixture was heated at 90 °C and the esterification was monitored on TLC until complete consumption of the starting material was observed. Solvent was then removed *in vacuo* and the reaction mixture was diluted with CH_2Cl_2 (30 mL) and washed with H_2O, CH_2Cl_2 (2x30 mL) and saturated aqueous $NaHCO_3$. The aqueous phase was extracted and the combined organic layers were dried over anhydrous Na_2SO_4, filtered and concentrated *in vacuo* to give the crude product. The crude mixture was purified by flash column chromatography over silica gel (eluent CH_2Cl_2 – MeOH, 9:1) to afford the product as a colourless solid recrystallised from EtOH.

II Methyl 3-hydroxynaphthalene-2-carboxylate

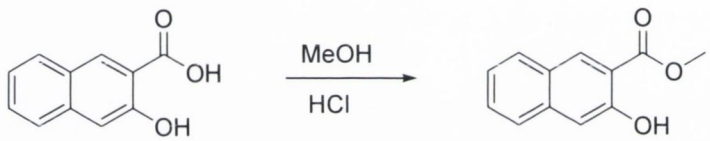

Yield: 2.62 g, 65%, brown solid (Flash Column; CH_2Cl_2 – MeOH, 9:1)
MP: 74-76°C **Lit. Ref**. [268] **Lit. MP**: 75-76 °C
IRϑ_{max} (KBr): 3562.51 (OH), 1658.73 (C=O), 1584.31, 1532.67 (C=C) cm^{-1}
^{1}H NMR (400 MHz, DMSO-d_6): δ ppm 3.47 (s, 3H, CH_3), 7.24 - 7.31 (m, 2H, Ar-H), 7.69 (s, 2H, Ar-H), 7.94 (d, 2H, *J*=7.21 Hz, Ar-H), 8.21 (s (br), 1H, OH)
^{13}C NMR (101 MHz, DMSO-d_6): δ ppm 47.89 (CH_3), 110.37 (CH), 112.57 (C), 121.97 (CH), 126.84 (CH), 128.84 (C), 129.21 (CH), 129.84 (CH), 131.93 (CH), 132.04 (C), 157.84 (C-OH), 164.67 (C=O)
HRMS (ESI): $C_{12}H_{10}NaO_3$ [M+ +Na] requires (m/e) 225.0528, found 225.0521 (-3.11 ppm)

General Procedure **Step 2**- *3-Hydroxynaphthalene-2-carbohydrazide*

To a solution of Methyl 3-hydroxynaphthalene-2-carboxylate, (2.02 g, 10 mmol) in EtOH (10 mL), hydrazine hydrate was added (1.245 mL, 40 mmol) and the reaction mixture was heated to 120 °C until complete precipitation of hydrazide occurred (15 min). Completion of the reaction was confirmed by TLC. The reaction mixture was allowed to cool to 20 °C, filtered and washed with hexane to give product as a beige powder, recrystallised from EtOH.

III 3-Hydroxynaphthalene-2-carbohydrazide

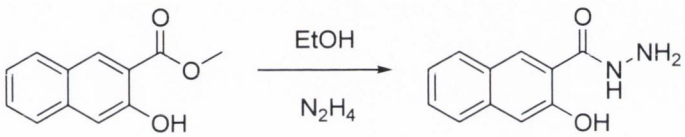

Yield: 1.99 g, 99%, light brown solid (Flash Column; CH_2Cl_2 – MeOH, 9:1)

MP: 201-209°C **Lit. Ref**. [269] **Lit. MP**: 208-210 °C

IRϑ_{max} (KBr): 3590.64 (OH), 3484.62 (NH), 3382.63 (NH_2), 1651.46 (C=O), 1567.46, 1506.32 (C=C) cm^{-1}

^{1}H NMR (400 MHz, DMSO-d_6): δ ppm 2.16 (s (br), 2H, NH_2), 7.16 (d, 2H, *J*=7.24 Hz, Ar-H), 7.21 - 7.26 (m, 2H, Ar-H), 7.84 (s, 1H, Ar-H), 7.96 (s, 1H, Ar-H), 8.15 (s (br), 1H, OH), 8.56 (s (br), 1 H, NH)

^{13}C NMR (101 MHz, DMSO-d_6): δ ppm 106.48 (CH), 114.27 (CH), 122.78 (C), 125.73 (CH), 126.83 (CH), 129.47 (CH), 130.47 (C), 133.78 (C), 156.47 (C-OH), 161.38 (C=O)

HRMS (ESI): $C_{11}H_{10}N_2NaO_2$ [M+ +Na] requires (m/e) 225.064 found at 225.0629 (+4.8 ppm)

General Procedure **Step 1**- *Methyl 2-naphthoate.*

2-naphthoic acid, (1.72 g, 10 mmol) was added to a solution of MeOH (20 mL) and HCl 37% (20 mL). The reaction mixture was heated at 90 °C and the esterification was monitored on TLC until complete consumption of the starting material was observed. Solvent was then removed *in vacuo* and the reaction mixture was diluted with CH_2Cl_2 (30 mL) and washed with H_2O, CH_2Cl_2 (2x30 mL) and saturated aqueous $NaHCO_3$. The aqueous phase was extracted and the combined organic layers were dried over anhydrous Na_2SO_4, filtered and concentrated *in vacuo* to give the crude product. The crude mixture was purified by flash column chromatography over silica gel (eluent CH_2Cl_2) to afford the product as a colourless solid recrystallised from MeOH.

IV Methyl 2-naphthoate

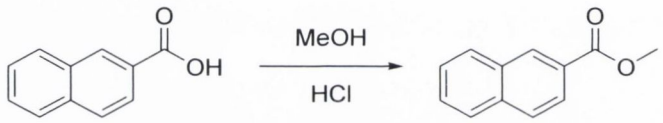

Yield: 1.19 g, 64%, light brown solid (Flash Column; CH_2Cl_2)

MP: 76-79°C **Lit. Ref.**[270] **Lit. MP**: 77-77.5 °C

IR ϑ_{max} (KBr): 1679.36 (C=O), 1594.27, 1542.46 (C=C) cm^{-1}

^{1}H NMR (400 MHz, DMSO-d_6): δ ppm 3.78 (s, 3H, CH_3), 7.36 - 7.42 (m, 2H, Ar-H), 7.73 (s, 2H, Ar-H), 7.83 – 7.89 (m, 2H, Ar-H), 8.48 (s, 1H, Ar-H)

^{13}C NMR (101 MHz, DMSO-d_6): δ ppm 51.63 (CH_3), 124.46 (CH), 125.96 (CH), 126.19 (C), 127.37 (CH), 128.41 (CH), 129.59 (CH), 132.78 (C), 136.54 (C), 165.34 (C=O)

HRMS (ESI): $C_{12}H_{10}O_2$ [M+] requires (m/e) 186.0681, found 186.0675 (3.22 ppm)

General Procedure **Step 2-** Microwave assisted synthesis of *2-Naphthohydrazide*
To a solution of Methyl 3-hydroxynaphthalene-2-carboxylate, (150 mg, 0.8 mmol) in EtOH (2 mL), hydrazine hydrate was added (0.0996 mL, 3.2 mmol) and the reaction mixture was heated in a Microwave reactor to 160 °C until complete precipitation of hydrazide occurred (60 min). Completion of the reaction was confirmed by TLC. The reaction mixture was allowed to cool to 20 °C, filtered and washed with hexane to give product as a white powder.

V 2-Naphthohydrazide

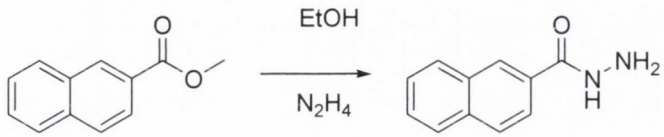

Yield: 0.126 g, 85%, white solid (Recrystallisation, EtOH)
MP: 147-152°C **Lit. Ref**.[271] **Lit. MP**: 147-148 °C
IRϑ_{max} (KBr): 3557.36 (OH), 3475.35 (NH), 3437.47 (NH_2), 1668.36 (C=O), 1536.48, 1511.58 (C=C) cm^{-1}
^{1}H NMR (400 MHz, DMSO-d_6): δ ppm 2.74 (s (br), 2H, NH_2), 7.33 (m, 2H, *J*=6.87 Hz, Ar-H), 7.56 (d, 2H, *J*=7.05 Ar-H), 7.79 (s, 1H, Ar-H), 8.11 – 8.17 (m, 2H, Ar-H), 8.56 (s (br), 1 H, NH)
^{13}C NMR (101 MHz, DMSO-d_6): δ ppm 122.58 (CH), 124.59 (CH), 125.36 (CH), 126.46 (CH), 127.26 (CH), 128.35 (CH), 129.28 (CH), 132.86 (C), 134.26 (C), 135.04 (C), 163.52 (C=O)
HRMS (ESI): $C_{11}H_{10}N_2O$ [M+] requires (m/e) 186.0793 found at 186.0787 (+3.22 ppm)

General Procedure **Step 3**- Synthesis of hydrazides

To a solution of 3-Hydroxynaphthalene-2-carbohydrazide, (1.534 g, 7.5 mmol) in EtOH (20 mL), the appropriate aryl aldehyde or aryl ketone was added (1.1713 g, 7.5 mmol), and the reaction was heated to 120 °C and monitored by TLC until complete consumption of the starting material was observed (6 h). The reaction mixture was allowed to cool to 20 °C, filtered and the product was washed with hexane to give a pale yellow powder identified as product. The product was purified further with recrystallisation from EtOH.

2 *(E)-N'-(5-Chloro-2-hydroxybenzylidene)-3-hydroxynaphthalene-2-carbohydrazide*

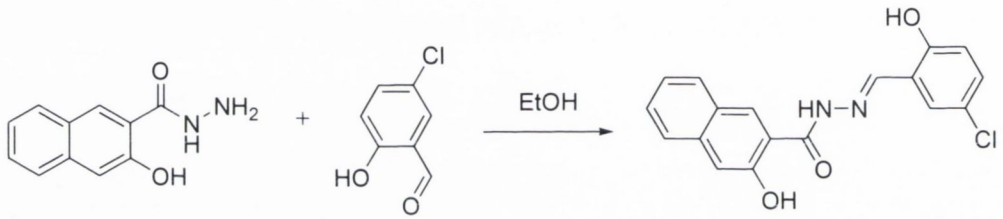

Yield: 2.39 g, 94 %, pale white powder (Recrystallisation, EtOH)

HPLC Purity: 94 % **MP:** 271-275°C **Lit. Ref**. [272]

IRϑ_{max} (KBr): 3534.29, 3516.94 (OH), 3395.73, 3263.76 (NH), 1657.62 (C=O), 1649.82 (C=C), 1630.01 (C=C), 1579.52, 653 (C-Cl) cm^{-1}

^{1}H NMR (400 MHz, DMSO-d6): δ ppm 6.98 (d, 1H, *J=8.76* Hz, Ar-H), δ 7.33 - 7.42 (m, 3H, Ar-H), δ 7.52 (t, 1H, *J=7.14* Hz, Ar-H), δ 7.69 (d, 1H, *J=2.52* Hz, CH), δ 7.77 (d, 1H, *J=8.28* Hz, Ar-H), δ 7.91 (d, 1H, *J=8.04* Hz, Ar-H), δ 8.46 (s, 1H, Ar-H), δ 8.66 (s, 1H, CH), δ 1.06 (s, 1H, OH), δ 11.25 (s, 1H, OH), δ 12.24 (s, 1H, NH)

^{13}C NMR (400 MHz, DMSO-d6): δ ppm 111.05 (CH), δ 118.75 (CH), δ 120.56 (C), δ 121.14 (CH), δ 123.51 (C), δ 124.31 (CH), δ 126.34 (C), δ 127.23 (CH), δ 128.00 (CH), δ 128.78 (CH), δ 129.14 (CH), δ 130.83 (CH), δ 131.46 (CH), 136.38 (C), δ 146.77 (C), 154.49 (C-O), δ 156.56 (C-O), δ 164.24 (C=O)

HRMS (ESI): $C_{18}H_{12}{}^{37}ClN_2O_3$ [M^- -H] requires (m/e) 339.0536, found 339.0548

3 *(E)-N'-(5-Bromo-2-hydroxybenzylidene)-3-hydroxynaphthalene-2-carbohydrazide*

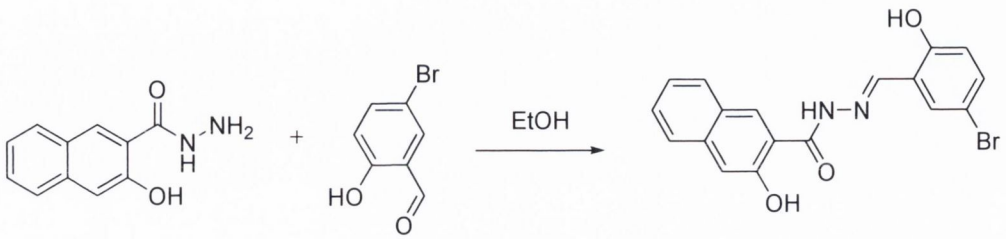

Yield: 2.76 g, 96 %, pale white powder (Recrystallisation, EtOH)

HPLC Purity: 93 % **MP:** 282-287°C **Lit. Ref**. [121]

IRϑ_{max} (KBr): 3591.16, 3488.94 (OH), 3433.34, 3356.57 (NH), 1644.73 (C=O), 1634.83 (C=C), 1621.60 (C=C), 1533.45, 793 (C-Br) cm^{-1}

^{1}H NMR (400 MHz, DMSO-d6): δ ppm 6.93 (d, 1H, *J=8.76* Hz, Ar-H), δ 7.34 (s, 1H, Ar-H), δ 7.36 - 7.40 (m, 1H, Ar-H), δ 7.45 (dd, 1H, J_1*=2.52* Hz, J_2*=6.28* Hz, Ar-H), δ 7.50 (d, 1H, *J=8.28* Hz, Ar-H), δ 7.77 (d, 1H, *J=8.28* Hz, Ar-H), δ 7.82 (d, 1H, *J=2.52* Hz, Ar-H), δ 7.91 (d, 1H, *J=8* Hz, Ar-H), δ 8.46 (s, 1H, Ar-H), δ 8.65 (s, 1H, CH), δ 11.06 (s, 1H, OH), δ 11.25 (s, 1H, OH), δ 12.23 (s, 1H, NH)

^{13}C NMR (400 MHz, DMSO-d6): δ ppm 110.98 (CH), δ 119.20 (C), δ 120.57 (CH), δ 121.75 (C), δ 124.31 (CH), δ 126.34 (C), δ 127.23 (CH), δ 128.78 (CH), δ 129.14 (CH), δ 130.83 (CH), 130.85 (C), δ 134.26 (CH), δ 136.38 (CH), δ 146.61 (C), δ 154.49 (C-O), δ 156.96 (C-O), δ 164.25 (C=O)

HRMS (ESI): $C_{18}H_{12}{}^{81}BrN_2O_3$ [M^- -H] requires (m/e) 383.0031, found 338.0085

6 (*E*)-3-hydroxy-N'-((2-hydroxynaphthalen-1-yl)methylene)naphthalene-2-carbohydrazide

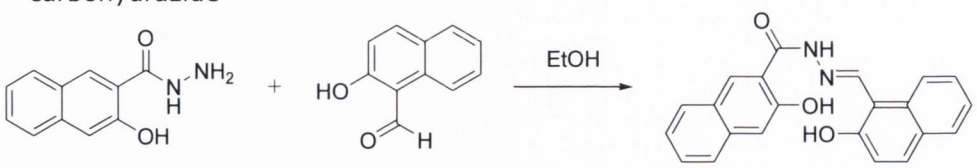

Yield: 2.14 g, 80%, yellow powder (Recrystallisation, EtOH)

HPLC Purity: 100 % **MP:** 312-315 °C **Lit. Ref**. [273]

IRϑ_{max} (KBr): 3562.96 (OH), 3521.27 (OH), 3459.26 (NH), 1642.63 (C=O), 1628.09 (C=C), 1605.73, 1594.83, 1529.48, 1459.64 cm^{-1}

^{1}H NMR (400 MHz, DMSO-d6): δ ppm 12.80 (s (br), 1H, NH), 11.37 (s (br), 1H, OH), 8.55 (s, 1H, H_{CN}), 8.36 (d, *J=8.52* Hz, 1H, H_1, CH), 7.97 (d, *J = 8.52* Hz, 1H, $H_{3'}$, Ar-H), 7.92 (d, *J = 8.04* Hz, 1H, $H_{8'}$, Ar-H), 7.81 (d, *J = 8* Hz, 1H, $H_{4'}$, Ar-H), 7.64 (t, *J = 7.54* Hz, 1H, $H_{5'}$, Ar-H), 7.55 (t, *J = 7.54* Hz, 1H, H_8, Ar-H), 7.44 - 7.36 (m, 3H, H_5, Ar-H), 7.28 (dd, J_1 = 3 Hz, J_2 = 3 Hz, 1H, $H_{6'}$, Ar-H), 7.58 (dd, J_1 = 3.28 Hz, J_2 = 3 Hz, 1H, $H_{7'}$, Ar-H), 7.53 (dd, J_1 = 8.2 Hz, J_2 = 7.5 Hz, 1H, H_6, Ar-H), 7.39 (dd, J_1 = 8.3 Hz, J_2 = 7.5 Hz, 1H, H_7, Ar-H), 7.36 (s (br), 1H, H_4, OH)

^{13}C NMR (400 MHz, DMSO-d6): δ ppm 163.8 (q, C_{CO}), 154.1 (q, C_3), 148.4 (q, C_{CN}), 135.8 (q Ar, C_{10}), 133.8 (q Ar, $C_{10'}$), 131.9 (q Ar, $C_{2'}$), 130.2 (CH Ar, C_1), 129.0 (CH Ar, $C_{1'}$), 128.6 (CH Ar, C_8), 128.5 (CH Ar, $C_{4'}$), 128.4 (CH Ar, $C_{8'}$), 128.2 (CH Ar, C_6), 127.8 (CH Ar, $C_{5'}$), 127.2 (CH Ar, $C_{6'}$), 126.8 (q Ar, C_9), 126.8 (q Ar, $C_{9'}$), 126.8 (CH Ar, $C_{7'}$), 125.8 (CH Ar, C_5), 123.8 (CH Ar, C_7), 122.7 (CH Ar, $C_{3'}$), 120.4 (q Ar, C_2), 110.5 (CH Ar, C_4)

HRMS (ESI): $C_{22}H_{16}N_2NaO_3$ [M^+ +Na] requires (m/e) 379.1059, found 379.1050 (-2.3 ppm)

7 (E)-3-Hydroxy-N'-(naphthalen-2-ylmethylene)-2-naphthohydrazide

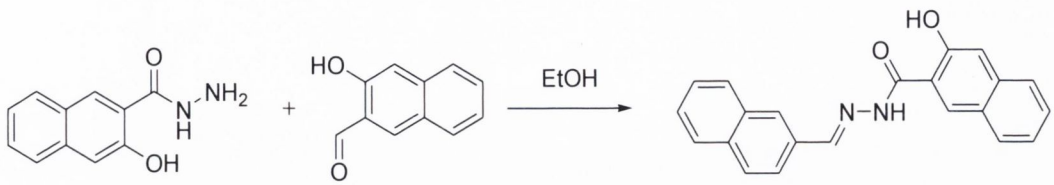

Yield: 2.19 g, 86%, pale yellow powder (Recrystallisation, EtOH)

HPLC Purity: 96 % **MP:** 276-280 °C **Lit. Ref**. [274]

IRϑ_{max} (KBr): 3439.73 (OH), 3329.37, 3054.38 (NH), 1625.69 (C=O), 1621.78 (C=C), 1563.74, 1544.83, 1521.84 cm^{-1}

^{1}H NMR (400 MHz, DMSO-d6): δ ppm 12.09 (s (br), 1H, NH), 11.33 (s (br), 1H, OH), 8.64 (s, 1H, H_{CN}), 8.50 (s, 1H, H_1, Ar-H), 8.21 (s, 1H, $H_{1'}$, Ar-H), 8.04 (d, J = 7.21 Hz, 1H, $H_{3'}$, Ar-H), 8.03 (d, J = 7.04 Hz, 1H, $H_{8'}$, Ar-H), 8.02 (d, J = 6.24 Hz, 1H, $H_{4'}$, Ar-H), 7.98 (d, J = 3.52 Hz, 1H, $H_{5'}$, Ar-H), 7.95 (d, J = 8.3 Hz, 1H, H_8, Ar-H), 7.79 (d, J = 8.2 Hz, 1H, H_5, Ar-H), 7.59 (dd, J_1 = 7.02 Hz, J_2 = 3.12 Hz, 1H, $H_{6'}$, Ar-H), 7.58 (dd, J_1 = 8.28 Hz, J_2 = 3 Hz, 1H, $H_{7'}$, Ar-H), 7.53 (dd, J_1 = 8.2 Hz, J_2 = 7.5 Hz, 1H, H_6, Ar-H), 7.39 (dd, J_1 = 8.3 Hz, J_2 = 7.5 Hz, 1H, H_7, Ar-H), 7.36 (s, 1H, H_4, Ar-H)

^{13}C NMR (400 MHz, DMSO-d6): δ ppm 163.8 (q, C_{CO}), 154.1 (q, C_3), 148.4 (q, C_{CN}), 135.8 (q Ar, C_{10}), 133.8 (q Ar, $C_{10'}$), 131.9 (q Ar, $C_{2'}$), 130.2 (CH Ar, C_1), 129.0 (CH Ar, $C_{1'}$), 128.6 (CH Ar, C_8), 128.5 (CH Ar, $C_{4'}$), 128.4 (CH Ar, $C_{8'}$), 128.2 (CH Ar, C_6), 127.8 (CH Ar, $C_{5'}$), 127.2 (CH Ar, $C_{6'}$), 126.8 (q Ar, C_9), 126.8 (q Ar, $C_{9'}$), 126.8 (CH Ar, $C_{7'}$), 125.8 (CH Ar, C_5), 123.8 (CH Ar, C_7), 122.7 (CH Ar, $C_{3'}$), 120.4 (q Ar, C_2), 110.5 (CH Ar, C_4)

HRMS (ESI): $C_{22}H_{17}N_2O_2$ [M^+ +H] requires (m/e) 341.1290, found 341.1296

8 (E)-3-Hydroxy-N'-(1-(naphthalen-2-yl)ethylidene)-2-naphthohydrazide

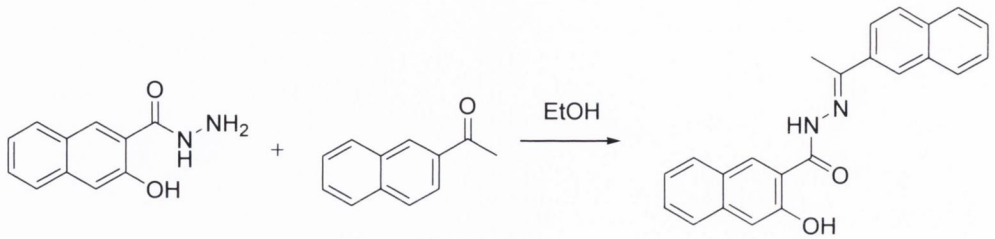

Yield: 2.23 g, 84%, pale yellow powder (Recrystallisation, EtOH)

HPLC Purity: 85 % **MP:** 275-280 °C **Lit. Ref**. [275]

IRϑ_{max} (KBr): 3369.86 (OH), 3248.71, 3052.55 (NH), 1657.45 (C=O), 1627.98 (C=C), 1595.30, 1564.47, 1512.89 cm^{-1}

^{1}H NMR (400 MHz, DMSO-d6): δ ppm 11.69 (s (br), 1H, OH), 11.67 (s (br), 1H, NH), 8.67 (s, 1H, H_1, Ar-H), 8.37 (s, 1H, $H_{1'}$, Ar-H), 8.20 (d, J = 8.52 Hz, 1H, $H_{3'}$, Ar-H), 8.05 (d, J = 7.14 Hz, 1H, $H_{8'}$, Ar-H), 8.02 (d, J = 8.0 Hz, 1H, H_8, Ar-H), 7.98 (d, J = 8.14 Hz, 1H, $H_{4'}$, Ar-H), 7.97 (d, J =7.24 Hz , 1H, $H_{5'}$, Ar-H), 7.80 (d, J = 8.0 Hz, 1H, H_5, Ar-H), 7.58 (dd, J_1 = 7.02 Hz, J_2 = 2.04 Hz , 1H, $H_{6'}$, Ar-H), 7.57 (dd, J_1 = 8.04 Hz, J_2 = 2.14 Hz, 1H, $H_{7'}$, Ar-H), 7.54 (dd, J_1 = 8.0 Hz, J_2 = 7.3 Hz, 1H, H_6, Ar-H), 7.40 (s, 1H, H_4, Ar-H), 7.39 (dd, J_1 = 8.0 Hz, J_2 = 7.3 Hz, 1H, H_7, Ar-H), 2.52 (s, 3H, H_{Me})

^{13}C NMR (400 MHz, DMSO-d6): δ ppm 161.6 (q, C_{CO}), 152.8 (q, C_3), 152.0 (q, C_{CN}), 135.8 (q Ar, C_{10}), 135.3 (q Ar, $C_{2'}$), 133.4 (q Ar, $C_{10'}$), 132.8 (q Ar, $C_{9'}$), 132.3 (CH Ar, C_1), 128.9 (CH Ar, C_8), 128.6 (CH Ar, $C_{8'}$), 128.3 (CH Ar, C_6), 127.8 (CH Ar, $C_{4'}$), 127.5 (CH Ar, $C_{5'}$), 127.2(q Ar, C_9), 126.9 (CH Ar, $C_{6'}$), 126.6 (CH Ar, $C_{1'}$), 126.5 (CH Ar, $C_{7'}$), 125.7 (CH Ar, C_5), 123.9 (CH Ar, C_7), 123.7 (CH Ar, $C_{3'}$), 120.8 (q Ar, C_2), 110.7 (CH Ar, C_4), 13.7 (CH_3)

HRMS (ESI): $C_{23}H_{19}N_2O_2$ [M^+ +H] requires (m/e) 355.1447, found 355.1459

9 (E/Z)-3-Hydroxy-N'-(naphthalen-2-yl(phenyl)methylene)-2-naphthohydrazide

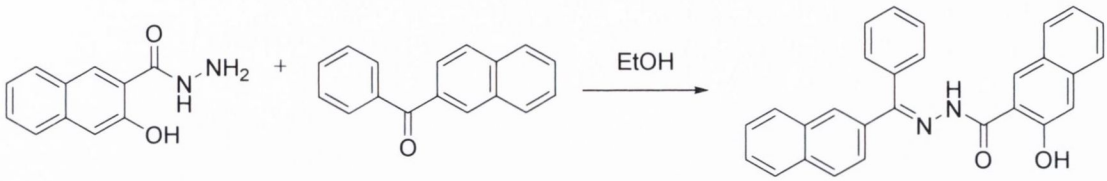

Yield: 0.16 g, 5%, pale brown resin (Recrystallisation, EtOH)

HPLC Purity: 96 % **MP:** 295-298 °C **Lit. Ref.** [276]

IRϑ_{max} (KBr): 3482.27 (OH), 3327.61, 3149.78 (NH), 3151.87, 3068.45 (CH), 1680.74 (C=O), 1641.83, 1610.42 (C=C), 1536.71, 1458.96 cm^{-1}

^{1}H NMR (400 MHz, DMSO-d6): δ ppm 11.56 (s (br), 1H, NH), 11.51 (s (br), 1H, NH), 11.06 (s (br), 1H, OH), 10.81 (s (br), 1H, OH), 8.68 (s, 1H, H_2), 8.66 (s, 1H, H_1), 7.71 (t, 1H, H_{21}), 7.44 (m, 1H, H_{32}), 7.73 (t, 1H, H_{20}), 8.20 (d, 1H, H_5), 7.97 (d, 1H, H_{18}), 7.96 (d, 1H, H_{19}), 7.86 (d, 1H, H_{22}), 8.07 (d, 1H, H_{26}), 7.43 (m, 1H, H_{27}), 7.49 (m, 1H, H_{30}), 7.46 (t, 1H, H_{31}), 7.49 (m, 1H, H_{29}), 7.69 (m, 1H, H_{28}), 8.01 (d, 1H, H_{25}), 8.10 (d, 1H, H_{24}), 8.05 (s, 1H, H_{23}), 7.96 (d, 1H, H_{17}), 7.59 (d, 1H, H_{15}), 7.69 (d, 1H, H_{16}), 7.57 (t, 1H, H_{14}), 7.64 (t, 1H, H_{13}), 7.52 (s, 1H, H_{12}), 7.69 (m, 1H, H_{10}), 7.63 (t, 1H, H_9), 7.51 (m, 1H, H_{11}), 7.35 (d, 1H, H_8), δ 7.33 (t, 1H, H_7), δ 8.14 (d, 1H, H_6), δ 7.21 (s, 1H, H_4), δ 7.10 (s, 1H, H_3)

^{13}C NMR (400 MHz, DMSO-d6): δ ppm 128.53 (CH Ar, C_{52}), 129.80 (CH Ar, C_{51}), 120.20 (CH Ar, C_{50}), 110.50 (CH Ar, C_{49}), 110.54 (CH Ar, C_{48}), 120.19 (CH Ar, C_{47}), 123.86 (CH Ar, C_{46}), 123.93 (CH Ar, C_{45}), 123.95 (CH Ar, C_{44}), 125.32 (CH Ar, C_{43}), 125.63 (CH Ar, C_{42}), 125.67 (CH Ar, C_{41}), 126.75 (CH Ar, C_{40}), 126.96 (CH Ar, C_{39}), 127.17 (CH Ar, C_{38}), 127.20 (CH Ar, C_{37}), 127.23 (CH Ar, C_{36}), 127.37 (CH Ar, C_{35}), 127.58 (CH Ar, C_{34}), 127.63 (CH Ar, C_{33}), 128.07 (CH Ar, C_{32}), 128.09 (CH Ar, C_{31}), 128.14 (CH Ar, C_{30}), 128.21 (CH Ar, C_{29}), 128.29 (CH Ar, C_{28}), 128.39 (CH Ar, C_{27}), 128.44 (CH Ar, C_{26}), 128.52 (CH Ar, C_{25}), 128.58 (CH Ar, C_{24}), 129.02 (CH Ar, C_{23}), 129.06 (CH Ar, C_{22}), 129.51 (CH Ar, C_{21}), 129.82 (CH Ar, C_{20}), 130.04 (CH Ar, C_{19}), 130.18 (CH Ar, C_{18}), 132.51 (CH Ar, C_{17}), 132.61 (CH Ar, C_{16}), 132.97 (CH Ar, C_{15}), 133.03 (CH Ar, C_{14}), 133.06 (CH Ar, C_{13}), 133.22 (CH Ar, C_{12}), 133.50 (CH Ar, C_{11}), 134.83 (CH Ar, C_{10}), 135.78 (CH Ar, C_9), 135.85 (CH Ar, C_8), 137.38 (CH Ar, C_7), 152.19 (CH Ar, C_6), 152.25 (CH Ar, C_5), 153.73 (CH Ar, C_4), 153.81 (CH Ar, C_3), 160.97 (CH Ar, C_2), 161.12 (CH Ar, C_1).

HRMS (ESI): $C_{28}H_{20}N_2NaO_2$ [M^+ +Na] requires (m/e) 439.14225, found 439.1410

26 *(E)-N'-(5-Chloro-2-hydroxybenzylidene)-2-naphthohydrazide*

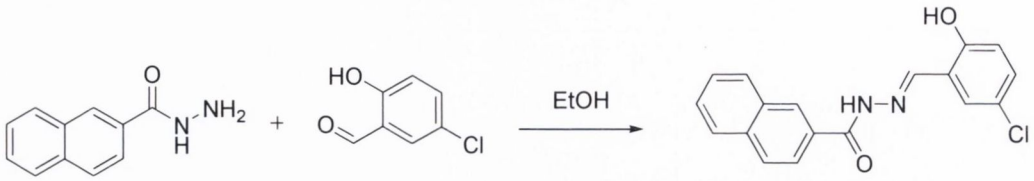

Yield: 0.36 g, 15 %, brown powder (Recrystallisation, EtOH)

HPLC Purity: 96 % **MP:** 253-262°C

IRϑ_{max} (KBr): 3592.73, 3495.83 (OH), 3362.15, 3383.63 (NH), 1664.74 (C=O), 1658.18 (C=C), 1624.83 (C=C), 1687.75, 1476.59, 1431.73 cm^{-1}

^{1}H NMR (400 MHz, DMSO-d6): δ ppm 6.88 (d, 1H, *J=8.52* Hz, Ar-H), δ 7.23 (d, 2H, *J=8.52* Hz, Ar-H), δ 7.56 (s, 2H, Ar-H), δ 7.94 (d, 2H, *J=7.52* Hz, Ar-H), δ 8.50 (s, 1H, Ar-H), δ 8.60 (s, 1H, Ar-H), δ 11.23 (s (br), 1H, OH), δ 12.30 (s (br), 1H, NH)

^{13}C NMR (400 MHz, DMSO-d6): δ ppm 118.25 (CH), δ 120.79 (C), δ 122.99 (CH), δ 124.25 (CH), δ 127.00 (CH), δ 127.51 (CH), δ 127.74 (CH), δ 128.08 (CH), δ 128.23 (2xCH), δ 128.97 (CH), δ 130.05 (CH), δ 130.81 (CH), δ 132.05 (C), δ 134.47 (C), δ 145.69 (CH), δ 156.04 (C-O), 163.01 (C=O)

HRMS (ESI): $C_{18}H_{12}{}^{35}ClN_2O_2$ [M^- -H] requires (m/e) 323.0587, found 323.065

27 (E)-N'-Benzylidene-3-hydroxynaphthalene-2-carbohydrazide

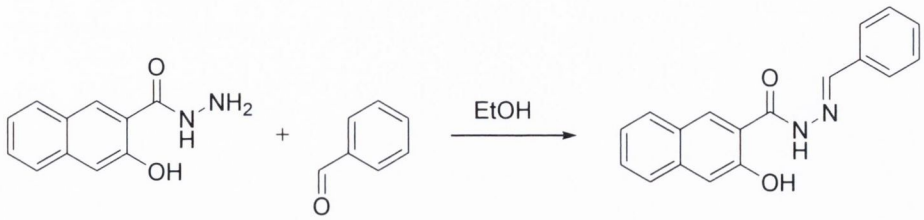

Yield: 1.85 g, 85%, pale brown powder (Recrystallisation, EtOH)

HPLC Purity: 100 % **MP:** 227-230 °C **Lit. Ref**. [277] **Lit. MP**: 224-225 °C

IRϑ_{max} (KBr): 3452.61 (OH), 3242.11, 3047.11 (NH), 1625.80 (C=O), 1631.09 (C=C), 1612.65 (C=C), 1560.54 cm^{-1}

^{1}H NMR (400 MHz, DMSO-d_6): δ ppm 11.99 (s (br), 1H, OH), 11.30 (s (br), 1H, NH), 8.48 (s, 1H, H_{CN}), 8.47 (s, 1H, H_1), 7.93 (d, J = 8.2 Hz, 1H, H_8), 7.79 (d, J = 7.2 Hz, 1H, $H_{2'}$), 7.78 (d, J = 7.2 Hz, 1H, H_5), 7.53 (dd, J_1 = 7.3 Hz, J_2 = 7.3 Hz, 1H, H_6), 7.50 (dd, J = 7.52 Hz, 1H, $H_{3'}$), 7.49 (ddd, J = 6.56 Hz, $H_{4'}$), 7.38 (dd, J_1 = 8.2 Hz, J_2 = 7.3 Hz, 1H, H_7), 7.34 (s, 1H, H_4)

^{13}C NMR (101 MHz, DMSO-d_6): δ ppm 163.8 (q, C_{CO}), 154.1 (q, C_3), 148.5 (q, C_{CN}), 135.8 (q Ar, C_{10}), 134.1 (q Ar, $C_{1'}$), 130.3 (CH Ar, $C_{4'}$), 130.2 (CH Ar, C_1), 128.9 (CH Ar, $C_{3'}$), 128.7 (CH Ar, C_8), 128.3 (CH Ar, C_6), 126.8 (CH Ar, $C_{2'}$), 126.8 (q Ar, C_9), 125.7 (CH Ar, C_5), 123.9 (CH Ar, C_7), 120.4 (q Ar, C_2), 110.6 (CH Ar, C_4)

HRMS (ESI): $C_{18}H_{15}N_2O_2$ [M^+ +H] requires (m/e) 291.1134, found 291.1141

28 *(E)-N'-(2-Hydroxybenzylidene)-3-hydroxynaphthalene-2-carbohydrazide*

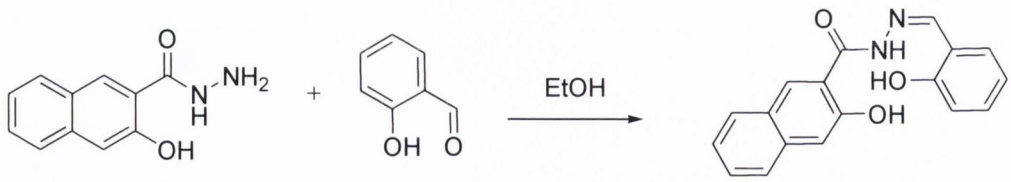

Yield: 2.06 g, 90 %, pale yellow powder (Recrystallisation, EtOH)

HPLC Purity: 97 % **MP:** 217-220 °C **Lit. Ref**. [278] **Lit. MP**: 215°C

IRϑ_{max} (KBr): 3478.00 (OH), 3351.84, 3256.37 (NH), 1659.67 (C=O), 1645.73 (C=C), 1632.34 (C=C), 1596.30, 1567.38 cm^{-1}

^{1}H NMR (400 MHz, DMSO-d6): δ ppm 5.63 (s (br), 1H, OH), 6.95 - 7.12 (m, 2H, Ar-H), δ 7.33 - 7.41 (m, 3H, Ar-H), δ 7.52 (d, 1H, *J=7.52*, Ar-H), δ 7.58 (d, 1H, *J= 6.52* Hz, Ar-H), δ 7.77 (d, 1H, *J=8.52*, Ar-H), δ 7.91 (d, 1H, *J=8.04*, Ar-H), δ 8.47 (s, 1H, Ar-H), δ 8.69 (s, 1H, CH), δ 11.22 (s (br), 1H, OH), δ 12.17 (s (br), 1H, NH)

^{13}C NMR (400 MHz, DMSO-d6): δ ppm 110.56 (CH), δ 116.45 (CH), δ 118.68 (C), δ 119.43 (CH), δ 120.07 (CH), δ 123.85 (C), δ 125.85 (CH), δ 126.76 (C), δ 128.31 (CH), δ 128.67 (CH), δ 129.41 (C), δ 130.33 (CH), δ 131.64 (CH), δ 135.89 (C), δ 148.71 (NCH), δ 154.01 (C-OH), δ 157.50 (C-OH), δ 163.56 (C=O)

HRMS (ESI): $C_{18}H_{14}N_2NaO_3$ [M^+ +Na] requires (m/e) 329.0902, found 329.0903 (3 ppm)

29 *(E)-N'-(2-Hydroxy-5-methylbenzylidene)-3-hydroxynaphthalene-2-carbohydrazide*

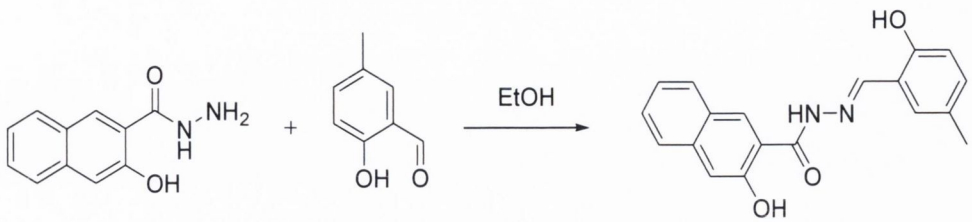

Yield: 1.98 g, 89 %, beige powder (Recrystallisation, EtOH)

HPLC Purity: 100 % **MP:** 254-258 °C

IRϑ_{max} (KBr): 3541.87 (OH), 3387.84, 3276.63 (NH), 1668.67 (C=O), 1657.41 (C=C), 1630.53 (C=C) cm^{-1}

^{1}H NMR (400 MHz, DMSO-d6): δ ppm 2.27 (s, 3H, CH_3), δ 6.86 (d, 1H, *J= 8.52*, Ar-H), δ 7.19 (dd, 1H, *J=1.76, J=1.72*, Ar-H), δ 7.35 - 7.40 (m, 3H, Ar-H), δ 7.51 - 7.59 (m, 1H, Ar-H), δ 7.77 (d, 1H, *J=8*, Ar-H), δ 7.92 (d, 1H, *J=8.04*, Ar-H), 8.16 (s, 1H, CH), 8.47 (s, 1H, Ar-H), δ 8.65 (s, 1H, OH)

^{13}C NMR (400 MHz, DMSO-d6): δ ppm 20.43 (CH_3), δ 111.05 (CH), δ 116.78 (CH), δ 118.81 (C), δ 120.46 (CH), δ 124.30 (C), δ 126.34 (CH), δ 127.23 (C), δ 128.44 (CH), δ 128.77 (C), δ 129.14 (CH), δ 129.67 (C), δ 130.80 (CH), δ 132.80 (CH), δ 136.37 (C), δ 149.11 (NCH), δ 154.57 (C-OH), δ 155.83 (C-OH), δ 164.08 (C=O)

HRMS (ESI): $C_{19}H_{16}N_2O_3$ [M^+ +Na] requires (m/e) 320.11609, found 329.0930

30 *(E)-N'-(5-tert-Butyl-2-hydroxybenzylidene)-3-hydroxynaphthalene-2-carbohydrazide*

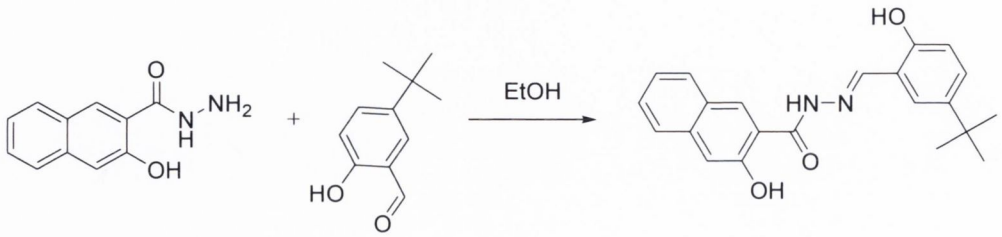

Yield: 2.25 g, 83 %, pale cream powder (Recrystallisation, EtOH)

HPLC Purity: 100 % **MP:** 247-250°C

IRϑ_{max} (KBr): 3411.76 (OH), 3321.93, 3164.32 (NH), 1636.78 (C=O), 1632.94 (C=C), 1626.36 (C=C), 1567.46 cm^{-1}

^{1}H NMR (400 MHz, DMSO-d6): δ ppm 1.15 (s, 9H, 3xCH_3), δ 6.90 (d, 1H, *J=8.52*, Ar-H), δ 7.35 - 7.41 (m, 2H, Ar-H), δ 7.53 (t, 2H, *J=7.28* Hz, Ar-H), δ 7.77 (s, 1H, Ar-H), δ 7.92 (s, 1H, Ar-H), δ 8.17 (s, 1H, Ar-H), δ 8.49 (s, 1H, Ar-H), δ 8.63 (s, 1H, NH), δ 11.30 (s, 1H, OH), δ 12.15 (s, 1H, OH)

^{13}C NMR (400 MHz, DMSO-d6): δ ppm 31.73 (CH_3), δ 34.27 (C), δ 111.04 (CH), δ 116.57 (CH), δ 118.36 (C), δ 120.59 (CH), δ 124.31 (CH), δ 125.95 (C), δ 126.34 (CH), δ 127.24 (CH), δ 128.76 (CH), δ 129.15 (CH), δ 129.35 (CH), δ 130.82 (CH), δ 136.35 (C), δ 141.99 (C), 149.58 (C), δ 154.48 (C-O), δ 155.83 (C-O), 163.95 (C=O)

HRMS (ESI): $C_{22}H_{21}N_2O_3$ [M^- -H] requires (m/e) 361.155, found 361.1566

31 *(E)-N'-(2, 5-dihydroxybenzylidene)-3-hydroxynaphthalene-2-carbohydrazide*

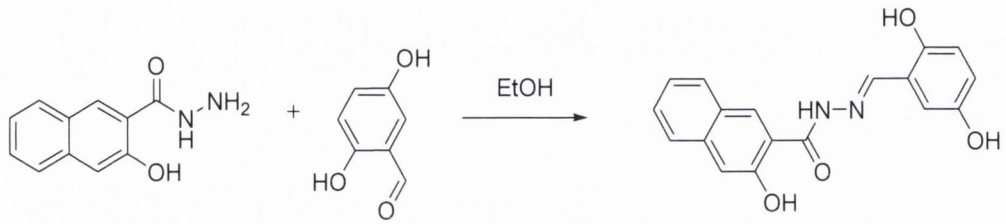

Yield: 2.15 g, 89 %, pale yellow powder (Recrystallisation, EtOH)

HPLC Purity: 100 % **MP:** 232-236 °C

IRϑ_{max} (KBr): 3585.36, 3560.61 3489.60 (OH), 3356.78, 3147.85 (NH), 1645.63 (C=O), 1653.12 (C=C), 1638.73 (C=C), 1544.52 cm^{-1}

^{1}H NMR (400 MHz, DMSO-d6): δ ppm 6.77 (t, 2H, *J=2.5* Hz, Ar-H), δ 7.03 (s, 1H, Ar-H), δ 7.34 - 77.41 (m, 2H, Ar-H), δ 7.53 (d, 1H, *J*=7.02 Hz, Ar-H), δ 7.77 (d, 1H, *J*=8.24 Hz, Ar-H), δ 7.91 (d, 1H, *J*=8.04 Hz, δ 8.48 (s, 1H, Ar-H), δ 8.62 (s, 1H, Ar-H), δ 9.04 (s, 1H, NH), δ 10.34 (s, 1H, OH), δ 11.33 (s, 1H, OH), δ 12.10 (s, 1H, OH)

^{13}C NMR (400 MHz, DMSO-d6): δ ppm 111.05 (CH), δ 114.08 (CH), δ 117.61 (CH), δ 119.46 (CH), δ 119.69 (C), δ 120.40 (CH), δ 124.30 (CH), δ 126.34 (CH), δ 127.22 (CH), δ 128.77 (CH), δ 129.14 (CH), δ 130.71 (C), δ 136.37 (C), δ 148.58 (C), δ 150.39 (C-O), δ 150.77 (C-O), δ 154.66 (C-O), δ 164.10 (C=O)

HRMS (ESI): $C_{18}H_{13}N_2O_4$ [M^- -H] requires (m/e) 321.0875, found 321.0865

32 *(E)-N'-(2-Hydroxy-5-methoxybenzylidene)-3-hydroxynaphthalene-2-carbohydrazide*

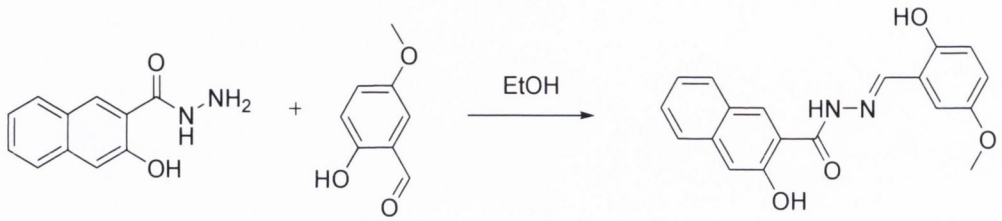

Yield: 2.39 g, 95 %, pale white powder (Recrystallisation, EtOH)

HPLC Purity: 100 % **MP:** 287-292°C **Lit. Ref**. [279]

IRϑ_{max} (KBr): 3528.72, 3488.65 (OH), 3356.81, 3250.04 (NH), 1648.62 (C=O), 1636.34 (C=C), 1620.46 (C=C), 1549.62, 1452.76 cm^{-1}

^{1}H NMR (400 MHz, DMSO-d6): δ ppm 3.75 (s, 3H, CH_3), δ 6.91 - 6.99 (m, 2H, Ar-H), δ 7.17 (d, 1H, *J=2.76* Hz, Ar-H), δ 7.34 - 7.41 (m, 2H, Ar-H), δ 7.51 (td, 2H, J_1= 1.28 Hz, J_2 = 8.28 Hz, J_3= 13.8 Hz, Ar-H), δ 7.77 (d, 1H, *J* = 8.28 Hz, Ar-H), δ 7.91 (d, 1H, *J*= 8.24 Hz, Ar-H), δ 8.47 (s, 1H, OH), δ 8.67 (s, 1H, OH)

^{13}C NMR (400 MHz, DMSO-d6): δ ppm 55.97 (CH_3), δ 111.04 (CH), δ 112.47 (CH), δ 117.81 (CH), δ 119.01 (CH), δ 119.40 (CH), δ 120.56 (CH), δ 124.30 (C), δ 126.34 (CH), δ 127.23 (CH), δ 128.76 (CH), δ 129.13 (CH), δ 130.74 (C), δ 136.36 (C), δ 148.49 (C), δ 152.03 (C-O), δ 152.63 (C-O), δ 154.56 (C-O), δ 164.11 (C=O)

HRMS (ESI): $C_{19}H_{15}N_2O_4$ [M^- -H] requires (m/e) 335.1032, found 335.1045

35 *(E)-N'-(2-Hydroxy-5-iodobenzylidene)-3-hydroxynaphthalene-2- carbohydrazide*

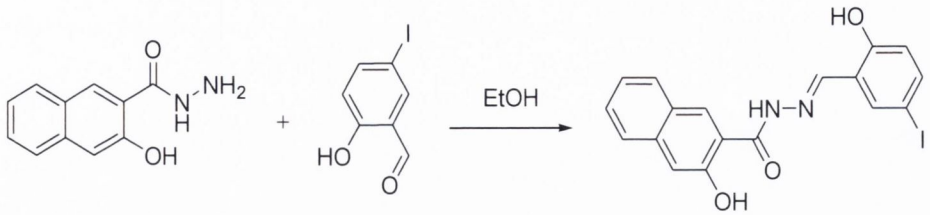

Yield: 3.10 g, 96 %, pale white powder (Recrystallisation, EtOH)

HPLC Purity: 100 % **MP:** 281-288°C

IRϑ_{max} (KBr): 3563.67, 3482.65 (OH), 3359.71, 3147.53 (NH), 1670.58 (C=O), 1642.69 (C=C), 1621.42 (C=C) cm^{-1}

^{1}H NMR (400 MHz, DMSO-d6): δ ppm 6.80 (d, 1H, *J* = 8.52 Hz, Ar-H), δ 7.34 – 7.40 (m, 2H, Ar-H), 7.52 (s, 1H, Ar-H), δ 7.58 (dd, 1H, J_1=2.28 Hz, J_2= 8.52 Hz, Ar-H), δ 7.77 (d, 1H, *J*= 8.28 Hz, Ar-H), δ 7.91 (d, 1H, *J*= 8.28 Hz, Ar-H), δ 7.97 (d, 1H, *J*= 2.24 Hz, Ar-H), 8.46 (s, 1H, Ar-H), δ 8.62 (s, 1H, CH), δ 11.23 (s, 1H, NH), δ 12.22 (s, 1H, OH)

^{13}C NMR (400 MHz, DMSO-d6): δ ppm 81.85 (C-I), δ 111.04 (CH), δ 119.58 (CH), δ 120.58 (C), δ 122.29 (CH), δ 124.31 (C), δ 126.34 (CH), δ 127.22 (CH), δ 128.77 (CH), δ 129.14 (CH), δ 130.81 (C), δ 136.38 (CH), δ 136.73 (CH), δ 139.99 (CH), δ 146.52 (C), δ 154.49 (C-O), δ 157.50 (C-O), δ 164.22 (C=O)

HRMS (ESI): $C_{18}H_{12}{}^{127}IN_2O_3$ [M^- -H] requires (m/e) 430.9893, found 430.9934

36 *(E)-N'-(2-Hydroxy-5-nitrobenzylidene)-3-hydroxynaphthalene-2- carbohydrazide*

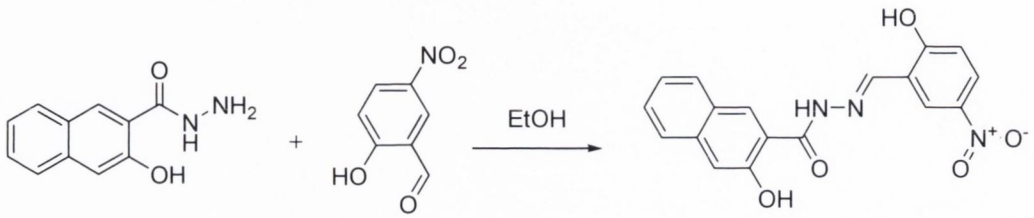

Yield: 2.50 g, 95 %, pale yellow powder (Recrystallisation, EtOH)

HPLC Purity: 82 % **MP:** 258-260°C **Lit. Ref**. [280]

IRϑ_{max} (KBr): 3435.38 (OH), 3352.83, 3141.70 (NH), 1693.58 (C=O), 1649.83 (C=C), 1625.74 (C=C), 1539.74 cm^{-1}

^{1}H NMR (400 MHz, DMSO-d6): δ ppm 7.13 (d, 1H, *J*= 9.04 Hz, Ar-H), δ 7.34 – 7.40 (m, 2H, Ar-H), δ 7.50 (td, 1H, J_1= 1 Hz, J_2 = 8.04 Hz, J_3= 14.04 Hz, Ar-H), δ 7.77 (d, 1H, *J*= 8.28 Hz, Ar-H), δ 7.91 (d, 1H, *J* = 8.24 Hz, Ar-H), δ 8.18 (dd, 1H, J_1= 3.02 Hz, J_2= 12.04 Hz, Ar-H), δ 8.46 (s, 1H, Ar-H), δ 8.61 (d, 1H, *J*= 2.76 Hz, Ar-H), δ 8.76 (s, 1H, CH), δ 12.29 (s, 1H, OH)

^{13}C NMR (400 MHz, DMSO-d6): δ ppm 111.03 (CH), δ 117.64 (CH), δ 120.43 (C), δ 120.70 (CH), δ 124.20 (CH), δ 124.32 (CH), δ 126.34 (CH), δ 127.23 (2xCH), δ 128.79 (CH), δ 129.13 (CH), δ 130.88 (C), δ 136.38 (C), δ 140.41 (CN), δ 145.26 (C), δ 154.41 (C-O), δ 163.11 (C-O), δ 164.34 (C=O)

HRMS (ESI): $C_{18}H_{12}N_3O_5$ [M^- -H] requires (m/e) 350.0777, found 350.0786

37 *(E)-N'-(2-Hydroxy-3-methylbenzylidene)-3-hydroxynaphthalene-2-carbohydrazide*

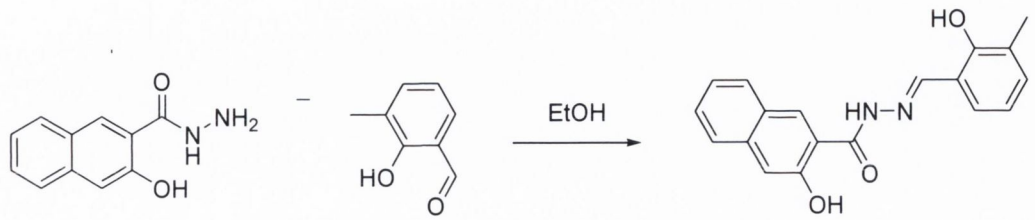

Yield: 2.11 g, 88 %, white powder (Recrystallisation, EtOH)

HPLC Purity: 97 % **MP:** 278-285 °C

IRϑ_{max} (KBr): 3537.62, 3450.72 (OH), 3384.71, 3294.73 (NH), 1648.79 (C=O), 1629.33 (C=C), 1615.64 (C=C), 1583.91 cm^{-1}

^{1}H NMR (400 MHz, DMSO-d6): δ ppm 2.24 (s, 3H, CH_3), δ 6.88 (t, 1H, *J=7.52* Hz, Ar-H), δ 7.23 (d, 1H, *J=7.28* Hz, Ar-H), δ 7.30 (d, 1H, *J=1* Hz, Ar-H), δ 7.36 - 7.41 (m, 2H, Ar-H), δ 7.51 - 7.58 (m, 1H, Ar-H), δ 7.78 (d, 1H, *J=8.24* Hz, Ar-H), δ 7.93 (d, 1H, *J=8* Hz, Ar-H), δ 8.48 (s, 1H, Ar-H), δ 8.64 (s, 1H, CH), δ 11.26 (s, 1H, OH), δ 11.90 (s, 1H, OH), δ 12.23 (s, 1H, NH)

^{13}C NMR (400 MHz, DMSO-d6): δ ppm 15.94 (CH_3), δ 111.06 (CH), 117.64 (C), δ 119.44 (CH), δ 120.55 (CH), δ 124.34 (CH), δ 125.54 (C), δ 126.34 (C), δ 127.28 (CH), δ 128.80 (CH), δ 129.17 (CH), δ 129.25 (CH), δ 131.03 (C), δ 133.09 (CH), δ 136.39 (C), δ 151.12 (C-O), δ 154.31 (C-O), δ 156.51 (C-O), δ 163.78 (C=O)

HRMS (ESI): $C_{19}H_{15}N_2O_3$ [M^- -H] requires (m/e) 319.1083, found 319.1081

38 *(E)-N'-(2-Hydroxy-3-methoxybenzylidene)-3-hydroxynaphthalene-2-carbohydrazide*

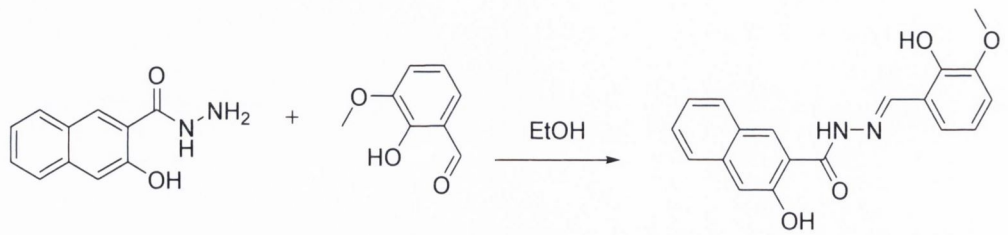

Yield: 2.14 g, 85 %, cream powder (Recrystallisation, EtOH)

HPLC Purity: 89 % **MP:** 288-291 °C **Lit. Ref**. [281]

IRϑ_{max} (KBr): 3467.81 (OH), 3372.25, 3284.17 (NH), 1646.78 (C=O), 1630.52 (C=C), 1609.36 (C=C), 1585.76, 1568.46 cm^{-1}

^{1}H NMR (400 MHz, DMSO-d6): δ ppm 3.84 (s, 3H, OCH_3), δ 6.87 (t, 1H, *J=7.9* Hz, Ar-H), δ 7.05 (dd, 1H, J_1*=1.24* Hz, J_2*=6.8* Hz, Ar-H), δ 7.19 (dd, 1H, J_1*=1.28* Hz, J_2*=6.78* Hz, Ar-H), δ 7.34 - 7.41 (m, 2H, Ar-H), δ 7.51 - 7.60 (m, 1H, Ar-H), δ 7.77 (d, 1H, *J=8.28* Hz, Ar-H), δ 7.91 (d, 1H, *J=8,* Ar-H), δ 8.47 (s, 1H, Ar-H), δ 8.71 (s, 1H, CH), δ 10.90 (s (br), 1H, OH), δ 11.29 (s (br), 1H, OH), δ 12.15 (s (br), 1H, NH)

^{13}C NMR (400 MHz, DMSO-d6): δ ppm 59.37 (s, 1H, OCH_3), 111.05 (CH), δ 114.43 (CH), δ 119.41 (CH), δ 119.58 (CH), δ 120.52 (CH), δ 121.16 (C), δ 124.30 (CH), δ 126.34 (CH), δ 127.24 (CH), δ 128.77 (CH), δ 129.14 (CH), δ 130.78 (C), δ 136.38 (C), δ 147.70 (C), δ 148.46 (C-O), δ 149.11 (C-O), δ 154.55 (C-O), δ 164.06 (C=O)

HRMS (ESI): $C_{19}H_{15}N_2O_4$ [M^- -H] requires (m/e) 335.1032, found 335.1028

39 *(E)-N'-(3-Chloro-2-hydroxybenzylidene)-3-hydroxynaphthalene-2-carbohydrazide*

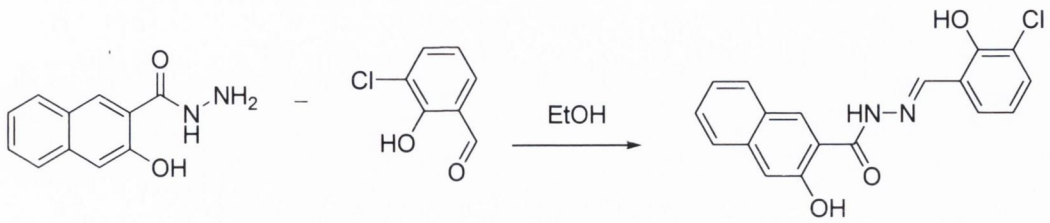

Yield: 2.34 g, 92 %, cream powder (Recrystallisation, EtOH)

HPLC Purity: 100 % **MP:** 238-244°C

IRϑ_{max} (KBr): 3537.62, 3516.74 (OH), 3346.95, 3257.82 (NH), 1662.78 (C=O), 1628.64 (C=C), 1621.44 (C=C), 1567.47, 1439.57 cm^{-1}

^{1}H NMR (400 MHz, DMSO-d6): δ ppm 6.97 (t, 1H, *J=7.8* Hz, Ar-H), δ 7.26 - 7.36 (m, 2H, Ar-H), δ 7.50 – 7.56 (m, 3H. Ar-H), δ 7.78 (d, 1H, *J=8.28* Hz, Ar-H), δ 7.93 (d, 1H, *J=8.04* Hz, Ar-H), δ 8.47 (s, 1H, CH), δ 8.68 (s, 1H, Ar-H), δ 9.11 (s (br), 1H, OH) δ 11.20 (s (br), 1H, OH), δ 12.40 (s (br), 1H, NH)

^{13}C NMR (400 MHz, DMSO-d6): δ ppm 111.20 (CH), δ 120.10 (C), δ 120.57 (CH), δ 120.73 (C), δ 120.86 (CH), δ 124.36 (CH), δ 126.35 (CH), δ 127.29 (CH), δ 128.83 (CH), δ 129.19 (CH), δ 130.01 (CH), δ 131.24 (CH), δ 131.95 (C), δ 136.40 (C), δ 149.57 (C), δ 153.77 (C-O), δ 154.10 (C-O), δ 163.80 (C=O)

HRMS (ESI): $C_{18}H_{12}{}^{35}ClN_2O_3$ [M^- -H] requires (m/e) 339.0536, found 339.0543

40 *(E)-N'-(5-Chloro-2-hydroxy-3-methoxybenzylidene)-3-hydroxynaphthalene-2-carbohydrazide*

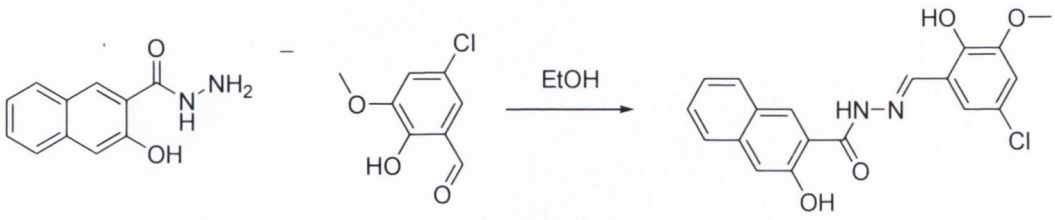

Yield: 2.71 g, 98 %, pale yellow powder (Recrystallisation, EtOH)

HPLC Purity: 100 % **MP:** 298-302°C **Lit. Ref**. [282]

IRϑ_{max} (KBr): 3514.83, 3492.73 (OH), 3274.65, 3127.43 (NH), 1656.49 (C=O), 1646.73 (C=C), 1614.62 (C=C), 631 (C-Cl) cm^{-1}

^{1}H NMR (400 MHz, DMSO-d6): δ ppm 3.86 (s, 3H, CH_3), δ 7.10 (d, 1H, *J=2.48* Hz, Ar-H), δ 7.29 - 7.34 (m, 3H, Ar-H), δ 7.52 (d, 1H, *J=7.52* Hz, Ar-H), δ 7.76 (d, 1H, *J=8.52* Hz, Ar-H), δ 7.90 (d, 1H, *J=8.52* Hz, Ar-H), δ 8.45 (s, 1H, Ar-H), δ 8.66 (s, 1H, CH), δ 10.84 (s, 1H, OH), δ 11.24 (s, 1H, OH), δ 12.20 (s, 1H, NH)

^{13}C NMR (400 MHz, DMSO-d6): δ ppm 56.25 (CH_3), δ 110.53 (CH), δ 113.50 (CH), δ 118.58 (C), δ 120.14 (CH), δ 120.19 (CH), δ 122.84 (CH), δ 123.83 (C), δ 125.87 (CH), δ 126.75 (C), δ 128.29 (CH), δ 128.66 (CH), δ 130.33 (C), δ 135.88 (C), δ 145.93 (C), δ 146.28 (C-O), δ 148.99 (C-O), δ 154.00 (C-O), δ 163.72 (C=O)

HRMS (ESI): $C_{19}H_{14}{}^{35}ClN_2O_4$ [M^- -H] requires (m/e) 369.0642, found 369.0721

41 *(E)-N'-(2-Methoxybenzylidene)-3-hydroxynaphthalene-2-carbohydrazide*

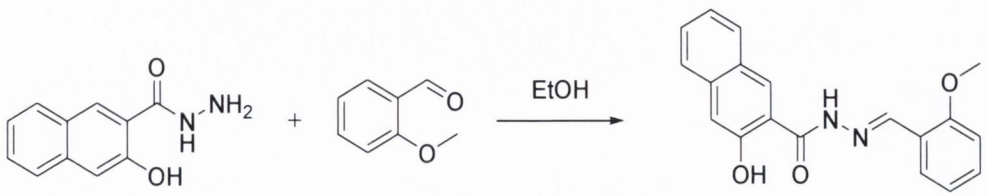

Yield: 1.95 g, 81 %, light beige powder (Recrystallisation, EtOH)

HPLC Purity: 96 % **MP:** 274-279°C **Lit. Ref**. [283]

IRϑ_{max} (KBr): 3436.28 (OH), 3356.73, 3239.62 (NH), 1639.92 (C=O), 1630.25 (C=C), 1619.29 (C=C), 1537.38 cm^{-1}

^{1}H NMR (400 MHz, DMSO-d6): δ ppm 3.89 (s, 3H, OCH_3), δ 7.04 (t, 1H, *J=7.52* Hz, Ar-H), δ 7.13 (d, 1H, *J=8.28* Hz, Ar-H), δ 7.33 (s, 1H, Ar-H), δ 7.36 - 7.40 (m, 1H, Ar-H), δ 7.44 - 7.49 (m, 1H, Ar-H), δ 7.50 - 7.59 (m, 1H, Ar-H), δ 7.77 (d, 1H, *J=8.28* Hz, Ar-H), δ 7.90 (m, 1H, Ar-H), δ 8.49 (s, 1H, Ar-H), δ 8.82 (s, 1H, Ar-H), δ 11.40 (s, 1H, CH), δ 12.07 (s (br), 1H, OH)

^{13}C NMR (400 MHz, DMSO-d6): δ ppm 56.20 (OCH_3), δ 111.08 (CH), δ 112.38 (CH), δ 120.20 (C), δ 121.28 (CH), δ 122.53 (CH), δ 124.27 (CH), δ 126.13 (CH), δ 126.34 (CH), δ 127.17 (CH), δ 128.75 (CH), δ 129.11 (CH), δ 130.34 (C), δ 132.35 (CH), δ 136.38 (C), δ 144.58 (C), δ 155.06 (C-O), δ 158.38 (C-O), δ 164.70 (C=O)

HRMS (ESI): $C_{19}H_{15}N_2O_3$ [M^- -H] requires (m/e) 319.1083, found 319.1087

42 *(E)-N'-(5-Bromo-2-methoxybenzylidene)-3-hydroxynaphthalene-2-carbohydrazide*

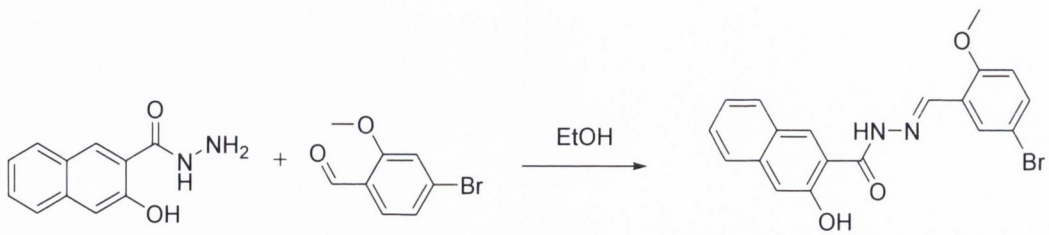

Yield: 2.48 g, 83 %, yellow powder (Recrystallisation, EtOH)

HPLC Purity: 94 % **MP:** 293-297°C **Lit. Ref.** [284]

IRϑ_{max} (KBr): 3582.59, 3452.61 (OH), 3368.82, 3175.84 (NH), 1690.83 (C=O), 1657.86 (C=C), 1654.69 (C=C), 1559.71 cm^{-1}

^{1}H NMR (400 MHz, DMSO-d6): δ ppm 3.89 (s, 3H, OCH_3), δ 7.12 (d, 1H, *J=9.04* Hz, Ar-H), δ 7.33 (s, 1H, Ar-H), δ 7.36 (d, 1H, *J=7* Hz, Ar-H), δ 7.50 – 7.56 (m, 1H, Ar-H), δ 7.60 (d, 1H, *J=2.52* Hz, Ar-H), δ 7.76 (d, 1H, *J=8.04* Hz, Ar-H), δ 7.90 (d, 1H, *J=8.04* Hz, Ar-H), 7.98 (d, 1H, *J=2.52* Hz, Ar-H), δ 8.46 (s, 1H, Ar-H), δ 8.73 (s, 1H, Ar-H), δ 11.29 (s (br), 1H, OH), δ 12.13 (s (br), 1H, NH)

^{13}C NMR (400 MHz, DMSO-d6): δ ppm 56.63 (CH_3), δ 111.06 (CH), δ 112.99 (C), δ 114.96 (CH), δ 120.47 (C), δ 124.28 (CH), δ 124.79 (CH), δ 126.34 (CH), δ 127.18 (CH), δ 128.04 (CH), δ 128.76 (CH), δ 129.11 (CH), δ 130.49 (C), δ 134.35 (C), δ 136.38 (CH), δ 142.74 (C), δ 154.81 (C-O), δ 157.49 (C-OCH_3), δ 164.69 (C=O)

HRMS (ESI): $C_{19}H_{14}{}^{79}BrN_2O_3$ [M^- -H] requires (m/e) 397.0188, found 397.0243

46 *(E)-N'-(1-(5-Chloro-2-hydroxyphenyl)ethylidene)-3-hydroxynaphthalene-2-carbohydrazide*

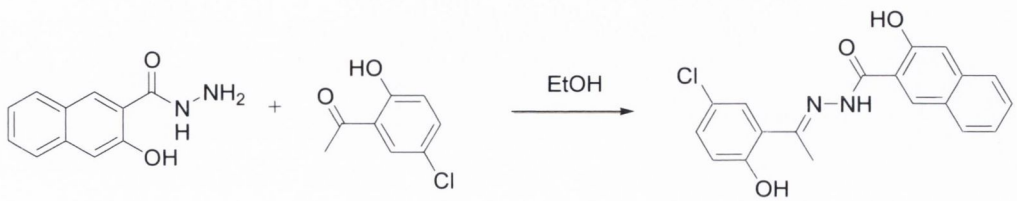

Yield: 1.22 g, 46 %, white powder (Recrystallisation, EtOH)

HPLC Purity: 86 % **MP:** 270-277°C **Lit. Ref.** [285]

IRϑ_{max} (KBr): 3552.91 (OH), 3481.21, 3278.17 (NH), 1674.27 (C=O), 1646.93 (C=C), 1622.59 (C=C), 1573.73 cm^{-1}

^{1}H NMR (400 MHz, DMSO-d6): δ ppm 2.48 (s, 3H, CH_3), δ 7.27 (s, 1H, Ar-H), δ 7.34 - 7.40 (m, 2H, Ar-H), δ 7.47 - 7.53 (m, 2H, Ar-H), δ 7.73 - 7.81 (m, 3H, Ar-H), δ 8.46 (s, 1H, Ar-H), δ 10.24 (s (br), 1H, OH), δ 11.90 (s (br), 1H, NH)

^{13}C NMR (400 MHz, DMSO-d6): δ ppm 13.89 (CH_3), δ 111.05 (CH), 118.52 (CH), δ 119.59 (C), δ 122.71 (CH), δ 124.09 (C), δ 124.41 (CH), δ 126.25 (C), δ 127.08 (CH), δ 128.56 (CH), δ 129.12 (CH), δ 129.46 (CH), δ 131.24 (C), δ 132.68 (CH), δ 136.28 (C), δ 153.32 (C-O), δ 155.47 (C-O), δ 157.85 (C=O), δ 167.46 (C)

HRMS (ESI): $C_{19}H_{14}{}^{35}ClN_2O_3$ [M^- -H] requires (m/e) 353.0693, found 353.0698

Theoretical Study. *Docking Studies of Structures* ***46, 27, 47, 28, 22 and 41***. Structure data was read from the PDB reference 1T73 containing the crystal structure of the androgen receptor ligand binding domain in complex with a FxxLF motif. Completion of missing atoms and preparation of the protein was performed with MOE, optimization of the hydrogen bond network and calculation of the charges was made by 'Protonate 3D' and 'Partial Charges' implemented in MOE using default parameters. Ligand conformations were generated with 'LowModeMD Search' method by MOE. The placement of the ligand within the site was guided by introducing three pharmacophoric constraints (aromatic/hydrophobic) into the three subpockets mimicking the protein:coactivator interaction. Docking was made by using the 'Induce Fit' protocol which includes protein sidechains in the refinement stage. Affinity DG function was used for scoring and AMBER 99 forcefield for the refinement of the poses.

Minimisation and MMPBSA Single Point Binding Energy of Structures ***46, 27, 47, 28, 22*** *and* ***41***. The docked poses were energy-minimized by using the AMBER software. The ff94SB and GAFF force fields were utilized for building the protein and the ligands, respectively. Systems were solvated adding a water explicit box of 12 Å around the centre. The minimizations were carried out in a multistep procedure restraining with a harmonic potential of force constant of 10, 5, 1 and 0.1 kcal/mol^2 Å^2, respectively. Finally, complexes were minimized without any restriction. MMPBSA approach was applied to minimized poses providing 'single point' binding energies (Poisson-Boltzmann, PB).

Molecular Dynamic Simulation and Energy Analysis of Compounds ***46, 27, 47, 28, 22 and 41***. After minimization, the selected complexes were gradually heated in the NVT ensemble (constant volume and temperature conditions) from 0 to 300K. Then, the systems were equilibrated for 50ps at a constant temperature of 300K by coupling the system to a thermal bath with Berendsen algorithm with a time coupling constant of 1ps, and a pressure of 1 atm (NPT). Then, the systems were simulated in the NVT ensemble for 40 ns. For the stable complexes, the last 5ns of production step were used for further energy analysis. Binding free energies were calculated using the molecular mechanics Poisson-Boltzmann surface area (MMPBSA) implemented in AMBER. Finally, Pairwise Free Energy Decomposition Analysis was performed to identify the key residues in the binding mode of our proposed most probable Bioactive Conformation.

6.0 Bibliography

1. Menendez, Carmen Avendano and J. Carlos, *Medicinal Chemistry of Anticancer Drugs*. Vol. 1. 2008: Elsevier Science. 400.
2. http://www.medicinenet.com/cancer/article (2012) *Warfarin therapy*.
3. Nelson, S. M. Ferguson, L. R.and Denny, W. A., *Cell Chromosome.* 3, 2004. **2**.
4. Bisell, M. J., and Radisky, D. , *Putting tumours in context.* Nat. Rev. Cancer, 2001. **1**(1): p. 46-54.
5. http://www.cancer.gov/cancerinfo/wyntk/breast (2012)
6. Bradbury, R. H. (ed), *Cancer.* Topics in Medicinal Chemistry, 2007. **1**(Springer-Verlag, Berlin Heidelberg).
7. Capdeville, R., Buchdunger, E., Zimmermann, J., and Matter, A., *STI571-Imatinib, a rationally developed targeted anticancer drug.* Nat. Rev. Drug Discovery, 2002. **1**(493-502).
8. Atkins, J. H., and Gershell, L. J., *A brief history of novel drug discovery technologies.* Nat Rev Drug Discov, 2003 **2**(4): p. 321-7.
9. Christoph C Lengauer, Luis A LA Diaz, and Saurabh S Saha, *Cancer drug discovery through collaboration.* Nat. Rev. Drug Discov., 2005. **4**(5): p. 375-80.
10. Toffoli, G., Cecchin, E., Corona, G., and Boiocchi, M., *Pharmacogenetics of irinotecan.* Curr. Med. Chem. Anti Cancer Agents, 2003. **3**(3): p. 225-37.
11. Torchilin, V. P., *Drug targeting.* European Journal of Pharmaceutical Sciences, 2000. **11**(2): p. S81–S91.
12. Society, American Cancer (2008) *Doxorubicin*. ACS.
13. Jain, R. K., *Cancer Metastasis Rev.* 1987. **6**: p. 559.
14. Gottesman, M. M. , Fojo, T. and Bates, S. E., *Multidrug resistance in cancer: role of ATP-dependent transporters.* Nat. Rev. Cancer, 2002. **2**(1): p. 48-58.
15. Nygren, P., and Larsson, R., *Overview of the clinical efficacy of investigational anticancer drugs.* J. Intern. Med., 2003. **253**(1): p. 46–75.
16. http://www.breastcancerireland.com/iopen24/the-facts-t-41.html (2012) *Breast cancer Ireland Facts*.
17. Jerzy E. Tyczynski, Freddie Bray, D. Maxwell Parkin, *Breast Cancer in Europe.* European Network of Cancer Registries International Agency for Research on Cancer ENCR Cancer Fact Sheets, 2002. **2**: p. 1-5.
18. McPherson K, Steel CM, Dixon JM, *Breast cancer - epidemiology,risk factors, and genetics.* BMJ, 2000. **321**(624): p. 8.
19. Brewster A, Helzlsouer K., *Breast cancer epidemiology, prevention, and early detection.* Current Opinion in Oncology, 2001. **13**(420): p. 25.
20. Vainio H, Bianchini F. (eds.), *Breast cancer screening.* IARC Handbooks of Cancer Prevention. IARCPress, Lyon, 2002.
21. (CGHFBC), Collaborative Group on Hormonal Factors in Breast Cancer, *Familial breast cancer: collaborative reanalysis of individual data from 52 epidemiological studies including 58209 women with breast cancer and 101986 women without the disease.* Lancet, 2001. **358**: p. 1389-99.
22. Emery J, Lucassen A, Murphy M., *Common hereditary cancers and implications for primary care.* Lancet, 2001. **358**: p. 56-63.
23. Heneghan H. M., P.R.S., Devaney A., Sweeney K., Malone C., McLaughlin R., Kerin M.J., *Evolution of breast cancer management in Ireland: A decade of change.* BMC Surgery, 2009. **9**(15).
24. Jennifer D Davis, S.-Y.L, *DNA damage and breast cancer.* World Journal of Clinical Oncology, 2011. **2**(9): p. 329-38.

25. http://www.webmd.com/breast-cancer/breast-cancer-types-er-positive-her2-positive (2012) *Types of Breast Cancer: ER Positive, HER2 Positive, and Triple Negative*. Breast Cancer Health Center.
26. Stephan, Pam (2011) *Paclitaxel (Taxol) - Chemotherapy Drug Profile*.
27. Institute, National Cancer (2013) *Cancer ER pos chemotherapy*. NCI
28. Institute, National Cancer (2008) *Methotrexate*. NCI
29. http://www.cancer.org/treatment/treatmentsandsideeffects/guidetocancerdrugs/methotrexate, FDA, ACS (2011) Methotrexate.
30. http://druginfosys.com/Drug.aspx?drugCode=315&DrugName=5-FU&type=1, (2012) 5-Fu. *Fluorouracil*.
31. Gemzar, *http://www.rxlist.com/gemzar-drug.htm.*
32. Orlando E. Silva, Stefano Zurrida, *Breast Cancer: a practical guide.* Elsevier Health Sciences, 2005.
33. K. David Voduc, Maggie C.U. Cheang, Scott Tyldesley, Karen Gelmon, Torsten O. Nielsen and, and Hagen Kennecke (2010) *Breast Cancer Subtypes and the Risk of Local and Regional Relapse*. American Society of Clinical Oncology
34. Roche (2010) *Herceptin*. Roche-Australia
35. Registry, National Cancer, *Age-standardised incidence rates, .* 2010.
36. (NCRI), National Cancer registry of Ireland (2011) *Cancer in Ireland 2011:*. Annual report of the National Cancer Registry
37. Casey Z, *EUI cancer-screening rates far off target, .* European Voice 22/1/2009.
38. Key T.J., V.P.K., Banks E., *Epidemiology of breast cancer. .* The Lancet, , 2001. **2** (Oncology): p. p. 132-140.
39. Del Re M, M.A., Simi P, Danesi R, *Pharmacogenetics of anti-estrogen treatment of breast cancer.* Cancer Treat. Rev, 2011
40. http://info.cancerresearchuk.org/cancerstats/types/breast/incidence/index.htm (2012) *Breast cancer, incidence*.
41. rates, Cancer survival (2013) *Cancer survival rates*.
42. Platet, Nadine, Anne Marie Cathiard, Michel Gleizes, and Marcel Garcia, *Estrogens and their receptors in breast cancer progression: a dual role in cancer proliferation and invasion.* Critical Reviews in Oncology/Hematology, 2004. **51**(1): p. 55-67.
43. Gust, Zhenlin Bai and Ronald, *Breast Cancer, Estrogen Receptor and Ligands.* Arch. Pharm. Chem. Life Sci., 2008. **342**: p. 133 - 149.
44. E. H. Kong, A. C. W. Pike, R. E. Hubbard, *Structure and mechanism of the oestrogen receptor.* Biochem. Soc. Trans., 2003. **31**: p. 56–59.
45. Edwards, D. P., *Regulation of signal transduction pathways by estrogen and progesterone.* Annu. Rev. Physiol., 2005. **67**: p. 335–376.
46. Yager, J. D., *Chapter 3: Endogenous Estrogens as Carcinogens Through Metabolic Activation.* J Natl Cancer Inst Monographs, 2000. **27**: p. 67–73.
47. R. X. Song, C. J. Barnes, Z.-G. Zhang, Y.-D. Bao, et al, *Proc. Natl. Acad. Sci. U.S.A.* 2004(101,): p. 2076–2081.
48. R. K. Dubey, E. K. Jackson, *J. Appl. Physiol.* 2001. **91**: p. 1868–1883.
49. Dr. U. R. Desai, *Estrogens.* Advanced Medicinal Chemistry, 2006.
50. H. P. Rang, M.M.D., *Rang and Dale's Pharmacology.* Churchill Livingstone. 2007: Elsevier. 829.
51. Lewis, J.S., Jordan V.C., *Selective estrogen receptor modulators (SERMs): mechanisms of anticarcinogenesis and drug resistance.* Mutation Research 2005(591): p. p. 247-263.
52. Nilsson, S., Koehler, K.F., Gustafsson, J., *Development of Subtype-selective Oestrogen receptor-based therapeutics.* Nature Reviews,, 2011. **10**(drug discovery): p. p. 778-792.

53. Pearce, Sandra Timm and V. Craig Jordan, *The biological role of estrogen receptors [alpha] and [beta] in cancer.* Critical Reviews in Oncology/Hematology, 2004. **50**(1): p. 3-22.
54. Monica Morrow, and V. Craig Jordan, *Tamoxifen, Raloxifene, and the Prevention of Breast Cancer*.* The Endocrine Society, Endocrine Reviews, 1999. **20**(3): p. 253–278.
55. Jordan, Woo-Chan Park and V. Craig, *Selective estrogen receptor modulators (SERMS).* Trends in Molecular Medicine, 2002. **8**(2): p. 82-88.
56. Watts, C. K. W. and Sutherland , R. L. , *Mol. Pharmacol.* 1987. **31**: p. 541.
57. C. Kent Osborne, M.D., *Tamoxifen in the Treatment of Breast Cancer.* Drug Therapy, 1998. **339**: p. 1609-1618
58. Young Chai Lim1, 2 Contact Information, Zeruesenay Desta1, David A. Flockhart1 and Todd C. Skaar, *Endoxifen (4-hydroxy-N-desmethyl-tamoxifen) has anti-estrogenic effects in breast cancer cells with potency similar to 4-hydroxy-tamoxifen Journal Cancer Chemotherapy and Pharmacology.* Cancer Chemotherapy and Pharmacology, 2004. **55**: p. 471-478.
59. N. Keely Ph.D., H.Dip.Sys.Analysis, Prof. M.J.Meegan Ph. D. M.R.S.C., C. Chem, *Design, synthesis and biochemistry of duai acting estrogen receptor conjugates – synthesis and antiestrogenic effects in human breast cancer cells.* Transfer School of Pharmacy and Pharmaceutical Sciences, Trinity College Dublin, 2007: p. 4.
60. Yu FL, et al.:, *A hypothesis on breast cancer.* The 22nd Congress of International Association for Breast Cancer Research, 2001.
61. Yu. F; and W, Bender., *The mechanism of tamoxifen in breast cancer prevention.* Breast Cancer Res., 2001. **3**(1).
62. Phillips DH, et al.:, *Carcinogenesis. 1994.* Düsseldorf, Germany, 13-16 June 2001. **15**: p. 793-795.
63. http://www.memidex.com/warfarin (2012) *Warfarin*.
64. Kufe DW, Pollock RE, Weichselbaum RR, et al., *Holland-Frei Cancer Medicine. 6th edition.* Hamilton (ON):, 2003: p. 2003.
65. Knabbe C, Lippman ME, Wakefield LM. et al, *Evidence that TGF-β is a hormonally regulated negative growth factor in human breast cancer cells.* Cell, 1987(48): p. 417–28.
66. Colletta AA, Wakefield LM, Howell LM. et al, *Antioestrogens induce the secretion of active TGF-β from human fetal fibroblasts.* Br J Cancer., 1990. **62**: p. 405–9.
67. Butta A, MacLennan K, Flanders KC. et al, *Induction of transforming growth factor β1 in human breast cancer in vivo following tamoxifen treatment.* Cancer Res, 1992. **52**: p. 4261–4.
68. Organization., Nolvadex Adjuvant Trial, *Controlled trial of tamoxifen as a single adjuvant agent in the management of early breast cancer.* Br J Cancer., 1988. **57**: p. 608–11.
69. Colletti RB, Roberts JD, Devlin JT, Copeland KC, *Effect of tamoxifen on plasma insulin-like growth factor I in patients with breast cancer.* Cancer Res., 1989. **49**: p. 1882–4.
70. Pollak MJ, Costantino C, Polychronakos SA. et al, *Effect of tamoxifen on serum insulin-like growth factor I levels in stage I breast cancer patients.* J Natl Cancer Inst. , 1990;(82:): p. 1693–7.
71. Jordan , V. C., *Tamoxifen: a most unlikely pioneering medicine.* Nat. Rev. Drug Discovery 2003. **2**(3): p. 205-13.
72. De. Medina, P., Favre, G., and Poirot, M. , *Multiple targeting by the antitumor drug tamoxifen.* Curr. Med. Chem. Anticancer Agents, 2004. **4**: p. 491-508.

73. Warri, 29. A.M., *Apoptosis in Tormifene Induced Growth Inhibition of human breast cancer cells In Vivo and In Vitro.* JNCI J Natl Cancer Inst, 1993. **85**(17): p. 1412-1418.
74. S.E., M.D.P.a.W., *The molecular mechanisms underlying the pharmacological actions of ER modulators: implications for new drug discovery in breast cancer.* Current Opinion in Pharmacology, 2010. **10:**(10): p. p. 620–628.
75. NCI (2011) *Study of Tamoxifen and Raloxifene (STAR) Trial*. National Surgical Adjuvant Breast and Bowel Project
76. Munster, Pamela N, *Arzoxifene: the development and clinical outcome of an ideal SERM.* Expert Opinion on Investigational Drugs, 2005. **15**(3): p. 317-326.
77. R. W. Downs Jr., A. M. Moffett, A. Ghosh, D. A. Cox, S. A. Dowsett and K. Harper, *Effects of Arzoxifene on bone, lipid markers, and safety parameters in postmenopausal women with low bone mass.* Osteoporosis International, 2009.
78. M. Carr. Ph.D., Prof. Mary J. Meegan Ph. D. M.R.S.C., C. Chem, *Development of the β-Lactam Structure as a scaffold for Biologicall Active Compounds.* School of Pharmacy, Trinity College Dublin, 2006. **1**: p. 17-20.
79. Poletti, Angelo, *Editorial: Searching for the Ideal SERM.* Pharmacological Research, 1999. **39**(5): p. 333.
80. Jr, Goldstein SR; Siddhanti S; Ciaccia AV; Plouffe L, *A pharmacological review of selective oestrogen receptor modulators.* Human reproduction update, 2000. **6**(3): p. 212-224.
81. McDonnell, Donald P. and Suzanne E. Wardell, *The molecular mechanisms underlying the pharmacological actions of ER modulators: implications for new drug discovery in breast cancer.* Current Opinion in Pharmacology, 2010. **10**(6): p. 620-628.
82. Rejnmark, L. and L. Mosekilde, *New and emerging antiresorptive treatments in osteoporosis.* Curr Drug Saf., 2011. **6**(2): p. 75-88.
83. Grubjesic, S., Moriarty, R.. M. and Pezzuto, J. M., *Medicinal chemistry of anticancer drugs.* Expert Opin. Ther. pat., 2002. **12**: p. 1647.
84. Li, P. K. and R. W. Brueggemeier, *7-substituted steroidal aromatase inhibitors: structure-activity relationships and molecular modeling.* J Enzyme Inhib., 1990. **4**(2): p. 113-20.
85. http://www.cancerresearchuk.org/cancer-help/about-cancer/treatment/cancer-drugs/exemestane (2012) *Exemestane (Aromasin)*.
86. R. Charles Coombes, M.D., Ph.D., Emma Hall, Ph.D., Lorna J. Gibson, M.Phil., Robert Paridaens, M.D., Ph.D.,, M.D. Jacek Jassem, Ph.D., Thierry Delozier, M.D., Stephen E. Jones, M.D., Isabel Alvarez, M.D.,, M.D. Gianfilippo Bertelli, Olaf Ortmann, M.D., Ph.D., Alan S. Coates, M.D., Emilio Bajetta, M.D., David Dodwell, M.D.,, M.D. Robert E. Coleman, Lesley J. Fallowfield, D.Phil., Elizabeth Mickiewicz, M.D., Jorn Andersen, D.M.Sc.,, M.D. Per E. Lønning, Ph.D., Giorgio Cocconi, M.D., Ph.D., Alan Stewart, M.D., Nick Stuart, D.M.,, M.Sc. Claire F. Snowdon, Marina Carpentieri, Ph.D., Giorgio Massimini, M.D., and Judith M. Bliss, M.Sc.,, and for the Intergroup Exemestane Study, *A Randomized Trial of Exemestane after Two to Three Years of Tamoxifen Therapy in Postmenopausal Women with Primary Breast Cancer.* The new england journal of medicine, 2004. **350**(11).
87. Coombes RC, Kilburn LS, Snowdon CF, Paridaens R, Coleman RE, Jones SE, Jassem J, Van de Velde CJ, Delozier T, Alvarez I, Del Mastro L, Ortmann O, Diedrich K, Coates AS, Bajetta E, Holmberg SB, Dodwell D, Mickiewicz E, Andersen J, Lønning PE, Cocconi G, Forbes J, Castiglione M, Stuart N, Stewart A, Fallowfield LJ, Bertelli G, Hall E, Bogle RG, Carpentieri M, Colajori E, Subar M, Ireland E, Bliss JM; Intergroup Exemestane Study., *Survival and safety of exemestane versus tamoxifen after 2-3 years' tamoxifen treatment (Intergroup*

Exemestane Study): a randomised controlled trial. Lancet. , 2007 Feb 17;. **369**((9561):): p. 559-70.

88. Bliss JM, Kilburn LS, Coleman RE, Forbes JF, Coates AS, Jones SE, Jassem J, Delozier T, Andersen J, Paridaens R, van de Velde CJ, Lønning PE, Morden J, Reise J, Cisar L, Menschik T, Coombes RC., *Disease-related outcomes with long-term follow-up: an updated analysis of the intergroup exemestane study.* J Clin Oncol. , 2012. **30**(7): p. 709-17. .
89. http://www.ceri.com/q_v7n2q3.htm
90. Jordan, V. C., *Chemoprevention of breast cancer with selective oestrogen-receptor modulators.* Nat Rev Cancer., 2007. **1**: p. 46-53.
91. Shaun R. Stauffera, Ying R. Huanga, Zachary D. Arona, Christopher J. Colettaa, Jun Sunb, Benita S. Katzenellenbogenb, c and John A. Katzenellenbogen, *Triarylpyrazoles with basic side chains: development of pyrazole-based estrogen receptor antagonists.* Bioorganic & Medicinal Chemistry, 2000. **9**(1): p. 151-161.
92. Lina K. Mehta, John Parrick, *The synthesis of three indolizine derivatives of interest as non-isomerizable analogues of tamoxifen.* Journal of Heterocyclic chemistry, 1994. **32**(2): p. 391-394.
93. Edmond Abrahamian, Peter C. Fox, Lars Nærum, Inge Thøger Christensen, Henning Thøgersen,and Robert D. Clark, *Efficient Generation, Storage, and Manipulation of Fully Flexible Pharmacophore Multiplets and Their Use in 3-D Similarity Searching.* J. Chem. Inf. Comput. Sci., 2003. **43**(2): p. 458–468.
94. Areias, Filipe, Marta Costa, Marian Castro, Jose Brea, Elisabet Gregori-Puigjane, M. Fernanda Proenca, Jordi Mestres, and Maria I. Loza, *New chromene scaffolds for adenosine A2A receptors: Synthesis, pharmacology and structure activity relationships.* European Journal of Medicinal Chemistry, 2012. **54**: p. 303-310.
95. Natsuki Ishizuka, * Ken-ichi Matsumura, Junko Kikuchi and Hiroshi Nakai, *A Novel Class of Endothelin-A Receptor Antagonists, (R)-2-(benzo[1,3]dioxol-5-yl)-6-isopropyloxy-2H-chromene-3-carboxylic Acids (S-1255). Conformational Analysis of Basic Structure, Crucial for ETA Antagonism, in Solution and Solid States.* Bioorganic & Medicinal Chemistry, 2002. **10**: p. 3965–3972.
96. Irini Akritopoulou-Zanze, Jyoti R. Patel, Kresna Hartandi, Jehrod Brenneman, Martin Winn, John K. Pratt, Marlene Grynfarb, Annika Goos-Nisson, Thomas W. von Gelderna and Philip R. Kyma, *Synthesis and biological evaluation of novel, selective, nonsteroidal glucocorticoid receptor antagonists.* Bioorganic & Medicinal Chemistry Letters, 2004. **14**: p. 2079–2082.
97. Tuncbilek, Meral, Saheyla Ozbey, Engin Kendi, Engin Yildirim, Kevser Erol, and Rahmiye Ertan, *Synthesis and X-ray crystal structure of the calcium channel antagonist: dimethyl 1,4-dihydro-2,6-dimethyl-4-[4'-(4H-4-oxo-1-benzopyran-2-yl)phenyl]-3,5-pyridine dicarboxylate.* Il Farmaco, 1999. **54**(10): p. 660-665.
98. Dandu, Reddeppa Reddy, Jacquelyn A. Lyons, Rita Raddatz, Zeqi Huang, Lisa D. Aimone, and Robert L. Hudkins, *Synthesis and evaluation of a new series of 1-cyclobutyl-6-(4-piperidyloxy)spiro[benzopyran-2,4-piperidine] derivatives as high affinity and selective histamine-3 receptor (H3R) antagonists.* Bioorganic & Medicinal Chemistry Letters, 2012. **22**(6): p. 2151-2153.
99. Farag, Nahla A., Shadia R. Mohamed, and Gamal A. H. Soliman, *Design, synthesis, and docking studies of novel benzopyrone derivatives as H1-antihistaminic agents.* Bioorganic & Medicinal Chemistry, 2008. **16**(19): p. 9009-9017.
100. Behrenswerth, Andrea, Nicole Volz, Jakob Torang, Sonja Hinz, Stefan Brase, and Christa E. Muller, *Synthesis and pharmacological evaluation of coumarin derivatives as cannabinoid receptor antagonists and inverse agonists.* Bioorganic & Medicinal Chemistry, 2009. **17**(7): p. 2842-2851.

101. Anderson, David R., Shridhar Hegde, Emily Reinhard, Leslie Gomez, William F. Vernier, Len Lee, Shuang Liu, Aruna Sambandam, Patricia A. Snider, and Liaqat Masih, *Aminocyanopyridine inhibitors of mitogen activated protein kinase-activated protein kinase 2 (MK-2).* Bioorganic & Medicinal Chemistry Letters, 2005. **15**(6): p. 1587-1590.
102. Leclercq, Guy and Yves Jacquot, *Interactions of isoflavones and other plant derived estrogens with estrogen receptors for prevention and treatment of breast cancer- Considerations concerning related efficacy and safety.* The Journal of Steroid Biochemistry and Molecular Biology, 2012(0).
103. Dhingra, K., *Antiestrogens - Tamoxifen, SERMs and beyond.* Invest New Drugs., 1999. **17**((3)): p. 285-311.
104. Sun, Wanying, Lovji D. Cama, Elizabeth T. Birzin, Sudha Warrier, Louis Locco, Ralph Mosley, Milton L. Hammond, and Susan P. Rohrer, *6H-Benzo[c]chromen-6-one derivatives as selective ER beta agonists.* Bioorganic & Medicinal Chemistry Letters, 2006. **16**(6): p. 1468-1472.
105. Al-Azzawi, AH Taylor and F, *Immunolocalisation of oestrogen receptor beta in human tissues.* J Mol Endocrinol, 2000 **24**: p. 145-155.
106. Andrzej M. Brzozowski, Ashley C. W. Pike, Zbigniew Dauter, Roderick E. Hubbard, Tomas Bonn, Owe Engström, Lars Öhman, Geoffrey L. Greene, Jan-Åke Gustafsson and Mats Carlquist, *Molecular basis of agonism and antagonism in the oestrogen receptor.* Nature, 1997. **389**: p. 753-758.
107. Chen, Ningyi, Nareshkumar Jain, Jiayi Xu, Michael Reuman, Xun Li, Ronald K. Russell, and Zhihua Sui, *Synthesis of novel tetracyclic chromenes through carbanion chemistry of 4-methyl coumarins.* Tetrahedron Letters, 2006. **47**(33): p. 5909-5913.
108. Lise B. Christiansen, Martin Wenckens, Paul S. Bury, Birgitte Gissel, Birgit S. Hansen, Susan M. Thorpe, Poul Jacobsen, Anders Kanstrup, Anker S. Jørgensen, Lars Nærum and Karsten Wassermann, *Synthesis and biological evaluation of novel thio-substituted chromanes as high-affinity partial agonists for the estrogen receptor.* Health Care Discovery & Preclinical Development, 2001.
109. Richardson, Timothy I., Jeffrey A. Dodge, Gregory L. Durst, Lance A. Pfeifer, Jikesh Shah, Yong Wang, Jim D. Durbin, Venkatesh Krishnan, and Bryan H. Norman, *Benzopyrans as selective estrogen receptor beta agonists (SERBAs). Part 3: Synthesis of cyclopentanone and cyclohexanone intermediates for C-ring modification.* Bioorganic & Medicinal Chemistry Letters, 2007. **17**(17): p. 4824-4828.
110. D.A. Egan, D. Cox, R. O'Kennedy, E. Moran, E. Prosser and R.D. Thornes, *The pharmacology, metabolism, analysis, and applications of coumarin and coumarin-related compounds.* Drugs Metab. Rev, 1990. **22**(5): p. 503-29.
111. G.R. Madhavan, V. Balraju, B. Mallesham, R. Chakrabarti and V.B. Lohray, *Novel coumarin derivatives of heterocyclic compounds as lipid-lowering agents.* Bioorg Med Chem Lett., 2003. **13**(15): p. 2547-51.
112. Paya, Miguel, Barry Halliwell, and J. R. S. Hoult, *Interactions of a series of coumarins with reactive oxygen species: Scavenging of superoxide, hypochlorous acid and hydroxyl radicals.* Biochemical Pharmacology, 1992. **44**(2): p. 205-214.
113. Reddy, Natala Srinivasa, Kiranmai Gumireddy, Muralidhar R. Mallireddigari, Stephen C. Cosenza, Padmavathi Venkatapuram, Stanley C. Bell, E. Premkumar Reddy, and M. V. Ramana Reddy, *Novel coumarin-3-(N-aryl)carboxamides arrest breast cancer cell growth by inhibiting ErbB-2 and ERK1.* Bioorganic & Medicinal Chemistry, 2005. **13**(9): p. 3141-3147.

114. Hiroshi Morita, Tomoka Dota and Jun'ichi Kobayashi, *Antimitotic activity of glaupalol-related coumarins from Glaucidium palmatum.* Bioorganic & Medicinal Chemistry Letters, 2004. **14**: p. 3665–3668.
115. N.S. Reddy, M.R. Mallireddigari, S. Cosenza, K. Gumireddy, S.C. Bell, E.P. Reddy and M.V.R. Reddy, *Synthesis of new coumarin 3-(N-aryl) sulfonamides and their anticancer activity.* Bioorg. Med. Chem. Lett, 2004. **4**(15): p. 4093-7.
116. Kemnitzer, William, Shailaja Kasibhatla, Songchun Jiang, Hong Zhang, Jianghong Zhao, Shaojuan Jia, Lifen Xu, Candace Crogan-Grundy, Réal Denis, Nancy Barriault, Louis Vaillancourt, Sylvie Charron, Jennifer Dodd, Giorgio Attardo, Denis Labrecque, Serge Lamothe, Henriette Gourdeau, Ben Tseng, John Drewe, and Sui Xiong Cai, *Discovery of 4-aryl-4H-chromenes as a new series of apoptosis inducers using a cell- and caspase-based high-throughput screening assay. 2. Structure-activity relationships of the 7- and 5-, 6-, 8-positions.* Bioorganic & Medicinal Chemistry Letters, 2005. **15**(21): p. 4745-4751.
117. Kasibhatla, S., H. Gourdeau, K. Meerovitch, J. Drewe, S. Reddy, L. Qiu, H. Zhang, F. Bergeron, D. Bouffard, Q. Yang, J. Herich, S. Lamothe, S. X. Cai, and B. Tseng, *Discovery and mechanism of action of a novel series of apoptosis inducers with potential vascular targeting activity.* Molecular Cancer Therapeutics, 2004. **3**(11): p. 1365-1373.
118. Das, Sonia G., Balasubramanian Srinivasan, David L. Hermanson, Nicholas P. Bleeker, Jignesh M. Doshi, Ruoping Tang, William T. Beck, and Chengguo Xing, *Structure Activity Relationship and Molecular Mechanisms of Ethyl 2-Amino-6-(3,5-dimethoxyphenyl)-4-(2-ethoxy-2-oxoethyl)-4H-chromene-3-carboxylate (CXL017) and Its Analogues.* Journal of Medicinal Chemistry, 2012. **54**(16): p. 5937-5948.
119. Ferlay, Jacques, Hai-Rim Shin, Freddie Bray, David Forman, Colin Mathers, and Donald Maxwell Parkin, *Estimates of worldwide burden of cancer in 2008: GLOBOCAN 2008.* International Journal of Cancer. **127**(12): p. 2893-2917.
120. Weinmann, Eckhard Ottow and Hilmar, *Nuclear Receptors as Drug Targets*. Methods and Principles in Medicinal Chemistry, ed. H.K. Raimund Mannhold, Gerd Folkers. Vol. 39. 2008: Wiley-VCH. p255.
121. Caboni, Laura; Kinsella, Gemma.; Blanco, Fernando; Fayne, Darren; Jagoe, William N.; Carr, Miriam; Williams, D. Clive; Meegan, Mary J.; Lloyd, David G, *"True" Antiandrogens-Selective Non-Ligand-Binding Pocket Disruptors of Androgen Receptor-Coactivator Interactions: Novel Tools for Prostate Cancer.* J. Med. Chem., 2012. **55**(4): p. 1635−1644.
122. Jung, M. E.; Ouk, S.; Yoo, D.; Sawyers, C. L.; Chen, C.; Tran, C.; Wongvipat, J. , *Structure-activity relationship for thiohydantoin androgen receptor antagonists for castration-resistant prostate cancer (CRPC).* J Med Chem, 2010. **53**: p. 2779-2796.
123. Xu L, Glass CK, Rosenfeld MG., *Coactivator and corepressor complexes in nuclear receptor function.* Curr Opin Genet Dev. , 1999 Apr;. **9**(2): p. 140-7.
124. Joseph B, Wallén-Mackenzie A, Benoit G, Murata T, Joodmardi E, Okret S, Perlmann T., *p57(Kip2) cooperates with Nurr1 in developing dopamine cells.* Proc Natl Acad Sci U S A. , 2003. **100**(26): p. 15619-24. .
125. Shiau AK, Barstad D, Loria PM, Cheng L, Kushner PJ, Agard DA, Greene GL., *The structural basis of estrogen receptor/coactivator recognition and the antagonism of this interaction by tamoxifen.* Cell. , 1998. **95**(7): p. 927-37.
126. Baker KD, Shewchuk LM, Kozlova T, Makishima M, Hassell A, Wisely B, Caravella JA, Lambert MH, Reinking JL, Krause H, Thummel CS, Willson TM, Mangelsdorf DJ., *The Drosophila orphan nuclear receptor DHR38 mediates an atypical ecdysteroid signaling pathway.* Cell. , 2003. **113**(6): p. 731-42.

127. Pfizer, Inc., US, *004367*. 2005.
128. Pfizer, Inc., US, *072043*. 2004.
129. Pfizer, Inc., US, *137228*. 2005.
130. Merck and Co. Inc., *US 7,196,076*.
131. Coleman, Paul, J.; and Lou Anne; Neilson, *ANDROGEN RECEPTOR MODULATORS AND METHODS OF USE THEREOF*, in *Nuclear receptors as drug targets, Eckhard Ottow and Hilmar Weinmann*, M.a.C. Inc., Editor. 2003: USA.
132. Lonard, D. M., O'Malley, B. W., *The expanding cosmos of nuclear receptor coactivators.* Cell., 2006 **125**(3): p. 411-4.
133. Tran, C.; Ouk, S.; Clegg, N. J.; Chen, Y.; Watson, P. A.; Arora, V.; Wongvipat, J.; Smith-Jones, P. M.; Yoo, D.; Kwon, A.; Wasielewska, T.; Welsbie, D.; Chen, C. D.; Higano, C. S.; Beer, T. M.; Hung, D. T.; Scher, H. I.; Jung, M. E.; Sawyers, C. L. , *Development of a second-generation antiandrogen for treatment of advanced prostate cancer.* . Science, 2009. **324**: p. 787-790.
134. Taplin, M. E.; Balk, S. P., *Androgen receptor: a key molecule in the progression of prostate cancer to hormone independence.* J Cell Biochem., 2004. **91**: p. 483-490.
135. Gregory CW, He B, Johnson RT, Ford OH, Mohler JL, French FS, Wilson EM, *A mechanism for androgen receptor-mediated prostate cancer recurrence after androgen deprivation therapy.* Cancer Res., 2001 **61**(11): p. 4315-9.
136. Folkertsma S, van Noort PI, Brandt RF, et al. , *The nuclear receptor ligand-binding domain: a family-based structure analysis.* Curr Med Chem., 2005. **12**(19): p. 1001-16.
137. Spellmeyer, D. C., Blaney, J . M. and Martin, E., *Computational approaches to chemical libraries.* Computer-assisted Molecular Modeling in Molecular Pharmacology, 1997.
138. Lyne, PD., *Structure-based virtual screening: an overview.* Drug Discov. Today, 2002. **7**: p. 1047-55.
139. Andrew J. S. Knox, Mary J. Meegan, Vladimir Sobolev, Dermot Frost, Daniela M. Zisterer, D. Clive Williams, and and David G. Lloyd, *Target Specific Virtual Screening: Optimization of an Estrogen Receptor Screening Platform.* J. Med. Chem, 2007. **50**: p. 5301-5310.
140. V. C. Jordan, *Antiestrogens and selective estrogen receptor modulators as multifunctional medicines.* Journal of medicinal chemistry 2003. **46**: p. 883-908.
141. C. Freddie, S. S. Larsen, M. Bartholomaeussen, A. Lykkesfeldt, *The effect of the new SERM Arzoxifene on growth and gene expression in MCF-7 breast cancer cells.* Molecular and Cellular Endocrinology, 2004. **219**(1-2): p. 27-36.
142. Daniel Lednicer, Lester A. Mitscher, *Organic Chemistry of Drug Synthesis*. Organic Chemistry of Drug Synthesis, ed. D. Lednicer. Vol. 1 - 7. 1985: Wiley-Interscience.
143. van Otterlo, Willem A. L., E. Lindani Ngidi, Samuel Kuzvidza, Garreth L. Morgans, Simon S. Moleele, and Charles B. de Koning, *Ring-closing metathesis for the synthesis of 2H- and 4H-chromenes.* Tetrahedron, 2005. **61**(42): p. 9996-10006.
144. Kazemi, Bagher, Shahrzad Javanshir, Ali Maleki, Mostafa Safari, and Hamid Reza Khavasi, *An efficient synthesis of 4H-chromene, 4H-pyran, and oxepine derivatives via one-pot three-component tandem reactions.* Tetrahedron Letters, 2012. **53**(51): p. 6977-6981.
145. Fernand Labrie, Pierre Champagne, Claude Labrie, Jean Roy, Jacques Laverdière, Louise Provencher, Martin Potvin, Yvan Drolet, Michael Pollak, Lawrence Panasci, Bernard L'Espérance, Jean Dufresne, Jean Latreille, Jean Robert, Benoit Samson, Jacques Jolivet, Louise Yelle, Lionel Cusan, Pierre

Diamond, and Bernard Candas, *Activity and Safety of the Antiestrogen EM-800, the Orally Active Precursor of Acolbifene, in Tamoxifen- Resistant Breast Cancer.* Journal of Clinical Oncology, 2004. **22**(5).

146. Gauthier, S., J. Cloutier, Y. L. Dory, A. Favre, J. Mailhot, C. Ouellet, A. Schwerdtfeger, Y. Merand, C. Martel, J. Simard, and F. Labrie, *Synthesis and structure-activity relationships of analogs of EM-652 (Acolbifene), a pure selective estrogen receptor modulator. Study of nitrogen substitution.* J Enzyme Inhib Med Chem, 2005. **20**(2): p. 165-77.
147. Lawrence, Nicholas J., Lucy A. Hepworth, David Rennison, Alan T. McGown, and John A. Hadfield, *Synthesis and anticancer activity of fluorinated analogues of combretastatin A-4.* Journal of Fluorine Chemistry, 2003. **123**(1): p. 101-108.
148. O'Kennedy, Aoife Lacy and Richard, *Studies on Coumarins and Coumarin-Related Compounds to Determine their Therapeutic Role in the Treatment of Cancer.* Current Pharmaceutical Design, 2004. **10**: p. 3797-3811.
149. Winuthayanon, W., P. Piyachaturawat, A. Suksamrarn, M. Ponglikitmongkol, Y. Arao, S. C. Hewitt, and K. S. Korach, *Diarylheptanoid phytoestrogens isolated from the medicinal plant Curcuma comosa: biologic actions in vitro and in vivo indicate estrogen receptor-dependent mechanisms.* Environ Health Perspect, 2009. **117**(7): p. 1155-61.
150. http://www.organic-chemistry.org/namedreactions/pechmann-condensation.shtm, (accessed 2012), *Pechmann condensation*. Organic chemistry portal
151. Bakhchinian, R., F. Terrier, S. Kirkiacharian, M. Resche-Rigon, F. Bouchoux, and E. Cerede, *Synthesis and relative binding affinity to human steroid receptors of substituted 3-aryloxycoumarins.* Farmaco, 2003. **58**(11): p. 1201-7.
152. Yang, Hua-Meng, Li Li, Ke-Zhi Jiang, Jian-Xiong Jiang, Guo-Qiao Lai, and Li-Wen Xu, *Highly enantioselective synthesis of warfarin and its analogs by means of cooperative LiClO4/DPEN-catalyzed Michael reaction: enantioselectivity enhancement and mechanism.* Tetrahedron, 2010. **66**(51): p. 9708-9713.
153. Ogliarolo, A., *Synthesis of phenylcoumarins.* Gazz. Chim. Ital., 1878. **9**: p. 428–432.
154. Kirkiacharian, Serge, Anh Tuan Lormier, Henri Chidiack, Francoise Bouchoux, and Evelyne Cerede, *Synthesis and binding affinity to human α and β estrogen receptors of various 7-hydroxycoumarins substituted at 4- and 3,4- positions.* Il Farmaco, 2004. **59**(12): p. 981-986.
155. Al-Maharik, Nawaf and Nigel P. Botting, *A new short synthesis of coumestrol and its application for the synthesis of [6,6a,11a-13C3]coumestrol.* Tetrahedron, 2004. **60**(7): p. 1637-1642.
156. Bhonoah, Yunas (1996) *Warfarin Synthesis*. Imperial College London
157. Theophil Eicher, Seigfried Hauptmann, *The Chemistry of Heterocycles.* WILEY-vch, 2003: p. 248 - 249.
158. Leeson, Paul (26 January 2012) *Drug discovery: Chemical beauty contest*. The Lipinski rule of five, 455–456 DOI: 10.1038/481455a
159. Sabbaghan, M. and Z. Hossaini, *A highly efficient green synthesis of N-alkyl 2-[(2-oxo-2-aryl ethyl) amino] benzamide derivatives from reaction of isatoic anhydride, primary amines and 2-bromoacethophenone.* Comb Chem High Throughput Screen, 2012. **15**(9): p. 745-8.
160. Wang, Jane L., David Limburg, Matthew J. Graneto, John Springer, Joseph Rogier Bruce Hamper, Subo Liao, Jennifer L. Pawlitz, Ravi G. Kurumbail, Timothy Maziasz, John J. Talley, James R. Kiefer, and Jeffery Carter, *The novel benzopyran class of selective cyclooxygenase-2 inhibitors. Part 2: The second clinical candidate having a shorter and favorable human half-life.* Bioorganic & Medicinal Chemistry Letters, 2010. **20**(23): p. 7159-7163.

161. ATCC (2012) *Cell Biology mammary gland; Breast Disease: adenocarcinoma*. MCF7 (ATCC® HTB-22™)
162. ATCC (2012) *Metastatic prostate carcinoma LNCaP clone FGC (ATCC® CRL-1740™)* LNCaP; ATCC
163. Anoopkumar-Dukie S, Carey JB, Conere T, O'Sullivan E, van Pelt FN, Allshire A., *Resazurin assay of radiation response in cultured cells.* Br J Radiol., 2005. **78**(934): p. 945-7.
164. O'Brien J, Wilson I, Orton T, Pognan F., *Investigation of the Alamar Blue (resazurin) fluorescent dye for the assessment of mammalian cell cytotoxicity.* Eur J Biochem., 2000. **267**(17): p. 5421-6.
165. Lee, J Cai and C W, *Tamoxifen inhibits nitrobenzylthioinosine-sensitive equilibrative uridine transport in human MCF-7 breast cancer cells.* Biochem J., 1996. **320**(3): p. 991–995.
166. Bank, RCSB Protein Data, *Human Estrogen Receptor Alpha Ligand-Binding Domain Compley with 4-Hydroxytamoxifen*, in PDB. 1998.
167. Brzozowski, A. M., A. C. Pike, Z. Dauter, R. E. Hubbard, T. Bonn, O. Engstrom, L. Ohman, G. L. Greene, J. A. Gustafsson, and M. Carlquist, *Molecular basis of agonism and antagonism in the oestrogen receptor.* Nature, 1997. **389**(6652): p. 753-8.
168. Bank, RCSB Protein Data, *Human Estrogen Receptor Alpha Ligand-Binding Domain Compley with Raloxifene.* PDB, 1997.
169. Olympus (2012) *TR-FRET Introductory Concepts*. Microscopy resource centre
170. assays, CISBIO (2012) *TR-Fret Basics*. htrf.com
171. Yeh, S.; Lin, H. K.; Kang, H. Y.; Thin, T. H.; Lin, M. F.; Chang, C., *HER2/Neu signal cascade to androgen receptor and its coactivators: a novel pathway by induction of androgen 270 target genes through MAP kinase in prostate cancer cells.* Proc Natl Acad Sci U S A, 1999. **96**.
172. Simeonov, A., A. Jadhav, C. J. Thomas, Y. Wang, R. Huang, N. T. Southall, P. Shinn, J. Smith, C. P. Austin, D. S. Auld, and J. Inglese, *Fluorescence spectroscopic profiling of compound libraries.* J. Med. Chem., 2008. **51**(8): p. 2363-71.
173. Thorne, N., D. S. Auld, and J. Inglese, *Apparent activity in high-throughput screening: origins of compound-dependent assay interference.* Curr Opin Chem Biol. **14**(3): p. 315-24.
174. Vedvik, K. L., H. C. Eliason, R. L. Hoffman, J. R. Gibson, K. R. Kupcho, R. L. Somberg, and K. W. Vogel, *Overcoming compound interference in fluorescence polarization-based kinase assays using far-red tracers.* Assay Drug Dev Technol, 2004. **2**(2): p. 193-203.
175. Turconi, S., K. Shea, S. Ashman, K. Fantom, D. L. Earnshaw, R. P. Bingham, U. M. Haupts, M. J. Brown, and A. J. Pope, *Real experiences of uHTS: a prototypic 1536-well fluorescence anisotropy-based uHTS screen and application of well-level quality control procedures.* J Biomol Screen, 2001. **6**(5): p. 275-90.
176. Holbeck, S.L., *Update on NCI in vitro drug screen utilities.* European Journal of Cancer, 2004. **40**: p. 785–793.
177. Jemal, A.; Siegel, R.; Ward, E.; Hao, Y.; Xu, J.; Murray, T.; Thun, M. J., *Cancer statistics.* CA Cancer J Clin, 2008.
178. Huggins, C.; Hodges, C. V., *Studies on prostatic cancer. I. The effect of castration, of estrogen and androgen injection on serum phosphatases in metastatic carcinoma of the prostate.* CA Cancer J Clin 1972. **22**: p. 232-240.
179. Heinlein, C. A.; Chang, C., *Androgen receptor in prostate cancer.* Endocr. Rev., 2004. **24**: p. 276-308.
180. Evans, R. M., *The steroid and thyroid hormone receptor superfamily.* Science 1988. **240**: p. 889–895.

181. Bain, D. L.; Heneghan, A. F.; Connaghan-Jones, K. D.; Miura, M. T., *Nuclear receptor structure: implications for function.* Annu. Rev. Physiol., 2007. **69**: p. 201–220.
182. He, B.; Kemppainen, J. A.; Voegel, J. J.; Gronemeyer, H.; Wilson, E. M. , *Activation function 2 in the human androgen receptor ligand binding domain mediates interdomain communication with the NH(2)-terminal domain.* . J Biol Chem, 1999. **274**: p. 37219-37225.
183. Heemers HV, Tindall DJ., *Androgen receptor (AR) coregulators: a diversity of functions converging on and regulating the AR transcriptional complex.* Endocr Rev, 2007. **28**: p. 778-808.
184. Heinlein, C. A.; Chang, C., *Androgen receptor (AR) coregulators: an overview.* Endocr Rev, 2002(23): p. 175-200.
185. Gomella, L. G.; Singh, J.; Lallas, C.; Trabulsi, E. J. , *Hormone therapy in the management of prostate cancer: evidence-based approaches.* Ther Adv Urol, 2010. **2**: p. 171-181.
186. Feldman, B. J.; Feldman, D., *The development of androgen-independent prostate cancer. Nat Rev Cancer.* Nat Rev Cancer, 2001. **1**: p. 34-45.
187. Chen, C. D.; Welsbie, D. S.; Tran, C.; Baek, S. H.; Chen, R.; Vessella, R.; Rosenfeld, M. G.; Sawyers, C. L. , *Molecular determinants of resistance to antiandrogen therapy.* Nat Med, 2004. **10**: p. 33-39.
188. Kawata, H.; Arai, S.; Nakagawa, T.; Ishikura, N.; Nishimoto, A.; Yoshino, H.; Shiraishi, T.; Tachibana, K.; Nakamura, R.; Sato, H., *Biological properties of androgen receptor pure antagonist for treatment of castration resistant prostate cancer: optimization from lead compound to CH5137291.* . Prostate, 2011. **71**: p. 1344-1356.
189. Sharifi, N., *New agents and strategies for the hormonal treatment of castration-resistant prostate cancer.* . Expert Opin Investig Drugs, 2010. **19**: p. 837-846.
190. Scher, H. I.; Beer, T. M.; Higano, C. S.; Anand, A.; Taplin, M. E.; Efstathiou, E.; Rathkopf, D.; Shelkey, J.; Yu, E. Y.; Alumkal, J.; Hung, D.; Hirmand, M.; Seely, L.; Morris, M. J.; Danila, D. C.; Humm, J.; Larson, S.; Fleisher, M.; Sawyers, C. L. , *Antitumour activity of MDV3100 in castration-resistant prostate cancer: a phase 1-2 study.* . Lancet 2010, , 2010. **375**: p. 1437-1446.
191. Attar, R. M.; Jure-Kunkel, M.; Balog, A.; Cvijic, M. E.; Dell-John, J.; Rizzo, C. A.; Schweizer, L.; Spires, T. E.; Platero, J. S.; Obermeier, M.; Shan, W.; Salvati, M. E.; Foster, W. R.; Dinchuk, J.; Chen, S. J.; Vite, G.; Kramer, R.; Gottardis, M. M. , *Discovery of BMS-641988, a novel and potent inhibitor of androgen receptor signaling for the treatment of prostate cancer.* Cancer Res, 2009. **69**: p. 6522-6530.
192. Rathkopf, D.; Liu, G.; Carducci, M. A.; Eisenberger, M. A.; Anand, A.; Morris, M. J.; Slovin, S. F.; Sasaki, Y.; Takahashi, S.; Ozono, S.; Fung, N. K.; Cheng, S.; Gan, J.; Gottardis, M.; Obermeier, M. T.; Reddy, J.; Zhang, S.; Vakkalagadda, B. J.; Alland, L.; Wilding, G.; Scher, H. I. , *Phase I dose-escalation study of the novel antiandrogen BMS-641988 in patients with castration-resistant prostate cancer.* Clin Cancer Res, 2011. **17**: p. 880-887.
193. Clegg, N. J.; Wongvipat, J.; Tran, C.; Ouk, S.; Dilhas, A.; Joseph, J.; Chen, Y.; Grillot, K.; Bischoff, E. D.; Cai, L.; Aparicio, A.; Dorow, S.; Arora, V.; Shao, G.; Qian, J.; Zhao, H.; Yang, G.; Cao, C.; Sensintaffar, J.; Wasielewska, T.; Herbert, M. R.; Bonnefous, C.; Darimont, B.; Scher, H. I.; Smith-Jones, P. M.; Klang, M.; Smith, N. D.; de Stanchina, E.; Wu, N.; Ouerfelli, O.; Rix, P.; Heyman, R.; Jung, M. E.; Sawyers, C. L.; Hager, J. H. , *ARN-509: a novel anti-androgen for prostate cancer treatment.* . Cancer Res, 2012. **72**: p. 1494–1503.

194. Estebanez-Perpina, E.; Arnold, L. A.; Nguyen, P.; Rodrigues, E. D.; Mar, E.; Bateman, R.; Pallai, P.; Shokat, K. M.; Baxter, J. D.; Guy, R. K.; Webb, P.; Fletterick, R. J. , *A surface on the androgen receptor that allosterically regulates coactivator binding.* Proc Natl Acad Sci U S A 2007. **104**: p. 16074-16079.
195. Buzon, V.; Carbo, L. R.; Estruch, S. B.; Fletterick, R. J.; Estebanez-Perpina, E. , *A conserved surface on the ligand binding domain of nuclear receptors for allosteric control.* . Mol Cell Endocrinol, 2011. **348**: p. 394-402.
196. Moore, T.W.; Mayne, C.G.; Katzenellenbogen, J.A. Minireview: *Not picking pockets: nuclear receptor alternate-site modulators (NRAMs).* Mol Endocrinol, 2009. **24**: p. 683-695.
197. Estebanez-Perpina, E.; Jouravel, N.; Fletterick, R.J., *Perspectives on designs of antiandrogens for prostate cancer.* Expert Opinion on Drug Discovery, 2007. **2**: p. 1341-1355.
198. Chang, C.Y.; McDonnell, D.P., *Androgen receptor-cofactor interactions as targets for new drug discovery.* . Trends Pharmacol Sci, 2005. **26**: p. 225-228.
199. Gunther, J.R.;Parent, A.A.; Katzenellenbogen, J.A., *Alternative inhibition of androgen receptor signaling: peptidomimetic pyrimidines as direct androgen receptor/coactivator disruptors.* ACS Chem Biol, 2009. **4**: p. 435- 440.
200. M.D., Sadar, *Small molecule inhibitors targeting the "achilles' heel" of androgen receptor activity.* Cancer Res, 2011. **71**: p. 1208-1213.
201. Chang, C.Y.; Abdo, J.; Hartney, T.; McDonnell, D.P. , *Development of peptide antagonists for the androgen receptor using combinatorial peptide phage display.* Mol Endocrinol, 2005. **19**: p. 2478-2490.
202. Dominguez-Seoane, M.; Petkau-Milroy, K.; Vaz , B.; Möcklinghoff, S.; Folkertsma, S.; Milroy, L.G.; Brunsveld, L. , *Structure–activity relationship studies of miniproteins targeting the androgen receptor–coactivator interaction* Med. Chem. Commun., 2013. **4**: p. 187-192.
203. Lack, N.A.; Axerio-Cilies, P.; Tavassoli, P.; Han, F.Q.; Chan, K.H., Feau, C.; LeBlanc, E.; Guns, E.T.; Guy, R.K.; Rennie, P.S.; Cherkasov, A. , *Targeting the binding function 3 (BF3) site of the human androgen receptor through virtual screening.* J Med Chem, 2011. **54**: p. 8563-8573.
204. Munuganti, R. S. N.; Leblanc, E. ; Axerio-Cilies, P.; Labriere, Ch.; Frewin, K.; Hassona, M. D. H.; Lack, N. A.; Li, H.; Ban, F.; Guns, E. T.; Young, R.; Rennie, P. S.; Cherkasov, A. , *Targeting the Binding Function 3 (BF3) Site of the Androgen Receptor Through Virtual Screening. 2. Development of 2-((2-phenoxyethyl) thio)-1H-benzimidazole Derivatives* J. Med. Chem., 2013. **56**: p. 1136–1148.
205. Karabatsos, G. J.; Graham, J. D.; Vane, F. M., *Syn-anti Isomer Determination of 2,4-Dinitrophenylhydrazones and Semicarbazones by N.M.R.* J. Am. Chem. Soc. , 1966. **84**: p. 753 - 755.
206. Karabatsos, G. J.; Shapiro, B. L.; Fleming, J. S.; Ratka, J. S., *Structural Studies by Nuclear Magnetic Resonance. II. Aldehyde 2,4- Dinitrophenylhydrazones.* J. Am. Chem. Soc., 1963. **85**: p. 2784–2788.
207. Karabatsos, G. J.; Hsi, N., *Structural studies by nuclear magnetic resonance-XI: Conformations and configurations of oxime o-methyl ethers.* Tetrahedron 1967. **23**: p. 1079–1095.
208. Minabe, M.; Takabayashi, Y.; Setta, Y.; Nakamura, H.; Kimura, T.; Tsubota, M., *Characterization of 9-(p-Substituted Benzylidenehydrazono)fluorenes.* Bull. Chem. Soc. Jpn., 1996. **69**: p. 3633–3638.
209. Ramanathan, S.; Lemal, D. M., *Conformational and configurational dynamics of a highly fluorinated hydrazone.* J. Org. Chem., 2007(72): p. 1566–1569.

210. Alkorta, I.; Blanco, F.; Elguero, J., *Barriers about Double Carbon-Nitrogen Bond in Imine Derivatives Aldimines, Oximes, Hydrazones, Azines.* Croat. Chim. Acta, 2009. **82**: p. 173–183.
211. Chapelle, J. P.; Elguero, J.; Jacquier, R.; Tarrago, G., *Studies on enehydrazines 2. Reaction of trimethylhydrazine with ketones – Formation of enehydrazines and N,N-dimethylhydrazones.* Bull. Soc. Chim. Fr., 1970: p. 3145–3146.
212. Lu, S. I. J., *Gibbs energy of activation for thermal isomerization of (1Z)-acetaldehyde hydrazone and (1Z)-acetaldehyde N,N-dimethylhydrazone by Gaussian-4 theory and CCSD(T)/CBS computations.* Comput. Chem., 2009. **30**: p. 2176–2180.
213. Trabelsi, M.; Salem, M.; Champagne, B., *Investigation of the configuration of alkyl phenyl ketone phenylhydrazones from ab initio 1H NMR chemical shifts.* Org. Biomol. Chem. , 2003. **1**: p. 3839–3844.
214. Langa, F.; de la Cruz, P.; Delgado, J. L.; Haley, M. M.; Shirtcliff, L.; Alkorta, I.; Elguero, J., *The structure of p-nitrophenylhydrazones of aldehydes: the case of the p-nitrophenylhydrazone of 2-diethylamino- 5-methoxy-2H-indazole-3-carboxaldehyde.* J. Mol. Struct., 2004. **699**: p. 17–21.
215. Savini, L.; Chiasserini, L.; Gaeta, A.; Pellerano, C., *Synthesis and anti-tubercular evaluation of 4-quinolylhydrazones.* Bioorg. Med. Chem., 2002. **10**: p. 2193–2198.
216. Wyrzykiewicz, E.; Prukala, D., *New Isomeric N-substituted Hydrazones of 2-, 3- and 4-Pyridinecarboxaldehydes.* J. Heterocycl. Chem., 1998. **35**: p. 381–387.
217. Brokaite, K.; Mickevicius, V.; Mikulskiene, G., *Synthesis and structural investigation of some 1,4-disubstituted-2-pyrrolidinones.* Arkivoc 2006. **ii**: p. 61–67.
218. Kuodis, Z.; Rutavicius, A.; Matijoska, A.; Eicher-Lorka, O., *Synthesis and isomerism of hydrazones of 2-(5-thioxo-4,5-dihydro- 1,3,4-thiadiazol-2-ylthio)acetohydrazide.* Centr. Eur. J. Chem., 2007. **5**: p. 996–1006.
219. Ershov, A. Y.; Lagoda, I. V.; Yakimovich, S. I.; Pakal'nis, V. V.; Zerova, I. V.; Dobrodumov, A. V.; Shamanin, V. V., *Tautomerism and conformational isomerism of mercaptoacetylhydrazones of aliphatic and aromatic aldehydes.* Russ. J. Org. Chem., 2009. **45**: p. 660–666.
220. Monfared, H. H.; Bikas, R.; Mayer, P., *(E)-3-Hydroxy-N'-(2-hydroxybenzylidene)-2-naphthohydrazide. .* Acta Crystallogr. (E), 2010. **66**: p. o236–o237.
221. Blanco, F., B. Egan, L. Caboni, J. Elguero, J. O'Brien, T. McCabe, D. Fayne, M. J. Meegan, and D. G. Lloyd, *Study of E/Z isomerization in a series of novel non-ligand binding pocket androgen receptor antagonists.* J Chem Inf Model, 2012. **52**(9): p. 2387-97.
222. CCDC, *Cambridge Crystallographic Data Centre, 12 Union Road, Cambridge CB2 1EZ, England.* Cambridge Crystallographic Data Centre, 2012.
223. H. H. Monfared, R. Bikas and P. Mayer, *(E)-3-Hydroxy-N'-(2-hydroxybenzylidene)-2-naphthohydrazide.* Acta Cryst., 2010. **66**: p. o236-o237.
224. Li, W.-Y. Liu and Y.-Z., *2-Hydroxyacetophenone 3-hydroxy-2-naphthoylhydrazone.* Acta Cryst., 2004. **60**: p. o694-o69.
225. Lei JT, Jiang YX, Tao LY, Huang SS, Zhang HL., *N'-(3-Eth-oxy-2-hydroxy-benzyl-idene)-3-hydroxy-naphthalene-2-carbohydrazide.* Acta Crystallogr Sect E Struct Rep Online., 2008. **64**(5): p. o909.
226. Caboni, Laura; Blanco, Fernando, *Biochemical evaluation of AR:coactivator interaction using TR-FRET techniques.* 2012.

227. Pope, A. J.; Haupts, U. M.; Moore, K. J., *Homogeneous fluorescence readouts for miniaturized high-throughput screening: theory and practice.* Drug Discov. Today., 1999. **4**: p. 350–362.
228. Gunther, J. R.; Du, Y.; Rhoden, E.; Lewis, I.; Revennaugh, B.; Moore, T. W.; Kim, S. H.; Dingledine, R.; Fu, H.; Katzenellenbogen, J. A., *A set of time-resolved fluorescence resonance energy transfer assays for the discovery of inhibitors of estrogen receptor-coactivator binding.* J. Biomol. Screen, 2009. **14**: p. 181–193.
229. Klokol, G. V.; Sharanina, L. G.; Nesterov, V. N.; Shklover, V. E.; Sharanin, Yu. A.; Struchkov, Yu. T., *Cyclization of nitriles. XXIII. Addition of active phenols to electron-deficient ethylenes with cyclization to 2-amino-4H-benzo[b]pyrans. Crystal structure of 2-amino-4-(2-fluorophenyl)-3-(ethoxycarbonyl)4H-naphtho[2,1-b]pyran* Zhurnal Organicheskoi Khimii, 1987. **23**(2): p. 412-21.
230. *Ambinter*, Chemical Library. *Supplier.*
231. Elagamey, Abdel Ghani A.; Sawllim, Salah Z.; El-Taweel, Fathy M. A.; Elnagdi, Mohamed H. , *Nitriles in heterocyclic synthesis: novel syntheses of benzo[b]pyrans, naphtho[1,2-b]pyrans, naphtho[2,1-b]pyrans, pyrano[3,2-h]quinolines and pyrano[3,2-c]quinolines* Collection of Czechoslovak Chemical Communications, 1988. **52**(7): p. 1534-8.
232. Elagamey, Abdel Ghani Ali; El-Taweel, Fathy Mohamed Abdel Aziz *Nitriles in heterocyclic synthesis: synthesis of condensed pyrans`.* Indian Journal of Chemistry, Section B: Organic Chemistry Including Medicinal Chemistry, 1990. **29B**(9): p. 885-6.
233. ALDRICH Chemical Company, Inc. *Supplier.*
234. Zhang, Li; Lu, Cui-fen; Yang, Gui-chun; Chen, Zu-xing *Novel synthesis of 2-amino-3-ethoxycarbonyl benzopyrans with onium salt as soluble support.* Chemical Research in Chinese Universities, 2011. **27**(3): p. 435-440.
235. *Ambinter*, Chemical Library. *Supplier.*
236. Ltd., Interbioscreen. Chemical Library. *Supplier.*
237. Krishnan, G. Rajesh; Sreekumar, Krishnapillai *First example of organocatalysis by polystyrene-supported PAMAM dendrimers: highly efficient and reusable catalyst for Knoevenagel condensations* European Journal of Organic Chemistry, 2008(28): p. 4763-4768.
238. Shah, K. J.; Genge, D. K.; Trivedi, J. J., *Substituted dicarboxylic acids. II. Synthesis of dichlorophenyl- and methoxynaphthylsuccinic acids.* Journal of the Indian Chemical Society, 1959. **36**: p. 54-6.
239. Database: ChemDB (University of California. Irvine), 2010.
240. S. Ayyad, F. El-Taweel, A. Elagamey and T. El-Mashad, *An Efficient and Convenient Synthesis of Certain 2-Thioxothiazole,2-oxo-1,2-dihydropridine, 2-Oxo-2H-pyran,2,4-diaminothiophene and Pyrazolo[5,1-c][1,2,4]triazine Derivatives Containing Antipyrine Moiety.* International Journal of Organic Chemistry, 2012. **2**(2): p. 135-142.
241. Ambinter, *Chemical Library Supplier.*
242. Ismail, M.M.F., Afinidad *Synthesis and biological evaluation of novel polysubstituted chromene, chromenopyrimidine and chromenotriazolopyrimidine derivatives.* Spanish Journal, 2004. **61** p. 334-340.
243. Chemical Library Supplier: MicroChemistry, *MicroChemistry Ltd.*
244. http://www.chemicalbook.com/ChemicalProductProperty_EN_CB6115807.htm, 70627-20-2 (CAS Reference)
245. Harris, Christopher M.; Hobson, Adrian D.; Wilson, Noel S. Assignee, *Preparation of 1-benzylazetidine-3-carboxylic acid derivatives as agonists and antagonists of the S1P5 receptor.* Abbott Laboratories, USA, 2010.

246. Marrapu, Vijay K.; Chaturvedi, Vinita; Singh, Shubhra; Singh, Shyam; Sinha, Sudhir; Bhandari, Kalpana *Novel aryloxy azolyl chalcones with potent activity against Mycobacterium tuberculosis H37Rv.* Eur J Med Chem., 2011. **46**(9): p. 4302-10.
247. Woo, Jacqueline C. S.; Cui, Sheng; Walker, Shawn D.; Faul, Margaret M. , *Asymmetric syntheses of a GPR40 receptor agonist via diastereoselective and enantioselective conjugate alkynylation.* Tetrahedron, 2010. **66**(26): p. 4730-4737.
248. Albers, Harald M. H. G.; Hendrickx, Loes J. D.; van Tol, Rob J. P.; Hausmann, Jens; Perrakis, Anastassis; Ovaa, Huib *Structure-Based Design of Novel Boronic Acid-Based Inhibitors of Autotaxin, .* J. Med. Chem., 2011. **54**(13): p. 4619–4626.
249. Kassem, Emad M.; El-Sawy, Eslam R.; Abd-Alla, Howaida I.; Mandour, Adel H.; Abdel-Mogeed, Dina; El-Safty, Mounir M. , *Synthesis, antimicrobial, and antiviral activities of some new 5-sulphonamido-8-hydroxyquinoline derivatives.* Arch Pharm Res., 2012. **35**(6): p. 955-64.
250. Ghorab, Mostafa M.; Al-Said, Mansour S. , *Anticancer activity of novel indenopyridine derivatives.* Archives of Pharmacal Research, 2012. **35**(6): p. 987-994
251. Kharas, Gregory B.; Hanawa, Emi; Lachenberg, Jamie; Brozek, Beata; Miramon, Patricia; Mojica, Audris C.; Colbert, Acheera C.; Crowell, Bridget T.; Madison, Ashley; Martinez, Amanda P. , *Novel Copolymers of Vinyl Acetate and Some Ring-Substituted 2-Phenyl-1,1-dicyanoethylenes.* Journal of Macromolecular Science, 2008. **45**(6): p. 420-424.
252. Sun, Qi; Shi, Lan-Xiang; Ge, Ze-Mei; Cheng, Tie-Ming; Li, Run-Tao *An efficient and green procedure for the Knoevenagel condensation catalyzed by urea.* Chinese Journal of Chemistry, 2005. **23**(6): p. 745–748.
253. Oskooie, Hossien A.; Heravi, Majid M.; Derikvand, Fatemeh; Khorasani, Marzieh; Bamoharram, Fatemeh F., *On water. An efficient Knoevenagel condensation using 12-tungstophosphoric acid as a reusable green catalyst.* Synthetic Communications, 2006. **36**: p. 2819-2823.
254. Gazit, Aviv; Yaish, Pnina; Gilon, Chaim; Levitzki, Alexander *Tyrphostins I: synthesis and biological activity of protein tyrosine kinase inhibitors.* Journal of medicinal chemistry, 1989. **32** p. 2344-2352
255. Jiang, Heng; Wang, Min; Song, Zhiguo; Gong, Hong *Inorganic zinc salts-catalyzed Knoevenagel condensation at room temperature without solvent.* Prep Biochem Biotechnol, 2009. **39**(2): p. 194-200.
256. Chen, Zhuo; Dong, Xian; Wu, Jian-Wei; Xie, Hui *An efficient and recyclable ionic liquid-supported proline catalyzed Knoevenagel condensation.* ISRN Organic Chemistry, 2011: p. 5.
257. Volmajer, Julija; Toplak, Renata; Bittner, Shmuel; Majcen Le Marechal, Alenka *2-Oxiranecarbonitriles in the synthesis of linked quinono heterocyclic derivatives.* ARKIVOC, 2003. **xiv**: p. 49-61.
258. Liu, Wei; Liu, Ye *Synergistic effect of an ionic liquid catalyst with two kinds of basic sites on Knoevenagel condensation.* 2008.
259. Weinberger, M. A.; Heggie, R. M.; Holmes, H. L, *Solvent effects in the nuclear magnetic resonance spectra of benzalmalononitriles.* Canadian Journal of Chemistry, 1965. **43**: p. 2585-2593.
260. Swaringen, Roy A., Jr.; Yeowell, David A.; Wisowaty, James C.; El-Sayad, Hassan A.; Stewart, Ellen L.; Darnofall, Michael E. , *Reaction of orthoformates with acidic methines.* Journal of organic chemistry, 1979. **44**: p. 4825-4829

261. Jin, Tong-Shou; Xiao, Jin-Chong; Wang, Su-Juan; Li, Tong-Shuang *Ultrasound-assisted synthesis of 2-amino-2-chromenes with cetyltrimethylammonium bromide in aqueous media.* Ultrasonics Sonochemistry, 2004. **11**(6): p. 393-7.
262. Seifi, Mohammad.; Sheibani, Hassan., *High surface area MgO as a highly effective heterogeneous base catalyst for three-component synthesis of tetrahydrobenzopyran and 3,4-dihydropyrano[c]chromene derivatives, in aqueous media.* Catalysis Letters, 2008. **126**: p. 275.
263. Heravi, Majid M.; Zakeri, Masoumeh; Mohammadi, Narges *Morpholine catalyzed one-pot multicomponent synthesis of compounds containing chromene core in water.* Chinese Journal of Chemistry, 2011. **29**(6): p. 1163–1166.
264. Shaterian, H. R.; Oveisi, A. R. , *A simple green approach to the synthesis of 2-amino-5-oxo-4,5-dihydropyrano[3,2-c]chromene-3-carbonitrile derivatives catalyzed by 3-hydroxypropanaminium acetate (HPAA) as a new ionic liquid.* Journal of the Iranian Chemical Society, 2011. **8**(2): p. 545-552.
265. Khurana, Jitender M.; Nand, Bhaskara; Saluja, Pooja *DBU: a highly efficient catalyst for one-pot synthesis of substituted 3,4-dihydropyrano[3,2-c]chromenes, dihydropyrano[4,3-b]pyranes, 2-amino-4H-benzo[h]chromenes and 2-amino-4H benzo[g]chromenes in aqueous medium.* Tetrahedron, 2010. **66**(30): p. 5637–5641.
266. Shi, Da-Qing; Wu, Nan; Zhuang, Qi-Ya *Synthesis of 2-amino-4-aryl-5-oxo-4,5-dihydropyrano[3,2-c]chromene derivatives catalysed by KF-montmorillonite.* Journal of Chemical Research, 2008. **9**(4): p. 542-545.
267. AsInEx, in *Chemical Library, Supplier: AsInEx*.
268. Tarbell, D. S.; Wargotz, Bernard *A rearrangement involving aromatization. The condensation of Δ^4-tetrahydrophthalaldehyde with diethyl acetonedicarboxylate.* J. Am. Chem. Soc., 1954. **76**(22): p. 5761–5767.
269. Jain, Asheesh K.; Gupta, Pradeep K.; Ganesan, K.; Pande, Ambuja; Malhotra, R. C. , *Rapid solvent-free synthesis of aromatic hydrazides under microwave irradiation.* Defence science journal, 2007. **57**(2): p. 267-270.
270. Cacchi, Sandro; Ciattini, Pier Giuseppe; Morera, Enrico; Ortar, Giorgio *Palladium-catalyzed carbonylation of aryl triflates. Synthesis of arenecarboxylic acid derivatives from phenols.* Tetrahedron Letters, 1986. **27**(33): p. Pages3931-4.
271. Brown, Ursula, M.; Carter, P. H.; Tomlinson, Muriel *Formyl compounds. II.* Journal of the Chemical Society, 1958 p. 1843-9.
272. You, Zhong-Lu; Shi, Da-Hua; Zhang, Ji-Cai; Ma, Yu-Ping; Wang, Che; Li, Kun *Synthesis, structures, and urease inhibitory activities of oxovanadium(V) complexes with Schiff bases.* Inorganica Chimica Acta, 2012. **384**: p. 51-61.
273. *1. (WO1994006280) Inhibitors of Metazoan Parasite Proteases, 31, 03, 1994, Internal publication with ISR A1 (08/1994) (1-4).*
274. CAS, *CAS Registry Number: 91997-94-3 & Depositor: ABI Chem, External ID: AC1NC1R3*
275. CAS, *CAS Registry Number: 316132-50-0 (CH3).*
276. Fernando Blanco, Billy Egan, Laura Caboni, José Elguero, John O'Brien, Thomas McCabe, Darren Fayne, David G. Lloyd, and Mary J. Meegan, *Study of E/Z Isomerization in a Series of Novel Non-ligand Binding Pocket Androgen Receptor Antagonists.* J. Chem. Inf. Model., 2012. **52**(9): p. 2387-97.
277. Franzen, Hartwig; Eichler, Th., *Replacement of Hydroxyl by the Hydrazine Group.* J. pr. Chem., 1909. **78**: p. 157-64.
278. Ganjali, Mohammad Reza; Norouzi, Parviz; Tamaddon, Atefeh; Adib, Mehdi *Nano-level monitoring of ytterbium(III) by a novel ytterbium(III) membrane sensor based on 3-hydroxy-N'-[(2-hydroxyphenyl) methylene]-2-*

naphthohydrazide. Sensors and Actuators B: Chemical, 200-6. **114**(2): p. 855-860.
279. Look, Gary Charles; Schultz, Lauri; Polozov, Alexandre Mikhaylovich; Bhagat, Nikhil; Wang, Jian; Zembower, David E.; Goure, William F.; Pray, Todd; Krafft, Grant A. Assignee, *Methods of inhibiting the formation of amyloid-beta diffusible ligands using acylhydrazide compounds*, in *Acumen Pharmaceuticals, Inc., USA* 2008, Acumen Pharmaceuticals, Inc., USA
280. *Chemical Library Supplier: ALDRICH Chemical Company, Inc.*
281. Osman, Mahar Mohamed; Ali, Gamila Yousef; *Complexes of cobalt(II), nickel(II), copper(II) and zinc(II) with 3-hydroxy-2-naphthoyl hydrazones of some aromatic aldehydes.* ACTA Chimica Academiae Scientarium Hungaricae, 1981. **108**(1): p. 13-23.
282. *Chemical Library Supplier: TimTec, Inc.*
283. Dogan, H. N.; Duran, A.; Rollas, S.; Sener, G.; Armutak, Y.; Keyer-Uysal, M. , *Synthesis and structure elucidation of some new hydrazones and oxadiazolines: anticonvulsant activities of 2-(3-acetyloxy-2-naphthyl)-4-acetyl-5-substituted-1,3,4-oxadiazolines.* Med Sci Res, 1998. **26**(11): p. 755-758.
284. Zhang, Mei; Xian, Dong-Mei; Li, Hai-Hua; Zhang, Ji-Cai; You, Zhong-Lu *Synthesis and Structures of Halo-Substituted Aroylhydrazones with Antimicrobial Activity.* Australian Journal of Chemistry 2012. **65**(4): p. 343-350.
285. Hapipah, M. A.; Zain, Sharifuddin M.; Jefrey, B. Wan; Rahuma, S. M.; Rohaiza, S. O. Sharifah; Abdullah, Noorlidah; Teoh, H., *Synthesis, structural characterization, electrochemical and antimicrobial studies of complexes from the NO ligating Schiff bases of furoic acid hydrazide.* Malaysian Journal of Science, 2004. **23**(1): p. 119-127.